FINAL REPORT
LONG-TERM MONITORING GROUNDWATER OPTIMIZATION AT SITE 133 EDWARDS AFB, CALIFORNIA USING THE GEOSTATISTICAL TEMPORAL/SPATIAL (GTS) ALGORITHM

CONTRACT NUMBER: F41624-00-D-8030
TASK ORDER 0062
TASK 5

May 2004

Submitted to:

HQ AFCEE/BCE
3300 Sidney Brooks Road
Brooks City-Base TX 78235

Submitted by:

Science Applications International Corporation
11251 Roger Bacon Drive
Reston, VA 20190

SAIC Project No. 06-6312-04-4567-005

This page left intentionally blank for duplicating purposes.

Table of Contents

Introduction **1**
Section 1. Executive Summary **2**
Section 2. Description of Site 133, Edwards AFB **3**
Section 2.1. Site Hydrogeology and Contaminant Sources 3
Section 2.2. Monitoring Network 4
Section 3. Temporal Optimization at Site 133 ..... **6**
Section 3.1. Data Preparation 6
Section 3.2. Temporal Methodology 9
Section 3.2.1. Temporal Variograms 9
Section 3.2.2. Iterative Thinning 12
Section 3.3. Trend Mapping 17
Section 3.4. Temporal Optimization Results 18
Section 3.4.1. Temporal Variograms 19
Section 3.4.2. Iterative Thinning 19
Section 3.4.3. Trend Maps 20
Section 4. Spatial Optimization **24**
Section 4.1. Data Preparation 24
Section 4.2. Methodology 25
Section 4.2.1. Declustered CDF 25
Section 4.2.2. Spatial Bandwidth and Search Radius 27
Section 4.2.3. Creating Base Maps with LWQR 28
Section 4.2.4. Constructing the Base Map 31
Section 4.2.5. Global Regression Weights 32
Section 4.2.6. Local and Global Variance Measures 34
Section 4.2.7. Iterative Elimination of Wells 34
Section 4.3. Spatial Optimization Results 35
Section 4.3.1. Global Measures of Redundancy 36
Section 4.3.2. Local Indications of Redundancy 38
Section 4.3.3. Base Map Accuracy 39
Section 5. Recommendations for Edwards AFB, Site 133 ..... **40**
Section 5.1 Recommendations Regarding Sampling Frequency 40
Section 5.2 Recommendations Regarding Spatial Redundancy 42
Section 5.3 Recommendations Regarding Siting of New Wells 50
Section 5.4. Cost Analysis and Summary 52
Section 5.4.1. Unit Cost Data 52
Section 5.4.2. Estimating Baseline (Current) Monitoring Costs 52
Section 5.4.3. Estimating Reductions in Monitoring Activity 53
Section 5.4.4. Estimating Sample Analysis Costs 53
Section 5.4.5. Estimating Project Level Monitoring Costs 54
Section 5.4.6. Checking the Baseline Cost Tables 55
Section 5.4.7. Estimate of Costs Savings 55
Section 6. References **57**

Appendices

Appendix 3-1 Temporal Optimization: Temporal Variograms
Appendix 3-2 Temporal Optimization: Iterative Fitting Overlays
Appendix 3-3 Temporal Optimization: Iterative Fitting Results
Appendix 3-4 Temporal Optimization: Trend Maps
Appendix 4-1 Spatial Optimization: Global Redundancy Measures
Appendix 4-2 Spatial Optimization: DIOXANE14 Indicator Difference Maps – Time Slice 1
Appendix 4-2 Spatial Optimization: DIOXANE14 Indicator Difference Maps – Time Slice 2
Appendix 4-2 Spatial Optimization: MN Indicator Difference Maps – Time Slice 1
Appendix 4-2 Spatial Optimization: MN Indicator Difference Maps – Time Slice 2
Appendix 4-2 Spatial Optimization: TCE Indicator Difference Maps – Time Slice 1
Appendix 4-2 Spatial Optimization: TCE Indicator Difference Maps – Time Slice 2
Appendix 4-3 Spatial Optimization: DIOXANE14 Local Variance Maps – Time Slice 1
Appendix 4-3 Spatial Optimization: DIOXANE14 Local Variance Maps – Time Slice 2
Appendix 4-3 Spatial Optimization: MN Local Variance Maps – Time Slice 1
Appendix 4-3 Spatial Optimization: MN Local Variance Maps – Time Slice 2
Appendix 4-3 Spatial Optimization: TCE Local Variance Maps – Time Slice 1
Appendix 4-3 Spatial Optimization: TCE Local Variance Maps – Time Slice 2
Appendix 4-4 Spatial Optimization: Base Concentration Maps
Appendix 5-1 Estimate of Cost Savings (MS Excel file)

Figures

Figure 5-1. Approximate Locations of Greatest Relative Local Uncertainty 51

Tables

Table 2-1. Existing Site 133 Baseline LTM Network (All measurements in feet)..... 4
Table 3-1. COC Detection Frequencies 7
Table 3-2. Well Detection Rates for Selected COCs 8
Table 3-3. Temporal Variogram Ranges and Recommended Sampling Interval 19
Table 3-4. Summary of Iterative Thinning Results, By COC and Well Location..... 21
Table 3-5. Estimated Trend Magnitudes and Confidence Intervals by COC and Well Location..... 22
Table 4-1. Parameters of Final Spatial Correlation Models 27
Table 4-2. Reference Concentrations and Corresponding Percentiles of Declustered CDF for Each COC 29
Table 4-4. Hypothetical LWQR Results for TCE..... 32
Table 5-1. Example Sampling Plan for the First Seven Quarters of the Optimized LTM Sampling Program 42
Table 5-2. Essential Monitoring Network Based on Analysis of All COCs 44
Table 5-3. Redundant Monitoring Wells Based on Analysis of All COCs 46
Table 5-4. Essential Monitoring Network Based on Analysis of TCE in 2001-2002 47
Table 5-5. Redundant Monitoring Wells Based on Analysis of TCE in 2001-2002 49
Table 5-6. Approximate Locations of Greatest Local Relative Uncertainty 51
Table 5-7A. Estimate of Cost Savings at Site 37..... 56
Table 5-7B. Estimate of Cost Savings at Site 133 57

This page left intentionally blank for duplicating purposes.

Long-Term Monitoring Groundwater Optimization at Site 133 Edwards AFB, California Using the Geostatistical Temporal/Spatial (GTS) Algorithm

Prepared by SAIC and MacStat Consulting, Ltd., May 2004

Introduction

This report summarizes the effort to optimize the existing long-term groundwater monitoring (LTM) network at Site 133 on Edwards Air Force Base in California. The optimization analysis is based on an application of the Geostatistical Temporal/Spatial (GTS) algorithm, which was designed for the Air Force Center for Environmental Excellence (AFCEE) by MacStat Consulting, Ltd. The analysis and the algorithm consist of two basic parts: a temporal optimization component and a spatial optimization component. The twin goals of the study are to determine, based on the existing sampling data and sampling network, 1) to what extent sampling frequencies at the site can be optimized so as to pare sampling and analysis budgets efficiently, and 2) to what extent locations within the sampling network can be optimized so that sampling information is not being collected at statistically redundant groundwater wells. Set against these goals is the overriding mandate that information critical to the success of the LTM program at Site 133 should not be sacrificed.

It should be noted that GTS is not designed around a traditional hypothesis testing framework. As an example, considering the spatial analysis, rather than deciding whether or not the mean concentration level at the site is above or below a fixed concentration limit, and then designing the monitoring network with the goal of balancing the risks of false positive and false negative decision errors, GTS is fundamentally aimed at balancing a different kind of trade-off. In particular, GTS assumes that the existing network of sampling locations is the 'most informative' available, and that a map of the spatial distribution of concentration levels based on all the existing sampling information is the most accurate map that can be estimated barring significant numbers of additional well locations. Under this presumption, GTS then balances the information lost in map accuracy against the savings in sampling and monitoring resources that otherwise would be spent maintaining the current network. Optimization is thus defined with respect to this accuracy-cost trade-off and not with respect to the false negative-false positive trade-off common to hypothesis testing.

The report is organized into six major sections. The first section is the executive summary of the optimization results and recommendations. The second section provides a brief description of the site and its existing groundwater monitoring scheme. The next two sections correspond to the temporal and spatial analyses respectively. As explained below, the temporal component is further divided into three parts: temporal variogram analysis, iterative fitting of individual wells, and trend mapping. The spatial analysis consists of a series of iterative steps. The site maps corresponding to these iterations are collected in appendices to the report. The fifth section of the report summarizes the

conclusions of the optimization effort, offers a number of recommendations, and provides a cost analysis at the site based on the optimization results. The final section provides relevant technical references.

Section 1. Executive Summary

After using the Geostatistical Temporal/Spatial (GTS) algorithm to optimize the long-term monitoring network at Site 133 on Edwards AFB, the following key results were found:

- GTS exploratory analyses were used to determine 2 to 3 'best' candidates for the optimization routine. The COCs were not chosen *primarily* on the basis of regulatory concern or health risk-exposure (although these factors were considered), but rather with the intent to include those parameters in the optimization routine that offered *the most statistical information* concerning temporal and spatial redundancy. The best such parameters typically exhibit larger detection rates and more widespread spatial occurrence. At Site 133, based on detection frequencies, per-well 'hit' rates, and spatial plotting of the maximum per-well concentration values, the most promising candidates appeared to be trichloroethylene (TCE) and manganese (MN). In addition, since 1,4-Dioxane (DIOXANE14) was of particular concern at Edwards AFB, and also showed a fairly widespread spatial distribution at the site, the final three optimization candidates were selected as TCE, MN, and DIOXANE14.

- The *common* sampling schedule for Site 133 as a whole ought to be adjusted. Temporal variograms generated by combining all the available sampling information indicate that the common sampling interval could be set to one sampling event every seven quarters (i.e., nearly biennial sampling) with little loss of statistical information, compared to current annual sampling regimen.

- The recommended operational sampling interval for wells analyzed by Iterative Fitting is generally 2-3 quarters. This number is shorter than the recommended sampling interval from the Temporal Variograms of approximately 7 quarters, probably for the reason that the number of wells eligible for Iterative Fitting was fairly limited. The Temporal Variogram procedure amalgamates sampling information across an entire collection of wells, and, therefore, does not *require* more than 2 sampling events from any given well in the set. Because relatively few wells could be optimized by Iterative Fitting, the overall GTS recommendation for the optimal sampling is based on the Temporal Variogram results.

- If the results of the GTS optimization analysis are implemented at Site 133, there ought to be a similar follow-up analysis conducted after 3 to 5 years in order to assess whether or not the same recommendations would still hold. However, any new sampling schedules should be implemented with care. The Temporal Variograms, for instance, depend significantly on having pairs of measurements from any given well with a variety of inter-event time intervals. With regard to sampling frequency, the Temporal Variograms depend significantly on having

pairs of measurements from any given well with a variety of inter-event time intervals. If all wells are sampled at the same time for each year of sampling after implementation, the range of between-sample intervals will be reduced, and consequently it will be much harder to construct a future Temporal Variogram to test the original recommendation. Instead, it is recommended that the overall set of wells be divided into sevenths, and that for each consecutive seven quarter span, a (different) quarter would be assigned at random for the sampling of each of these seven well subsets. As an example, the first subset might be sampled during the sixth quarter, while the second and third subsets are sampled during the fourth quarter, and so. Although more operationally cumbersome, such an approach would greatly facilitate the construction of future Temporal Variograms. For while each well would be sampled only once during the 7-quarter interval, there would be some variation in the times between sampling events (some would be even shorter than the current annual sampling plan). **Table 5-1** in **Section 5.1** illustrates a possible schedule for the first five years after implementation.

- The spatial optimization analysis at Site 133 revealed varying levels of spatial redundancy. For the 1999-2000 data, a 'safe' level of redundancy appeared to be about 13-27% of the total well network. For the most recent TCE data, this safe level increased to approximately 33-40%.

- 28 wells were listed as potentially redundant across the COCs, amounting to 20 ercent of the total baseline well set. Considering only the most recent TCE data, 48 wells might be considered redundant or 34% of the baseline LTM network.

- The GTS optimization algorithm can offer potentially significant cost savings over the existing LTM program at Site 133. Accurate estimates of plume magnitude and extent can be made using fewer wells than the current network and sampling at a lower frequency than presently in place. Estimates of specific potential cost savings off the total annual project budget range from 54-62%, amounting to between roughly $230,000 and $266,000 per year.

Section 2. Description of Site 133, Edwards AFB

Section 2.1. Site Hydrogeology and Contaminant Sources

Edwards Air Force Base was placed on the National Priority List (NPL) in 1990. As of 1999, site investigations had identified over 460 sites and other areas of concern on the base. Site 133 includes groundwater contamination beneath, down gradient, and upgradient of the AFRL CE Yard, extending under the AFRL landfill. The CE Yard is located at the southern extent of Saturn Boulevard at the southeastern corner of Titan Road. Sources for the Site 133 groundwater plume include storage and disposal practices at CE Yard facilities including a Waste Discharge Area located south of Building 8405 and the Drum Storage Area located approximately 50 feet south of the Waste Discharge Area. In addition, disposal practices at other sites located up gradient or cross gradient of the CE Yard have contributed to groundwater contamination within the Site 133 groundwater plume.

The subsurface geology at the CE Yard is characterized as fractured crystalline bedrock (quartz monzonite) overlain by weathered bedrock and a thin veneer of alluvial material. In wells drilled at the site, weathered bedrock has varied in thickness from 1 foot to 52 feet with depth to competent bedrock ranging from 3 feet below ground surface (bgs) to 55 feet bgs. Groundwater occurs in fractured granitic bedrock. Groundwater flow direction is generally to the south.

Section 2.2. Monitoring Network

Based on recent monitoring data, the existing monitoring network used as a baseline for the optimization analyses at Site 133 includes 140 wells as listed in **Table 2-1**. It should be noted that this list includes 48 wells labeled as part of Site 37, immediately to the west and slightly to the south of the main source area for Site 133. All the wells on this list were used as the baseline LTM network for purposes of estimating the cost savings that would accrue from the GTS optimization analysis. These wells are generally sampled once per year. Available data for this analysis covered the period from 1994 to Fall 2002, with somewhat sparse data from the years 1994 to 1997. The most typical constituents of concern (COCs) collected at the site are listed in **Section 3.1, Data Preparation**.

Groundwater is collected at Site 133 generally from bedrock wells, mostly screened in the competent bedrock zone. The depths of screened intervals range from approximately 14 feet to approximately 335 feet below ground surface (bgs). The ground surface itself varies across well locations by almost 400 feet. As only 11 wells are screened in weathered bedrock, the spatial optimization analysis could only be performed on the data set as a whole, considered as three-dimensional site volume, rather than as separate two-dimensional (areal) horizons.

Table 2-1. Existing Site 133 Baseline LTM Network (All measurements in feet)

Note: Sample Elevation is recorded as either a sample specific elevation or as the midpoint depth of a screen typically 10 feet in length

WELL_ID	EASTING	NORTHING	DEPTH	SAMPLE ELEVATION
120-MW01	6652723	2153458.5	101.8	2692.99
120-MW02	6652130.9	2153339.6	61.9	2726.79
120-MW03	6651337.7	2152768.1	115.8	2652.46
120-MW04	6651735.6	2152507.9	55	2723.04
120-MW05	6650388.3	2151854.7	23	2716.86
120-MW06	6652141.75	2153319.04	250	2538.28
120-MW07	6650852.17	2152945.68	32.5	2762.59
120-MW08	6652750.96	2152340.57	37.5	2730.02
120-MW10	6650536.74	2152200.72	65.4	2686.64
120-MW11	6652278.25	2153729.5	152.6	2645.49
120-MW12	6651527.93	2153167.6	31.5	2744.61
120-MW13	6652214.94	2152507.03	35.4	2748.22
120-MW14	6650132.24	2151472.04	43	2696
120-MW15	6650620.62	2152200.14	335.3	2410.87
121-MW09	6651912.58	2153099	46.4	2735.77
13-MW01	6656146.61	2157842.87	20.5	2886.3
13-MW02	6656649.44	2158078.61	40	2878
13-MW03	6656323.57	2159449.3	22	2930.3
13-MW04	6655406.52	2158401.88	26	2901.6
13-MW05	6656632.9	2160353.8	27	2953.63
13-MW06	6655321.7	2159854.1	24	2937.72
13-MW07	6654089.7	2159897.8	55	2922.67

WELL_ID	EASTING	NORTHING	DEPTH	SAMPLE ELEVATION
13-MW08	6656164.3	2157833	54	2852.91
13-MW09	6656144.9	2157235.9	22	2873.57
13-MW10	6655350.7	2155550.5	31	2834.26
13-MW11	6655989.68	2158806.51	51.3	2888.47
13-MW12	6654159.09	2158121.11	82	2886.33
13-MW14	6656174.57	2157261.67	105	2790.86
13-MW15	6654926.59	2153986.48	55	2790.28
13-MW16	6657790.69	2155492.4	128	2793.01
13-MW17	6655939.48	2160078.21	29	2935.41
13-MW18	6653506.98	2155883.04	51	2815.3
13-MW19	6657720.46	2153313.3	73	2803.98
13-MW20	6654728.85	2151622.06	65	2741.91
13-MW21	6656211.83	2157285.19	190	2708.8
13-MW22	6653229.32	2154153.85	111	2701.74
13-MW23	6653442.94	2152798.48	52	2756.33
13-MW24	6658576.31	2159688.48	97	2865.42
13-MW25	6658386.08	2158308.38	177	2772.8
13-MW26	6651314.69	2154738.49	33	2793.95
13-MW27	6652743.71	2150936.77	132	2644.28
13-MW28	6657809.27	2150910.93	174	2673.61
13-MW29	6651212.73	2150312.18	120	2616.04
13-MW30	6652676.18	2148799.17	98	2650.33
13-OW01	6656097.65	2157893.59	51.5	2858.6
13-OW02	6656164.23	2157884.83	39	2868.81
133-EW01	6656161.84	2157868.56	38	2870.28
133-EW02	6655214.64	2159794.78	100.5	2860.45
133-EW03	6655305.23	2160521.65	93	2887.89
133-MW01	6655449.52	2160136.78	24	2943.5
133-MW02	6655319.75	2160548.27	23	2958.14
133-MW03	6655312.52	2160355.27	25	2951.6
133-OW02	6655472.92	2159672.48	144.8	2810.74
133-OW03	6655669.17	2160547.37	153	2824.72
133-OW04	6655481.06	2160764.7	147.8	2836.97
133-OW05	6655493.74	2160905.92	145	2844.19
137-MW01	6655897.42	2161189.79	27.5	2965.16
145-MW01	6654111.54	2161135.42	49.5	2962.03
150-MW01	6655386.97	2161438.46	77	2922.69
150-MW02	6654870.46	2162277.68	82	2945.43
150-MW03	6655413.74	2161724.15	48	2961.52
150-MW04	6655265.22	2161802.34	87	2925.59
150-MW05	6654634.19	2161710.37	50.5	2962.04
150-MW06	6655096.71	2162722.82	171.5	2869.3
151-MW01	6656285.37	2161754.63	46	2966.67
153-MW01	6655973.8	2161598.28	47	2962.95
153-MW02	6656349.31	2161244.74	41	2956.27
153-MW03	6655954.34	2160838.96	18	2968.48
153-MW04	6655496.54	2160896.33	34	2955.03
153-MW05	6656017.29	2161943.61	55	2959.22
153-MW06	6655878.59	2160995.46	31	2960.94
153-MW07	6656085.42	2160933.32	48	2944.9
153-MW08	6655987.71	2161597.48	164.5	2845.72
153-MW09	6655312.52	2160535.45	256.5	2724.59
153-MW10	6655758.31	2162485.49	80.5	2951.14
162-MW01	6650280.52	2163457.13	113	2714.05
162-MW03	6650257.23	2162992.58	136.5	2730.57
162-MW04	6650231.23	2163008.36	283	2581.17
171-MW05	6651599.48	2161231.21	42	3027.29
177-MW03	6659169.43	2163818.37	83.1	2843.66
177-MW04	6658753.47	2163604.67	107.4	2839.34
177-MW06	6659098.2	2163891.3	75	2850.77
177-MW07	6659383.87	2163969.71	55.5	2857.43
177-MW08	6659263.57	2163836.95	66	2856.96
177-MW09	6659765.8	2163875.19	102.9	2798.67
177-MW20	6659372.85	2163991.21	173.5	2739.11
186-MW01	6655261.26	2160512.43	25	2955.75
186-MW02	6655250.35	2160582.13	25	2956.22
26-MW01	6657052.3	2160152.99	25	2947.4
26-MW08	6656935.29	2160875.76	33	2970.72

WELL_ID	EASTING	NORTHING	DEPTH	SAMPLE ELEVATION
32-MW01	6656137.82	2163712.03	105	2944.86
32-MW02	6656723.24	2163939.8	68	2941.45
32-MW03A	6656147.09	2163707.83	85.5	2964.34
32-MW03B	6656147.34	2163707.93	85.5	2964.34
32-MW04	6656434.84	2163538.27	86.5	2949.94
36-MW01	6650391.53	2162254.45	225	2734.42
36-MW02	6651229.12	2162847.48	243	2800.07
36-MW03	6650596.86	2162814.45	147	2750.14
36-MW04	6651339.93	2162397.37	264	2853.87
37-DEW01	6651889.9	2160869.9	70.5	2975.05
37-EW01	6652489.61	2160922.45	145	2888.78
37-EW02	6652665.97	2160754.3	66	2960.17
37-EW03	6652605.78	2160645.8	78	2945.32
37-EW04	6651878.68	2160063.02	83	2926.05
37-EW05	6652155.29	2160459.05	73	2952.24
37-EW06	6651943.4	2160872.3	82.5	2960.96
37-EW07	6651625.85	2161270.56	47.4	3023.12
37-EW08	6651621.13	2161237.59	242.5	2827.41
37-MW01	6651884.3	2161228.9	42	3015.84
37-MW02	6651465.8	2160972.4	88	2975.26
37-MW04	6652722.9	2160566.7	57	2962.73
37-MW05	6652153.5	2159651	34	2959.59
37-MW06	6651906.29	2160884.05	57.5	2986
37-MW07	6653906.26	2160643.43	53	2947.11
37-MW08	6651306.09	2160000.14	78	2936.58
37-MW09	6652142.69	2158127.06	35	2898.06
37-MW10	6651433.07	2161768.84	194	2892.4
37-MW11	6652498.83	2160924.92	110	2923.53
37-MW12	6650910.55	2158461.84	190	2763.28
37-MW13	6651459.98	2156587.43	29	2847.69
37-MW14	6652680.28	2160754.33	247	2779.43
37-MW15	6652173.3	2160215.67	70	2945.1
37-MW16	6652756.65	2160806.78	125	2901.63
37-MW17	6652298.39	2160318.27	80	2943.83
37-MW18	6653367.62	2160136.44	43	2955.48
37-MW19	6651672.68	2160164.69	242.5	2775.91
37-MW21	6652844.51	2161142.47	41	2993.99
37-MW22	6650356.65	2155556.95	80	2734.06
37-MW23	6650514.68	2159669.4	179	2826.21
37-MW24	6650924.8	2160777.8	159.5	2928.4
37-MW25	6653223.1	2159466.8	269.5	2747.4
37-MW26	6651372.3	2161323.8	94.5	2979.6
37-MW27	6651693.5	2161585.1	170.5	2900.76
37-MW28	6651796	2161436.4	105.5	2963.28
37-MW29	6651367	2161160.4	119.5	2953.01
37-OW02	6651888.3	2160830.3	153	2891.45
37-OW03	6652708.52	2160755.68	76	2950.04
37-OW05	6652449	2160449.98	145	2886.39
37-OW06	6651723.87	2160131.89	70.5	2945.3
396-MW02	6656450.36	2160682.79	14	2970.97

Section 3. Temporal Optimization at Site 133

Section 3.1. Data Preparation

Data queries were made by AFCEE and Earth Tech of all available electronic sampling records from Site 133. Data covered the period from 1994 until September 2002. In order to better gauge sources of variability — especially spatial variation — among the chemical data, data queries specifically asked for field duplicates as well as normal environmental samples.

Overall, the subsequent database included just over 16,000 records covering the following 23 constituents of concern (COC): arsenic (AS), benzene (BZ), toluene (BZME), chromium (CR), 1,2-dichloroethane (DCA12), 1,1-dichloroethene (DCE11), cis-1,2-dichloroethene (DCE12C), 1,2-t-dichloroethene (DCE12T), 1,4-dioxane (DIOXANE14), ethylbenzene (EBZ), iron (FE), mercury (HG), manganese (MN), naphthalene (NAPH), nickel (NI), NNSM, perchlorate (PCATE), perchloroethene (PCE), selenium (SE), TBUTMEE, 1,1,1-trichloroethane (TCA111), trichloroethene (TCE), and TL. These COCs were noted in site documents and reports as chemicals being monitored at Site 133 and that had been detected in laboratory analyses of sampling data. Initial detection rates by sample record for these COCs are given in **Table 3-1**.

Table 3-1. COC Detection Frequencies

COC	Rate of Detection (%)
MN	91.6
TCE	86.7
AS	77.4
NNSM	74.7
NI	74.4
SE	72.8
FE	70.5
PCE	67.5
DIOXANE14	65.3
CR	57.7
PCATE	46.1
HG	45.2
DCE12C	38.2
DCE11	19.3
TL	13.9
TBUTMEE	8.2
DCE12T	6.5
DCA12	4.5
NAPH	3.9
BZ	3.7
TCA111	2.5
BZME	1.9
EBZ	0.9

Based on these detection rates and initial time series plots of the raw data, nine COCs were initially eliminated from consideration as not exhibiting enough statistical variation for meaningful analysis: BZ, BZME, DCA12, DCE12T, EBZ, NAPH, TBUTMEE, TCA111, and TL. Exploratory plots of the remaining constituents indicated that the following eight COCs exhibited poorer spatial coverage across the site and poorer (i.e., highly discontinuous) trends over time: CR, DCE11, DCE12C, FE, HG, NNSM, PCATE, and SE. Consequently, these constituents were also eliminated from subsequent analysis.

The final six constituents were further examined by computing per-well detection rates, that is, the fraction of wells for a given compound with at least one detection, along with per-well detection rates above specific concentration levels of interest (usually a primary or secondary MCL). Summaries of these statistics are given in **Table 3-2** below:

Table 3-2. Well Detection Rates for Selected COCs

COC	Well Hit Rate (%)	Level (ppb)	Hits > Level (%)
AS	89.7	50 (MCL)	14.4
DIOXANE14	60.6	5	26.0
MN	100.0	50 (MCL)	80.4
NI	72.2	100 (MCL)	45.4
PCE	75.7	5 (MCL)	62.9
TCE	86.4	5 (MCL)	72.9

Based on these summaries and additional time series plots of the remaining COCs, the most promising candidates for the GTS optimization routine appeared to be TCE among the VOCs and MN among the metals. Spatial plotting of the maximum per-well concentration values was then conducted to determine the crude spatial distribution of the hits for each parameter. These plots generally confirmed that these two parameters had the most widespread spatial distribution at Site 133. Another parameter of particular concern at Edwards AFB was 1,4-Dioxane. It also showed a fairly widespread spatial distribution at the site, and so was included in the analysis. Thus, the final three optimization candidates were TCE, MN, and DIOXANE14.

Note in this regard that one of the purposes of the initial exploratory analysis was to determine 2 to 3 ‘best’ candidates for the optimization routine. Including a larger number of COCs significantly increases the amount of work required to run the GTS algorithm without typically improving the results. The aim is *not* to determine which COCs to monitor, but rather to include only those parameters in the optimization routine that offer *the most statistical information* concerning temporal and spatial redundancy. The best such parameters typically exhibit larger detection rates and more widespread spatial occurrence.

Another preparation step that was taken to prepare the remaining data for temporal optimization was to average values for a given sampling date by duplicate status and across multiple depths (when they existed). That is, if a given well on a given date had both normal samples and field duplicates and/or had multiple samples collected at different depths, all of these values were averaged in order to create a single analysis value for that well and sampling event. The major reason for doing this was to ensure that estimates of the typical interval between samples were not biased downward by the presence of multiple samples on a given date. Most of the wells and sampling dates only included a single sample at depth, so to include all the sample records without this averaging step would tend to skew the results.

As a final note, non-detects were handled prior to analysis by converting them to half the listed reporting limit (RL). In addition, part of the temporal analysis required keeping track of which samples were non-detects and which were detections. For single, non-averaged samples this posed no difficulty. But for values that were averaged across duplicate status and/or depth, if any of the samples to be averaged were 'hits,' the average value was also considered a hit. If all were non-detects, the average value was also labeled a non-detect.

Section 3.2. Temporal Methodology

The temporal optimization analysis in GTS consists of three basic components: 1) temporal variograms applied to groups of wells, 2) iterative thinning of individual wells, and 3) trend mapping over specific time periods. Each of these components is explained below. Note again that the temporal analysis is *not* designed to determine which well locations might be redundant and perhaps unnecessary to the LTM program. Rather, the major goal of the temporal portion of GTS is to examine and optimize well sampling frequencies for *currently existing* locations.

Section 3.2.1. Temporal Variograms

The first piece of the GTS temporal puzzle is the Temporal Variogram. The Temporal Variogram technique is designed to optimize sampling frequencies simultaneously over a *group* of well locations. These locations might represent all wells at a given site, those connected with a particular regulatory unit, or even selected wells that are part of a treatment system network. Whatever the grouping, the Temporal Variogram aims to provide a single optimal sampling interval that can be applied to every well within the group. Thus, this technique can be particularly helpful when a site manager wants to establish uniform operational sampling schedules at the site, and the optimization of individual well frequencies is not deemed as high a priority.

Results from the Temporal Variogram should not be viewed as optimal for any *single* well. The Temporal Variogram in GTS combines data from all wells in the group in its construction. Consequently, it attempts to find an optimal sampling interval, *on average*, for the group. Some individual wells might be better optimized with shorter or longer sampling intervals. Nevertheless, when a uniform sampling frequency is desired, the Temporal Variogram can provide a reasonable way to estimate it for the well group simultaneously.

Another advantage of the Temporal Variogram as employed in GTS is that even wells with very little sampling data can be included in its construction. The trend fitting methods for individual wells explained in **Section 3.2.2** generally require at least 8 or more distinct sampling events to provide a reasonable fit. With the temporal variogram, any well with at least two distinct sampling events can be included.

The Temporal Variogram is constructed using nested pairs of concentration measurements from each well in the group. By nested what is meant is that given a particular location, all pairs of measurements are formed for that well and one-half the squared difference is

then computed for each pair. Pairs are never formed *across* distinct wells, which would introduce unwanted spatial variability, but rather are *nested within* wells. This allows an independent estimate of temporal variability from each well. Then, to allow the inclusion of wells with only minimal amounts of sampling data, and to gauge average temporal variation for the group as a whole, the squared differences are amalgamated together into a single set of *pair differences* for the entire group.

In previous versions of GTS, a Temporal Variogram was actually constructed for each well, but then a weighted average of the individual variograms was formed to get the final overall Temporal Variogram. In the current version of GTS, this process is streamlined by simply estimating the final variogram from the entire unweighted set of half-squared pair differences. In this fashion, wells with more data are naturally given greater weight in the final Temporal Variogram (since they contribute more pairs), while well locations with less data are given some, but lesser weight.

The Temporal Variogram itself is simply a graph of a unitless variogram measure plotted against time, or more specifically, against the time lag between successive sampling events. It is estimated using locally-weighted quadratic regression (LWQR), taking the half-squared difference pairs as the *y*-variable and the time lag or time difference between sampling event pairs as the *x*-variable. All sampling dates at Site 133 were converted into number of weeks since a reference date prior to any actual historical sampling. The time lag differences were thus expressed in number of *weeks* between sampling events.

As explained in more detail in **Section 3.2.2** on the use of LWQR in Iterative Fitting, the GTS analyst must choose an appropriate bandwidth parameter prior to estimating the Temporal Variogram. However, testing of various data sets has shown that smaller bandwidths do not do a good job of capturing the most important features of the variogram. Instead larger bandwidths provide better and more interpretable results.

For this reason, all the Site 133 Temporal Variograms were computed at two larger bandwidths: 50% and 70%. Both of these estimated fits are graphed for each constituent in **Appendix 3-1**.The use of LWQR also allowed the estimation of confidence bands around the fit, in order to better gauge possible variation in the estimate. Confidence bands were constructed for both bandwidths; however, for visual clarity only the 50% bandwidth confidence bands are actually plotted on the graphs in **Appendix 3-1**. Sometimes the LWQR fit at the 70% bandwidth is different enough from the 50% bandwidth fit as to make the former estimate fall outside the confidence bands (as can be seen in the Temporal Variogram for DIOXANE14). Nonetheless, as described below, the key to comparing results at different bandwidths is not whether the *magnitude* of the Temporal Variogram differs from one bandwidth to the next, but instead whether the fundamental *shapes* of the variograms differ. Generally, at Site 133 they did not.

A couple of additional technical points are important to the Temporal Variogram methodology. First, concentration outliers can skew the results of the Temporal Variogram as much as they can skew the Iterative Thinning routine (as explained in **Section 3.2.2**). Because of this possibility, Tukey's box plot rule (also described in **Section 3.2.2**) was run on the concentration data from each well, both on the raw and logged scales of

measurement. Again, as with Iterative Thinning, only data values that were tagged as outliers on *both* scales were excluded from the Temporal Variogram computations.

In addition, to avoid the problem of some wells having vastly different average concentration levels (and thus contributing vastly different squared-difference pair contributions to the Temporal Variogram), each well's data was temporarily re-scaled to have a maximum of one before doing the Temporal Variogram calculations and fitting. Thus, every well in the group was put more or less on an 'equal footing' in terms of its concentration range.

Another potential problem involved non-detects. Prior testing of the Temporal Variogram has shown that wells with too many non-detects exhibit too little temporal variation to be of help in estimating the Temporal Variogram. For this reason, all wells with less than a 30% detection rate are excluded from the variogram computations.

Finally, two different types of Temporal Variograms were computed on the Site 133 data: the *mean* variogram and the *median* variogram. In each case, the LWQR procedure looks at a neighborhood of half-squared-difference pairs surrounding a time lag point to be estimated. However, in the case of the mean variogram, the local regression estimate attempts to pinpoint the arithmetic average of the difference pairs, while in the case of the median variogram, a similar estimate is made on the *ranks* of the set of difference pairs rather than the pair values themselves. Comparisons of these variogram types showed that the mean variogram rarely offered interpretable results, mainly because it was too erratic, while the median variogram was typically more promising and well-behaved. Consequently, the Temporal Variograms of **Appendix 3-1** only include the median variogram results.

The ultimate goal when analyzing a Temporal Variogram is to identify an approximate *range* in its structure. That is, at what point (if any) does the variogram start to 'level out' and remain at roughly a constant level? Ideally, any variogram offers a measure of correlation between the measured data and either time or space. For cases of positive temporal or spatial correlation, such a linkage is evidenced on the variogram by small values for small lags (either *time* lags between sampling events for the Temporal Variogram or, more commonly, *distance* lags between well locations when constructing variograms for a geostatistical analysis) and larger values for large lags. Small values on a variogram are typically indicative of a high degree of correlation, while higher values represent a loss of correlation and greater statistical independence.

On many variograms, there is a point at which larger lags no longer lead to larger variogram values. It is at this point that the range is identified. The magnitude of the leveled-out portion of the variogram is known as its *sill*. Lags at least as large as the range — and thereby associated with the sill — are thought to represent sampling pairs having essentially no statistical correlation. Smaller lags on the other hand, having variogram values smaller than the sill, represent pairs which are correlated to some degree and therefore contain a certain level of statistical redundancy in the information they offer.

It is for this reason that GTS sets the optimal sampling interval for a group of wells as the *range* of the Temporal Variogram, if it can be identified. Sampling intervals smaller than the range are associated with somewhat correlated, and therefore redundant, sampling

results. On the other hand, sampling intervals at least as large at the range tend to be uncorrelated, and therefore — from a statistical standpoint — optimal in the sense that consecutive samples collected at such lags will provide the shortest sampling interval at which the maximal statistical information per sample is achieved.

Bear in mind that while the Temporal Variogram is a useful tool, it is not without its caveats. Sometimes a range cannot be reliably identified, often because some of the wells in the group do not possess the same basic temporal correlation structure as other wells. In other cases, a range may be identified, yet the result is different from that estimated via Iterative Thinning. This can happen in part because the Temporal Variogram tries to optimize a group of locations *on average*, rather than individually. It can also occur if only a smaller number of wells have enough sampling data to be included in the Iterative Fitting analysis, yet are included in the Temporal Variogram computations. In fact, this last situation seems to have occurred at Site 133, where relatively few wells were eligible for Iterative Fitting.

Section 3.2.2. Iterative Thinning

Iterative Thinning refers to the technique by which the well sampling frequencies at *individual* wells are optimized. Because each location is analyzed separately, it is quite possible to have a different recommended sampling interval for each well after applying the Iterative Thinning routine. Nevertheless, GTS looks at the optimized sampling intervals as a whole and adjusts the recommended common operational sampling frequency for either all the wells treated as a single group, or each subgroup of related wells, based on the median optimal sampling interval for that group or subgroup.

The Iterative Thinning process is based on a relatively simple idea: 1) take the existing, historical data for a given well location and constituent, 2) determine the current average sampling frequency and sampling interval, 3) fit a trend to these initial data along with statistical confidence bounds around this trend, 4) iteratively remove, at random, certain fractions of the original data, and 5) re-estimate the trend based on the reduced dataset to determine whether or not the trend still lies within the original confidence bounds. If too much of the new trend falls outside the confidence limits, stop removing data and compute a new, optimized sampling frequency and sampling interval based on the portion of data removed.

The original version of GTS fit trends during Iterative Thinning by way of Sen's slope statistic, a non-parametric estimate of the slope of a linear trend. Although useful, Sen's statistic is not highly informative for cases of more complicated, non-linear trends. Previously, this meant that the GTS analyst would have to 'screen out' those wells which did not exhibit roughly linear trends over time. Since then, GTS has been modified to estimate the initial trend via a statistical technique known as locally-weighted quadratic regression (LWQR; see Loader, 1999). This procedure is readily able to fit complex trends and confidence bounds around those trends. Moreover, the data requirements for using LWQR are quite similar to Sen's slope method, and the process can be automated to essentially the same degree.

To perform the Iterative Thinning, LWQR was used to construct an initial trend and 90% confidence bounds around this trend. Also, the baseline sampling frequency was computed

over the entire record of sampling at the well, and the baseline sampling interval was estimated by averaging the set of intervals between consecutive samples. As will be noted below, greater emphasis was given to more recent sampling information when constructing these baselines, especially if any large gaps appeared within the sampling record. Still, it is quite possible that the baseline sampling interval for a given well may not directly correspond to the nominal operational sampling schedule currently being used. The Iterative Thinning routine is data driven, and includes as much useful trend information as is possible, even if contributed by, for instance, multiple contractors operating under different sampling schedules or goals.

Once the initial trend was fit, data points were removed at random in systematic increments of 5% at each level, up to a maximum of 95%. At each stage, the trend was re-estimated on the reduced dataset and then compared to the initial confidence bounds. Since data points were removed randomly, and it was therefore possible that only points from one portion of the existing sampling record might be removed, the same removal process was repeated 500 times at each removal level, each iteration with a new set of randomly chosen points. This step helped to ensure that the trend results were not artifacts of the removal process, but really reflected what kind of trend estimate was possible at each stage of removal.

Another advantage to using LWQR in this way is that it can readily account for seasonal fluctuations or seasonal trends. Because local regression is used to estimate non-linear trends in the original or baseline data at a given well, it does a good job of identifying seasonal patterns in the initial estimate. Then, since subsequent trends computed on the reduced data-sets are compared to the baseline estimate, if a dominant seasonal fluctuation cannot be identified in the reduced data, the iterative fitting procedure will register such a result as a loss of accuracy and perhaps conclude that too much data has been removed from that well.

Because 500 new trends were fit to the reduced data at each removal level, key statistical summaries were used to express the results. These include the median trend value (calculated at a series of dates throughout the sampling record), the lower quartile (i.e., 25^{th} percentile) trend value, and the upper quartile (i.e., 75^{th} percentile) trend value. The median trend summaries are plotted on the graphs in **Appendix 3-2** for two specific removal levels: the percentage at which too much data has been removed to adequately reconstruct the original trend, and the removal level just below this, which represents the optimal stopping point for the Iterative Thinning algorithm. Thus, for example, at well 13-MW14 for TCE, the initial trend is plotted in blue with 90% confidence bounds around this trend shaded in light blue, the median fit of the set of new trends when 20% of the data has been removed is plotted in red, and the median fit of the optimal stopping point of 15% removal is plotted in green. This same pattern and color scheme was used for all of the **Appendix 3-2** graphs.

The other summary plotted on each **Appendix 3-2** graph is the pair of upper and lower quartile fits (identified by red dashed traces) on the reduced data when too much sampling information was removed. These statistics are quite important for a couple of reasons. First, the upper quartile represents the point which is exceeded by 25% of all the new

trend values (and the same for the lower quartile on the low end of the concentration range). If this trace falls outside the original confidence bounds, it demonstrates that at least a quarter of the new trend values constructed from the reduced data were outside the initial confidence limits. This can happen even when the *median* trend fit doesn't look that bad, especially in the case where the new trend value is 'swinging wildly' from iteration to iteration above and below the initial fit, causing the median fit to fall somewhere near the original trend, but at the expense of substantial variability in the 500 trend fits at that removal level. Therefore it can be quite informative to compare the lower and upper quartile fit traces against the original confidence bounds. Sometimes there are key stretches of the data record where these fits lie outside the confidence band, indicating too much variability in the fitting process to allow for reliable trend reconstruction.

Second, the difference between the upper and lower quartile fits — also known as the *interquartile range* or IQR — was computed at each fitting point along the sampling record and averaged across the fitting points to form the *average* IQR. This statistic offers a numerical indication of the typical level of variation exhibited among the 500 trend fits computed at a given removal level. It is also plotted against removal level (i.e., fraction of data removed) for each well and parameter in the graphs of **Appendix 3-3**. There the average IQR typically increases as more of the data is removed, up until and often beyond the optimal stopping point.

Note however that the average IQR is not a fail-safe indicator. In some cases, this statistic begins to *drop* near to or beyond the optimal stopping point, rather than continuing to increase. The primary reason for such behavior is that when enough data is removed — and depending on the configuration of the original time series — the re-estimated trend can, instead of 'swinging' above and below the initial fit, merely stay either consistently above or below the original trend, leading to a lower than expected difference between the upper and lower quartile fits.

It is for this reason that the optimal stopping point was chosen not on the basis of the average IQR, but rather by determining what fraction of the new trend values fell outside the original 90% confidence band. For Site 133, a threshold of 25% was chosen, meaning that too much removal was judged to have occurred whenever at least 25% of the reduced-data trend values fell beyond the initial confidence bounds. While the choice of threshold is somewhat arbitrary, tests of the data at Site 133 and at other sites have shown that it gives generally good results. However, it may not be the *ideal* threshold for each and every time series. Remember, the overall goal in Iterative Thinning is to determine how much data can be removed (and thus how much the interval between sampling events can be lengthened) and still allow one to reconstruct the *major* features of the original trend. Some 'finer' features of the time series trend are undoubtedly lost when less data is collected, but often it is quite difficult to determine whether these features are 'real' or simply due to measurement and/or field variation in the data. It may also be the case that certain transient features are less important to the needs of the long-term monitoring program and therefore do not need to be estimated as carefully.

To graphically illustrate at what point the 'out-of-bounds' fraction of new trend values exceeded the threshold of 25%, a graph of this measure plotted against removal level is

provided for each well and COC in **Appendix 3-3**. Both this graph and the plot of the average IQR are denoted by red traces and set in the top panel of the page for each well. Also on these graphs is a vertical reference line indicating the optimal stopping point of data removal as determined by the Iterative Thinning routine. In the bottom panel are two graphs representing optimal sampling interval (in green) and optimal sampling frequency (in blue). These graphs were constructed by adjusting the baseline sampling interval and baseline frequency according to the amount of data 'thinned' at each removal level. Also included are two reference lines indicating the optimal stopping point and the optimal interval or sampling frequency associated with that stopping point. Hence, again referring to TCE at well 13-MW14, the baseline sampling interval is just over 33 weeks between sampling events, while the optimal interval is found to be almost 39 weeks. Conversely, the baseline sampling frequency at this well is approximately 0.0312 samples per week (approximately 1.6 samples per year), compared to a recommended optimal frequency of approximately 0.0268 samples per week (1.4 samples per year).

Data Screening prior to LWQR

It is important to note certain steps that were necessary to apply the locally-weighted quadratic regression technique. While extremely flexible as a statistical tool, its flexibility comes with certain restrictions and assumptions. First, prior testing of the GTS algorithm has demonstrated that reliable fitting of an initial trend, and especially, confidence bounds around that trend, are almost impossible with less than 8 to 10 sample measurements (that is, data from distinct sampling events). Because of this, well locations with fewer sampling events at Site 133 were automatically screened out of the Iterative Thinning routine and do not appear in the graphs of **Appendices 3-2** and **3-3**.

Furthermore, large data gaps in the sampling record are also troublesome to the LWQR algorithm and tend to cause artifactual looking trends. For this reason, historical sampling data prior to a large gap were screened from that well's time series before fitting. In this case, a large gap was defined as an outlier among the set of time-lags between consecutive sampling events using *Tukey's box plot outlier rule*, where a sampling gap outlier is identified whenever the lag exceeds the upper 'hinge' of the box plot of time-lags. (The upper hinge is defined as the upper quartile plus 1.5 times the interquartile range [IQR] of the box plot.)

Another data feature that can significantly affect the trend estimate is the presence of concentration outliers. The modified GTS algorithm screens these values prior to fitting with LWQR by again using Tukey's box plot rule, this time on the concentration values. To ensure that only very significant outliers are identified and removed, two passes of the box plot test are run, once on the raw data and once on the logged concentrations. Only samples that are identified as outliers on *both* scales are screened from the time series prior to fitting.

A final screening check is made for wells with no observable variation, typically in the case where all the data for a time series are non-detects with a common reporting limit (RL). Although LWQR can estimate a (flat) trend to such data, it is impossible to construct a confidence band around the trend or to determine an optimal stopping point for data removal. These latter statistics require the measurements to exhibit some

variation (the same is true of other trend estimation methods). Because of this, wells with no observable variation are screened from the Iterative Thinning routine. In addition, the data at some wells — after removing apparent concentration outliers and sampling events prior to large data gaps — only consist of a string of identically-valued non-detects. These wells are consequently also screened from Iterative Thinning.

After running these automated checks, the results are re-checked manually by the GTS analyst by examining a time series plot of each well with possible outliers, data gaps, and stretches of no variation identified. Occasionally, it is necessary to add or remove one or more outliers or data gaps, in order to improve the fitting process.

Trend Fitting with LWQR

After screening the time series measurements for data gaps, concentration outliers, and observable variation, one final step was needed before constructing the initial trend estimates. That step was to choose a *bandwidth* for fitting. LWQR works by estimating the trend value at a given fitting point (i.e., a particular date within the range of dates between the start and end of the sampling record) using a weighted linear combination of the known sample values close to the fitting point. What must be selected by the analyst is how many neighboring sample measurements to use. In GTS this is done by selecting a *bandwidth parameter* that represents the fraction of known samples to be included in the neighborhood of any given fitting point. These bandwidths typically range from 40% to 80%, depending, among other things, on the number of points in the time series and its shape.

In order to automate the GTS routines as much as possible, especially when there are a large number of wells to analyze, every attempt is made to simplify the choice of bandwidth. In general, the higher the bandwidth, the greater the amount of 'smoothing' that will occur within the fitted trend. Too high a bandwidth and the trend may 'miss' important peaks and valleys in the time series. Too low a bandwidth and the trend may exhibit artifactual jumps and/or dips between known sample values. It can also occur that the fitted trend mostly 'disregards' the known data altogether, leading to highly inaccurate trend estimates.

To guard against these scenarios, it is important to run a 'pre-flight' check of the LWQR fits at several possible bandwidths prior to running the Iterative Thinning routine. This pre-flighting is done in two basic ways: 1) visually comparing the estimated fits obtained by systematically changing the bandwidth for each well, and 2) computing diagnostic checks of the *residuals* obtained when the trend is estimated at each known sample value and the known value is subtracted from this estimate. Again the goal is to automate this process as much as possible. However, some visual inspection of the pre-flight results at each well is still necessary.

As to the first pre-flight check, plots of the known sampling data can be overlaid with LWQR trend estimates at several possible bandwidths. In this setting, one should look for a 'visually pleasing' fit, one that captures the major features of the overall trend, and especially to exclude fits that are clearly bad.

The second pre-flight check, that of residuals, includes the following calculations: Mallow's CP statistic, correlation of the residuals with date of sampling, skewness of the residuals, and Filliben's probability plot correlation coefficient. Each of these statistics is designed to provide a numerical indication of the goodness of the estimated trend relative to a given bandwidth. In GTS, these residual diagnostic measures are plotted simultaneously against bandwidth in order to search for the most appropriate fitting neighborhood. None of them, however, is fail-safe by themselves.

Mallow's CP statistic is a scaled measure of the sum of squared residuals. Lower values of Mallow's CP usually indicate a better fit. However, it is possible to have a very low Mallow's CP and yet a visually unacceptable fit between known sample values. This occurs for instance when the estimated trend 'goes right through' each known sampling value, yet has improbable 'squiggles' or curves *between* sampling points. The correlation with sampling date is used to check whether the fit is worse over certain portions of the sampling record than others. Values close to zero are best. The skewness coefficient is used to check for 'lopsidedness' in the distribution of residuals. LWQR works best when the *residual* distribution is symmetric and normally distributed, so skewness values closer to zero are better. Along the same lines, Filliben's correlation coefficient is a test of normality that can be used to check the shape of the residual distribution. Coefficient values closer to one are best.

As noted, none of the residual diagnostic measures are fool-proof by themselves. They can even give conflicting indications for the same time series in some situations. Nevertheless, examined together along with graphs of the possible fits by bandwidth, an acceptable initial trend estimate can almost always be found.

Section 3.3. Trend Mapping

One of the natural by-products of constructing the initial trend fits at each well location during Iterative Fitting is the ability to create a *map* of the trend estimates for any specific time period. In order to construct the confidence band around the initial fit on the known sample data, LWQR creates an estimate not only of the trend value at each fitting point, but also the local *first derivative* or *slope*. These local slopes can then be averaged in an appropriate way to determine the general direction and magnitude of the trend for a given portion of the sampling record.

At Site 133, three different time windows were chosen for estimating average trend slopes: 1) the historical trend, based on all the available and usable data at a well location, 2) the recent trend, based on data collected since the start of 2000, and 3) the newest trend, based on the four latest sampling measurements. Each of these trends was also characterized as increasing (with an average slope > 0) or decreasing/flat (with an average slope no greater than 0).

To actually estimate the typical slope, the *median* slope value is selected from the set of fitting points falling within the specified time period. This is done to ensure that the dominant trend direction is identified. With non-linear trends, there can be short periods of very steep trends that do not represent the dominant direction of the trend over the time

interval in question. The *mean* slope can be then skewed by a few very large local slope values, whereas the *median* slope tends to be resistant to this problem.

In addition, it is possible to compute a non-parametric confidence interval around the median slope, in order to characterize the *strength* of each trend. Using a 95% nominal target confidence level, each trend can then be characterized as either fairly 'sure' or 'unsure,' depending on whether the confidence interval around the slope contained the value zero.

Finally, all of this trend information can be mapped by well location. The maps presented in **Appendix 3-4** offer for each designated time period a spatial representation of the types of trends at Site 133, along with an indication of their strength and relative magnitude. Specifically, increasing trends are listed in red and pink, with trends surely above 0 identified in red, and less sure increases in pink. Flat or decreasing trends are colored in blue and light blue, with surely decreasing trends in blue and less sure trends (including flat trends) in light blue.

Also on these maps is an indication of the *relative* magnitude of each trend. To do this, the actual slope estimates were divided into quintiles (each quintile representing 20% of the ranked slope estimates). Then, an increasing series of symbol sizes was assigned to the set of quintiles for plotting purposes. Consequently, the largest red symbols on the trend maps, for example, represent increases in the top 20% of magnitude, while the smallest red symbols designate increases in the lowest 20% of magnitude. The same patterns apply to the other trends. The largest blue symbols represent those trends that exhibited the largest decreases, while the smallest blue symbols represent the smallest downward trends. And so on.

It is important to note that the trend maps do not provide information specific to the optimal adjustment of sampling frequencies. Rather, the maps provide an overview of where at the site different kinds of trends are occurring and how probable it is that the trends represent something 'real.' They can also be used to potentially augment or confirm patterns of plume movement or change over time, and perhaps to help identify areas of the site where additional sampling might be helpful. Still, it must be remembered that the LWQR fits are only constructed at wells with at least 8 usable sampling events. At Site 133, only a relatively small number of wells met this requirement, and then, with the exception of a single well, only for TCE, but not for MN or DIOXANE14. Consequently, it is difficult to gain an adequate overall picture of the apparent trends in concentration levels.

Section 3.4. Temporal Optimization Results

The temporal optimization results at Site 133 are contained in a series of graphs and tables. Overall, there is room to adjust and optimize sampling frequencies within the long-term monitoring (LTM) program. A number of the monitoring wells could have their sampling frequencies reduced by at least 15-30% yet retain the most useful statistical information concerning their long-term trends. It would also be possible to adjust the *common* sampling schedule for Site 133 as a whole. Temporal variograms generated by combining all the available sampling information indicate that the common

sampling interval could be set to one sampling event every 7 quarters with little loss of statistical information, compared to current annual sampling regimen.

Section 3.4.1. Temporal Variograms

The Temporal Variograms for Site 133 are contained in the graphs of **Appendix 3-1**. There is one Temporal Variogram per COC. As can be seen from graphs for TCE and MN, there appears to be a smooth increase of the variogram up to a lag of approximately 90 weeks. Each graph then flattens out. The Temporal Variogram for DIOXANE14 is more problematic. In that case, the graph exhibits peaks and valleys, but no real sill. Because of this, it is not clear how to best interpret the results for this constituent. Results by COC are listed in **Table 3-3** below.

Table 3-3. Temporal Variogram Ranges and Recommended Sampling Interval

Temporal Variogram Range			Optimal Sampling Interval
DIOX	**MN**	**TCE**	
Unknown	90 wks	90–100 wks	7 qtrs

It should be noted that the recommendations on sampling frequency for Site 133 are strictly data driven. Other regulatory or engineering considerations may need to be accommodated in the assignment of final sampling schedules. Still, the sampling intervals listed below in **Table 3-3** offer a summary of the statistical information provided by the available data, and how that information can be used to adjust operations at the site.

Section 3.4.2. Iterative Thinning

Mention has already been made of the graphs in **Appendices 3-2** and **3-3**. These appendices provide the visual results of the Iterative Thinning process. As described above, **Appendix 3-2** includes a time series graph of each eligible well, overlaid with the initial trend fit, a confidence band around that trend, and selected results of the Iterative Thinning routine, including an indication of the optimal stopping point for data removal. These results are further detailed in the graphs of **Appendix 3-3**, where for each well and COC there are four plots: 1) the percentage of trend fits on the reduced data that fall outside the initial confidence band, plotted against the percent of data removed; 2) the average interquartile range (IQR) of the reduced-data trend fits, plotted against percent of data removed; 3) the optimal average sampling interval, plotted against percent of data removed; and 4) the optimal average sampling frequency, plotted against percent of data removed.

Key numerical portions of this same information are summarized in **Table 3-4**. There for each well, the optimal and recommended sampling intervals and frequencies are summarized for the three COCs input into GTS. It will be noted that only TCE could be optimized at these wells with the exception of location 171-MW05.

The suggested operational sampling interval for the wells that could be analyzed by Iterative Fitting is generally 2-3 quarters. This number is of course shorter than the recommended sampling interval from the Temporal Variograms of approximately 7 quarters. The most probable reason for this difference is that the number of wells used in

the constructing the Temporal Variograms was much greater than the number eligible for Iterative Fitting. The Temporal Variogram procedure amalgamates sampling information across an entire collection of wells, and, therefore, does not *require* more than 2 sampling events from any given well in the set. Because relatively few wells could be optimized by Iterative Fitting, the overall GTS recommendation for the optimal sampling is based on the Temporal Variogram results.

Section 3.4.3. Trend Maps

The trend maps themselves have been described above (a graph for each time period is contained in **Appendix 3-4**). Since these trends are a by-product of the Iterative Fitting process, only those wells and COCs eligible for Iterative Fitting show up on these maps. At Site 133, this means that maps could only be produced for TCE at a small subset of the site locations. The wells that are mapped generally show — both historically and more recently — increasing trends in TCE, especially in and around the site 37 well locations. Even where the trends are too uncertain statistically to identify a definite direction with confidence (as denoted by the light pink and light blue shading), the nominal trends are still by and large on the upswing.

Specific numerical information about the estimated trend magnitudes — including confidence bounds around each trend — by well is listed in **Table 3-5**.

Table 3-4. Summary of Iterative Thinning Results, By COC and Well Location

Notes: CUT = optimal data removal percentage; OUTPCT = fraction of estimated trend pts outside confidence band; INTERVAL = optimal sampling interval (in weeks); FREQ = optimal sampling frequency per week; AVE-IQR = average interquartile range across 500 iterative fits; PROPOSED = closest operational sampling interval (in quarters) to the minimum optimal sampling interval (e.g., 3Q = 3 quarters)

WELL_ID	EASTING (ft)	NORTHING (ft)	COC	CUT	OUTPCT	INTERVAL (wks)	FREQ (#/wk)	AVE-IQR (ppb)	PROPOSED
13-MW14	6656174.57	2157261.67	TCE	0.15	0.202	38.77	0.0268	179.60	3Q
13-MW21	6656211.83	2157285.19	TCE	0.10	0.227	37.00	0.0282	1.04	3Q
133-EW03	6655305.23	2160521.65	TCE	0.35	0.242	8.15	0.1220	5829.00	1Q
133-MW01	6655449.52	2160136.78	TCE	0.15	0.193	51.70	0.0193	91.10	4Q
133-MW02	6655319.75	2160548.27	TCE	0.20	0.219	31.34	0.0324	1358.00	2Q
171-MW05	6651599.48	2161231.21	MN	0.45	0.235	115.89	0.0089	77.16	9Q
171-MW05	6651599.48	2161231.21	TCE	0.25	0.218	38.87	0.0255	164.00	3Q
177-MW03	6659169.43	2163818.37	TCE	0.20	0.201	40.64	0.0256	24.66	3Q
177-MW04	6658753.47	2163604.67	TCE	0.10	0.187	36.05	0.0289	3.56	3Q
177-MW07	6659383.87	2163969.71	TCE	0.15	0.247	45.12	0.0230	85.58	3Q
26-MW08	6656935.29	2160875.76	TCE	0.30	0.231	78.30	0.0131	118.70	6Q
37-EW02	6652665.97	2160754.30	TCE	0.15	0.236	24.16	0.0414	13.43	2Q
37-EW03	6652605.78	2160645.80	TCE	0.50	0.214	40.74	0.0243	106.90	3Q
37-EW04	6651878.68	2160063.02	TCE	0.15	0.200	21.92	0.0464	9.79	2Q
37-EW05	6652155.29	2160459.05	TCE	0.15	0.182	24.37	0.0417	9.23	2Q
37-EW06	6651943.40	2160872.30	TCE	0.15	0.249	25.81	0.0392	52.14	2Q
37-MW04	6652722.90	2160566.70	TCE	0.35	0.219	35.48	0.0279	111.70	3Q
37-MW06	6651906.29	2160884.05	TCE	0.10	0.183	27.29	0.0376	15.67	2Q
37-MW10	6651433.07	2161768.84	TCE	0.05	0.145	41.75	0.0250	0.04	3Q
37-MW14	6652680.28	2160754.33	TCE	0.30	0.226	27.84	0.0356	285.10	2Q
37-MW15	6652173.30	2160215.67	TCE	0.20	0.207	29.06	0.0344	7.00	2Q
37-MW16	6652756.65	2160806.78	TCE	0.20	0.226	28.10	0.0361	27.35	2Q
37-MW17	6652298.39	2160318.27	TCE	0.20	0.234	28.18	0.0358	8.35	2Q
37-OW03	6652708.52	2160755.68	TCE	0.10	0.168	25.35	0.0399	2.79	2Q

Table 3-5. Estimated Trend Magnitudes and Confidence Intervals by COC and Well Location

Notes: Historical = all data; Latest = last 4 sampling events
CONF-LEV = Achieved confidence level of non-parametric confidence interval around median slope
TREND = estimated magnitude of median slope (ppb/week);
LOWER-LIMIT = lower 95% confidence bound on trend magnitude (ppb/week)
UPPER-LIMIT = upper 95% confidence bound on trend magnitude (ppb/week)

WELLID	EASTING	NORTHING	COC	TYPE	CONF-LEV	TREND	LOWER-LIMIT	UPPER-LIMIT
13-MW14	6656174.57	2157261.67	TCE	Historical	0.976	-3.7780	-8.3854	1.7675
13-MW14	6656174.57	2157261.67	TCE	Post-1999	0.951	-3.7780	-4.5099	-0.3742
13-MW14	6656174.57	2157261.67	TCE	Latest	0.978	-1.6303	-4.3542	4.8209
13-MW21	6656211.83	2157285.19	TCE	Historical	0.976	0.0495	0.0046	0.0718
13-MW21	6656211.83	2157285.19	TCE	Post-1999	0.951	0.0362	0.0046	0.0531
13-MW21	6656211.83	2157285.19	TCE	Latest	0.978	0.0168	-0.0073	0.0531
133-EW03	6655305.23	2160521.65	TCE	Historical	0.953	129.3565	13.6649	212.5277
133-EW03	6655305.23	2160521.65	TCE	Post-1999	0.976	119.5072	-21.0371	212.5277
133-EW03	6655305.23	2160521.65	TCE	Latest	0.959	119.5072	-3.6861	198.6587
133-MW01	6655449.52	2160136.78	TCE	Historical	0.962	-0.8374	-4.8708	0.0120
133-MW01	6655449.52	2160136.78	TCE	Post-1999	0.978	-9.0015	-14.6299	-0.4965
133-MW01	6655449.52	2160136.78	TCE	Latest	0.979	-12.4924	-15.7073	-6.1749
133-MW02	6655319.75	2160548.27	TCE	Historical	0.965	-2.2217	-26.4147	28.9619
133-MW02	6655319.75	2160548.27	TCE	Post-1999	0.983	25.9767	-30.0692	42.4351
133-MW02	6655319.75	2160548.27	TCE	Latest	0.969	-18.7582	-98.4651	29.0809
171-MW05	6651599.48	2161231.21	TCE	Historical	0.969	14.3327	9.3297	15.4879
171-MW05	6651599.48	2161231.21	TCE	Post-1999	0.969	15.7941	14.7588	16.2892
171-MW05	6651599.48	2161231.21	TCE	Latest	0.961	14.7588	14.3327	17.4333
177-MW03	6659169.43	2163818.37	TCE	Historical	0.976	0.1262	-0.0330	0.3073
177-MW03	6659169.43	2163818.37	TCE	Post-1999	0.979	-0.0740	-0.2304	0.3073
177-MW03	6659169.43	2163818.37	TCE	Latest	0.978	0.0116	-0.2295	0.4299
177-MW04	6658753.47	2163604.67	TCE	Historical	0.976	-0.1115	-0.2563	-0.0531
177-MW04	6658753.47	2163604.67	TCE	Post-1999	0.979	-0.0634	-0.1772	-0.0237
177-MW04	6658753.47	2163604.67	TCE	Latest	0.978	-0.0798	-0.2138	-0.0369
177-MW07	6659383.87	2163969.71	TCE	Historical	0.976	0.5090	-1.2890	3.9058
177-MW07	6659383.87	2163969.71	TCE	Post-1999	0.987	2.6796	0.2655	7.3614
177-MW07	6659383.87	2163969.71	TCE	Latest	0.987	2.6796	0.2655	7.3614
26-MW08	6656935.29	2160875.76	TCE	Historical	0.965	-0.2658	-0.4285	-0.0161
26-MW08	6656935.29	2160875.76	TCE	Post-1999	0.979	-0.6524	-2.4761	0.2805
26-MW08	6656935.29	2160875.76	TCE	Latest	0.979	-0.6524	-2.4761	0.2805
37-EW02	6652665.97	2160754.30	TCE	Historical	0.962	-0.0733	-0.7354	0.6345
37-EW02	6652665.97	2160754.30	TCE	Post-1999	0.971	0.3803	-0.7824	0.7288
37-EW02	6652665.97	2160754.30	TCE	Latest	0.987	0.6817	-0.7354	1.0069
37-EW03	6652605.78	2160645.80	TCE	Historical	0.962	-0.3997	-1.2170	0.4086

37-EW03	6652605.78	2160645.80	TCE	Post-1999	0.971	0.1056	-1.1662	0.6797
37-EW03	6652605.78	2160645.80	TCE	Latest	0.987	0.7218	-1.3311	1.1637
37-EW04	6651878.68	2160063.02	TCE	Historical	0.953	0.0630	-0.2155	0.2446
37-EW04	6651878.68	2160063.02	TCE	Post-1999	0.976	0.1883	-0.0054	0.3551
37-EW04	6651878.68	2160063.02	TCE	Latest	0.979	0.3273	0.1328	0.5285
37-EW05	6652155.29	2160459.05	TCE	Historical	0.965	-0.2879	-0.5306	0.1296
37-EW05	6652155.29	2160459.05	TCE	Post-1999	0.971	0.0663	-0.4712	0.1919
37-EW05	6652155.29	2160459.05	TCE	Latest	0.987	0.2075	0.0986	0.5150
37-EW06	6651943.40	2160872.30	TCE	Historical	0.953	1.9076	-0.7764	2.2139
37-EW06	6651943.40	2160872.30	TCE	Post-1999	0.957	-0.3775	-2.6760	3.7618
37-EW06	6651943.40	2160872.30	TCE	Latest	0.987	2.6084	-14.4363	35.2107
37-MW04	6652722.90	2160566.70	TCE	Historical	0.962	-1.0372	-1.5619	-0.1356
37-MW04	6652722.90	2160566.70	TCE	Post-1999	0.965	-0.0308	-0.7126	0.3797
37-MW04	6652722.90	2160566.70	TCE	Latest	0.978	0.3797	-0.1222	0.9163
37-MW06	6651906.29	2160884.05	TCE	Historical	0.965	0.7703	0.2695	1.1006
37-MW06	6651906.29	2160884.05	TCE	Post-1999	0.983	0.3736	-1.1508	1.0342
37-MW06	6651906.29	2160884.05	TCE	Latest	0.961	0.5080	-3.3076	1.1006
37-MW10	6651433.07	2161768.84	TCE	Historical	0.976	0.0004	-0.0009	0.0013
37-MW10	6651433.07	2161768.84	TCE	Post-1999	0.987	-0.0009	-0.0026	0.0004
37-MW10	6651433.07	2161768.84	TCE	Latest	0.965	-0.0010	-0.0025	0.0001
37-MW14	6652680.28	2160754.33	TCE	Historical	0.960	0.1727	0.1311	0.2175
37-MW14	6652680.28	2160754.33	TCE	Post-1999	0.981	0.1212	-0.1140	0.9965
37-MW14	6652680.28	2160754.33	TCE	Latest	0.987	0.8256	-0.7124	2.6814
37-MW15	6652173.30	2160215.67	TCE	Historical	0.962	-0.1359	-0.2085	-0.0408
37-MW15	6652173.30	2160215.67	TCE	Post-1999	0.965	-0.0604	-0.2349	0.0904
37-MW15	6652173.30	2160215.67	TCE	Latest	0.978	0.0904	-0.2349	0.5898
37-MW16	6652756.65	2160806.78	TCE	Historical	0.953	1.3037	0.3970	2.0276
37-MW16	6652756.65	2160806.78	TCE	Post-1999	0.977	1.5811	-0.1447	3.9864
37-MW16	6652756.65	2160806.78	TCE	Latest	0.978	3.9864	2.0276	6.3894
37-MW17	6652298.39	2160318.27	TCE	Historical	0.953	0.0215	-0.0561	0.1495
37-MW17	6652298.39	2160318.27	TCE	Post-1999	0.977	0.1636	0.0215	0.3120
37-MW17	6652298.39	2160318.27	TCE	Latest	0.978	0.1986	0.0017	0.4434
37-OW03	6652708.52	2160755.68	TCE	Historical	0.953	-0.0476	-0.7150	0.6410
37-OW03	6652708.52	2160755.68	TCE	Post-1999	0.977	-0.3973	-1.9959	0.4731
37-OW03	6652708.52	2160755.68	TCE	Latest	0.978	0.0702	-1.1023	1.6812

Section 4. Spatial Optimization

This section summarizes the spatial statistical analyses conducted at Site 133 on long-term groundwater monitoring (LTM) data using the spatial component of the GTS algorithm. The main goal of this portion of the study was to determine whether there are statistical redundancies within the spatial network of well locations being monitored at Site 133, and to make recommendations as to which current wells might be "pulled out" of the network, or at least sampled very infrequently. The purpose in doing so is to optimize the LTM program by determining whether there are resources being poured into sampling and analysis that might be pared without sacrificing critical information.

A secondary goal of the spatial analysis is to determine whether there are specific areas at Site 133 where the siting of additional wells would provide important, unknown information about contaminant extent. By "eliminating" redundant wells from "over-sampled" areas and then potentially adding wells to other areas of "undercoverage," the spatial network can be optimized in the sense that monitoring wells are effectively placed to capture key information about the contaminant plume(s).

This section includes descriptions of 1) what data preparations were made for input to the GTS spatial algorithm; 2) the GTS spatial algorithm itself, including changes made to the algorithm since the last published version (Cameron and Hunter, 2002); and 3) results of the Site 133 spatial analysis.

Section 4.1. Data Preparation

As discussed in **Section 3.1**, data queries were made for all chemical analytical data collected from wells Site 133. Exploratory statistical analyses were then performed to pare the initial list of possible constituents to 2 to 3 candidate constituents of concern (COC). As mentioned previously, including a large number of COCs significantly increases the amount of work required to run the GTS algorithm without typically improving the results. So the goal was to include only those parameters in the optimization routine that offer *the most statistical information* concerning temporal and spatial redundancy. The best such parameters typically exhibit larger detection rates and more widespread spatial occurrence.

Overall, the most promising candidates at Site 133 were TCE (the single best candidate), MN, and DIOXANE14. These three were chosen for the optimization analysis. Other COCs had much lower detection rates and/or poorer spatial distributions, or were considered of lesser importance.

Unlike the temporal analysis, where sampling data at a given well and date but collected over multiple depths were averaged so as to ensure that there was only one value per sampling event per well, the spatial analysis was designed to be three-dimensional in nature. What that meant was that every sample measurement was assigned not only an easting and northing, but also a depth and elevation value. Only data that could be placed within three-dimensional space could be utilized in the analysis. Data points missing any of these components were excluded.

The other major step in the data preparation was to divide the available data for each COC into two separate "time slices." The first time slice consisted of all measurements procured during 1999 and 2000. The second covered all measurements sampled from 2001 and 2002. Data prior to these years were not used in the spatial analysis in part to ensure that the most current well network was optimized. There was also evidence that the magnitude of the plume of contamination was changing, almost certainly increasing for TCE, from the first time slice to the second.

The reason for analyzing separate time slices was three-fold: 1) because the character and extent of contamination is likely to change over time, yet maps of a site represent only "snapshots," it is important to analyze data from a limited time frame in order to create reasonably accurate maps; 2) unless sampling events are highly regimented and all wells are sampled at the same time and during the same sampling event, it may be impossible to include a full representation of the spatial well network if only a specific sampling event is analyzed, as opposed to a "slice" of time that includes a limited range of events; 3) to help ensure that well locations are optimized over the life of the LTM program and not simply for a given sampling event, wells are only identified as potentially redundant if they exhibit redundancy across time slices (note, however, that newer wells might not have any data for earlier time slices; such wells would exhibit redundancy only in more recent time slices).

In practical terms at Site 133, with 3 COCs and two time slices per COC, six distinct data sets were analyzed under the spatial optimization algorithm. This allowed for a six-fold comparison of redundancy in identifying wells that were either "essential" or potentially "redundant" in their statistical information. On a final note, as in the temporal analysis, non-detects were handled by converting them to half the listed reporting limit (RL).

Section 4.2. Methodology

The heart of the spatial optimization analysis in GTS consists of the following basic steps: 1) estimation of a declustered, univariate cumulative distribution of concentration values for each COC; 2) determination of an appropriate spatial bandwidth; 3) creation of a base map using locally-weighted quadratic regression and all existing site data; 4) calculation of a global regression weight at each well; and 5) iterative elimination of wells with the lowest global regression weights and re-estimation of the site map based on the reduced data set. Each of these steps is explained below.

Section 4.2.1. Declustered CDF

The first task of the spatial analysis was to determine an appropriate univariate distribution of concentration values for each COC. At many contaminated sites, the measurement data may range over several orders of magnitude. As importantly, there is a complex, three-dimensional spatial distribution associated with these values, dependent both on the nature of the subsurface and the intensity and location of the contaminant plume(s). High concentrations tend to cluster together, although not uniformly and not necessarily in a predictable fashion. Because of this reality, most standard geospatial techniques, including typical forms of kriging, can suffer in their ability to produce reasonable site maps. Univariate and parametric forms of kriging, in particular, such as ordinary or lognormal kriging, often have great difficulty accurately reproducing the

highs and lows of widely spread concentration ranges. Except that is, at known data locations, where kriging "honors" the data by exactly reproducing it.

A better strategy is to use a non-parametric form of spatial analysis, such as probability kriging or perhaps even quantile kriging. Probability kriging transforms the original concentration data into a series of indicator variables and another variable representing the uniform scores of the original data. Each indicator is a binary 0-1 variable associated with a particular reference concentration level. All samples with values no greater than the reference level are converted to ones and all values larger than the reference level are converted to zeros. The basic idea is to convert each data value into known probabilities: if the reference level is, for example, 10 ppb, an indicator value of one means it is certain that the data point in question does not exceed 10 ppb (the probability of not exceeding the reference level being equal to one), while an indicator value of zero means that the actual concentration is certainly greater than 10 ppb (the probability of not exceeding the reference being zero).

Typically in probability kriging a series of increasing reference levels is used to define key portions of the actual concentration range (e.g., 5 ppb, 100 ppb, 1,000 ppb, 5,000 ppb, 10,000 ppb). Indicator variables are defined for each reference level and kriging is performed on each indicator. The ultimate goal at each unknown map location is to form a weighted combination of the known 0's and 1's to estimate a probability that the unknown location does not exceed the reference level. Then, by having such probabilities in hand for the entire series of indicators, a reasonable estimate can be made of the actual concentration at the unknown location (more on that below).

To improve these estimates, probability kriging employs an extra variable computed as the *uniform scores* of the original concentration distribution. This transformation simply orders the data and converts each value to its rank divided by the data set sample size, thus giving a transformed value between 0 and 1. Higher values thus have uniform scores closer to 1 while low values have uniform scores closer to 0.

The same strategy is used in quantile kriging. While no indicator variables are formed as in probability kriging, kriging is performed on the uniform scores directly instead of the actual concentrations, leading to kriged estimates between 0 and 1. These estimates can then be thought of as percentiles, since they represent a probability of not exceeding a certain concentration level. The concentration level itself is known as the *quantile* associated with the particular percentile, hence the name quantile kriging. So for example, if the kriged estimate were 0.7, the estimated value at that location would represent the 70^{th} percentile of the possible distribution of concentration measurements.

To actually re-transform these percentile estimates back to the original concentration scale, some form of the cumulative distribution of concentration measurements must be used. Unfortunately, because sampling in contaminated areas is often done to "chase the plume," clusters of high values are often over-represented in the raw, univariate concentration distribution, biasing the results. A better solution is to make use of the *declustered cumulative distribution* or declustered CDF for short. The declustered CDF

adjusts the raw distribution for spatial clustering and generally offers a more accurate estimate of the true concentration distribution.

While a variety of techniques exist to form the declustered CDF, the one utilized in GTS is based on a method for finding declustering weights (Bourgault, 1999). In this method, simple quantile kriging is performed on the set of known measurements, not to estimate *unknown* locations, but rather to *cross-validate* the *known* ones. This is done by temporarily removing a known value from the data set and then calculating a kriged estimate at that spot using the remaining data (otherwise known as "leave-one-out" cross-validation or jackknifing). As it turns out, the local kriging variance associated with each data location being cross-validated can be considered a *declustering weight*: higher variances represent locations with minimal spatial clustering while lower variances represent locations with significant clustering. By then weighting the original concentrations according to these declustering weights, the declustered CDF is formed as the resulting weighted univariate distribution.

To perform the actual cross-validation and simple quantile kriging, two preparation steps had to be accomplished. One was to convert the original data into uniform scores. The other was to develop a three-dimensional model of spatial covariance for the uniform scores. This was accomplished by analyzing omnidirectional variograms of the uniform scores for each of the three COCs and fitting appropriate spatial correlation models to these plots. Parameters for each model are provided in **Table 4-1** below.

Table 4-1. Parameters of Final Spatial Correlation Models

COC	Nugget	Spherical Component		Exponential Component		Gaussian Component	
		Sill	Range	Sill	Range	Sill	Range
DIOX	0.57	0.135	700	0.32	6900	—	—
MN	0.68	0.11	600	0.33	10000	—	—
TCE	0.53	0.33	1000	0.22	10000	—	—

The result of this step was a declustered univariate CDF for each COC. Note that this cumulative distribution of concentration values was designed to represent the range of concentrations that could be observed at Site 133. As such, the declustered CDF includes data from the entire time period under consideration, from 1999 through 2002. Furthermore, as will be explained below, the declustered CDF was ultimately used to derive concentration estimates of each COC along a grid of unknown locations encompassing what will be termed the *optimization box*.

Section 4.2.2. Spatial Bandwidth and Search Radius

An important step to building an estimated site map is to choose a *spatial bandwidth*. The fitting procedure used in the current version of GTS, namely *locally-weighted quadratic regression* (LWQR), works by estimating the surface value at a given unknown grid location using a weighted linear combination of the known sample values close to the grid point. The analyst must select, however, how many neighboring sample measurements to use. In GTS this is done by selecting a *bandwidth parameter* that represents the

fraction of known samples to be included in the neighborhood of any given grid point. For a one-dimensional time series, these bandwidths typically range from 40% to 80%. With volumetric or three-dimensional data, roughly equivalent bandwidths (in terms of data density included in the neighborhood per unit of volume) are on the order of 10% to 40%.

In general, the higher the bandwidth, the greater the amount of 'smoothing' that will occur over the estimated surface. Too high a bandwidth and the surface trend may 'miss' important peaks and valleys. Too low a bandwidth and the surface trend may exhibit artifactual jumps and/or dips between known sample values.

To guard against these scenarios, it is important to run a 'pre-flight' check of the LWQR fits at several possible bandwidths prior to constructing a base map of the site. This pre-flighting is done by computing diagnostic checks of the *residuals* obtained when the surface trend is estimated at each known sample location and the known value is subtracted from this estimate.

Using GTS, several tests of the surface residuals are made, including the following calculations: Mallow's CP statistic, correlation of the residuals with the estimated surface trend, average bias of the residuals, and Filliben's probability plot correlation coefficient. Each of these statistics is designed to provide a numerical indication of the goodness of the estimated trend relative to a given bandwidth. In GTS, these residual diagnostic measures are plotted simultaneously against bandwidth in order to search for the most appropriate fitting neighborhood. The residuals are also plotted in space to look for obvious anomalies or areas of substantial lack of fit.

Mallow's CP statistic is a scaled measure of the sum of squared residuals. Lower values of Mallow's CP usually indicate a better fit. The correlation with the estimated surface trend is used to check whether the fit is worse over certain ranges of the variable being estimated than others. Values close to zero are best. Values close to zero are also good when examining the average bias, which simply measures the average difference between the estimated surface value and the known measurement. Filliben's correlation coefficient is a test of normality that can be used to check the shape and symmetry of the residual distribution. LWQR works best when the *residual* distribution is symmetric and normally distributed. Coefficient values closer to one are best.

Taken together, it is usually possible to find an acceptable bandwidth with which to construct the surface maps. At Site 133, a value of 12% was deemed a reasonably good choice for both time slices of TCE. That simply means that the nearest one-eighth of the data measurements were used to help estimate the unknown grid point, regardless of their distance from that location. For MN, a bandwidth of 15% was used for the first time slice and a bandwidth of 20% was used for the second. For DIOXANE14, a bandwidth of 20% was used for both time slices.

Section 4.2.3. Creating Base Maps with LWQR

Once a bandwidth is chosen, the next task is to create a three-dimensional base map for each COC and time slice. The base map under GTS serves as the primary means by which degrees of spatial redundancy are assessed. Not only is a baseline established as

each COC is mapped across the site area, but measures of local and global variance are also computed. At each further iteration of the GTS algorithm, new maps created from reductions in the original data set are compared to the base map to determine how much plume information has been lost and at what price in increased map uncertainty. For this reason, it is important to try and build as accurate a base map as possible.

The previously published version of GTS employed a fairly simple strategy for creating base maps (and subsequent maps). In order to 1) avoid data complexity, 2) handle large fractions of non-detect values, and to 3) aid in the fitting of spatial covariance models, all measurements were converted to a single indicator variable (i.e., zeros and ones), where the reference concentration level was taken as either the detection/reporting limit or a regulatory limit (such as an MCL). Base maps constructed from these indicators were not re-converted to concentrations, but rather represented maps of the probability that the true concentration was below the reference level. As such, these maps did not provide detailed information about plume intensity, but still were useful for assessing spatial redundancy. However, a significant amount of statistical information concerning the spatial distribution of contaminants was not utilized.

In the current version of GTS, the attempt is made to map the plume or contaminant distribution more completely. This is done by converting the sample concentrations into a series of 10 indicator variables, with each reference concentration representing a key quantile of the original, univariate declustered CDF, as shown in **Table 4-2** below. The goal here is not to choose specific regulatory limits as reference values, but rather levels that adequately 'divide' or 'span' the univariate distribution of COC concentrations, paying particular attention to the often highly skewed upper end of these distributions.

Table 4-2. Reference Concentrations and Corresponding Percentiles of Declustered CDF for Each COC

Indicator Variable	DIOXANE14		MN		TCE	
	Reference Conc (ppb)	Percentile	Reference Conc (ppb)	Percentile	Reference Conc (ppb)	Percentile
I-1	0.5	0.416	10	0.139	2	0.204
I-2	2.5	0.597	50	0.345	45	0.452
I-3	5	0.733	100	0.532	100	0.597
I-4	7.5	0.823	150	0.606	250	0.711
I-5	10	0.859	300	0.721	500	0.782
I-6	15	0.892	500	0.856	1000	0.831
I-7	30	0.924	650	0.908	2500	0.905
I-8	50	0.948	800	0.948	4000	0.954
I-9	100	0.974	1000	0.971	8000	0.983
I-10	300	0.990	2000	0.994	12000	0.992

It should also be noted that at the lower end of the concentration range, the reference percentiles are not always equally distributed. At many sites, including Site 133, there is often a significant fraction of non-detects at a common reporting limit. This can lead to large jumps in the declustered CDF.

Another facet of the previous version of GTS was that all analyses were conducted in two-dimensional (2D) space. Depth information was simply ignored or collapsed so that all well locations were treated as if they resided in a 2D plane. Furthermore, the technique used to estimate the base map (and all subsequent maps) was ordinary indicator kriging. Kriging takes a neighborhood of known values around an unknown grid point and solves a set of simultaneous linear equations to find the "best" estimate for that grid point. The known locations are "honored" in the sense that a kriged estimate at a known location returns the original data value. In this way, kriging can be thought of as a kind of *spatial interpolator*, where grid points between known locations are interpolated based on the known values.

A key aspect of the kriging method is that it fundamentally depends on having a spatial covariance model that adequately describes the strength of the spatial correlation between adjacent sample points. Much effort in fact can be devoted to analyzing the empirical spatial correlation measure (typically called the variogram or semi-variogram) and then developing an appropriate mathematical model of the spatial covariance.

In order to streamline this process, a different technique has been incorporated into the GTS algorithm: *locally-weighted quadratic regression* (LWQR). Like kriging, LWQR takes a neighborhood of sample values located near an unknown grid point and solves a system of linear equations to determine the optimal estimate. Like kriging, LWQR is a kind of linear estimator. Both techniques assign numerical weights to the sample values in the neighborhood and form the new estimate as a weighted average of the sample values. However, there are also a number of differences.

For one, kriging requires that all the sample data have distinct locations in space. Otherwise the kriging algorithm does not return a solution. In practice, if some locations have multiple measurements during a given time slice (say from distinct sampling events), these values must first be averaged or pre-processed in such a way that only a single value is used for kriging. Some information about the individual measurements and data variability is necessarily lost in this step. LWQR has no similar requirement. So multiple values at a given well or given sampling location are OK.

Second, kriging, as mentioned above, is a spatial interpolator which honors the known data values. LWQR is instead a *smoother*. Applied to spatial fields, LWQR attempts to find the best overall surface to *fit* the available sample points, but it does not require that any individual data value be honored. The best analogy is standard linear regression. When a best-fitting line is estimated for a time series or an XY-scatterplot, the line may or may not exactly pass through any given individual value. Nevertheless, the line is chosen to minimize the sum of squared deviations from it and to fit the overall trend. In a similar way, the standard version of LWQR is designed to determine the best-fitting quadratic surface through the sample points, but will not *necessarily* pass through any one of them exactly.

In practical terms, LWQR attempts to fit the best overall surface to the sample data while implicitly assuming that the measured samples may not precisely fit the surface trend either due to error or some other source of variation. Standard forms of kriging basically assume that all sample data are known exactly. Of course, there is no guarantee that some

measurements might not include elements of laboratory or sampling error. Variation is also introduced by the fact that the groundwater quality and/or plume intensity may change slightly from one sampling event to the next.

A third difference is that LWQR does not require prior development of a spatial covariance model. With LWQR, a locally-quadratic surface is fit to each grid point. Spatial correlation is incorporated in this method not through an explicit prior correlation model, but rather through the apparent *curvature* in the sample points themselves. The quadratic surface is fit to this curvature, the degree of curvature potentially changing with each grid point. In this way, spatial clustering *is* accommodated by the LWQR technique.

Section 4.2.4. Constructing the Base Map

To actually build the base maps at Site 133, a volume surrounding the site was constructed and a rectangular grid imposed on this volume. This volume is termed the *optimization box* in GTS. Often the optimization box will not precisely coincide with the site boundaries, or may not include some peripheral wells, but the aim is to have the box match the site boundaries fairly closely. Peripheral wells are included in the neighborhoods of sample points associated with some of the nearby grid locations. In this way, those wells do get included in the optimization analysis.

The specific coordinate ranges of the optimization box for Site 133 are listed in **Table 4-3** below. Note that due to the surface topography, it may occur that nodes on the upper layer of the grid are sometimes higher than ground level. In addition, approximate elevation constraints were imposed on the box to ensure that depths well below competent bedrock and the subsequent groundwater aquifer were not included in the optimization grid.

Table 4-3. Boundaries of Optimization Box

Direction	Minimum	Maximum	Step Size
Easting	6,650,200 ft	6,659,000 ft	400 ft
Northing	2,151,000 ft	2,163,400 ft	400 ft
Elevation	2,370 ft	3,050 ft	40 ft

At each grid node, an LWQR estimate was made using each of the ten indicator variables in turn. At each indicator level, the zeros and ones corresponding to the sample data were employed to compute an estimate of the probability that the reference concentration level had not been exceeded. Repeating this process for each indicator then gave a series of ten probability values at each grid node, representing updated information helping to “bracket” the best estimate of the concentration at that node. As an example of this process, consider the following hypothetical results for TCE at node 10 as shown in **Table 4-4**.

Table 4-4. Hypothetical LWQR Results for TCE

COC	Indicator Variable	Reference Level (ppb)	LWQR Result
TCE	I-1	2	0.10
TCE	I-2	45	0.20
TCE	I-3	100	0.25
TCE	I-4	250	0.28
TCE	I-5	500	0.36
TCE	I-6	1000	0.45
TCE	I-7	2500	0.78
TCE	I-8	4000	0.95
TCE	I-9	8000	0.99
TCE	I-10	12000	0.99

Based on the LWQR results, there would be only a 10% probability that the true concentration fell below 2 ppb, a 20% chance that the true concentration was below 45 ppb, a 25% chance that the true value was below 100 ppb, a 28% chance that the true value was below 250 ppb, a 36% chance that the true value was below 500 ppb, a 45% chance that the true value was below 1000 ppb, a 78% chance that the value was below 2500 ppb, a 95% chance that the true value was below 4000 ppb, and a 99% probability that the value was below 8000 ppb or greater. The most likely range would therefore be between 1000 ppb and 2500 ppb.

To actually determine a concentration estimate for this hypothetical grid node, the approach taken in GTS is to update the univariate declustered CDF using the LWQR results for the series of indicators. This leads to what is known as the *conditional* cumulative distribution function or CCDF. The basic idea is to *condition* or *adjust* the overall univariate distribution of measured values using the updated information provided by the LWQR indicator results. So, for instance, in the hypothetical example above, the declustered CDF for TCE indicates that 90.5% of all the available TCE measurements at Site 133 were no greater than 2500 ppb (see previous table). At the hypothetical grid node being estimated, however, the probability that the true value does not exceed 2500 ppb is only 78%. Therefore, the overall univariate CDF must be updated so that values less than 2500 ppb only occur 78% of the time *at this grid node*. In this manner, an updated CCDF can be calculated independently for each grid node and estimates of the (locally-varying) true mean concentration made across the site using the formula:

$$\hat{v} = \sum_i v_i \left(CCDF(v_i) - CCDF(v_{i-1}) \right)$$

where v_i indexes the observed concentration values from the declustered, univariate CDF, and CCDF(v_i) represents the updated or conditional CDF probability associated with v_i.

Section 4.2.5. Global Regression Weights

In addition to the base map built from the LWQR estimates, another key output is the computation of global regression weights. The vector of global regression weights

associates each known well location with a numerical index representing that well's overall relative contribution to the base map. Positive global regression weights represent wells that are more influential in the base map estimation; negative or zero weights represent wells which play a smaller, more redundant statistical role in the creation of the map. Thus, the global regression weights serve to identify degrees of spatial redundancy among the set of existing well locations.

The global regression weights are calculated by accumulating in an appropriate way a series of intermediate vectors known as the *local* regression weights. These intermediate weights are a by-product formed when computing the estimated probability of non-exceedance for each indicator variable at a given grid node: the LWQR results are manipulated to compute what is known as the *local weight diagram*. The weight diagram is a vector of numerical weights, one per sample measurement in the search neighborhood, such that the probability of non-exceedance for a specific indicator level is proportional to a weighted average of the product of the sample indicator values and the weight diagram. Thus the weight diagram represents the set of local regression weights that gets applied to the observed indicator data to produce the LWQR estimate.

There are two important things to note about the local weight diagram. First, each grid node involves a different set of neighborhood samples, but across the site as a whole, any given sample value is likely to be used in the neighborhood of a number of distinct grid nodes. Thus, the search neighborhoods tend to overlap as one "moves about" the grid. Second, the local weights in LWQR, while they sum to one, are not necessarily positive.

With these items in mind, how are the global regression weights then computed from the local weights? First, the local weight vectors are augmented to give *zero* weight to any sample location located outside the search neighborhood for that grid node. This numerically represents the fact that samples outside the neighborhood have no influence (positive or negative) on the LWQR result for the node being estimated. Second, the augmented local weight vectors are averaged across all the grid nodes *by* sample location. This means that given a known sample location at well X, the local weights associated with that location (one per grid node, with some possibly equaling zero) are summed and then divided by the total number of nodes. Finally the averaged weights are adjusted for wells with multiple sampling depths. Here the weights are summed across depths for each well. Weights at wells with only a single sampling depth remain unchanged.

After all these steps are completed, *there is exactly one weight per well location*, and it is this numerical vector that is deemed the set of global regression weights. The term global is used because the final weights are built by averaging the local influence on the base map of each sample across the grid, and hence, across the site as a whole. With this vector in hand, the wells are then ranked according to their statistical influence on the base map. Wells with higher global regression weights are deemed more essential to the map estimate, while those with lower weights are deemed least essential and thus potentially redundant.

Section 4.2.6. Local and Global Variance Measures

In addition to forming the basis for the global regression weights, the local regression weights are also useful for estimating relative local and global variance measures. These measures provide a way to assess the relative degree of statistical uncertainty associated with a given map estimate. First, a local uncertainty measure is computed at each grid node using the local weight diagram and the following formula:

$$locvar(w_k) = \sum_i \left| lx^i(w_k) \right|^2$$

where w_k denotes the kth grid node, i indexes the sample values in the search neighborhood around the kth node, and lx represents the local regression weight vector.

Because a different relative local variance is computed at each grid node, the set of local variances can be mapped, much like the base map of concentration estimates. One can also determine from such a variance map whether there are certain areas of the site where the local variance is particularly high, representing places of greater statistical uncertainty connected with the mapped concentration estimate.

With the local variances in hand, GTS also computes a global variance measure for the site as a whole. To do this, the local variances are simply summed across the set of grid nodes, using the following formula:

$$gvar = \sum_k locvar(w_k)$$

where, as before, w_k denotes the kth grid node and the summation is taken over the entire grid.

The reason why the global variance is valuable is that it provides a single numerical summary of the total relative statistical uncertainty associated with a given configuration of well locations. In other words, the global variance from the base map — utilizing all the original well locations — can be compared against the global variance computed from estimating the same map on a reduced or different set of well locations. Increases in global uncertainty then represent configurations that are less statistically reliable.

Section 4.2.7. Iterative Elimination of Wells

Given that the global regression weights provide a *relative* but not an *absolute* measure of spatial redundancy, it is important to use other measures to test how many wells are actually redundant and what degree of redundancy should be tolerated. The global regression weights therefore provide a *strategy* for identifying potentially redundant wells. However, the acid test is to see how accurately maps can be estimated when these possibly redundant wells are temporarily removed from the data set.

To accomplish this goal in a systematic fashion, GTS uses the following procedure. First, the remaining wells are sorted by global regression weight. Second, the subset with the lowest five to ten percent of global regression weight scores are flagged and removed from the data. Then LWQR is used on the reduced data set to re-estimate the site map.

Comparing this re-estimated map to the original base map, three basic statistical quantities are measured: 1) change in global regression variance; 2) changes in local node-specific variances, including tracking of the percentage of nodes with local variances greater than a pre-defined threshold; and 3) changes in the mapped concentration estimates.

The same process is repeated several times by removing five to ten percent of the lowest ranked well locations (that is, ranked by global regression weight) at each incremental iteration. In this fashion, a small number of wells is temporarily eliminated at each step, until the map estimates show obvious deterioration and the variance measures show substantial change.

The final step in the spatial analysis is to review the results of the iterative well location removal algorithm and to decide at what point the re-estimated maps have deteriorated beyond a reasonable level. Such a decision is necessarily somewhat subjective. However, it is often helpful to examine the rate of deterioration in the maps and the rate of change in the global and local variance measures as a function of the percentage of well locations that has been removed.

Once a "stopping point" has been decided, only wells deemed potentially redundant at the *previous* removal step are ultimately tagged as redundant for that COC and time slice. Then the lists of redundant wells are compared across the COCs and time slices in order to determine that subset of locations which is consistently redundant. These wells then make up the final redundancy list for the site.

One final thing to note is that the global regression weights are recomputed at each stage of removal and therefore are not "fixed" measures of redundancy. Wells with higher global weights at one stage, and thus considered important enough to "keep in the mix" of essential wells, might have low global weights at a subsequent stage. Because of this, rankings based on the global regression weights are only meaningful relative to the particular removal stage at which they are computed.

Section 4.3. Spatial Optimization Results

The spatial optimization results are contained in a series of graphs and tables. Overall, the spatial analysis of the two time slices (1999-2000 and 2001-2002) at Site 133 revealed different levels of spatial redundancy. For the earlier data, a 'safe' level of redundancy amounted to between 13% and 27% of the well network, depending on the COC. For the second time slice, redundancy levels for all three COCs were judged at between 33% to 40%. Because of the wide spatial spread and intensity of TCE at Site 133, and due to the apparently changing nature of the groundwater contaminant plume, the overall recommendation from the GTS analysis identifies approximately 35% of the well network locations as redundant.

When matching lists of redundant wells across the COCs, 28 wells were identified as potentially redundant, amounting to 20 percent of the total well set. For the most recent TCE data (2001-2002 data) — these data being deemed the most critical — 48 wells were identified as redundant, or 34% of the baseline network.

Potentially, *from strictly a statistical point of view*, all of these redundant wells ought to be eliminated from the Site 133 LTM network. However, other considerations must be factored in before making any such decisions. The spatial analysis here only considers statistical contributions of each well to concentration maps of the site. It does not consider other purposes for these wells. Some of them may be essential for other engineering, site characterization, or treatment reasons. Each potentially redundant well should be reviewed by site geologists and hydrologists to determine if such overriding factors exist.

Section 4.3.1. Global Measures of Redundancy

To help assess redundancy at a global level, the graphs in **Appendix 4-1** were prepared. These graphs plot selected summary statistics from the spatial mapping exercise against the percentage of wells that was removed from the data for each COC. Examination of these graphs can provide one indication of when 'too much' data has been removed (that is, when a reasonable level of statistical redundancy has been exceeded), especially if the trend is flat or very gentle at first (say for lower fractions of data removal), but then begins to trend more sharply at some increased level of data removal.

The first measure of global redundancy is given in the first figure for each COC in **Appendix 4-1**. These graphs plot the trend in global variance for each COC and each time slice. In general, the global variance might be expected to increase as more data is removed and the maps are re-estimated. In other words, less data equals less certainty and higher variance. However, this pattern does not always occur. At some grid nodes, the estimated variance tends to 'blow up,' leading to a much higher global variance value even at low removal levels. This artifact makes the global variance measures harder to interpret.

Overall, the global variance patterns, while not ideal, show a substantial jump for TCE after a 33% removal in the second time slice. For MN and DIOXANE14, a jump also occurs after 40% removal for 2001-2002. DIOXANE14 also exhibits an increase in global variance after 27% removal during 1999-2000.

Additional measures of global redundancy are shown in the second two figures for each COC in **Appendix 4-1**. The first of these documents the change in two measures: the percentage of voxels (i.e., three-dimensional pixels) with very high grid-node-specific local variances (denoted REDUCED-VARPCT on the plots) and the average level of difference between the estimated indicator values from the reduced data set and those of the base map (denoted AVE-IDIFF). The first of these (i.e., REDUCED-VARPCT) simply counts across the site grid the percentage of estimated nodes where the local variance value was determined to be in the extreme upper tail of the distribution of local variances. As the fraction of data removal increases, the percentage of extreme local variances would also be expected to increase.

The second measure (i.e., AVE-IDIFF) was computed by taking the difference at each of the five indicator levels between the reduced data set indicator estimate and the corresponding base map indicator estimate. These indicator differences were then averaged across the five indicator levels and finally averaged again across all the nodes on the site grid. The interpretation of the average indicator difference is as follows: each indicator variable corresponds to a particular concentration level from the overall

declustered CDF (for instance, the first indicator for TCE corresponds to a concentration value of 2 ppb). The indicator estimate after mapping the site with LWQR is the probability of not exceeding this reference concentration value. To the extent that the indicator estimates at a particular grid node for both the base map and the reduced-data map are the same, both maps then provide the same statistical information about the expected concentration level at that node. On the other hand, if the indicator estimates differ, the estimated concentration values will also differ, leading the reduced-data map to differ in pattern and magnitude from the base map. Averaged across all the nodes on the site grid, the average indicator difference then provides a summary measure of how much change is to be expected between the base and reduced-data maps.

For all the COCs, there is no particular pattern to the REDUCED-VARPCT measure. In fact it is generally flat to declining in overall trend as more data is removed. The reason for this appears to be connected with how the LWQR method estimates variance. Because the estimated variability depends fundamentally on the observed concentration values, if enough of the pre-existing variation has been removed at a given step (by not including wells with more variable sampling data), the local variances may begin to drop, leading sometimes to a lower overall global variance, and a smaller percentage of grid nodes with very high local variance values. This pattern can be seen for instance in some of the graphs in **Appendix 4-3**.

The average indicator difference measure (AVE-IDIFF) traces a more complicated, but also more informative, pattern. *Negative* values of this measure signify an overall *over*-estimation of the site grid on the reduced-data set compared to the base map. *Positive* values signify an overall *under*-estimation. For TCE, AVE-IDIFF remains quite close to zero during 1999-2000 until more than 40% of the wells have been removed. The pattern for the second time slice is harder to interpret. For MN, the sharpest changes in AVE-IDIFF occur after about 13% removal for 1999-2000, and after about 40-47% removal for 2001-2002. For DIOXANE14, AVE-IDIFF appears to exhibit more significant changes after about 27% removal for both time slices.

The final set of global redundancy measures are denoted by MEAN-MISCLASS, TRIM-MISCLASS, and PCT-IDIFF. MEAN-MISCLASS refers to the percentage of voxels or nodes that were classified one way relative to a regulatory limit or other pre-specified concentration level on the base map but are classified the *opposite* way on the reduced-data map. For example, using the MCL of 5 ppb for TCE, approximately 12% of all the estimated grid nodes were *misclassified* when 7% of the wells were removed in time slice one. That percentage rises to just over 20% by the time 40% of the wells have been removed. TRIM-MISCLASS is a measure closely related to MEAN-MISCLASS, except that instead of classifying voxels on the basis of the estimated mean concentration, the classification is done using the estimated *trimmed mean*, cutting off 10% of the lower and upper tails of the updated, conditional CDF. For the most part, MEAN-MISCLASS and TRIM-MISCLASS tend to give similar results at Site 133.

While the percentage of such misclassifications increases as expected with increased data removal, the trends do not always provide a clear way to measure a specific degree of acceptable redundancy. Instead of flat or nearly flat trend followed at greater levels of

removal by a sharp increase, the majority of the increase often occurs right away at the lowest removal levels. Still, there is an indication of a more noticeable jump in misclassifications after approximately 40-47% removal for TCE in both time slices, and perhaps DIOXANE14 during 2001-2002.

PCT-IDIFF is an additional measure of how much the reduced-data map indicator estimates differ from the base map indicator estimates. It counts the percentage of nodes at which at least one reduced-data indicator differs from the corresponding base map indicator by at least 0.5 (remember that all the indicator estimates are between 0 and 1; a difference of at least 0.5 is thus a large change in the estimated probability of non-exceedance for the associated reference concentration level). Unfortunately, while PCT-IDIFF again trends upward with increased data removal for all three COCs and both time slices, there is little evidence of any 'flat' portions of the trends upon which to judge degrees of redundancy, with the possible exception of MN after a 40% removal in the second time slice.

Section 4.3.2. Local Indications of Redundancy

While global measures of redundancy can be useful, they do not provide the full story. Global misclassification rates for example do not indicate *where* the misclassification is occurring or to what degree. Only actual maps of the site can provide this type of information. To this end, two sets of maps are provided for each COC and time slice. The first documents, at each level of data removal, the differences in the local indicator values between the base map and each reduced-data map (see **Appendix 4-2**) Local areas of overestimation (corresponding to *negative* indicator differences) are shaded in orange and red. Local areas of underestimation (corresponding to *positive* indicator differences) are shaded in blue. By comparing these maps relative to the increase in the amount of data removed, one can assess at what point too many local areas of over- and under-estimation 'pop-up.'

The second set of maps (see **Appendix 4-3**) details in a similar way what changes occur in the local variance with increasing data removal. Are there particular areas of the site at which the local uncertainty is unacceptably high? Do the areas with high local variance change as more data is removed? Do new areas emerge? All these questions can be assessed by viewing the maps in **Appendix 4-3**.

In general, the maps in **Appendix 4-2** support the conclusion that too much local information is lost from the base map when the data removal fraction rises above approximately 13-27% for the data collected during 2000-2001. For the second time slice, the results suggest a 'safe' level of redundancy of perhaps 33-40%. Please note that judgments about redundancy are necessarily somewhat subjective. The maps in **Appendix 4-2** should be viewed in a series, with an eye as to when large tracts of severe over-estimation and under-estimation begin to occur. Small pockets of estimation bias and perhaps smaller 'hotspots' are sometimes apparent even at low levels of removal. This is a consequence of the fact that hard information is lost when well locations are removed from the data base. However, the optimization analysis works to minimize the unavoidable loss of statistical information, and to balance this loss against the gain in resource savings that might be achieved.

The maps in **Appendix 4-3** are more problematic. The most common pattern exhibited by the local variance maps is an increase in areas of both very high variability and, simultaneously, areas of very low variability. As noted in **Section 4.3.1**, this is probably due to the fact that when a larger percentage of the wells have been removed, there are large swatches of the site where the nearest sample measurements are fairly uniform in concentration level, leading to a low variability estimate. At other locations, there is less data available to use in the estimates (or perhaps the remaining data do not vary in a continuous manner) and so the variation is quite high. In any event, the local variance maps, especially for the more recent data, do not provide much help at Site 133 in assessing degrees of redundancy. For the first time slice, the largest change in the local variance pattern and the largest increase in local variance 'hotspots' seems to appear after 20-27% removal. This observation is reasonably consistent with the analysis of the indicator difference maps for 1999-2000 discussed above.

One important thing to note about the maps in **Appendices 4-2** and **4-3** is that they are presented as two-dimensional "plan-view" contour surfaces. The actual map estimates at Site 133 were three-dimensional, as noted earlier. However, it is difficult to adequately visualize three-dimensional data within a static report. To solve this difficulty, all the indicator difference and local variance maps were first *averaged over depth* in order to provide two-dimensional projections of the three-dimensional surface estimates. Some information is of course lost when such averaging is done. Nevertheless, the results can be presented and visualized much more easily.

Section 4.3.3. Base Map Accuracy

In **Appendix 4-4**, there is a base map of the estimated concentrations for each COC, overlaid with a scatter plot of the actual data locations used in the analysis. Both the base map and the scatter plot of actual data are colored by contour level. One can see from this representation that most of the observed data levels correspond reasonably well with the surrounding nearby base map estimates. There are, however, some notable exceptions.

A couple of major reasons account for areas where there appears to be poor base map accuracy. First, the two-dimensional base map representation is again averaged over depth, but is in reality three-dimensional. Often the plume areas lie below the ground surface, but appear to be at ground level on the 2D surface map. Although unavoidable, this averaging process affects to some degree how well the observed data appear to "match" the estimated contours on the base map. Along the same lines, many more individual samples were used in the base map construction than show up on the base maps in **Appendix 4-4**. Deeper sample values are sometimes 'hidden' by shallower, but nearby, locations due to the scaling and size of the maps. This is especially apparent for the 2001-2002 TCE data near the Site 133 source area. In the database, there are several TCE measurements above 30,000 ppb that are 'hidden' on the base map by much smaller, shallower values in the same vicinity.

Second, locally-weighted quadratic regression is, as was noted earlier, a smoothing technique rather than a spatial interpolator. Because of this, the estimated surface may not precisely equal the value of any given observed data point. This will especially be true in those cases where one nearby sample is quite high while its neighbor is quite low.

Ultimately, having an accurate base map is an important key to a successful spatial optimization analysis using GTS. As noted, all assessments of redundancy flow from a comparison between the base map and subsequent maps constructed from reduced-data sets. Although it is likely that the GTS algorithm is 'robust' to some base map inaccuracy, it is certainly the case that spatial redundancy cannot be judged fairly unless the base map matches the actual data to a reasonable degree.

The base maps generated using LWQR may or may not adequately coincide with similar hand-drawn maps created by project geologists. The estimated base maps from the spatial analysis are strictly data driven and do not account for special features of the terrain or hydrogeology.

Section 5. Recommendations for Edwards AFB, Site 133

Section 5.1 Recommendations Regarding Sampling Frequency

It has already been noted in **Section 3** from the temporal analysis that the operational sampling frequency at Site 133 ought to be reduced from annually to once every seven quarters. This recommendation is based on the Temporal Variograms discussed in **Section 3.2**. What was not discussed is how this sampling schedule can be translated into a site-specific sampling plan. The recommended sampling strategy is discussed in more detail below.

With regard to sampling frequency, construction of the Temporal Variograms requires pairs of measurements from any given well with a variety of inter-event time intervals. If the wells are sampled at regular intervals (e.g., every seven quarters) after implementation, the range of between-sample intervals would not have the required variety of inter-event time intervals, and consequently it would be much harder to construct a future Temporal Variogram to test the original recommendation. Therefore, a key goal of the sampling strategy is to ensure that each well is sampled at irregular intervals over time. This involves 'mixing up' or randomizing the distribution of inter-event sampling intervals to facilitate a similar follow-up analysis after 3 to 5 years to assess whether or not the initial recommendations would still hold.

Full implementation of the sampling strategy may not, however, be practical for certain wells that need to be sampled together or in a particular sequence. To make the sampling procedure as operationally efficient as possible, but without sacrificing the goal of at least partially 'mixing up' or randomizing the distribution of inter-event sampling intervals, one could also group the wells into clusters that would be sampled simultaneously. This might be needed, for instance, if 'cleaner' wells needed to be sampled prior to 'dirtier' wells, or perhaps for other logistical reasons. In this case, each cluster would be treated as a single well in the randomization scheme discussed below. Care should be taken, however, to ensure that individual clusters are not so large as to make the final sampling groups highly unbalanced.

It is recommended that a sampling plan be developed using the following three-step process to ensure sufficient variety of inter-event sampling intervals:

> **Step 1** – Randomly divide the group of essential monitoring wells into seven approximately equal-size groups (e.g., Group 1, Group 2, Group 3, etc.). This process would be akin to representing each well as a ball, and then randomly dropping each ball into one of seven different urns, until all the balls are used up. In practical terms, the easiest way to achieve such random assignment — and to ensure that each group is of roughly equal size — is to list the wells in any order (say on a spreadsheet), draw a random number between 0 and 1 for each well from either a computer, calculator, or random number table, list the random numbers beside each well, sort the list in order of the random values, then assign the wells at the top of the sorted list comprising the first one-seventh of the total to the first urn (Group 1), the second listed chunk of one-seventh to the second urn (Group 2), and so on.
>
> **Step 2** – Randomly assign Group 1 to one of the seven consecutive quarters of the new sampling program. Repeat this process until all seven well groups have been assigned to one of the seven quarters. Note that it will be quite possible to have more than one of the well groups sampled during the same quarter. This means, in other words, that the quarter for sampling is chosen independently for each of the seven well groups.
>
> **Step 3** – At the start of each successive seven-quarter interval, repeat steps 1 and 2. This step ensures that no single well will be sampled at precisely the same time during each sampling round.

Example Sampling Schedule for Wells Listed in Table 5-2 (112 wells):

Step 1- Randomly divide the set of wells (112 wells) into seven equal groups. (To do this, assign a random number between 0 and 1 to each well, sort the list of wells in order by the random numbers, place the first 16 of the sorted wells in Group 1, the next 16 in Group 2, etc.), as shown in the example below. *Note that this table is for illustrative purposes, and site managers should construct their own well grouping to address any site-specific operational considerations* (such as the need to sample certain wells together or in a particular sequence).

Example of Random Grouping of Wells Listed in Table 5-2						
Group 1	**Group 2**	**Group 3**	**Group 4**	**Group 5**	**Group 6**	**Group 7**
133-MW02	37-EW07	37-MW12	150-MW01	120-MW02	133-MW03	37-MW26
120-MW14	37-MW24	26-MW01	13-MW24	150-MW03	120-MW07	37-EW03
32-MW03A	36-MW04	13-MW17	13-MW10	37-MW29	13-MW09	13-MW27
37-OW06	37-MW08	37-MW14	153-MW06	177-MW08	13-MW06	37-MW16
13-MW22	13-MW07	177-MW04	133-EW03	36-MW03	13-MW30	153-MW08
37-EW08	37-MW15	37-MW22	13-MW28	133-OW02	120-MW11	13-MW01
162-MW04	13-MW11	162-MW01	37-MW04	133-OW05	13-MW08	153-MW05
36-MW01	13-MW18	13-MW29	37-MW06	120-MW05	186-MW02	150-MW06
177-MW09	133-OW04	13-MW16	177-MW06	13-MW20	177-MW20	37-EW04
13-MW23	37-MW05	13-MW25	37-MW11	133-MW01	153-MW09	153-MW04
162-MW03	37-MW01	37-OW05	120-MW03	37-MW02	120-MW13	120-MW06
37-EW02	120-MW10	37-MW07	137-MW01	177-MW07	171-MW05	186-MW01
120-MW15	37-MW17	37-MW23	13-MW21	13-MW12	150-MW05	37-MW25
37-OW02	177-MW03	37-EW05	37-MW21	121-MW09	13-MW04	133-OW03
13-MW19	120-MW04	26-MW08	153-MW03	37-MW13	37-EW06	13-MW26
32-MW02	133-EW02	13-MW05	13-MW03	120-MW12	13-MW14	37-MW19

Step 2 - Randomly assign each group (Group 1, Group 2, etc.) to one of seven quarters to develop the first seven-quarter sampling schedule. See **Table 5-1**. Note that during some quarters, it is possible that no sampling will be required. (To do this, pick a random sampling quarter – e.g., using a handheld calculator – between one and seven, and assign the Group 1 wells to that quarter. Repeat this process for each of the remaining Groups).

Table 5-1. Example Sampling Plan for the First Seven Quarters of the Optimized LTM Sampling Program

Year 1				Year 2		
First Quarter	**Second Quarter**	**Third Quarter**	**Fourth Quarter**	**Fifth Quarter**	**Sixth Quarter**	**Seventh Quarter**
Group 5	Group 4	Group 2	Group 3 and Group 6	Group 1	No Sampling	No Sampling

Thus, all wells will be sampled once every seven-quarters. Per **Step 3**, the steps are repeated to develop a new sampling schedule each subsequent seven-quarter sampling plan. (In this example, the next seven-quarter period would start in Year 2, Fourth Quarter).

Section 5.2 Recommendations Regarding Spatial Redundancy

The ultimate decision about when 'too much' data has been removed is somewhat subjective. But, based on the GTS spatial analysis, and considering both the global measures of redundancy and the maps of local indicator differences, at least 30 wells and perhaps as many as 50, could be considered as redundant to the Site 133 LTM program. This leaves 90 to 110 wells from the baseline list as ones that should remain in the monitoring program. Specific lists of wells essential to the LTM program are provided in **Tables 5-2** and **5-4**. **Table 5-2** is a list of essential wells based on using all three COCs from the spatial analysis. **Table 5-4** is a smaller list based on the results of most recent TCE data.

Given the importance of TCE as a 'driver' of the contaminant plume at Site 133, this analysis recommends that the second of these monitoring networks be implemented.

Note that in each of these tables, the last column assigns a relative ranking of the statistical importance of each well, classified as HIGH, MED(IUM), or LOW. These rankings (at least for **Table 5-2**) reflect whether or not the well was consistently deemed essential in each time slice for at least one COC and had a positive average global regression weight (HIGH), was consistently deemed essential but had a non-positive average global regression weight (MED), or was deemed essential only in certain time slices (LOW).

Complementing these tables are lists of statistically redundant wells culled from each thread of the analysis. **Table 5-3** lists the redundant wells derived from an analysis using all three COCs, while **Table 5-5** is a longer list of redundant wells derived from the results of the TCE analysis.

Several wells from Site 37 were included in baseline list for the general Site 133 area. These wells were used in the optimization routine and run through the cost analysis presented in **Section 5.4** below. The proposed reductions in the monitoring networks in **Table 5-2** and **5-4** therefore include wells from both areas. Of note, the base maps in **Appendix 4-4** document that the majority of the 1,4-dioxane contamination and most of the manganese plume occur within or near the Site 37 area.

It should also be noted that for the purposes of long-term follow-up analysis, if redundant wells are removed from regular long-term monitoring, they should ideally not be decommissioned. Rather, prior to a multi-year follow-up review, the same wells ought to be sampled again to determine whether or not the original recommendations are still valid. Thus, these wells would still be sampled very infrequently, say once every 3 to 5 years.

Lastly, it is important to reiterate that the recommendations concerning redundant wells are highly data-driven. Groundwater wells can serve multiple purposes and may be important for reasons other than long-term monitoring. Because of this, all of the potentially redundant wells should be evaluated by site geologists and regulators to ensure that other goals of the Site 133 LTM program are not compromised.

Table 5-2. Essential Monitoring Network Based on Analysis of All COCs (All measurements in feet)

Note: RANKING refers to relative statistical importance; HIGH = wells deemed essential in both time slices and having positive average global regression weights at optimal removal stage; MED = wells deemed essential in both time slices but having non-positive average global regression weights; LOW = wells deemed essential in only one of two time slices

WELL_ID	EASTING	NORTHING	DEPTH	SCREEN ELEVATION	RANKING
120-MW03	6651337.7	2152768.1	115.8	2652.46	HIGH
120-MW05	6650388.3	2151854.7	23	2716.86	HIGH
120-MW11	6652278.25	2153729.5	152.6	2645.49	HIGH
120-MW12	6651527.93	2153167.6	31.5	2744.61	HIGH
120-MW13	6652214.94	2152507.03	35.4	2748.22	HIGH
120-MW14	6650132.24	2151472.04	43	2696	HIGH
13-MW04	6655406.52	2158401.88	26	2901.6	HIGH
13-MW07	6654089.7	2159897.8	55	2922.67	HIGH
13-MW09	6656144.9	2157235.9	22	2873.57	HIGH
13-MW10	6655350.7	2155550.5	31	2834.26	HIGH
13-MW14	6656174.57	2157261.67	105	2790.86	HIGH
13-MW18	6653506.98	2155883.04	51	2815.3	HIGH
13-MW19	6657720.46	2153313.3	73	2803.98	HIGH
13-MW20	6654728.85	2151622.06	65	2741.91	HIGH
13-MW24	6658576.31	2159688.48	97	2865.42	HIGH
13-MW25	6658386.08	2158308.38	177	2772.8	HIGH
13-MW27	6652743.71	2150936.77	132	2644.28	HIGH
13-MW28	6657809.27	2150910.93	174	2673.61	HIGH
133-EW02	6655214.64	2159794.78	100.5	2860.45	HIGH
162-MW01	6650280.52	2163457.13	113	2714.05	HIGH
177-MW04	6658753.47	2163604.67	107.4	2839.34	HIGH
177-MW07	6659383.87	2163969.71	55.5	2857.43	HIGH
177-MW08	6659263.57	2163836.95	66	2856.96	HIGH
26-MW08	6656935.29	2160875.76	33	2970.72	HIGH
32-MW03A	6656147.09	2163707.83	85.5	2964.34	HIGH
36-MW01	6650391.53	2162254.45	225	2734.42	HIGH
37-EW03	6652605.78	2160645.8	78	2945.32	HIGH
37-EW05	6652155.29	2160459.05	73	2952.24	HIGH
37-EW06	6651943.4	2160872.3	82.5	2960.96	HIGH
37-EW08	6651621.13	2161237.59	242.5	2827.41	HIGH
37-MW05	6652153.5	2159651	34	2959.59	HIGH
37-MW07	6653906.26	2160643.43	53	2947.11	HIGH
37-MW12	6650910.55	2158461.84	190	2763.28	HIGH
37-MW15	6652173.3	2160215.67	70	2945.1	HIGH
37-MW16	6652756.65	2160806.78	125	2901.63	HIGH
37-MW17	6652298.39	2160318.27	80	2943.83	HIGH
37-MW19	6651672.68	2160164.69	242.5	2775.91	HIGH
37-MW22	6650356.65	2155556.95	80	2734.06	HIGH
37-MW23	6650514.68	2159669.4	179	2826.21	HIGH
37-MW24	6650924.8	2160777.8	159.5	2928.4	HIGH
37-MW25	6653223.1	2159466.8	269.5	2747.4	HIGH
37-OW05	6652449	2160449.98	145	2886.39	HIGH
120-MW07	6650852.17	2152945.68	32.5	2762.59	MED
120-MW10	6650536.74	2152200.72	65.4	2686.64	MED
13-MW26	6651314.69	2154738.49	33	2793.95	MED
150-MW01	6655386.97	2161438.46	77	2922.69	MED
153-MW04	6655496.54	2160896.33	34	2955.03	MED
153-MW08	6655987.71	2161597.48	164.5	2845.72	MED
177-MW09	6659765.8	2163875.19	102.9	2798.67	MED
32-MW02	6656723.24	2163939.8	68	2941.45	MED
37-EW02	6652665.97	2160754.3	66	2960.17	MED
37-EW04	6651878.68	2160063.02	83	2926.05	MED
37-MW04	6652722.9	2160566.7	57	2962.73	MED
37-MW08	6651306.09	2160000.14	78	2936.58	MED
37-MW14	6652680.28	2160754.33	247	2779.43	MED
37-OW02	6651888.3	2160830.3	153	2891.45	MED

WELL_ID	EASTING	NORTHING	DEPTH	SCREEN ELEVATION	RANKING
37-OW06	6651723.87	2160131.89	70.5	2945.3	MED
120-MW02	6652130.9	2153339.6	61.9	2726.79	LOW
120-MW04	6651735.6	2152507.9	55	2723.04	LOW
120-MW06	6652141.75	2153319.04	250	2538.28	LOW
120-MW15	6650620.62	2152200.14	335.3	2410.87	LOW
121-MW09	6651912.58	2153099	46.4	2735.77	LOW
13-MW01	6656146.61	2157842.87	20.5	2886.3	LOW
13-MW03	6656323.57	2159449.3	22	2930.3	LOW
13-MW05	6656632.9	2160353.8	27	2953.63	LOW
13-MW06	6655321.7	2159854.1	24	2937.72	LOW
13-MW08	6656164.3	2157833	54	2852.91	LOW
13-MW11	6655989.68	2158806.51	51.3	2888.47	LOW
13-MW12	6654159.09	2158121.11	82	2886.33	LOW
13-MW16	6657790.69	2155492.4	128	2793.01	LOW
13-MW17	6655939.48	2160078.21	29	2935.41	LOW
13-MW21	6656211.83	2157285.19	190	2708.8	LOW
13-MW22	6653229.32	2154153.85	111	2701.74	LOW
13-MW23	6653442.94	2152798.48	52	2756.33	LOW
13-MW29	6651212.73	2150312.18	120	2616.04	LOW
13-MW30	6652676.18	2148799.17	98	2650.33	LOW
133-EW03	6655305.23	2160521.65	93	2887.89	LOW
133-MW01	6655449.52	2160136.78	24	2943.5	LOW
133-MW02	6655319.75	2160548.27	23	2958.14	LOW
133-MW03	6655312.52	2160355.27	25	2951.6	LOW
133-OW02	6655472.92	2159672.48	144.8	2810.74	LOW
133-OW03	6655669.17	2160547.37	153	2824.72	LOW
133-OW04	6655481.06	2160764.7	147.8	2836.97	LOW
133-OW05	6655493.74	2160905.92	145	2844.19	LOW
137-MW01	6655897.42	2161189.79	27.5	2965.16	LOW
150-MW03	6655413.74	2161724.15	48	2961.52	LOW
150-MW05	6654634.19	2161710.37	50.5	2962.04	LOW
150-MW06	6655096.71	2162722.82	171.5	2869.3	LOW
153-MW03	6655954.34	2160838.96	18	2968.48	LOW
153-MW05	6656017.29	2161943.61	55	2959.22	LOW
153-MW06	6655878.59	2160995.46	31	2960.94	LOW
153-MW09	6655312.52	2160535.45	256.5	2724.59	LOW
162-MW03	6650257.23	2162992.58	136.5	2730.57	LOW
162-MW04	6650231.23	2163008.36	283	2581.17	LOW
171-MW05	6651599.48	2161231.21	42	3027.29	LOW
177-MW03	6659169.43	2163818.37	83.1	2843.66	LOW
177-MW06	6659098.2	2163891.3	75	2850.77	LOW
177-MW20	6659372.85	2163991.21	173.5	2739.11	LOW
186-MW01	6655261.26	2160512.43	25	2955.75	LOW
186-MW02	6655250.35	2160582.13	25	2956.22	LOW
26-MW01	6657052.3	2160152.99	25	2947.4	LOW
36-MW03	6650596.86	2162814.45	147	2750.14	LOW
36-MW04	6651339.93	2162397.37	264	2853.87	LOW
37-EW07	6651625.85	2161270.56	47.4	3023.12	LOW
37-MW01	6651884.3	2161228.9	42	3015.84	LOW
37-MW02	6651465.8	2160972.4	88	2975.26	LOW
37-MW06	6651906.29	2160884.05	57.5	2986	LOW
37-MW11	6652498.83	2160924.92	110	2923.53	LOW
37-MW13	6651459.98	2156587.43	29	2847.69	LOW
37-MW21	6652844.51	2161142.47	41	2993.99	LOW
37-MW26	6651372.3	2161323.8	94.5	2979.6	LOW
37-MW29	6651367	2161160.4	119.5	2953.01	LOW

Table 5-3. Redundant Monitoring Wells Based on Analysis of All COCs (All measurements in ft)

WELL_ID	EASTING	NORTHING	DEPTH	SCREEN ELEVATION
120-MW01	6652723	2153458.5	101.8	2692.99
120-MW08	6652750.96	2152340.57	37.5	2730.02
13-MW02	6656649.44	2158078.61	40	2878
13-MW15	6654926.59	2153986.48	55	2790.28
13-OW01	6656097.65	2157893.59	51.5	2858.6
13-OW02	6656164.23	2157884.83	39	2868.81
133-EW01	6656161.84	2157868.56	38	2870.28
145-MW01	6654111.54	2161135.42	49.5	2962.03
150-MW02	6654870.46	2162277.68	82	2945.43
150-MW04	6655265.22	2161802.34	87	2925.59
151-MW01	6656285.37	2161754.63	46	2966.67
153-MW01	6655973.8	2161598.28	47	2962.95
153-MW02	6656349.31	2161244.74	41	2956.27
153-MW07	6656085.42	2160933.32	48	2944.9
153-MW10	6655758.31	2162485.49	80.5	2951.14
32-MW01	6656137.82	2163712.03	105	2944.86
32-MW03B	6656147.34	2163707.93	85.5	2964.34
32-MW04	6656434.84	2163538.27	86.5	2949.94
36-MW02	6651229.12	2162847.48	243	2800.07
37-DEW01	6651889.9	2160869.9	70.5	2975.05
37-EW01	6652489.61	2160922.45	145	2888.78
37-MW09	6652142.69	2158127.06	35	2898.06
37-MW10	6651433.07	2161768.84	194	2892.4
37-MW18	6653367.62	2160136.44	43	2955.48
37-MW27	6651693.5	2161585.1	170.5	2900.76
37-MW28	6651796	2161436.4	105.5	2963.28
37-OW03	6652708.52	2160755.68	76	2950.04
396-MW02	6656450.36	2160682.79	14	2970.97

Table 5-4. Essential Monitoring Network Based on Analysis of TCE in 2001-2002 (All measurements in feet)

Note: RANKING refers to relative statistical importance; HIGH = wells with highest (positive) global regression weights; MED = wells with mid-range, non-negative global regression weights; LOW = wells with negative global regression weights

WELL_ID	EASTING	NORTHING	DEPTH	SCREEN ELEVATION	RANKING
120-MW06	6652141.75	2153319.04	250	2538.28	HIGH
120-MW07	6650852.17	2152945.68	32.5	2762.59	HIGH
120-MW11	6652278.25	2153729.5	152.6	2645.49	HIGH
120-MW12	6651527.93	2153167.6	31.5	2744.61	HIGH
120-MW13	6652214.94	2152507.03	35.4	2748.22	HIGH
13-MW04	6655406.52	2158401.88	26	2901.6	HIGH
13-MW07	6654089.7	2159897.8	55	2922.67	HIGH
13-MW09	6656144.9	2157235.9	22	2873.57	HIGH
13-MW10	6655350.7	2155550.5	31	2834.26	HIGH
13-MW12	6654159.09	2158121.11	82	2886.33	HIGH
13-MW18	6653506.98	2155883.04	51	2815.3	HIGH
13-MW20	6654728.85	2151622.06	65	2741.91	HIGH
13-MW21	6656211.83	2157285.19	190	2708.8	HIGH
13-MW24	6658576.31	2159688.48	97	2865.42	HIGH
133-EW03	6655305.23	2160521.65	93	2887.89	HIGH
133-OW02	6655472.92	2159672.48	144.8	2810.74	HIGH
133-OW05	6655493.74	2160905.92	145	2844.19	HIGH
153-MW03	6655954.34	2160838.96	18	2968.48	HIGH
153-MW08	6655987.71	2161597.48	164.5	2845.72	HIGH
162-MW01	6650280.52	2163457.13	113	2714.05	HIGH
177-MW07	6659383.87	2163969.71	55.5	2857.43	HIGH
177-MW08	6659263.57	2163836.95	66	2856.96	HIGH
36-MW01	6650391.53	2162254.45	225	2734.42	HIGH
37-EW06	6651943.4	2160872.3	82.5	2960.96	HIGH
37-EW08	6651621.13	2161237.59	242.5	2827.41	HIGH
37-MW05	6652153.5	2159651	34	2959.59	HIGH
37-MW07	6653906.26	2160643.43	53	2947.11	HIGH
37-MW12	6650910.55	2158461.84	190	2763.28	HIGH
37-MW16	6652756.65	2160806.78	125	2901.63	HIGH
37-MW23	6650514.68	2159669.4	179	2826.21	HIGH
37-MW26	6651372.3	2161323.8	94.5	2979.6	HIGH
120-MW05	6650388.3	2151854.7	23	2716.86	MED
120-MW14	6650132.24	2151472.04	43	2696	MED
120-MW15	6650620.62	2152200.14	335.3	2410.87	MED
13-MW16	6657790.69	2155492.4	128	2793.01	MED
13-MW19	6657720.46	2153313.3	73	2803.98	MED
13-MW26	6651314.69	2154738.49	33	2793.95	MED
13-MW28	6657809.27	2150910.93	174	2673.61	MED
13-MW29	6651212.73	2150312.18	120	2616.04	MED
133-EW02	6655214.64	2159794.78	100.5	2860.45	MED
133-MW01	6655449.52	2160136.78	24	2943.5	MED
133-MW03	6655312.52	2160355.27	25	2951.6	MED
133-OW03	6655669.17	2160547.37	153	2824.72	MED
153-MW09	6655312.52	2160535.45	256.5	2724.59	MED
162-MW04	6650231.23	2163008.36	283	2581.17	MED
177-MW04	6658753.47	2163604.67	107.4	2839.34	MED
177-MW20	6659372.85	2163991.21	173.5	2739.11	MED
32-MW02	6656723.24	2163939.8	68	2941.45	MED
32-MW03A	6656147.09	2163707.83	85.5	2964.34	MED
37-EW03	6652605.78	2160645.8	78	2945.32	MED
37-EW04	6651878.68	2160063.02	83	2926.05	MED
37-EW05	6652155.29	2160459.05	73	2952.24	MED
37-MW15	6652173.3	2160215.67	70	2945.1	MED
37-MW19	6651672.68	2160164.69	242.5	2775.91	MED
37-MW22	6650356.65	2155556.95	80	2734.06	MED
37-MW24	6650924.8	2160777.8	159.5	2928.4	MED
37-MW25	6653223.1	2159466.8	269.5	2747.4	MED
37-OW05	6652449	2160449.98	145	2886.39	MED

WELL_ID	EASTING	NORTHING	DEPTH	SCREEN ELEVATION	RANKING
120-MW02	6652130.9	2153339.6	61.9	2726.79	LOW
120-MW03	6651337.7	2152768.1	115.8	2652.46	LOW
120-MW04	6651735.6	2152507.9	55	2723.04	LOW
120-MW10	6650536.74	2152200.72	65.4	2686.64	LOW
13-MW01	6656146.61	2157842.87	20.5	2886.3	LOW
13-MW03	6656323.57	2159449.3	22	2930.3	LOW
13-MW06	6655321.7	2159854.1	24	2937.72	LOW
13-MW08	6656164.3	2157833	54	2852.91	LOW
13-MW14	6656174.57	2157261.67	105	2790.86	LOW
13-MW17	6655939.48	2160078.21	29	2935.41	LOW
13-MW22	6653229.32	2154153.85	111	2701.74	LOW
13-MW23	6653442.94	2152798.48	52	2756.33	LOW
13-MW25	6658386.08	2158308.38	177	2772.8	LOW
13-MW27	6652743.71	2150936.77	132	2644.28	LOW
13-MW30	6652676.18	2148799.17	98	2650.33	LOW
133-MW02	6655319.75	2160548.27	23	2958.14	LOW
137-MW01	6655897.42	2161189.79	27.5	2965.16	LOW
150-MW01	6655386.97	2161438.46	77	2922.69	LOW
153-MW04	6655496.54	2160896.33	34	2955.03	LOW
162-MW03	6650257.23	2162992.58	136.5	2730.57	LOW
171-MW05	6651599.48	2161231.21	42	3027.29	LOW
177-MW06	6659098.2	2163891.3	75	2850.77	LOW
177-MW09	6659765.8	2163875.19	102.9	2798.67	LOW
186-MW01	6655261.26	2160512.43	25	2955.75	LOW
26-MW08	6656935.29	2160875.76	33	2970.72	LOW
36-MW03	6650596.86	2162814.45	147	2750.14	LOW
37-EW02	6652665.97	2160754.3	66	2960.17	LOW
37-MW04	6652722.9	2160566.7	57	2962.73	LOW
37-MW08	6651306.09	2160000.14	78	2936.58	LOW
37-MW14	6652680.28	2160754.33	247	2779.43	LOW
37-MW17	6652298.39	2160318.27	80	2943.83	LOW
37-MW29	6651367	2161160.4	119.5	2953.01	LOW
37-OW02	6651888.3	2160830.3	153	2891.45	LOW
37-OW06	6651723.87	2160131.89	70.5	2945.3	LOW

Table 5-5. Redundant Monitoring Wells Based on Analysis of TCE in 2001-2002 (All measurements in ft)

WELL_ID	EASTING	NORTHING	DEPTH	SCREEN ELEVATION
120-MW01	6652723	2153458.5	101.8	2692.99
120-MW08	6652750.96	2152340.57	37.5	2730.02
121-MW09	6651912.58	2153099	46.4	2735.77
13-MW02	6656649.44	2158078.61	40	2878
13-MW05	6656632.9	2160353.8	27	2953.63
13-MW11	6655989.68	2158806.51	51.3	2888.47
13-MW15	6654926.59	2153986.48	55	2790.28
13-OW01	6656097.65	2157893.59	51.5	2858.6
13-OW02	6656164.23	2157884.83	39	2868.81
133-EW01	6656161.84	2157868.56	38	2870.28
133-OW04	6655481.06	2160764.7	147.8	2836.97
145-MW01	6654111.54	2161135.42	49.5	2962.03
150-MW02	6654870.46	2162277.68	82	2945.43
150-MW03	6655413.74	2161724.15	48	2961.52
150-MW04	6655265.22	2161802.34	87	2925.59
150-MW05	6654634.19	2161710.37	50.5	2962.04
150-MW06	6655096.71	2162722.82	171.5	2869.3
151-MW01	6656285.37	2161754.63	46	2966.67
153-MW01	6655973.8	2161598.28	47	2962.95
153-MW02	6656349.31	2161244.74	41	2956.27
153-MW05	6656017.29	2161943.61	55	2959.22
153-MW06	6655878.59	2160995.46	31	2960.94
153-MW07	6656085.42	2160933.32	48	2944.9
153-MW10	6655758.31	2162485.49	80.5	2951.14
177-MW03	6659169.43	2163818.37	83.1	2843.66
186-MW02	6655250.35	2160582.13	25	2956.22
26-MW01	6657052.3	2160152.99	25	2947.4
32-MW01	6656137.82	2163712.03	105	2944.86
32-MW03B	6656147.34	2163707.93	85.5	2964.34
32-MW04	6656434.84	2163538.27	86.5	2949.94
36-MW02	6651229.12	2162847.48	243	2800.07
36-MW04	6651339.93	2162397.37	264	2853.87
37-DEW01	6651889.9	2160869.9	70.5	2975.05
37-EW01	6652489.61	2160922.45	145	2888.78
37-EW07	6651625.85	2161270.56	47.4	3023.12
37-MW01	6651884.3	2161228.9	42	3015.84
37-MW02	6651465.8	2160972.4	88	2975.26
37-MW06	6651906.29	2160884.05	57.5	2986
37-MW09	6652142.69	2158127.06	35	2898.06
37-MW10	6651433.07	2161768.84	194	2892.4
37-MW11	6652498.83	2160924.92	110	2923.53
37-MW13	6651459.98	2156587.43	29	2847.69
37-MW18	6653367.62	2160136.44	43	2955.48
37-MW21	6652844.51	2161142.47	41	2993.99
37-MW27	6651693.5	2161585.1	170.5	2900.76
37-MW28	6651796	2161436.4	105.5	2963.28
37-OW03	6652708.52	2160755.68	76	2950.04
396-MW02	6656450.36	2160682.79	14	2970.97

Section 5.3 Recommendations Regarding Siting of New Wells

While the primary motivation for the spatial analysis at Site 133 was to identify potentially redundant wells, a secondary goal was to locate areas of the site where additional wells might provide significant improvements in accuracy of the estimated site maps and thus improved information on the nature and extent of the groundwater plume(s). In GTS, the most straightforward way to do this is to examine the local variance *base maps* for each time slice and COC. There the local variances offer an indication of the relative *local uncertainty* associated with the mapped grid estimates. The higher the local uncertainty at a particular spot, the greater the benefit to siting a new well in that location.

It should be noted that high local uncertainty arises from two basic sources using the LWQR estimation technique. First, there may be areas of data sparsity. Estimates in these spots tend to be uncertain because few wells are sited there. Secondly, there may be areas of data inconsistency, where nearby wells exhibit strongly different concentration levels. This second phenomenon occurs wells with very low concentrations are located near wells with much higher measurements. High local uncertainty at grid nodes in these areas is then a result of the inconsistency of the known data located within the search neighborhood. In such cases, it may not be advantageous to site a new well nearby to several existing well locations, especially since the inconsistency might be due to the complex pattern of groundwater flow through the subsurface.

The approximate locations exhibiting the greatest local uncertainty are listed below in **Table 5-6** and graphed in **Figure 5-1**. Any of these spots might serve as locations for the siting of additional wells, but particularly those locations where nearby wells are sparse. Please note, however, that since the determination of local variance depends *both* upon the spatial configuration of the well network *and* the actual concentration values at those locations, it cannot be determined *a priori* exactly which additional sites would provide the greatest informational benefit, nor to what degree the accuracy would be improved. In addition, **Table 5-6** and **Figure 5-1** take no account of physical obstacles at the site (e.g., buildings) that might preclude siting of wells in the listed locations.

It should also be noted that the locations in **Table 5-6** are not ranked in any particular order. Operationally, more weight could be given to those four locations found to exhibit high local uncertainty when using the more recent data of time slice two (2001-2002). At this point, though, there is no reliable way within the GTS algorithm to reliably rank or distinguish between locations of uncertainty found from the TCE analysis versus the manganese analysis or the 1,4-dioxane analysis. Furthermore, high local uncertainty, for instance in TCE, does not mean there is high local uncertainty for other COCs not included in the optimization at those locations. However, given the fact that COCs are chosen for optimization in part because they exhibit more frequent and widespread spatial occurrence than other available chemical parameters, it is not unreasonable to assume that these same locations would be good candidates for sampling of other pertinent COCs.

Table 5-6. Approximate Locations of Greatest Local Relative Uncertainty

COC	Time Slice	Easting (ft)	Northing (ft)
TCE	1999-2000	6,657,800	2,162,200
	2001-2002	6,652,400	2,161,400
MN	1999-2000	6,651,000	2,157,400
		6.651,800	2,159,800
		6.653,400	2,162,200
	2001-2002	6.650,500	2,156,200
DIOX	2001-2002	6,651,400	2,161,000
		6,659,000	2,157,800

Figure 5-1. Approximate Locations of Greatest Relative Local Uncertainty

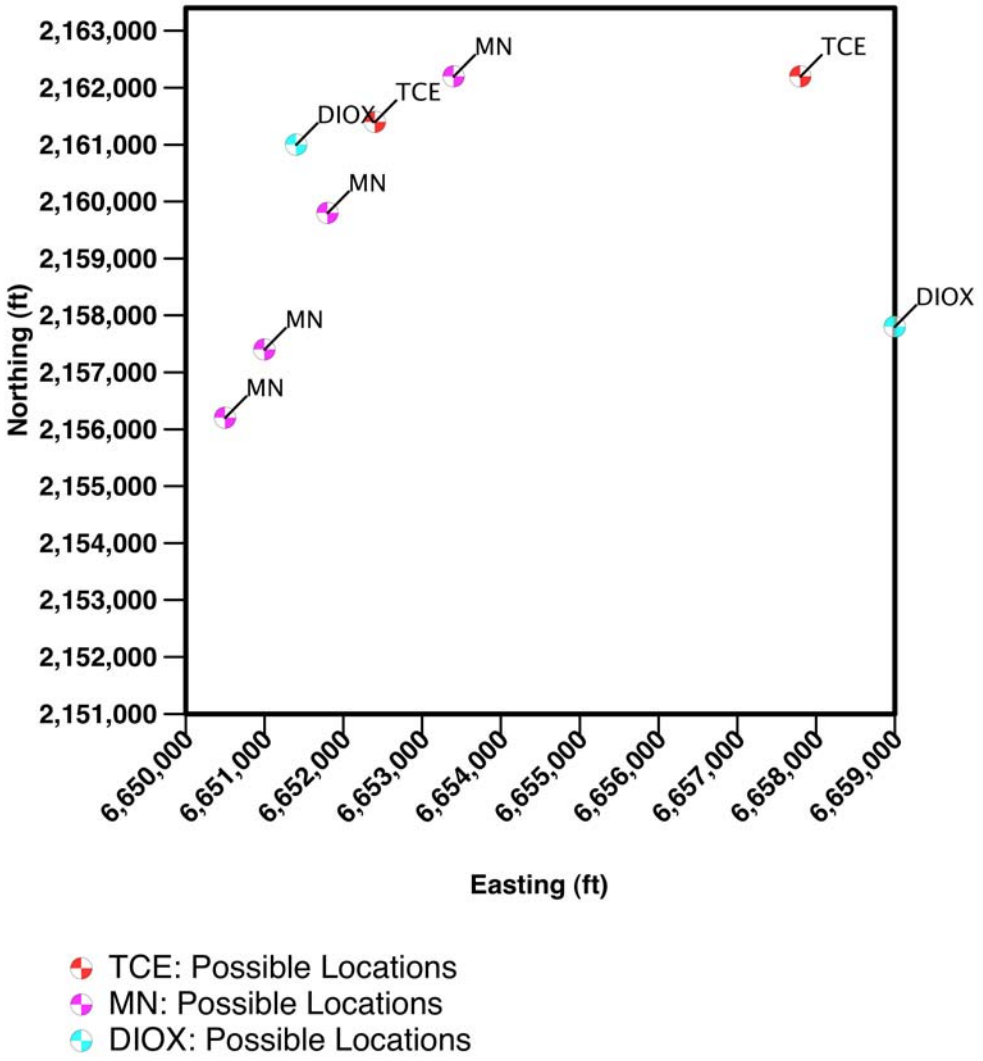

Section 5.4. Cost Analysis and Summary

This section describes the methodology for developing credible estimates of annualized cost savings that might result from the implementation of a GTS-optimized monitoring program. The approach is based on a simple cost model. To calculate a cost savings, two cost estimates are required for comparison. The first is the baseline (current) costs, including fixed and variable costs; the second is the projected cost under the optimized program. Cost savings are estimated based on the difference between annual baseline monitoring costs and projected annual costs under the optimized program, expressed in terms of current dollars and percent reduction from baseline.

Earth Tech, an Air Force contractor, provided the monitoring and cost data for the current (baseline) monitoring program at Edwards AFB Sites 37 and 133 in the form of groundwater monitoring reports (GMR) and cost data tables.

Section 5.4.1. Unit Cost Data

Prior to development of the estimate of current (baseline) annual monitoring costs, it was necessary to derive unit costs for the various monitoring activities including labor to purge and sample wells, sample management/data validation, sample analysis, travel and per diem, rented and purchased/material and equipment, preparation of groundwater monitoring reports, and project management and administration.

Earth Tech provided tables of costs for conducting quarterly sampling and analysis, including costs for analysis of field samples and quality assurance samples (e.g., duplicate samples, IDWs, and trip blanks) for various COCs. Separate tables were provided for each round of sampling and analysis or for groups of events conducted between 1999 and 2002. Unit costs for sampling and analysis were derived from the most recent sampling event for each COC.

Earth Tech provided estimates for sample management and labor costs, courier and shipping charges, as well costs for preparing electronic data deliverables and raw data packages. These costs were provided on a quarterly basis rather than per COC sampled basis. Estimates also were provided for costs of activities that support the monitoring program such as: management of data validation, travel and per diem expenses, preparation of groundwater monitoring reports, the rental and purchase of material and equipment, and overall project management and administration.

Section 5.4.2. Estimating Baseline (Current) Monitoring Costs

An estimate of current monitoring costs was needed to serve as a baseline for the purpose of estimating cost savings under an optimized plan. SAIC identified COCs to include in the baseline program using the sampling data provided by Earth Tech covering the period between the third quarter of 1998 and the second quarter of 2003. The data show that the wells samples and the COCs monitored vary from year to year. Furthermore, Earth Tech switched from semi-annual to annual monitoring in 2003[1]. As a result of this change, the COCs monitored during 2003 were judged to be the most representative of current (baseline) monitoring program. However, the last year for which cost data were provided

[1] Based on phone conversation with Sarah Grossi of Earth Tech, on February 23, 2004.

is 2002. Both years (2002 and 2003) had similar sets of wells being monitored, although there were more COC samples taken during 2003. Therefore, the last two years of monitoring data, 2002 and 2003, were used to create a baseline. If a COC was monitored at a given well during either of those two years, that COC was assumed to be monitored at the same well in future years.

Next, it was necessary to establish the baseline cost for the specific set of wells included in the optimization study. For the baseline program to be directly comparable to the optimized program, only the wells from the Earth Tech data that were also used for the optimization study were included in the baseline. The set of wells listed in the Earth Tech data was not identical to the set of wells included in the optimization study, therefore, some extrapolations and assumptions were required to derive the COCs (or classes of COCs) monitored at each well and the frequency of monitoring under the baseline scenario. When the Earth Tech data for 2002 or 2003 showed that a COC was sampled for at all the wells, then it was assumed that it would be sampled for at the wells included only in the optimization study data. The resulting baseline could then be used to estimate cost savings from the implementation of the optimization results.

Section 5.4.3. Estimating Reductions in Monitoring Activity

The goal of the optimization analysis is to determine when sampling is occurring more frequently than necessary and which wells are spatially redundant. Therefore, results of the optimization analysis are expressed in terms of reduced sampling frequencies and the retirement of specific wells. The first step in estimating cost savings was to estimate the reduction in samples collected as a result of the elimination of specific wells from the LTM program. The second step was to account for any changes in sampling frequency. Because the monitoring at Sites 37 and 133 is now conducted on an annual basis, the monitoring for the baseline cost estimate assumes annual monitoring of each well. The optimization results suggest monitoring could be reduced to once every seven quarters. So for the two optimization scenarios the total number samples taken annually was adjusted to reflect the reduction in overall sampling frequency.

Section 5.4.4. Estimating Sample Analysis Costs

The GMR cost tables provided by Earth Tech indicated sample analysis costs expressed in terms of the number of wells sampled for each category of COC listed. These tables were used to develop sample analysis costs for each COC. The cost tables cover the years 1999 through 2002. For each COC the most recent sample analysis cost was used. For most COCs this was the 2002 cost. All COC sample analysis costs were then adjusted to June 2003 dollars[2]. These costs were then increased by 8.6 % to account for fee. Additional sample analysis costs include shipping and handling costs such as: raw data packaging, electronic data deliverables, courier trips, and express mail shipments.

In the baseline, the number of total samples for each COC needs to include any quality assurance samples taken. The number of additional quality assurance samples taken for each COC, was not included in either the optimization study data or the Earth Tech sampling data. Therefore, to estimate quality assurance samples taken during future

[2] All costs were adjusted for inflation based on Table 2a of the Employment Cost Index using the Professional specialty and technical occupations category. ftp://ftp.bls.gov/pub/suppl/ECI.ECHISTRY.TXT

monitoring efforts, the number quality assurance samples needed to be expressed as a ratio of normal samples taken. The ratio of quality assurance samples to normal samples for each COC are averages based on information from the GMR cost tables.

Section 5.4.5. Estimating Project Level Monitoring Costs

Ultimately to capture the total costs savings, all costs need to be expressed in initial terms of dollars per sample taken or dollars per well monitored. By developing the sampling baseline for each well, reductions in wells and monitoring frequencies can be translated directly into reductions in sample analysis costs. However, reductions in the total number of samples taken are not readily translated into cost savings for all activities associated with the monitoring effort. On going monitoring projects require many activities to be performed in addition to sample analysis. These additional activities, such as monitoring labor and drafting reports are significant project costs. To estimate the cost savings from reductions in these activities the cost for each of these activities had to be expressed in terms of annual reductions in either total samples taken or total wells monitored.

In each of the Earth Tech reports the labor burden was expressed in terms of the number of days required for sampling and in a total dollar amount. Both the labor cost and days varied between reports when considered in terms of total wells sampled or total samples taken. The rate of wells sampled per day ranged from 3- 9 wells per day for Site 37 and 3- 5 wells per day for Site 133. However, the Earth Tech cost information did not contain labor rates, making it difficult to consider labor costs in terms of days worked. It was assumed that monitoring labor would be very sensitive to the total number of samples taken. So monitoring labor costs from the 2002 GMR tables were adjusted to 2003 dollars and then divided by total samples taken in 2002 to derive an average labor cost per sample. By multiplying these costs by the total annual samples estimated for the baseline the annual monitoring labor costs can be estimated for the baseline. In **Appendix 5-1**, **Tables 5-7.A2**, **5-7.A3**, and **5-7.A4** show the sampling costs for the baseline and two optimization scenarios for Site 37. **Appendix 5-1 Tables 5-7.C2**, **5-7.C3**, and **5-7.C4** show the sampling costs for the baseline and two optimization scenarios for Site 133.

Sample management and data validation are two activities that are assumed to also be sensitive to the total number of samples taken. The cost for these activities from the 2002 GMR tables was adjusted for inflation and divided by total samples taken. The resulting costs are now expressed in terms of the total annual samples taken. These costs were then multiplied by the total annual samples estimated for the baseline and optimization scenarios, to derive total annual cost estimates.

The cost for other activities such as: travel and per diem reimbursements; drafting the Groundwater Monitoring Reports; and the rental and purchase of material and equipment were considered less sensitive to total number of samples taken. These activity costs were adjusted for inflation and then divided by the total number of wells monitored in 2002 to derive costs per well. The GMR cost tables estimated total project management and administration costs to be 10% of monitoring labor, sample management, and report development costs. **Tables 5-7.B2b**, **5-7.B3b**, and **5-7.B4b** in **Appendix 5-1** show the project level costs for the baseline and two optimization scenarios for Site 37. **Appendix**

5-1 Tables 5-7.D2b, **5-7.D3b**, and **5-7.D4b** show the project level costs for the baseline and two optimization scenarios for Site 133.

Section 5.4.6. Checking the Baseline Cost Tables

A comparison of baseline monitoring costs with the monitoring costs under the two optimization scenarios, provides an estimate of potential cost savings. However, the reliability of the cost savings estimates is based on how well the baseline represents actual conditions. As mentioned, the baseline contains additional wells at each site that were not included in the Earth Tech data or the GMR cost tables. So the resulting baseline cost estimate cannot be directly compared to annual costs in the GMR tables.

In order to check the baseline cost estimates, the Earth Tech sampling data for 2002 was entered into the baseline tables to see if the resulting cost estimates would match the costs reported in the 2002 GMR tables. After the costs from the 2002 GMR tables were adjusted to 2003 dollars, the comparison showed that the baseline tables estimated the reported 2002 costs to within 1.5% for Site 37 and 1.7% for Site 133. The discrepancy is due to the number of quality assurance samples estimated by the baseline tables. These estimates are based average percentages from the GMRs from 1999 to 2002, and are slightly higher than the actual number reported in the 2002 GMR cost table. In **Appendix 5-1**, **Tables 5-7.A1**, **5-7.B1**, **5-7.C1** and **5-7.D1** show the results of entering the 2002 sampling data into the baseline cost tables.

Section 5.4.7. Estimate of Costs Savings

Although the measurement data at Site 133 are challenging, the temporal and spatial analyses demonstrate that the GTS optimization algorithm can offer potentially significant cost savings over the existing LTM program. Decent estimates of plume magnitude and extent can be made using fewer wells than the current network and sampling at a lower frequency than presently in place. Estimates of specific potential cost savings of course depend on how many wells are actually deemed redundant after further review by project managers and regulators, and to what extent sampling frequencies can be reduced to levels recommended in the temporal analysis. Nevertheless, **Tables 5-7A** and **5-7B** below (for the wells connected with Site 37 and for the remaining wells connected with Site 133, respectively) offer two estimates of the savings that might be achieved, based on costs of the current network, and also assuming that one of the two reduced monitoring networks is implemented at Site 133.

The baseline for Site 37 estimates that 367 samples will be taken from 48 wells annually at a total cost of approximately $141,000. Under the first optimization scenario (utilizing only TCE data from 2001-2002), 146 samples would be taken from 18 wells annually for a total cost of approximately $54,000 (an annual cost savings of 61.4 percent). Under the second optimization scenario (utilizing all the COCs), an estimated 182 samples would be taken from 22 wells annually for a total cost of approximately $68,000 (an annual cost savings of 51.4 percent).

The baseline annual monitoring scenario for Site 133 assumes that on average 751 samples are taken from 92 wells at a total cost of approximately $286,000. Under the first optimization scenario (2001-2002 TCE data), 284 samples would be taken from 35 wells

annually for a total cost of approximately $106,000 (an annual cost savings of 62.9 percent). Under the second optimization scenario (all COCs), an estimated 342 samples would be taken from 42 wells annually for a total cost of approximately $128,000 (an annual cost savings of 55.4 percent).

Table 5-7A. Estimate of Cost Savings at Site 37

Edwards Air Force Base (Site 37)			
	Baseline	Optimization 1 (based on TCE data only)	Optimization 2 (based on all COCs)
Wells Monitored (total)	**48**	**31**	**39**
Samples Collected Annually	**367**	**146**	**182**
Annual Costs			
Sample Management and Coordination Labor	$37,688	$15,043	$18,734
Analytical Costs	$41,950	$16,456	$20,886
Courier & Shipping Costs	$968	$387	$481
Electronic Data Deliverable & Raw Data Package	$3,859	$1,491	$1,918
Subtotal Sampling and Analysis Costs	**$84,465**	**$33,377**	**$42,020**
Sample Management/Data Validation	$1,973	$726	$914
Travel And Per Diem	$5,452	$2,007	$2,525
Groundwater Monitoring Reports	$38,166	$14,050	$17,676
Rented and Purchased/Material and Equipment	$2,726	$1,004	$1,263
Project Management and Administration	$7,783	$3,123	$3,948
Total Annual Project Cost	**$140,565**	**$54,286**	**$68,344**
Potential Cost Savings		**$86,279**	**$72,221**
Percentage Reduction in Project Costs		**61.38%**	**51.38%**

Table 5-7B. Estimate of Cost Savings at Site 133

Edwards Air Force Base (Site 133)			
	Baseline	Optimization 1 (based on TCE data only)	Optimization 2 (based on all COCs)
Wells Monitored (total)	**92**	**61**	**73**
Samples Collected Annually	**751**	**284**	**342**
Annual Costs			
Sample Management and Coordination Labor	$112,846	$42,753	$51,373
Analytical Costs	$80,097	$29,536	$35,841
Courier & Shipping Costs	$4,341	$1,645	$1,976
Electronic Data Deliverable & Raw Data Package	$6,058	$2,140	$2,637
Subtotal Sampling and Analysis Costs	**$203,341**	**$76,074**	**$91,828**
Sample Management/Data Validation	$3,458	$1,307	$1,564
Travel And Per Diem	$7,838	$2,962	$3,545
Groundwater Monitoring Reports	$47,026	$17,773	$21,269
Rented and Purchased/Material and Equipment	$7,838	$2,962	$3,545
Project Management and Administration	$16,333	$4,862	$5,867
Total Annual Project Cost	**$285,833**	**$105,939**	**$127,618**
Potential Cost Savings		**$179,894**	**$158,216**
Percentage Reduction in Annual Monitoring Costs		**62.94%**	**55.35%**

Section 6. References

Bourgault, G. (1997) Spatial declustering weights. *Mathematical Geology*, 29:277-290.

Cameron, K. & Hunter, P. (2002) Using spatial models and kriging techniques to optimize long-term groundwater monitoring networks: a case study. *Environmetrics*, 13:629-656.

Edwards AFB IRP (2001) IRP Update: Base Tests Common Cleanup Solution at Uncommon Site. (www.edwards.af.mil/penvmng/Documents/factsheets/ERP/133may2001.pdf)

Edwards AFB IRP (2000) The Edwards Air Force Base Installation Restoration Program: An Investment Report. (www.edwards.af.mil/penvmng/Documents/Investment/invest.pdf)

Loader, C. (1999) *Local Regression and Likelihood*. New York: Springer-Verlag.

Appendix 3.1
Temporal Variograms

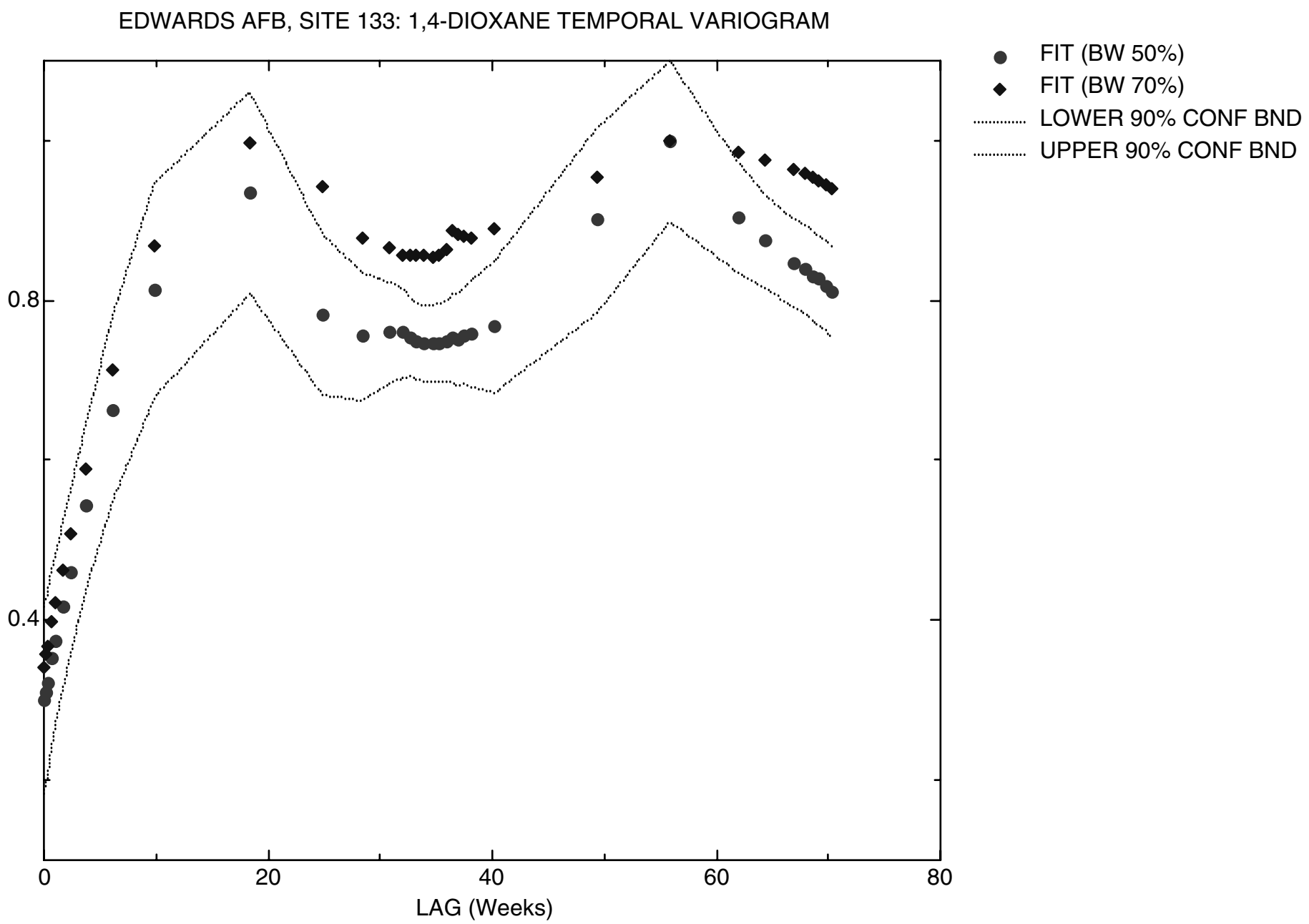
EDWARDS AFB, SITE 133: 1,4-DIOXANE TEMPORAL VARIOGRAM
FIT (BW 50%)
FIT (BW 70%)
LOWER 90% CONF BND
UPPER 90% CONF BND
0.8
0.4
0
20
40
60
80
LAG (Weeks)

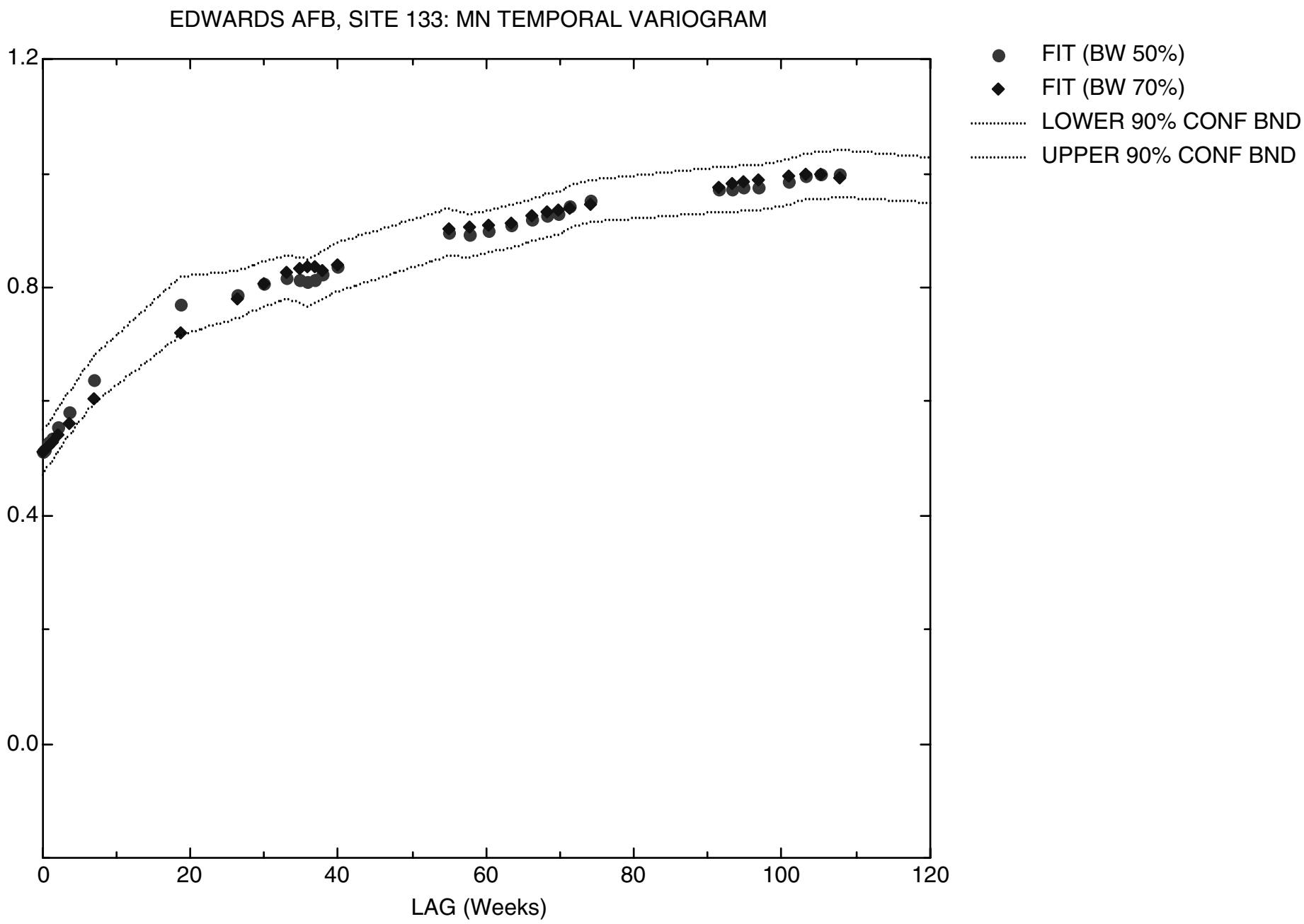
EDWARDS AFB, SITE 133: MN TEMPORAL VARIOGRAM
1.2
0.8
0.4
0.0
0
20
40
60
80
100
120
LAG (Weeks)
FIT (BW 50%)
FIT (BW 70%)
LOWER 90% CONF BND
UPPER 90% CONF BND

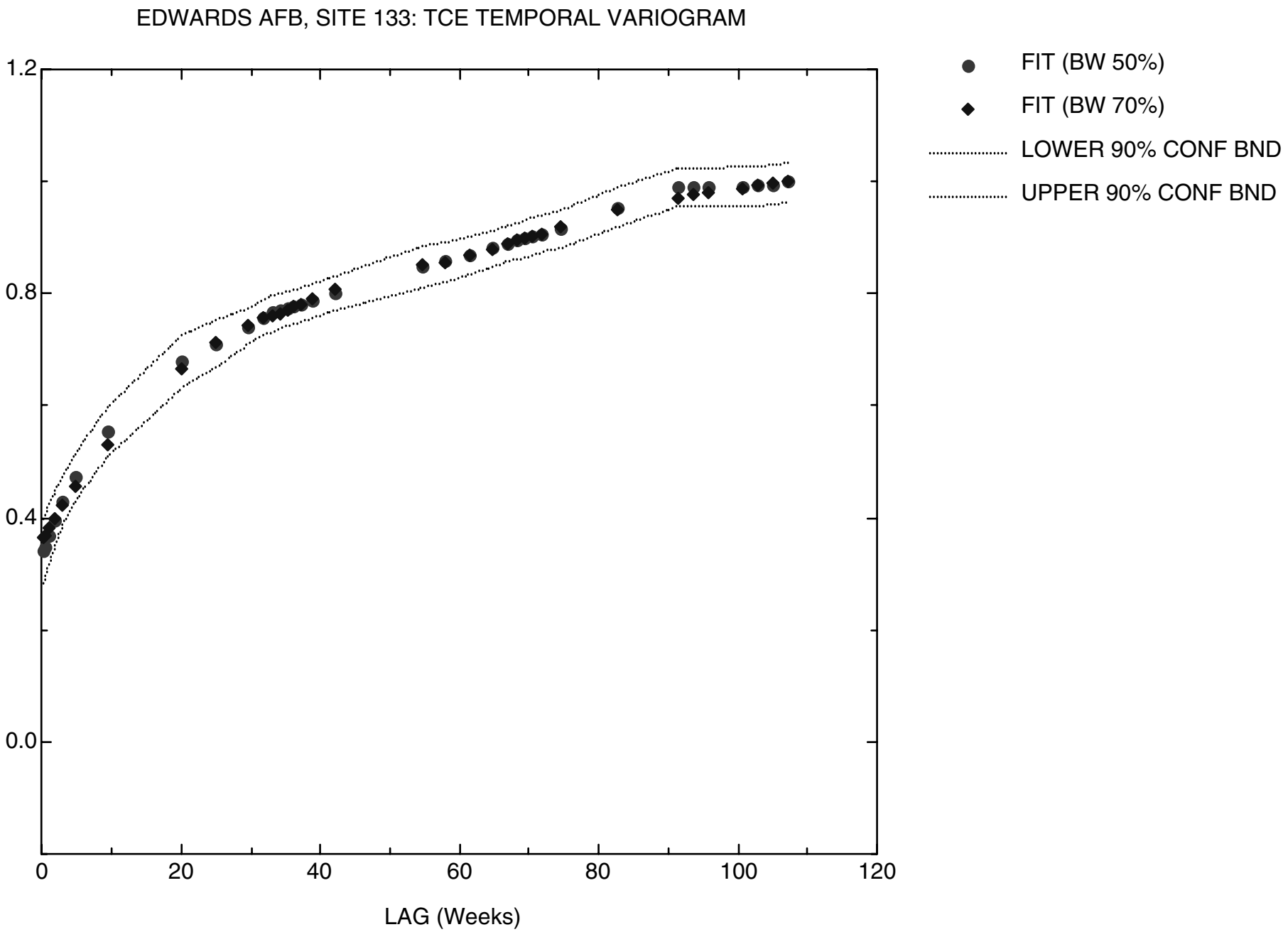
EDWARDS AFB, SITE 133: TCE TEMPORAL VARIOGRAM
1.2
0.8
0.4
0.0
0
20
40
60
80
100
120
LAG (Weeks)
FIT (BW 50%)
FIT (BW 70%)
LOWER 90% CONF BND
UPPER 90% CONF BND

Appendix 3.1
Temporal Variograms

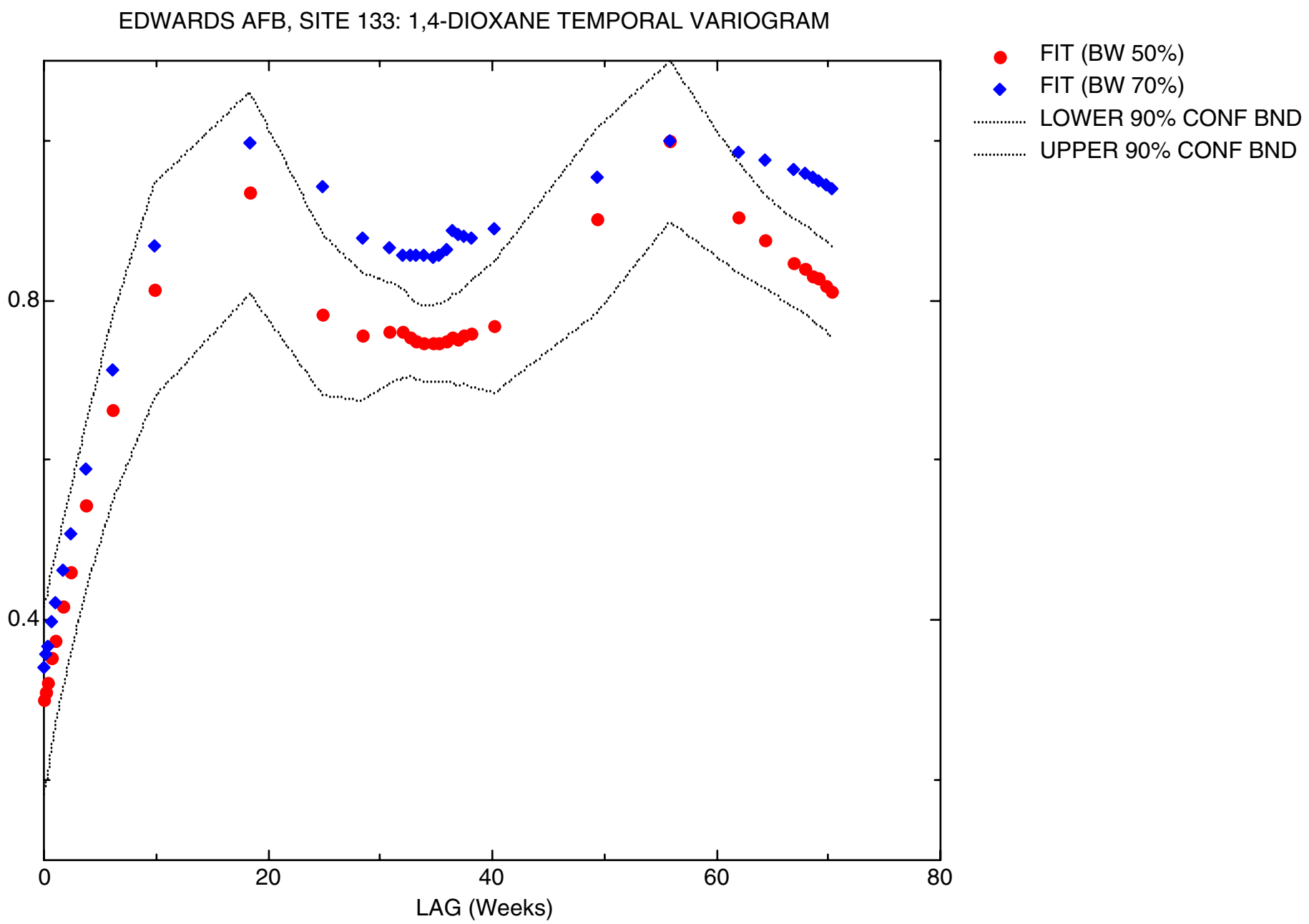
EDWARDS AFB, SITE 133: 1,4-DIOXANE TEMPORAL VARIOGRAM
FIT (BW 50%)
FIT (BW 70%)
LOWER 90% CONF BND
UPPER 90% CONF BND
0.8
0.4
0
20
40
60
80
LAG (Weeks)

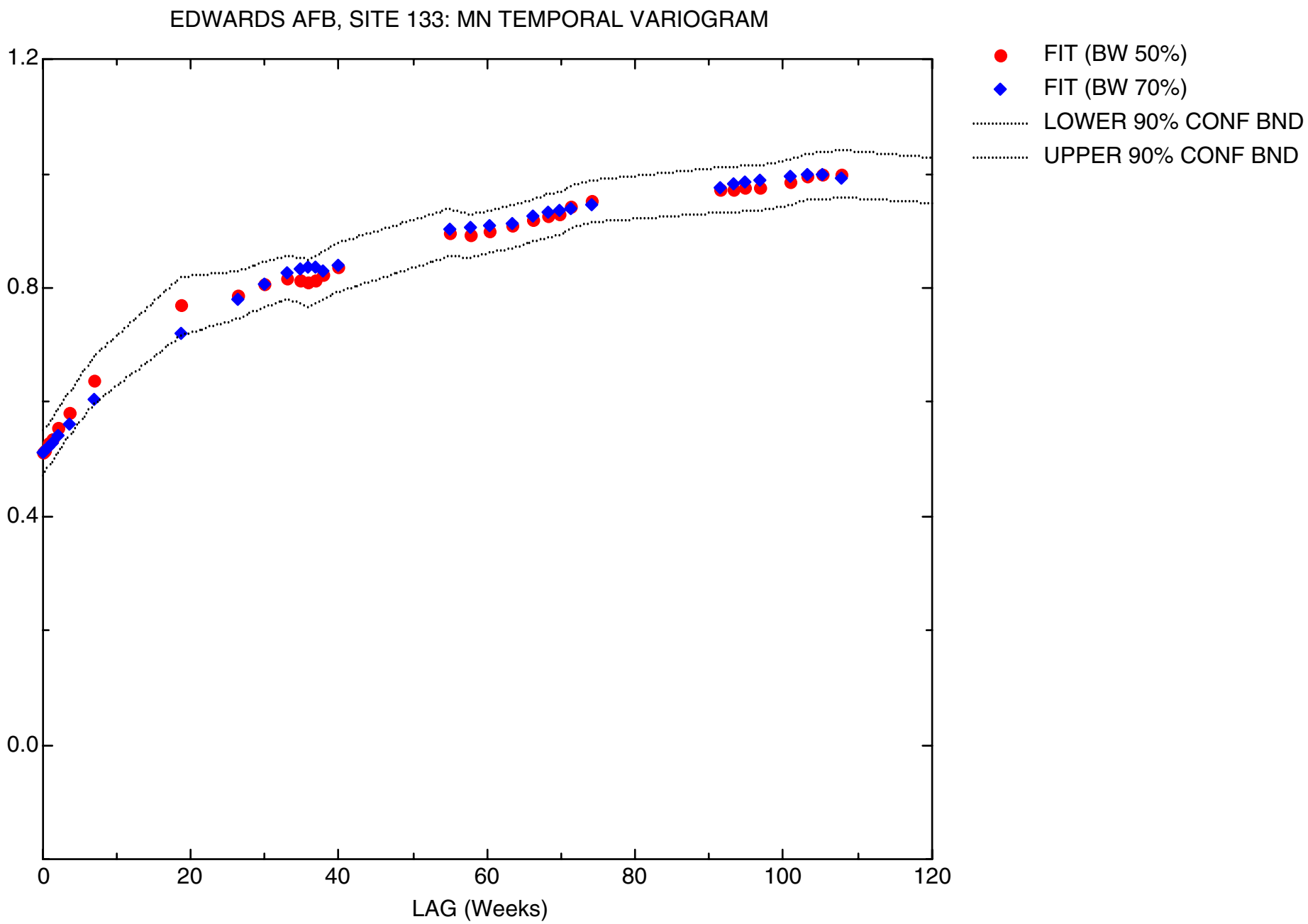
EDWARDS AFB, SITE 133: MN TEMPORAL VARIOGRAM
1.2
0.8
0.4
0.0
0
20
40
60
80
100
120
LAG (Weeks)
FIT (BW 50%)
FIT (BW 70%)
LOWER 90% CONF BND
UPPER 90% CONF BND

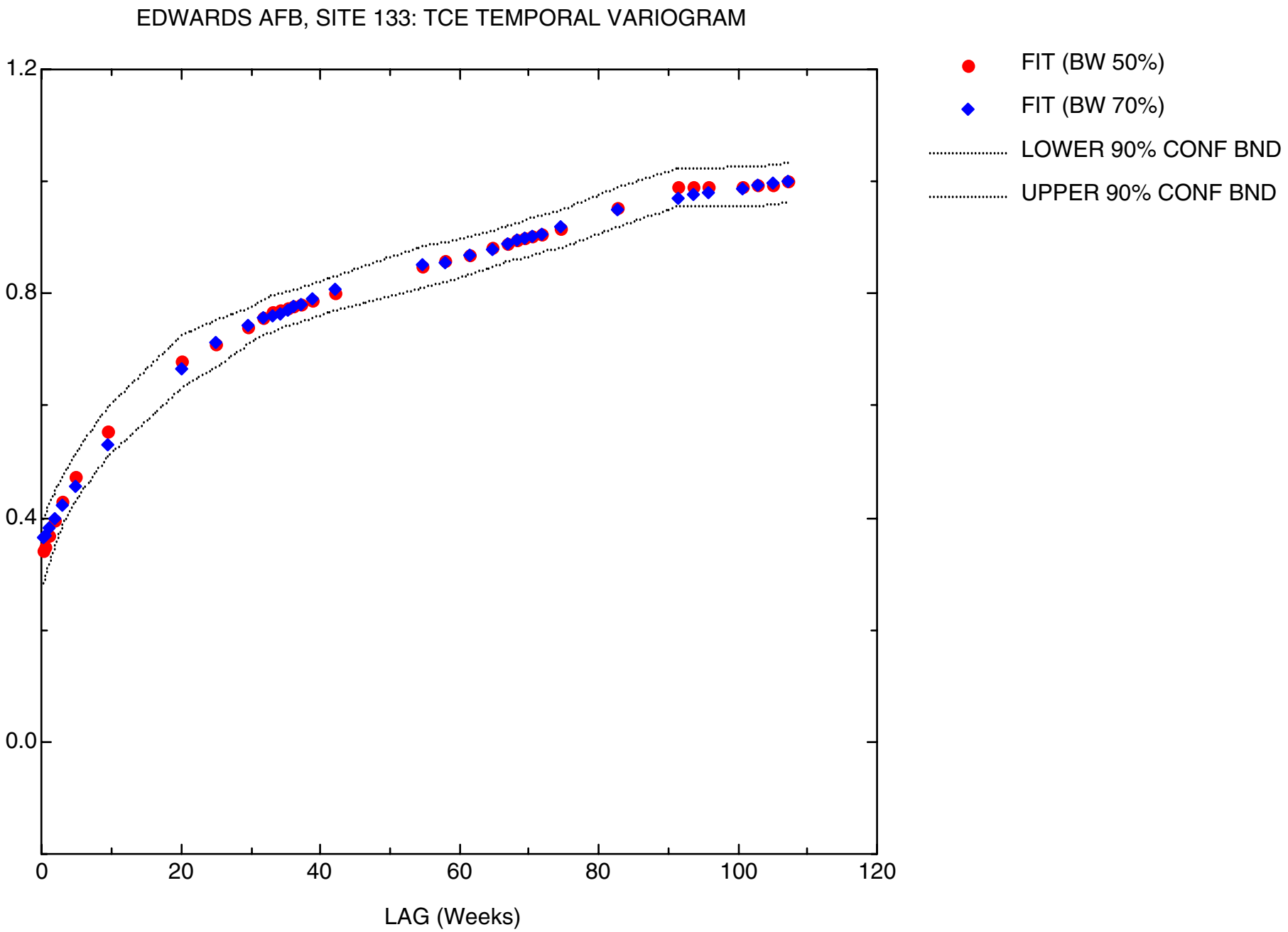
EDWARDS AFB, SITE 133: TCE TEMPORAL VARIOGRAM
1.2
0.8
0.4
0.0
0
20
40
60
80
100
120
LAG (Weeks)
FIT (BW 50%)
FIT (BW 70%)
LOWER 90% CONF BND
UPPER 90% CONF BND

Appendix 3.3
Iterative Fitting Results

TCE

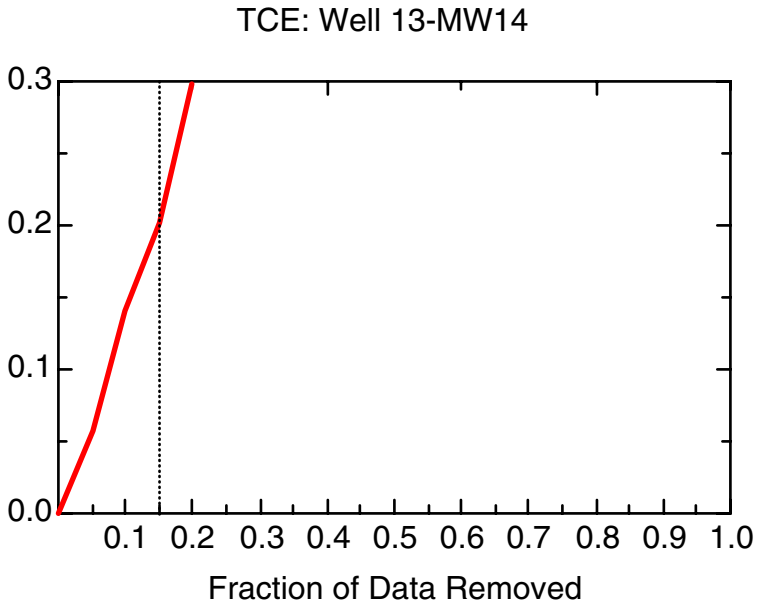
TCE: Well 13-MW14
0.3
0.2
0.1
0.0
0.1 0.2 0.3 0.4 0.5 0.6 0.7 0.8 0.9 1.0
Fraction of Data Removed

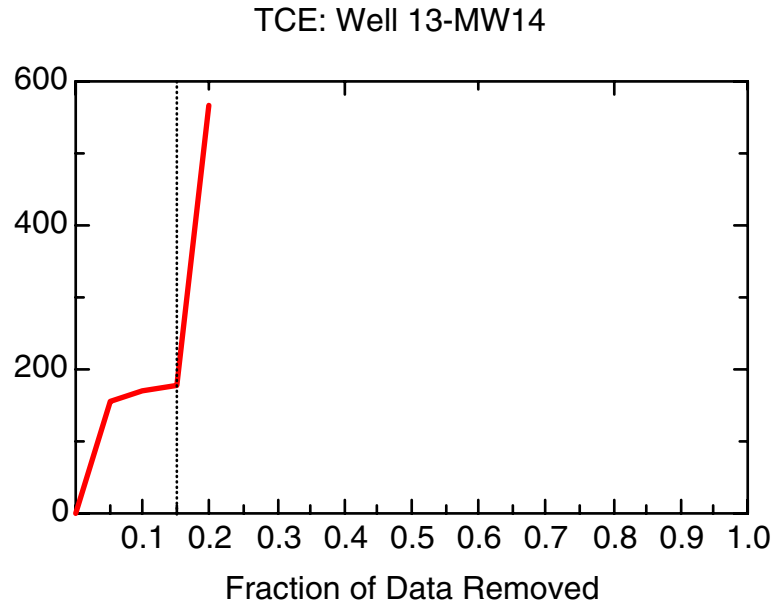
TCE: Well 13-MW14
600
400
200
0
0.1 0.2 0.3 0.4 0.5 0.6 0.7 0.8 0.9 1.0
Fraction of Data Removed

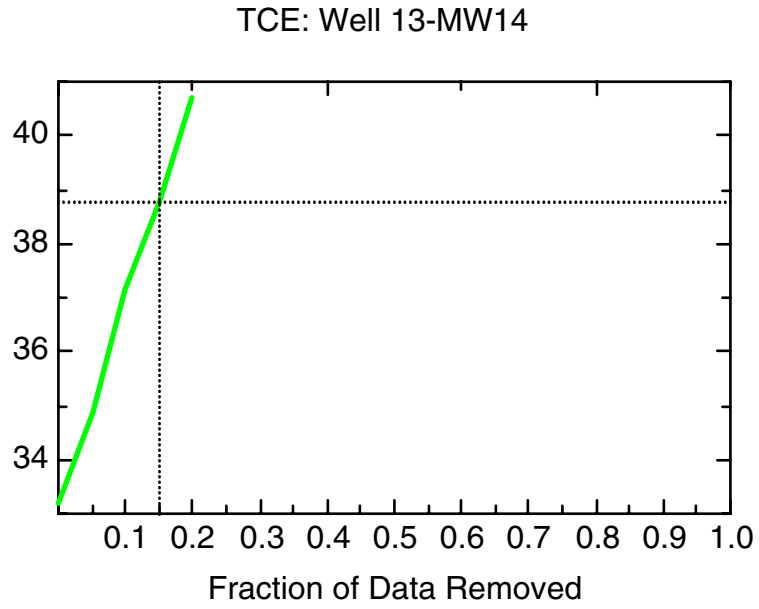
TCE: Well 13-MW14
40
38
36
34
0.1 0.2 0.3 0.4 0.5 0.6 0.7 0.8 0.9 1.0
Fraction of Data Removed

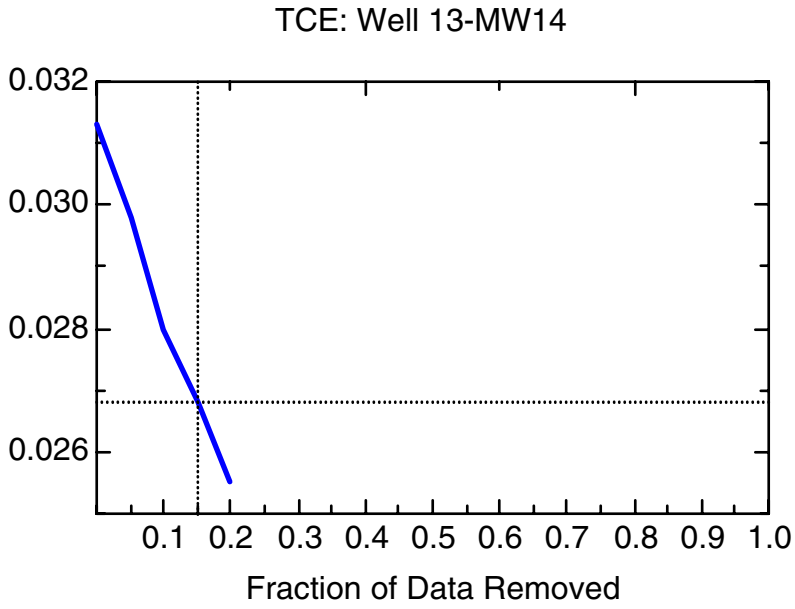
TCE: Well 13-MW14
0.032
0.030
0.028
0.026
0.1 0.2 0.3 0.4 0.5 0.6 0.7 0.8 0.9 1.0
Fraction of Data Removed

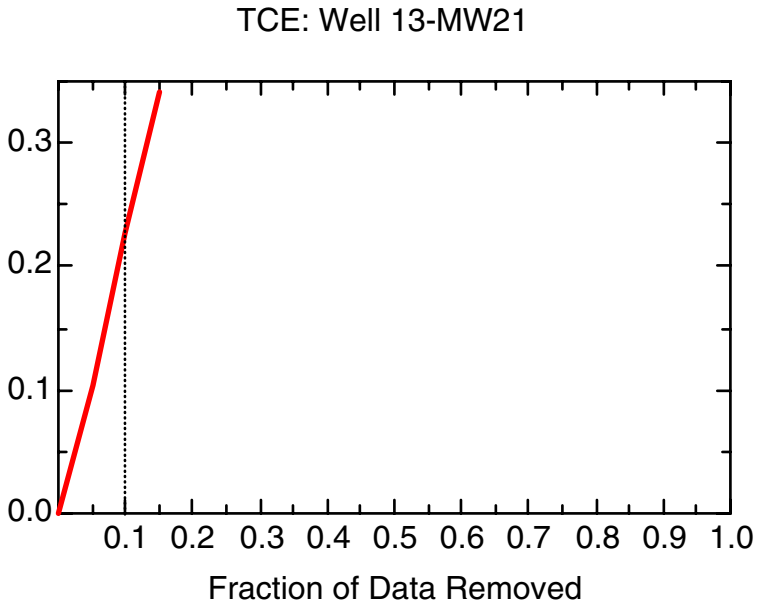
TCE: Well 13-MW21
0.3
0.2
0.1
0.0
0.1 0.2 0.3 0.4 0.5 0.6 0.7 0.8 0.9 1.0
Fraction of Data Removed

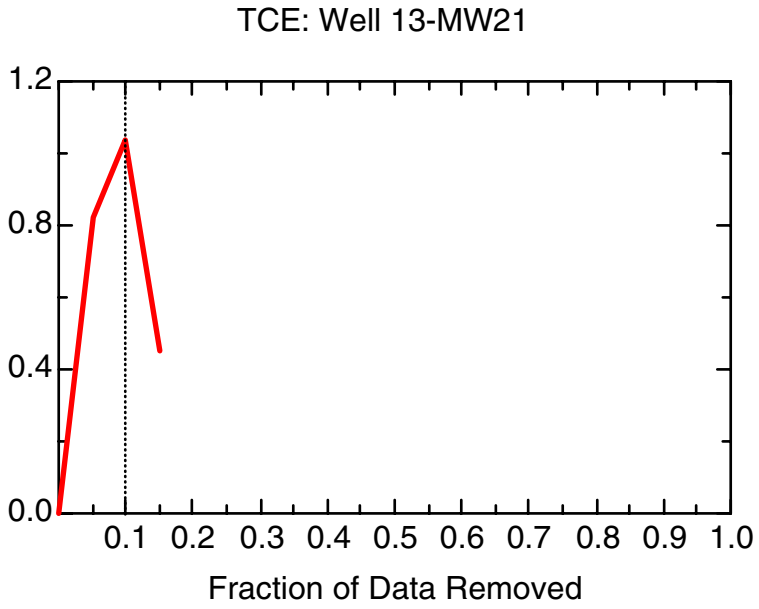
TCE: Well 13-MW21
1.2
0.8
0.4
0.0
0.1 0.2 0.3 0.4 0.5 0.6 0.7 0.8 0.9 1.0
Fraction of Data Removed

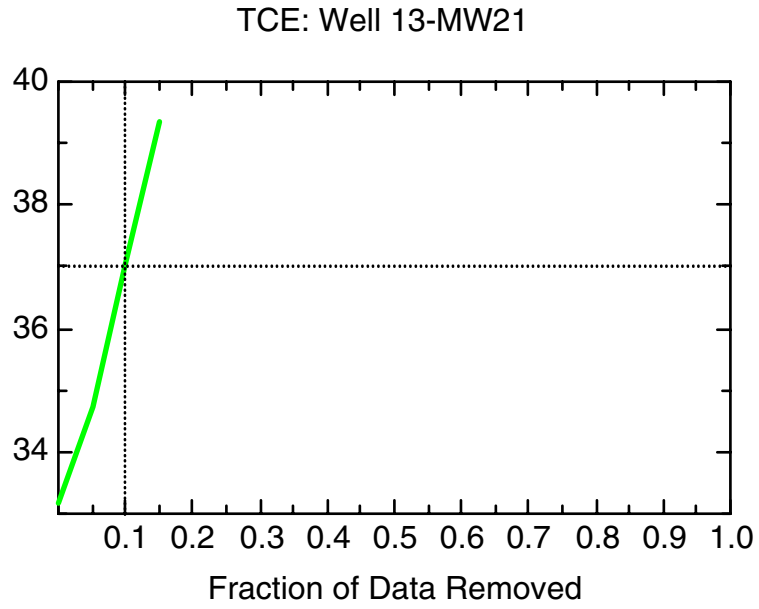
TCE: Well 13-MW21
40
38
36
34
0.1 0.2 0.3 0.4 0.5 0.6 0.7 0.8 0.9 1.0
Fraction of Data Removed

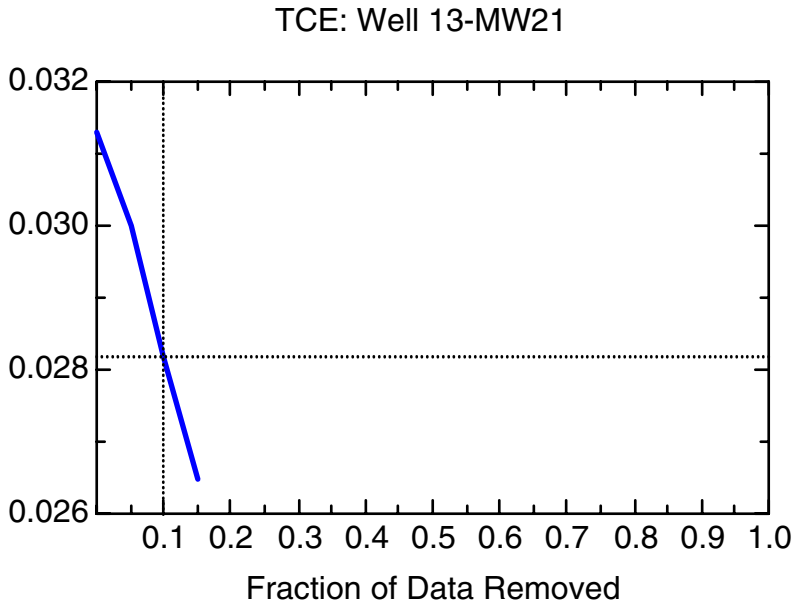
TCE: Well 13-MW21
0.032
0.030
0.028
0.026
0.1 0.2 0.3 0.4 0.5 0.6 0.7 0.8 0.9 1.0
Fraction of Data Removed

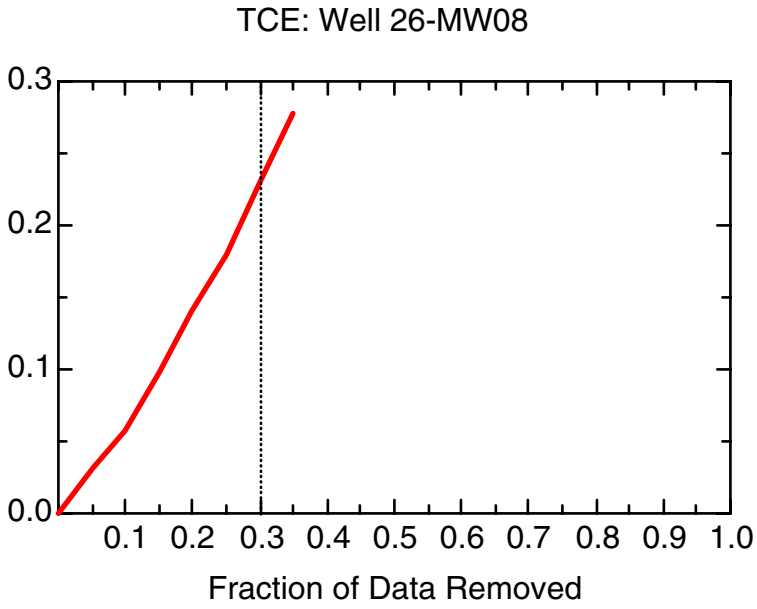
TCE: Well 26-MW08
0.3
0.2
0.1
0.0
0.1 0.2 0.3 0.4 0.5 0.6 0.7 0.8 0.9 1.0
Fraction of Data Removed

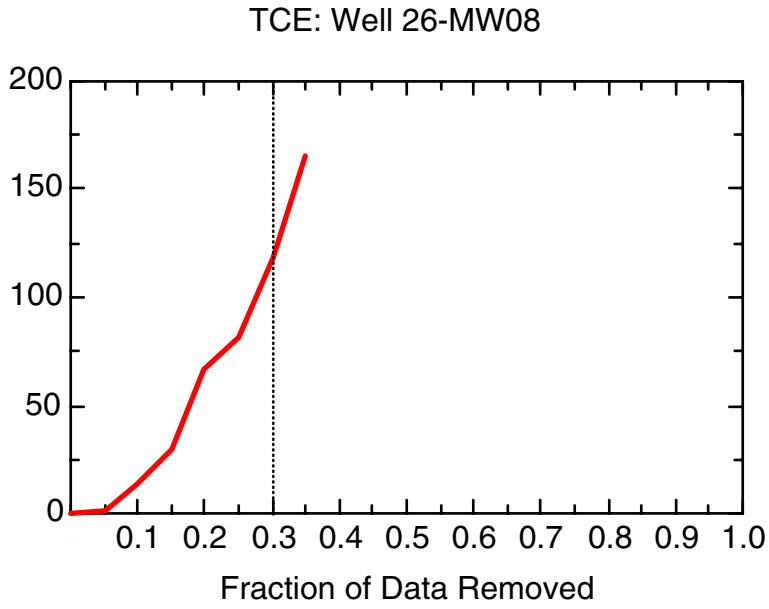
TCE: Well 26-MW08
200
150
100
50
0
0.1 0.2 0.3 0.4 0.5 0.6 0.7 0.8 0.9 1.0
Fraction of Data Removed

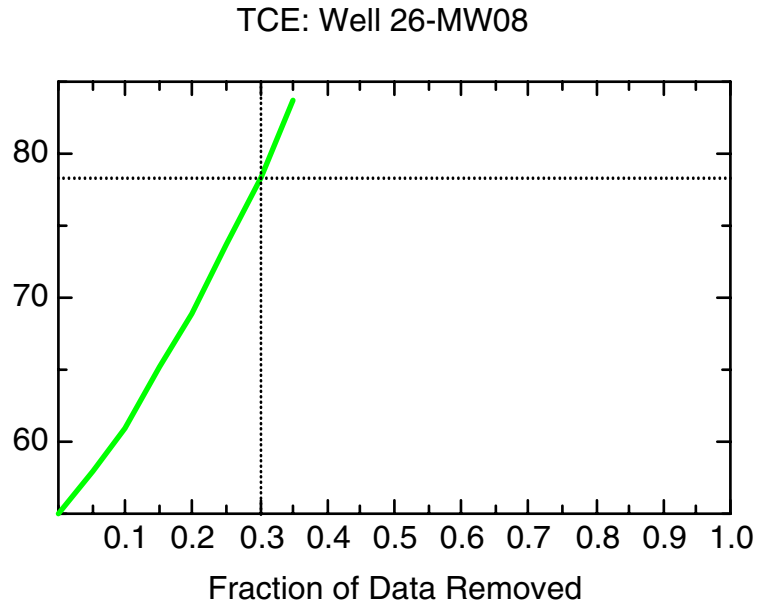
TCE: Well 26-MW08
80
70
60
0.1 0.2 0.3 0.4 0.5 0.6 0.7 0.8 0.9 1.0
Fraction of Data Removed

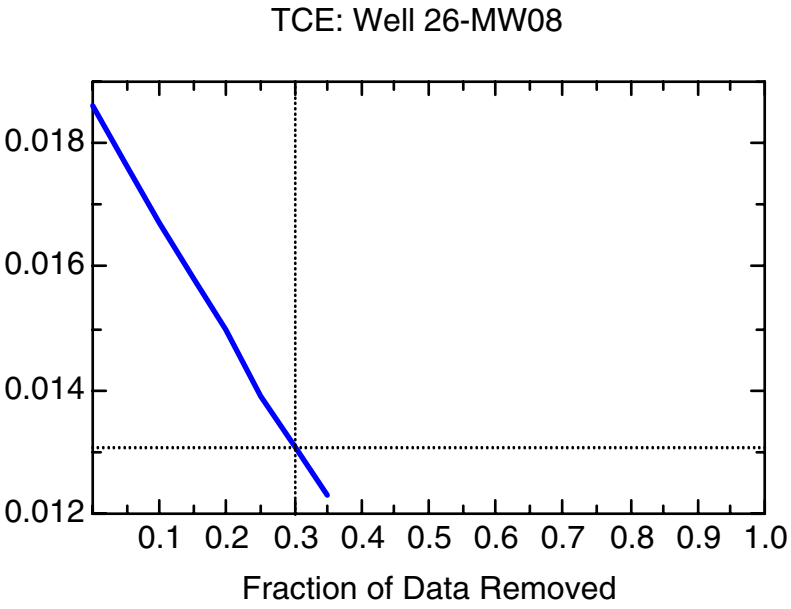
TCE: Well 26-MW08
0.018
0.016
0.014
0.012
0.1 0.2 0.3 0.4 0.5 0.6 0.7 0.8 0.9 1.0
Fraction of Data Removed

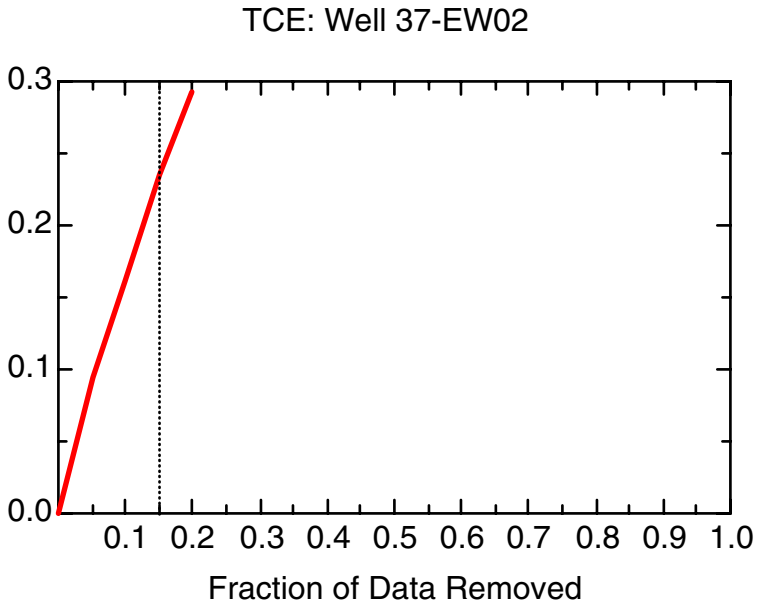
TCE: Well 37-EW02
0.3
0.2
0.1
0.0
0.1 0.2 0.3 0.4 0.5 0.6 0.7 0.8 0.9 1.0
Fraction of Data Removed

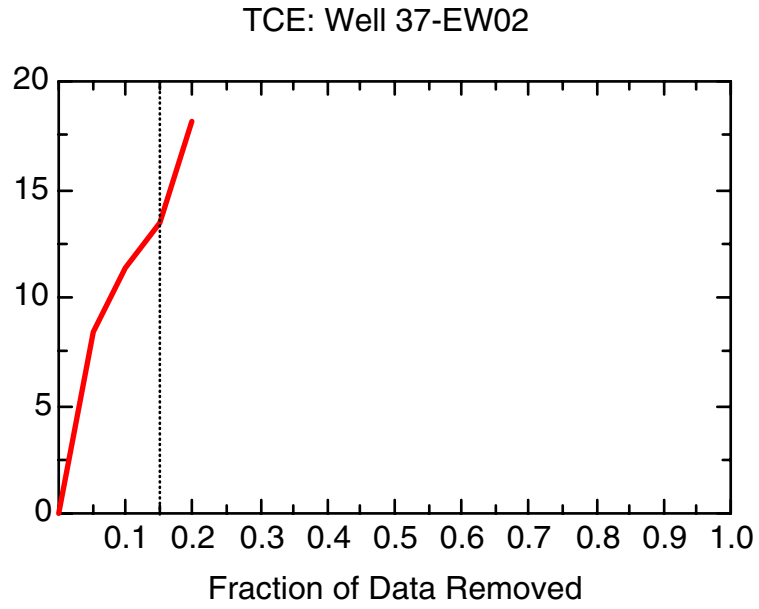
TCE: Well 37-EW02
20
15
10
5
0
0.1 0.2 0.3 0.4 0.5 0.6 0.7 0.8 0.9 1.0
Fraction of Data Removed

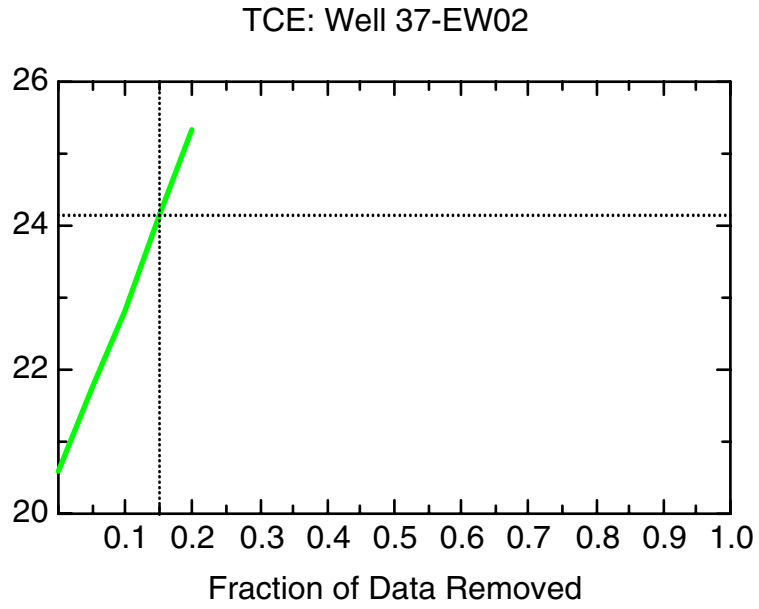
TCE: Well 37-EW02
26
24
22
20
0.1 0.2 0.3 0.4 0.5 0.6 0.7 0.8 0.9 1.0
Fraction of Data Removed

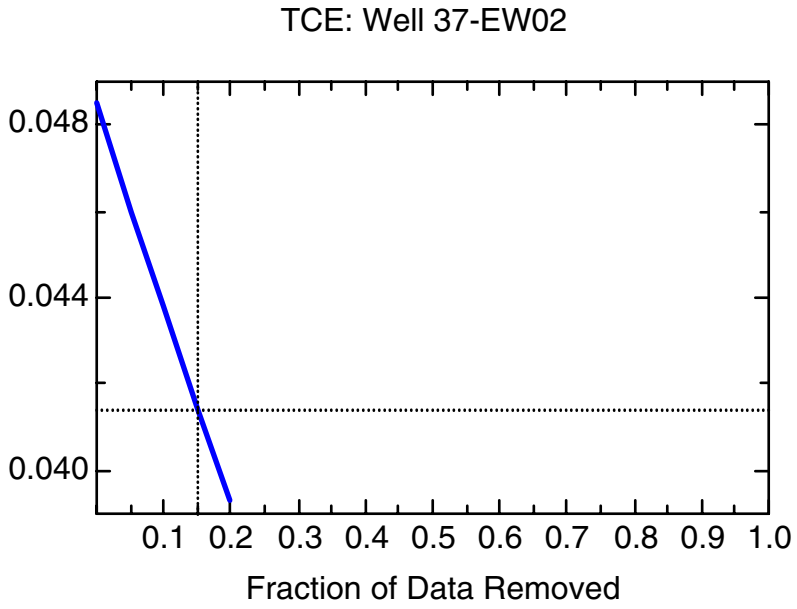
TCE: Well 37-EW02
0.048
0.044
0.040
0.1 0.2 0.3 0.4 0.5 0.6 0.7 0.8 0.9 1.0
Fraction of Data Removed

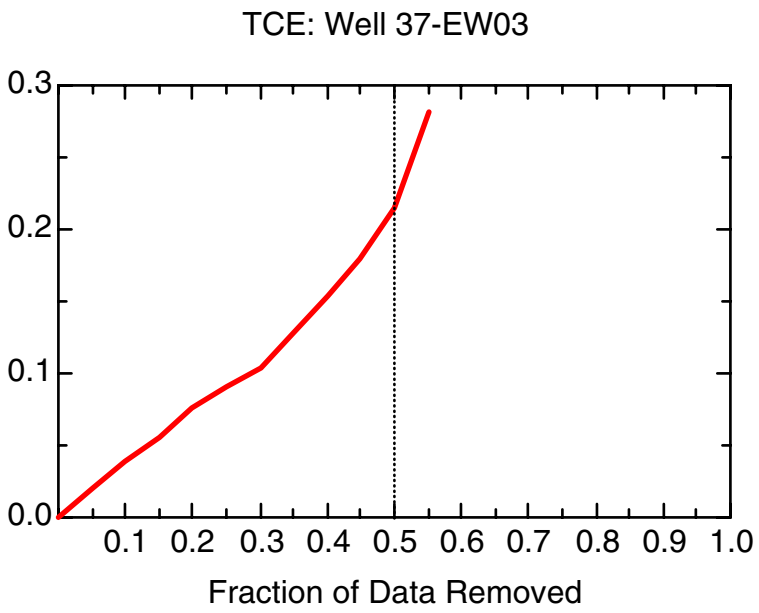
TCE: Well 37-EW03
0.3
0.2
0.1
0.0
0.1 0.2 0.3 0.4 0.5 0.6 0.7 0.8 0.9 1.0
Fraction of Data Removed

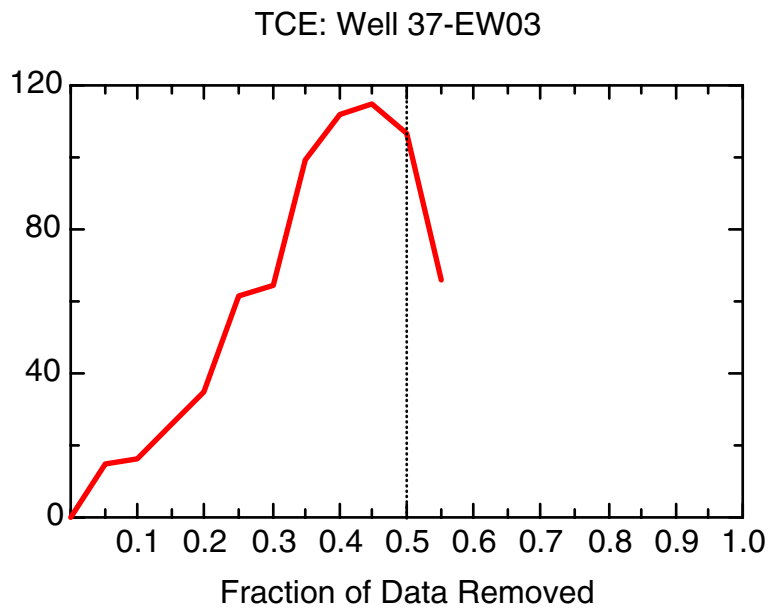
TCE: Well 37-EW03
120
80
40
0
0.1 0.2 0.3 0.4 0.5 0.6 0.7 0.8 0.9 1.0
Fraction of Data Removed

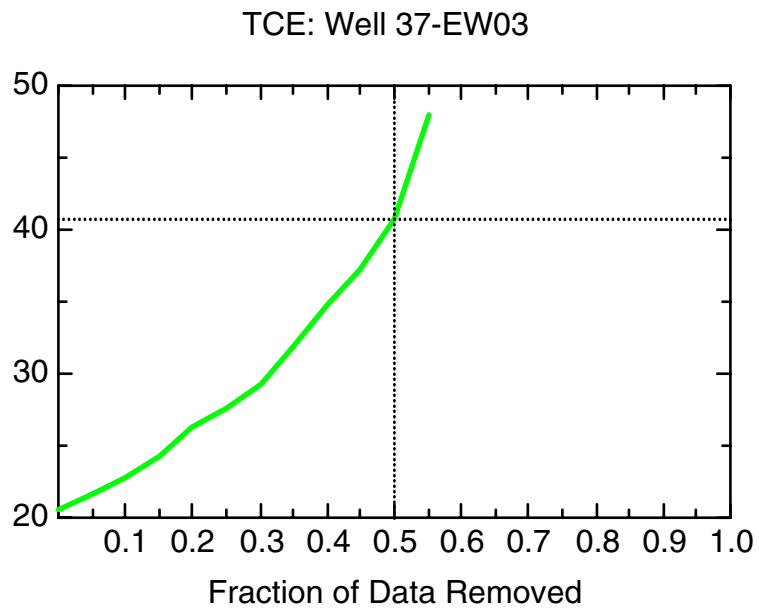
TCE: Well 37-EW03
50
40
30
20
0.1 0.2 0.3 0.4 0.5 0.6 0.7 0.8 0.9 1.0
Fraction of Data Removed

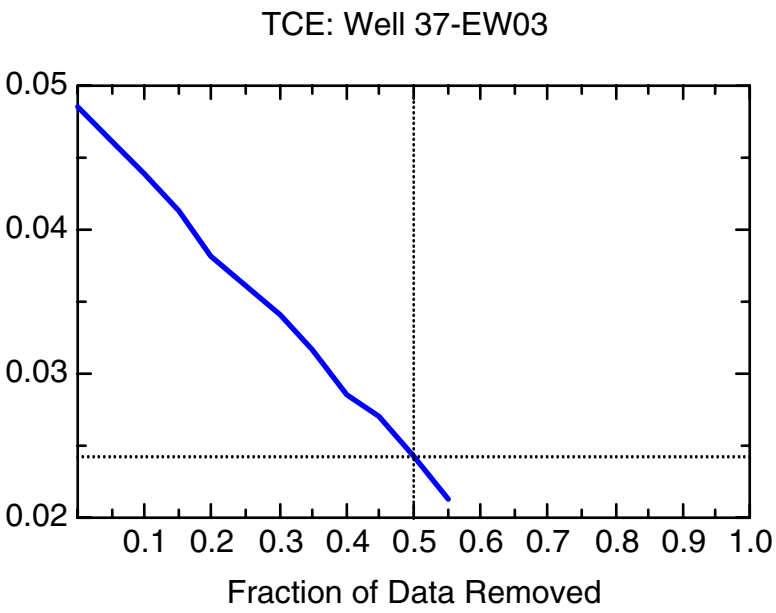
TCE: Well 37-EW03
0.05
0.04
0.03
0.02
0.1 0.2 0.3 0.4 0.5 0.6 0.7 0.8 0.9 1.0
Fraction of Data Removed

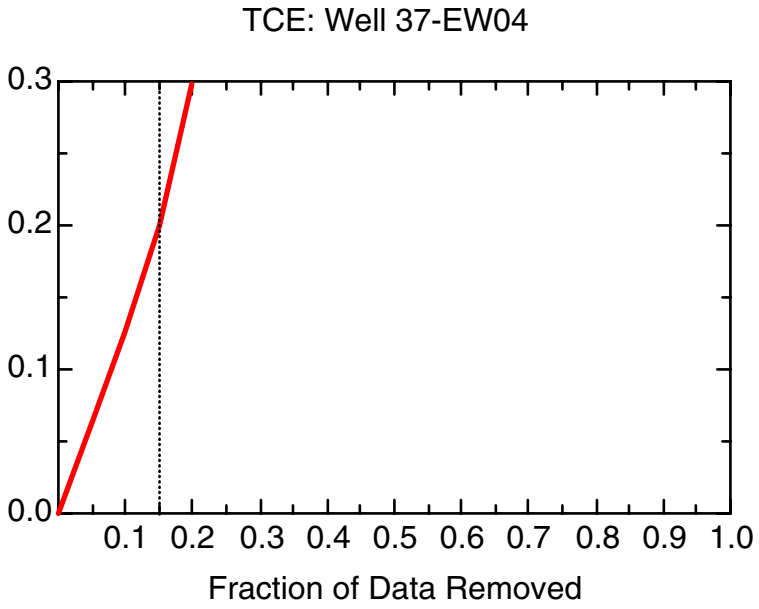
TCE: Well 37-EW04
0.3
0.2
0.1
0.0
0.1 0.2 0.3 0.4 0.5 0.6 0.7 0.8 0.9 1.0
Fraction of Data Removed

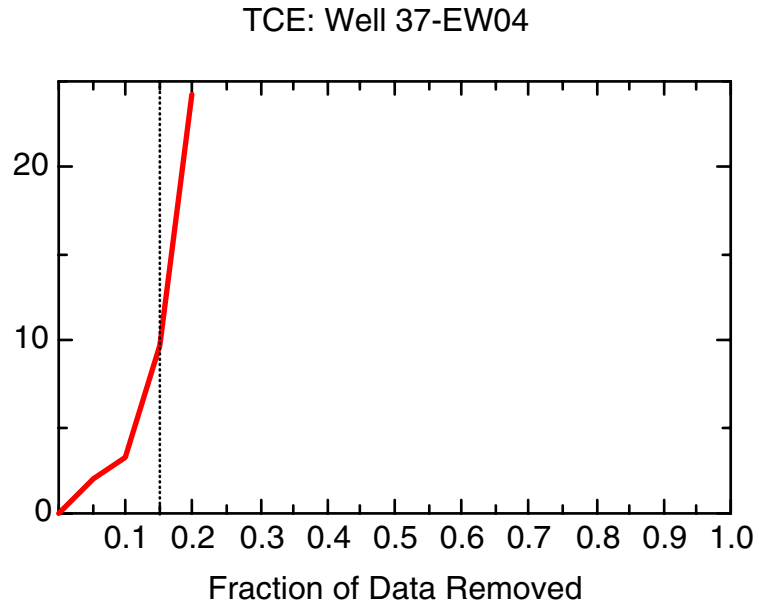
TCE: Well 37-EW04
20
10
0
0.1 0.2 0.3 0.4 0.5 0.6 0.7 0.8 0.9 1.0
Fraction of Data Removed

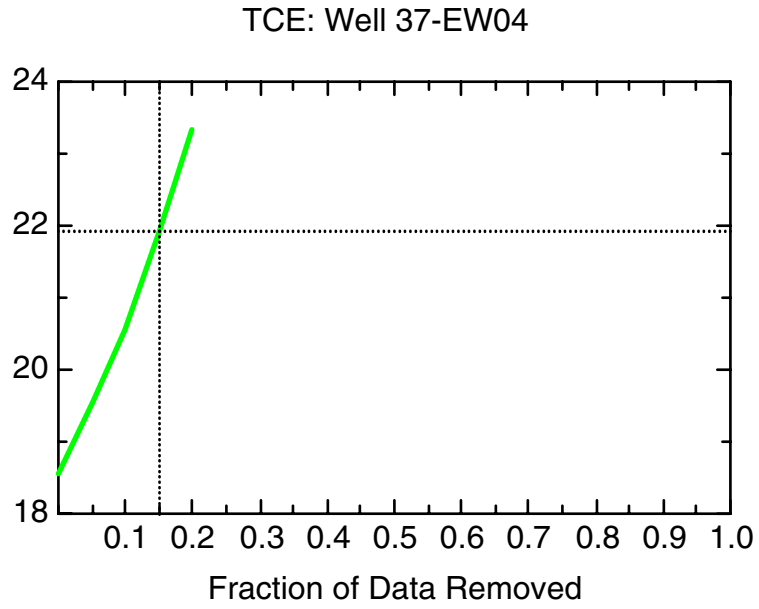
TCE: Well 37-EW04
24
22
20
18
0.1 0.2 0.3 0.4 0.5 0.6 0.7 0.8 0.9 1.0
Fraction of Data Removed

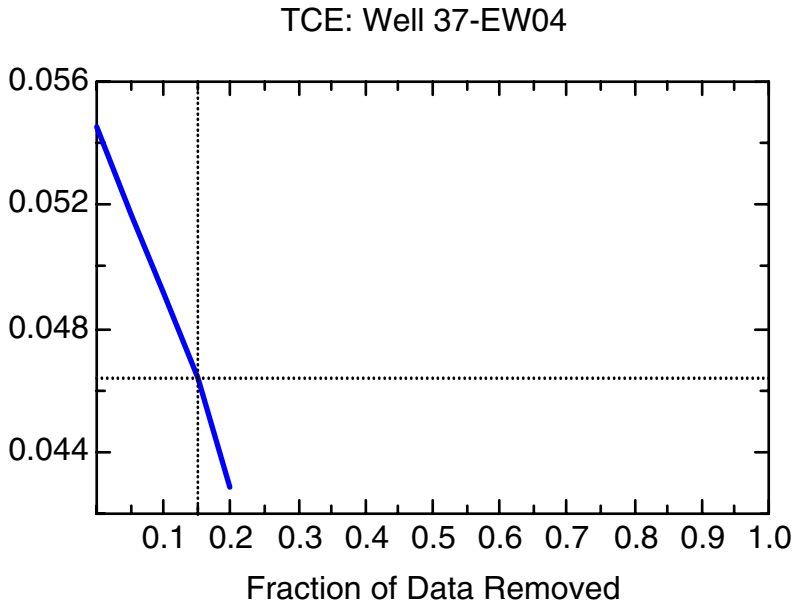
TCE: Well 37-EW04
0.056
0.052
0.048
0.044
0.1 0.2 0.3 0.4 0.5 0.6 0.7 0.8 0.9 1.0
Fraction of Data Removed

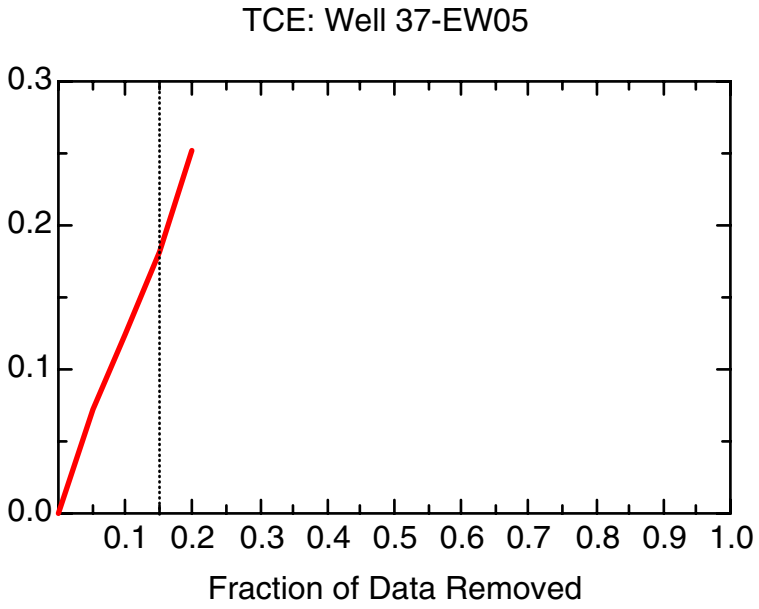
TCE: Well 37-EW05
0.3
0.2
0.1
0.0
0.1 0.2 0.3 0.4 0.5 0.6 0.7 0.8 0.9 1.0
Fraction of Data Removed

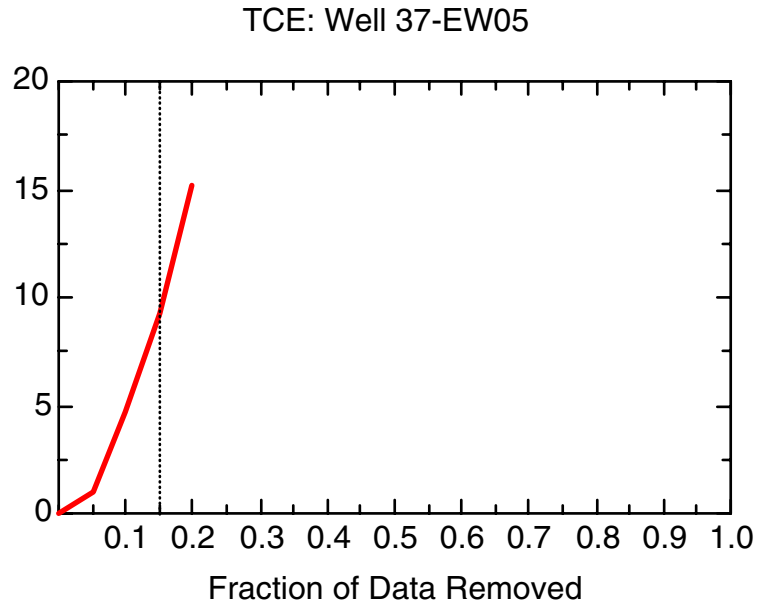
TCE: Well 37-EW05
20
15
10
5
0
0.1 0.2 0.3 0.4 0.5 0.6 0.7 0.8 0.9 1.0
Fraction of Data Removed

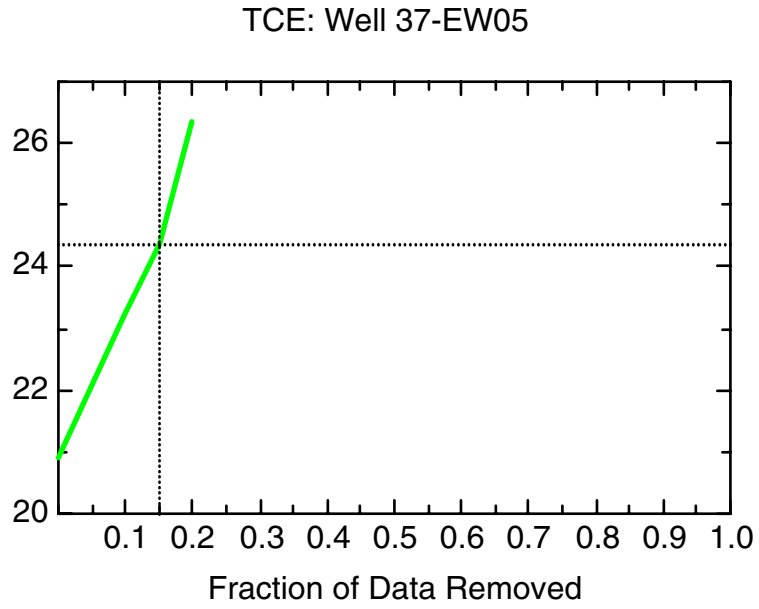
TCE: Well 37-EW05
26
24
22
20
0.1 0.2 0.3 0.4 0.5 0.6 0.7 0.8 0.9 1.0
Fraction of Data Removed

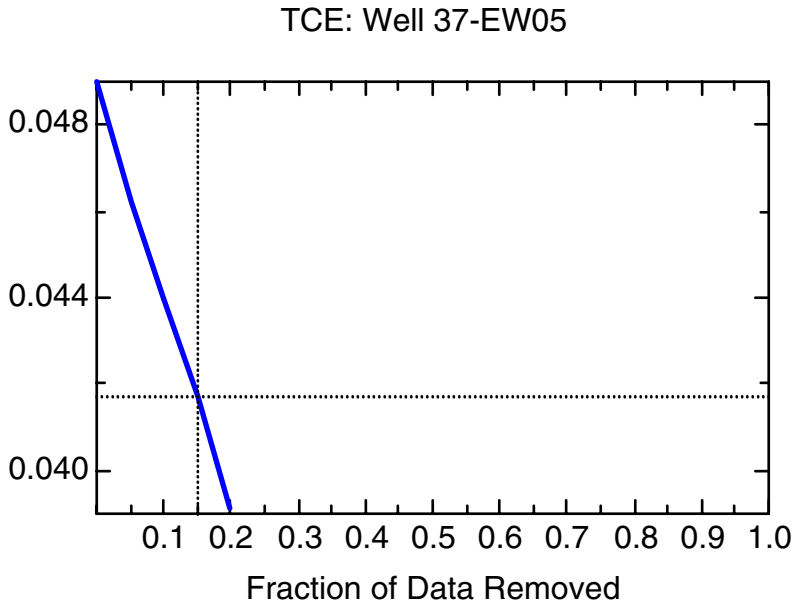
TCE: Well 37-EW05
0.048
0.044
0.040
0.1 0.2 0.3 0.4 0.5 0.6 0.7 0.8 0.9 1.0
Fraction of Data Removed

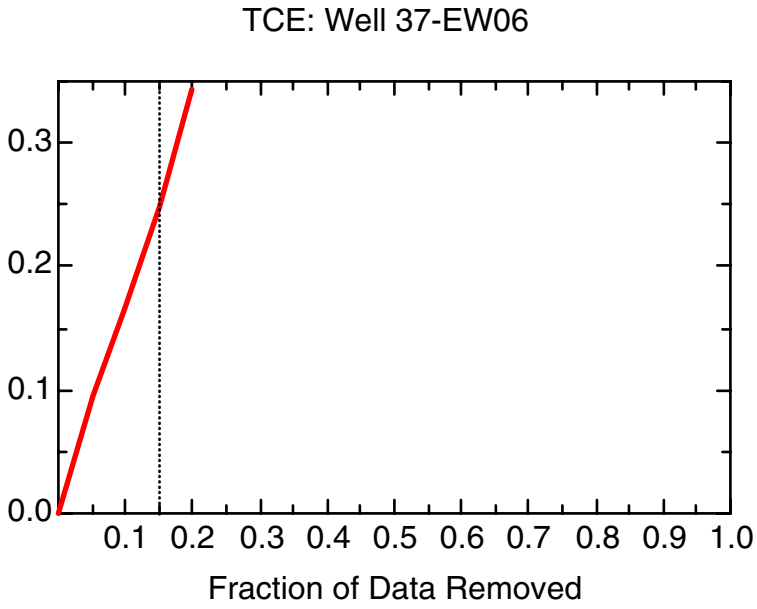
TCE: Well 37-EW06
0.3
0.2
0.1
0.0
0.1 0.2 0.3 0.4 0.5 0.6 0.7 0.8 0.9 1.0
Fraction of Data Removed

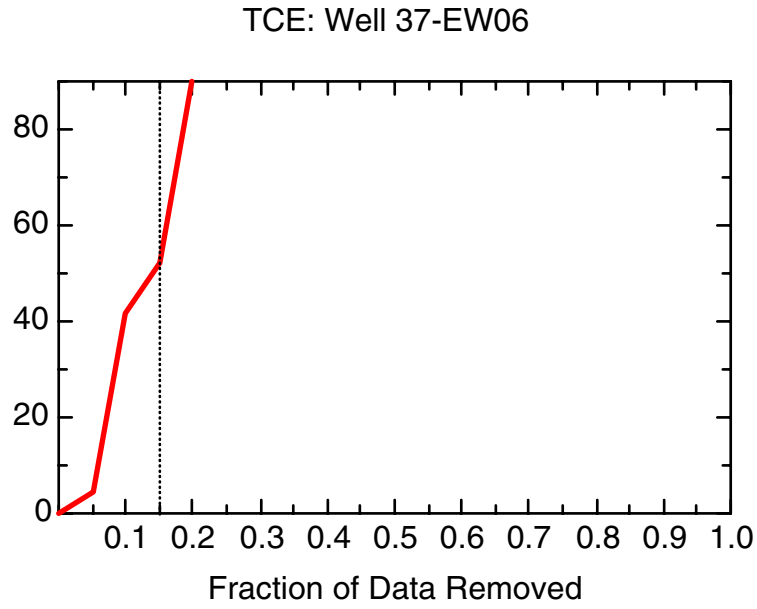
TCE: Well 37-EW06
80
60
40
20
0
0.1 0.2 0.3 0.4 0.5 0.6 0.7 0.8 0.9 1.0
Fraction of Data Removed

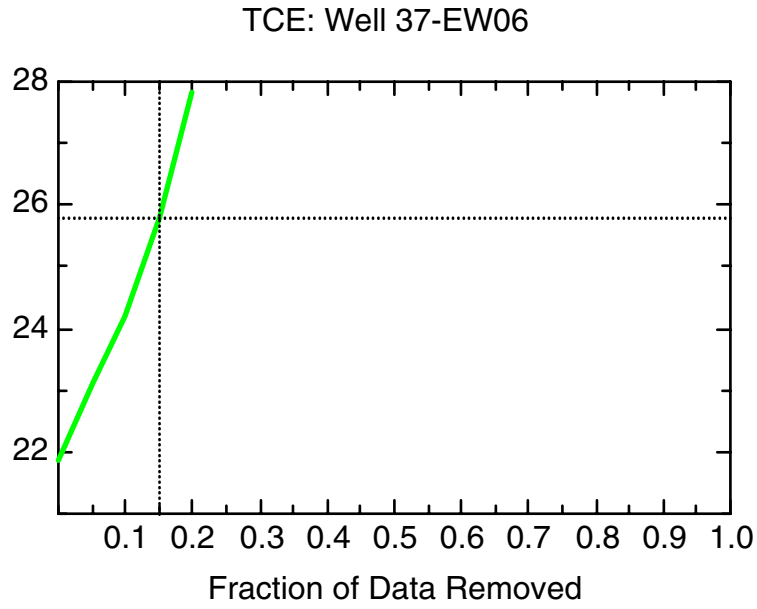
TCE: Well 37-EW06
28
26
24
22
0.1 0.2 0.3 0.4 0.5 0.6 0.7 0.8 0.9 1.0
Fraction of Data Removed

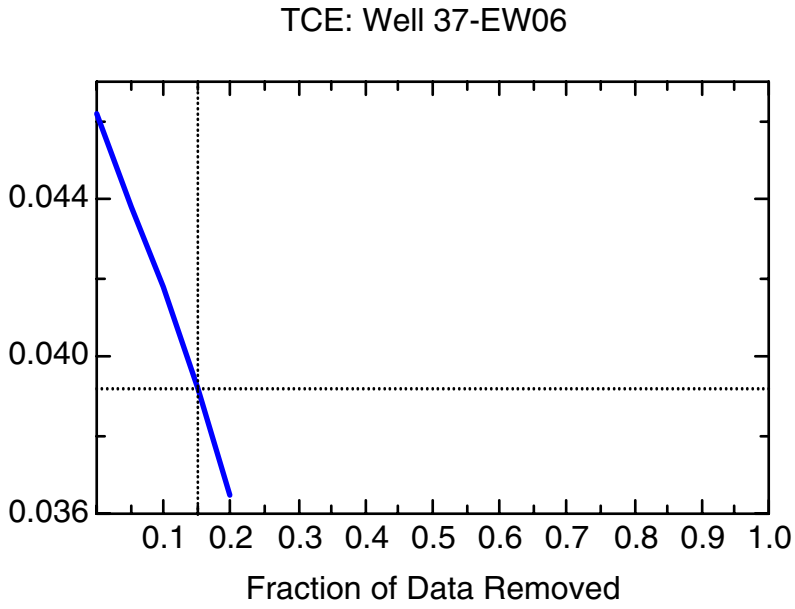
TCE: Well 37-EW06
0.044
0.040
0.036
0.1 0.2 0.3 0.4 0.5 0.6 0.7 0.8 0.9 1.0
Fraction of Data Removed

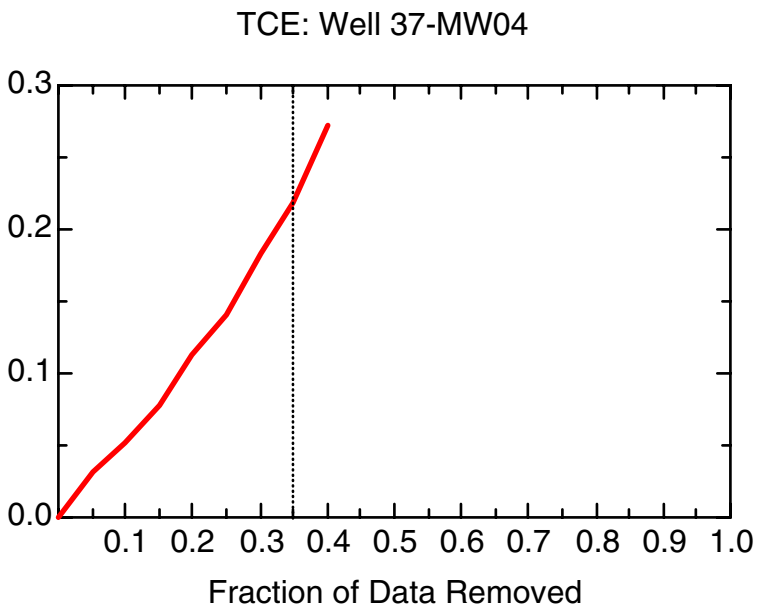
TCE: Well 37-MW04
0.3
0.2
0.1
0.0
0.1 0.2 0.3 0.4 0.5 0.6 0.7 0.8 0.9 1.0
Fraction of Data Removed

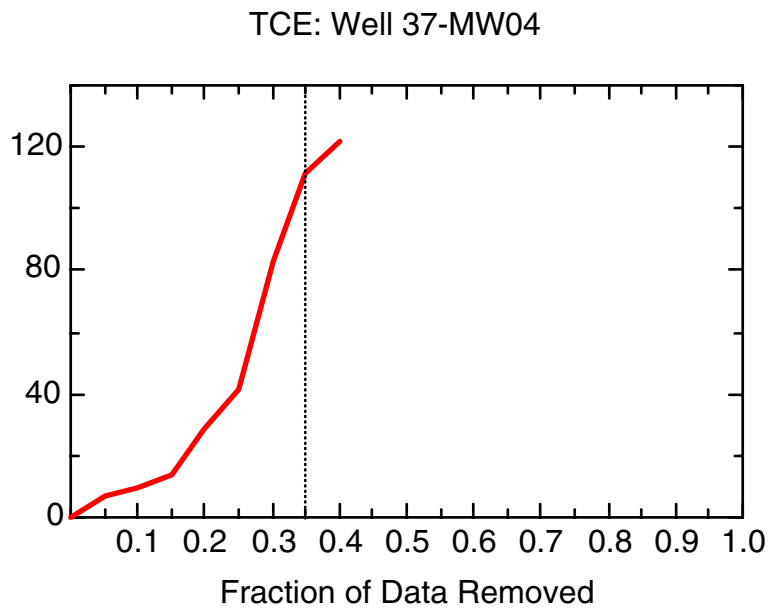
TCE: Well 37-MW04
120
80
40
0
0.1 0.2 0.3 0.4 0.5 0.6 0.7 0.8 0.9 1.0
Fraction of Data Removed

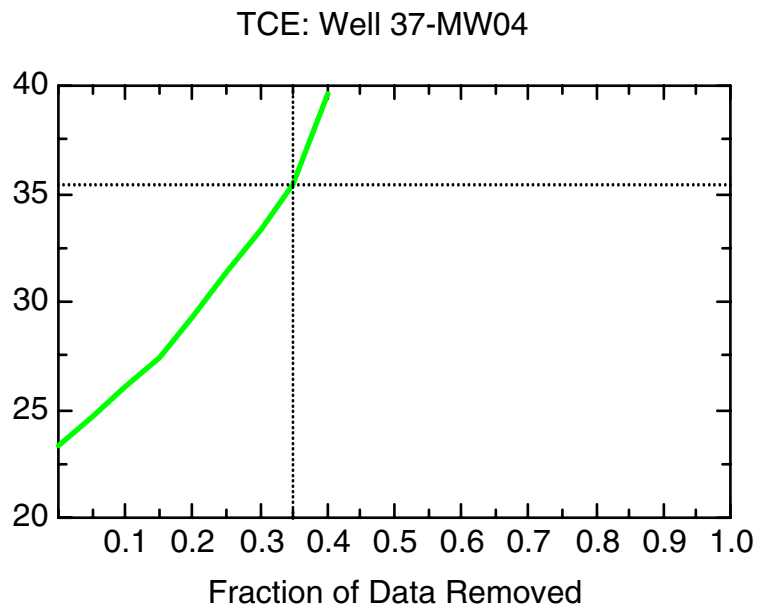
TCE: Well 37-MW04
40
35
30
25
20
0.1 0.2 0.3 0.4 0.5 0.6 0.7 0.8 0.9 1.0
Fraction of Data Removed

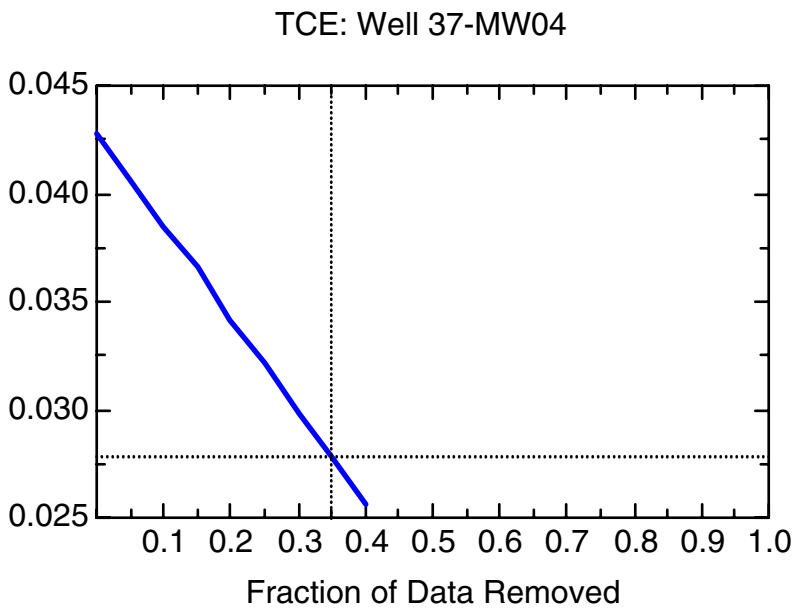
TCE: Well 37-MW04
0.045
0.040
0.035
0.030
0.025
0.1 0.2 0.3 0.4 0.5 0.6 0.7 0.8 0.9 1.0
Fraction of Data Removed

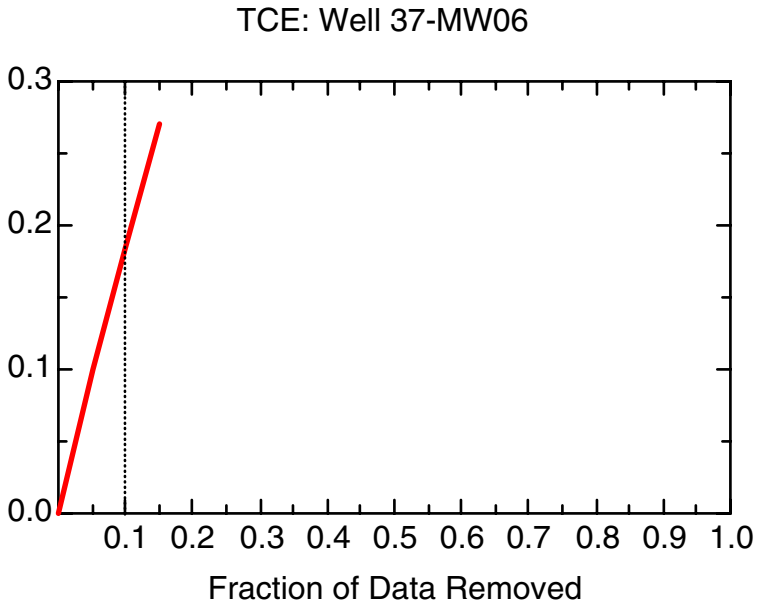
TCE: Well 37-MW06
0.3
0.2
0.1
0.0
0.1 0.2 0.3 0.4 0.5 0.6 0.7 0.8 0.9 1.0
Fraction of Data Removed

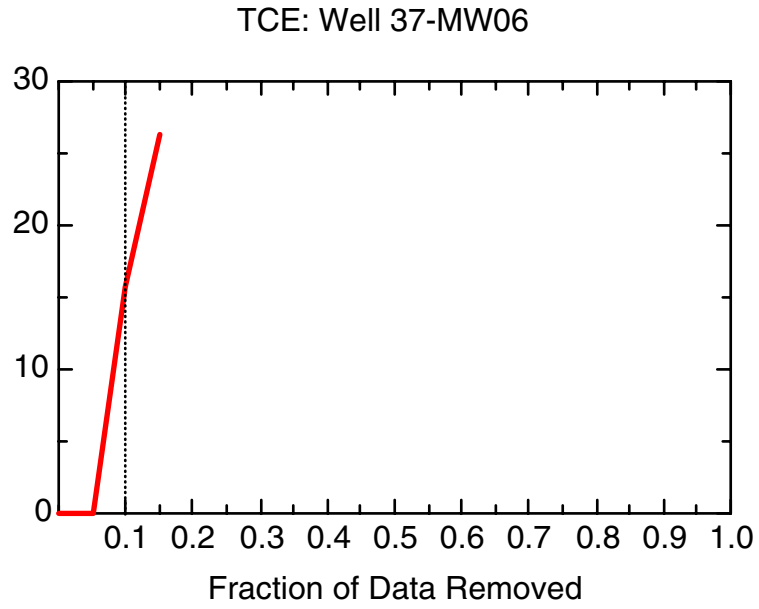
TCE: Well 37-MW06
30
20
10
0
0.1 0.2 0.3 0.4 0.5 0.6 0.7 0.8 0.9 1.0
Fraction of Data Removed

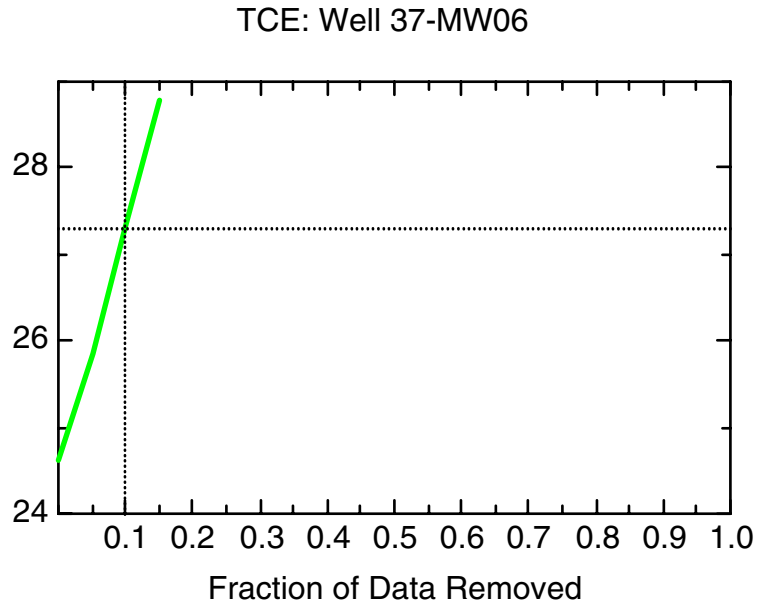
TCE: Well 37-MW06
28
26
24
0.1 0.2 0.3 0.4 0.5 0.6 0.7 0.8 0.9 1.0
Fraction of Data Removed

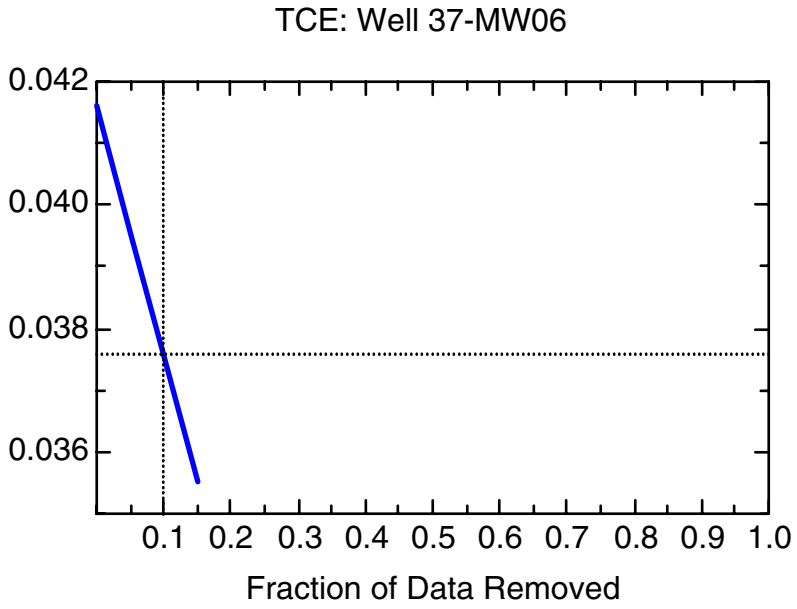
TCE: Well 37-MW06
0.042
0.040
0.038
0.036
0.1 0.2 0.3 0.4 0.5 0.6 0.7 0.8 0.9 1.0
Fraction of Data Removed

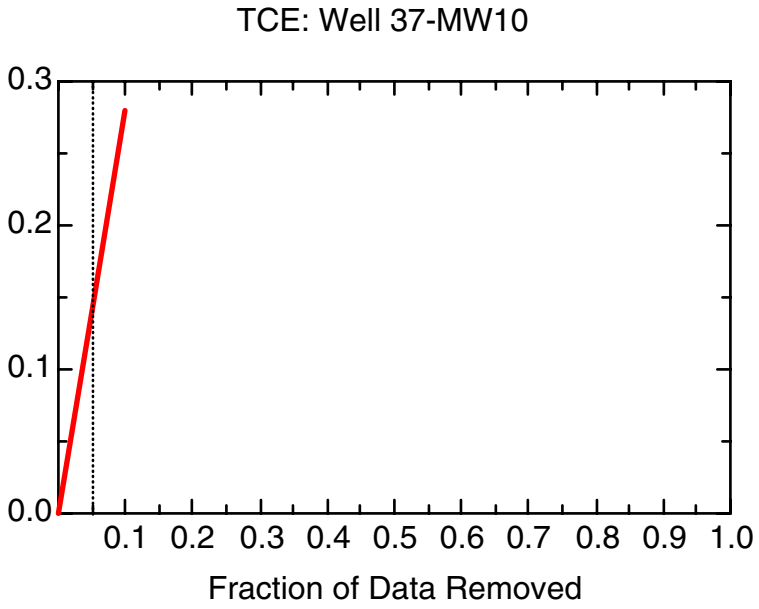
TCE: Well 37-MW10
0.3
0.2
0.1
0.0
0.1 0.2 0.3 0.4 0.5 0.6 0.7 0.8 0.9 1.0
Fraction of Data Removed

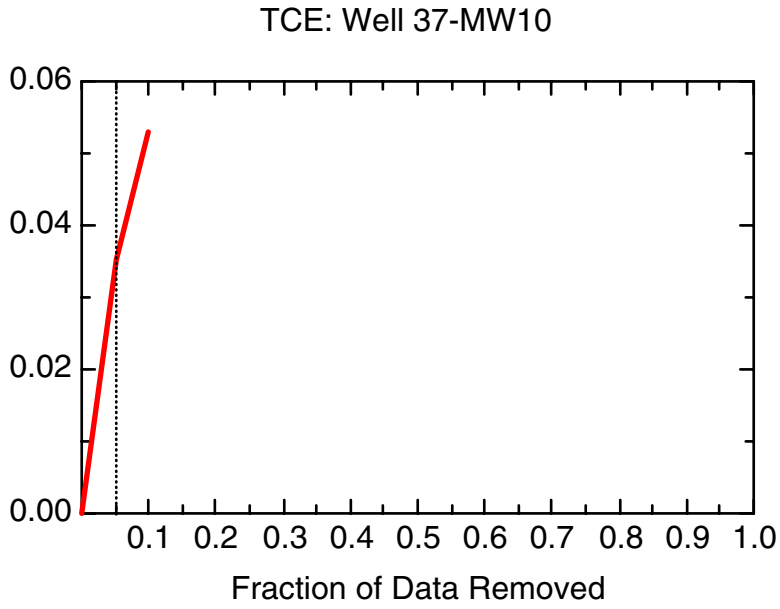
TCE: Well 37-MW10
0.06
0.04
0.02
0.00
0.1 0.2 0.3 0.4 0.5 0.6 0.7 0.8 0.9 1.0
Fraction of Data Removed

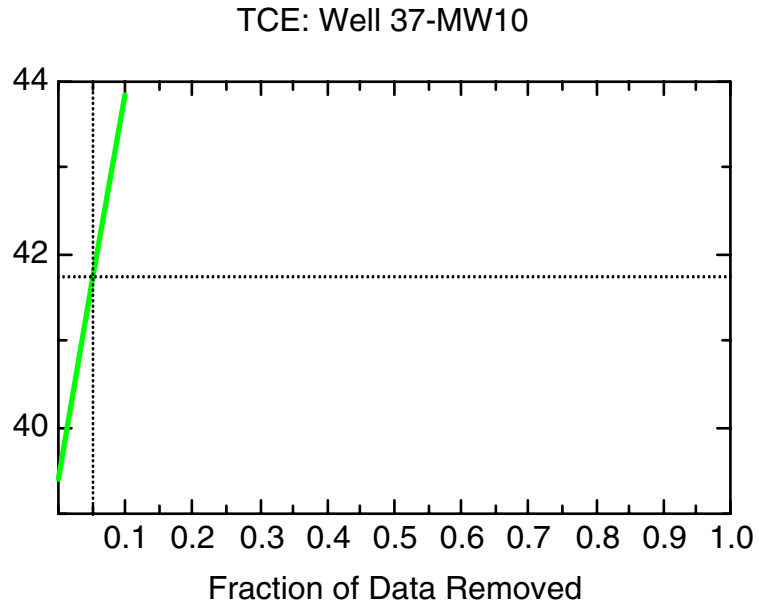
TCE: Well 37-MW10
44
42
40
0.1 0.2 0.3 0.4 0.5 0.6 0.7 0.8 0.9 1.0
Fraction of Data Removed

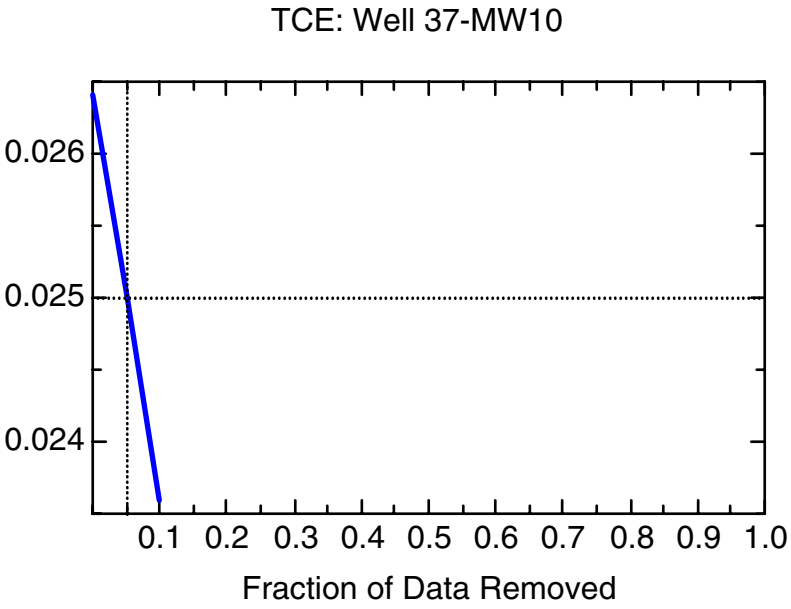
TCE: Well 37-MW10
0.026
0.025
0.024
0.1 0.2 0.3 0.4 0.5 0.6 0.7 0.8 0.9 1.0
Fraction of Data Removed

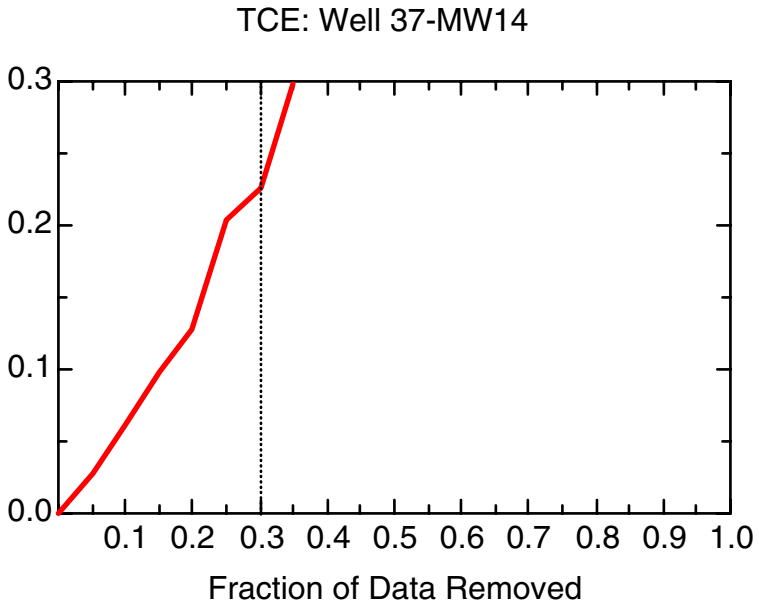
TCE: Well 37-MW14
0.3
0.2
0.1
0.0
0.1 0.2 0.3 0.4 0.5 0.6 0.7 0.8 0.9 1.0
Fraction of Data Removed

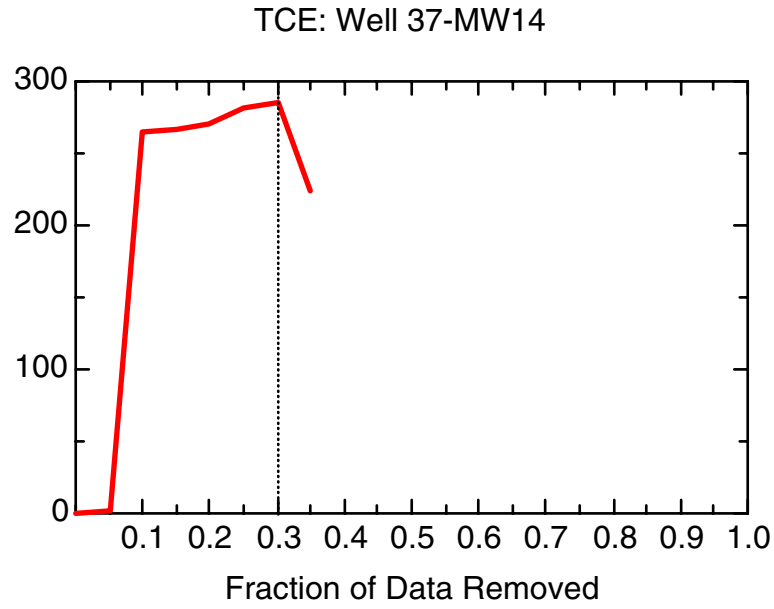
TCE: Well 37-MW14
300
200
100
0
0.1 0.2 0.3 0.4 0.5 0.6 0.7 0.8 0.9 1.0
Fraction of Data Removed

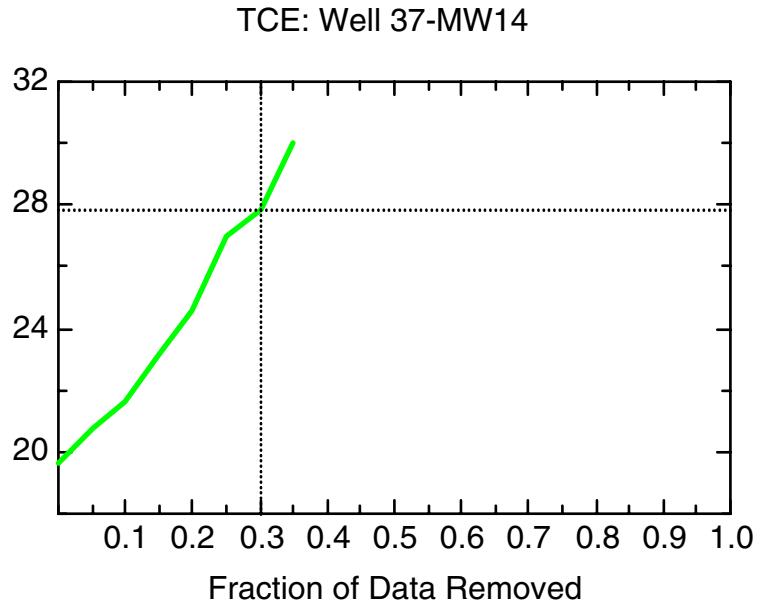
TCE: Well 37-MW14
32
28
24
20
0.1 0.2 0.3 0.4 0.5 0.6 0.7 0.8 0.9 1.0
Fraction of Data Removed

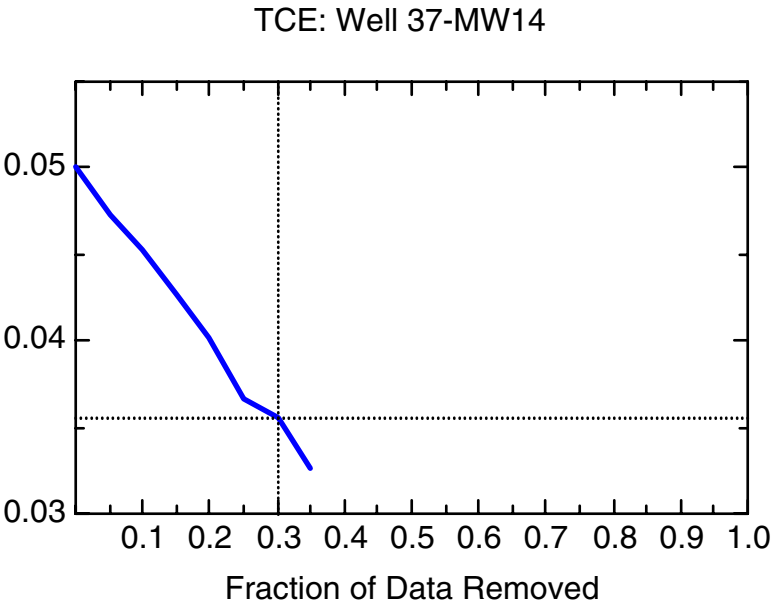
TCE: Well 37-MW14
0.05
0.04
0.03
0.1 0.2 0.3 0.4 0.5 0.6 0.7 0.8 0.9 1.0
Fraction of Data Removed

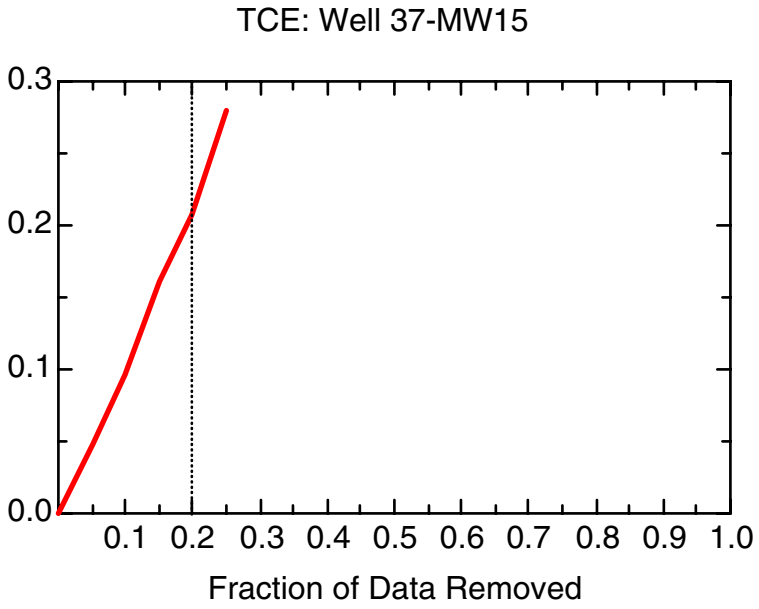
TCE: Well 37-MW15
0.3
0.2
0.1
0.0
0.1 0.2 0.3 0.4 0.5 0.6 0.7 0.8 0.9 1.0
Fraction of Data Removed

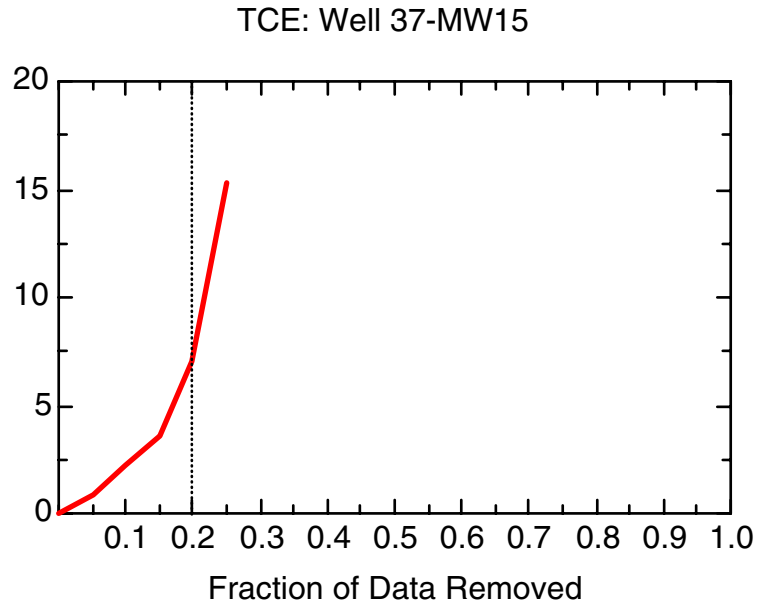
TCE: Well 37-MW15
20
15
10
5
0
0.1 0.2 0.3 0.4 0.5 0.6 0.7 0.8 0.9 1.0
Fraction of Data Removed

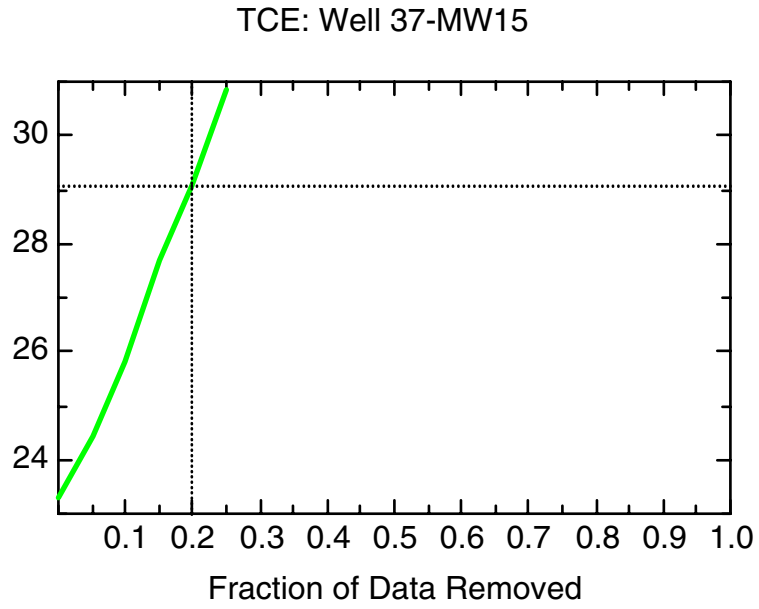
TCE: Well 37-MW15
30
28
26
24
0.1 0.2 0.3 0.4 0.5 0.6 0.7 0.8 0.9 1.0
Fraction of Data Removed

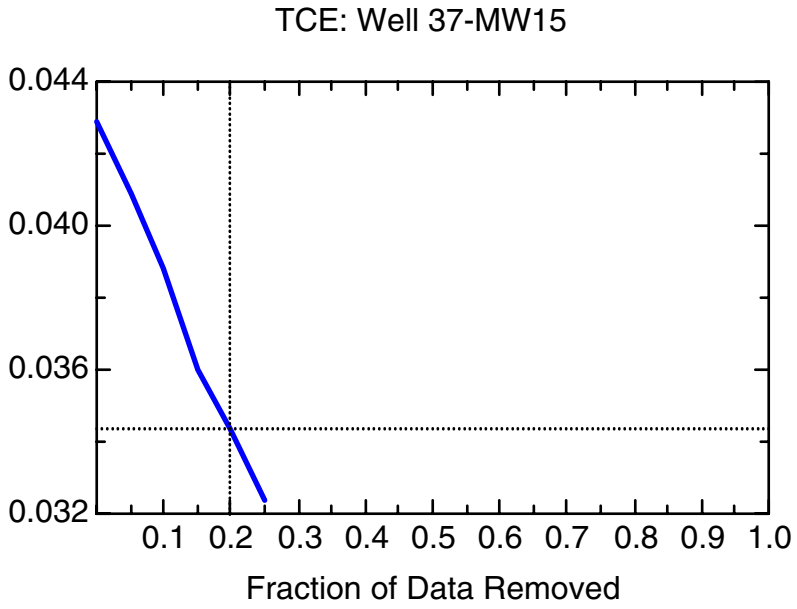
TCE: Well 37-MW15
0.044
0.040
0.036
0.032
0.1 0.2 0.3 0.4 0.5 0.6 0.7 0.8 0.9 1.0
Fraction of Data Removed

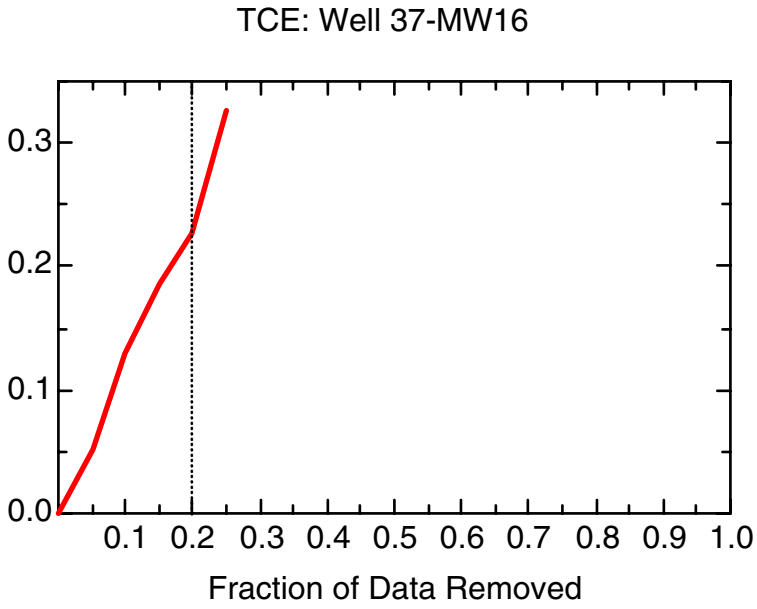
TCE: Well 37-MW16
0.3
0.2
0.1
0.0
0.1 0.2 0.3 0.4 0.5 0.6 0.7 0.8 0.9 1.0
Fraction of Data Removed

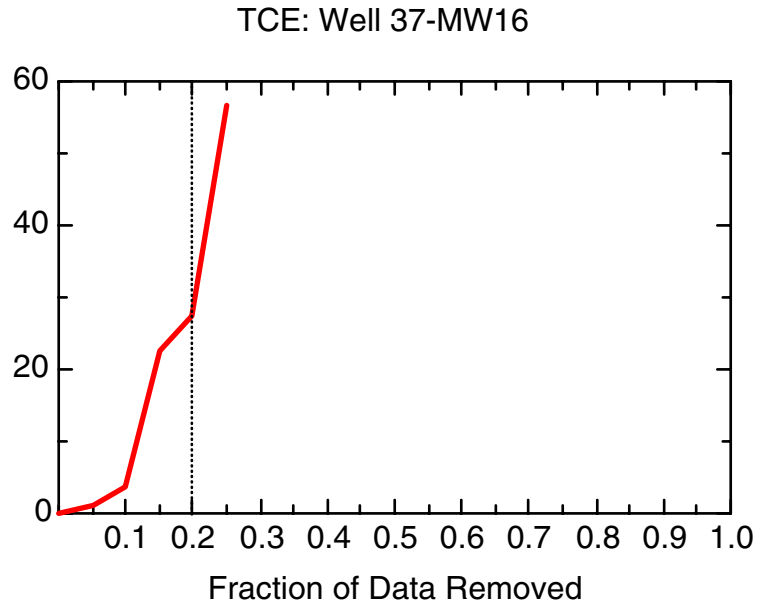
TCE: Well 37-MW16
60
40
20
0
0.1 0.2 0.3 0.4 0.5 0.6 0.7 0.8 0.9 1.0
Fraction of Data Removed

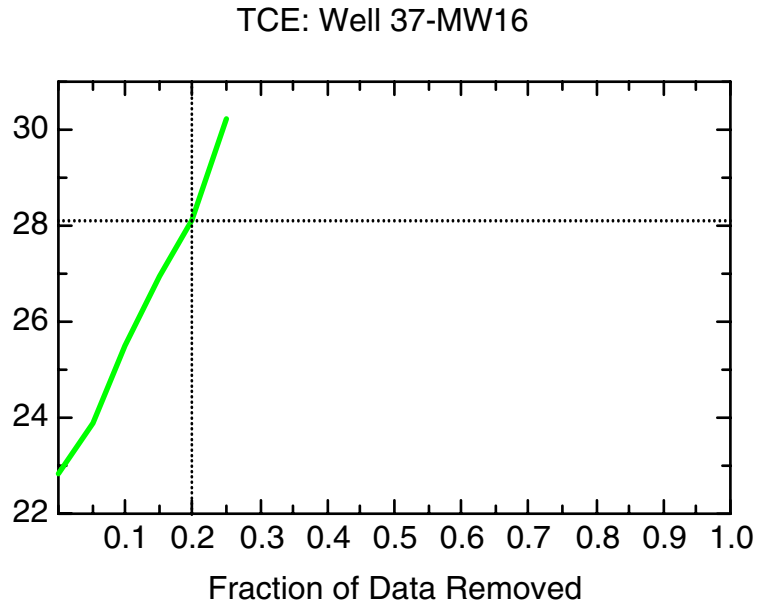
TCE: Well 37-MW16
30
28
26
24
22
0.1 0.2 0.3 0.4 0.5 0.6 0.7 0.8 0.9 1.0
Fraction of Data Removed

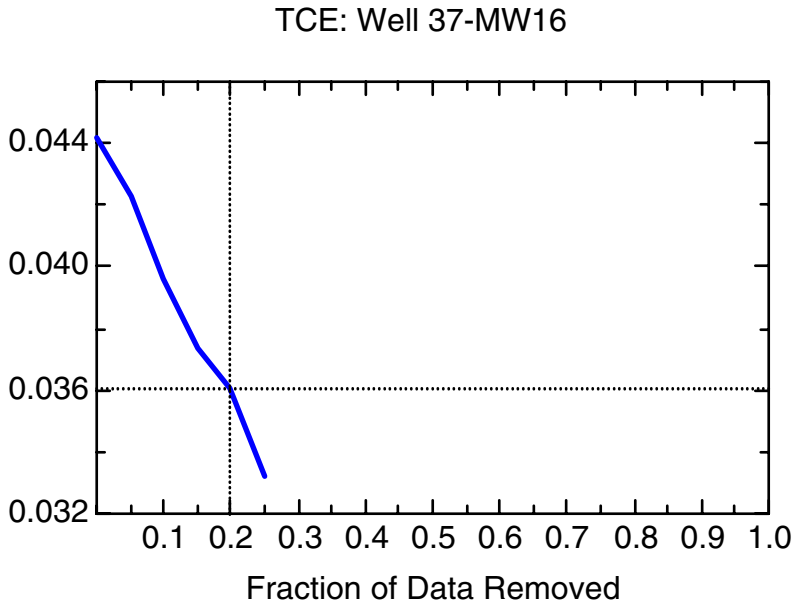
TCE: Well 37-MW16
0.044
0.040
0.036
0.032
0.1 0.2 0.3 0.4 0.5 0.6 0.7 0.8 0.9 1.0
Fraction of Data Removed

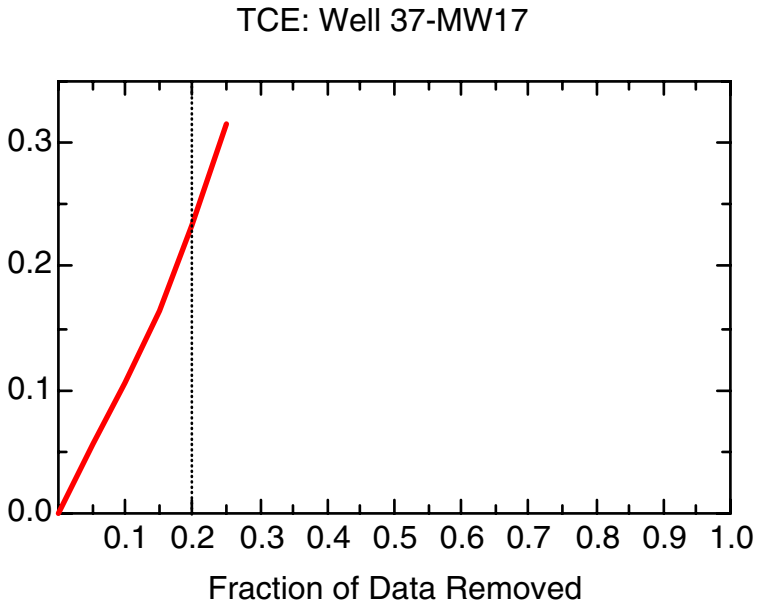
TCE: Well 37-MW17
0.3
0.2
0.1
0.0
0.1 0.2 0.3 0.4 0.5 0.6 0.7 0.8 0.9 1.0
Fraction of Data Removed

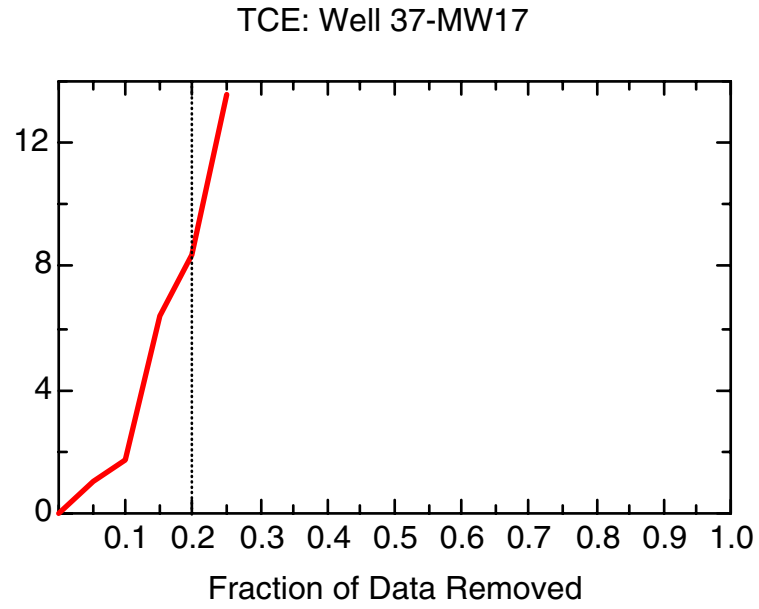
TCE: Well 37-MW17
12
8
4
0
0.1 0.2 0.3 0.4 0.5 0.6 0.7 0.8 0.9 1.0
Fraction of Data Removed

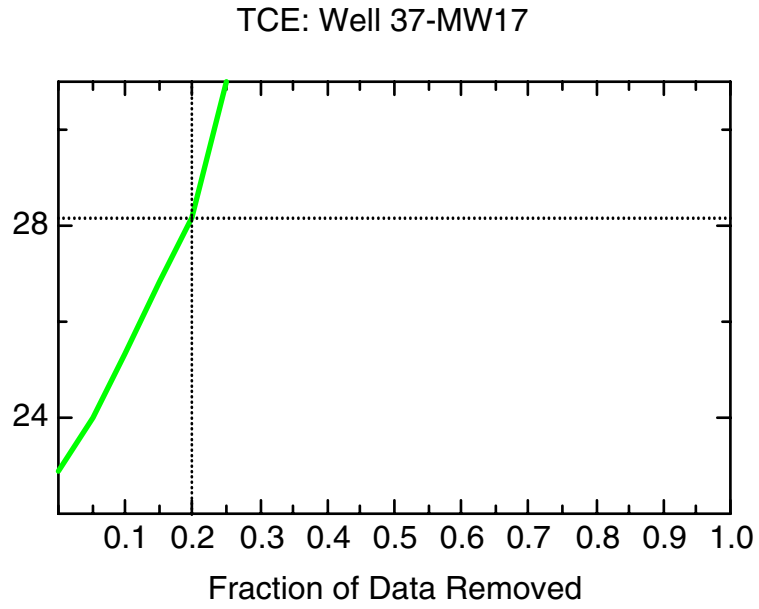
TCE: Well 37-MW17
28
24
0.1 0.2 0.3 0.4 0.5 0.6 0.7 0.8 0.9 1.0
Fraction of Data Removed

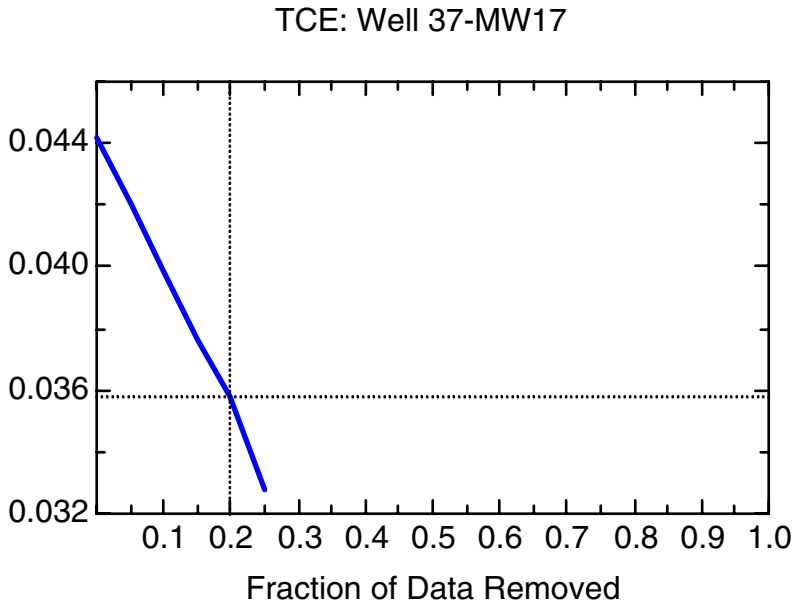
TCE: Well 37-MW17
0.044
0.040
0.036
0.032
0.1 0.2 0.3 0.4 0.5 0.6 0.7 0.8 0.9 1.0
Fraction of Data Removed

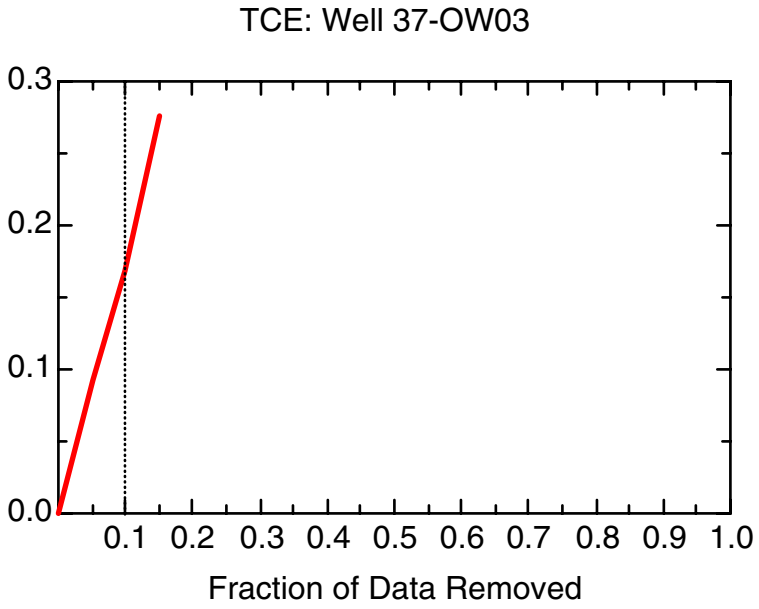
TCE: Well 37-OW03
0.3
0.2
0.1
0.0
0.1 0.2 0.3 0.4 0.5 0.6 0.7 0.8 0.9 1.0
Fraction of Data Removed

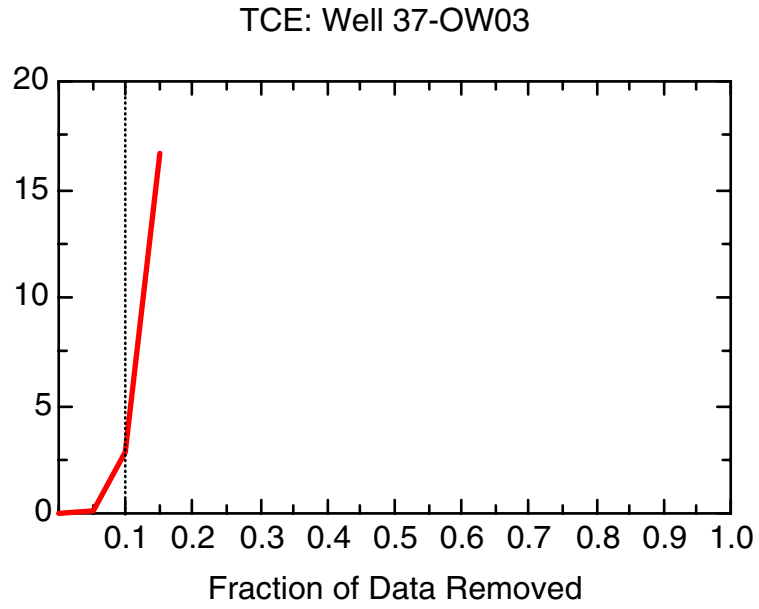
TCE: Well 37-OW03
20
15
10
5
0
0.1 0.2 0.3 0.4 0.5 0.6 0.7 0.8 0.9 1.0
Fraction of Data Removed

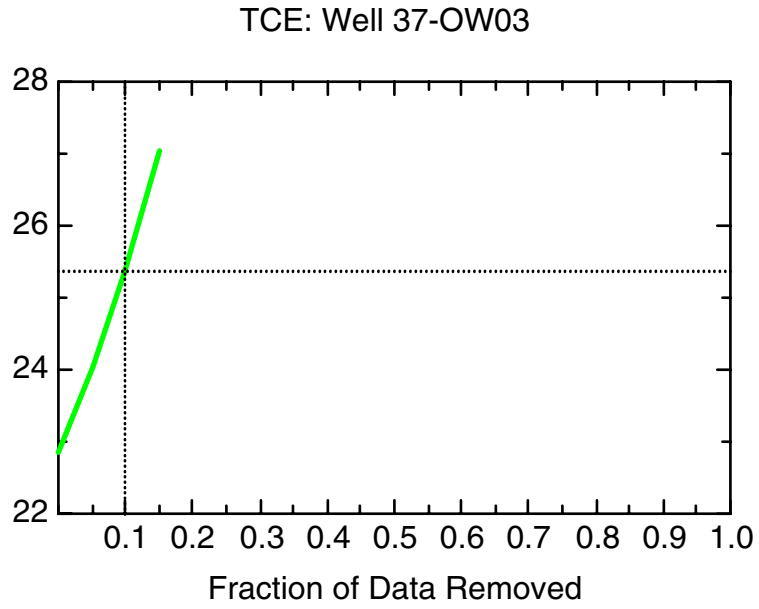
TCE: Well 37-OW03
28
26
24
22
0.1 0.2 0.3 0.4 0.5 0.6 0.7 0.8 0.9 1.0
Fraction of Data Removed

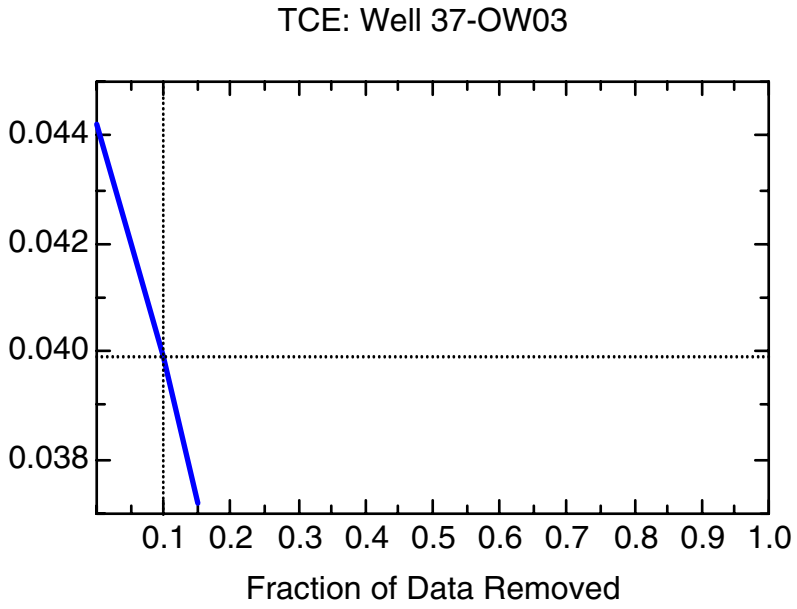
TCE: Well 37-OW03
0.044
0.042
0.040
0.038
0.1 0.2 0.3 0.4 0.5 0.6 0.7 0.8 0.9 1.0
Fraction of Data Removed

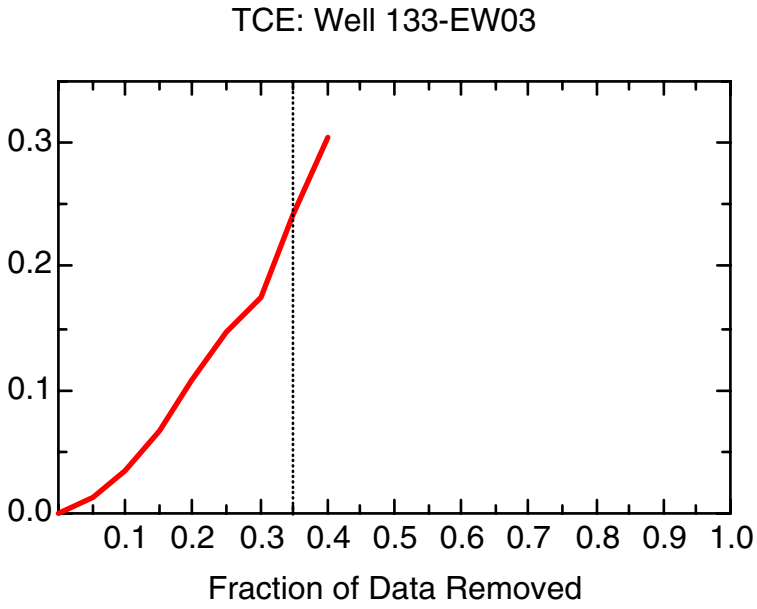
TCE: Well 133-EW03
0.3
0.2
0.1
0.0
0.1 0.2 0.3 0.4 0.5 0.6 0.7 0.8 0.9 1.0
Fraction of Data Removed

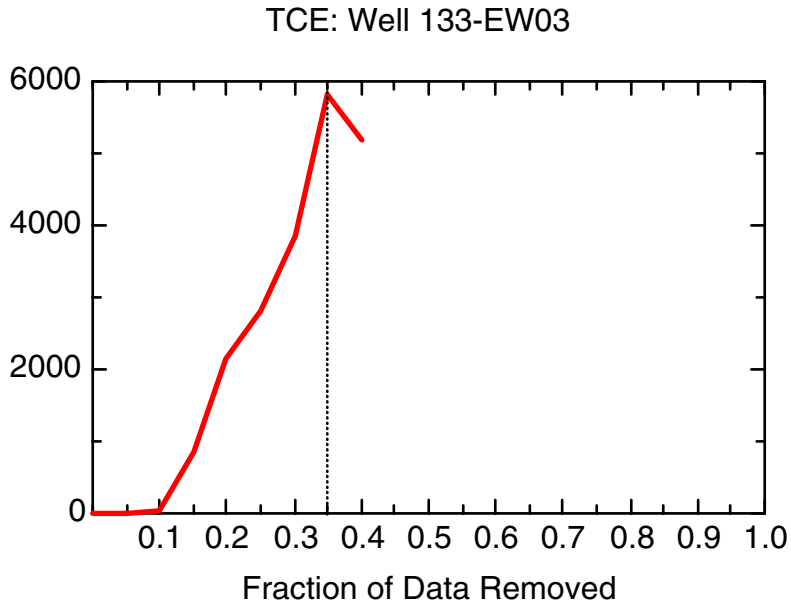
TCE: Well 133-EW03
6000
4000
2000
0
0.1 0.2 0.3 0.4 0.5 0.6 0.7 0.8 0.9 1.0
Fraction of Data Removed

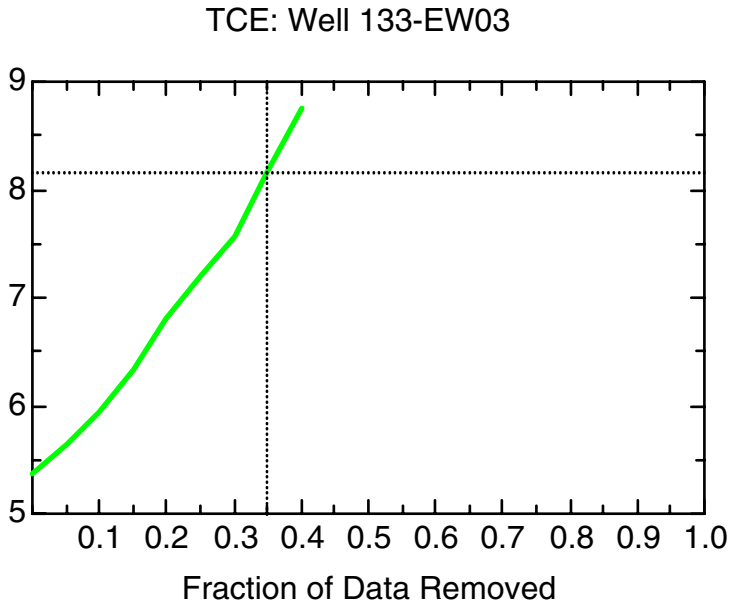
TCE: Well 133-EW03
9
8
7
6
5
0.1 0.2 0.3 0.4 0.5 0.6 0.7 0.8 0.9 1.0
Fraction of Data Removed

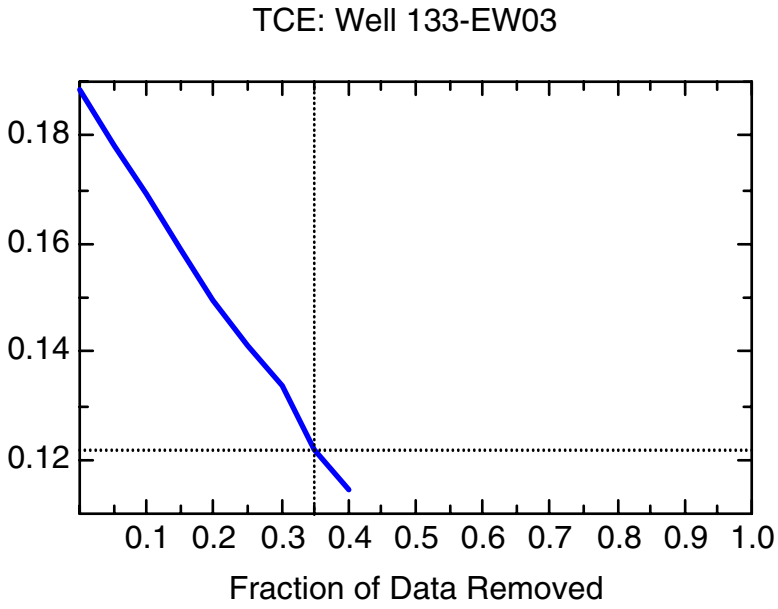
TCE: Well 133-EW03
0.18
0.16
0.14
0.12
0.1 0.2 0.3 0.4 0.5 0.6 0.7 0.8 0.9 1.0
Fraction of Data Removed

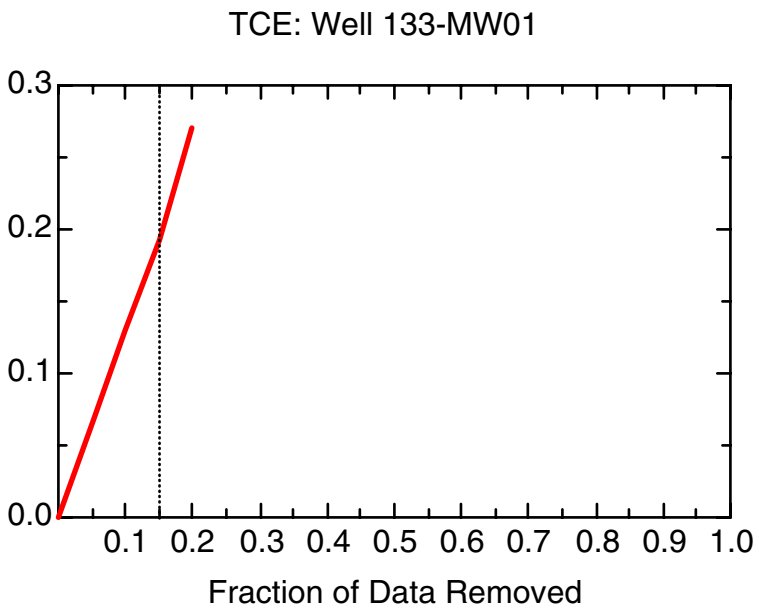
TCE: Well 133-MW01
0.3
0.2
0.1
0.0
0.1 0.2 0.3 0.4 0.5 0.6 0.7 0.8 0.9 1.0
Fraction of Data Removed

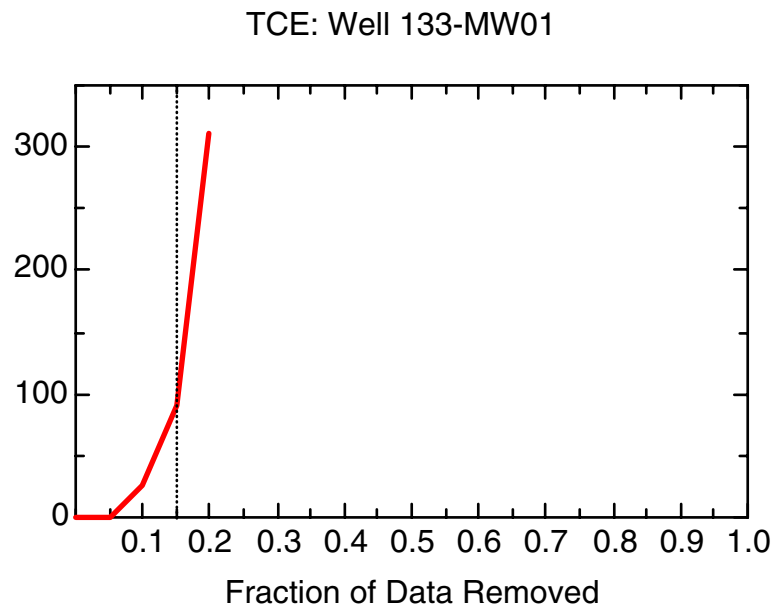
TCE: Well 133-MW01
300
200
100
0
0.1 0.2 0.3 0.4 0.5 0.6 0.7 0.8 0.9 1.0
Fraction of Data Removed

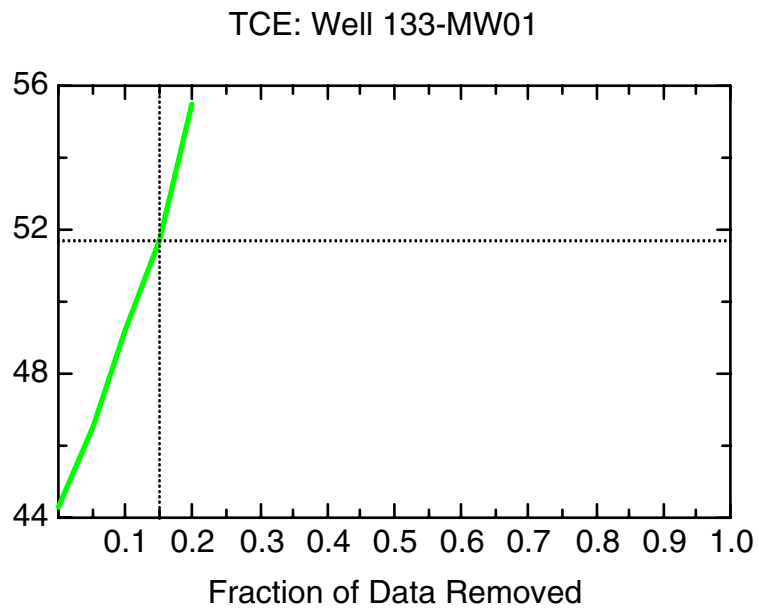
TCE: Well 133-MW01
56
52
48
44
0.1 0.2 0.3 0.4 0.5 0.6 0.7 0.8 0.9 1.0
Fraction of Data Removed

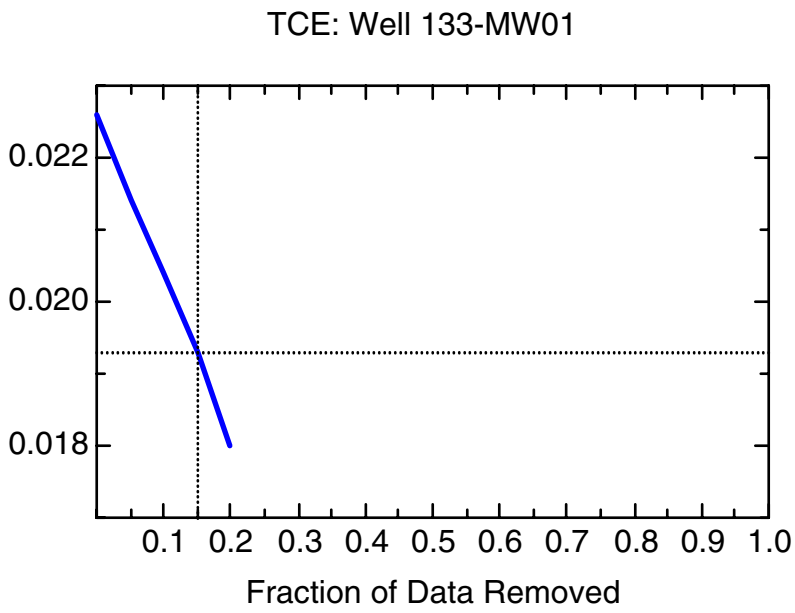
TCE: Well 133-MW01
0.022
0.020
0.018
0.1 0.2 0.3 0.4 0.5 0.6 0.7 0.8 0.9 1.0
Fraction of Data Removed

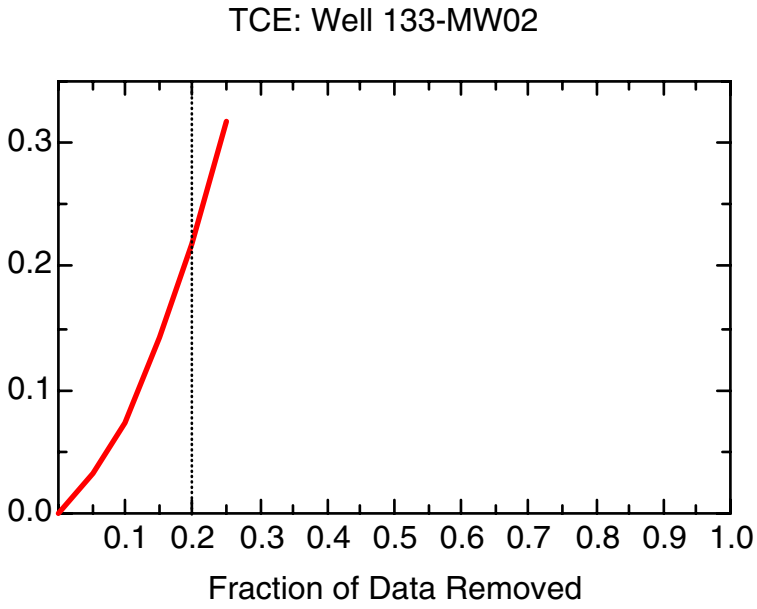
TCE: Well 133-MW02
0.3
0.2
0.1
0.0
0.1 0.2 0.3 0.4 0.5 0.6 0.7 0.8 0.9 1.0
Fraction of Data Removed

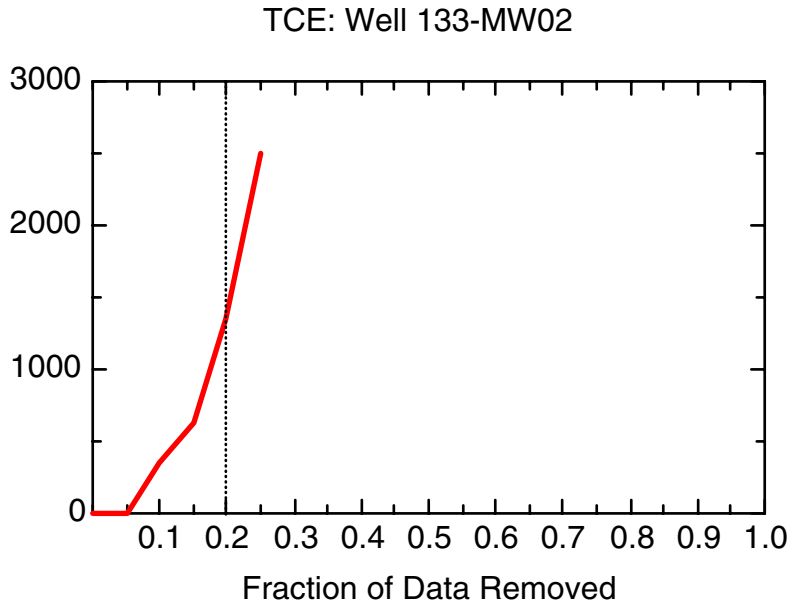
TCE: Well 133-MW02
3000
2000
1000
0
0.1 0.2 0.3 0.4 0.5 0.6 0.7 0.8 0.9 1.0
Fraction of Data Removed

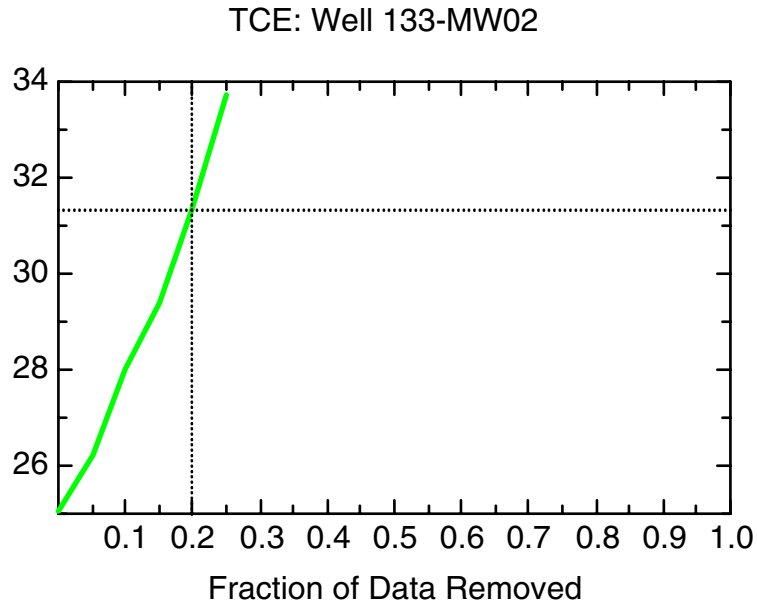
TCE: Well 133-MW02
34
32
30
28
26
0.1 0.2 0.3 0.4 0.5 0.6 0.7 0.8 0.9 1.0
Fraction of Data Removed

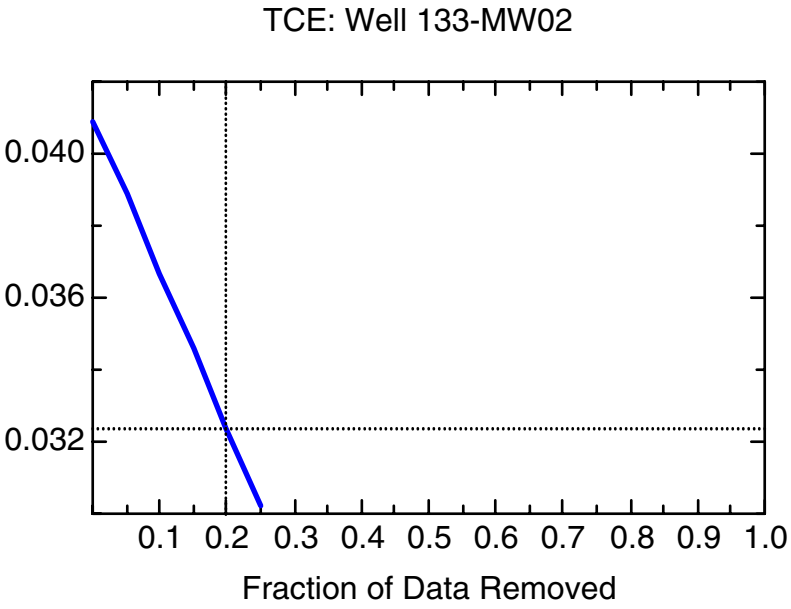
TCE: Well 133-MW02
0.040
0.036
0.032
0.1 0.2 0.3 0.4 0.5 0.6 0.7 0.8 0.9 1.0
Fraction of Data Removed

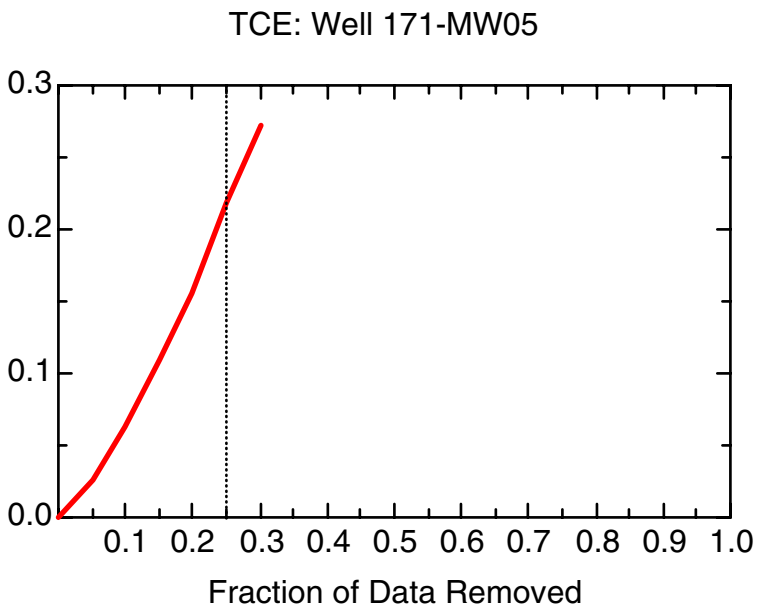
TCE: Well 171-MW05
0.3
0.2
0.1
0.0
0.1 0.2 0.3 0.4 0.5 0.6 0.7 0.8 0.9 1.0
Fraction of Data Removed

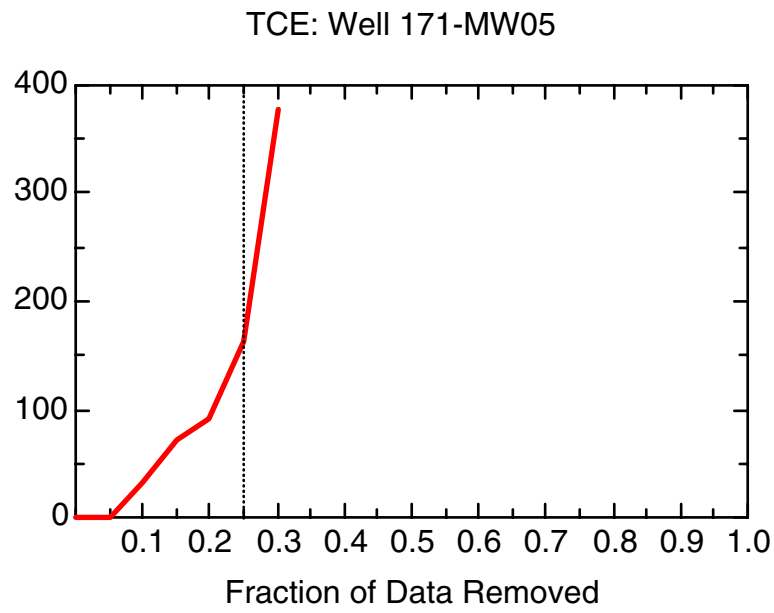
TCE: Well 171-MW05
400
300
200
100
0
0.1 0.2 0.3 0.4 0.5 0.6 0.7 0.8 0.9 1.0
Fraction of Data Removed

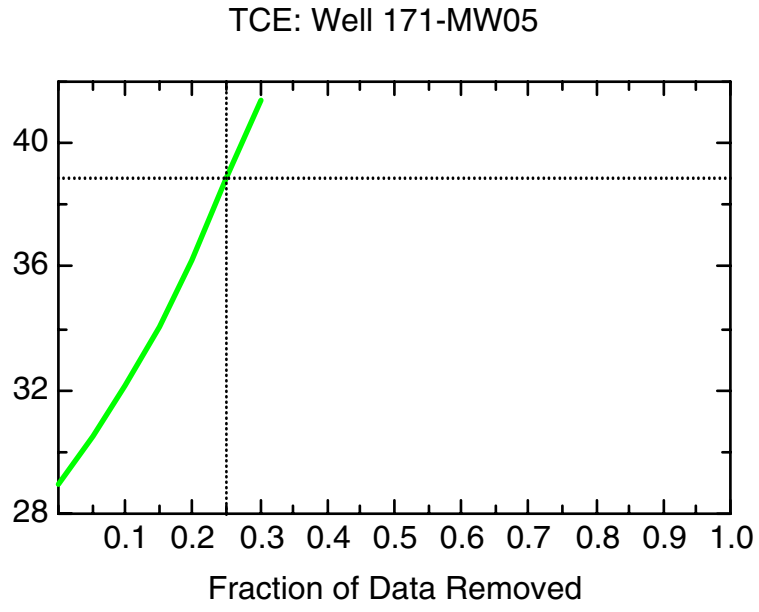
TCE: Well 171-MW05
40
36
32
28
0.1 0.2 0.3 0.4 0.5 0.6 0.7 0.8 0.9 1.0
Fraction of Data Removed

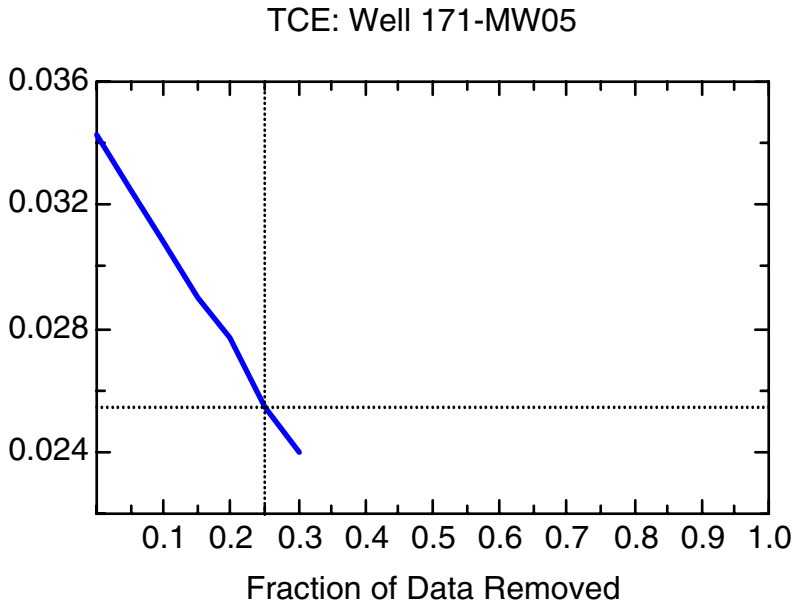
TCE: Well 171-MW05
0.036
0.032
0.028
0.024
0.1 0.2 0.3 0.4 0.5 0.6 0.7 0.8 0.9 1.0
Fraction of Data Removed

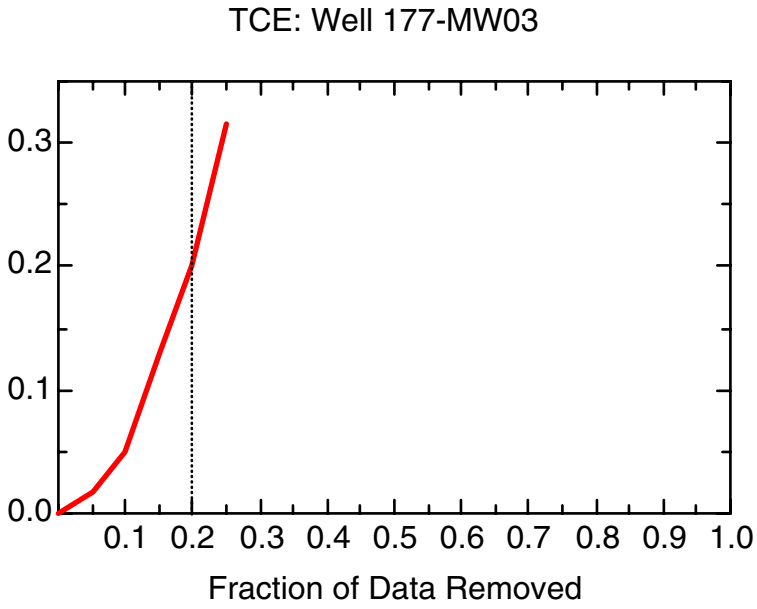
TCE: Well 177-MW03
0.3
0.2
0.1
0.0
0.1 0.2 0.3 0.4 0.5 0.6 0.7 0.8 0.9 1.0
Fraction of Data Removed

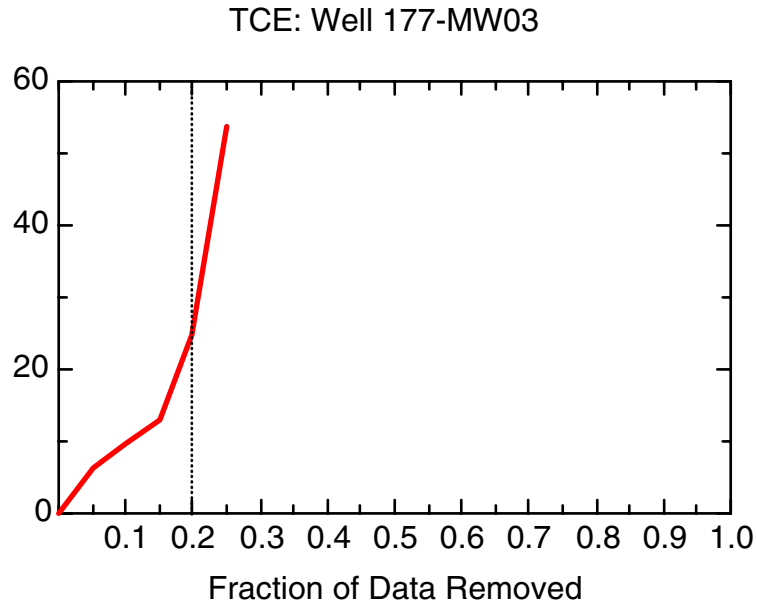
TCE: Well 177-MW03
60
40
20
0
0.1 0.2 0.3 0.4 0.5 0.6 0.7 0.8 0.9 1.0
Fraction of Data Removed

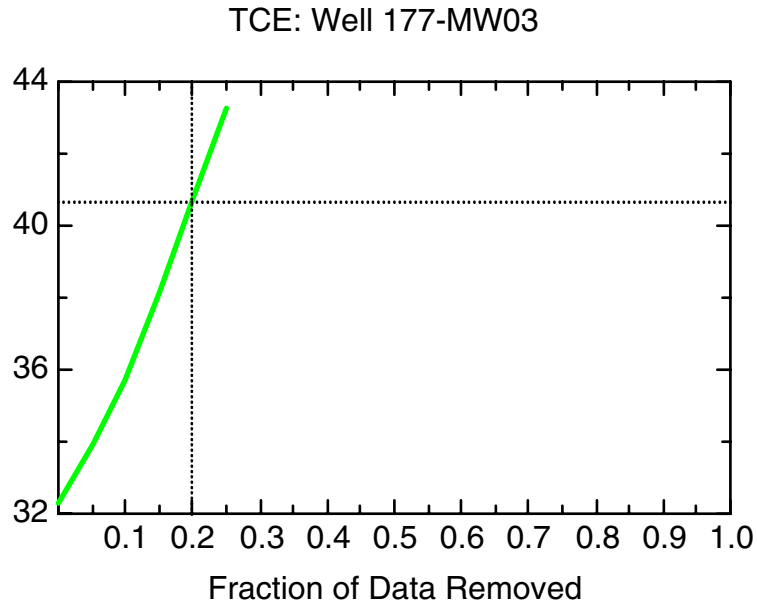
TCE: Well 177-MW03
44
40
36
32
0.1 0.2 0.3 0.4 0.5 0.6 0.7 0.8 0.9 1.0
Fraction of Data Removed

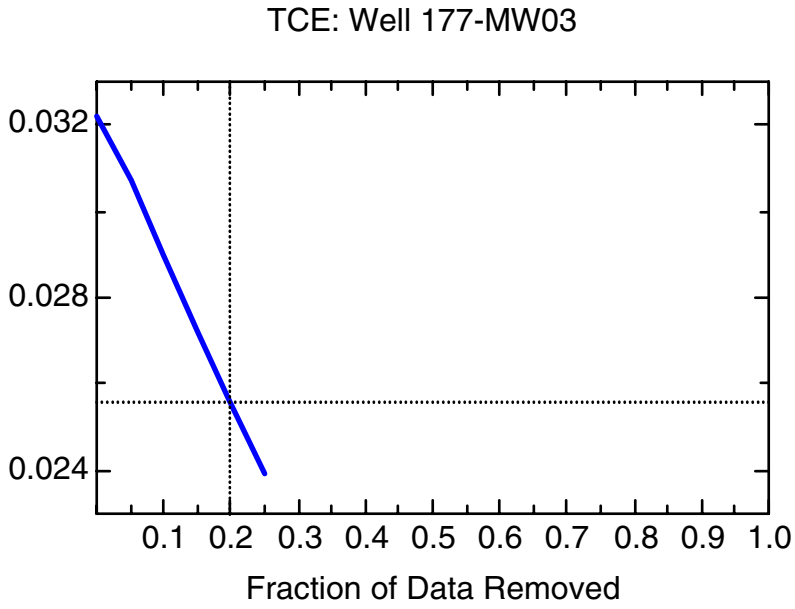
TCE: Well 177-MW03
0.032
0.028
0.024
0.1 0.2 0.3 0.4 0.5 0.6 0.7 0.8 0.9 1.0
Fraction of Data Removed

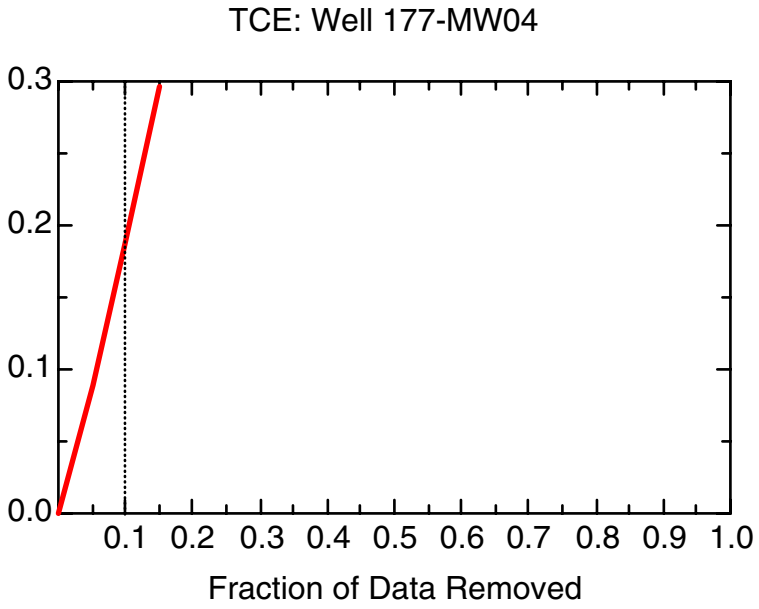
TCE: Well 177-MW04
0.3
0.2
0.1
0.0
0.1 0.2 0.3 0.4 0.5 0.6 0.7 0.8 0.9 1.0
Fraction of Data Removed

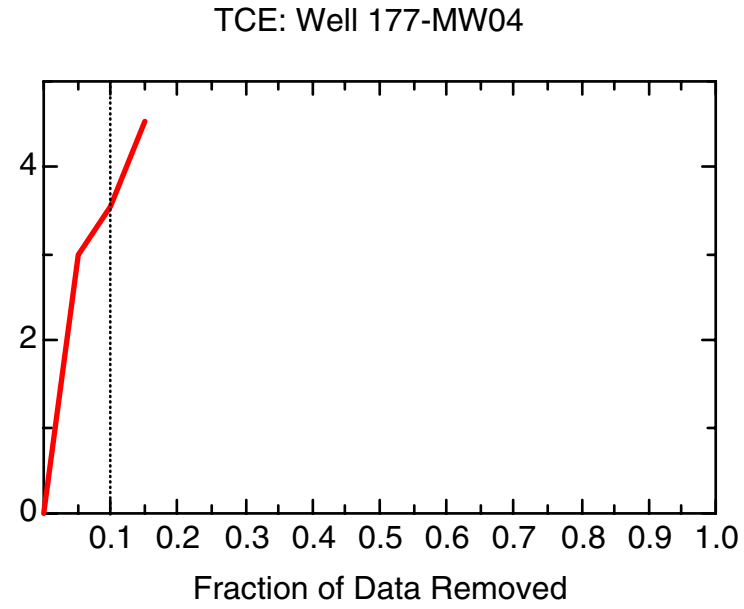
TCE: Well 177-MW04
4
2
0
0.1 0.2 0.3 0.4 0.5 0.6 0.7 0.8 0.9 1.0
Fraction of Data Removed

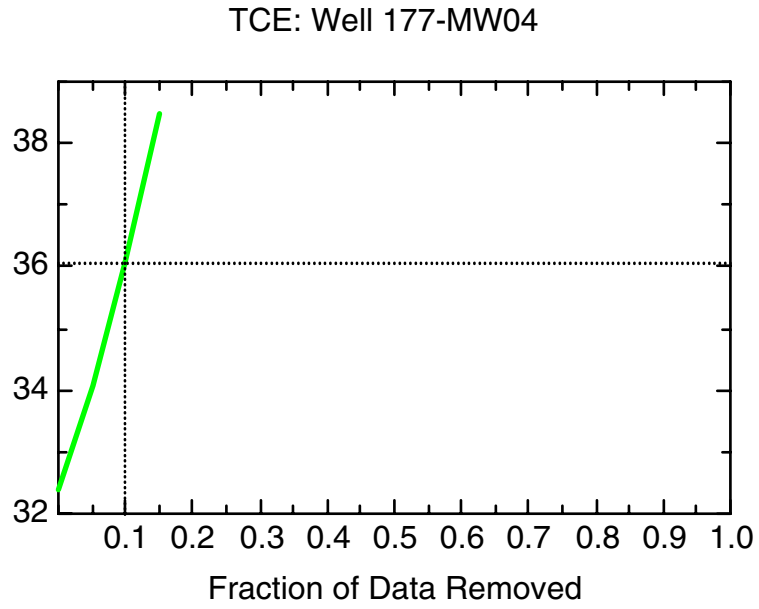
TCE: Well 177-MW04
38
36
34
32
0.1 0.2 0.3 0.4 0.5 0.6 0.7 0.8 0.9 1.0
Fraction of Data Removed

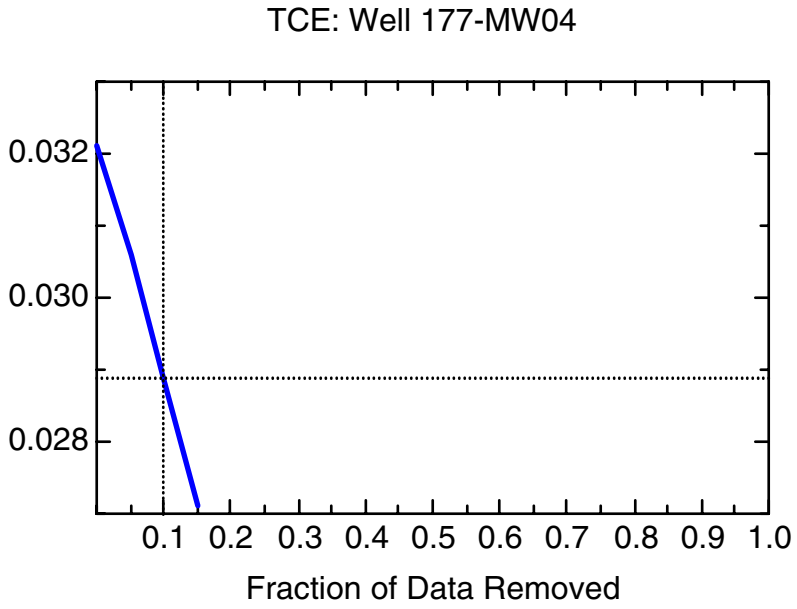
TCE: Well 177-MW04
0.032
0.030
0.028
0.1 0.2 0.3 0.4 0.5 0.6 0.7 0.8 0.9 1.0
Fraction of Data Removed

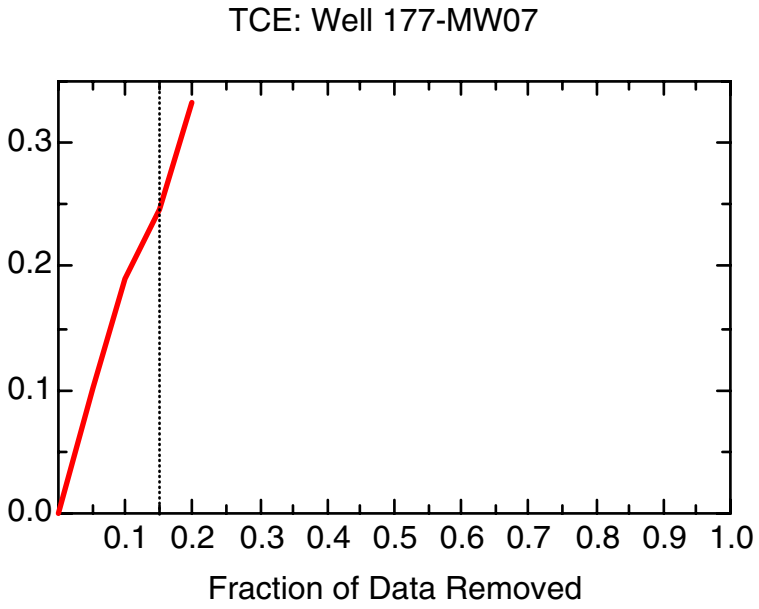
TCE: Well 177-MW07
0.3
0.2
0.1
0.0
0.1 0.2 0.3 0.4 0.5 0.6 0.7 0.8 0.9 1.0
Fraction of Data Removed

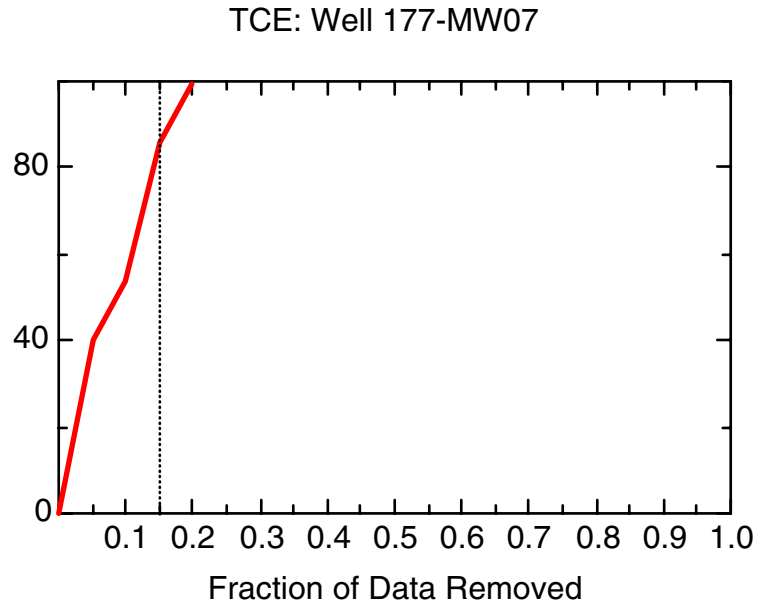
TCE: Well 177-MW07
80
40
0
0.1 0.2 0.3 0.4 0.5 0.6 0.7 0.8 0.9 1.0
Fraction of Data Removed

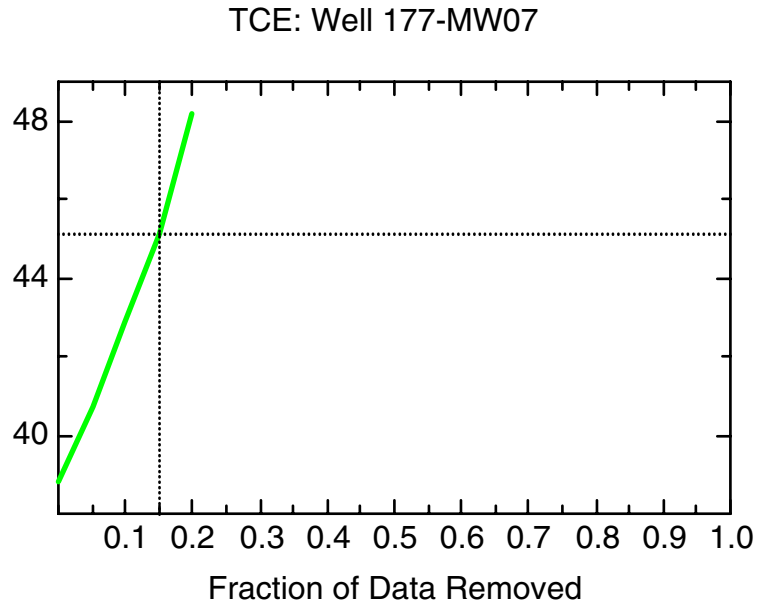
TCE: Well 177-MW07
48
44
40
0.1 0.2 0.3 0.4 0.5 0.6 0.7 0.8 0.9 1.0
Fraction of Data Removed

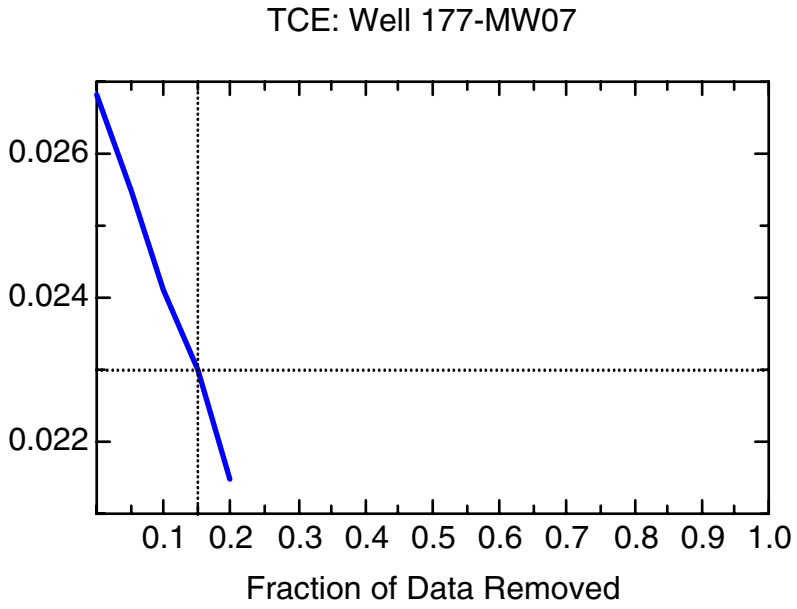
TCE: Well 177-MW07
0.026
0.024
0.022
0.1 0.2 0.3 0.4 0.5 0.6 0.7 0.8 0.9 1.0
Fraction of Data Removed

MN

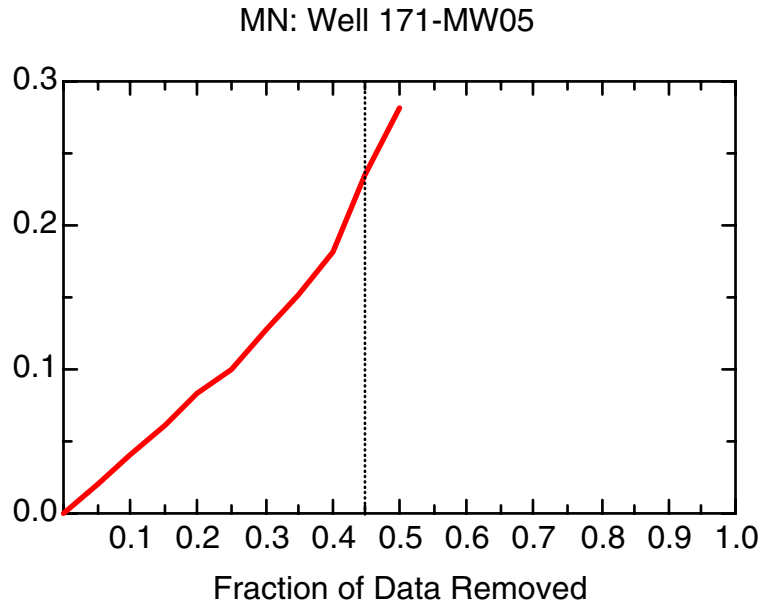
MN: Well 171-MW05
0.3
0.2
0.1
0.0
0.1 0.2 0.3 0.4 0.5 0.6 0.7 0.8 0.9 1.0
Fraction of Data Removed

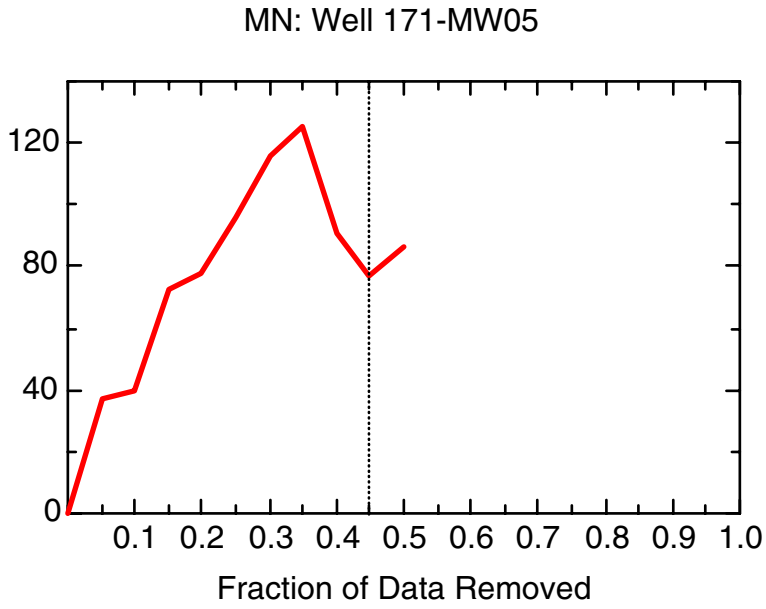
MN: Well 171-MW05
120
80
40
0
0.1 0.2 0.3 0.4 0.5 0.6 0.7 0.8 0.9 1.0
Fraction of Data Removed

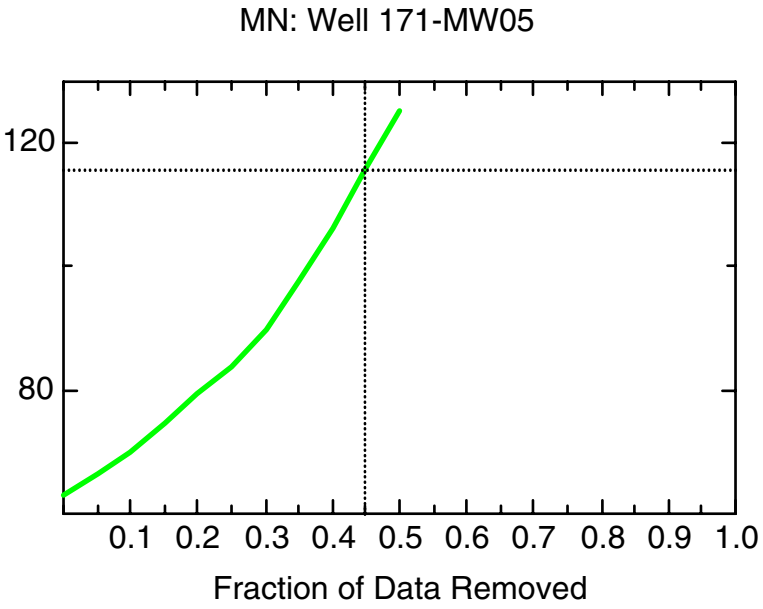
MN: Well 171-MW05
120
80
0.1 0.2 0.3 0.4 0.5 0.6 0.7 0.8 0.9 1.0
Fraction of Data Removed

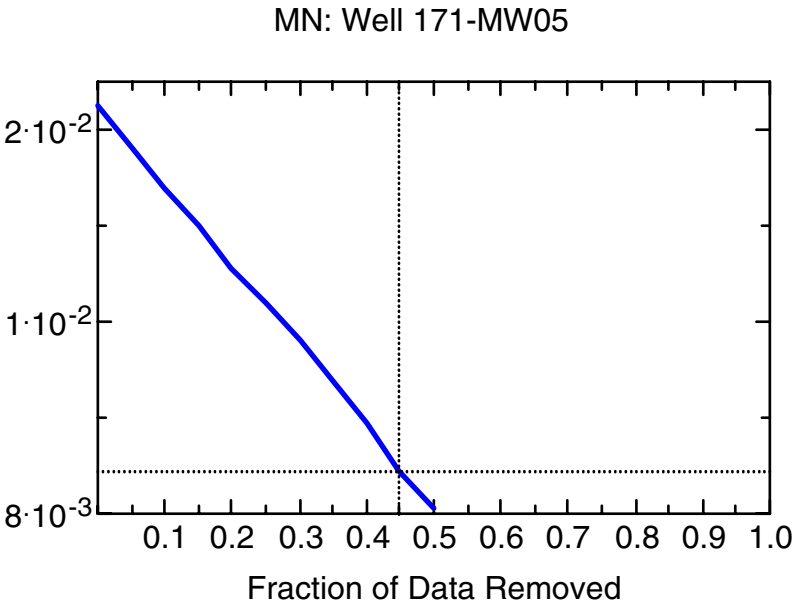
MN: Well 171-MW05
2·10-2
1·10-2
8·10-3
0.1 0.2 0.3 0.4 0.5 0.6 0.7 0.8 0.9 1.0
Fraction of Data Removed

Appendix 3.4
Trend Maps

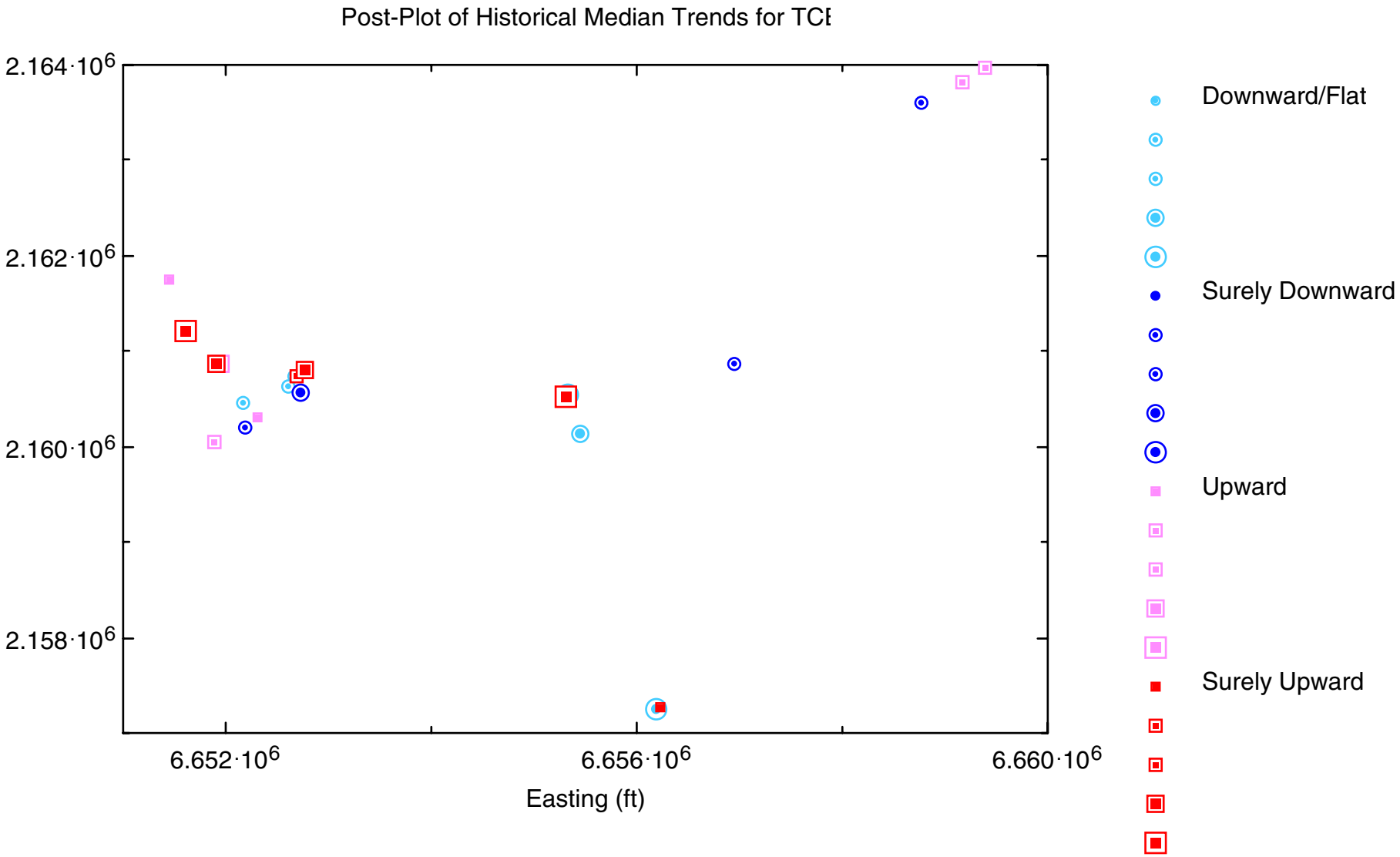
Post-Plot of Historical Median Trends for TCE
2.164·10^6
2.162·10^6
2.160·10^6
2.158·10^6
6.652·10^6
6.656·10^6
6.660·10^6
Easting (ft)
Downward/Flat
Surely Downward
Upward
Surely Upward

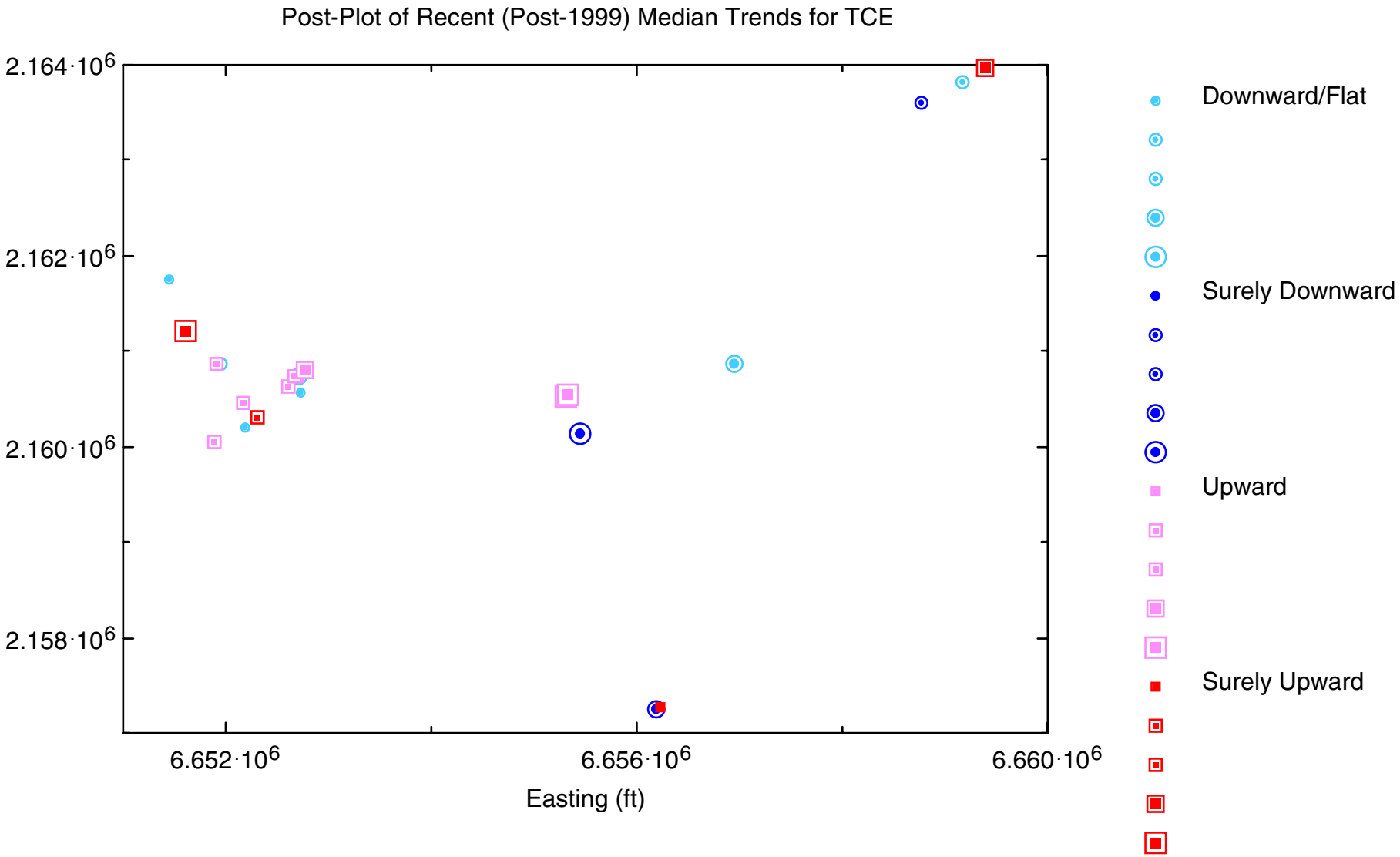
Post-Plot of Recent (Post-1999) Median Trends for TCE
2.164·10^6
2.162·10^6
2.160·10^6
2.158·10^6
6.652·10^6
6.656·10^6
6.660·10^6
Easting (ft)
Downward/Flat
Surely Downward
Upward
Surely Upward

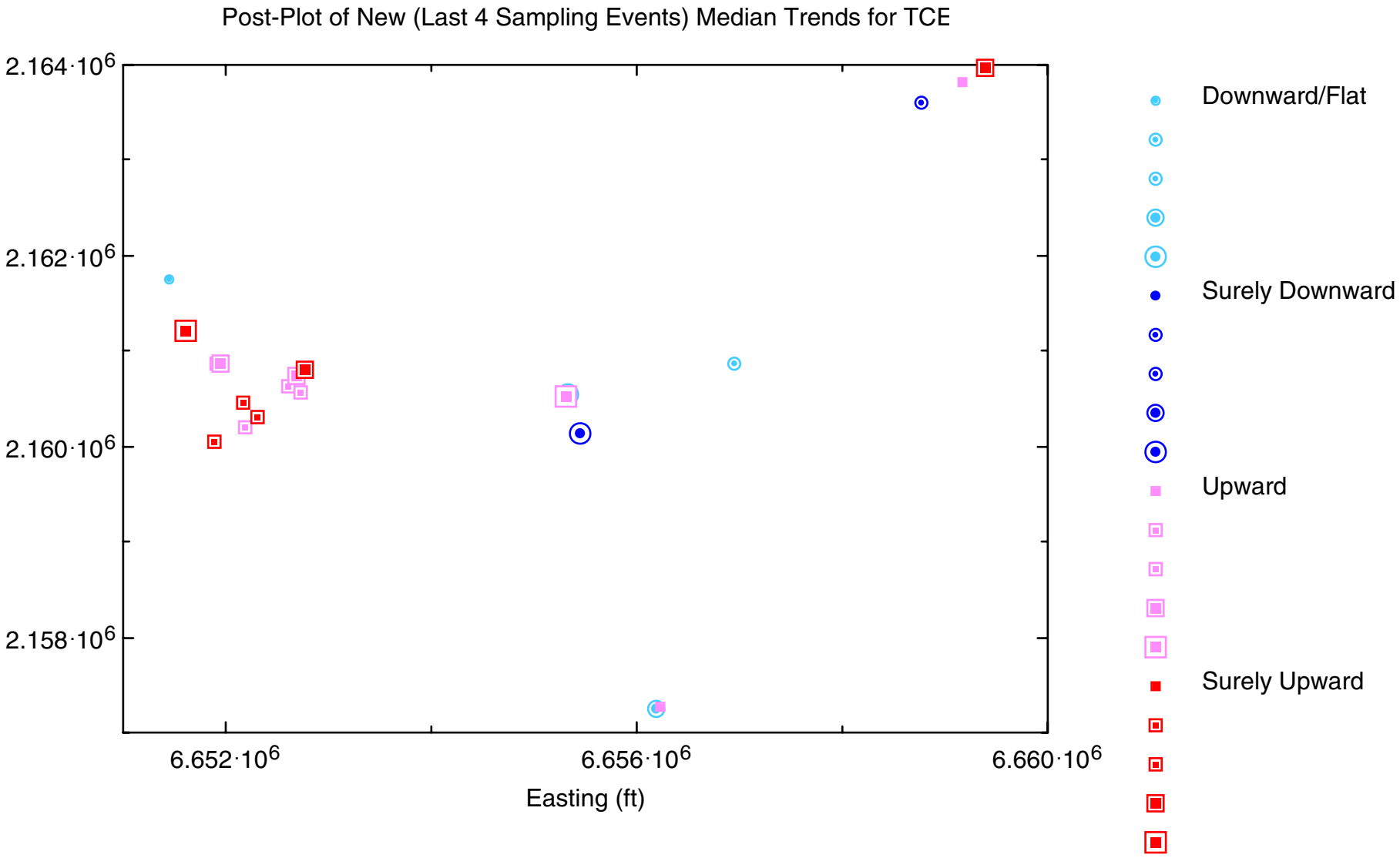
Post-Plot of New (Last 4 Sampling Events) Median Trends for TCE
2.164·10^6
2.162·10^6
2.160·10^6
2.158·10^6
6.652·10^6
6.656·10^6
6.660·10^6
Easting (ft)
Downward/Flat
Surely Downward
Upward
Surely Upward

Appendix 4.1
Global Redundancy Measures

TCE

EDWARDS AFB, SITE 133: TCE TRENDS IN GLOBAL VARIANCE

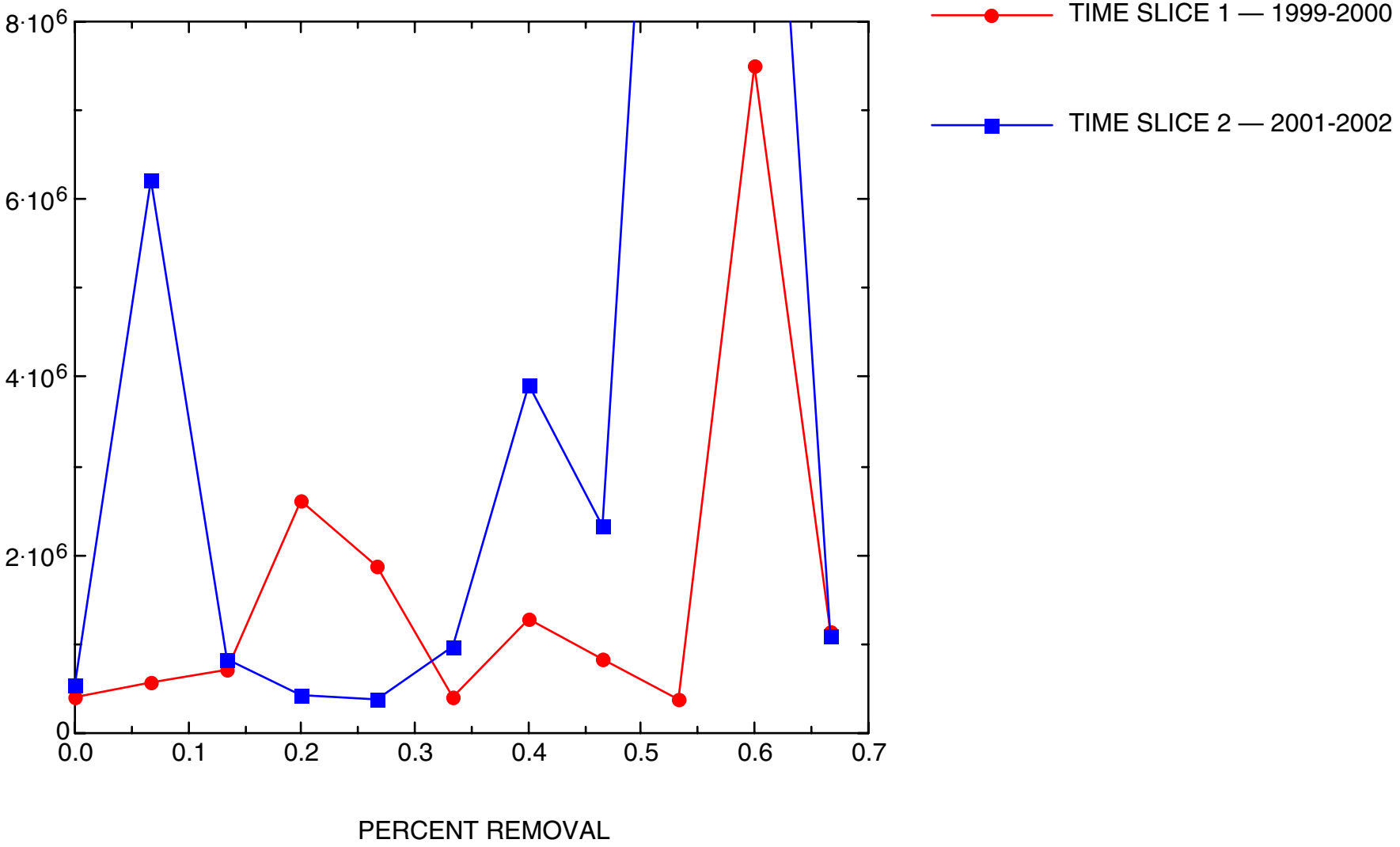

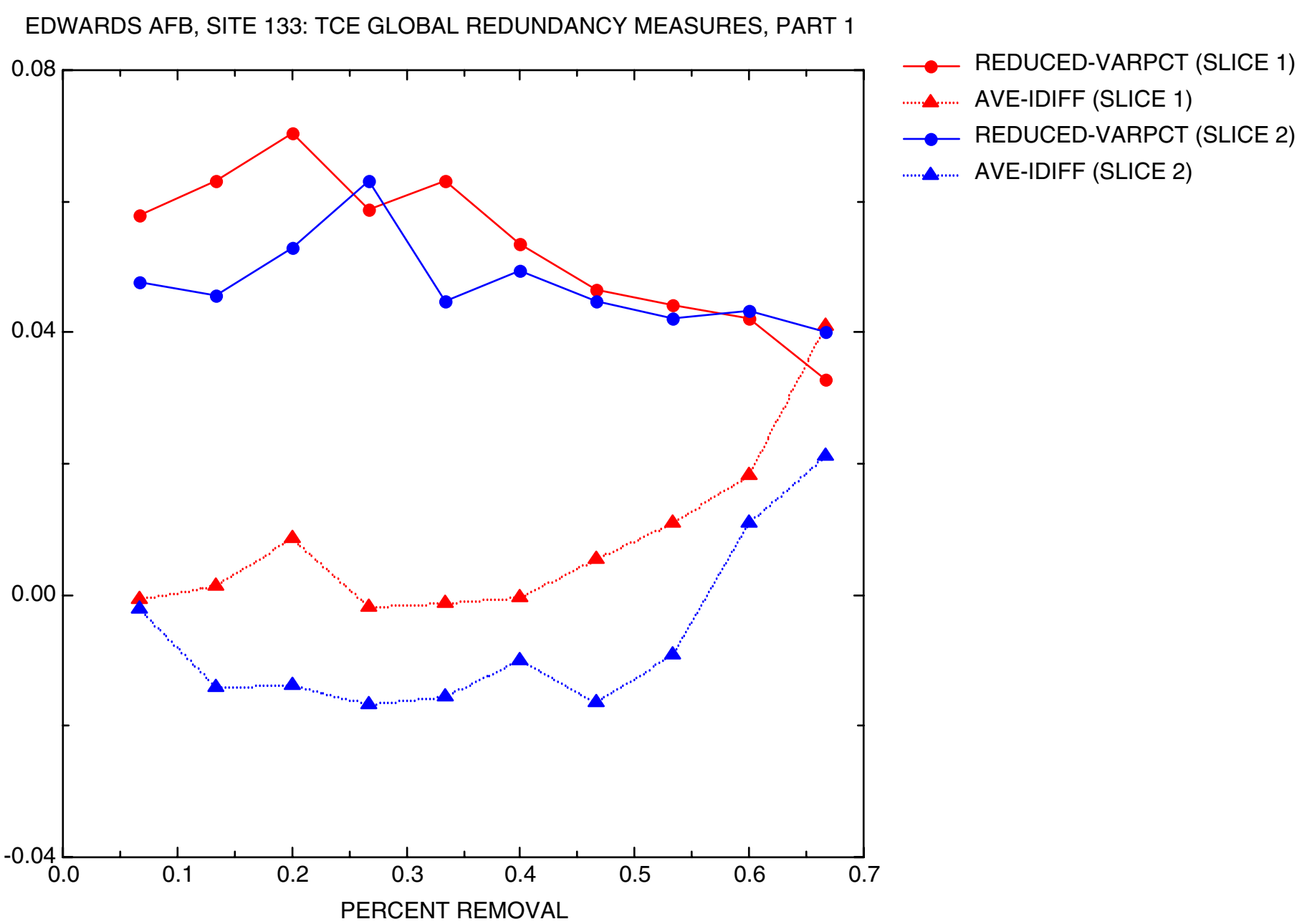
EDWARDS AFB, SITE 133: TCE GLOBAL REDUNDANCY MEASURES, PART 1
0.08
0.04
0.00
-0.04
0.0
0.1
0.2
0.3
0.4
0.5
0.6
0.7
PERCENT REMOVAL
REDUCED-VARPCT (SLICE 1)
AVE-IDIFF (SLICE 1)
REDUCED-VARPCT (SLICE 2)
AVE-IDIFF (SLICE 2)

EDWARDS AFB, SITE 133: TCE GLOBAL REDUNDANCY MEASURES, PART 2

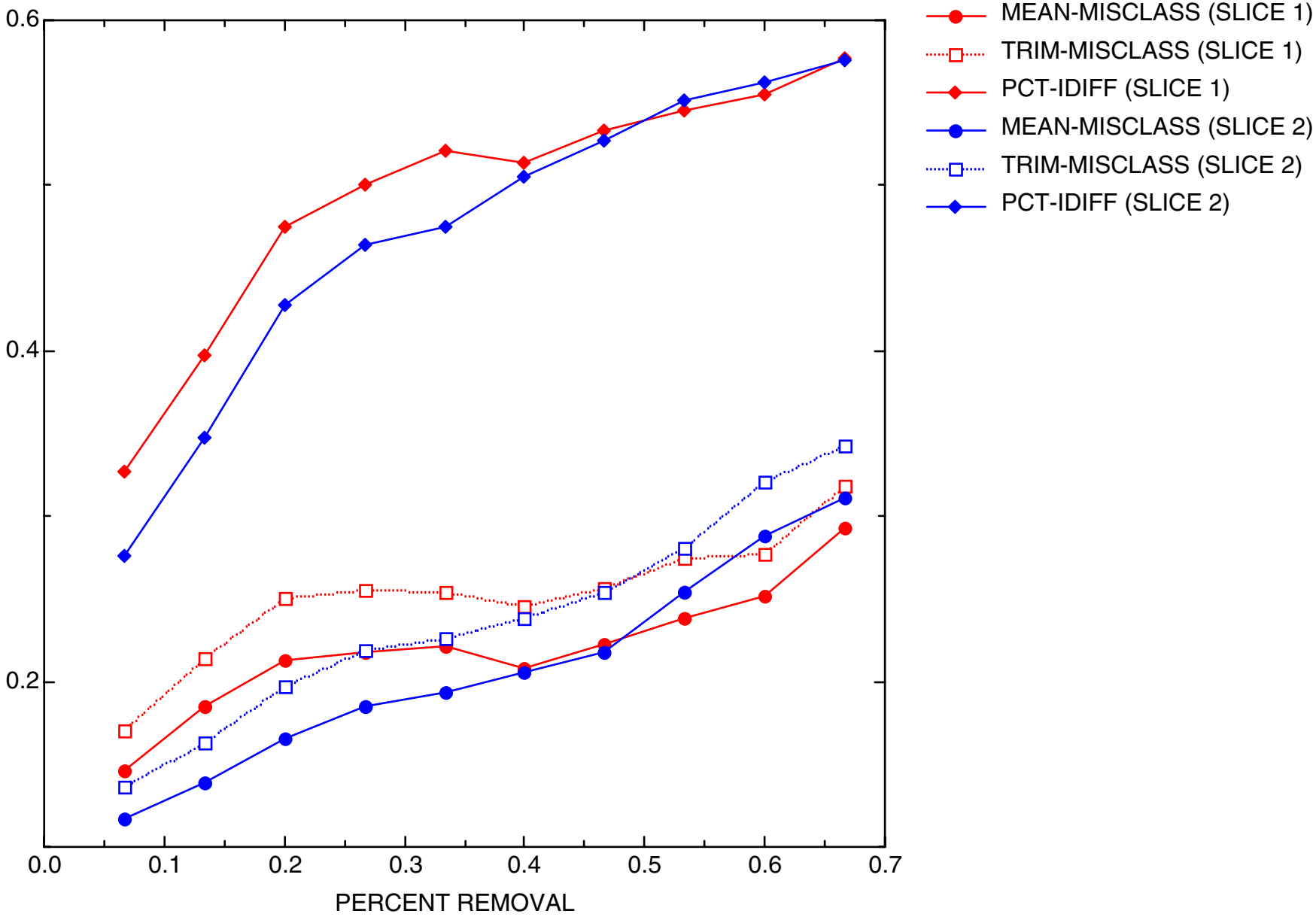

MN

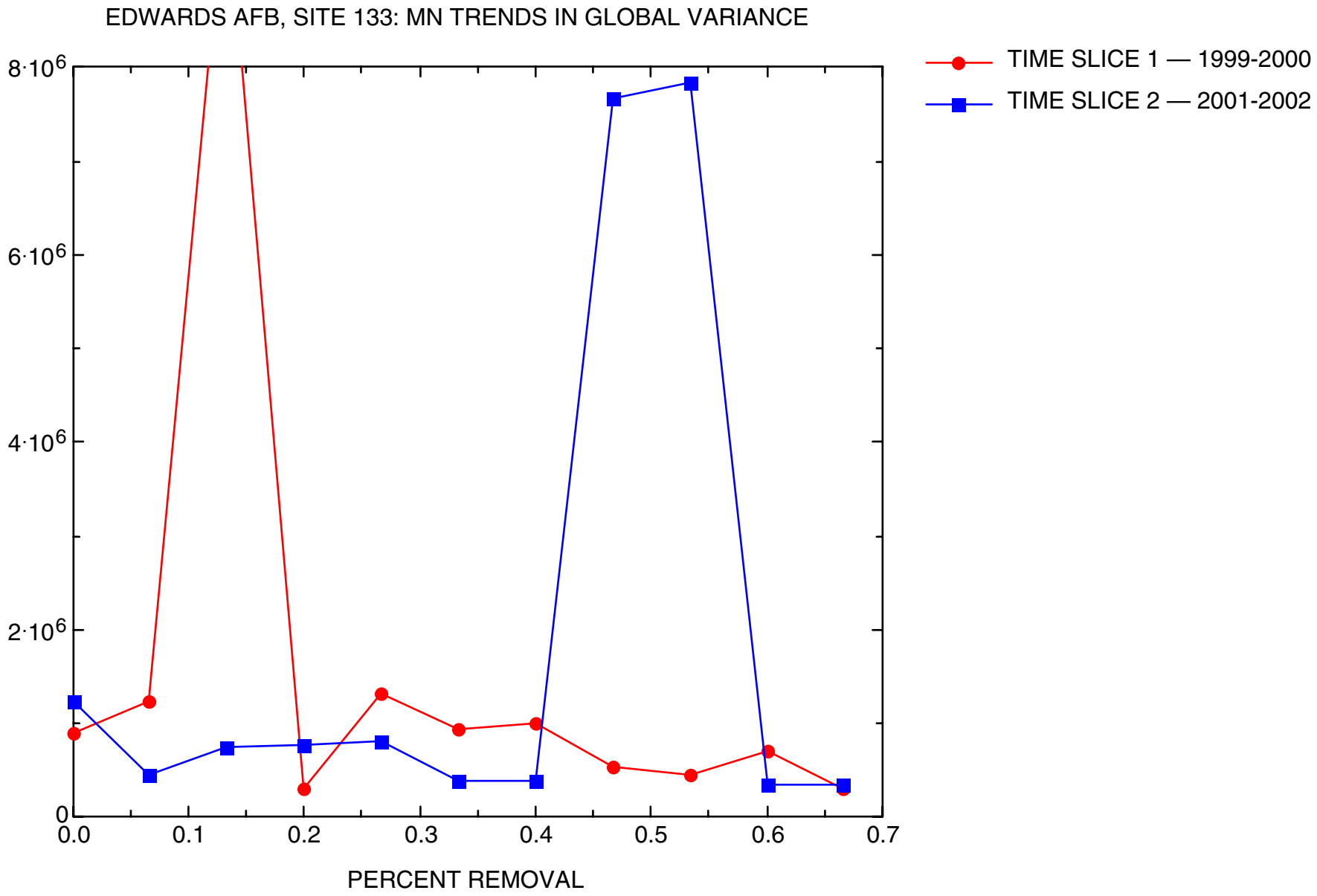
EDWARDS AFB, SITE 133: MN TRENDS IN GLOBAL VARIANCE
TIME SLICE 1 — 1999-2000
TIME SLICE 2 — 2001-2002
8·10^6
6·10^6
4·10^6
2·10^6
0
0.0
0.1
0.2
0.3
0.4
0.5
0.6
0.7
PERCENT REMOVAL

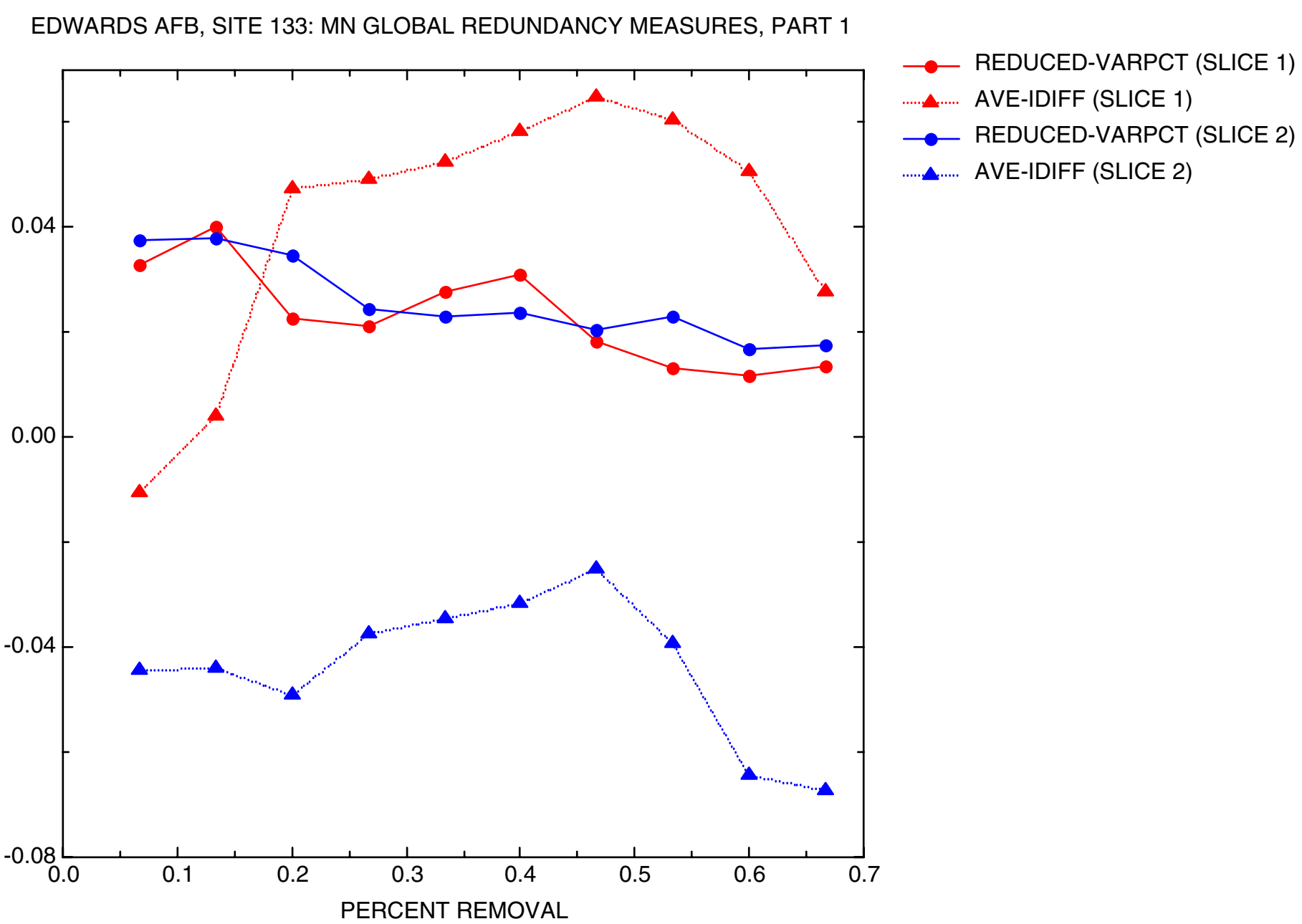
EDWARDS AFB, SITE 133: MN GLOBAL REDUNDANCY MEASURES, PART 1
REDUCED-VARPCT (SLICE 1)
AVE-IDIFF (SLICE 1)
REDUCED-VARPCT (SLICE 2)
AVE-IDIFF (SLICE 2)
0.04
0.00
-0.04
-0.08
0.0
0.1
0.2
0.3
0.4
0.5
0.6
0.7
PERCENT REMOVAL

EDWARDS AFB, SITE 133: MN GLOBAL REDUNDANCY MEASURES, PART 2

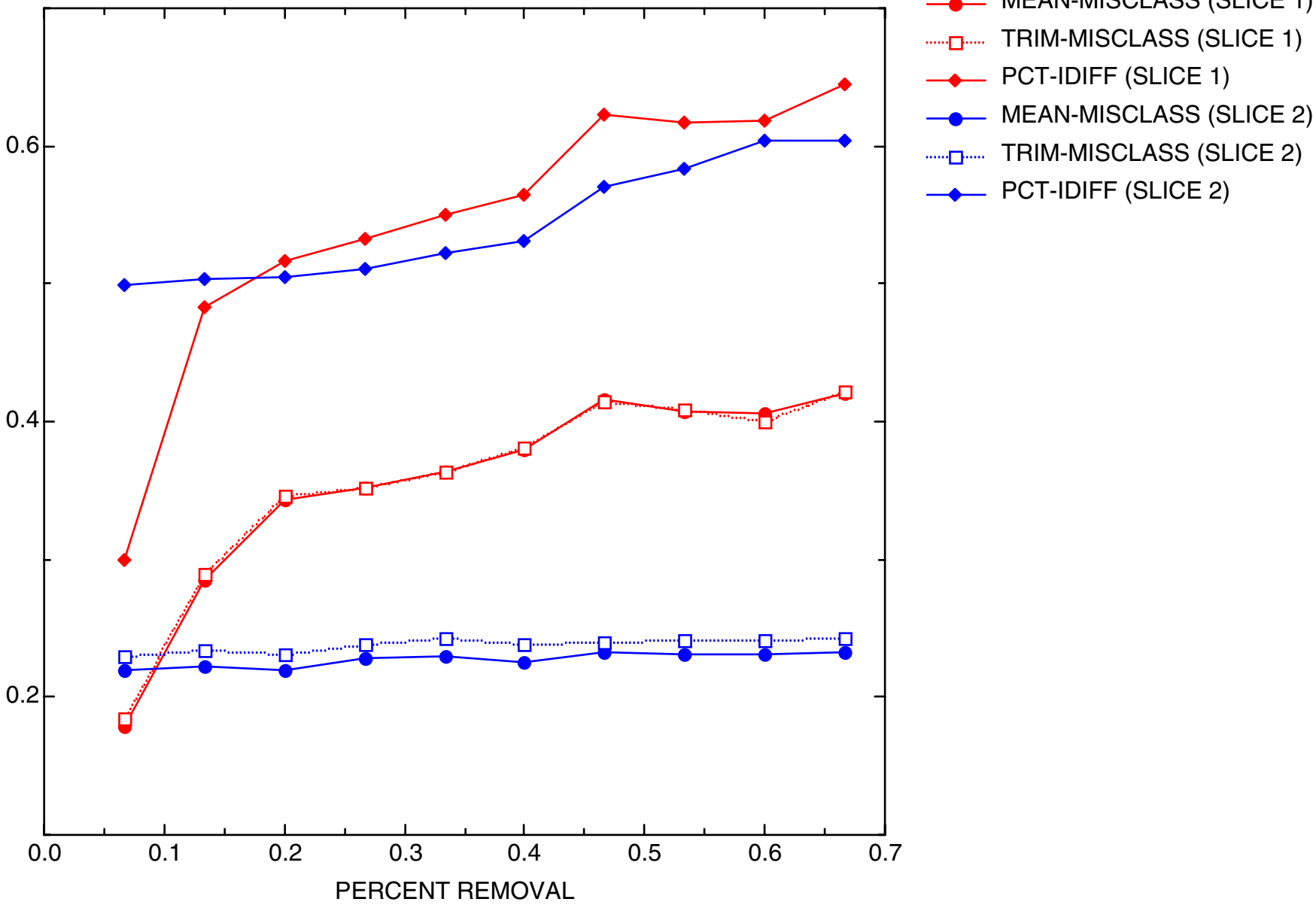

DIOXANE14

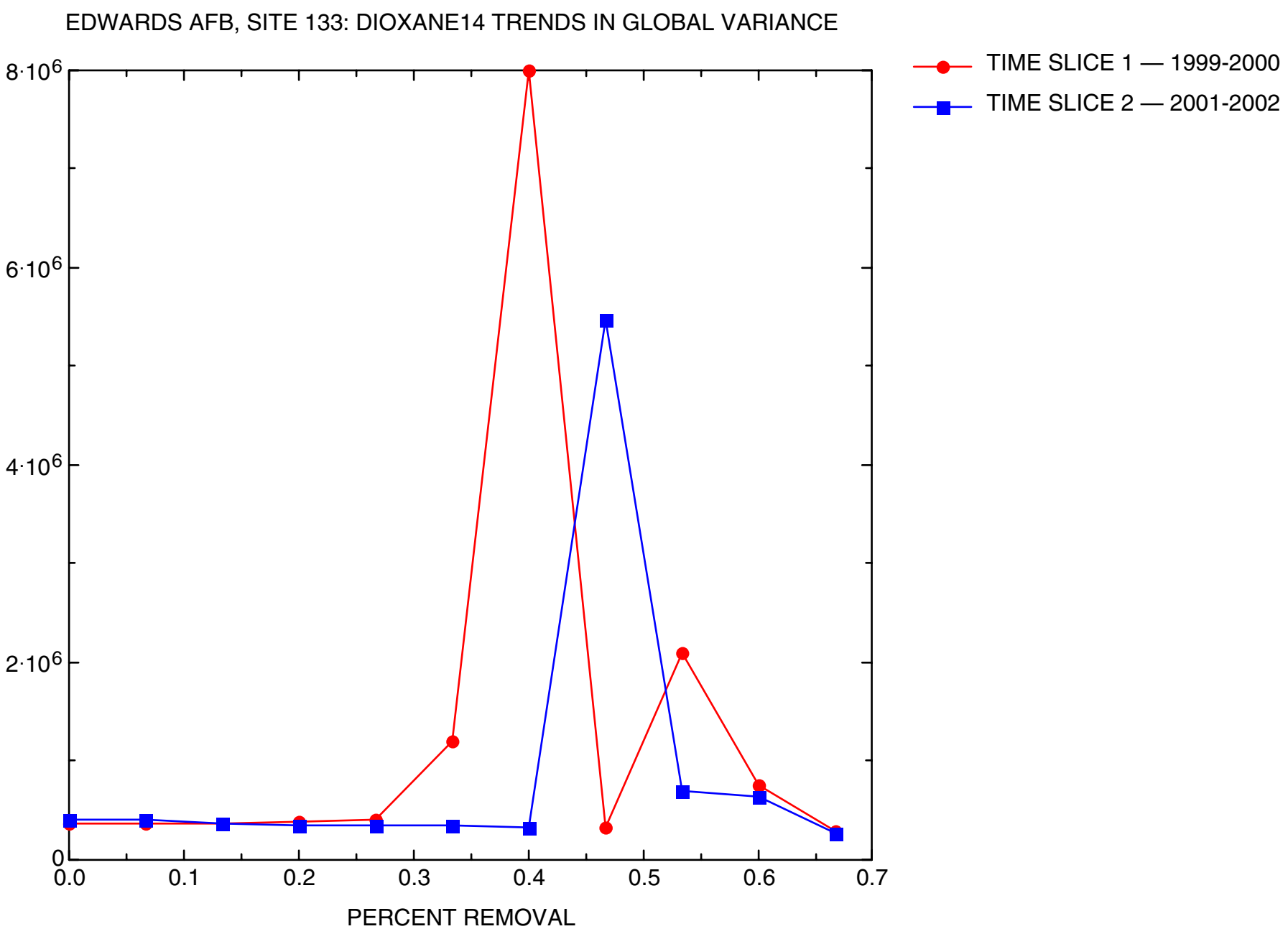
EDWARDS AFB, SITE 133: DIOXANE14 TRENDS IN GLOBAL VARIANCE
TIME SLICE 1 — 1999-2000
TIME SLICE 2 — 2001-2002
8·10^6
6·10^6
4·10^6
2·10^6
0
0.0
0.1
0.2
0.3
0.4
0.5
0.6
0.7
PERCENT REMOVAL

EDWARDS AFB, SITE 133: DIOXANE14 GLOBAL REDUNDANCY MEASURES, PART 1

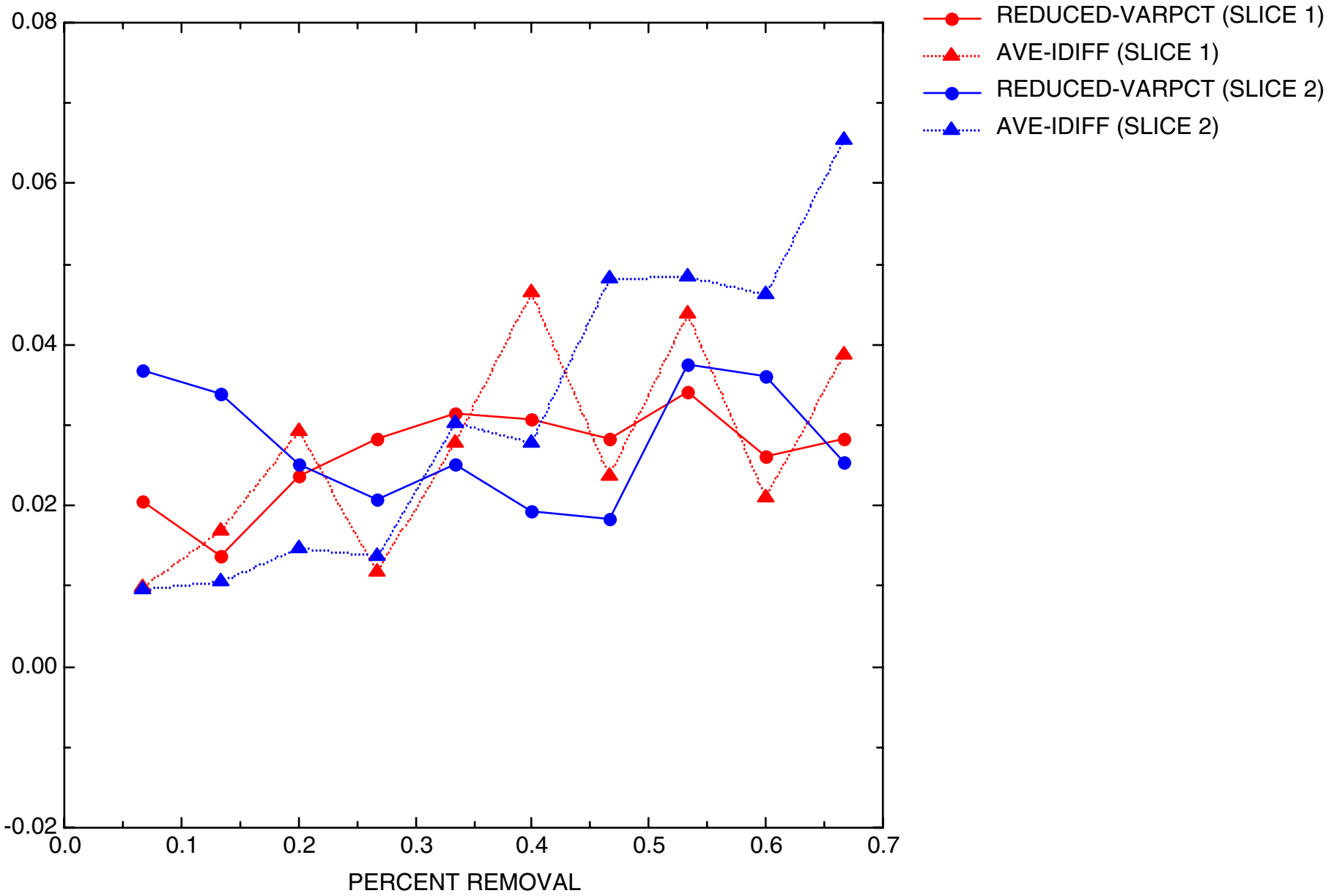

EDWARDS AFB, SITE 133: DIOXANE14 GLOBAL REDUNDANCY MEASURES, PART 2

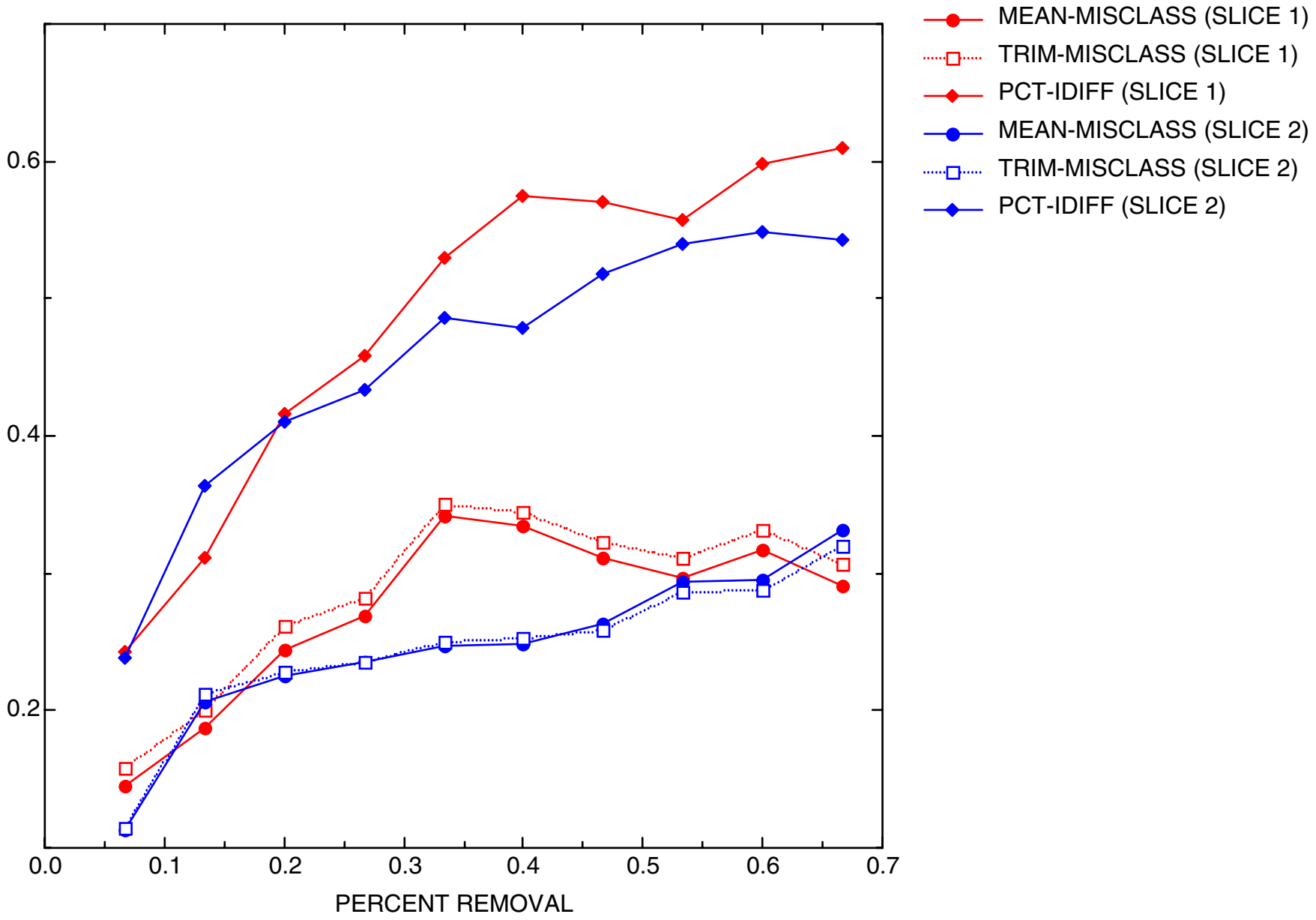

Appendix 4.2
DIOXANE14 Indicator Difference Maps
Time Slice 1

Site 133: DIOXANE14 Indicator Differences, 1999-2000, 7% Removal

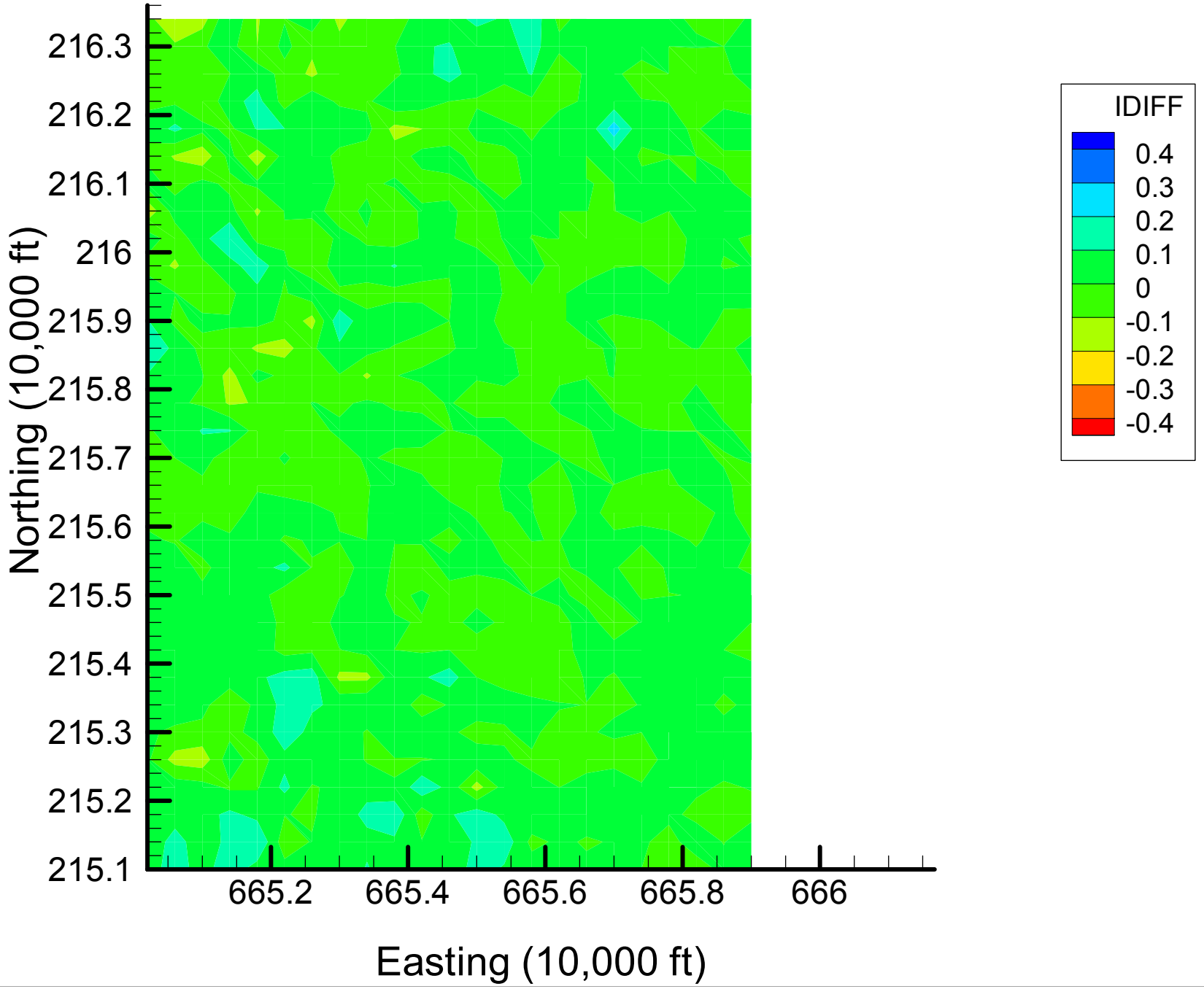

Site 133: DIOXANE14 Indicator Differences, 1999-2000, 13% Removal

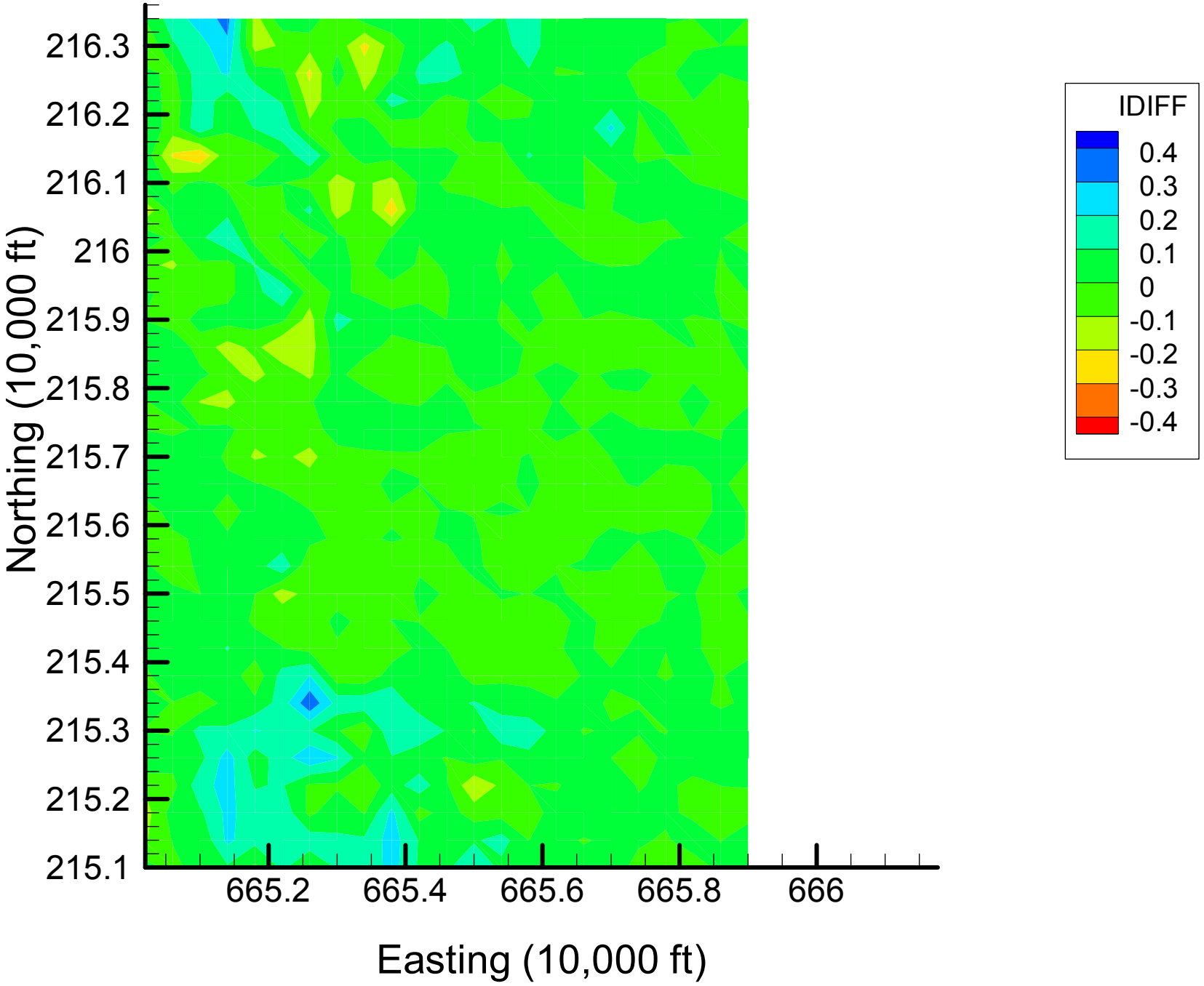

Site 133: DIOXANE14 Indicator Differences, 1999-2000, 20% Removal

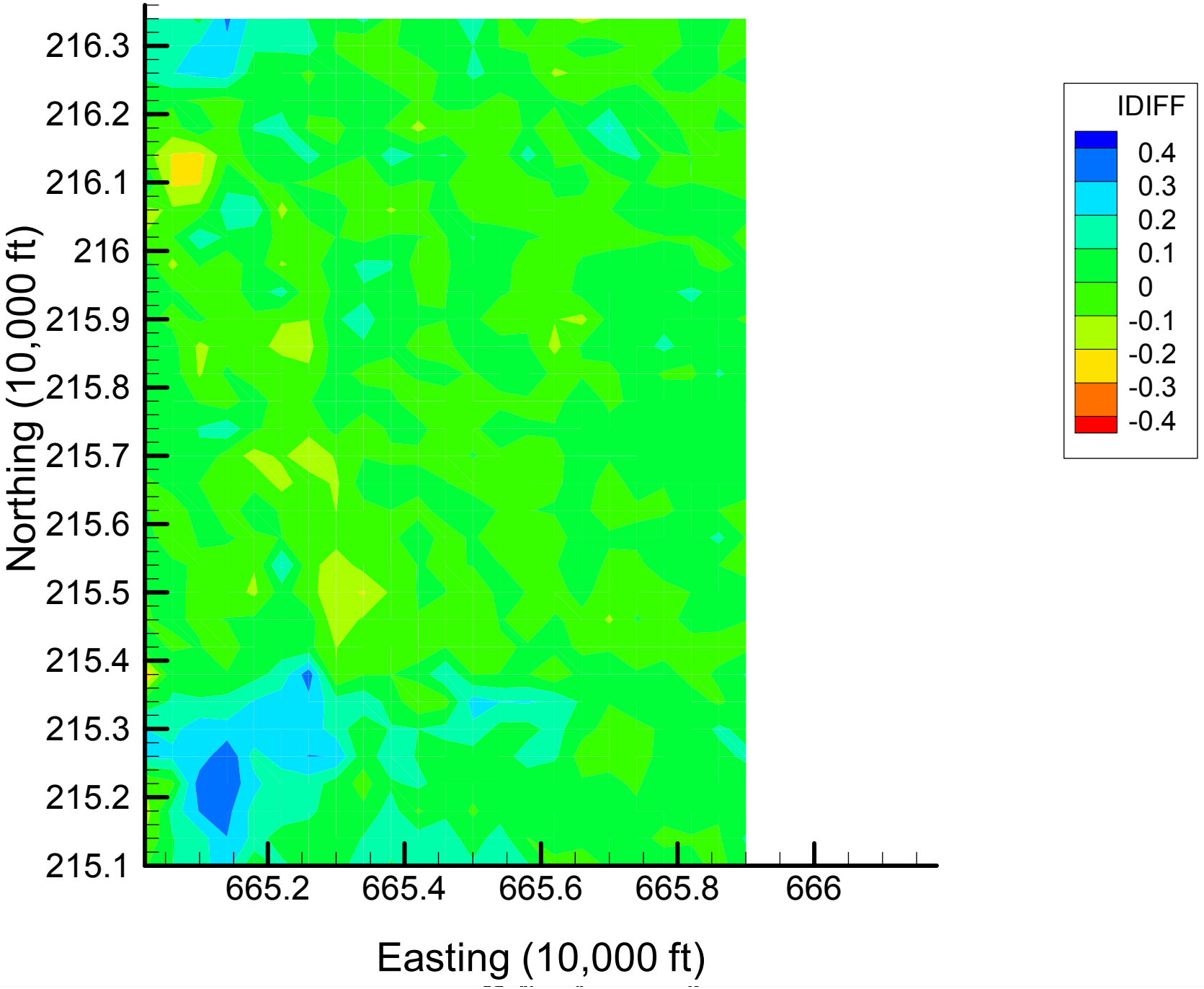

Site 133: DIOXANE14 Indicator Differences, 1999-2000, 27% Removal

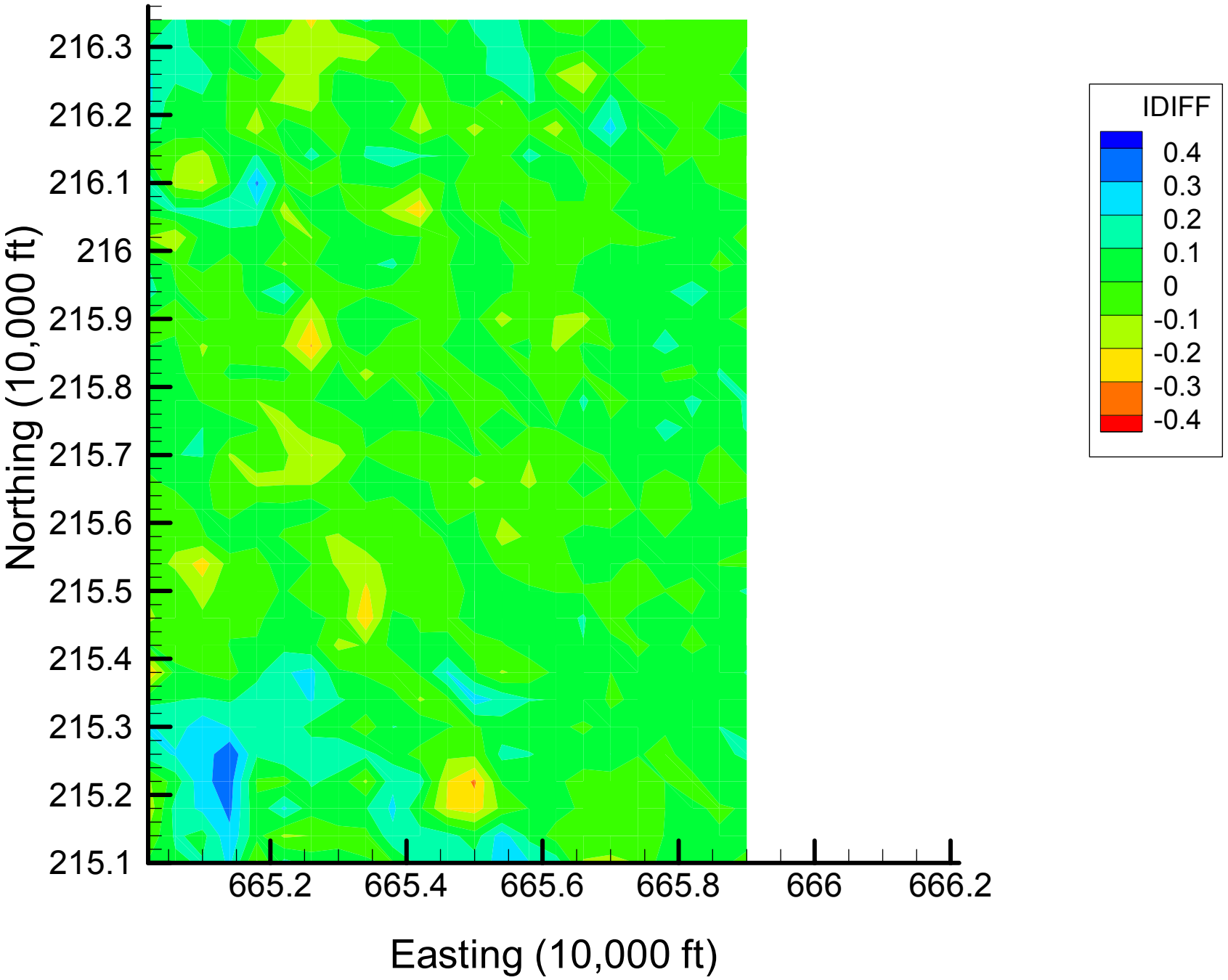

Site 133: DIOXANE14 Indicator Differences, 1999-2000, 33% Removal

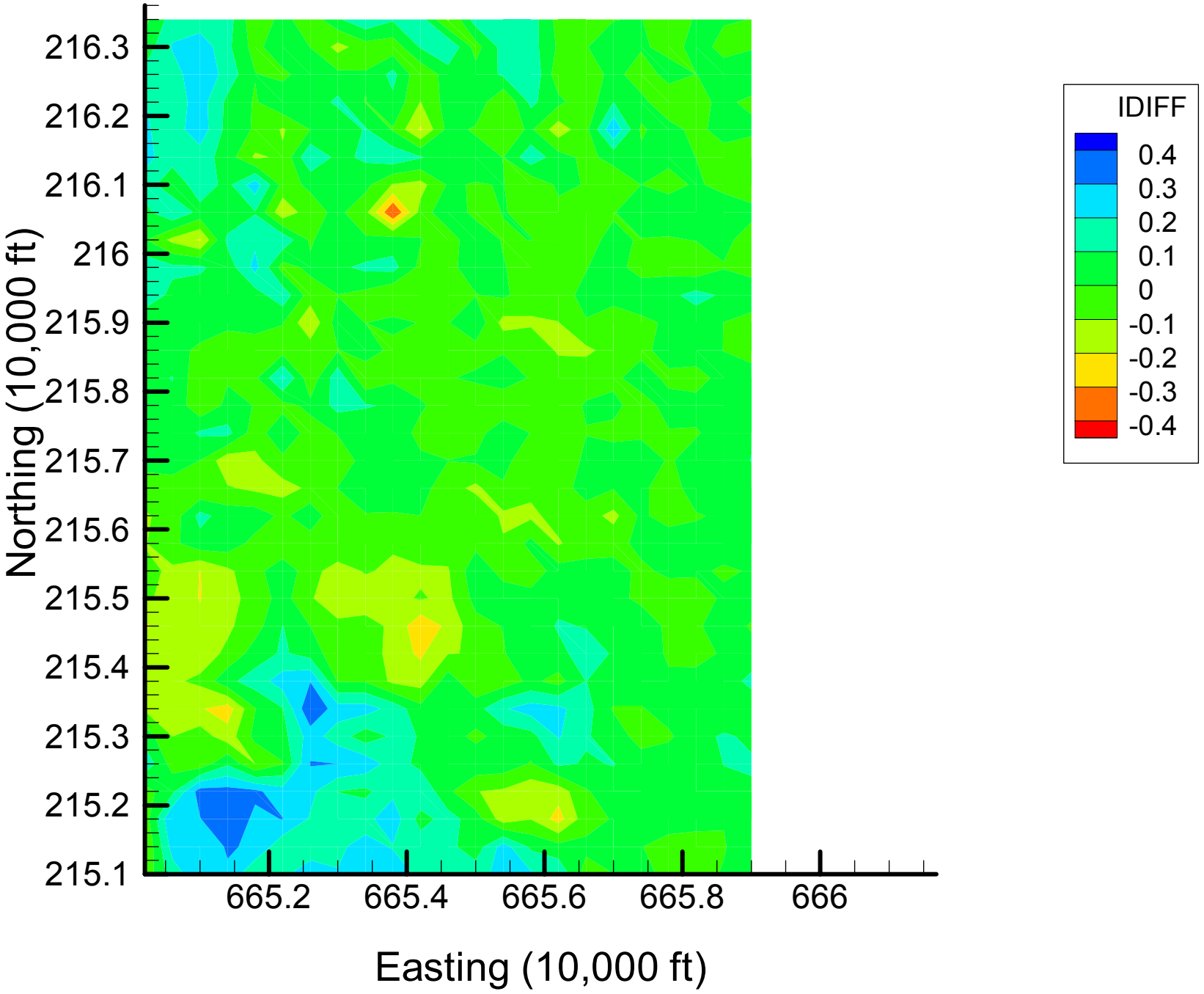

Site 133: DIOXANE14 Indicator Differences, 1999-2000, 40% Removal

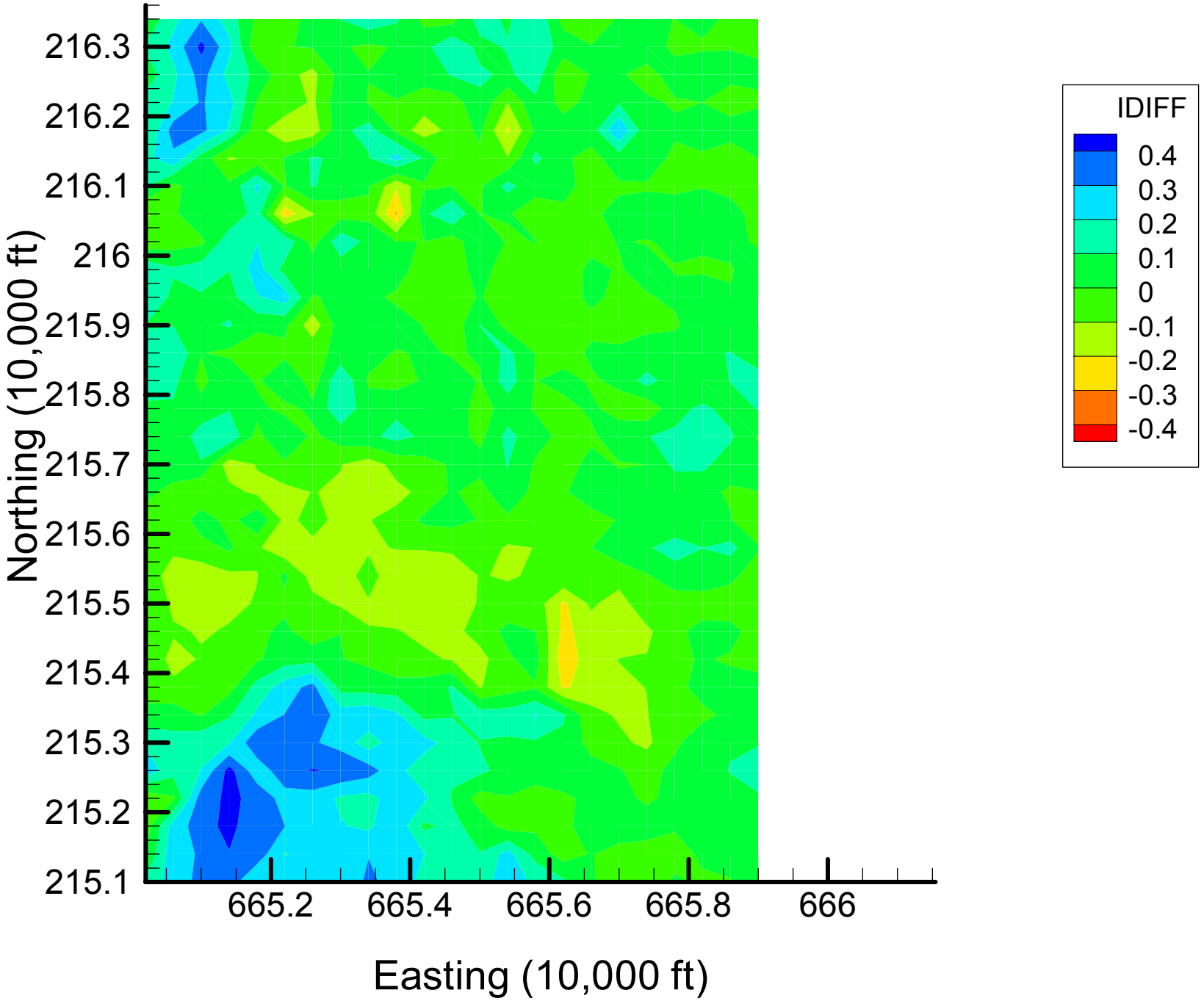

Site 133: DIOXANE14 Indicator Differences, 1999-2000, 47% Removal

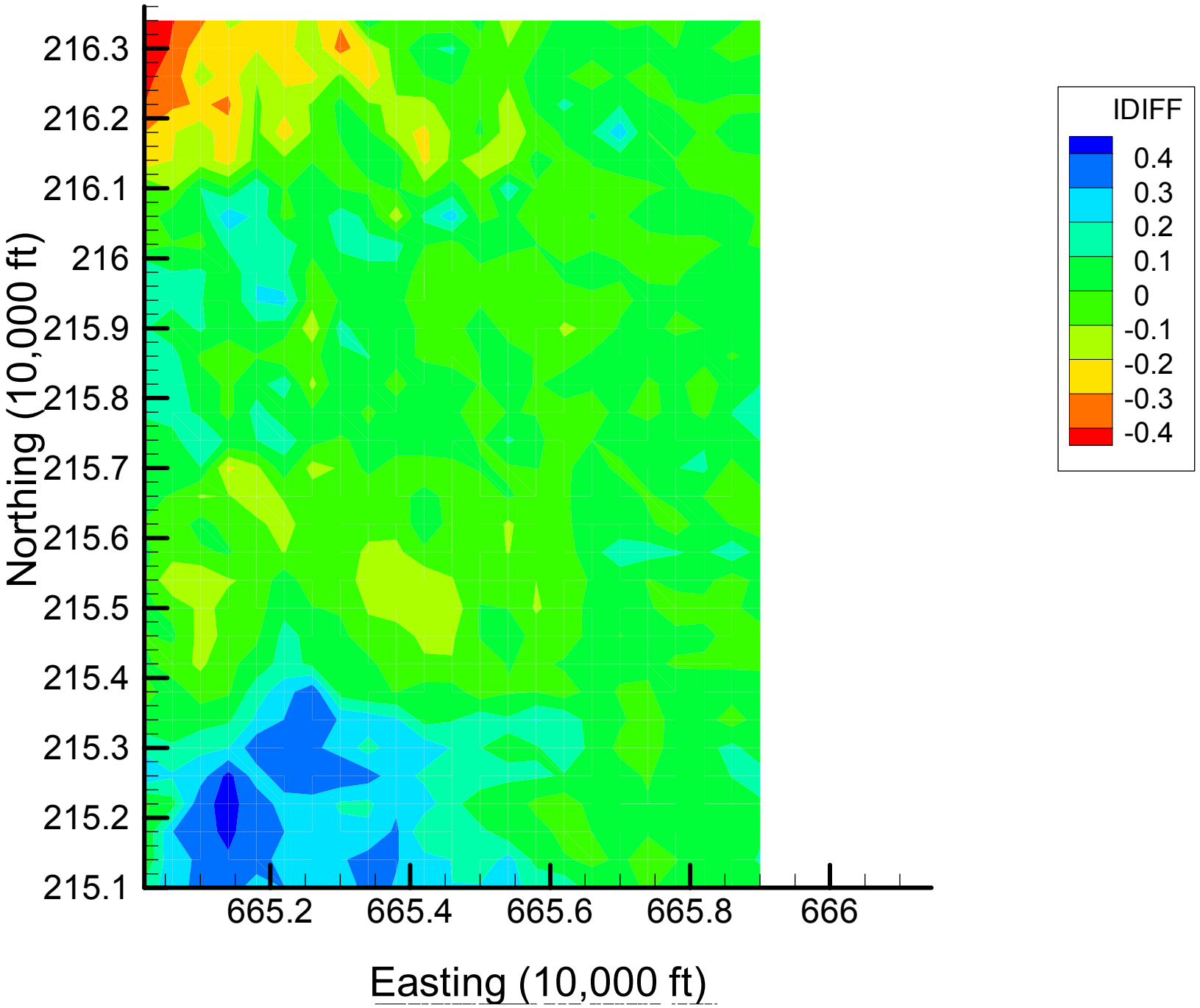

Site 133: DIOXANE14 Indicator Differences, 1999-2000, 53% Removal

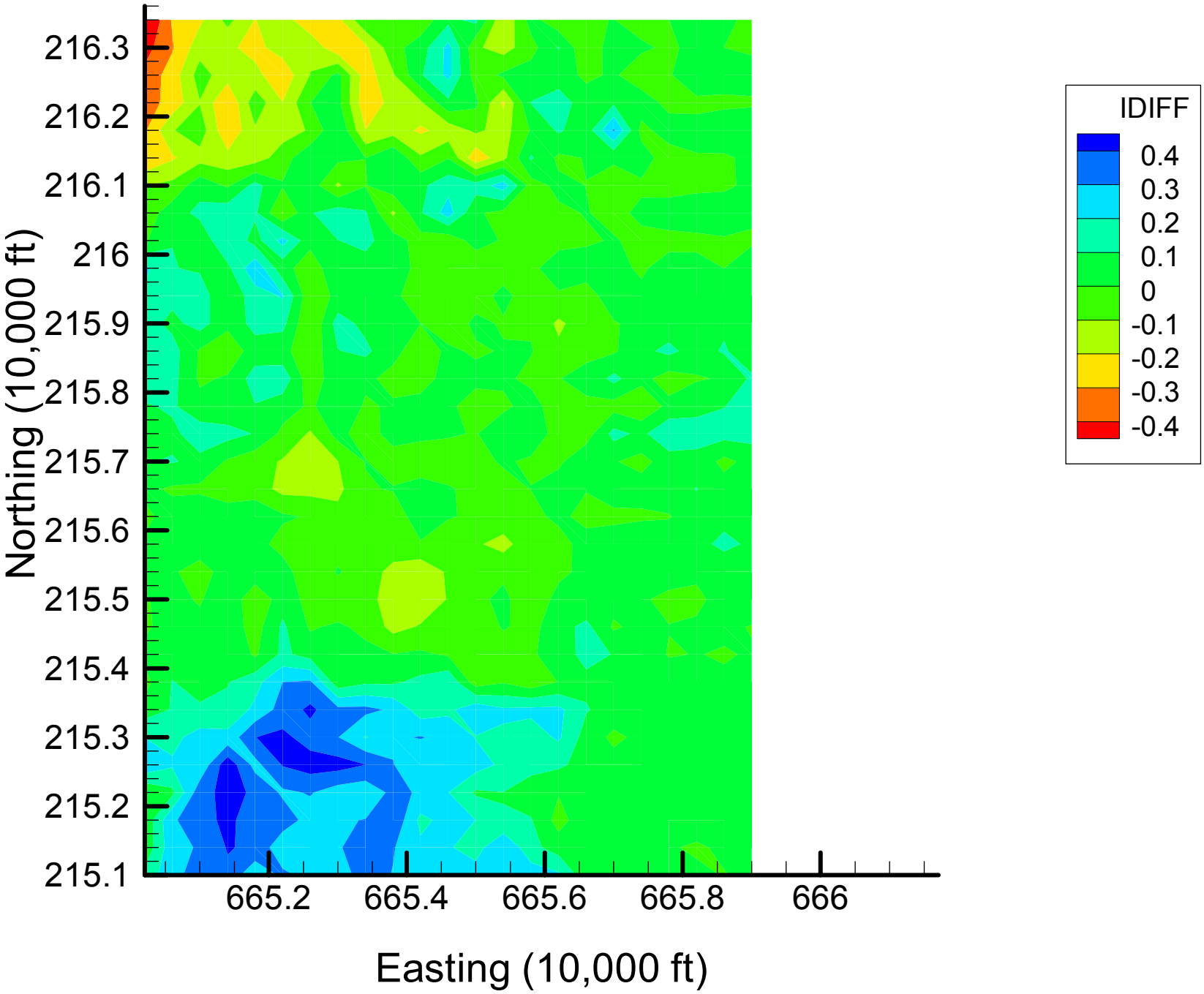

Site 133: DIOXANE14 Indicator Differences, 1999-2000, 60% Removal

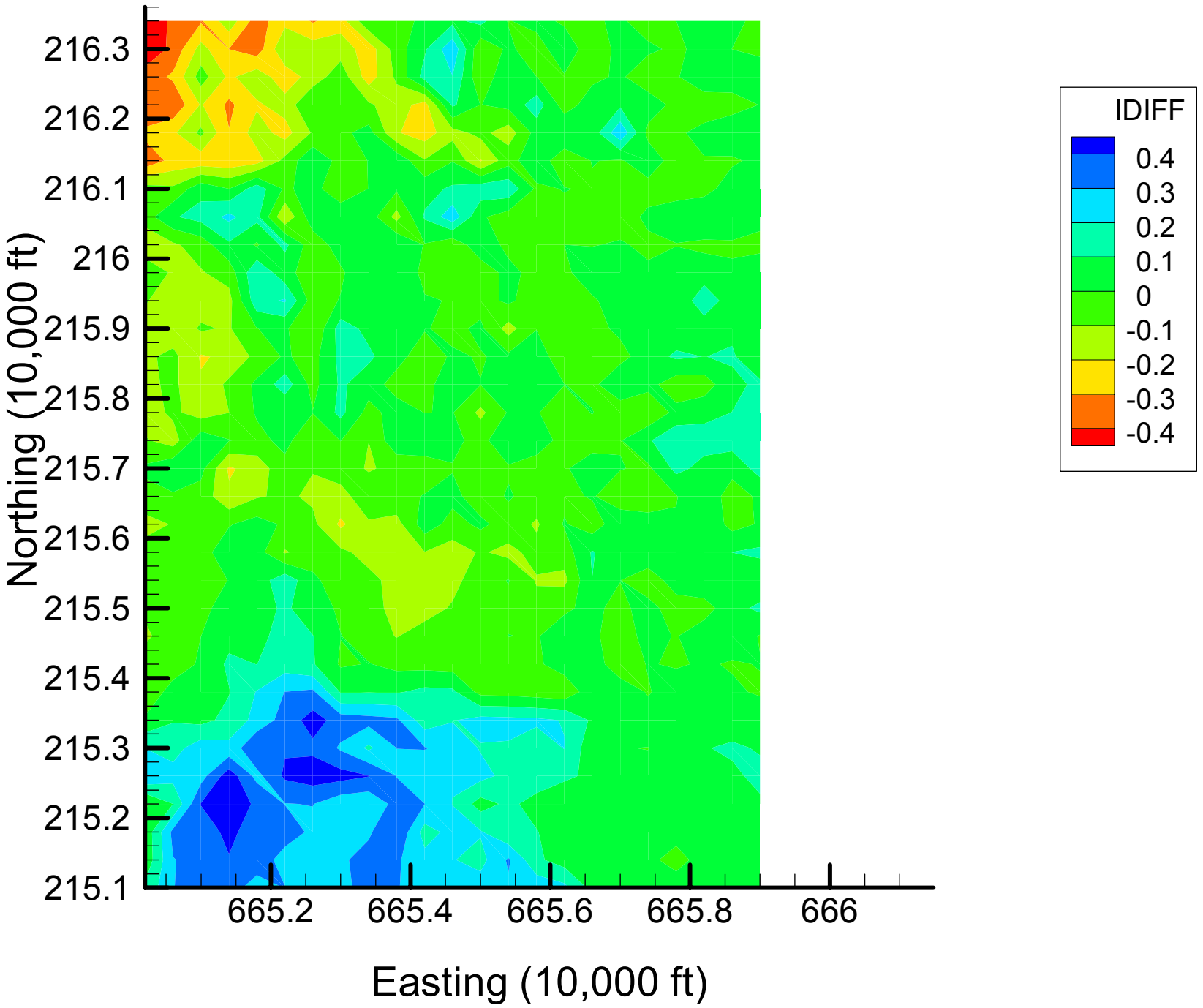

Site 133: DIOXANE14 Indicator Differences, 1999-2000, 67% Removal

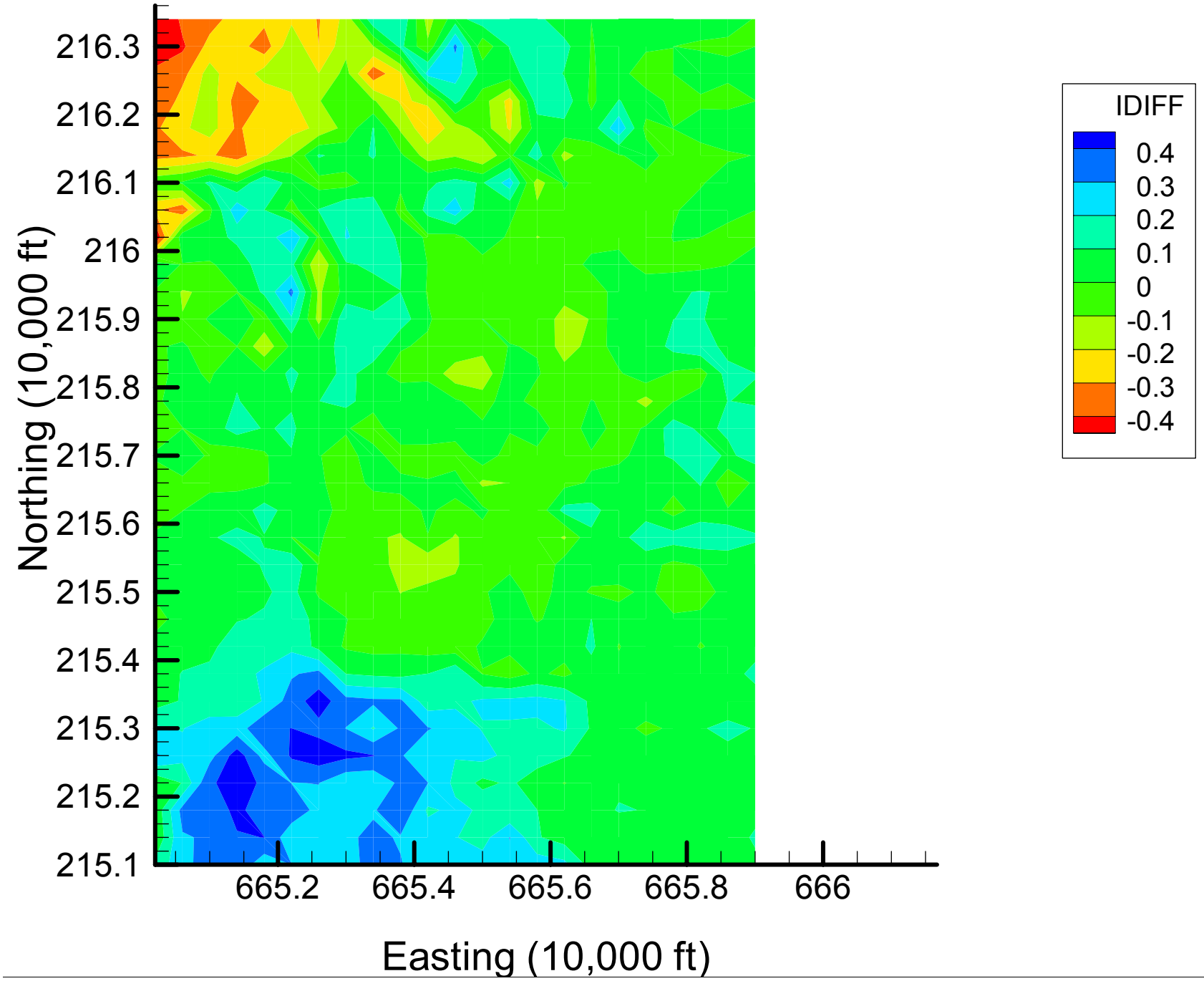

Appendix 4.2
DIOXANE14 Indicator Difference Maps
Time Slice 2

Site 133: DIOXANE14 Indicator Differences, 2001-2002, 7% Removal

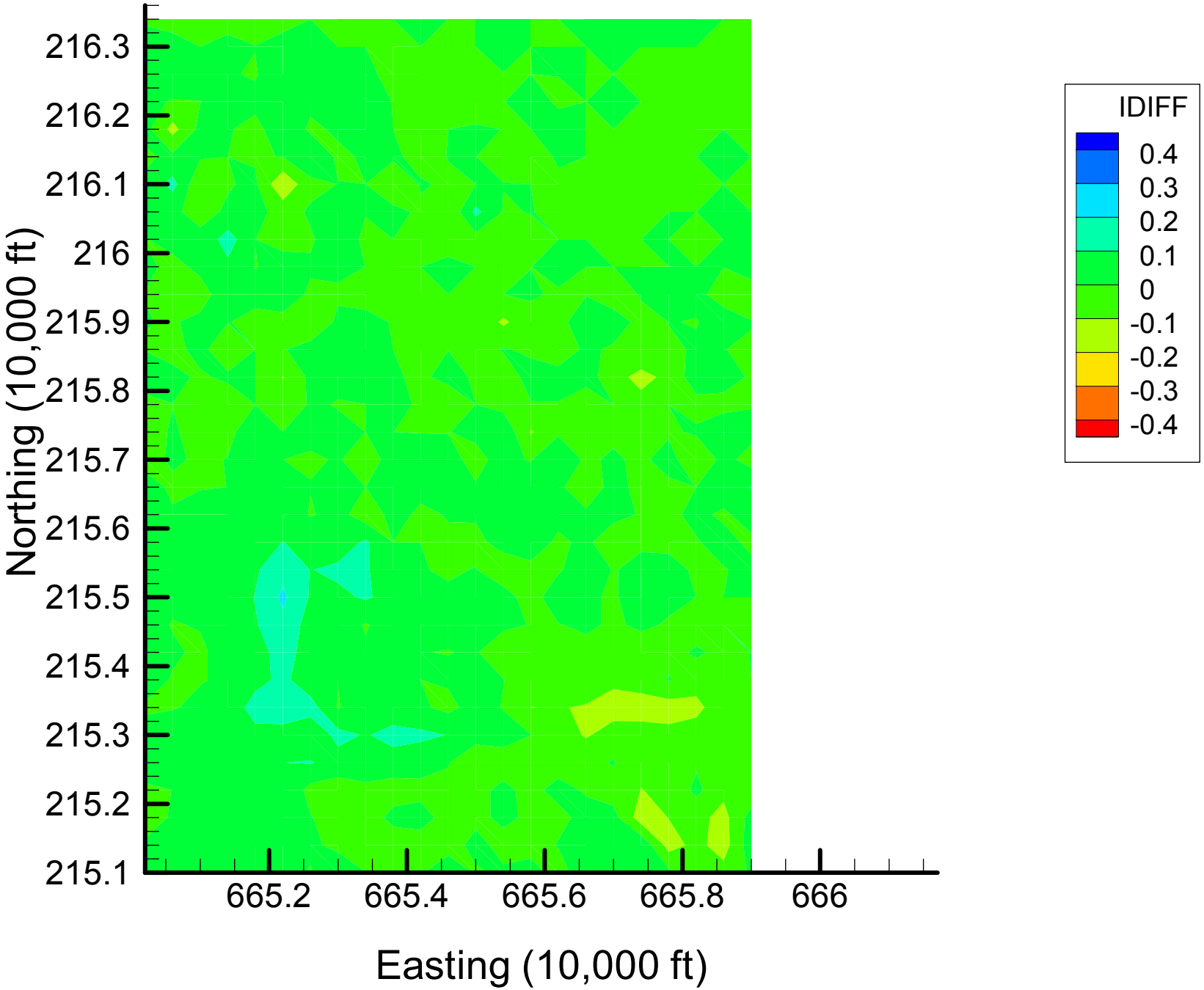

Site 133: DIOXANE14 Indicator Differences, 2001-2002, 13% Removal

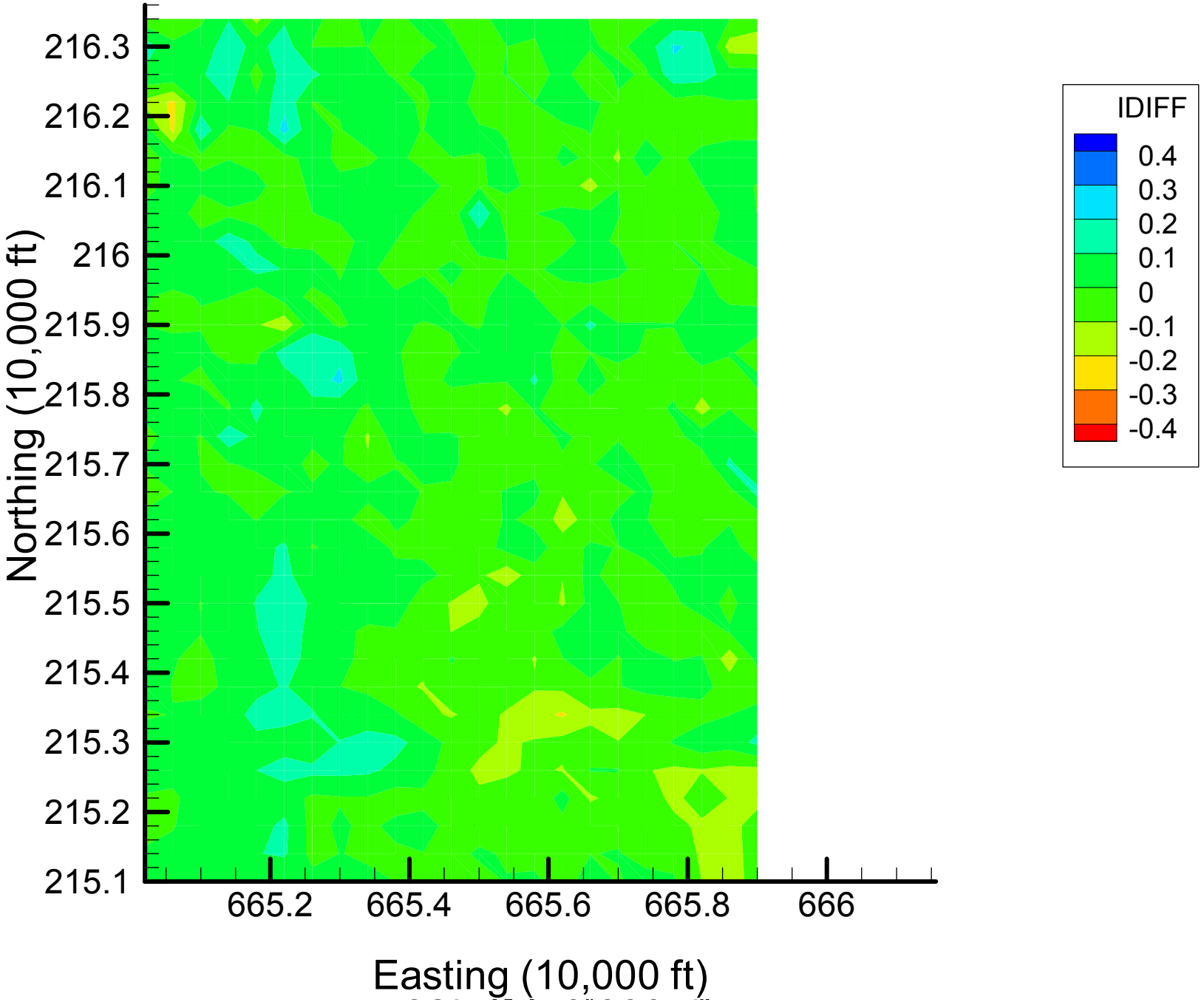

Site 133: DIOXANE14 Indicator Differences, 2001-2002, 20% Removal

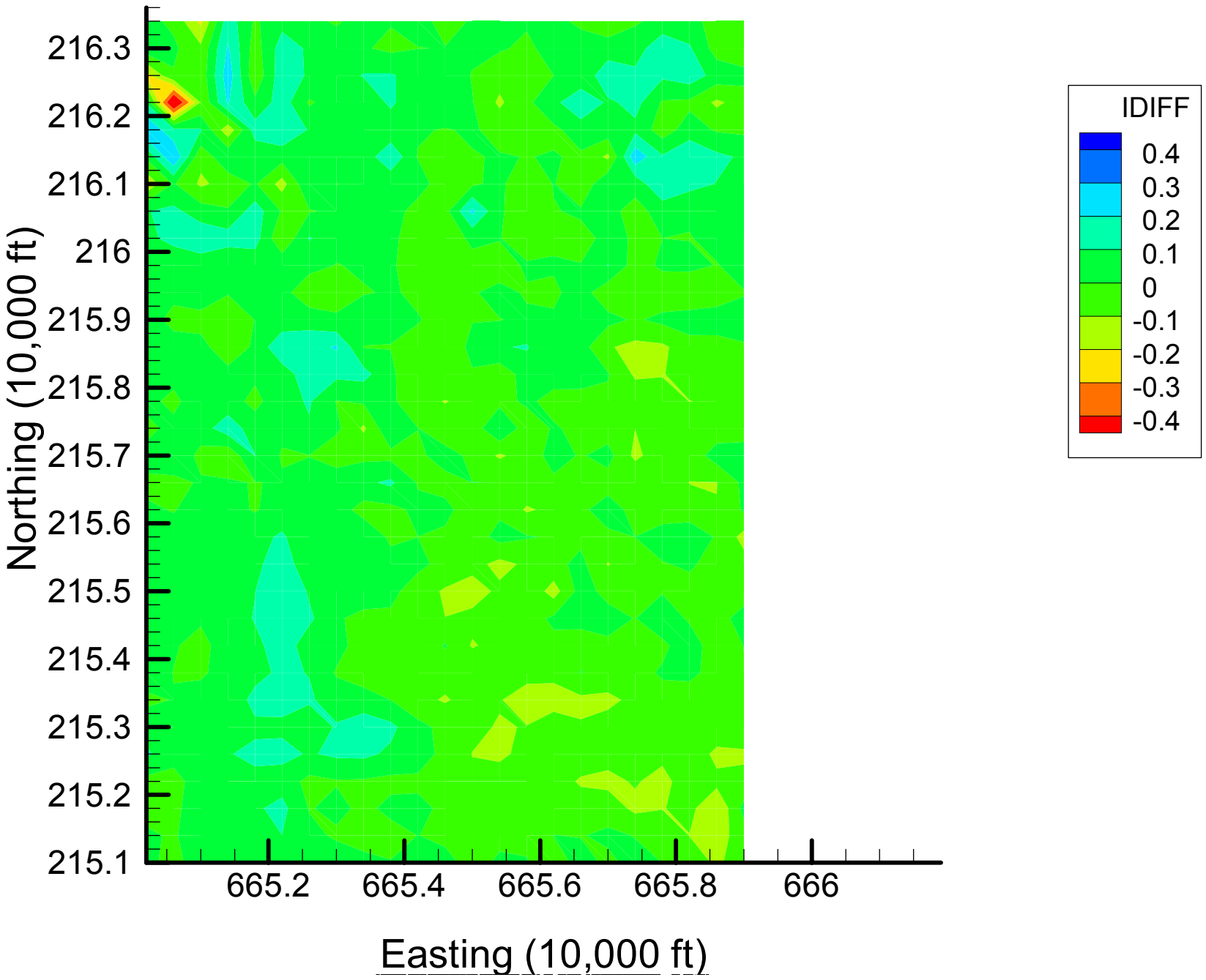

Site 133: DIOXANE14 Indicator Differences, 2001-2002, 27% Removal

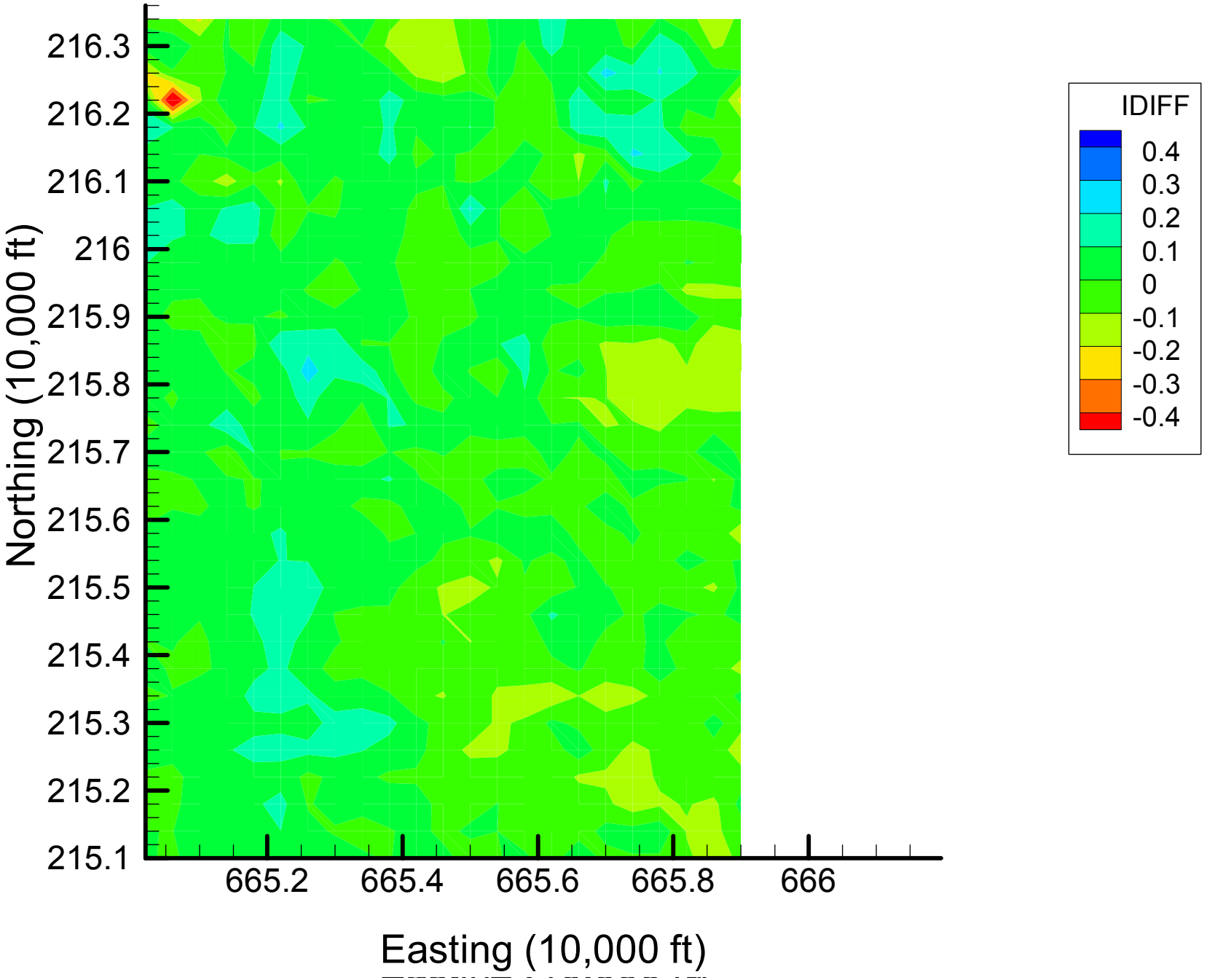

Site 133: DIOXANE14 Indicator Differences, 2001-2002, 33% Removal

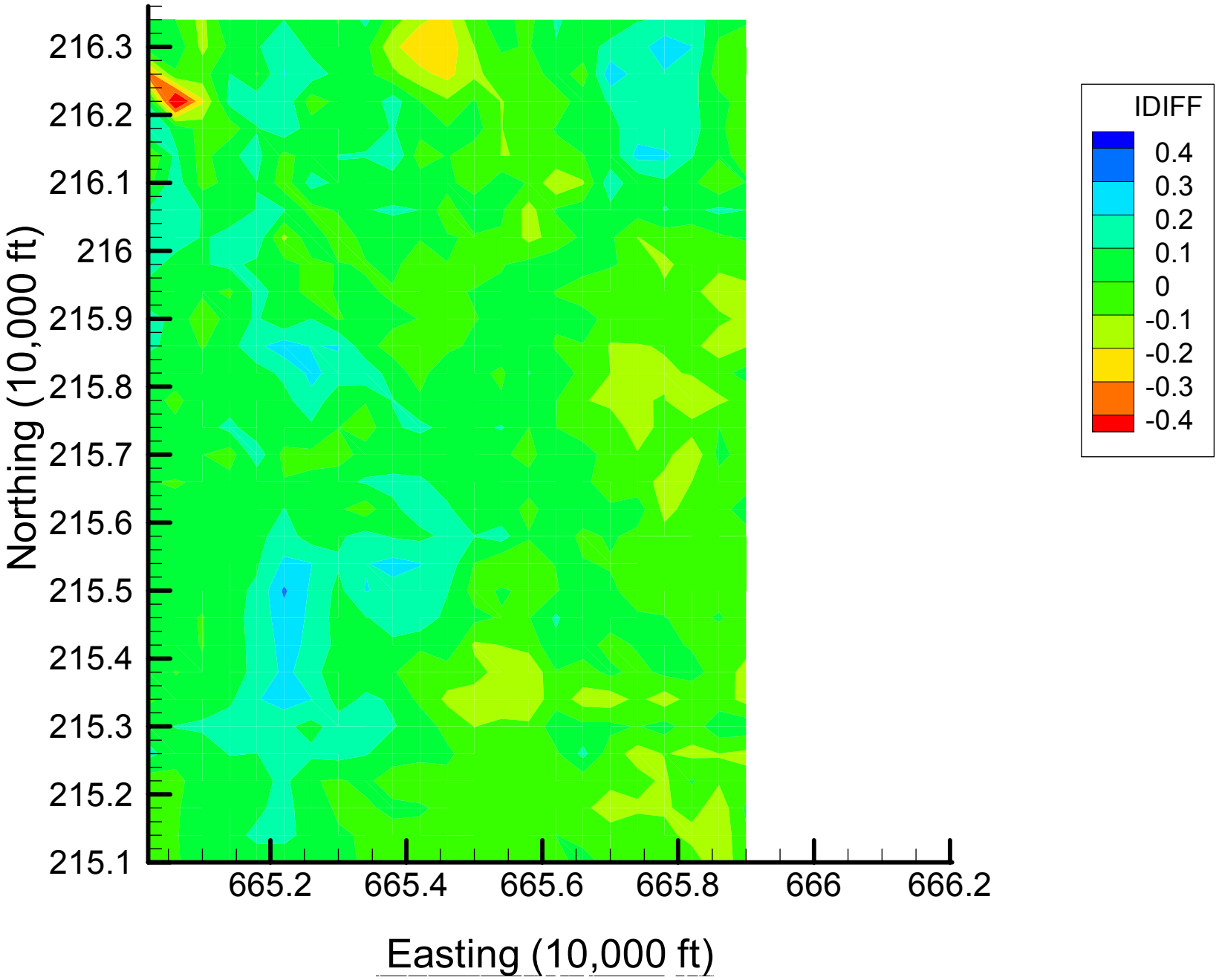

Site 133: DIOXANE14 Indicator Differences, 2001-2002, 40% Removal

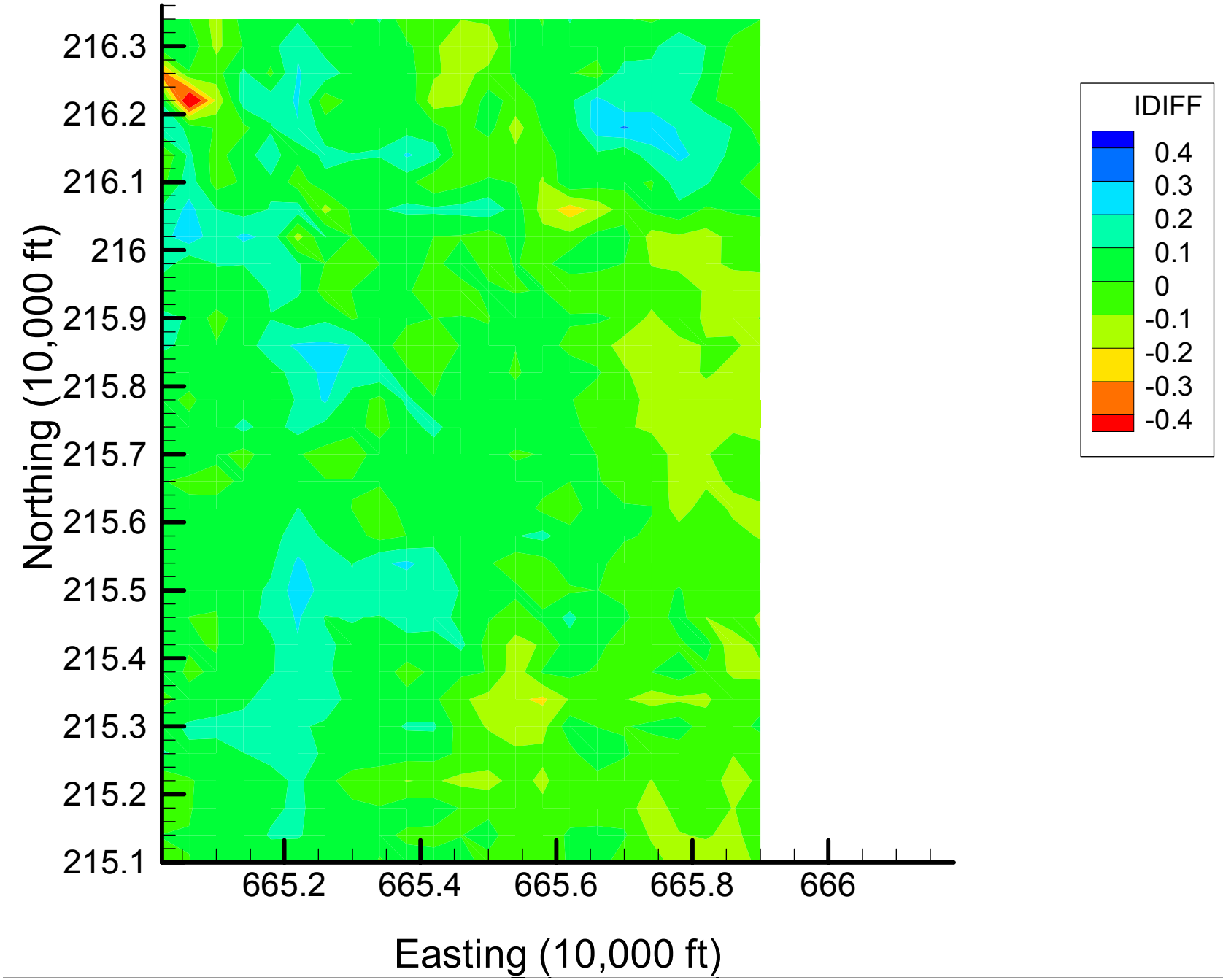

Site 133: DIOXANE14 Indicator Differences, 2001-2002, 47% Removal

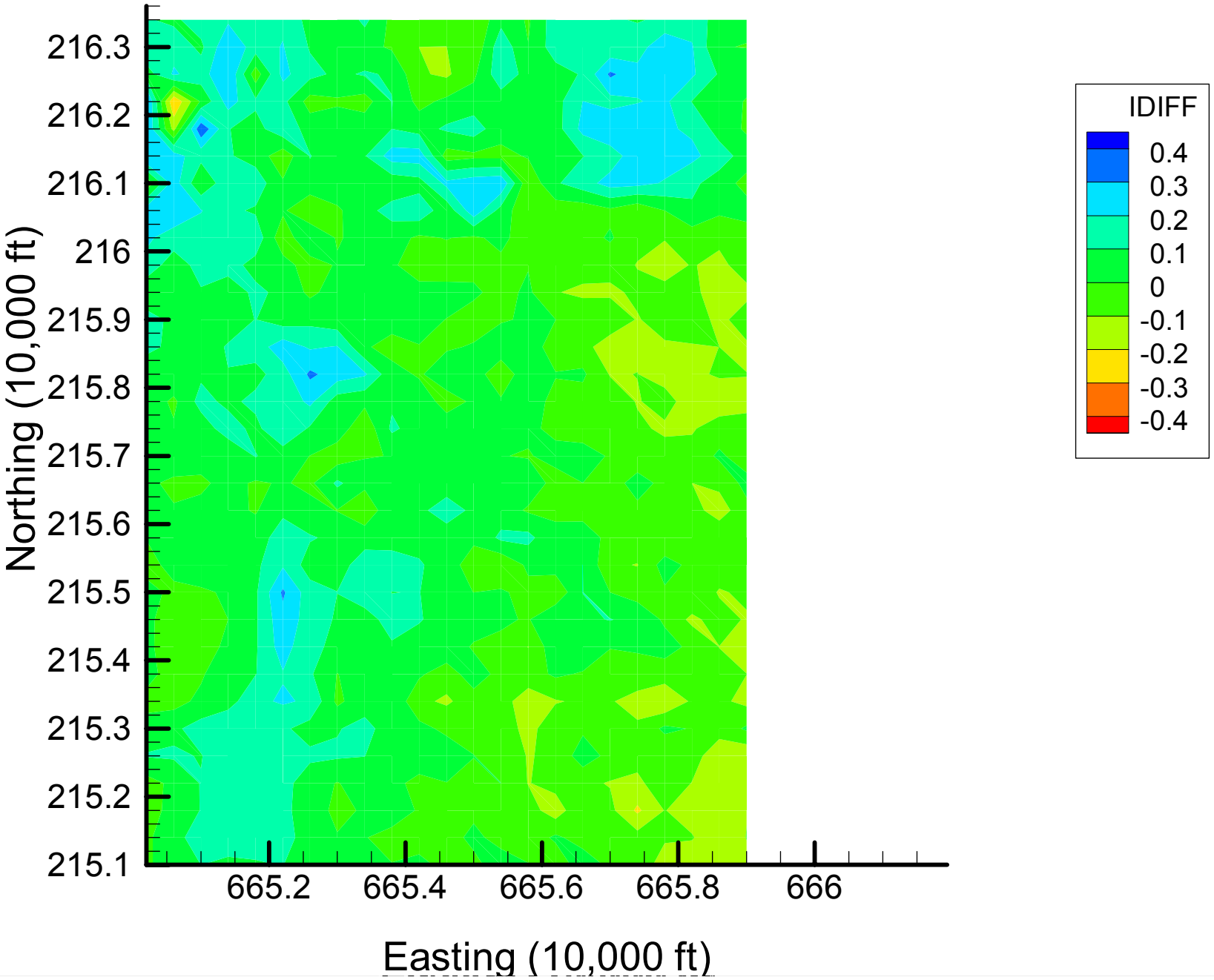

Site 133: DIOXANE14 Indicator Differences, 2001-2002, 53% Removal

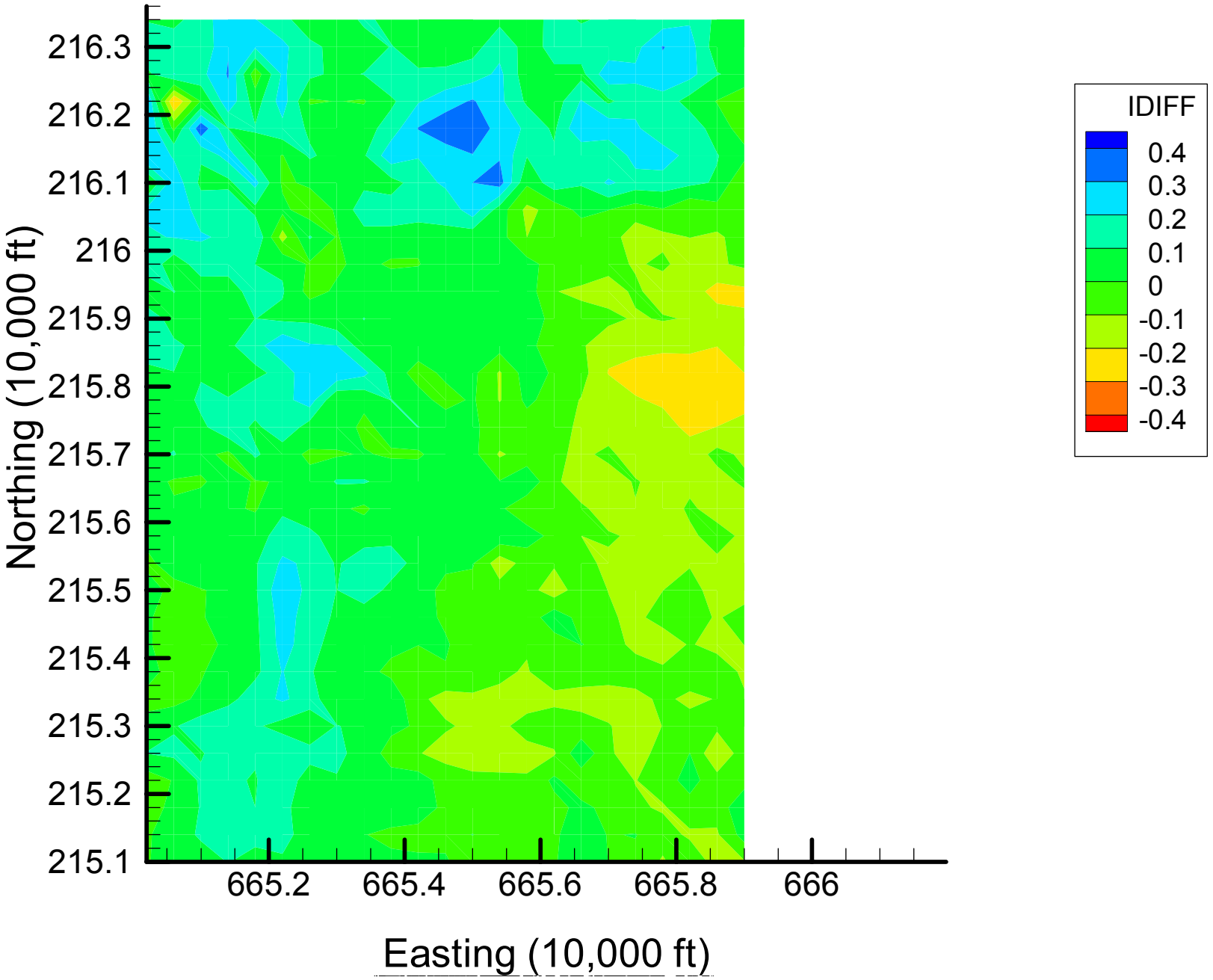

Site 133: DIOXANE14 Indicator Differences, 2001-2002, 60% Removal

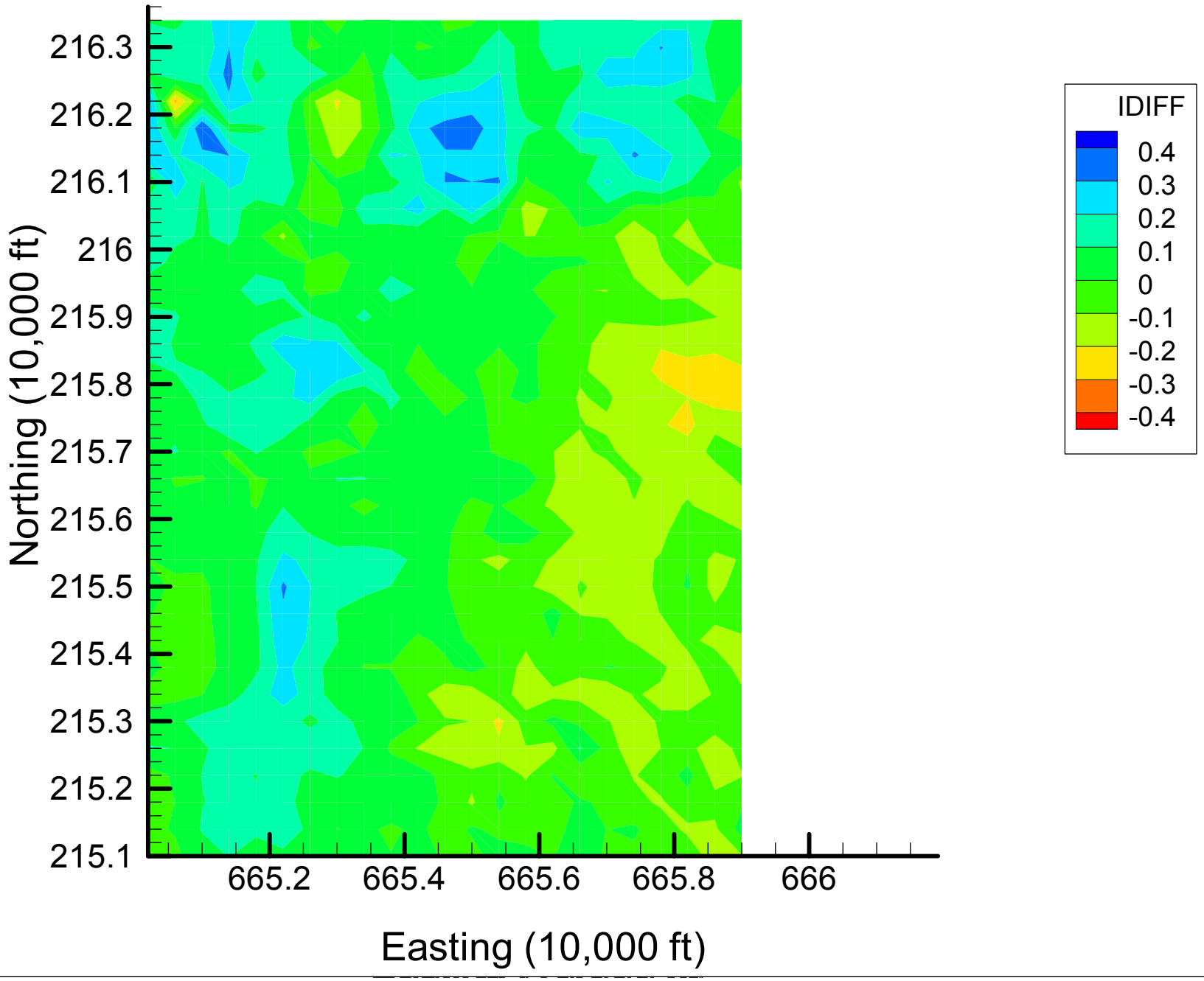

Site 133: DIOXANE14 Indicator Differences, 2001-2002, 67% Removal

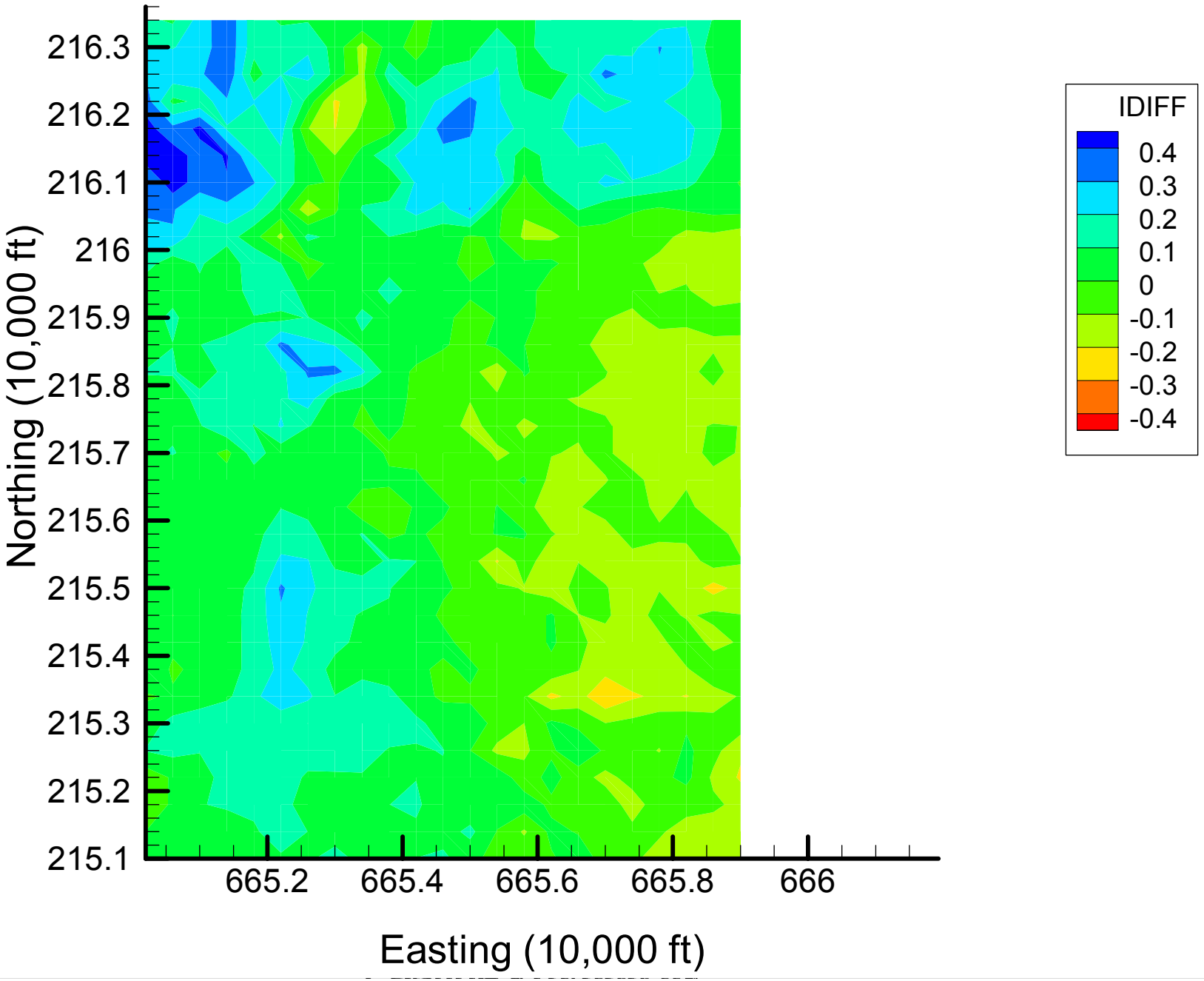

Appendix 4.2
MN Indicator Difference Maps
Time Slice 1

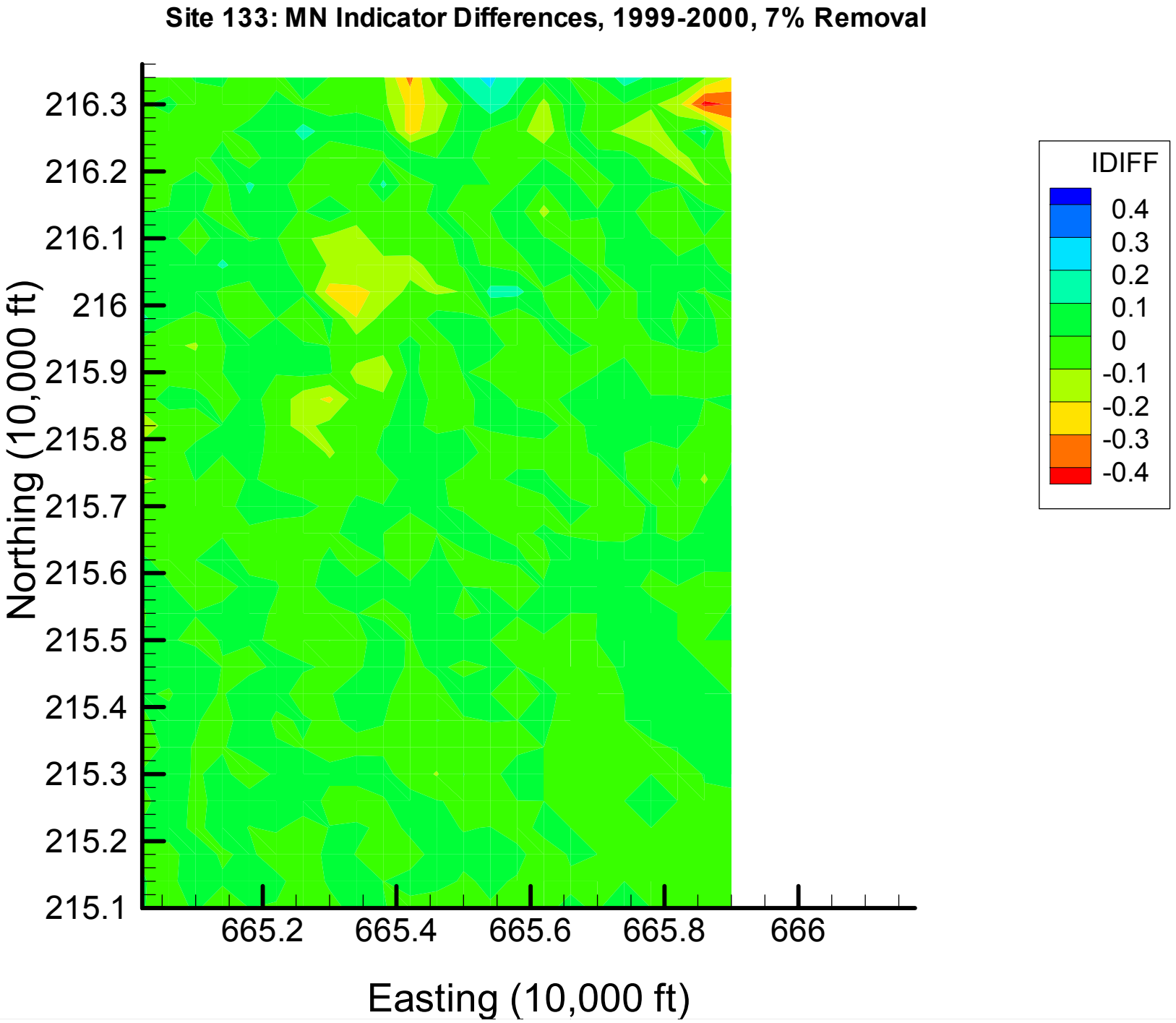
Site 133: MN Indicator Differences, 1999-2000, 7% Removal
IDIFF
0.4
0.3
0.2
0.1
0
-0.1
-0.2
-0.3
-0.4
Northing (10,000 ft)
216.3
216.2
216.1
216
215.9
215.8
215.7
215.6
215.5
215.4
215.3
215.2
215.1
665.2
665.4
665.6
665.8
666
Easting (10,000 ft)

Site 133: MN Indicator Differences, 1999-2000, 13% Removal

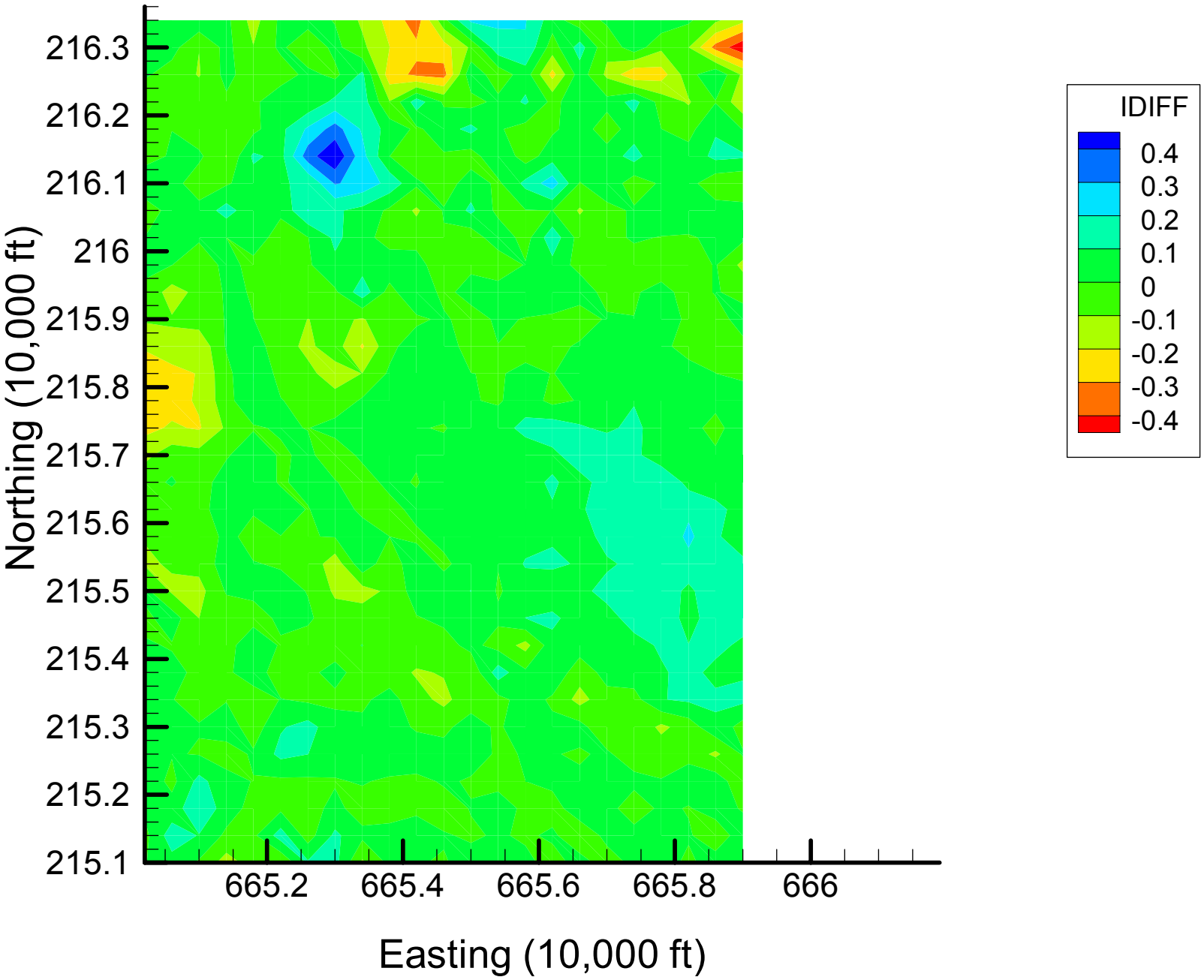

Site 133: MN Indicator Differences, 1999-2000, 20% Removal

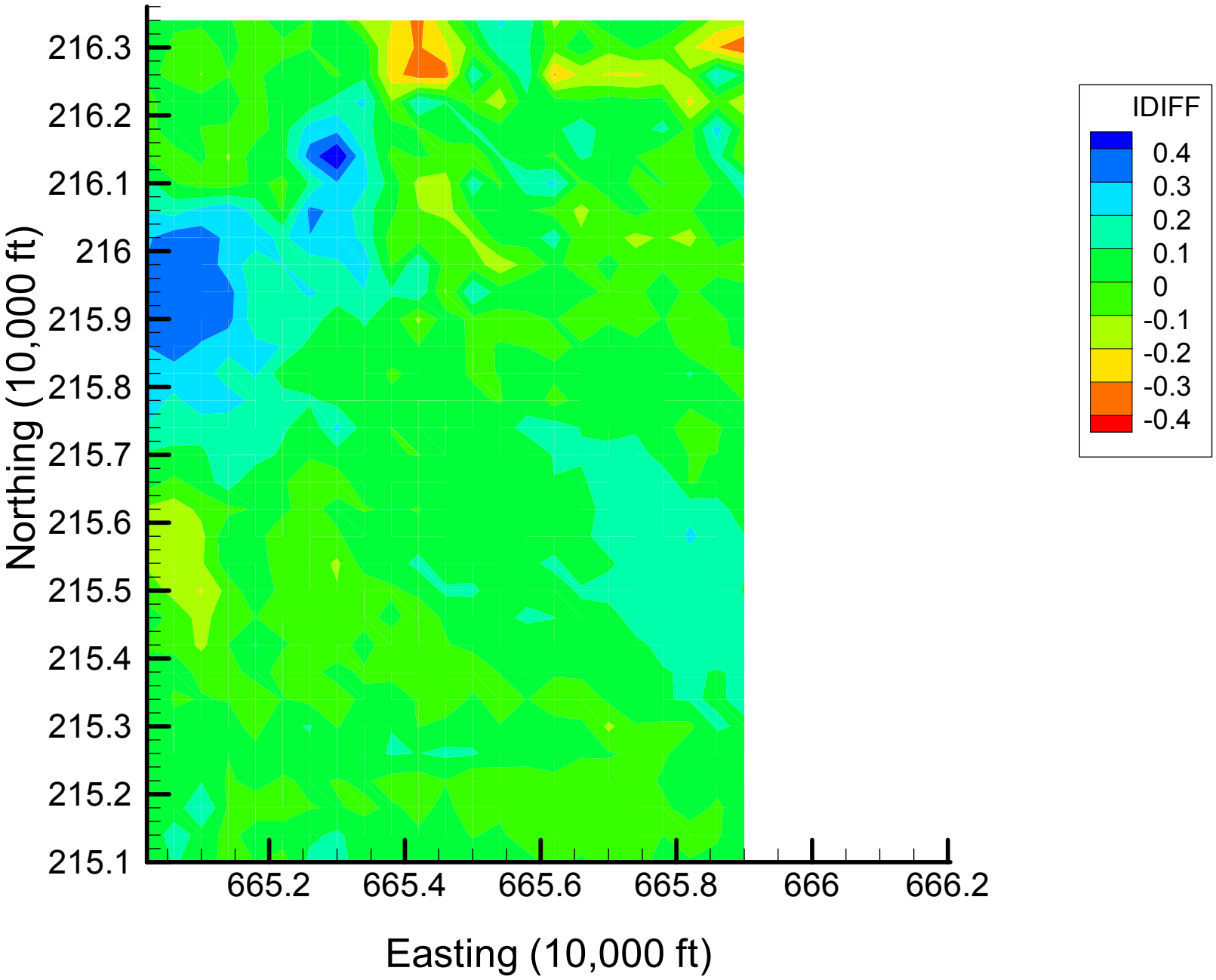

Site 133: MN Indicator Differences, 1999-2000, 27% Removal

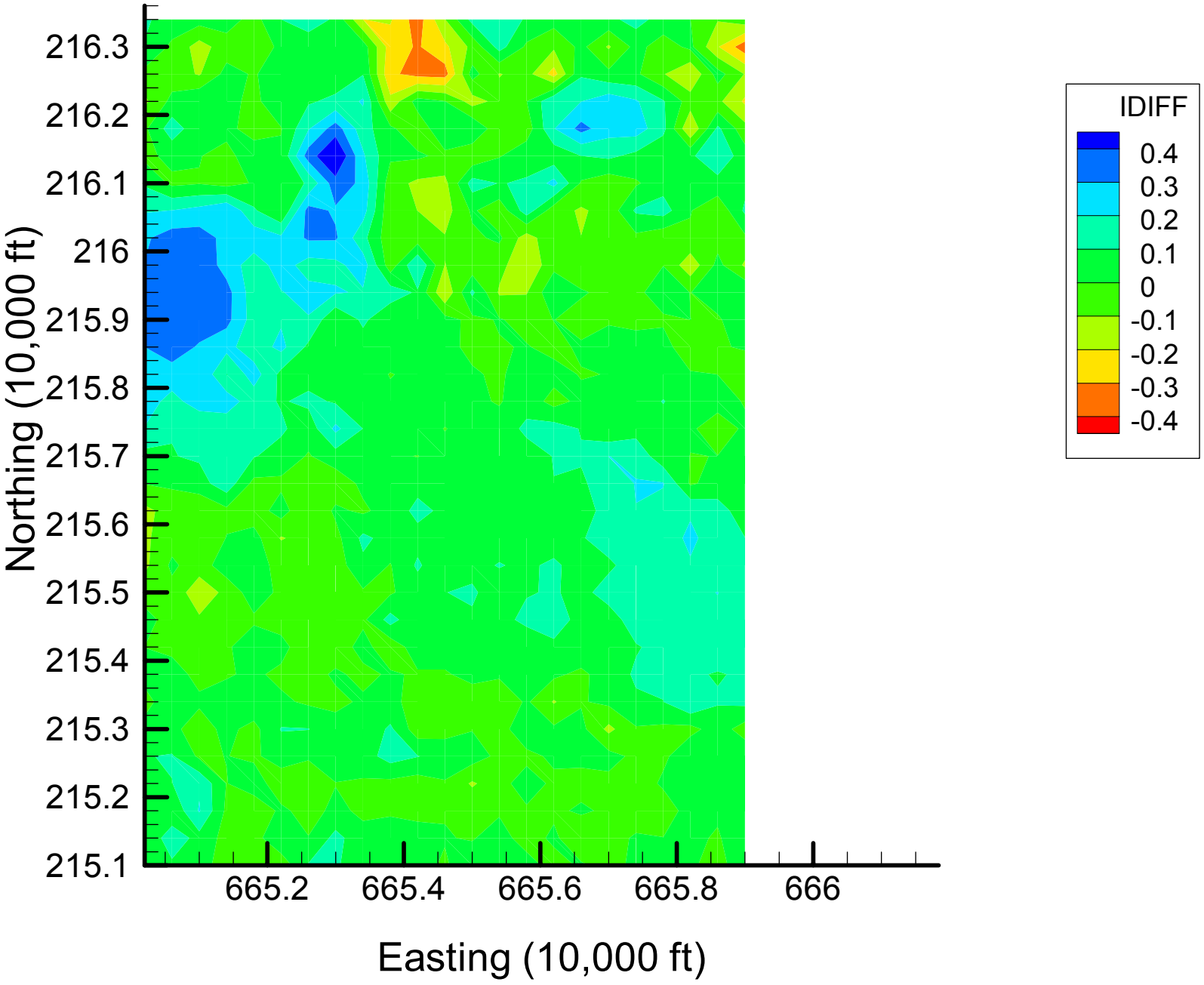

Site 133: MN Indicator Differences, 1999-2000, 33% Removal

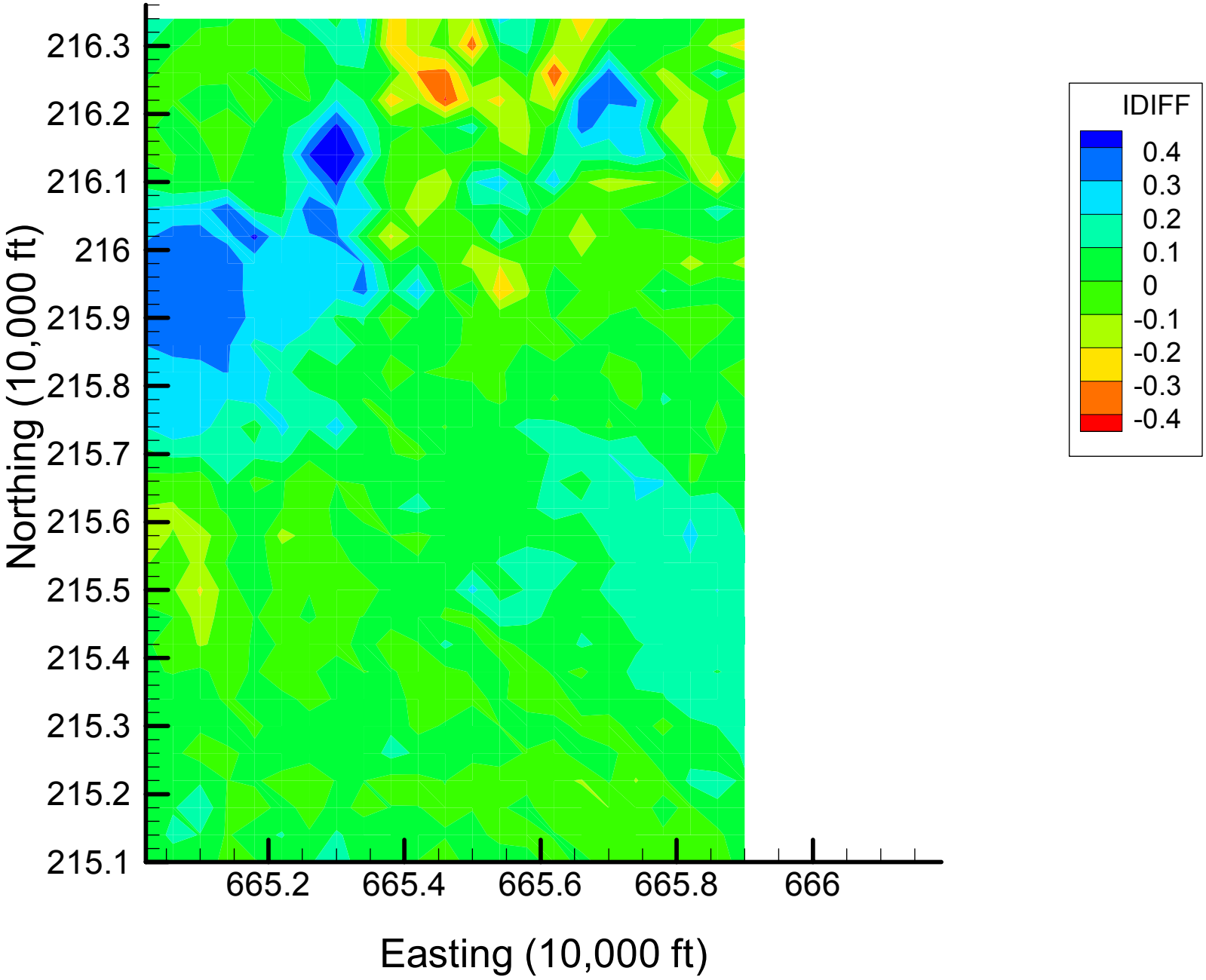

Site 133: MN Indicator Differences, 1999-2000, 40% Removal

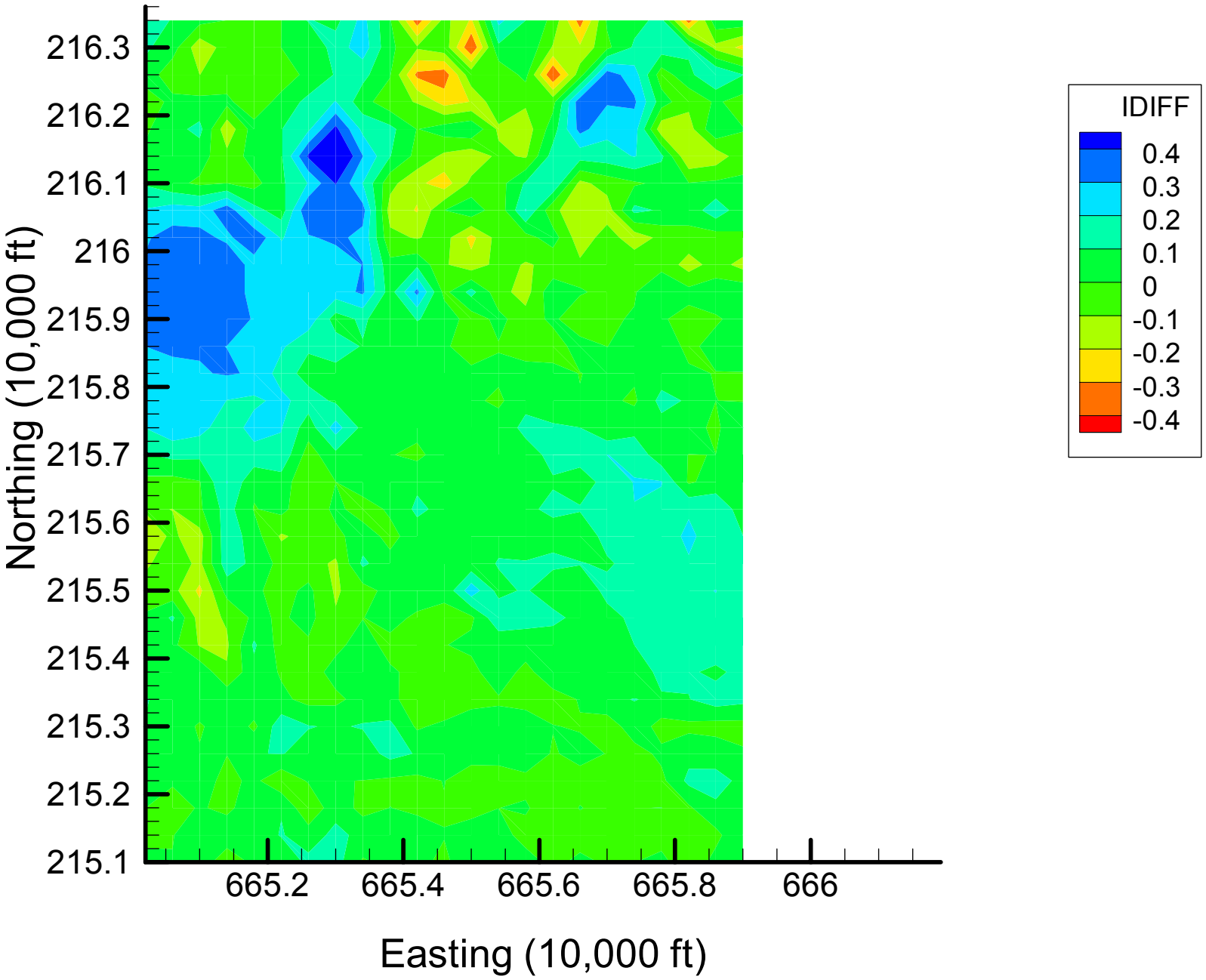

Site 133: MN Indicator Differences, 1999-2000, 47% Removal

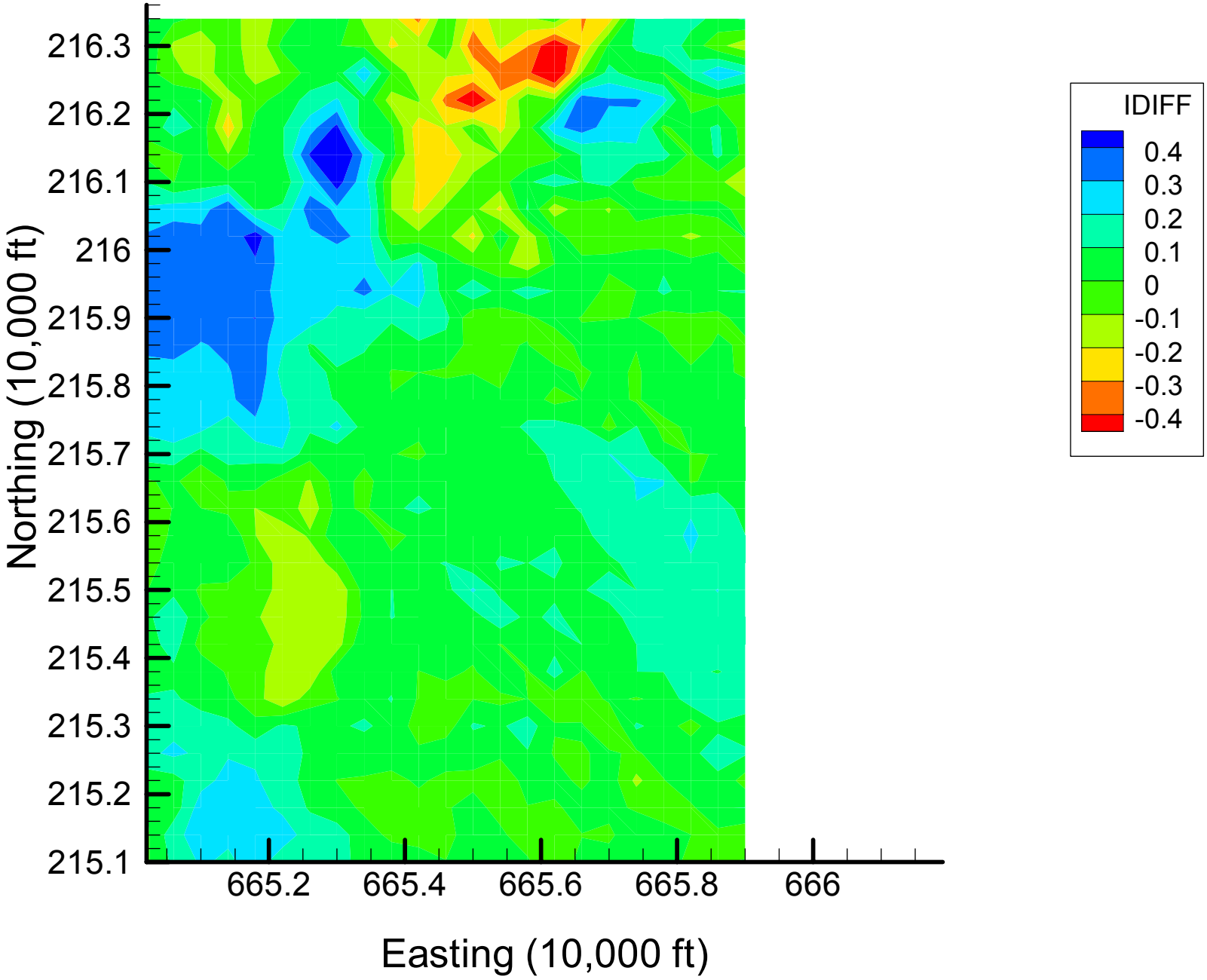

Site 133: MN Indicator Differences, 1999-2000, 53% Removal

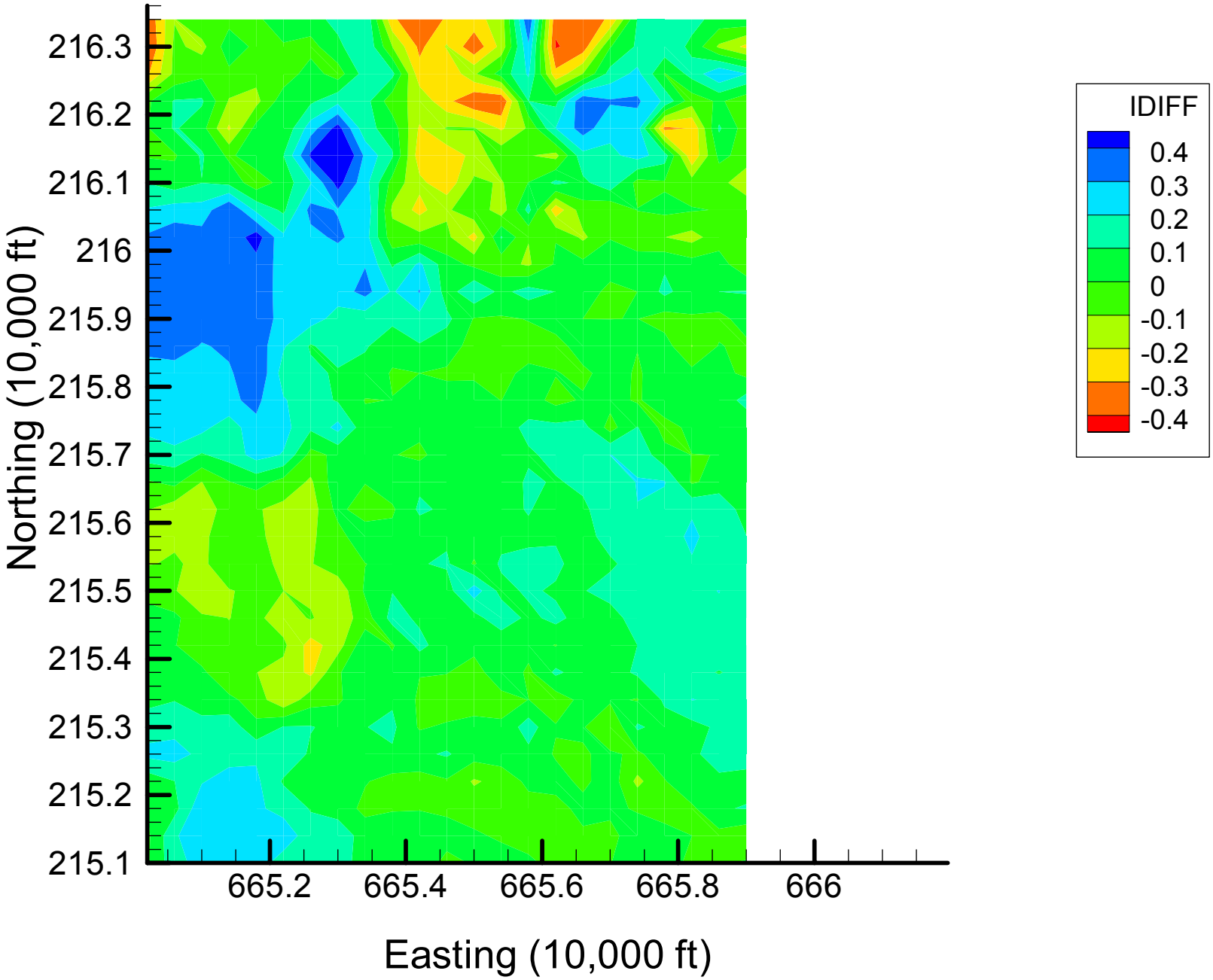

Site 133: MN Indicator Differences, 1999-2000, 60% Removal

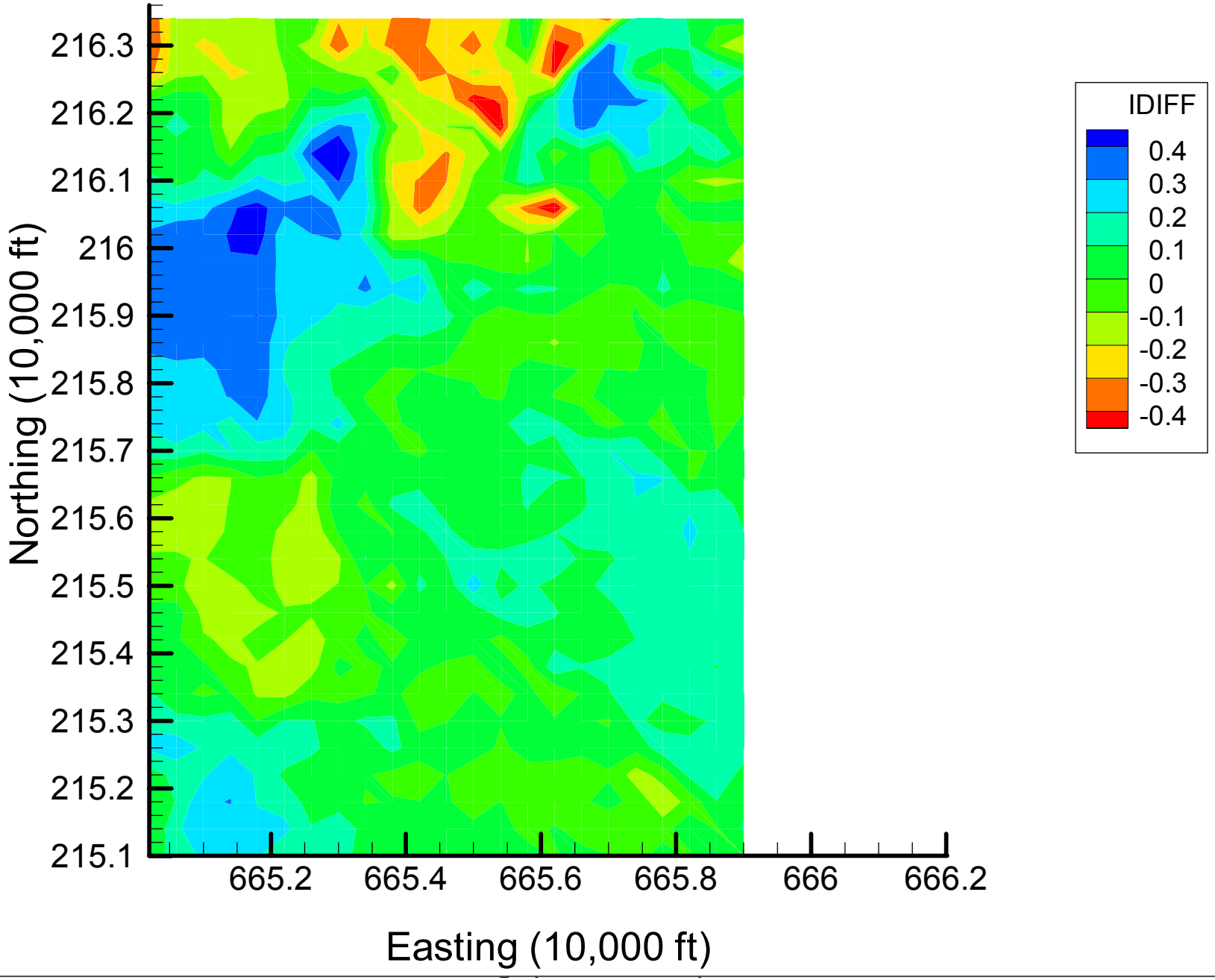

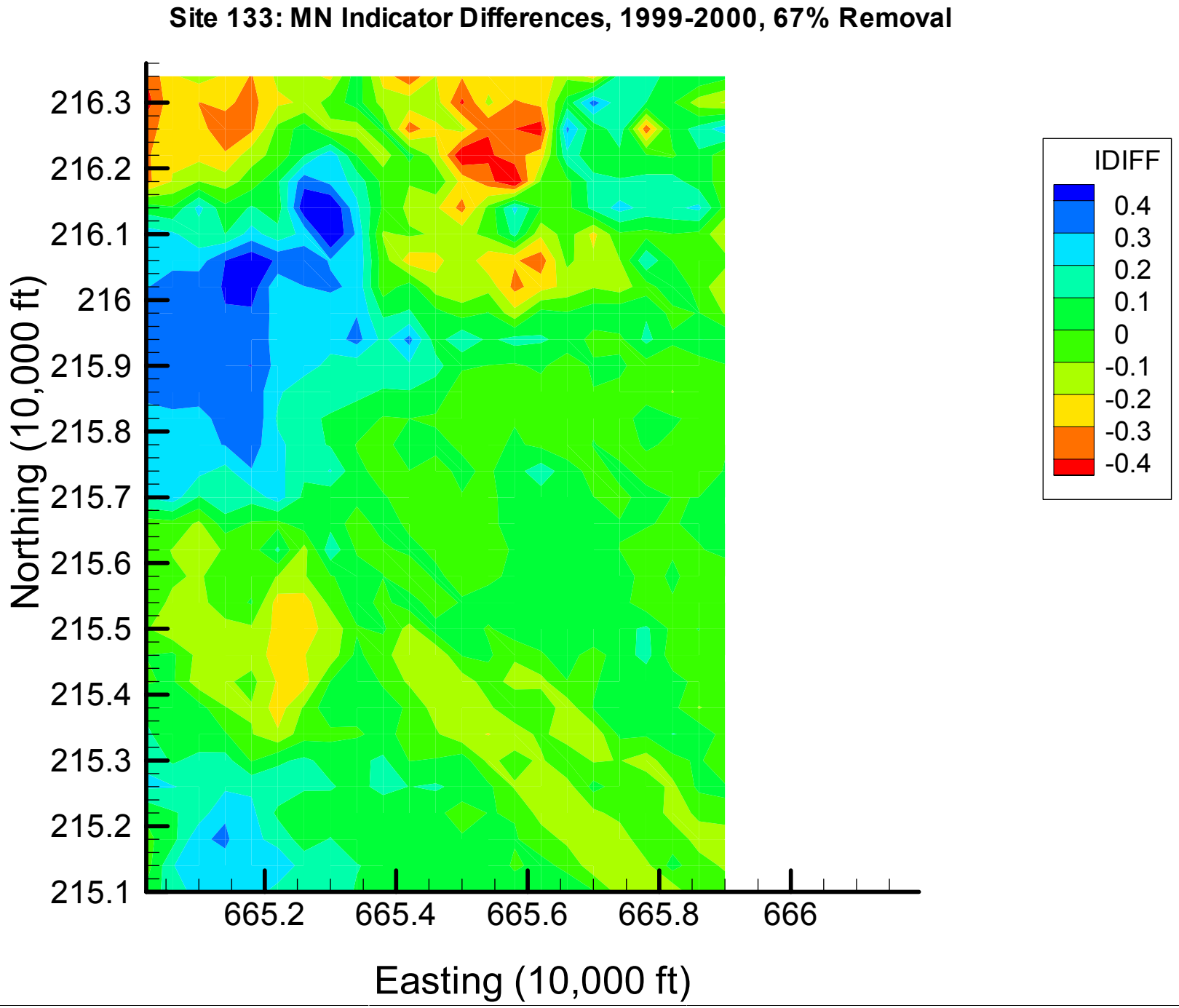
Site 133: MN Indicator Differences, 1999-2000, 67% Removal
Northing (10,000 ft)
216.3
216.2
216.1
216
215.9
215.8
215.7
215.6
215.5
215.4
215.3
215.2
215.1
665.2
665.4
665.6
665.8
666
Easting (10,000 ft)
IDIFF
0.4
0.3
0.2
0.1
0
-0.1
-0.2
-0.3
-0.4

Appendix 4.2
MN Indicator Difference Maps
Time Slice 2

Site 133: MN Indicator Differences, 2001-2002, 7% Removal

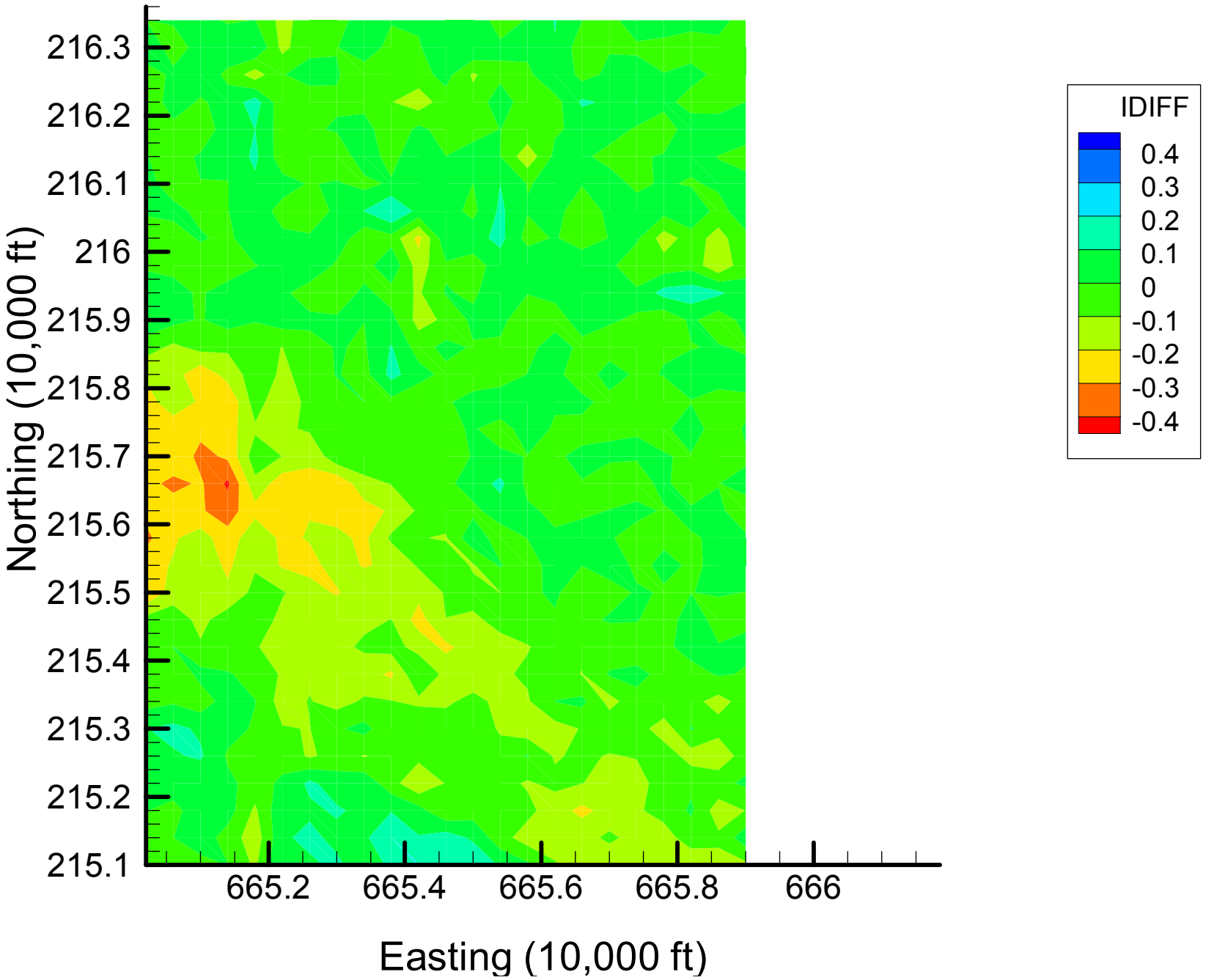

Site 133: MN Indicator Differences, 2001-2002, 13% Removal

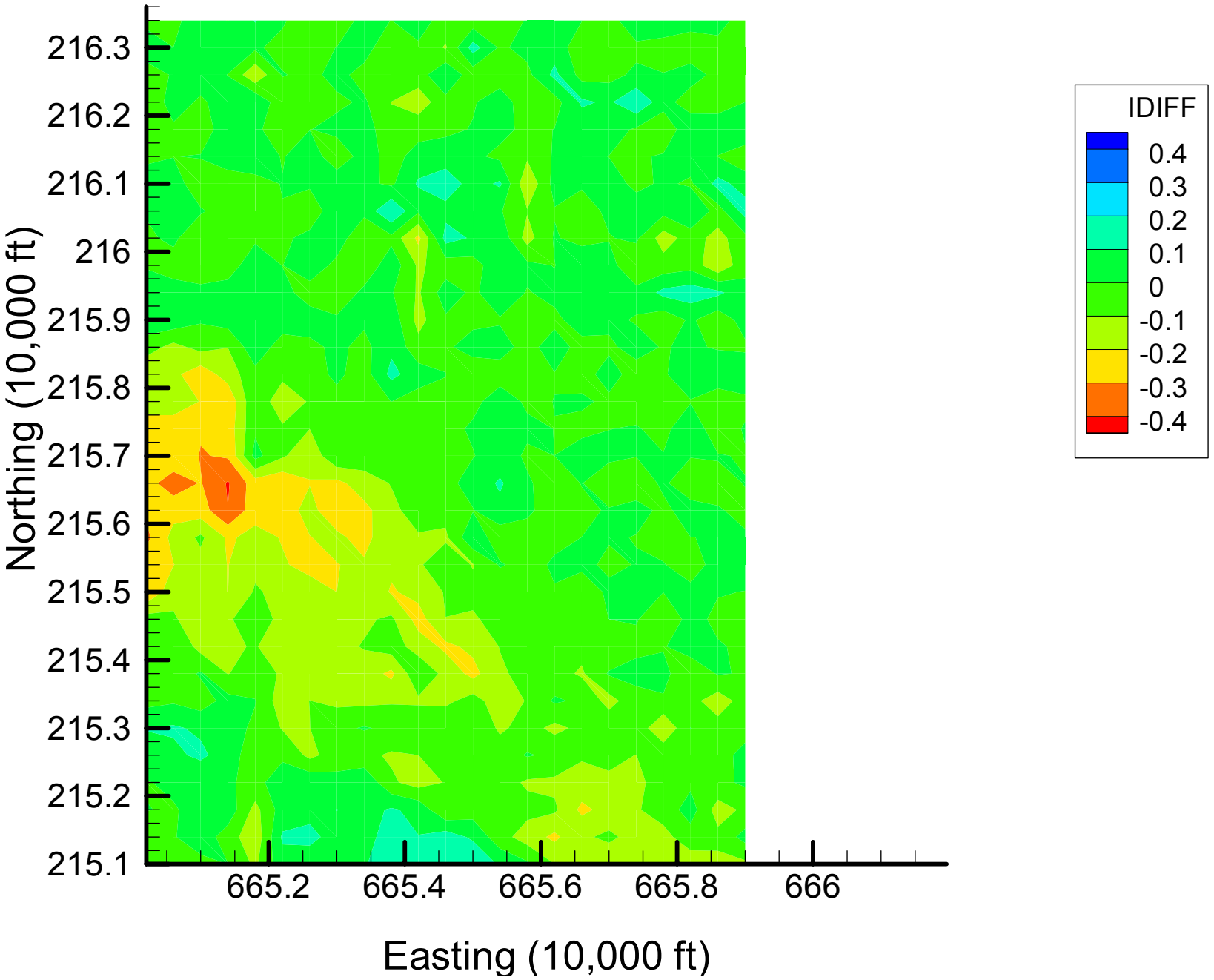

Site 133: MN Indicator Differences, 2001-2002, 20% Removal

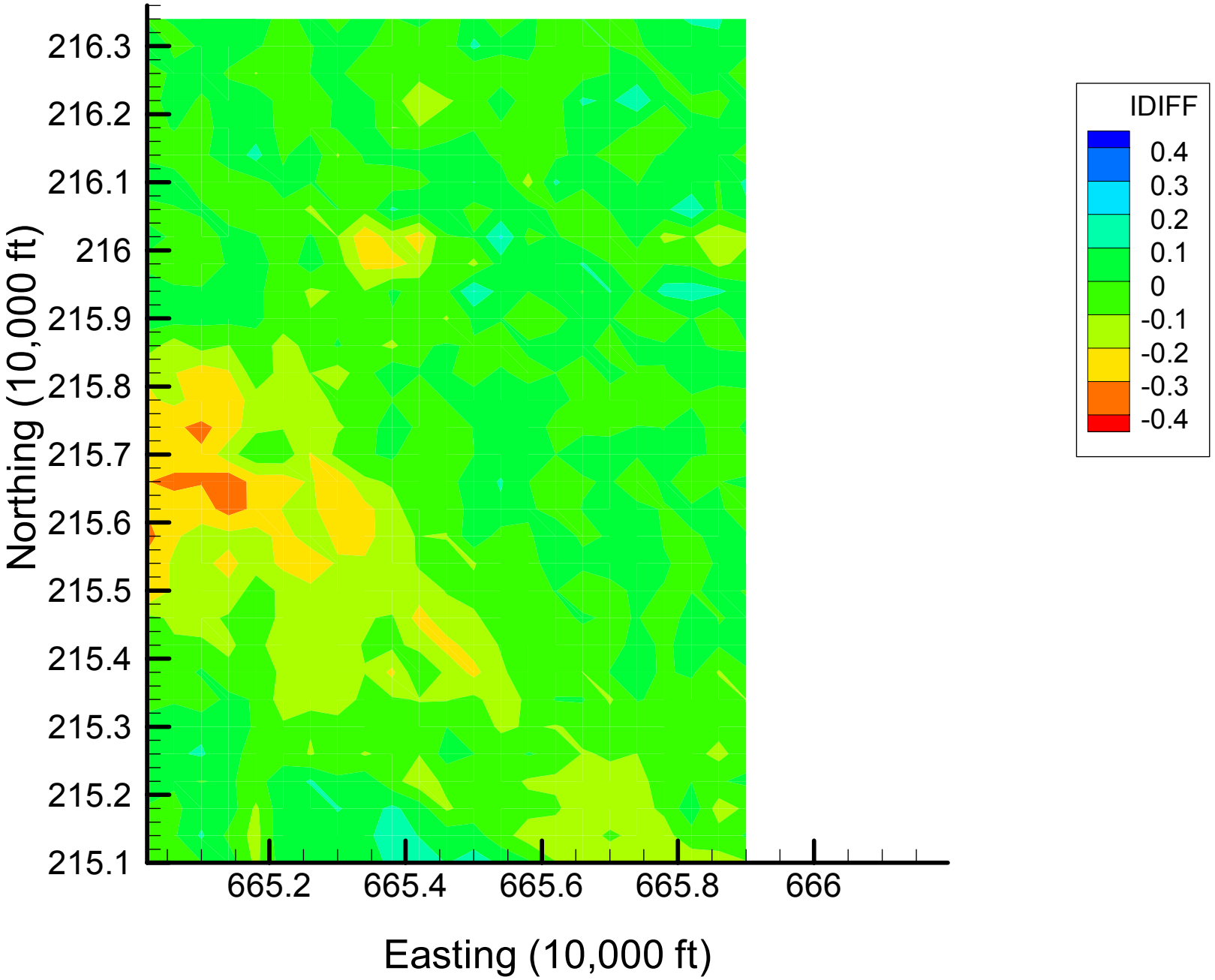

Site 133: MN Indicator Differences, 2001-2002, 27% Removal

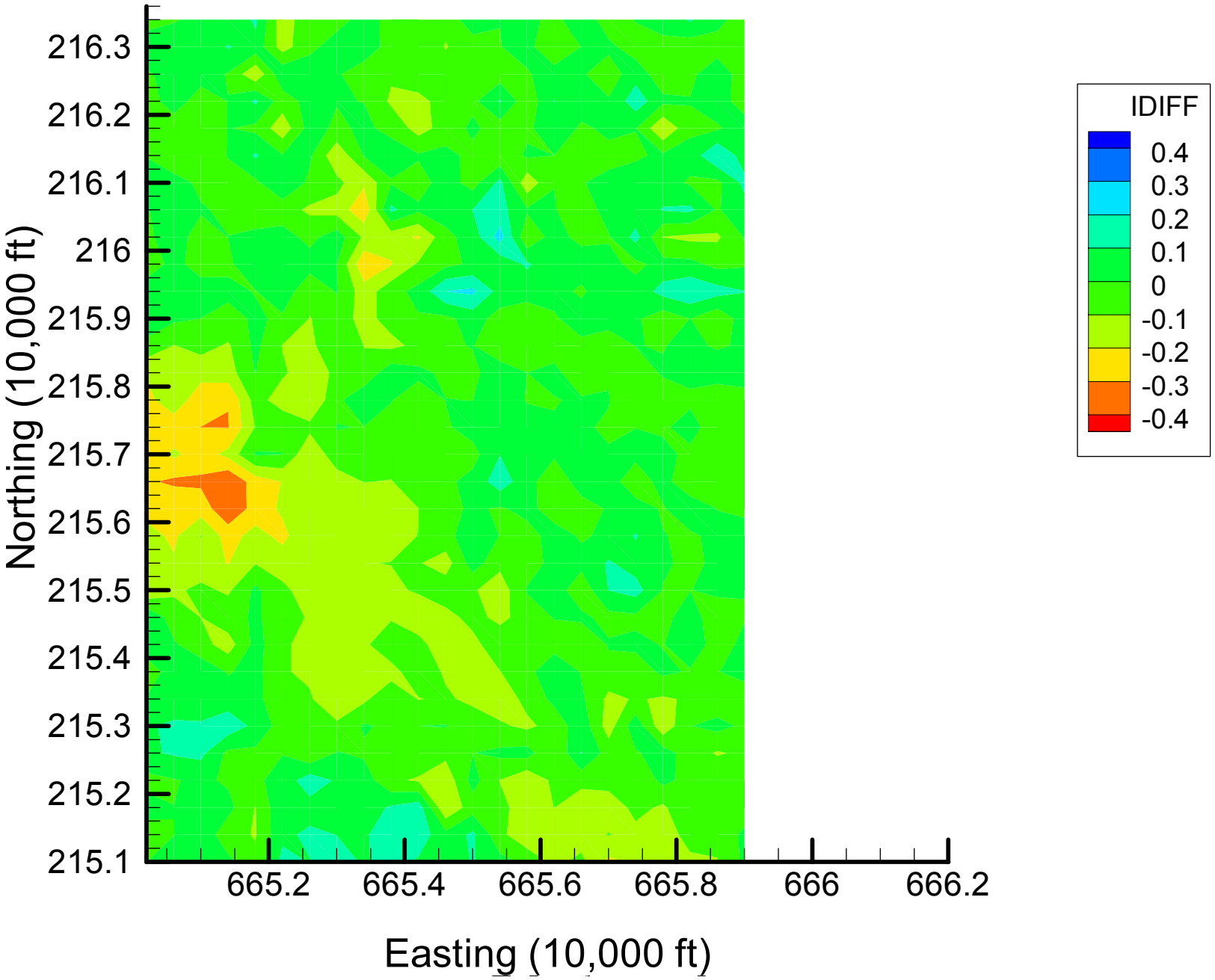

Site 133: MN Indicator Differences, 2001-2002, 33% Removal

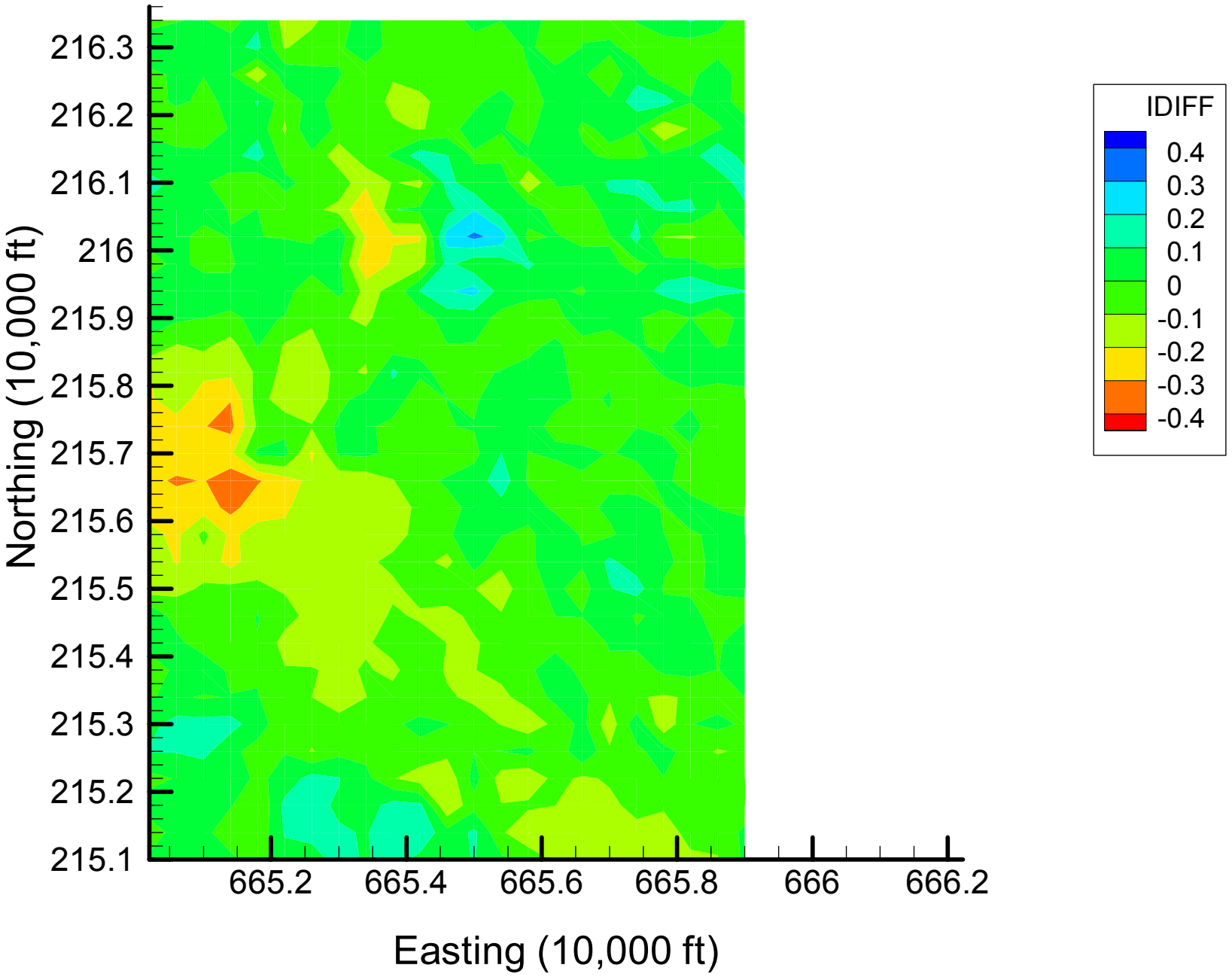

Site 133: MN Indicator Differences, 2001-2002, 40% Removal

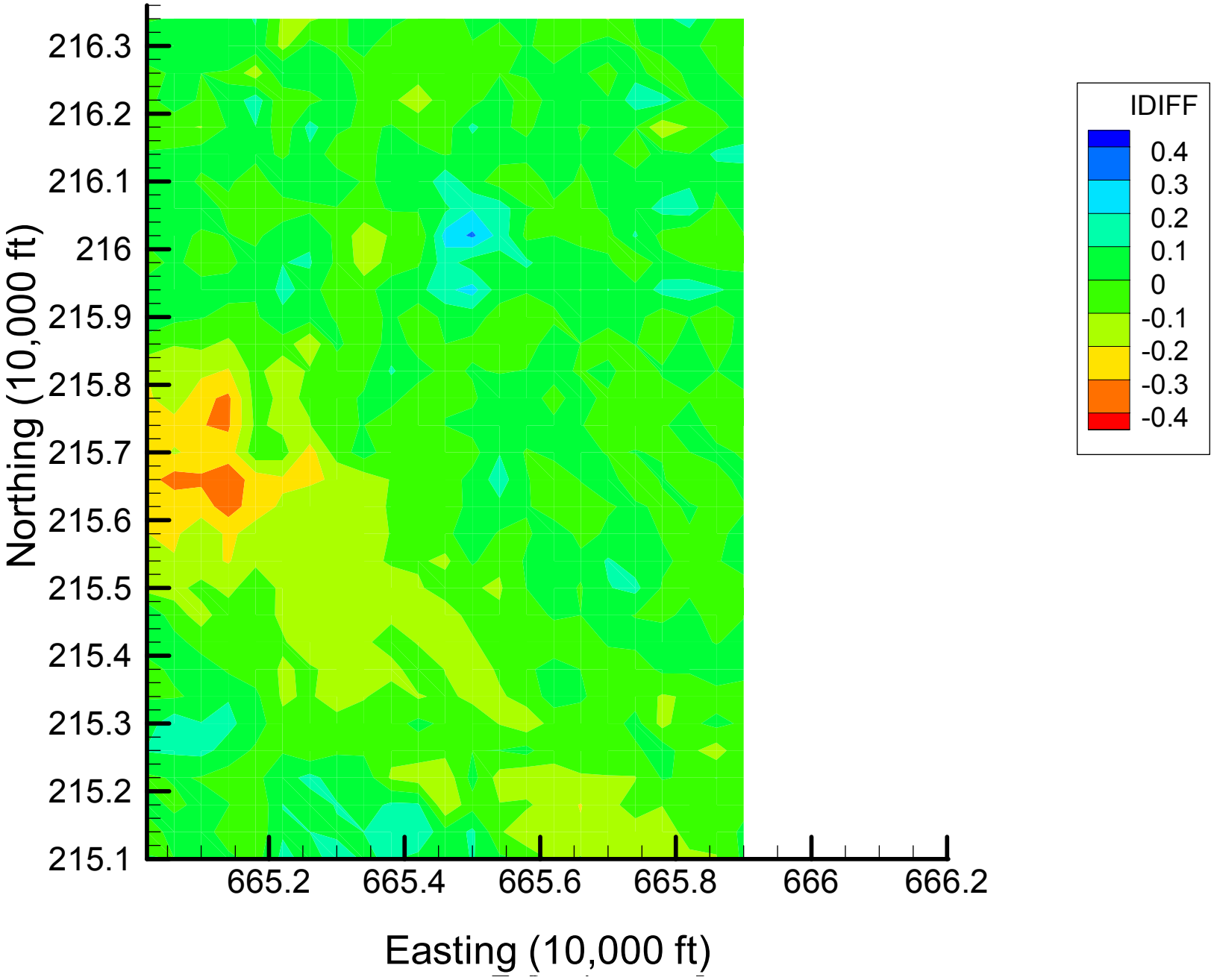

Site 133: MN Indicator Differences, 2001-2002, 47% Removal

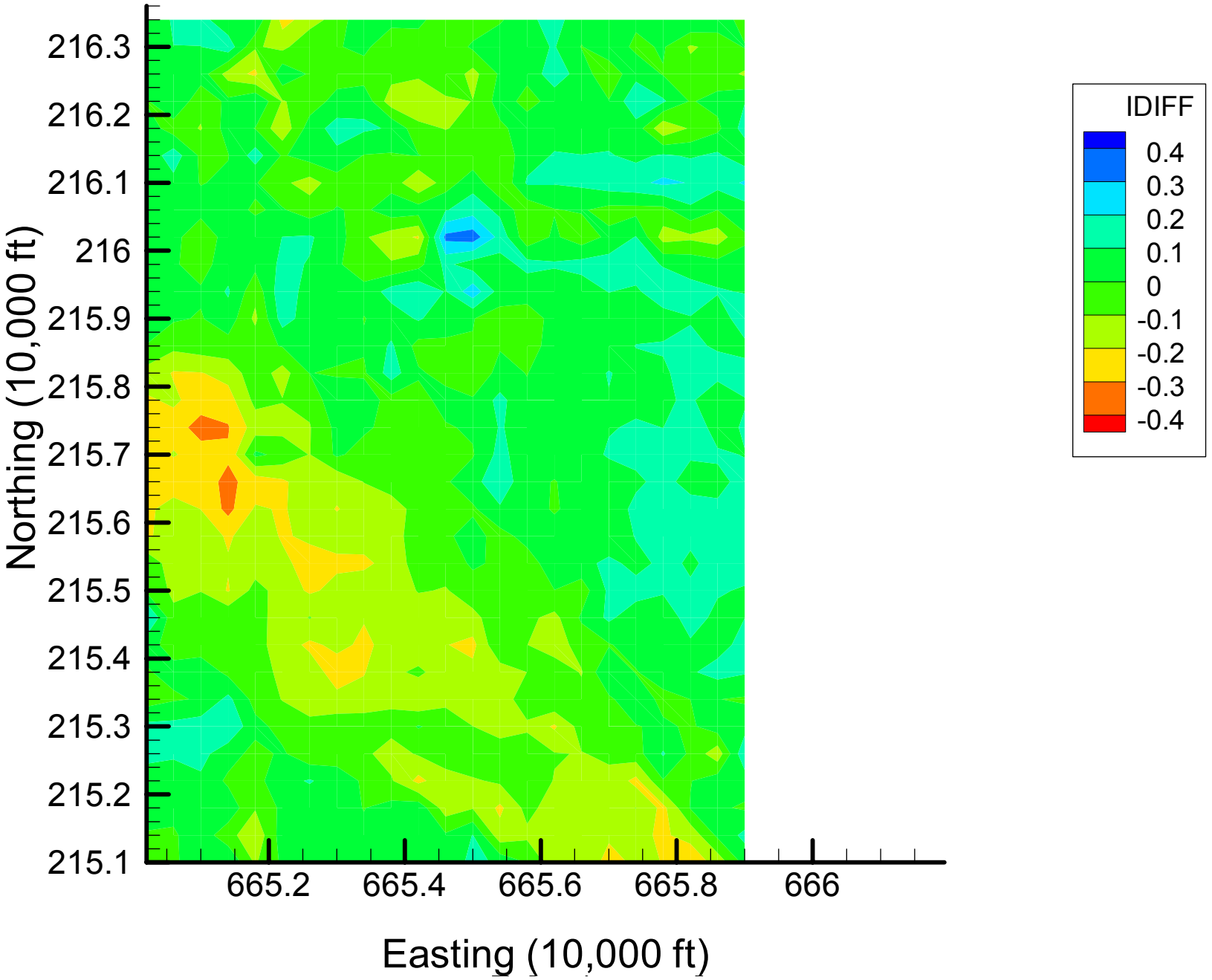

Site 133: MN Indicator Differences, 2001-2002, 53% Removal

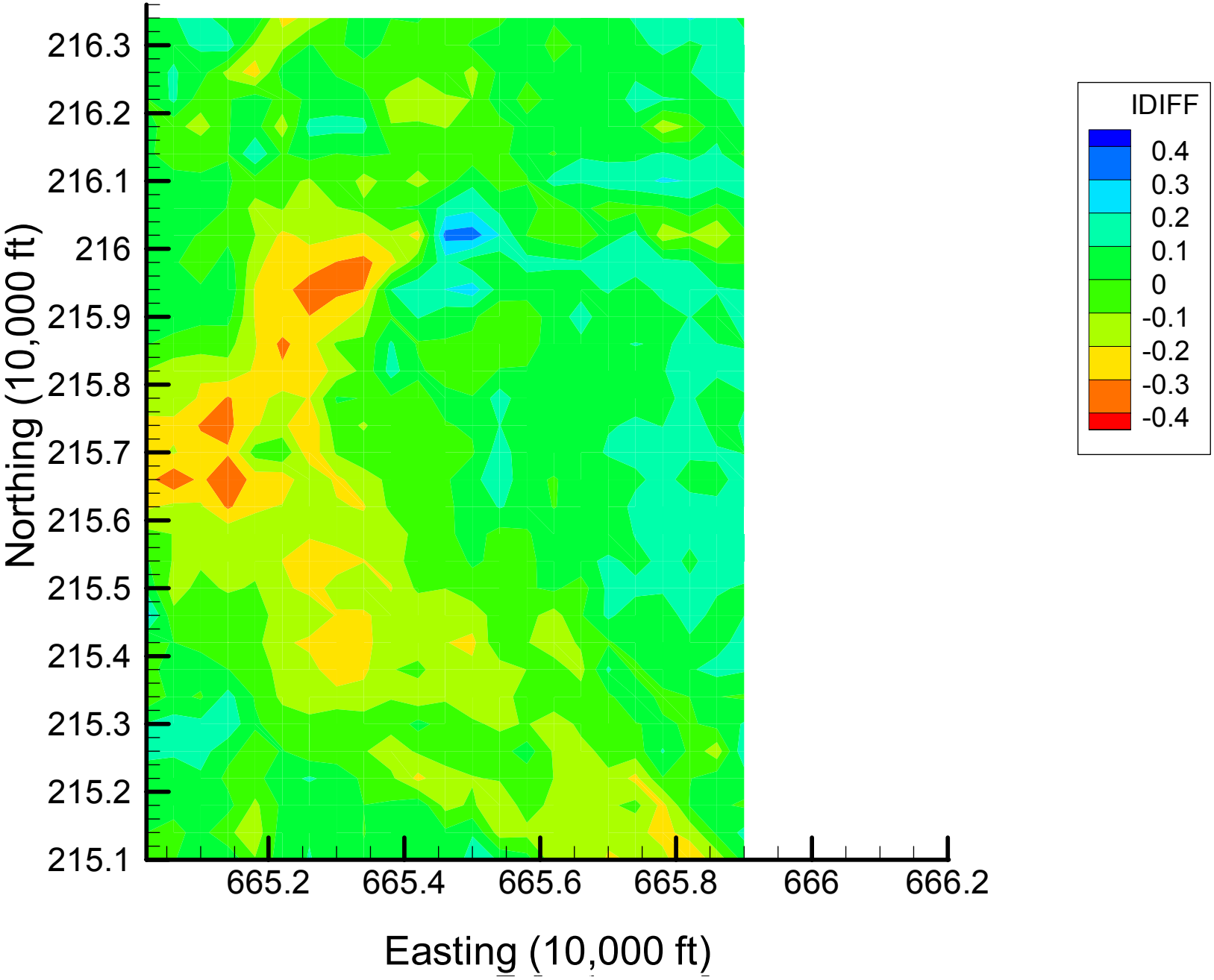

Site 133: MN Indicator Differences, 2001-2002, 60% Removal

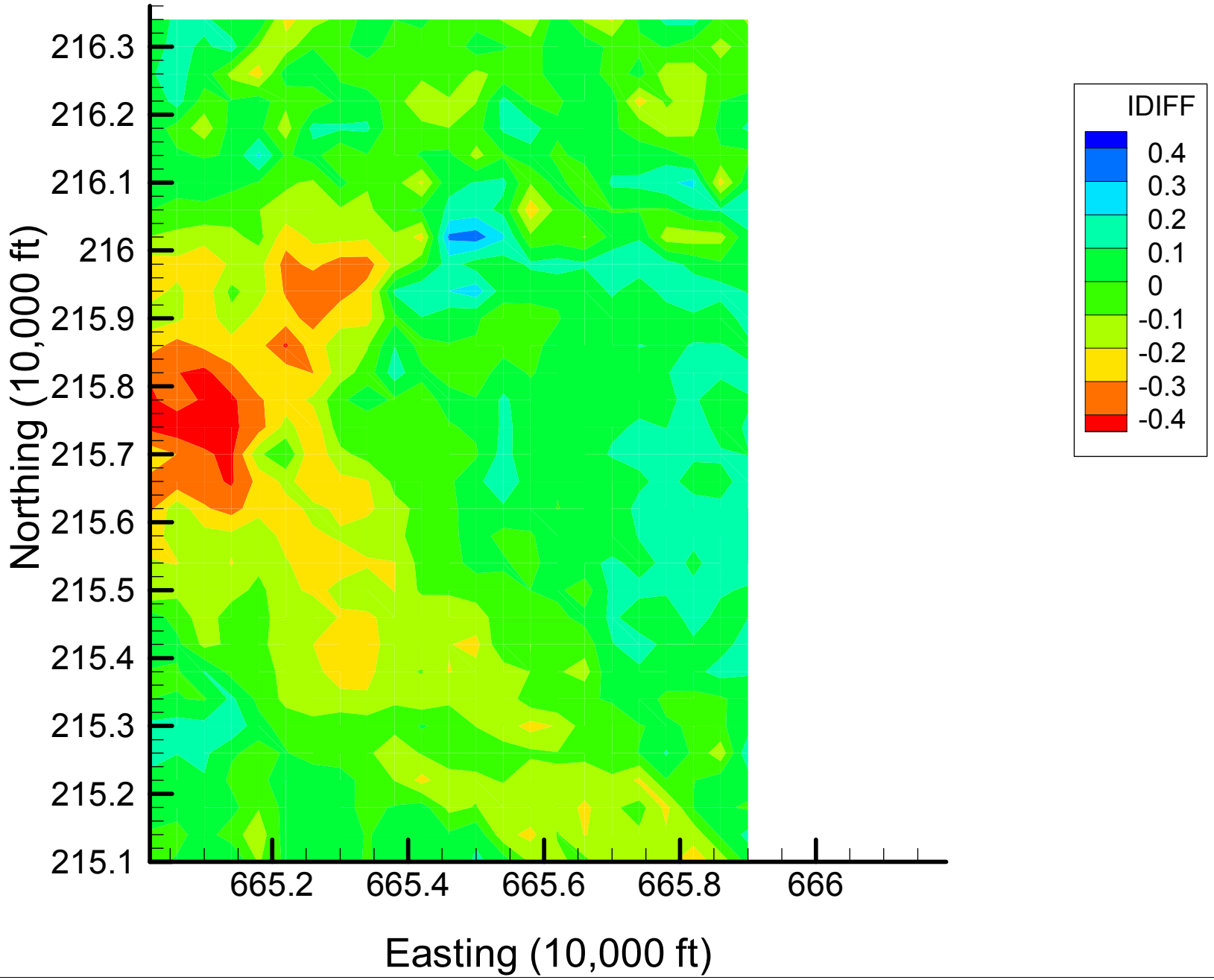

Site 133: MN Indicator Differences, 2001-2002, 67% Removal

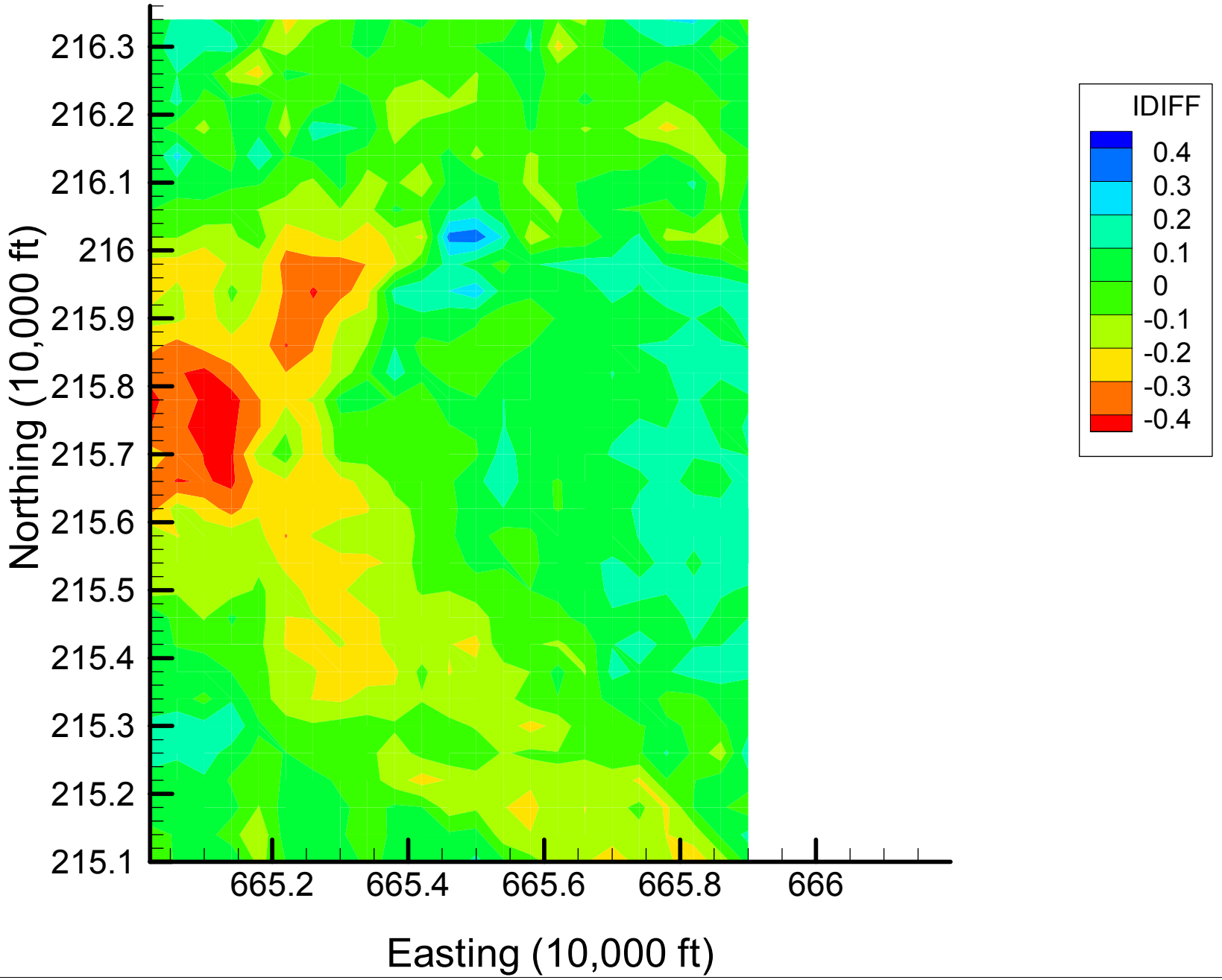

Appendix 4.2
TCE Indicator Difference Maps
Time Slice 1

Site 133: TCE Indicator Differences, 1999-2000, 7% Removal

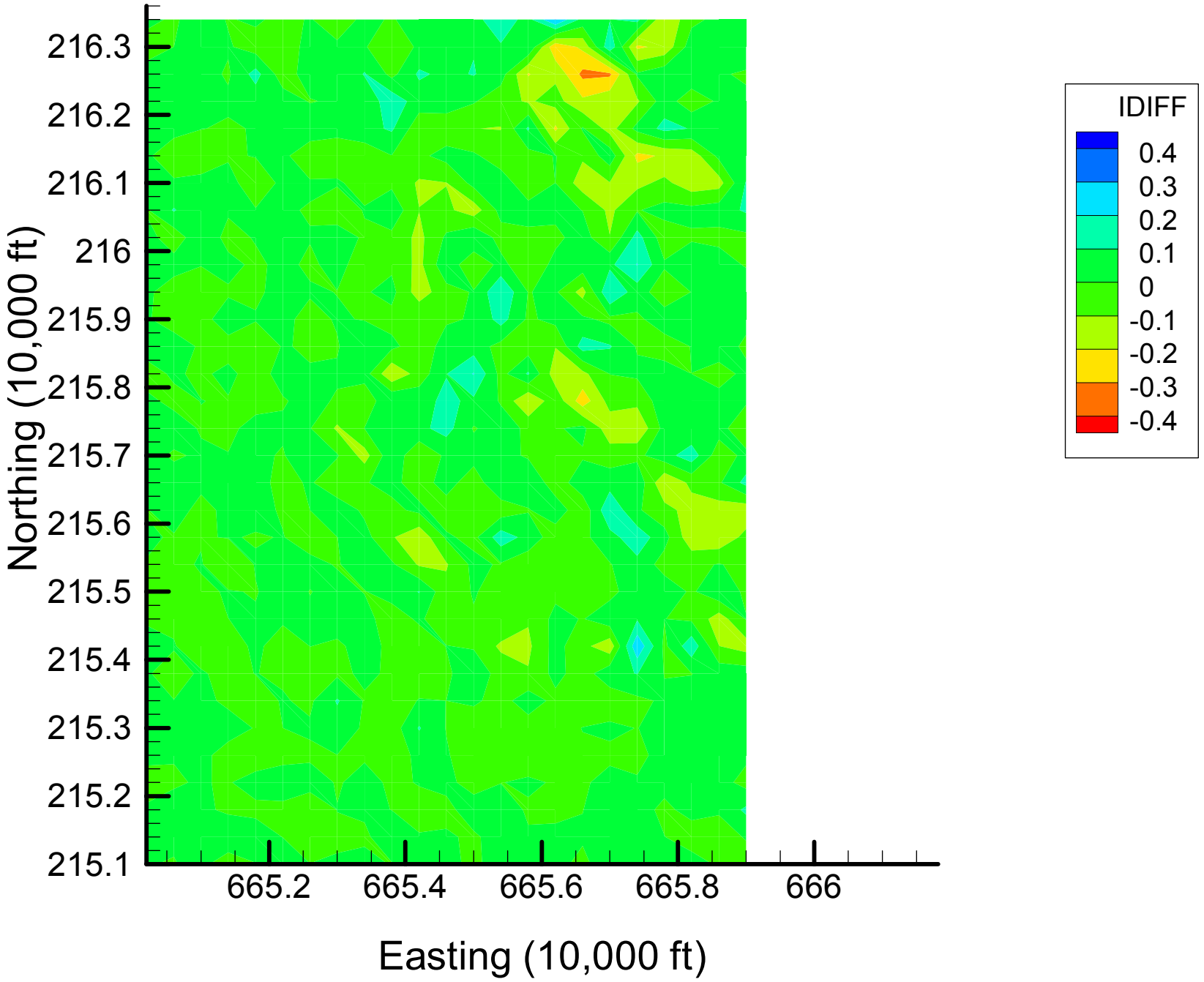

Site 133: TCE Indicator Differences, 1999-2000, 13% Removal

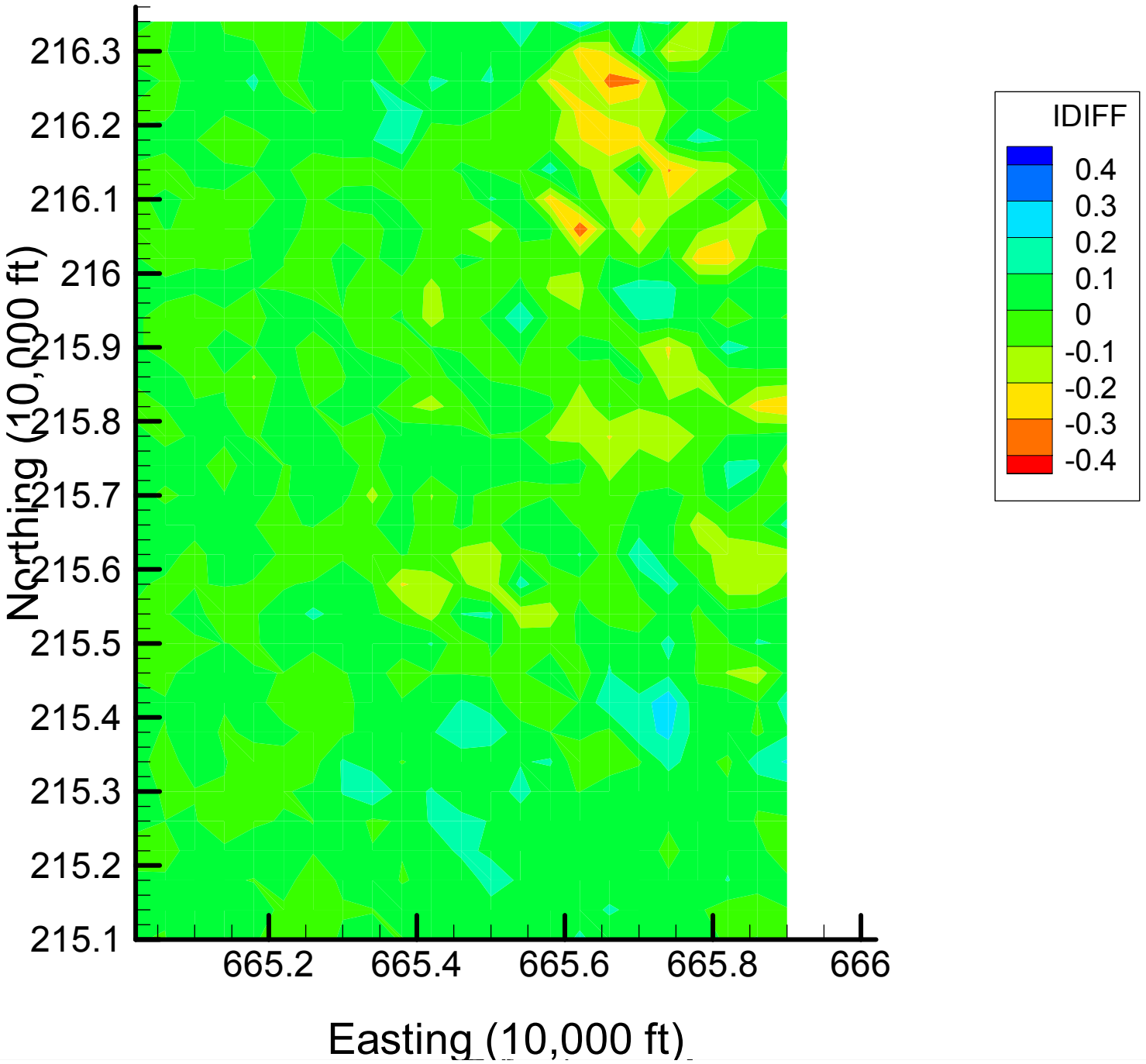

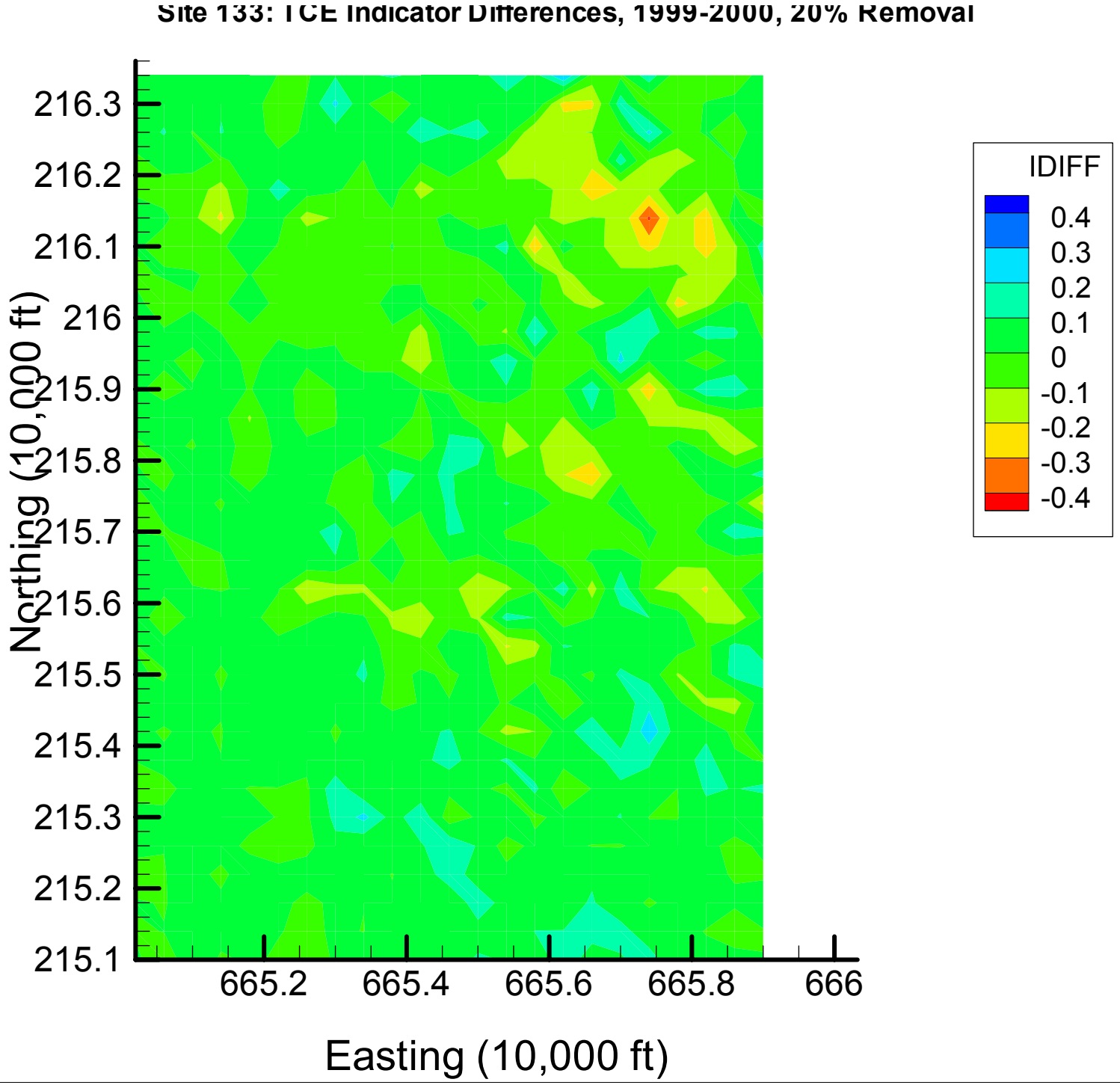
Site 133: TCE Indicator Differences, 1999-2000, 20% Removal
IDIFF
0.4
0.3
0.2
0.1
0
-0.1
-0.2
-0.3
-0.4
Northing (10,000 ft)
216.3
216.2
216.1
216
215.9
215.8
215.7
215.6
215.5
215.4
215.3
215.2
215.1
665.2
665.4
665.6
665.8
666
Easting (10,000 ft)

Site 133: TCE Indicator Differences, 1999-2000, 27% Removal

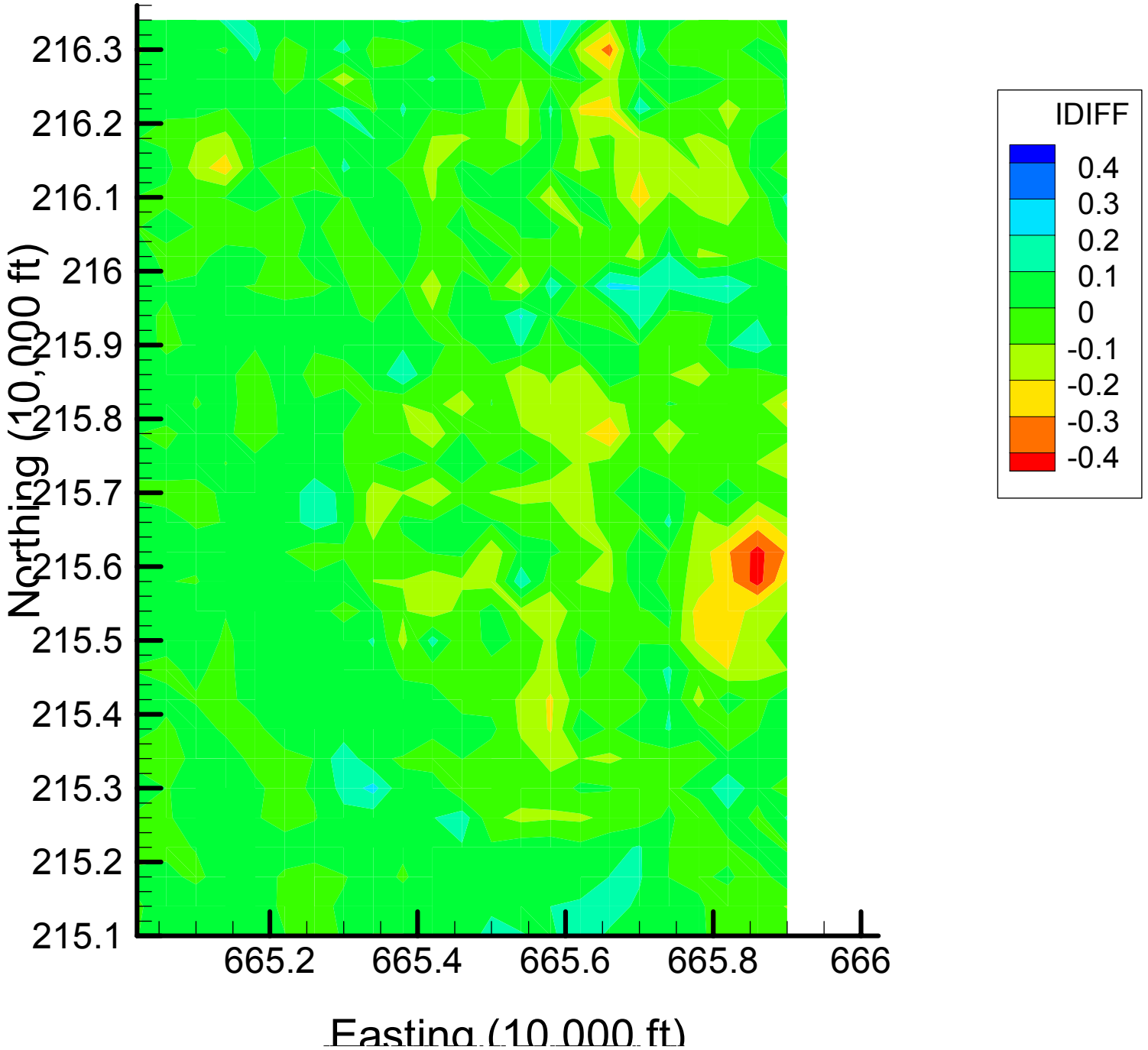

Site 133: TCE Indicator Differences, 1999-2000, 33% Removal

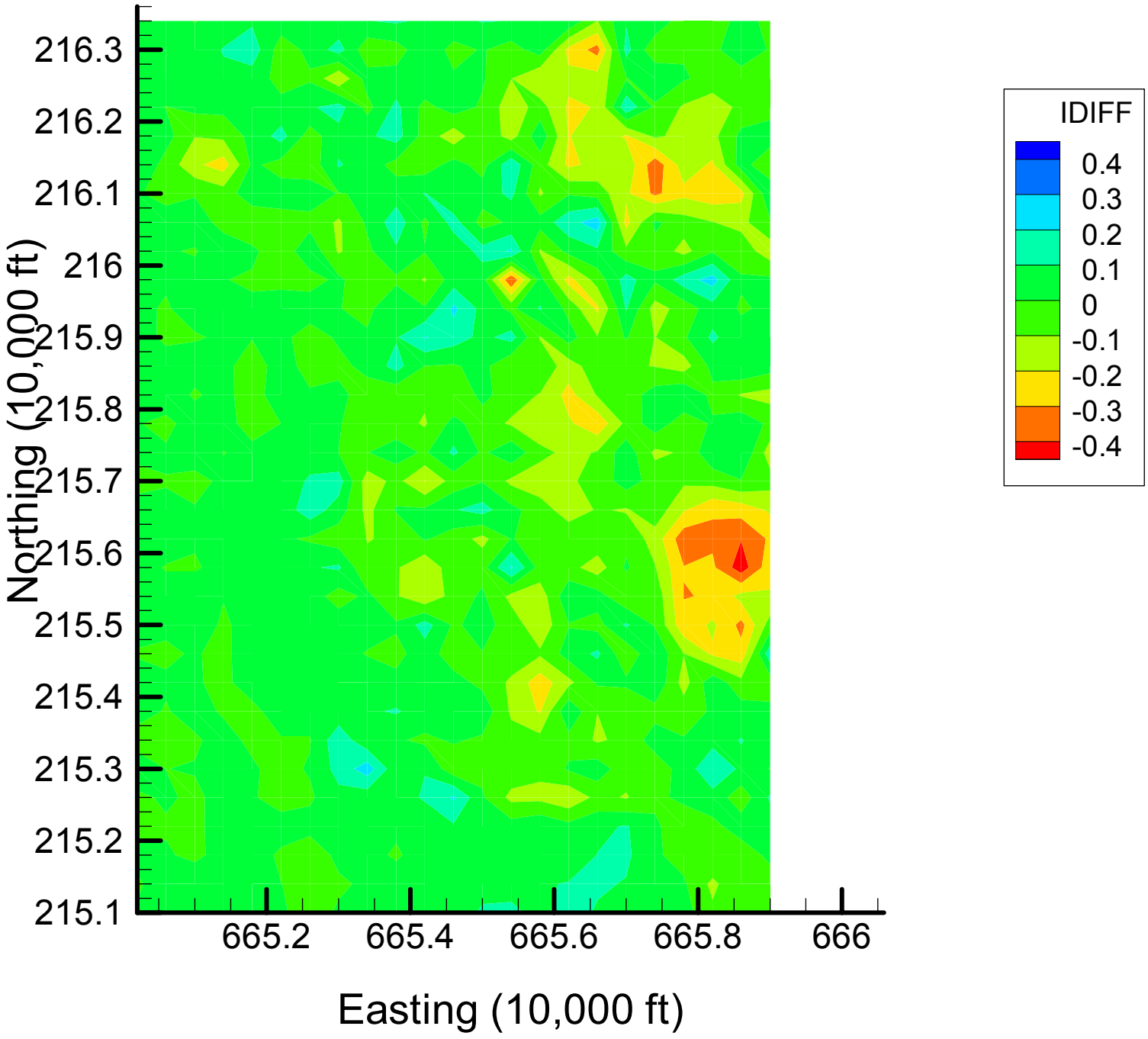

Site 133: TCE Indicator Differences, 1999-2000, 40% Removal

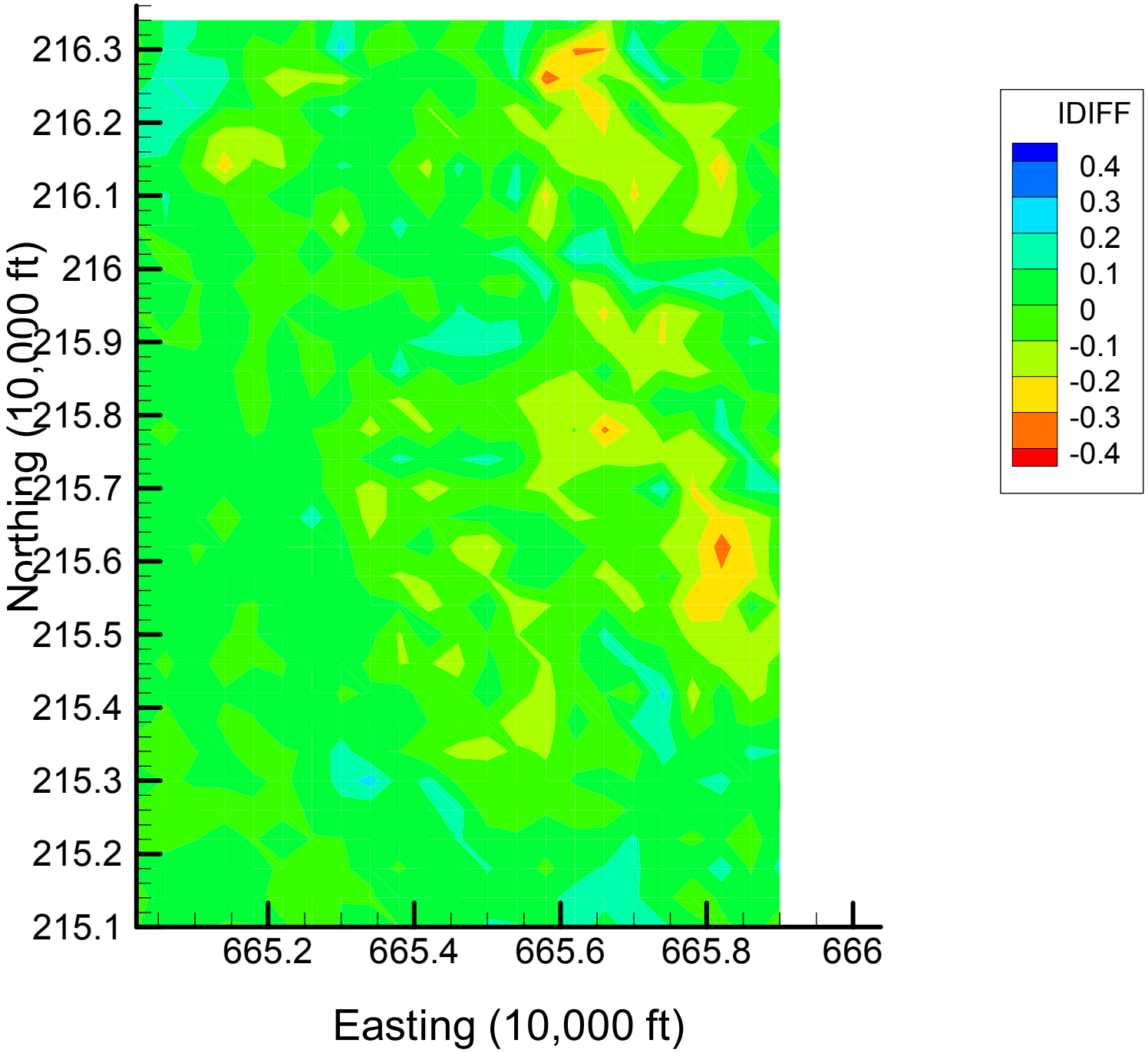

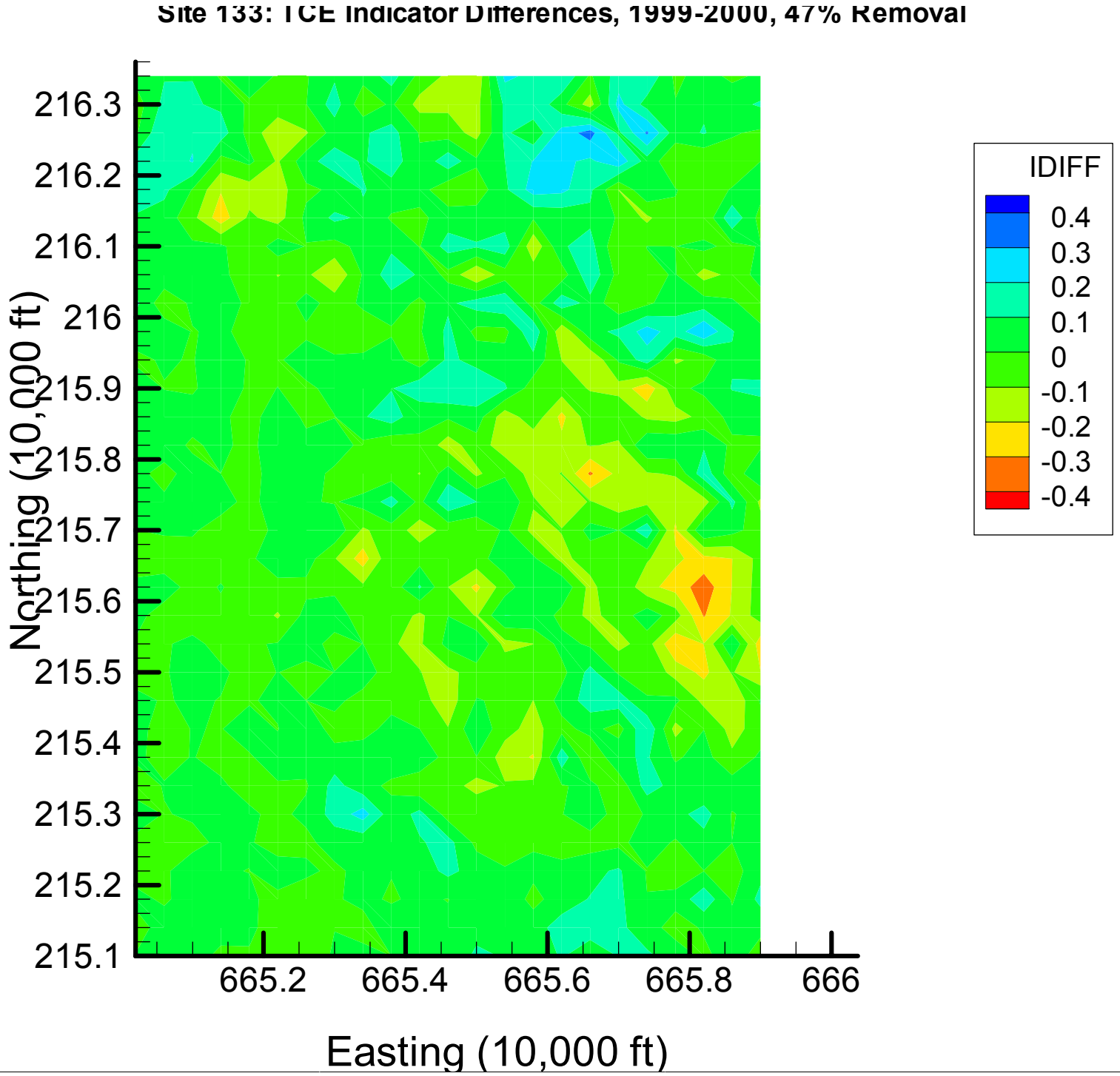
Site 133: TCE Indicator Differences, 1999-2000, 47% Removal
IDIFF
0.4
0.3
0.2
0.1
0
-0.1
-0.2
-0.3
-0.4
Northing (10,000 ft)
216.3
216.2
216.1
216
215.9
215.8
215.7
215.6
215.5
215.4
215.3
215.2
215.1
665.2
665.4
665.6
665.8
666
Easting (10,000 ft)

Site 133: TCE Indicator Differences, 1999-2000, 53% Removal

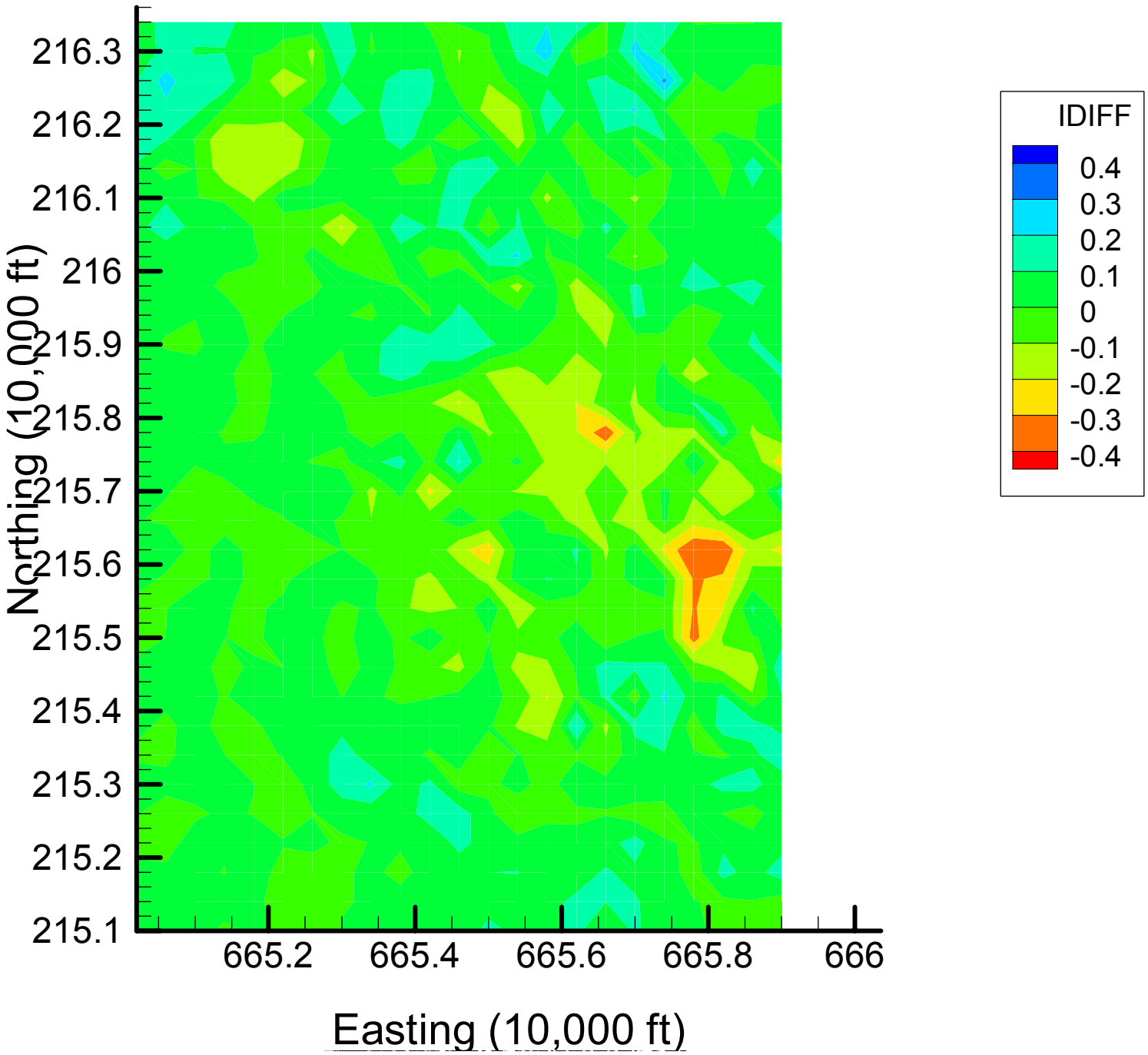

Site 133: TCE Indicator Differences, 1999-2000, 60% Removal

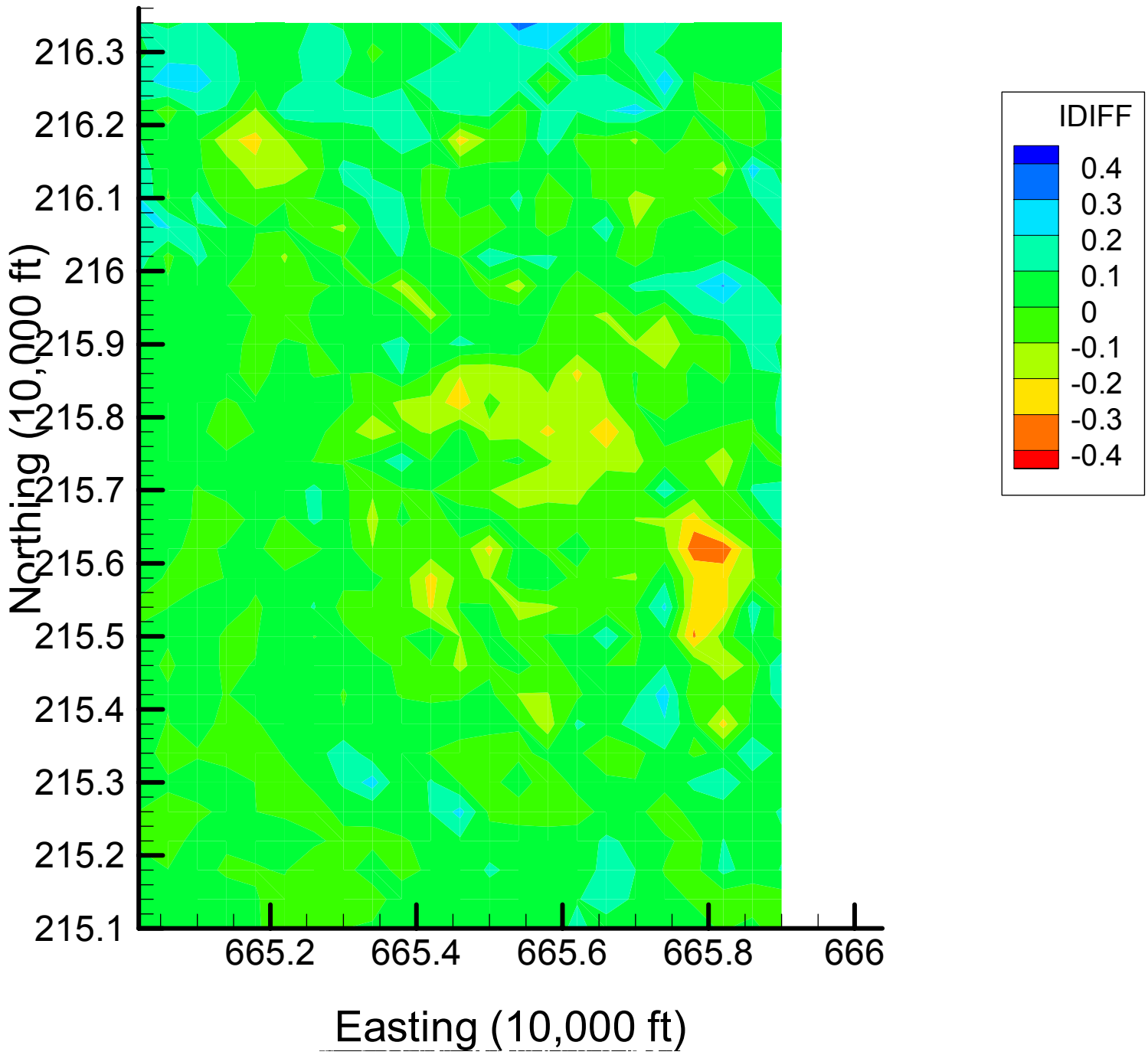

Site 133: TCE Indicator Differences, 1999-2000, 67% Removal

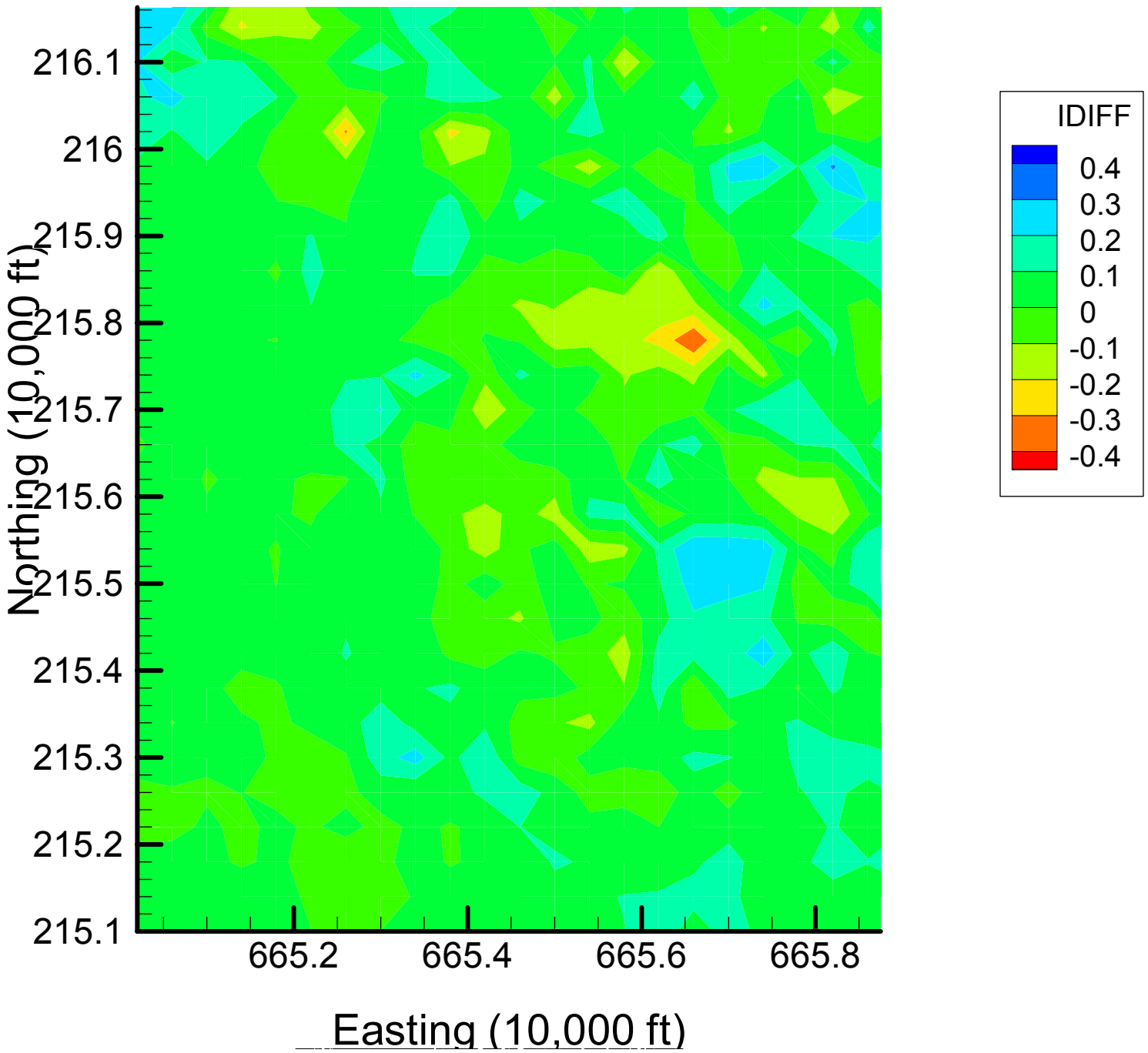

Appendix 4.2
TCE Indicator Difference Maps
Time Slice 2

Site 133: TCE Indicator Differences, 2001-2002, 7% Removal

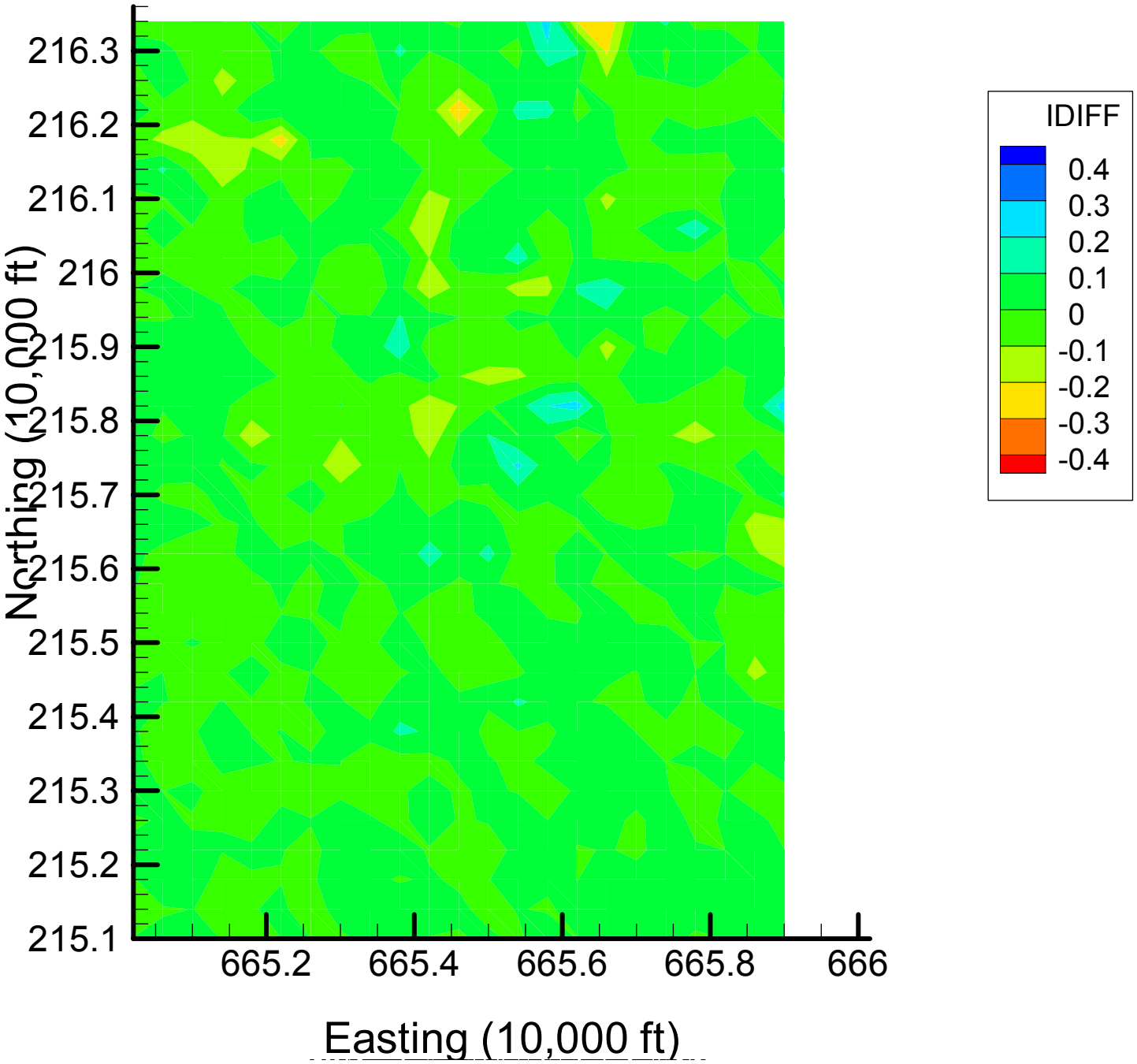

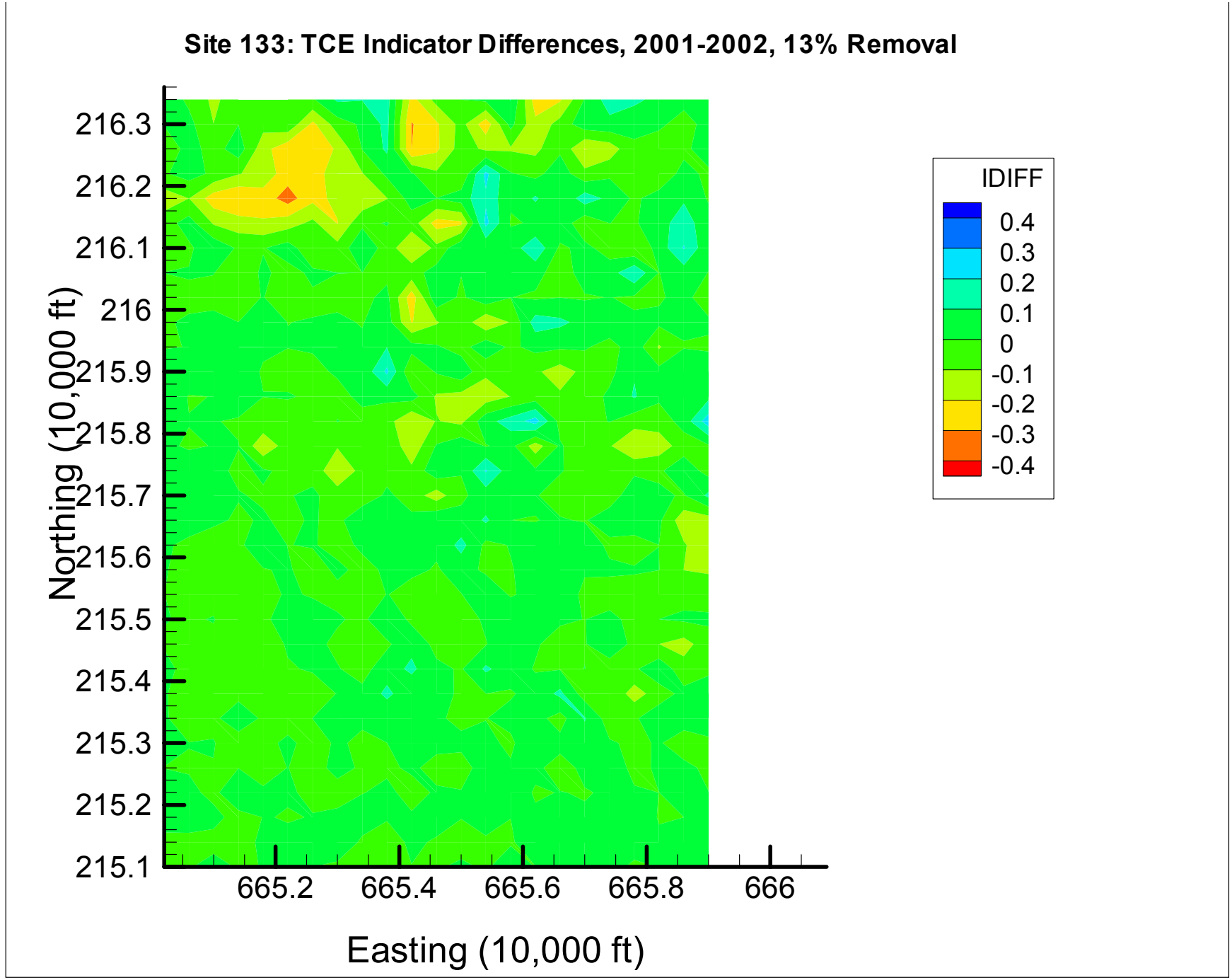
Site 133: TCE Indicator Differences, 2001-2002, 13% Removal
IDIFF
0.4
0.3
0.2
0.1
0
-0.1
-0.2
-0.3
-0.4
Northing (10,000 ft)
216.3
216.2
216.1
216
215.9
215.8
215.7
215.6
215.5
215.4
215.3
215.2
215.1
665.2
665.4
665.6
665.8
666
Easting (10,000 ft)

Site 133: TCE Indicator Differences, 2001-2002, 20% Removal

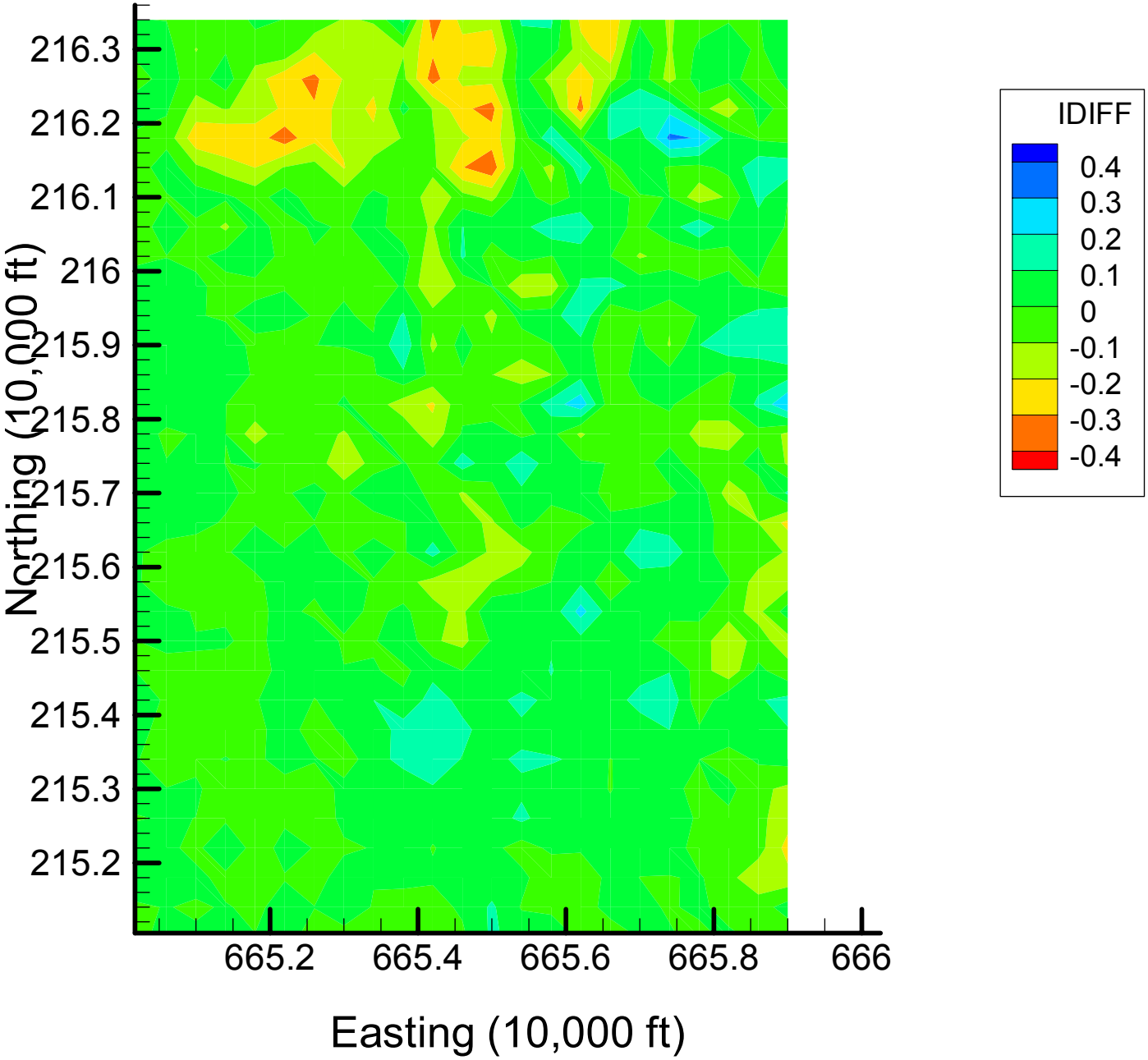

Site 133: TCE Indicator Differences, 2001-2002, 27% Removal

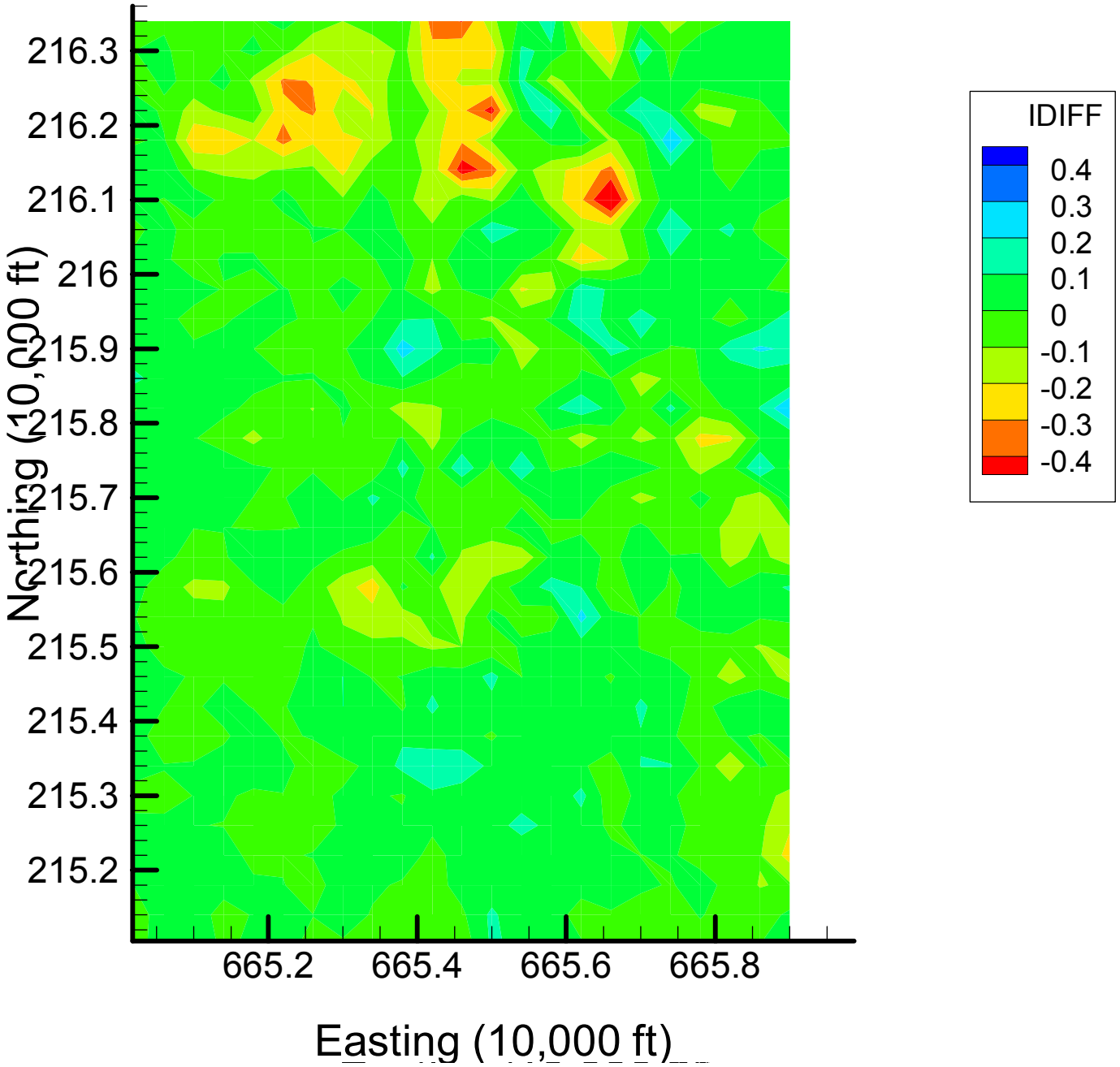

Site 133: TCE Indicator Differences, 2001-2002, 33% Removal

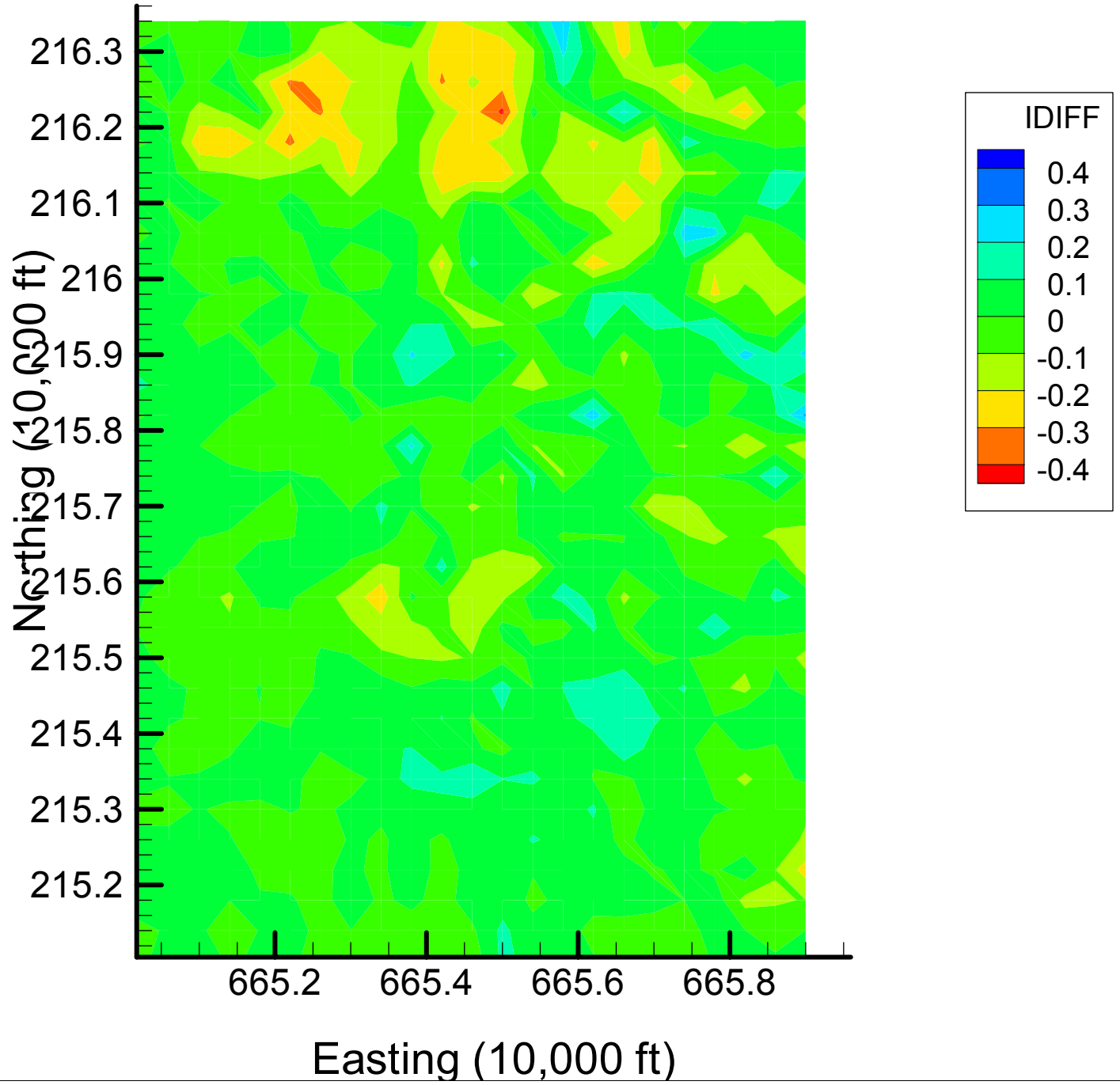

Site 133: TCE Indicator Differences, 2001-2002, 40% Removal

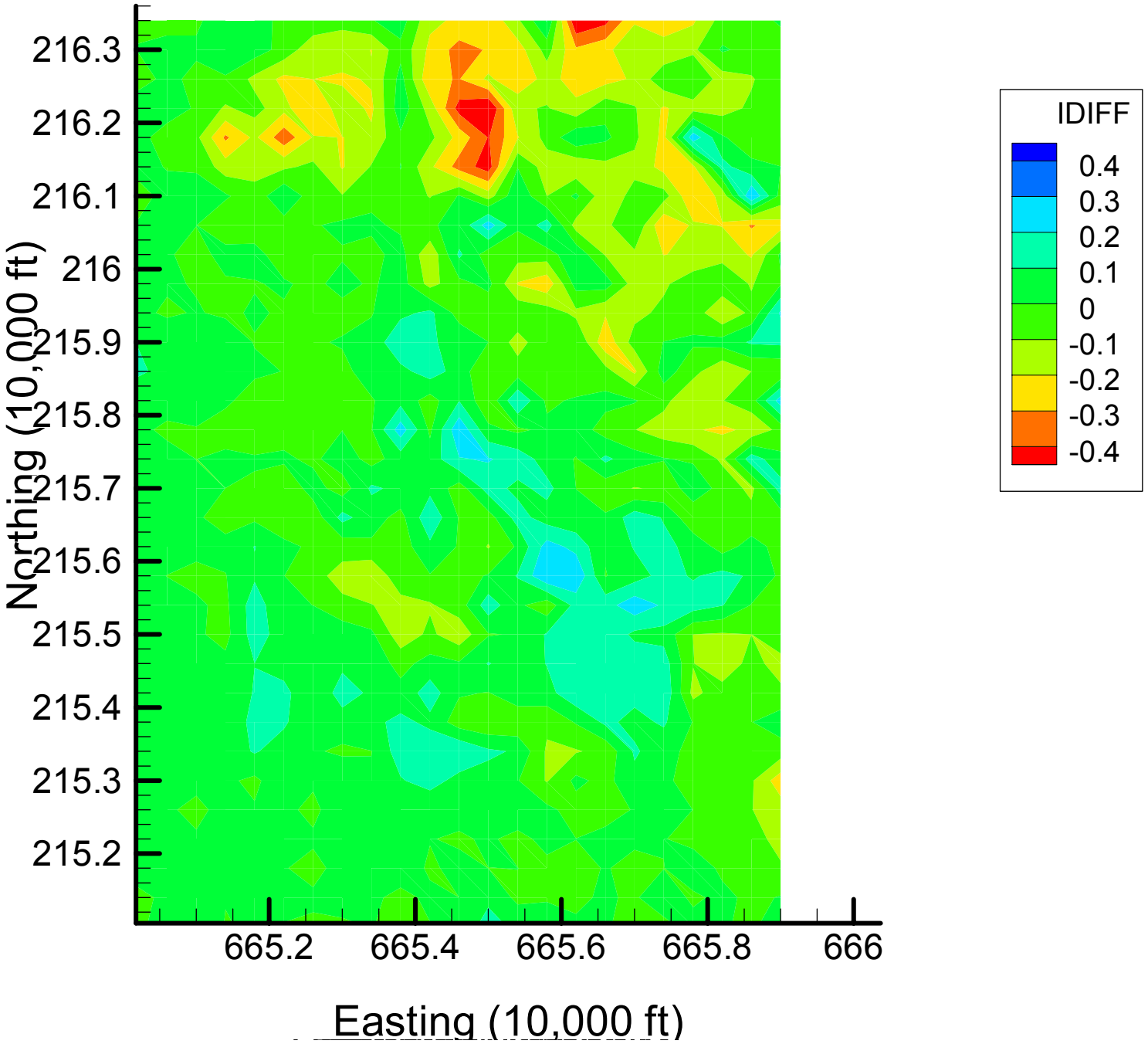

Site 133: TCE Indicator Differences, 2001-2002, 47% Removal

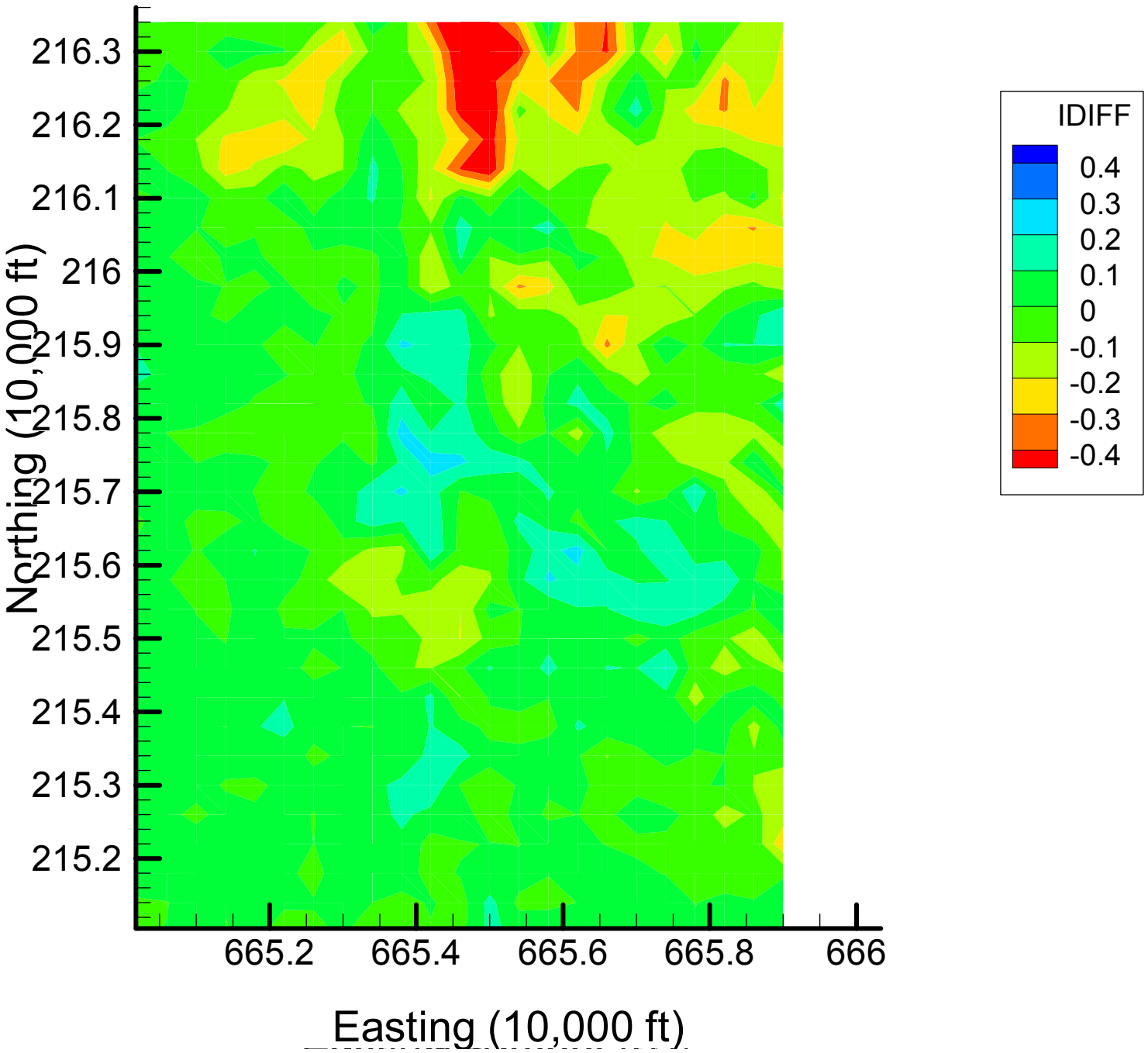

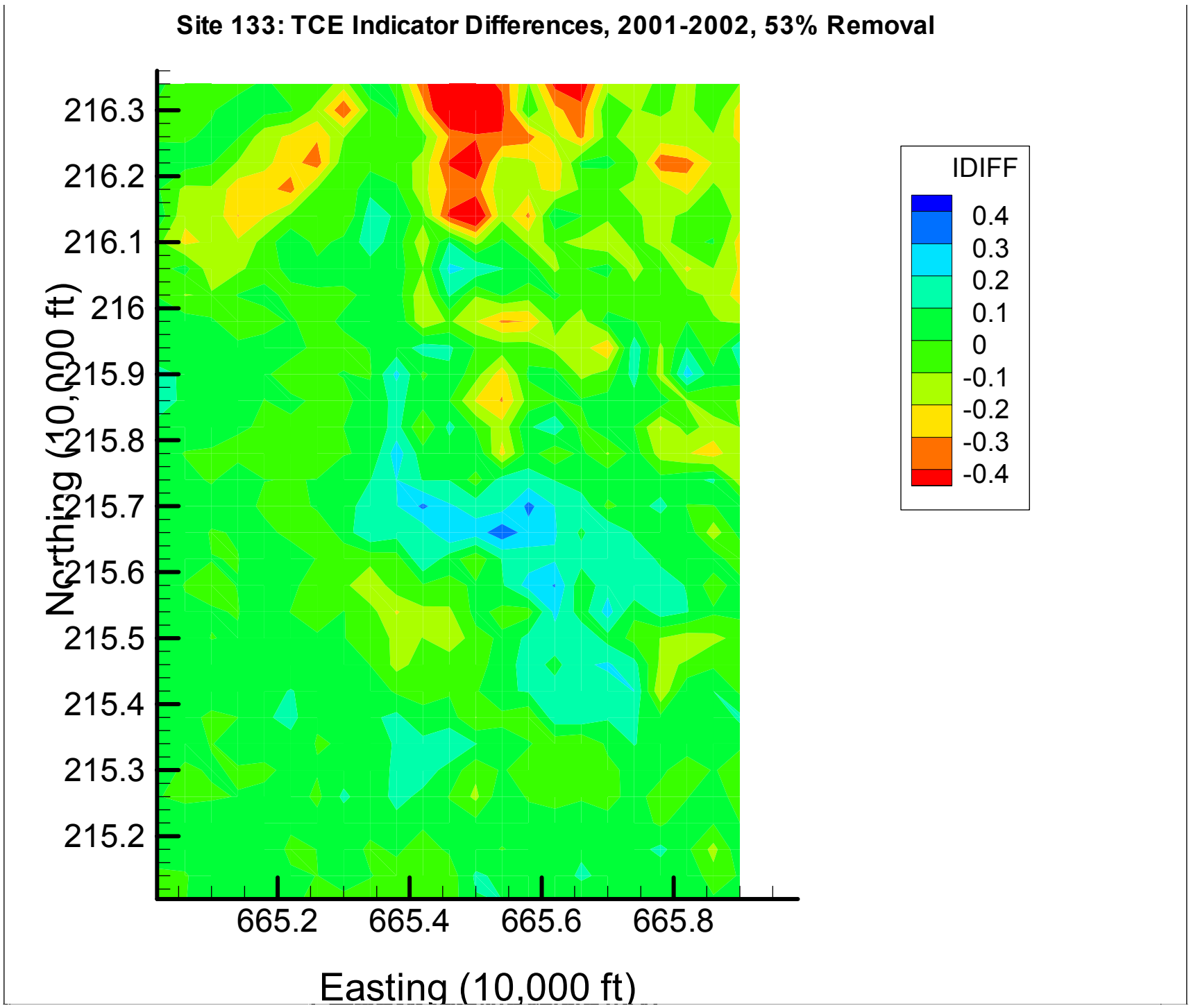
Site 133: TCE Indicator Differences, 2001-2002, 53% Removal
IDIFF
0.4
0.3
0.2
0.1
0
-0.1
-0.2
-0.3
-0.4
216.3
216.2
216.1
216
215.9
215.8
215.7
215.6
215.5
215.4
215.3
215.2
Northing (10,000 ft)
665.2
665.4
665.6
665.8
Easting (10,000 ft)

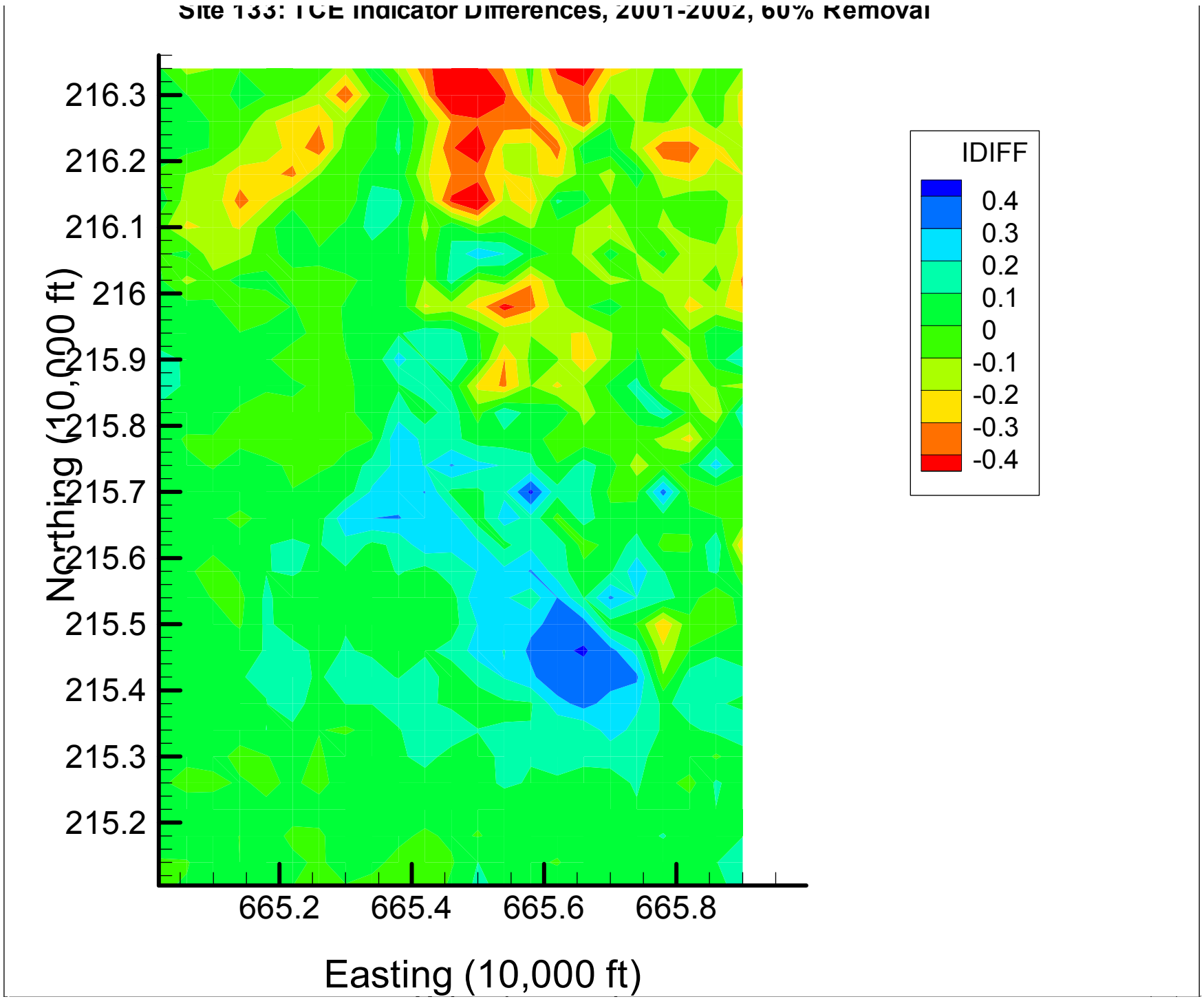
Site 133: TCE Indicator Differences, 2001-2002, 60% Removal
IDIFF
0.4
0.3
0.2
0.1
0
-0.1
-0.2
-0.3
-0.4
Northing (10,000 ft)
216.3
216.2
216.1
216
215.9
215.8
215.7
215.6
215.5
215.4
215.3
215.2
665.2
665.4
665.6
665.8
Easting (10,000 ft)

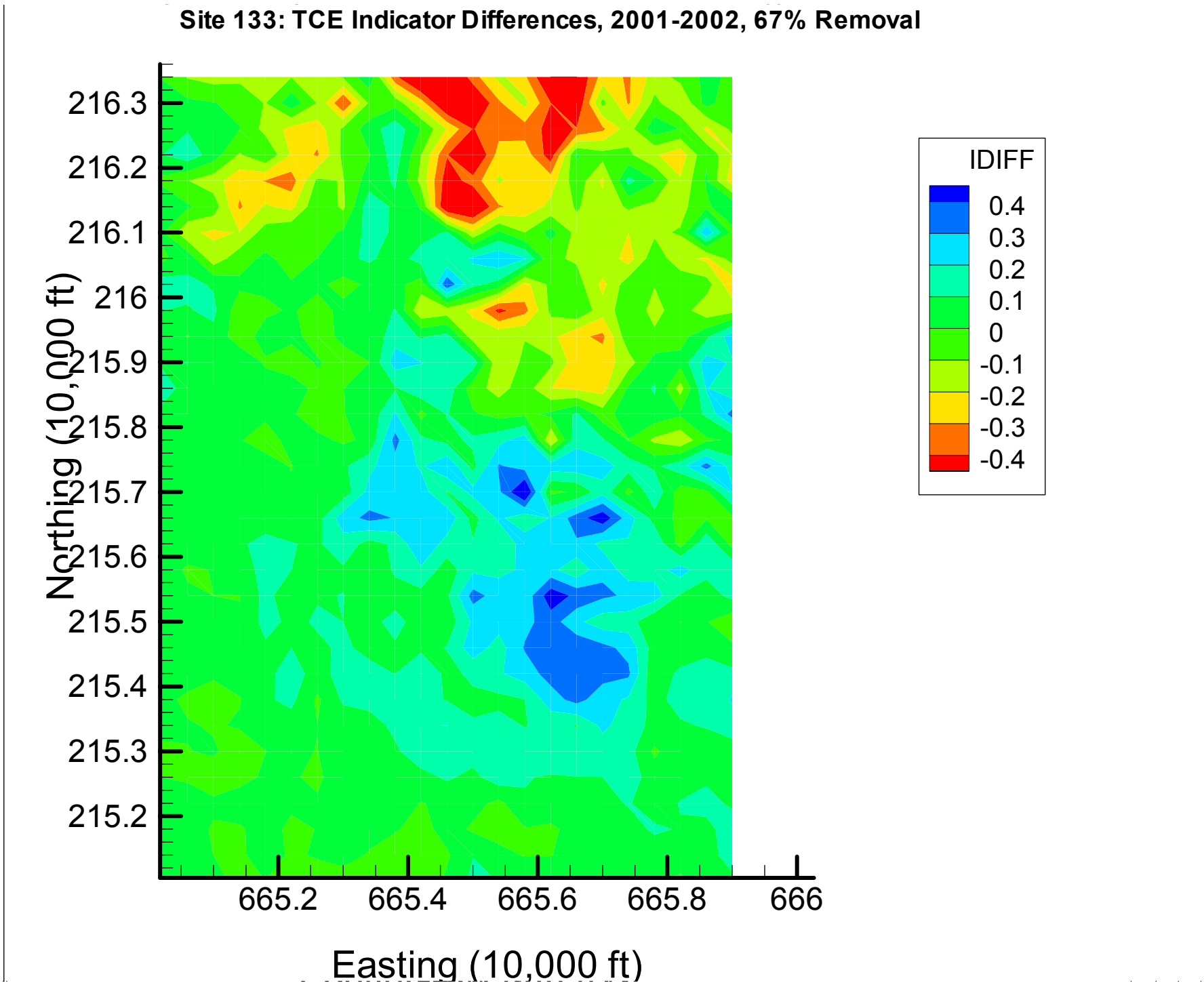
Site 133: TCE Indicator Differences, 2001-2002, 67% Removal
IDIFF
0.4
0.3
0.2
0.1
0
-0.1
-0.2
-0.3
-0.4
Northing (10,000 ft)
216.3
216.2
216.1
216
215.9
215.8
215.7
215.6
215.5
215.4
215.3
215.2
665.2
665.4
665.6
665.8
666
Easting (10,000 ft)

Appendix 4.3
DIOXANE14 Local Variance Maps
Time Slice 1

Site 133: DIOXANE14 Local Variances, 1999-2000, Base Map

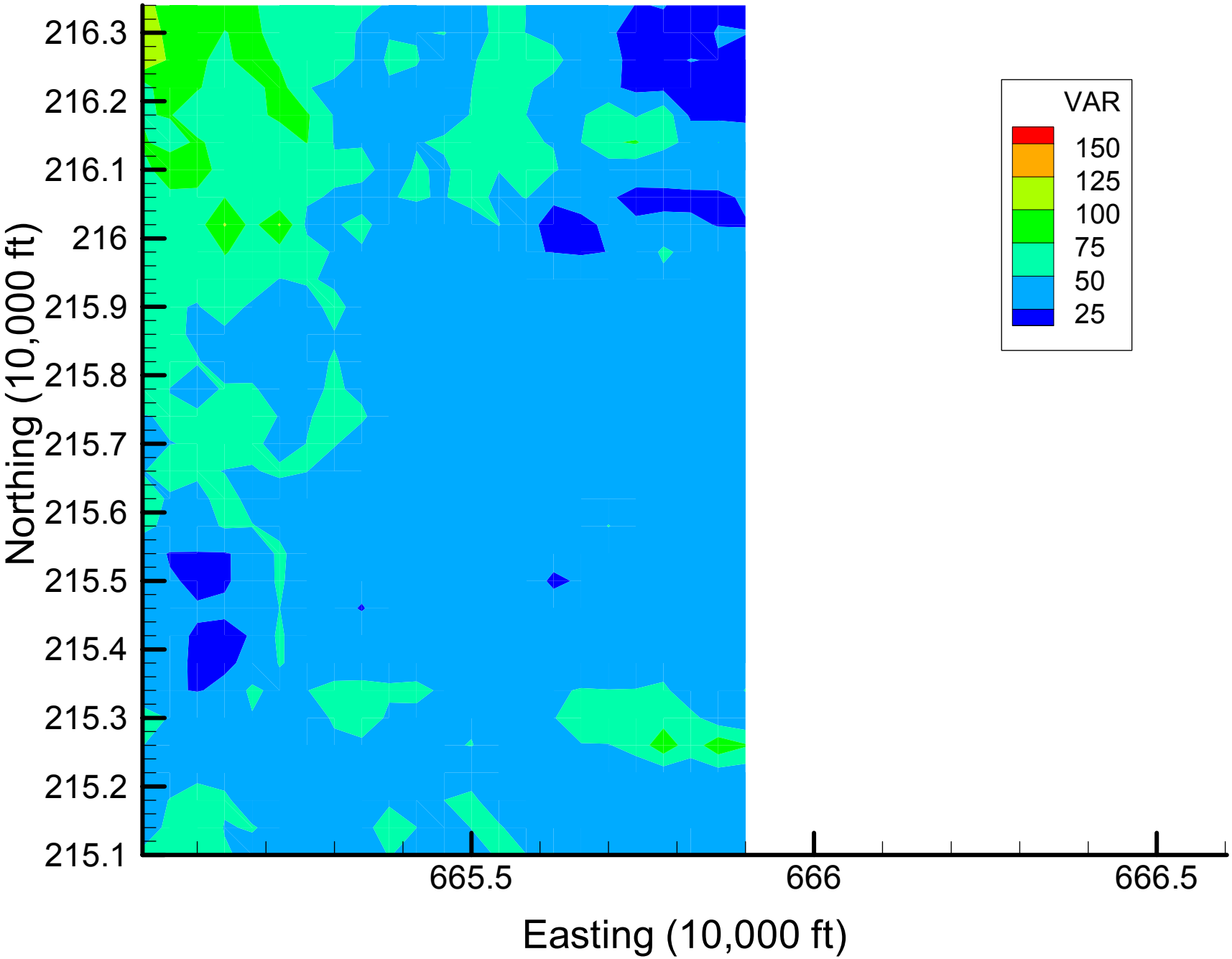

Site 133: DIOXANE14 Local Variances, 1999-2000, 7% Removal

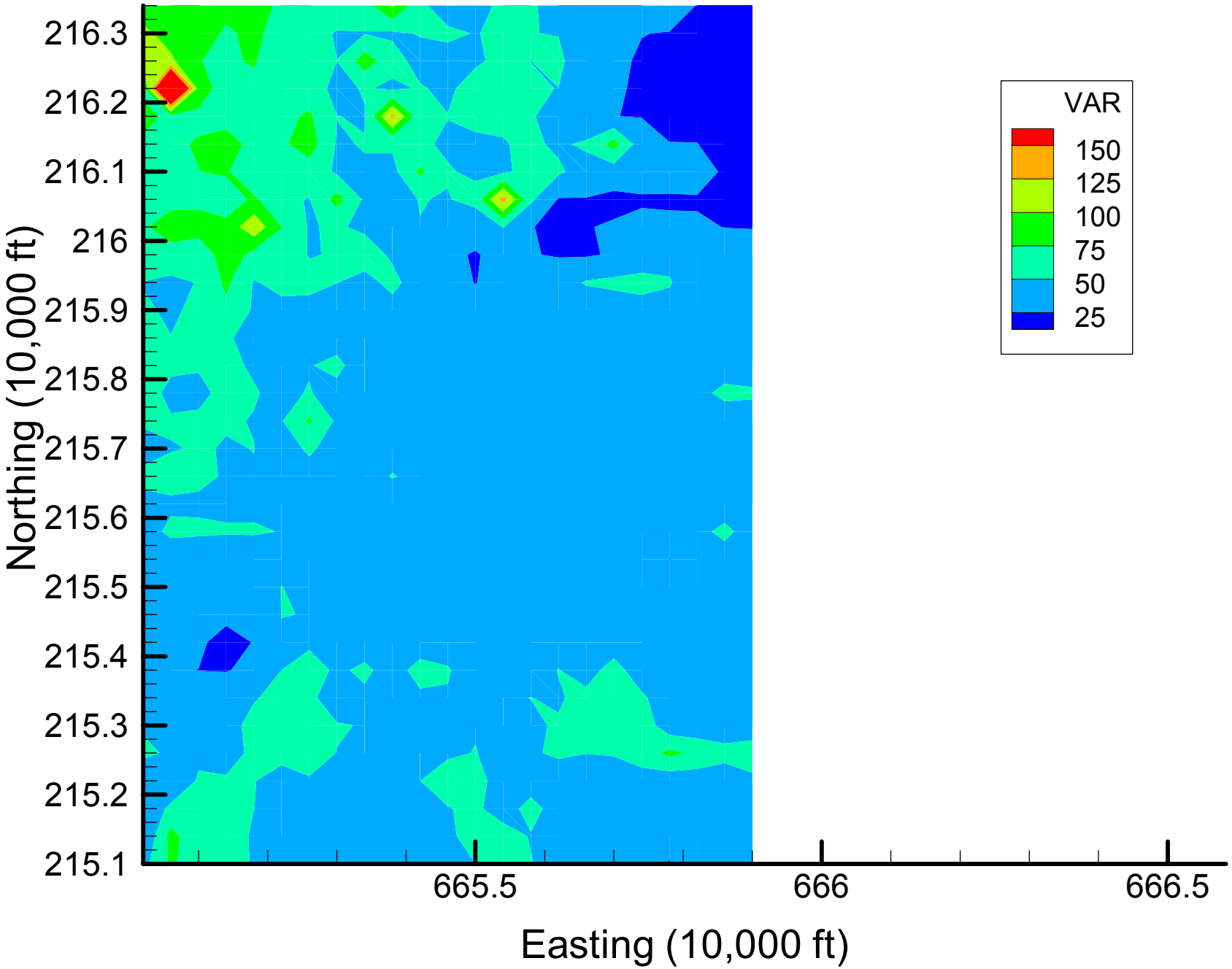

Site 133: DIOXANE14 Local Variances, 1999-2000, 13% Removal

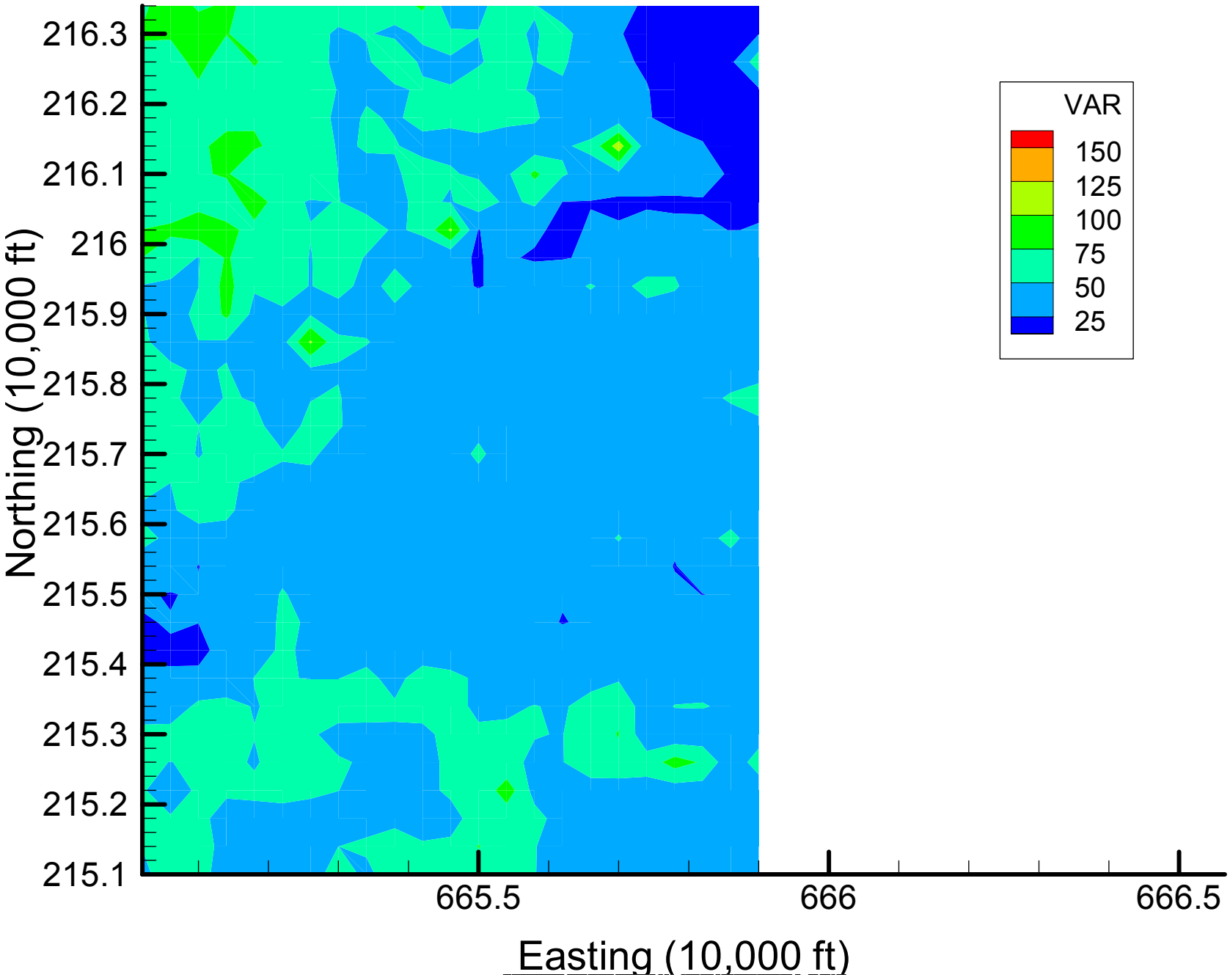

Site 133: DIOXANE14 Local Variances, 1999-2000, 20% Removal

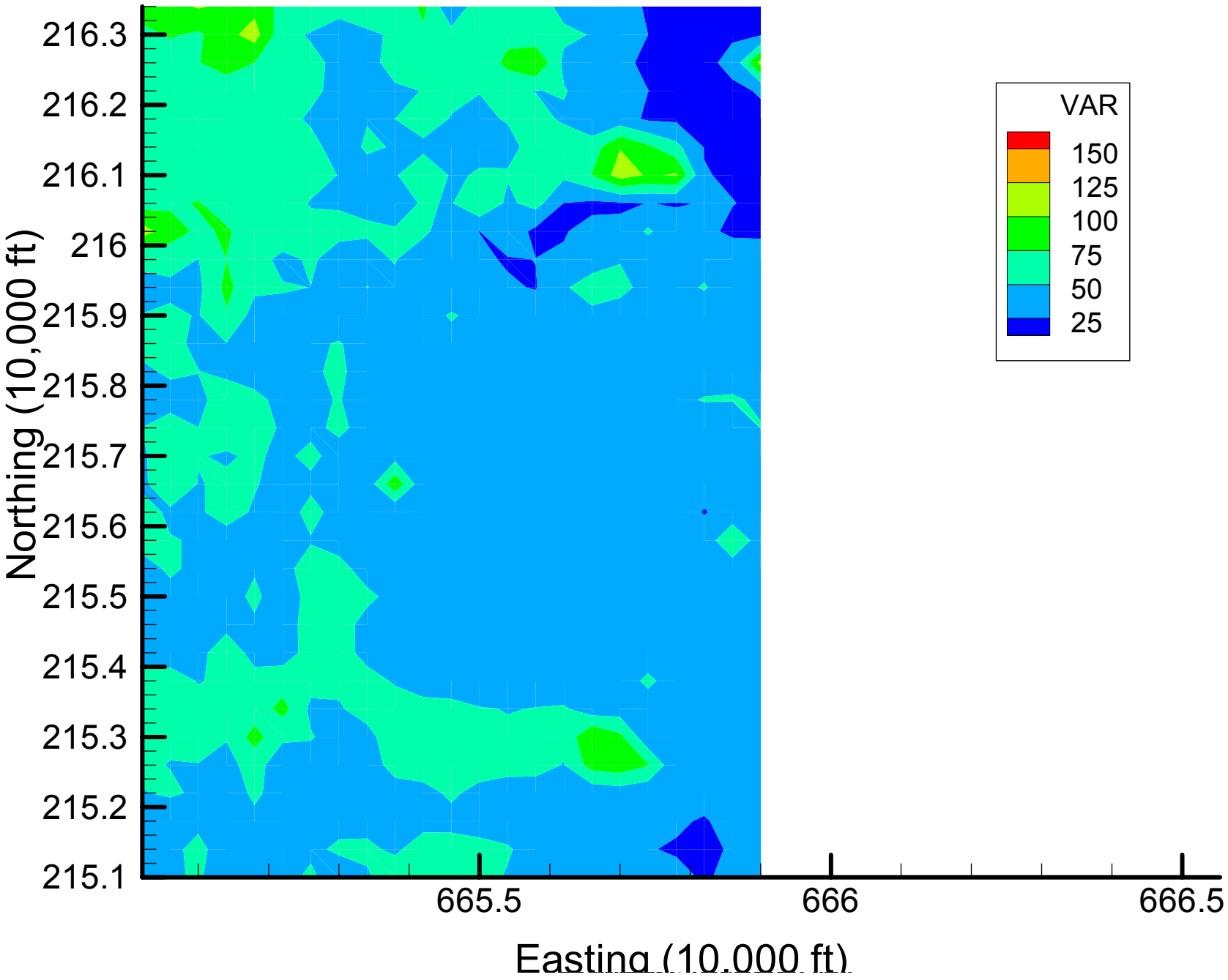

Site 133: DIOXANE14 Local Variances, 1999-2000, 27% Removal

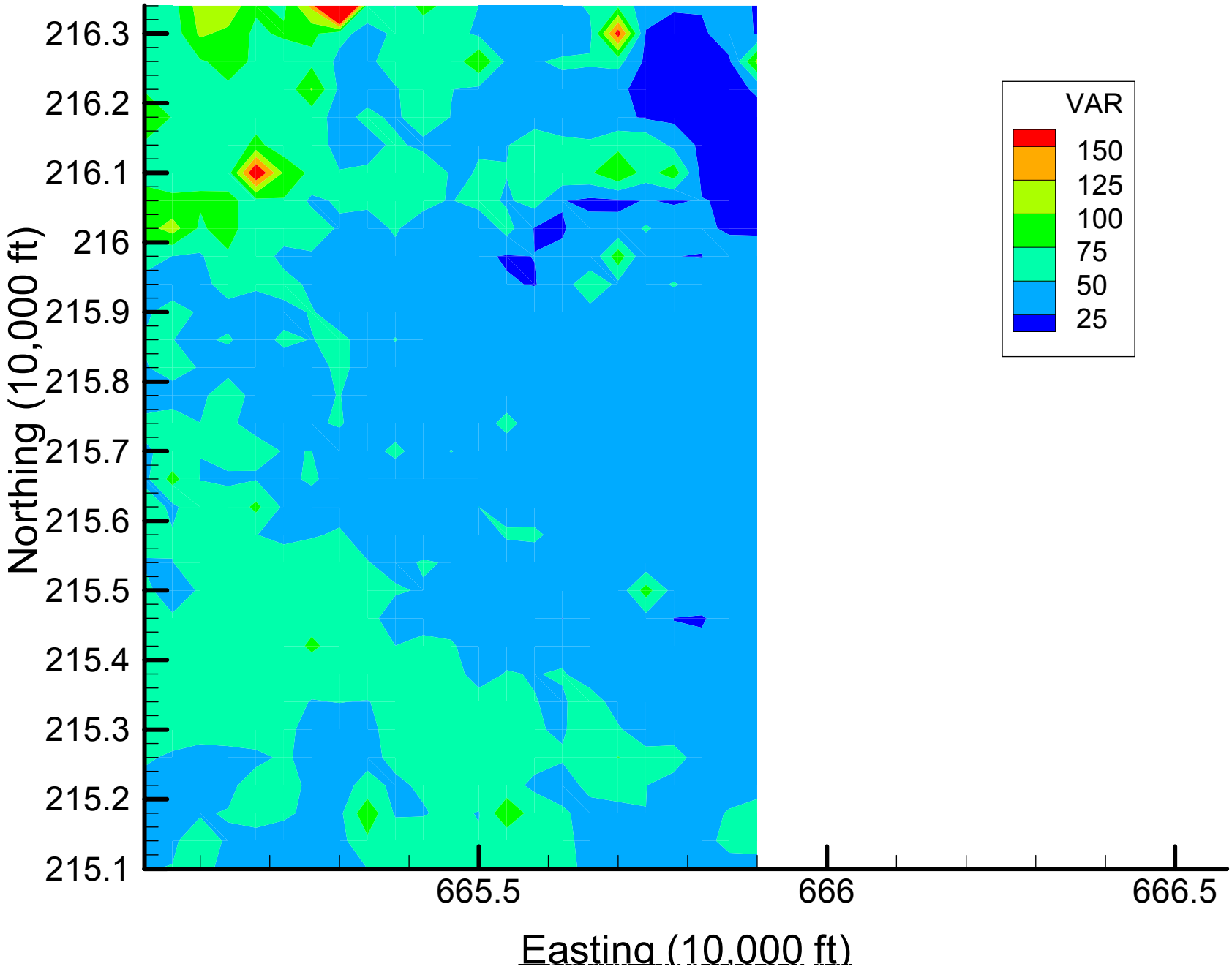

Site 133: DIOXANE14 Local Variances, 1999-2000, 33% Removal

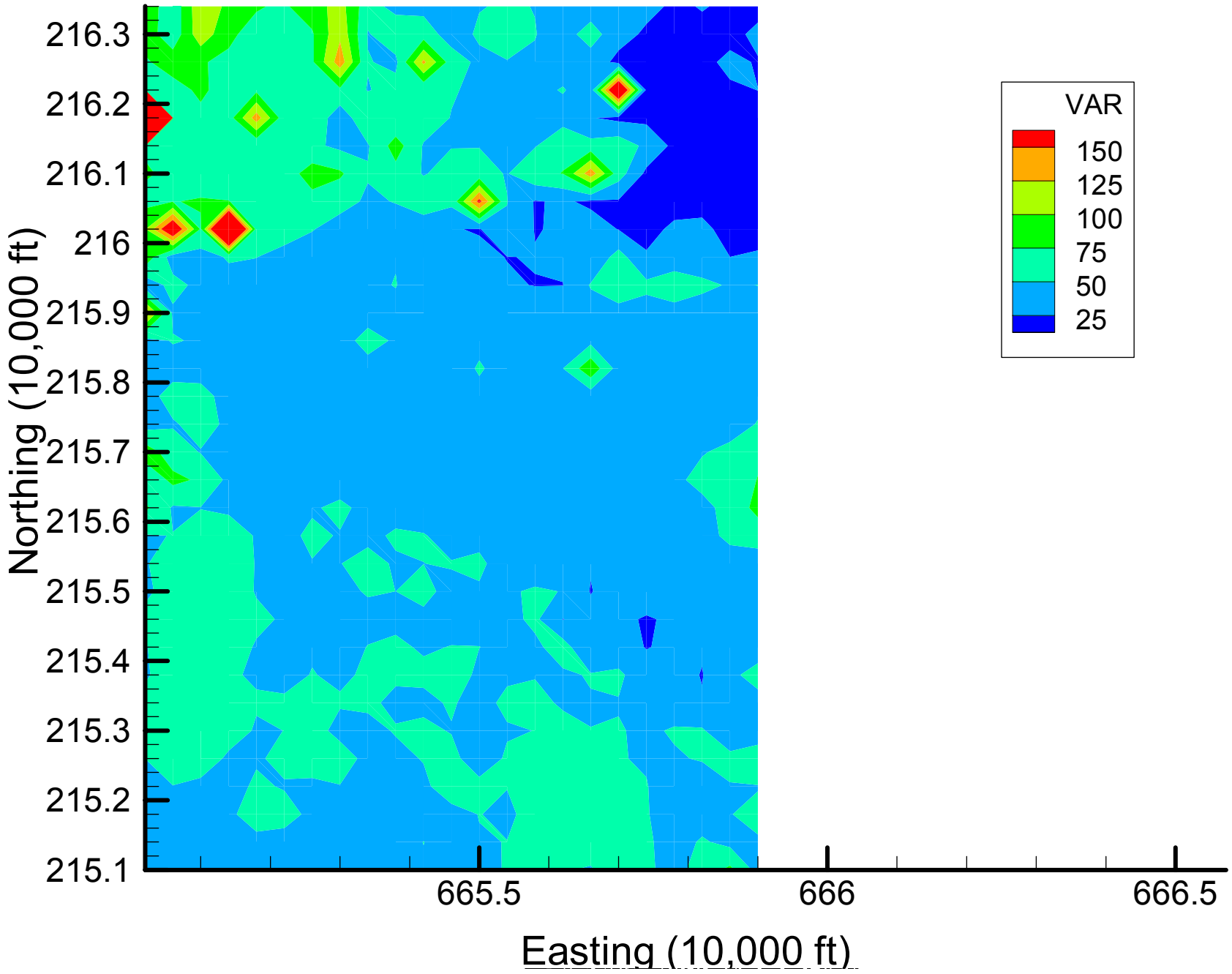

Site 133: DIOXANE14 Local Variances, 1999-2000, 40% Removal

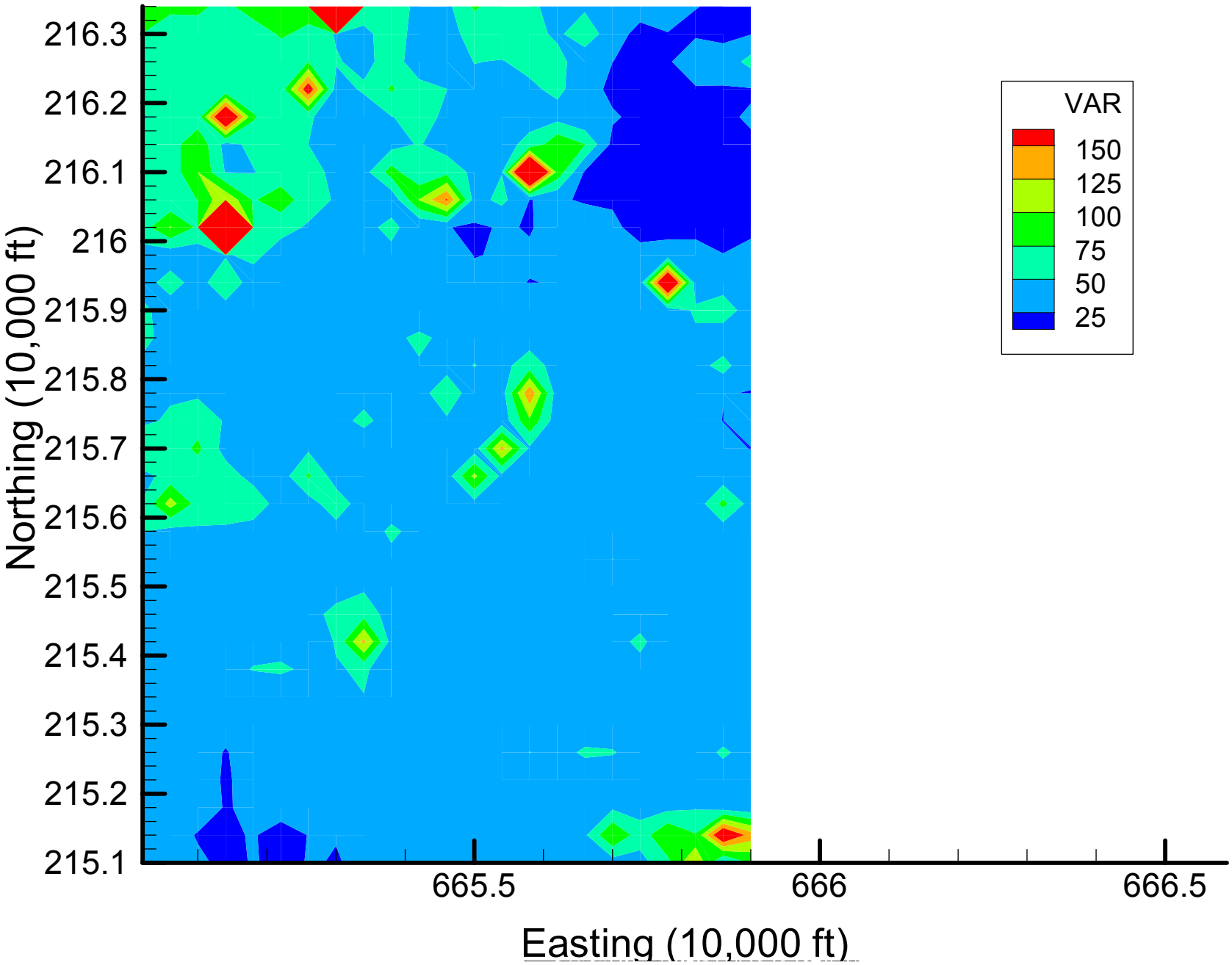

Site 133: DIOXANE14 Local Variances, 1999-2000, 47% Removal

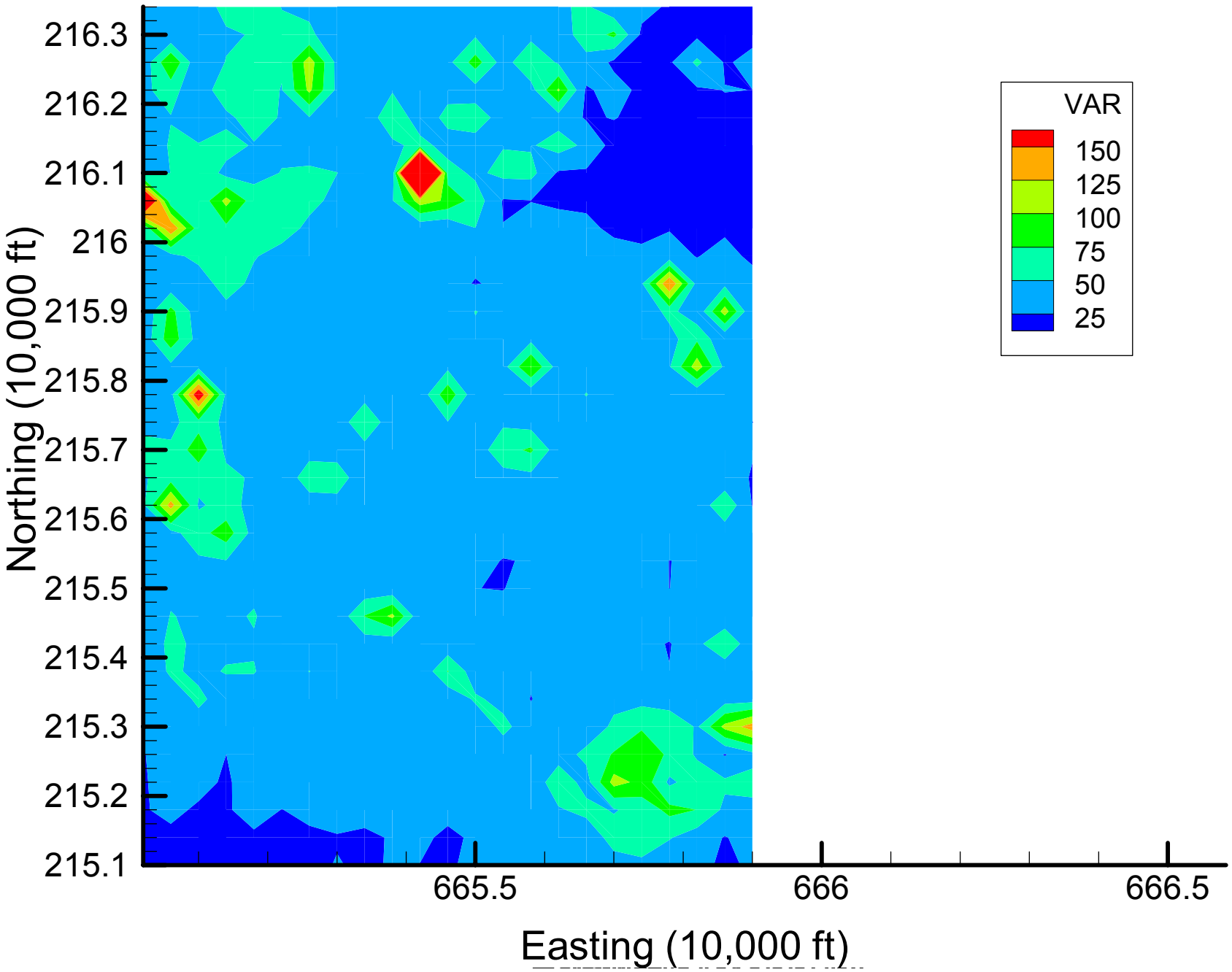

Site 133: DIOXANE14 Local Variances, 1999-2000, 53% Removal

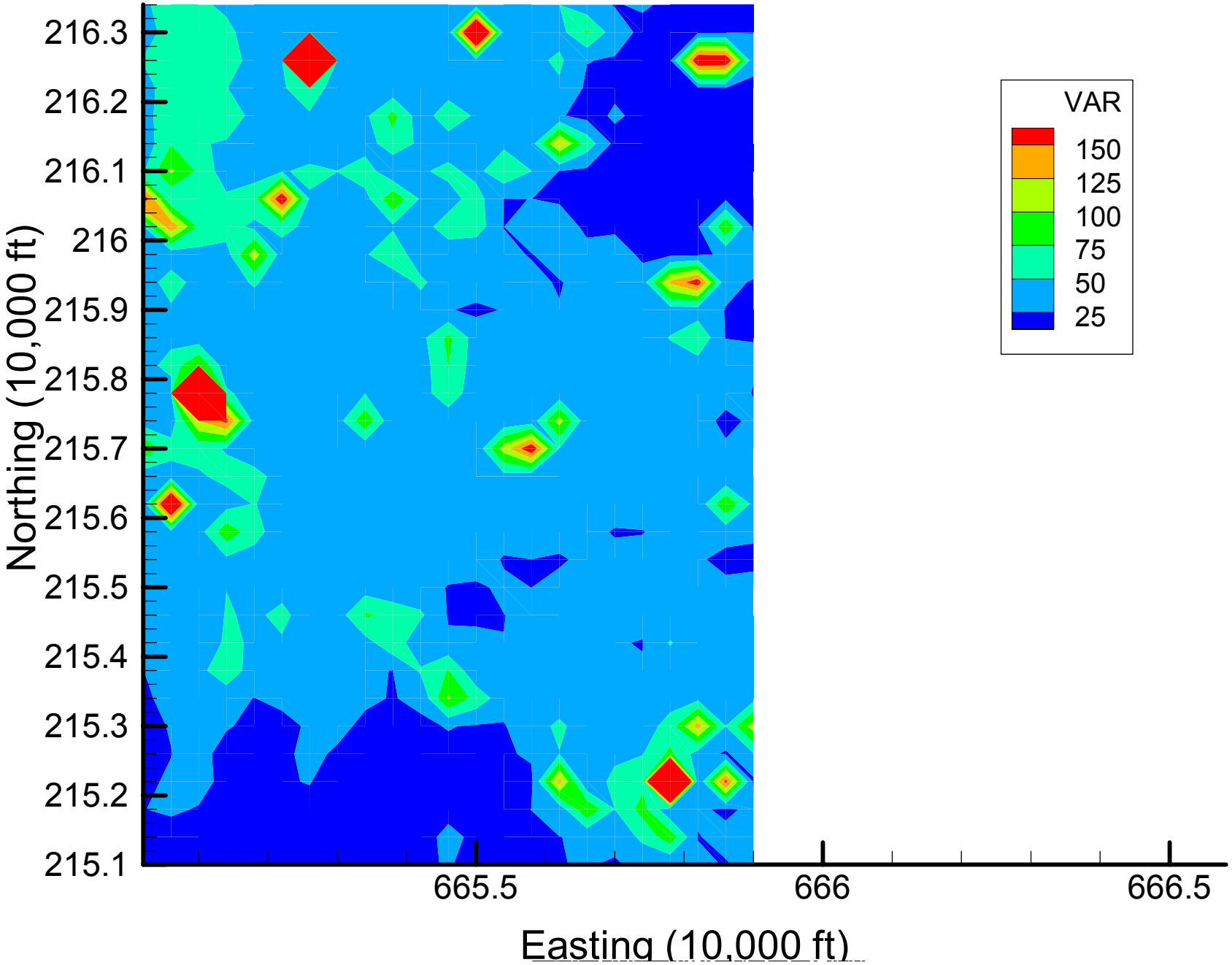

Site 133: DIOXANE14 Local Variances, 1999-2000, 60% Removal

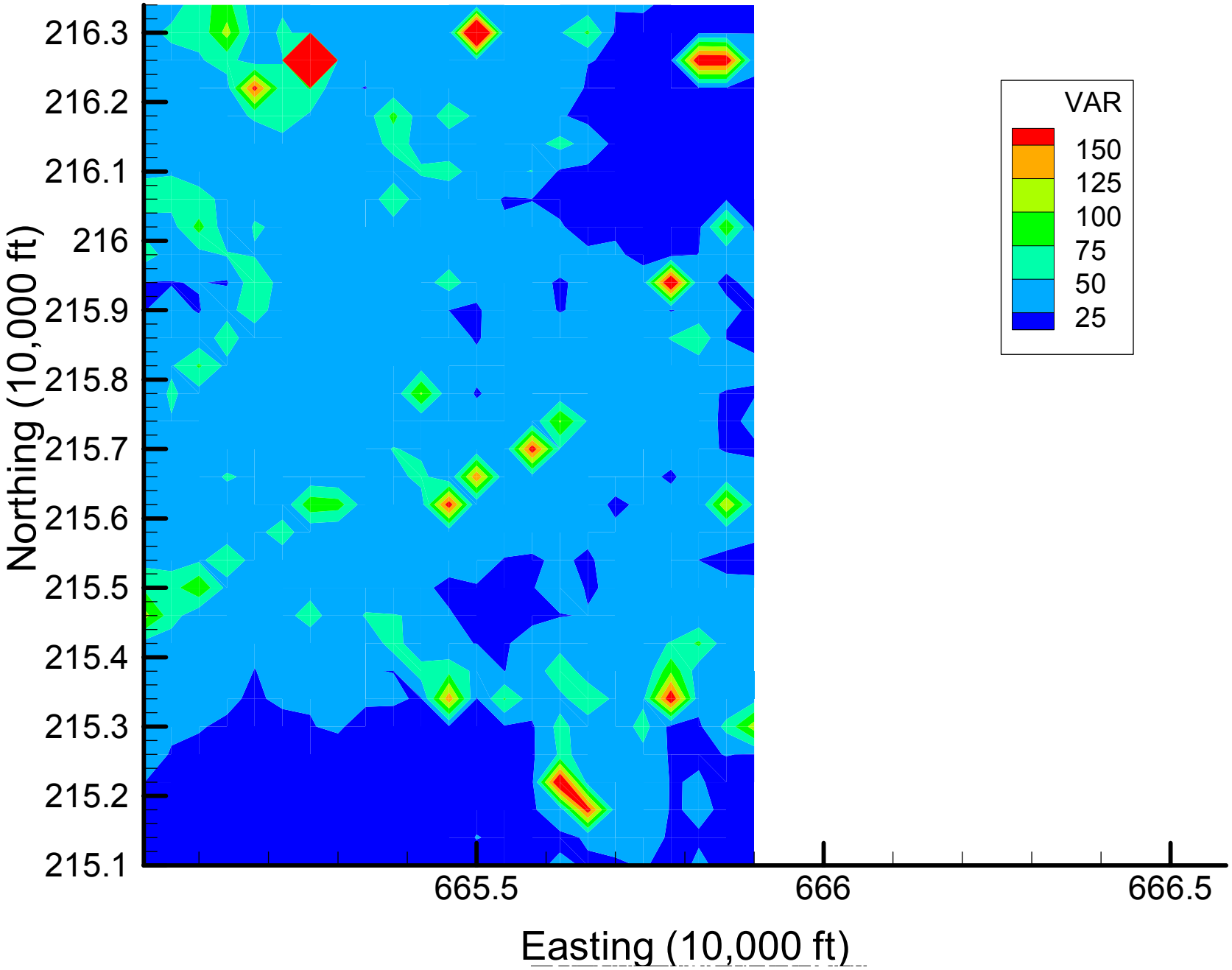

Site 133: DIOXANE14 Local Variances, 1999-2000, 67% Removal

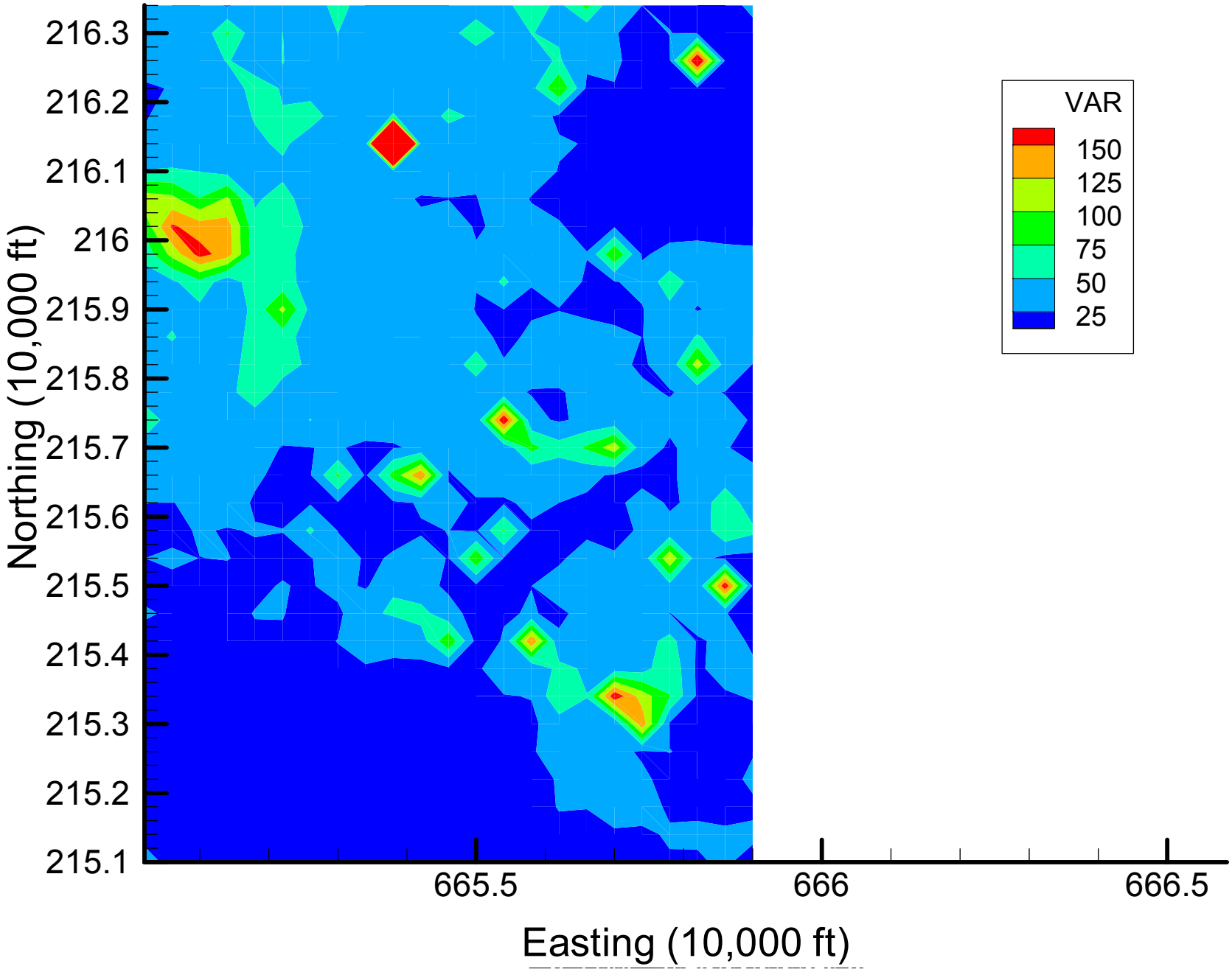

Appendix 4.3
DIOXANE14 Local Variance Maps
Time Slice 2

Site 133: DIOXANE14 Local Variances, 2001-2002, Base Map

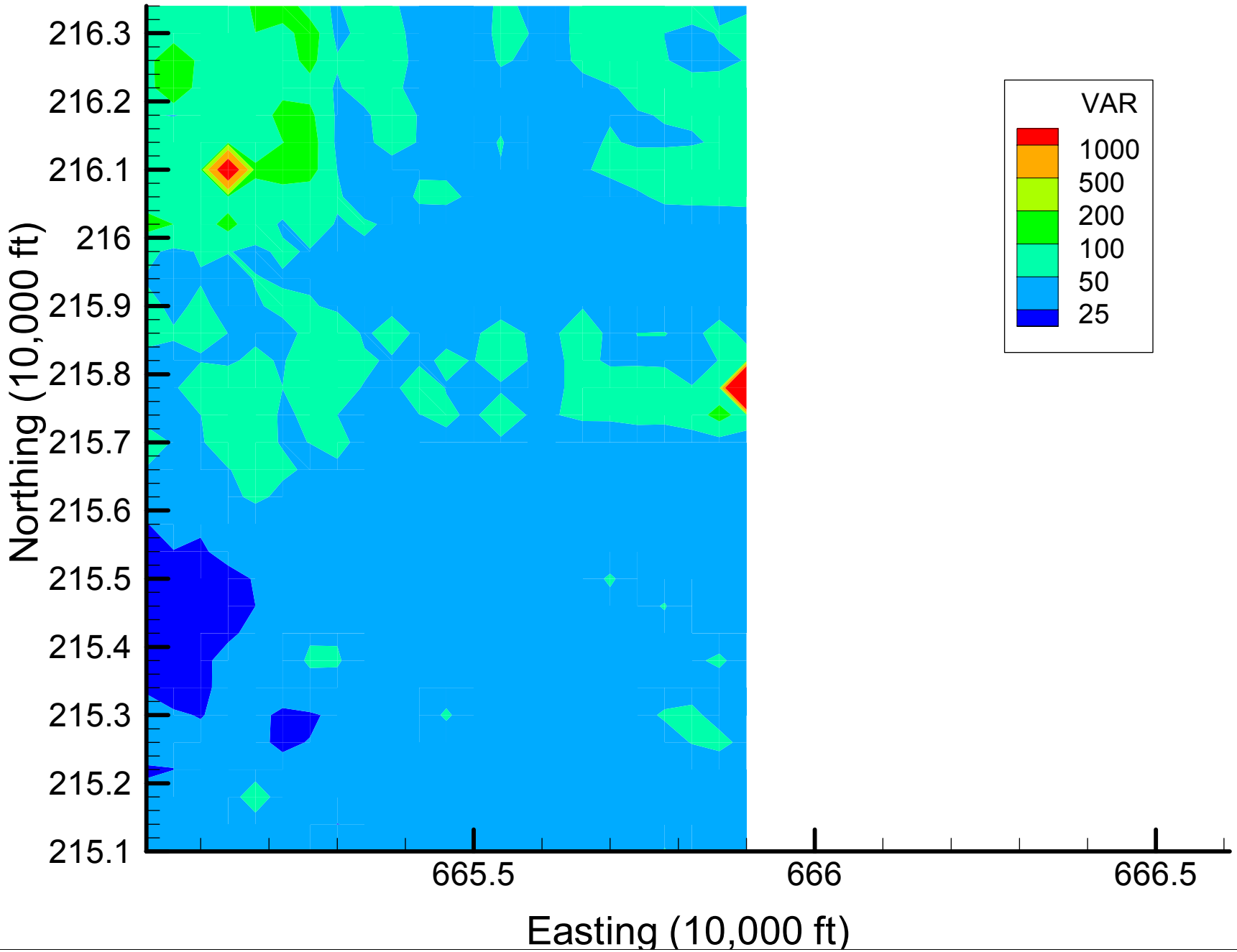

Site 133: DIOXANE14 Local Variances, 2001-2002, 7% Removal

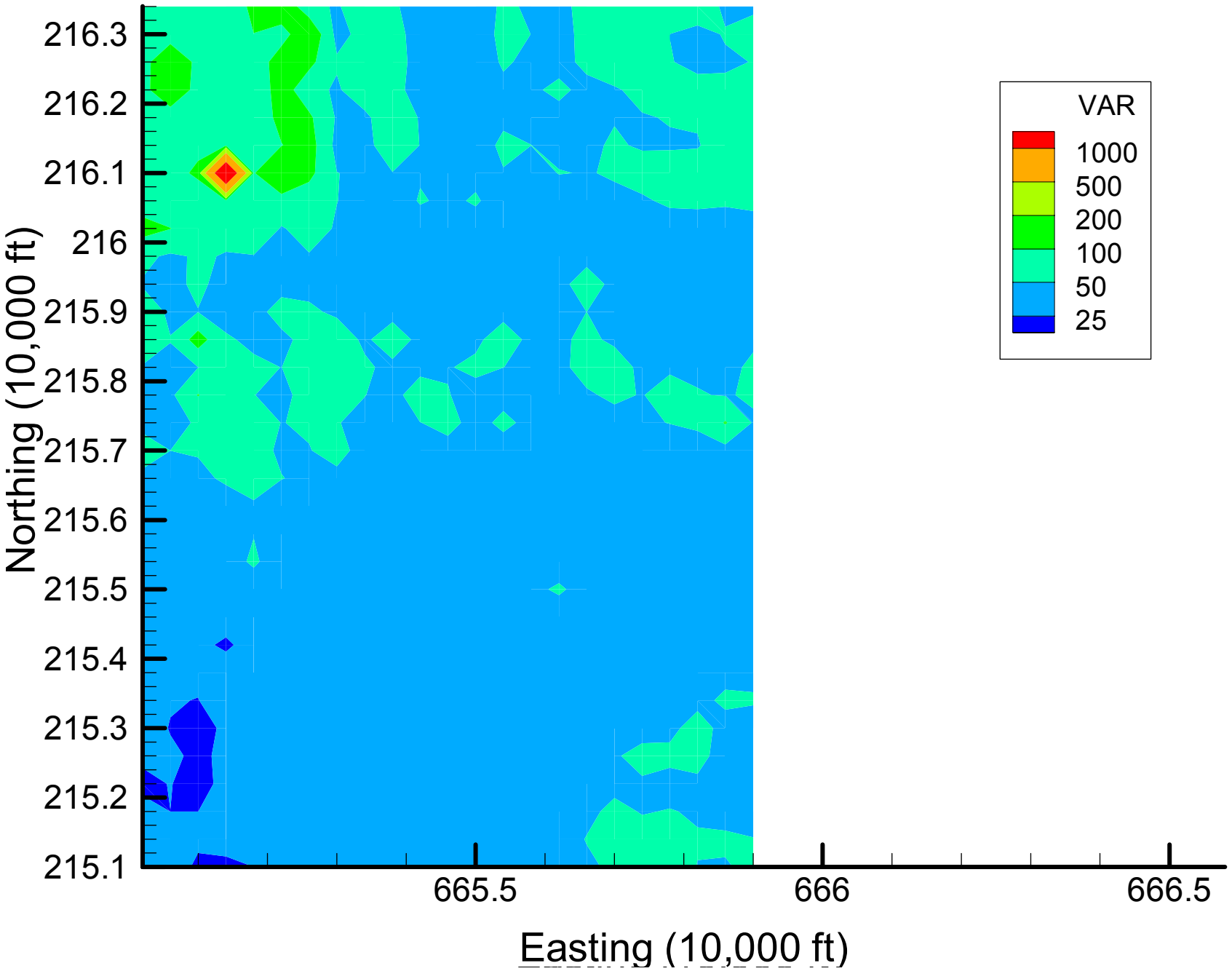

Site 133: DIOXANE14 Local Variances, 2001-2002, 13% Removal

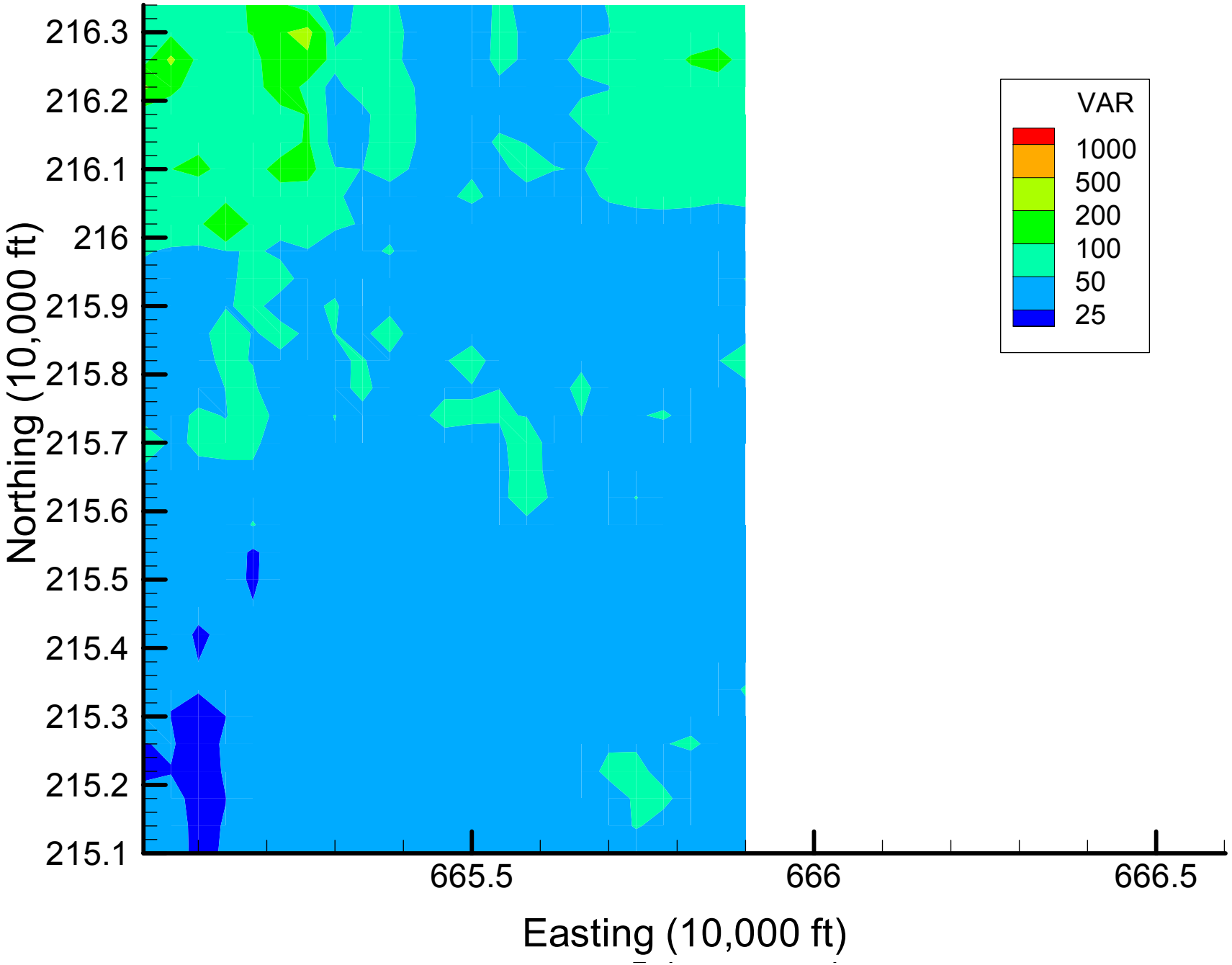

Site 133: DIOXANE14 Local Variances, 2001-2002, 20% Removal

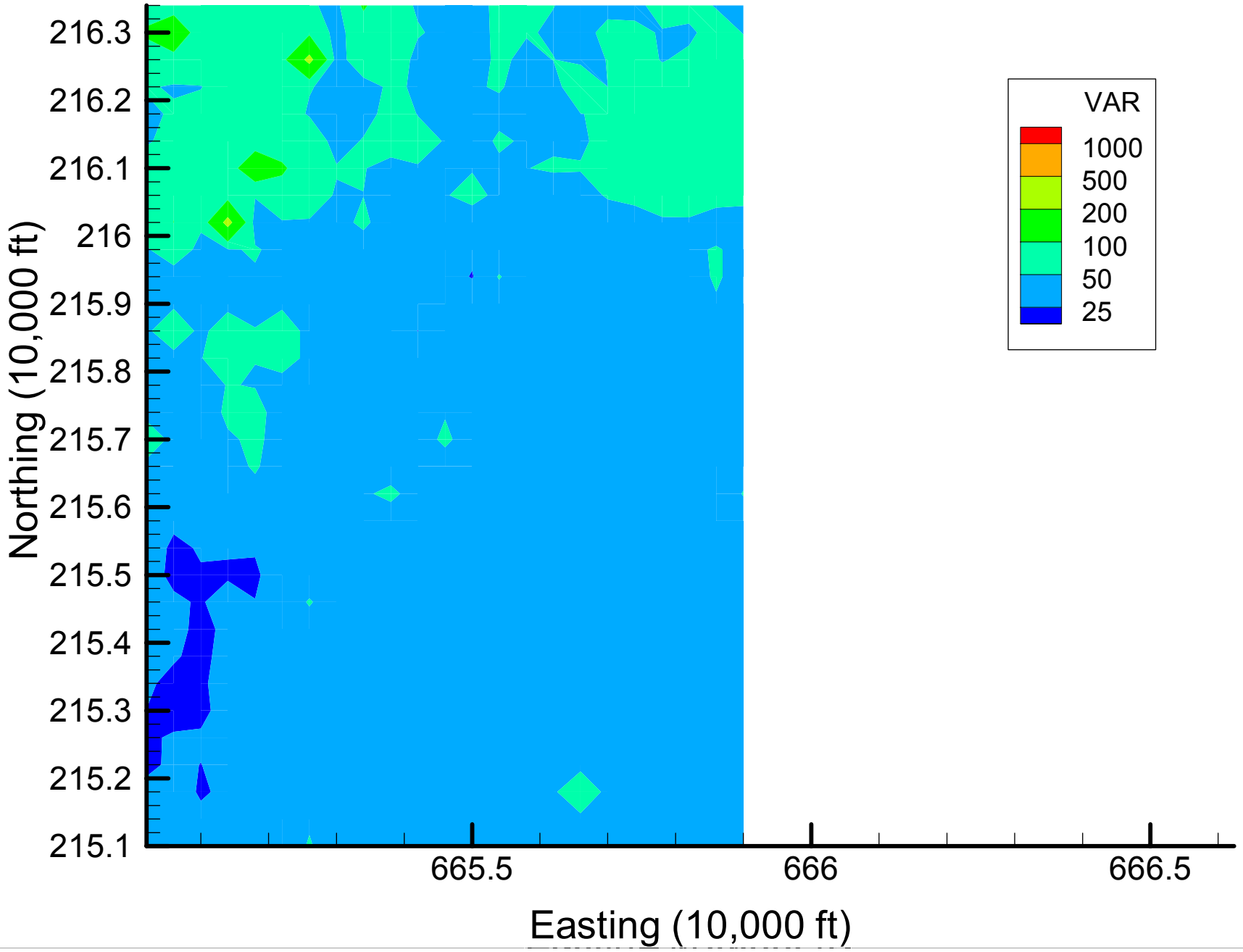

Site 133: DIOXANE14 Local Variances, 2001-2002, 27% Removal

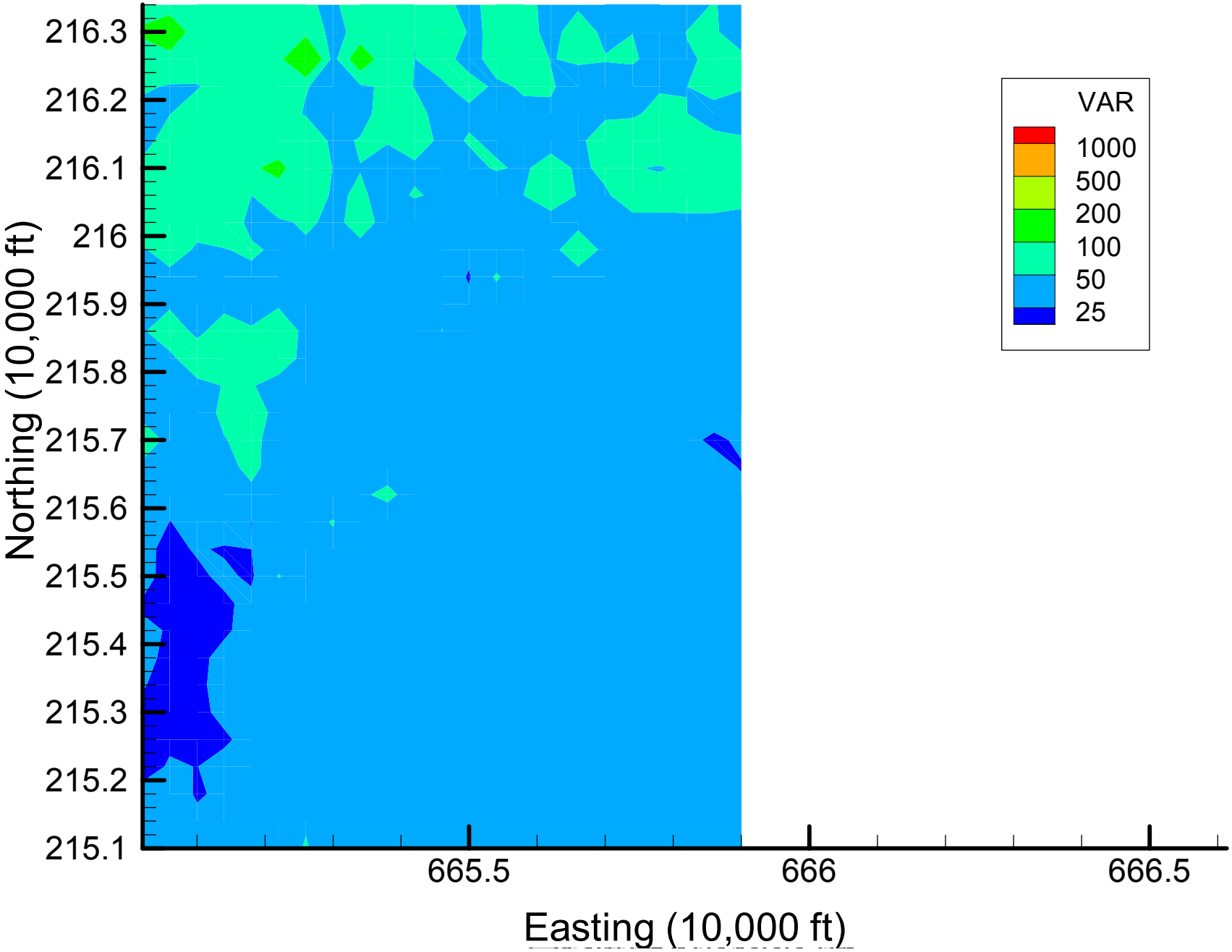

Site 133: DIOXANE14 Local Variances, 2001-2002, 33% Removal

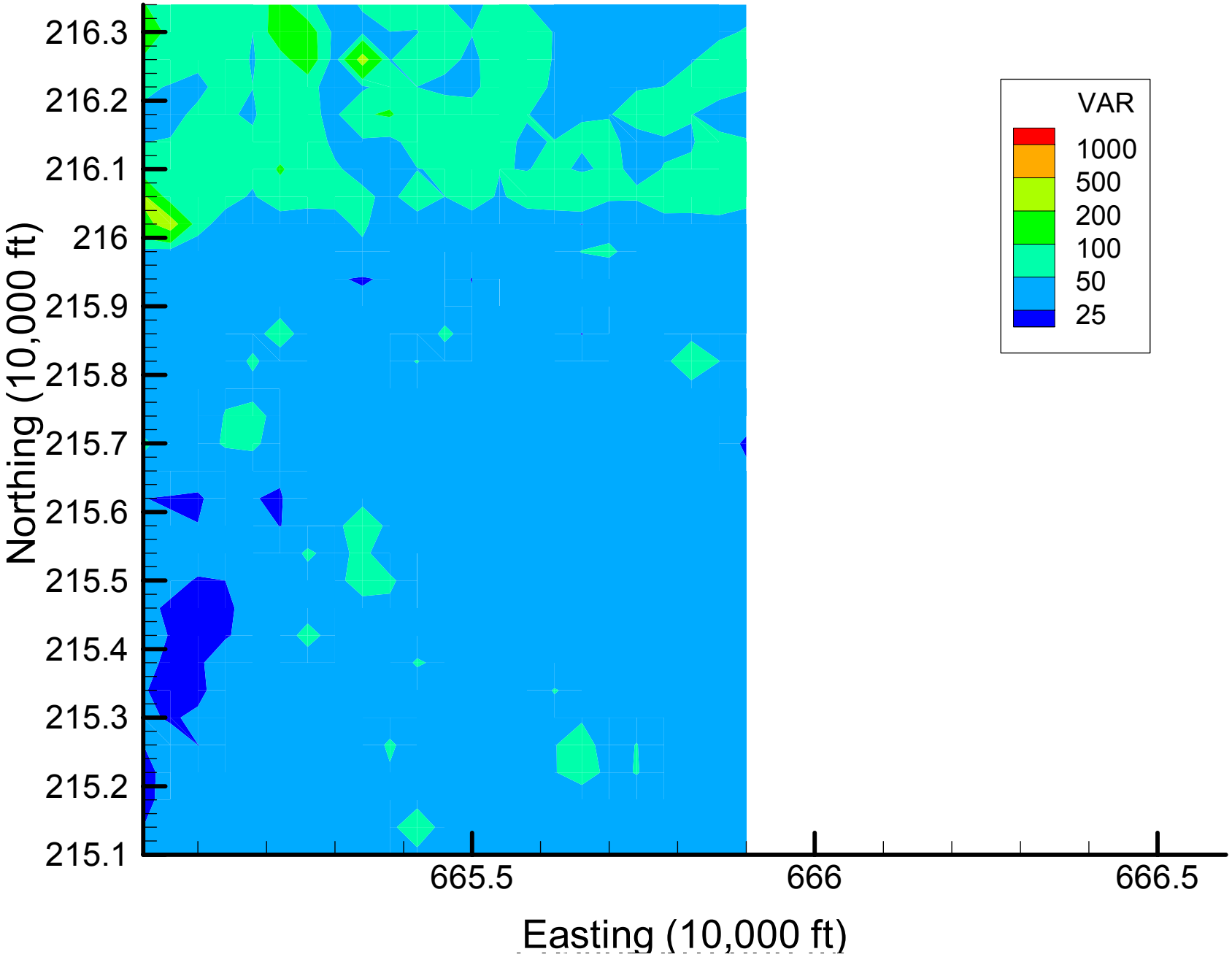

Site 133: DIOXANE14 Local Variances, 2001-2002, 40% Removal

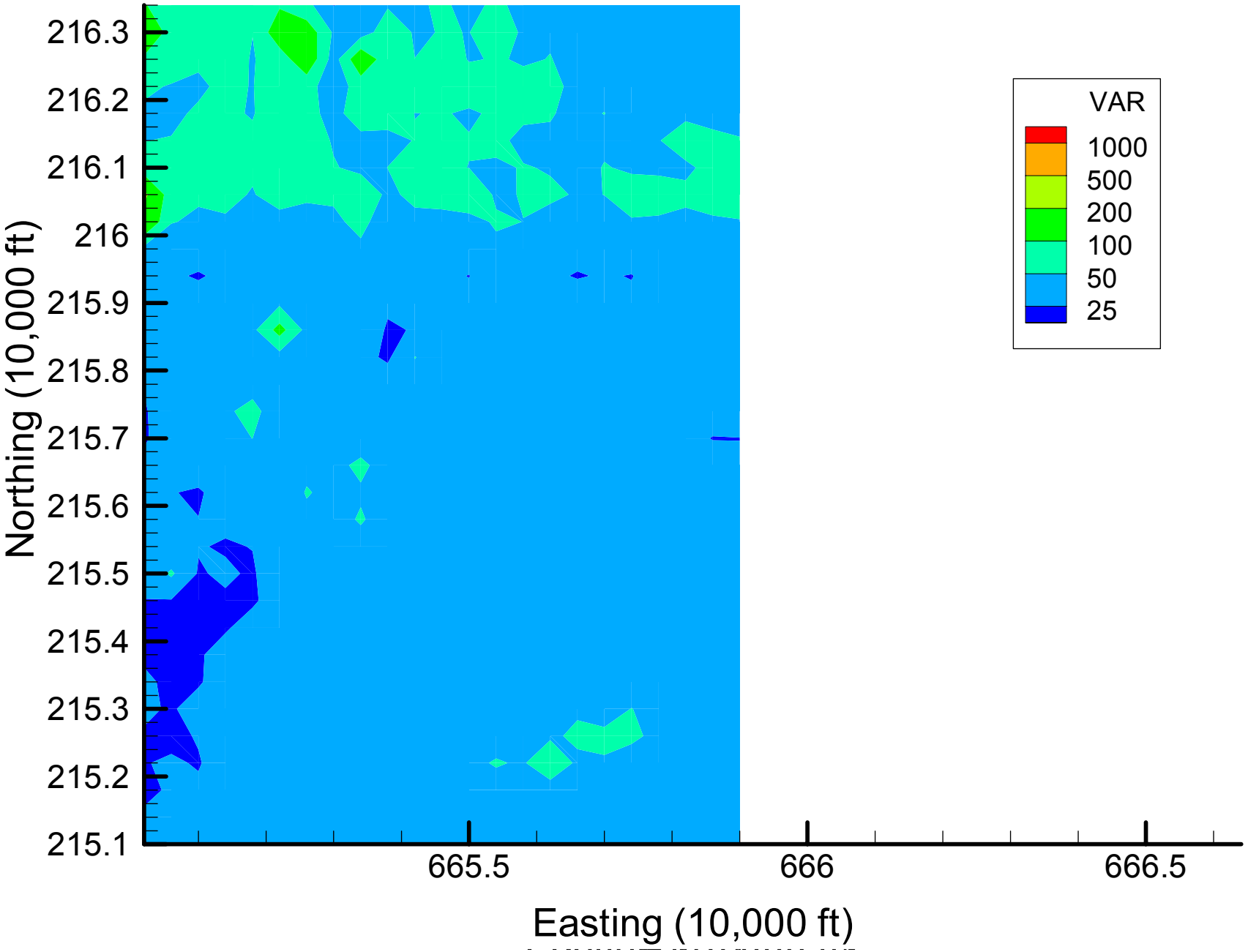

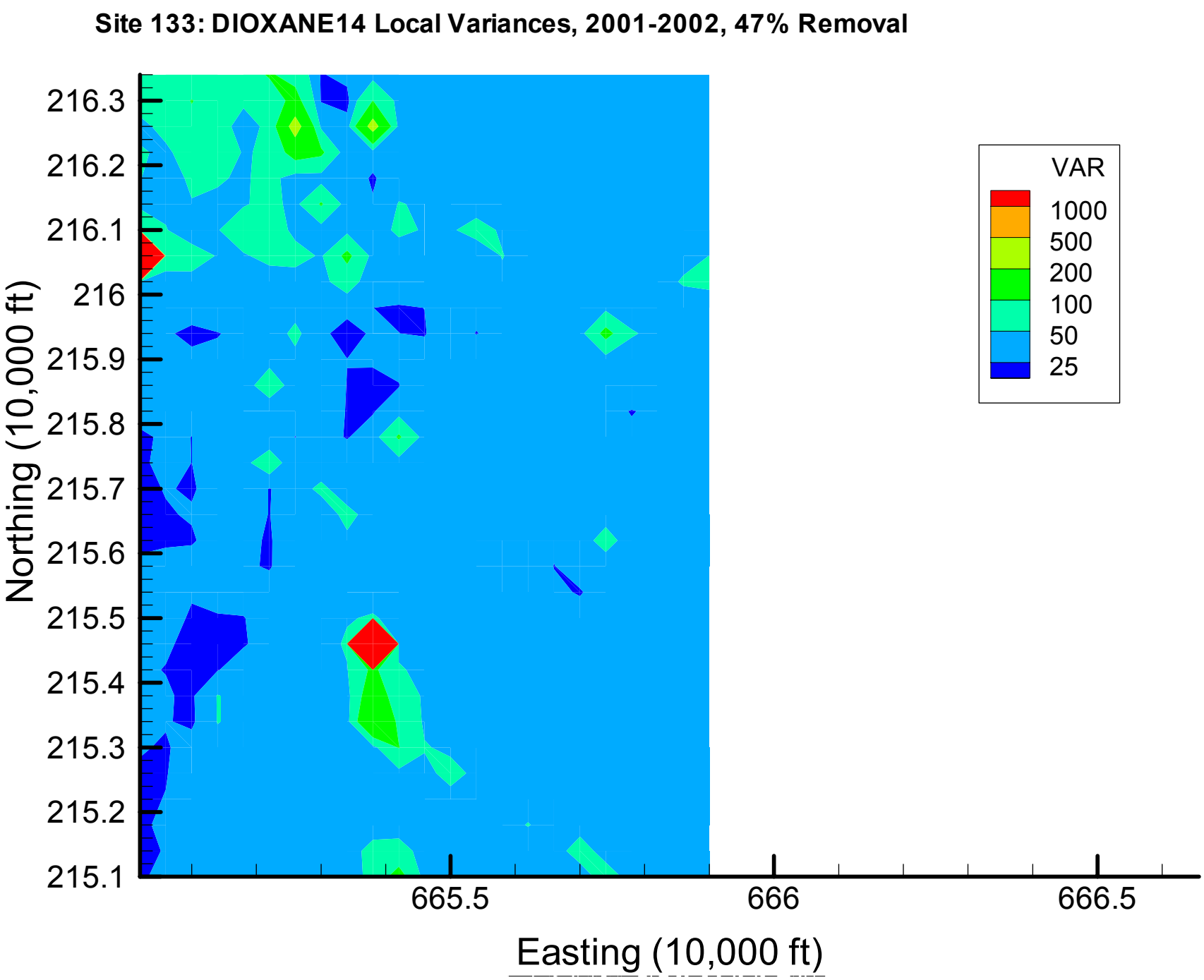
Site 133: DIOXANE14 Local Variances, 2001-2002, 47% Removal
VAR
1000
500
200
100
50
25
Northing (10,000 ft)
216.3
216.2
216.1
216
215.9
215.8
215.7
215.6
215.5
215.4
215.3
215.2
215.1
665.5
666
666.5
Easting (10,000 ft)

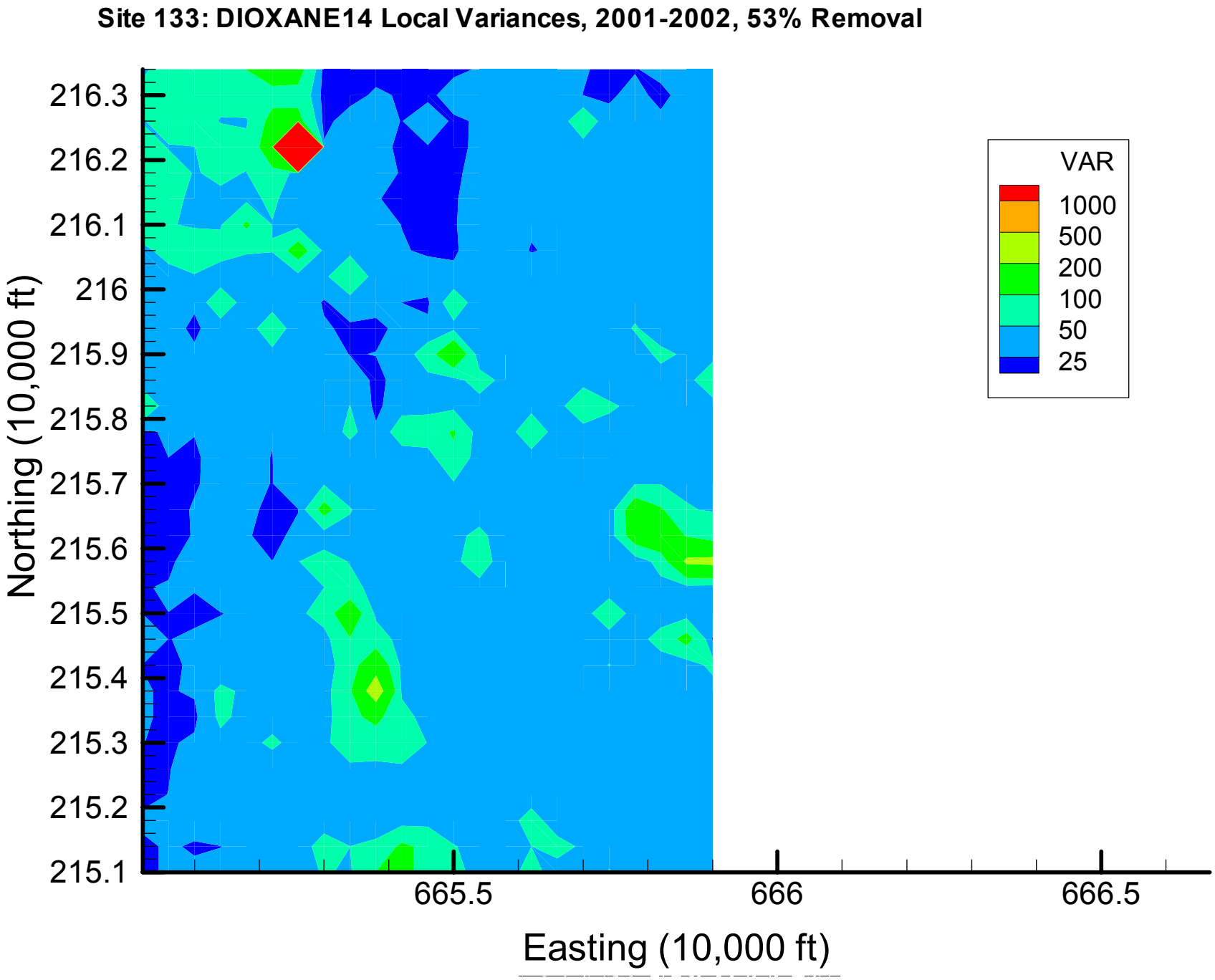
Site 133: DIOXANE14 Local Variances, 2001-2002, 53% Removal
VAR
1000
500
200
100
50
25
Northing (10,000 ft)
216.3
216.2
216.1
216
215.9
215.8
215.7
215.6
215.5
215.4
215.3
215.2
215.1
665.5
666
666.5
Easting (10,000 ft)

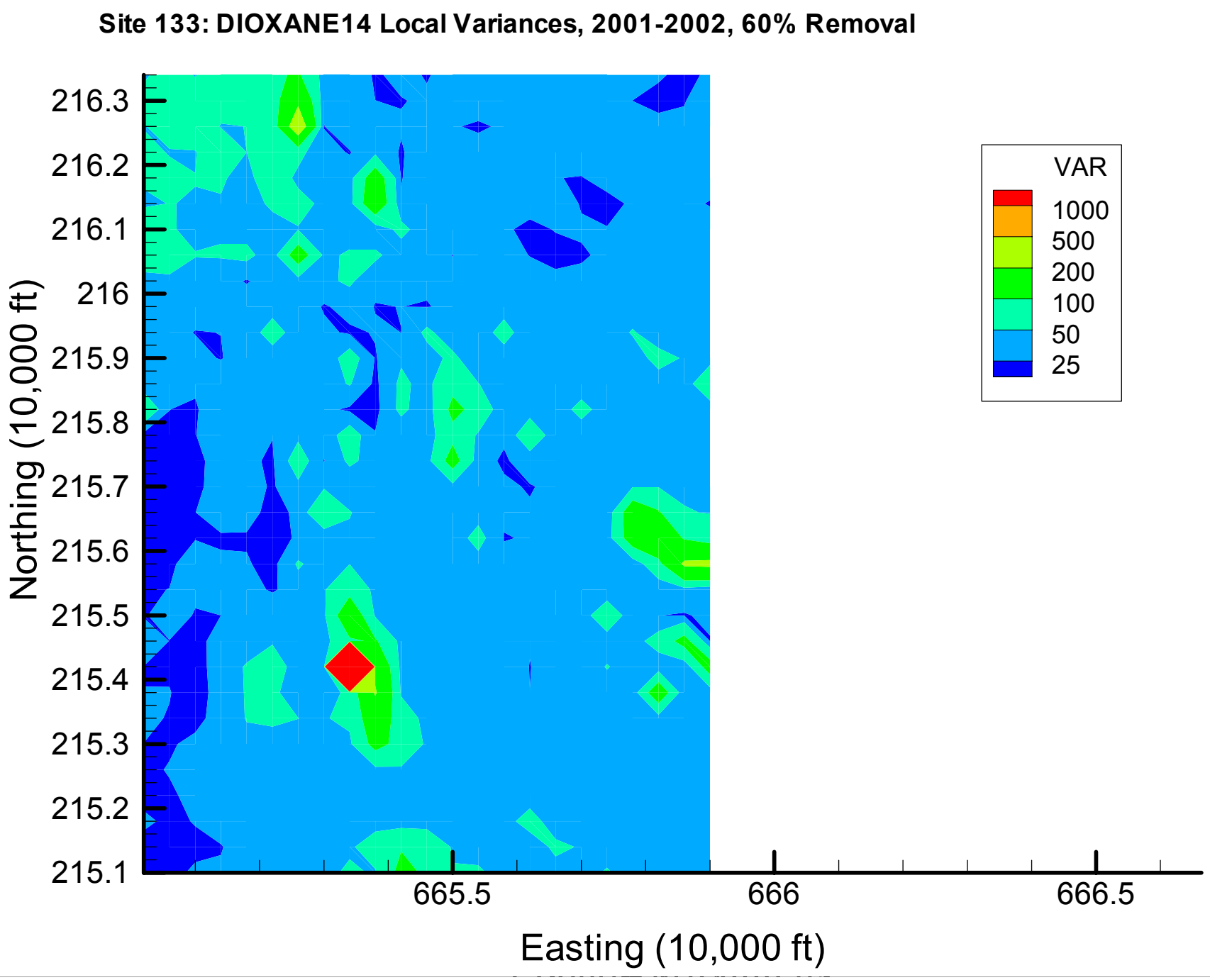
Site 133: DIOXANE14 Local Variances, 2001-2002, 60% Removal
VAR
1000
500
200
100
50
25
Northing (10,000 ft)
216.3
216.2
216.1
216
215.9
215.8
215.7
215.6
215.5
215.4
215.3
215.2
215.1
665.5
666
666.5
Easting (10,000 ft)

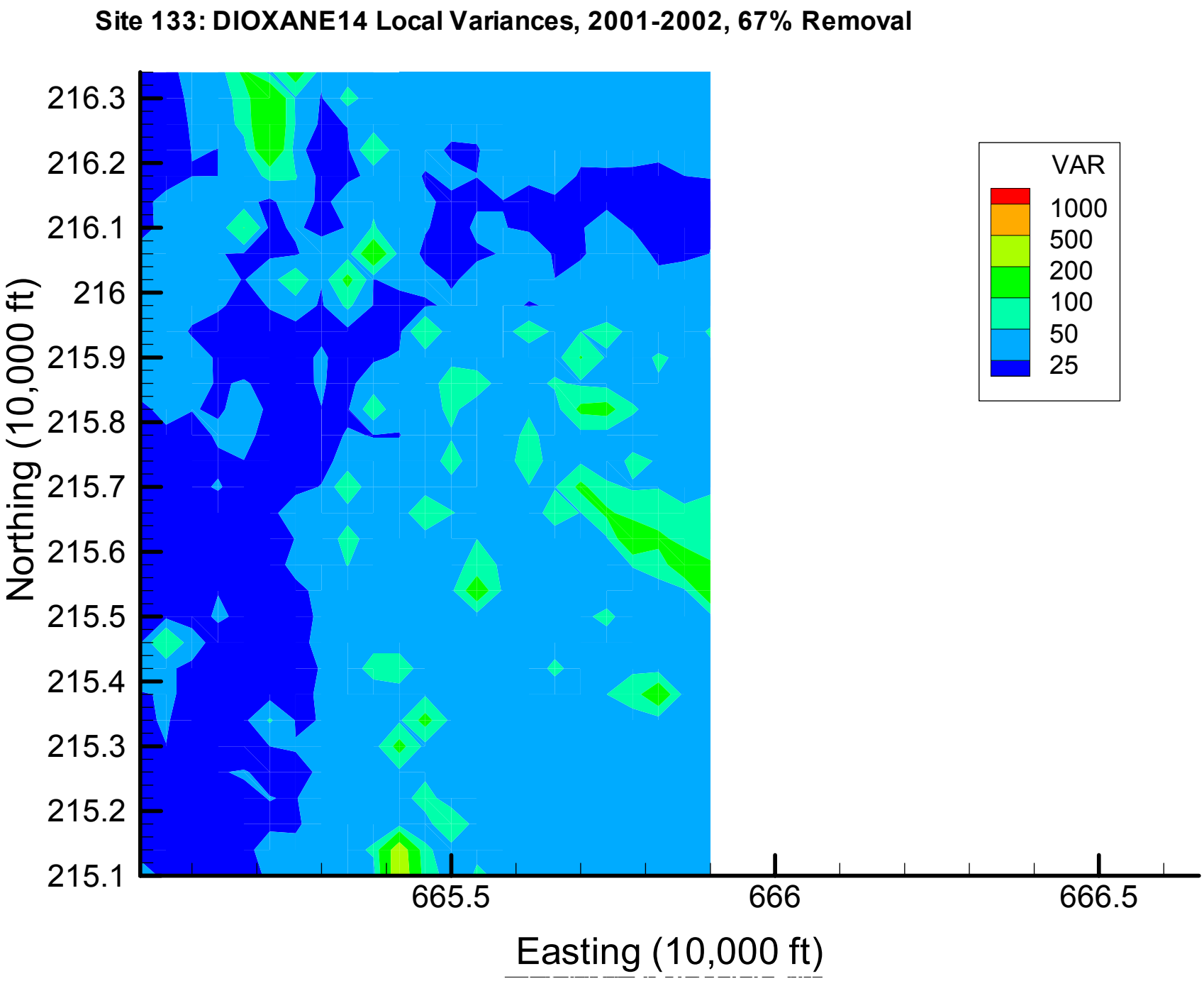
Site 133: DIOXANE14 Local Variances, 2001-2002, 67% Removal
VAR
1000
500
200
100
50
25
Northing (10,000 ft)
216.3
216.2
216.1
216
215.9
215.8
215.7
215.6
215.5
215.4
215.3
215.2
215.1
665.5
666
666.5
Easting (10,000 ft)

Appendix 4.3
MN Local Variance Maps
Time Slice 1

Site 133: MN Local Variances, 1999-2000, Base Map

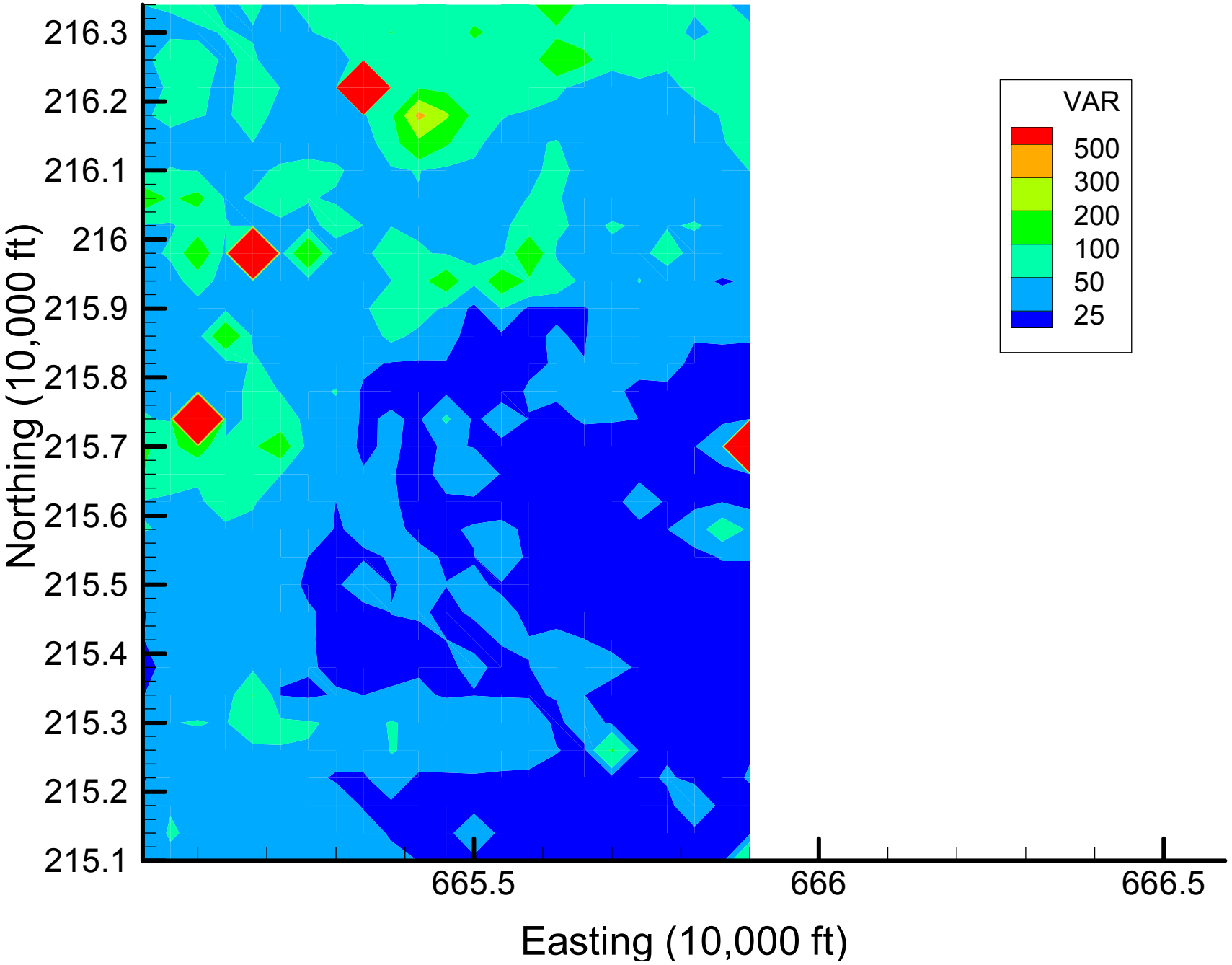

Site 133: MN Local Variances, 1999-2000, 7% Removal

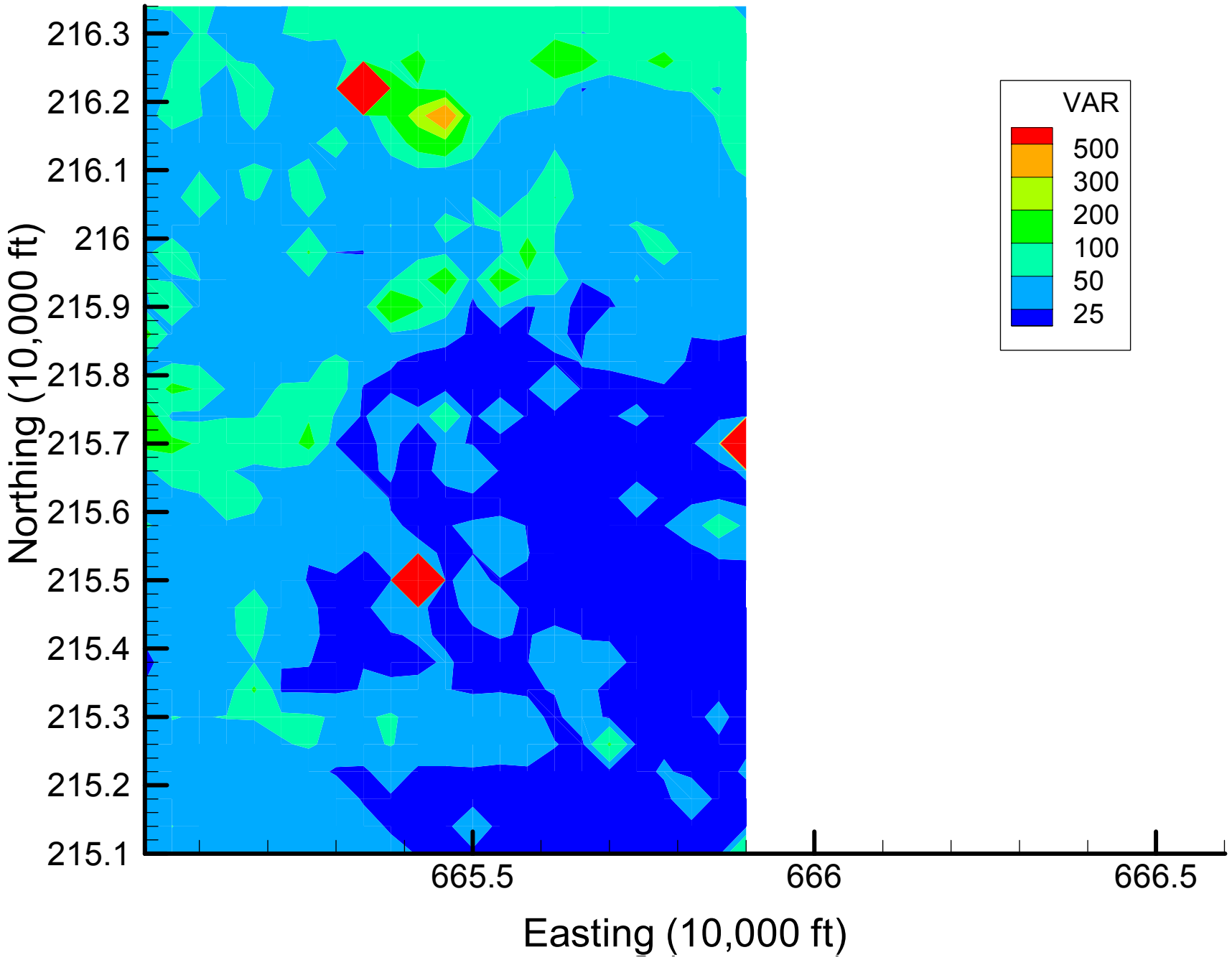

Site 133: MN Local Variances, 1999-2000, 13% Removal

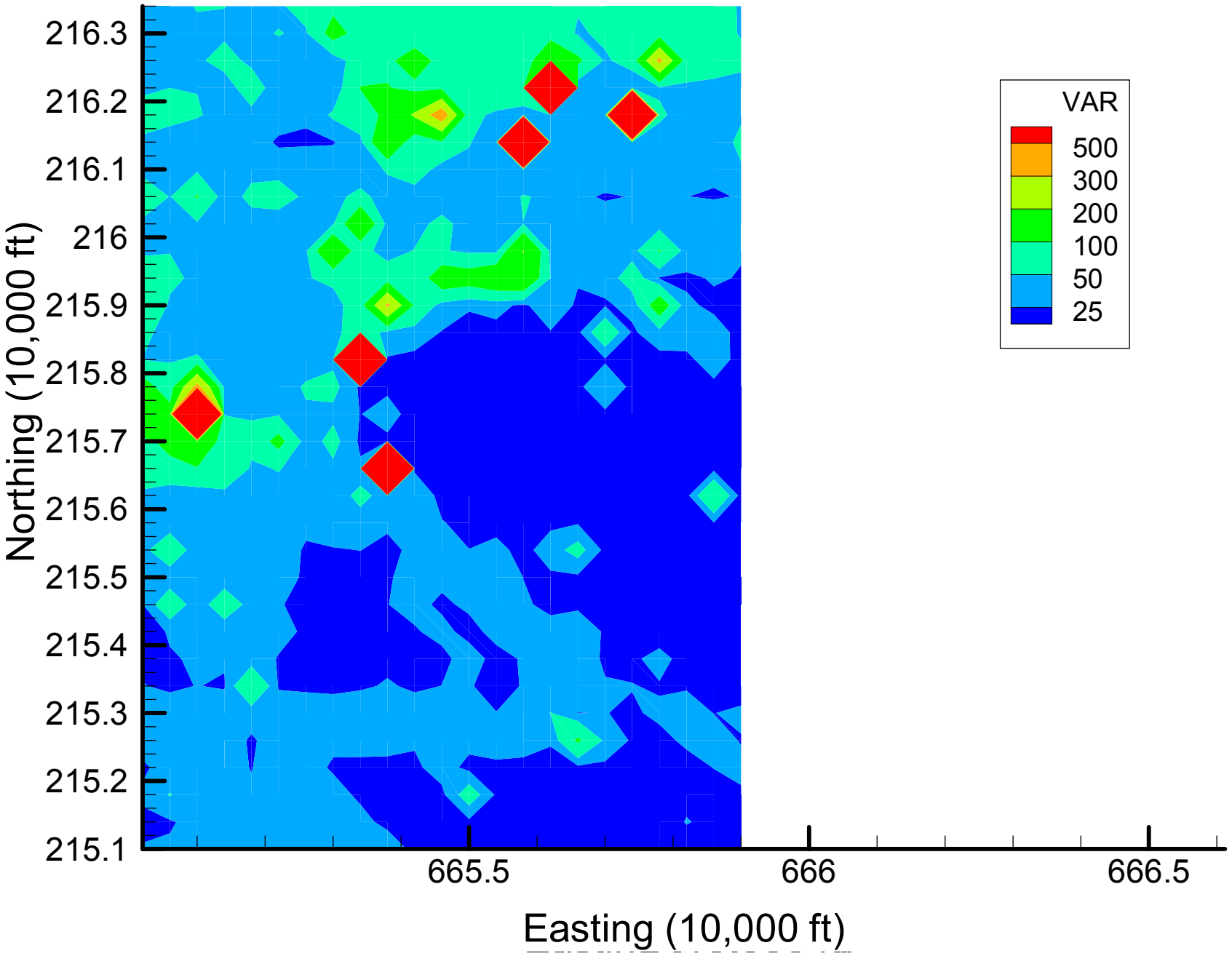

Site 133: MN Local Variances, 1999-2000, 20% Removal

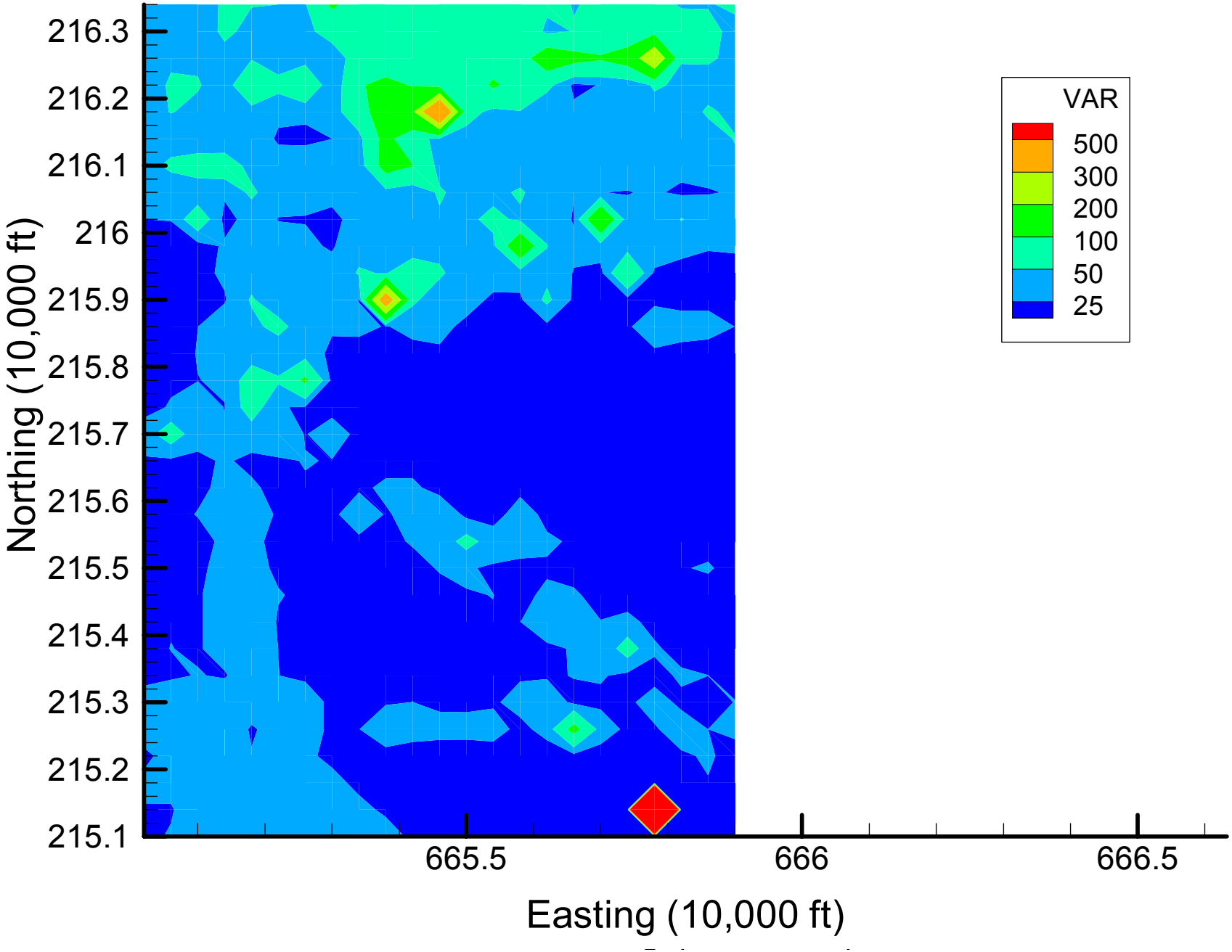

Site 133: MN Local Variances, 1999-2000, 27% Removal

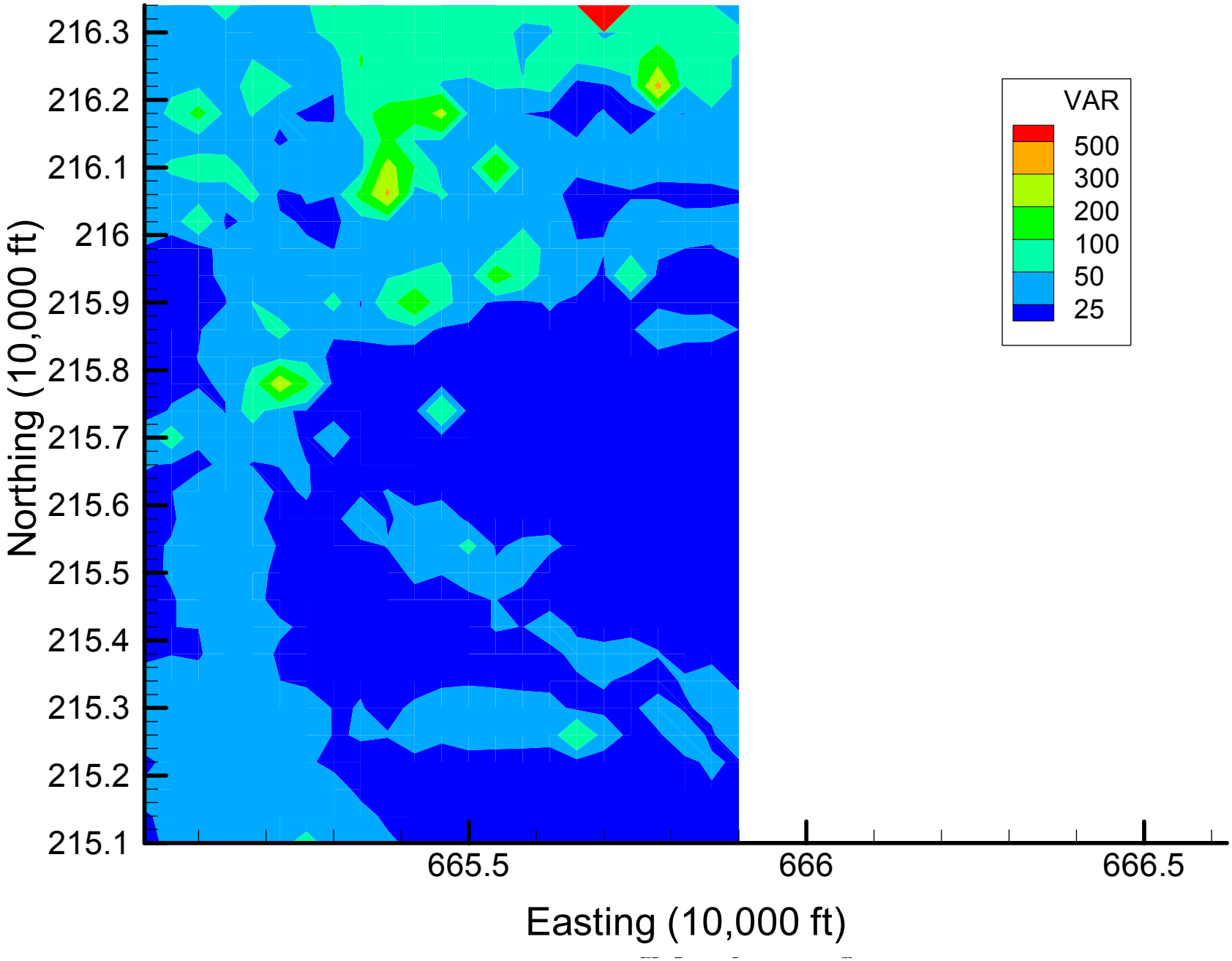

Site 133: MN Local Variances, 1999-2000, 33% Removal

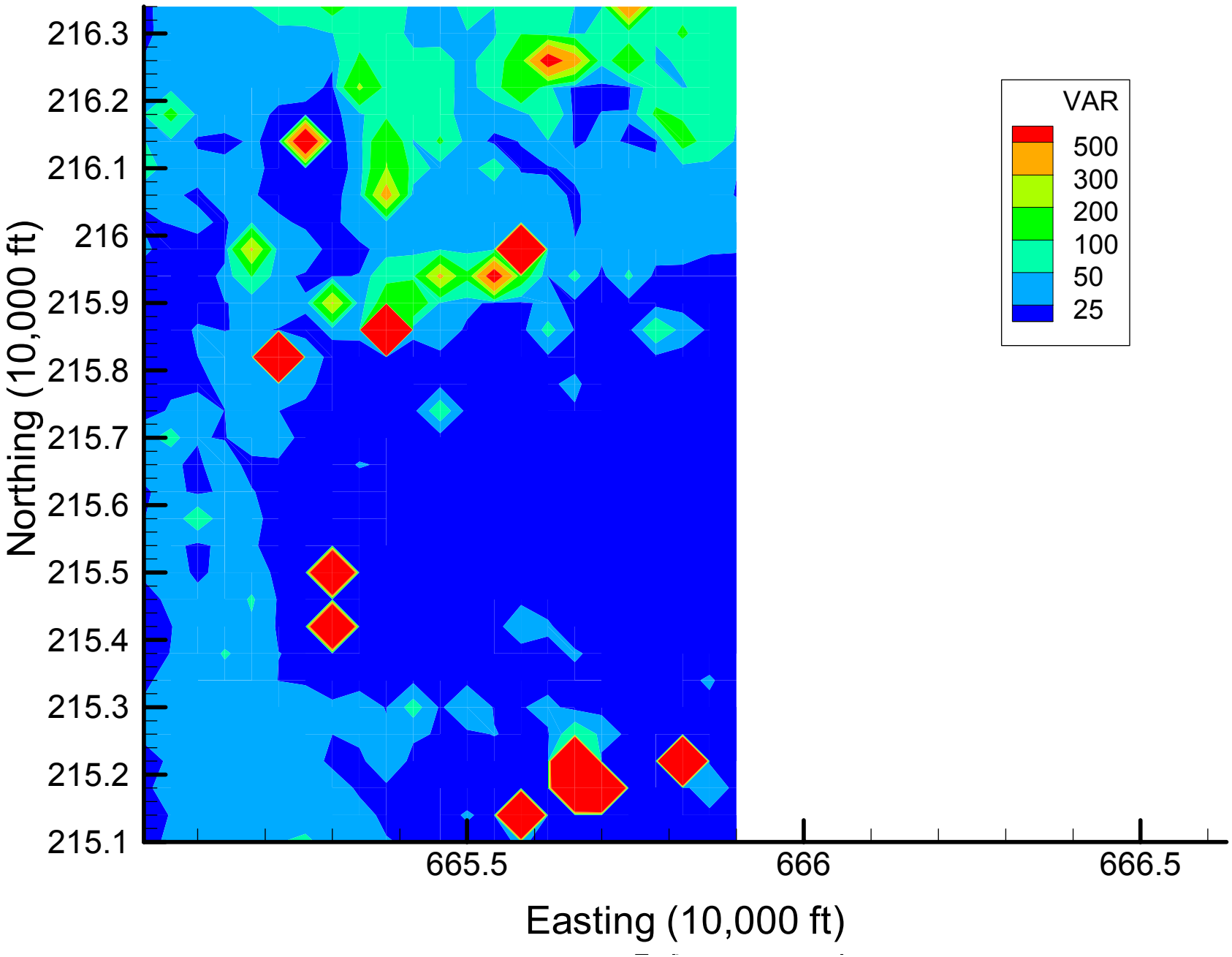

Site 133: MN Local Variances, 1999-2000, 40% Removal

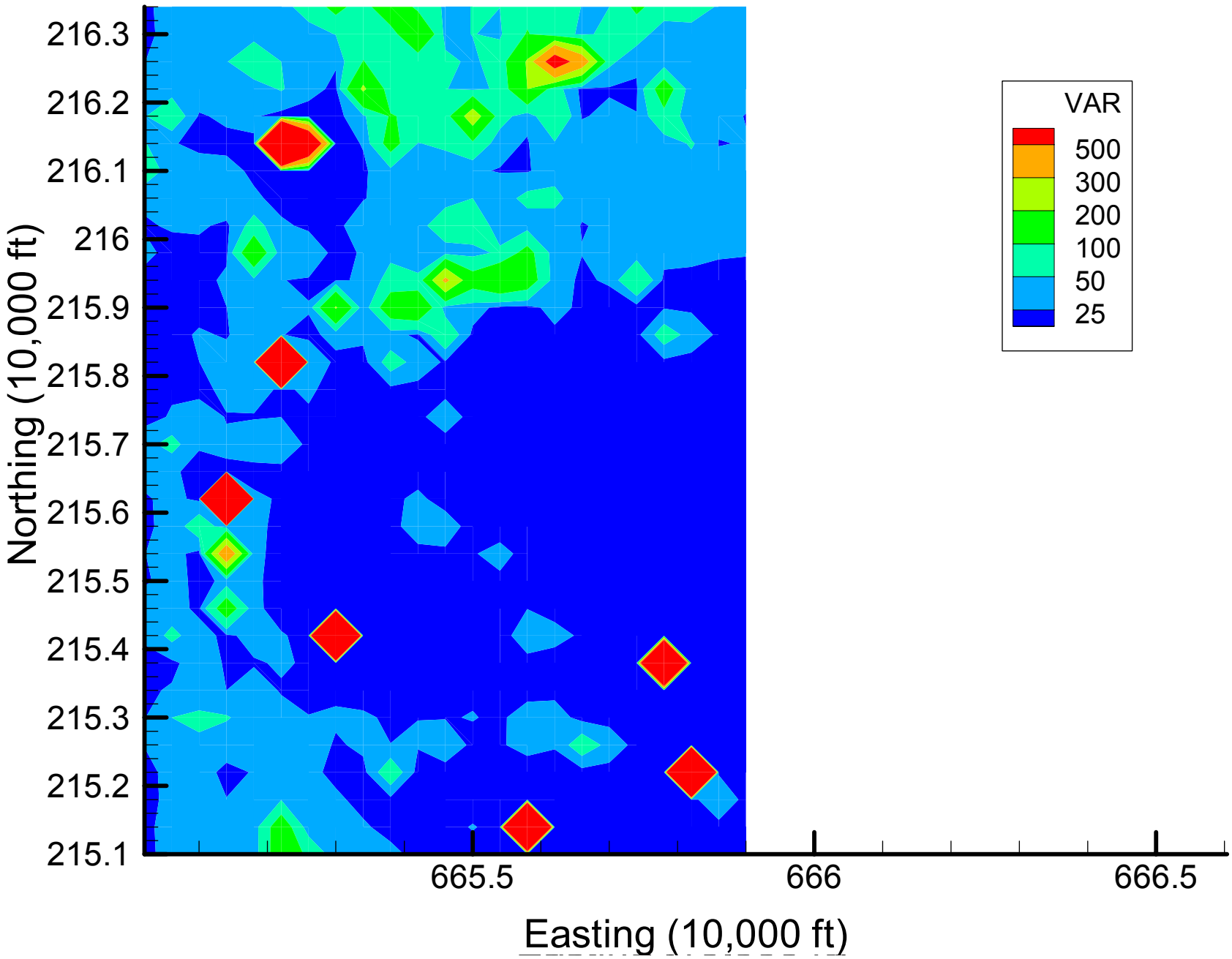

Site 133: MN Local Variances, 1999-2000, 47% Removal

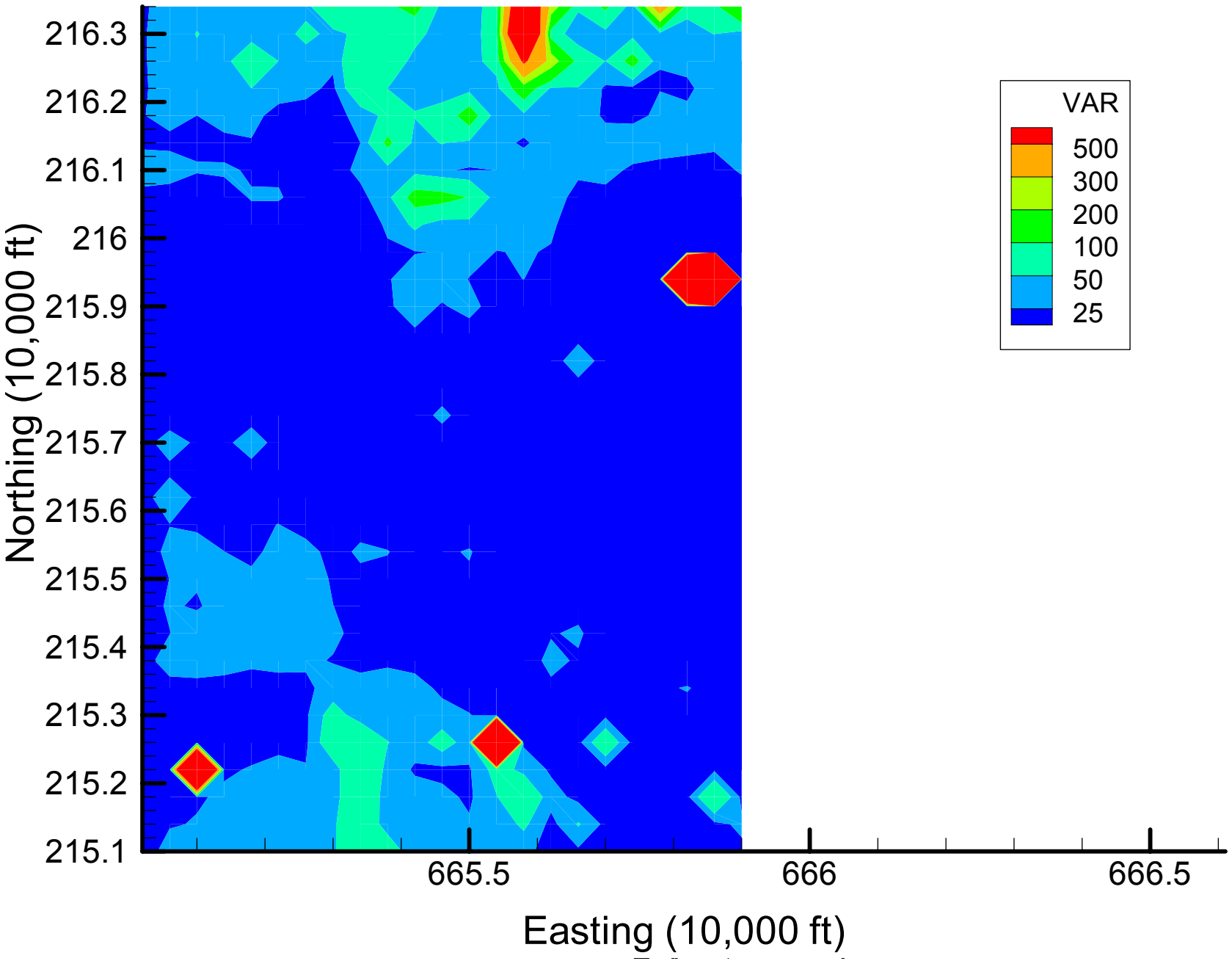

Site 133: MN Local Variances, 1999-2000, 53% Removal

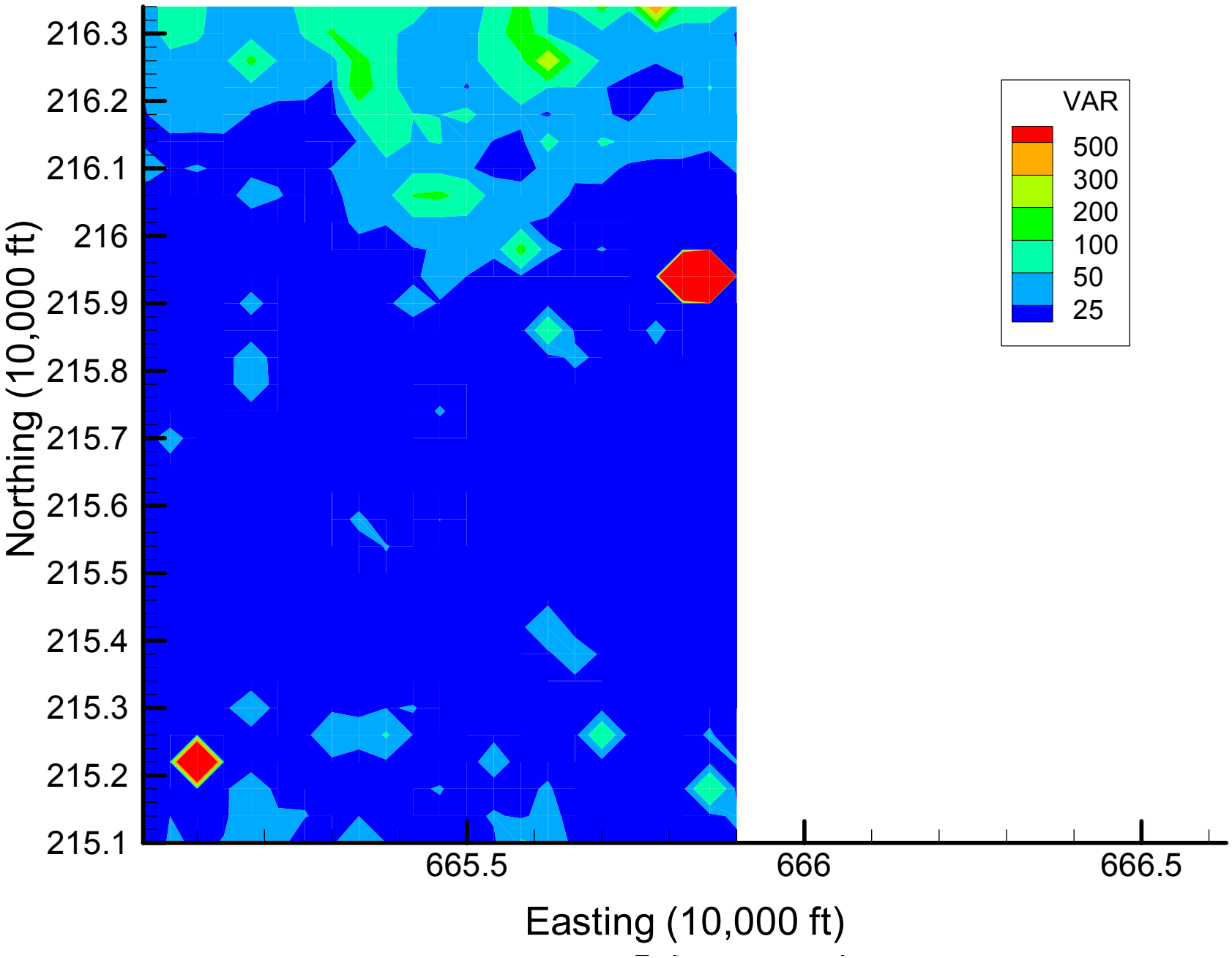

Site 133: MN Local Variances, 1999-2000, 60% Removal

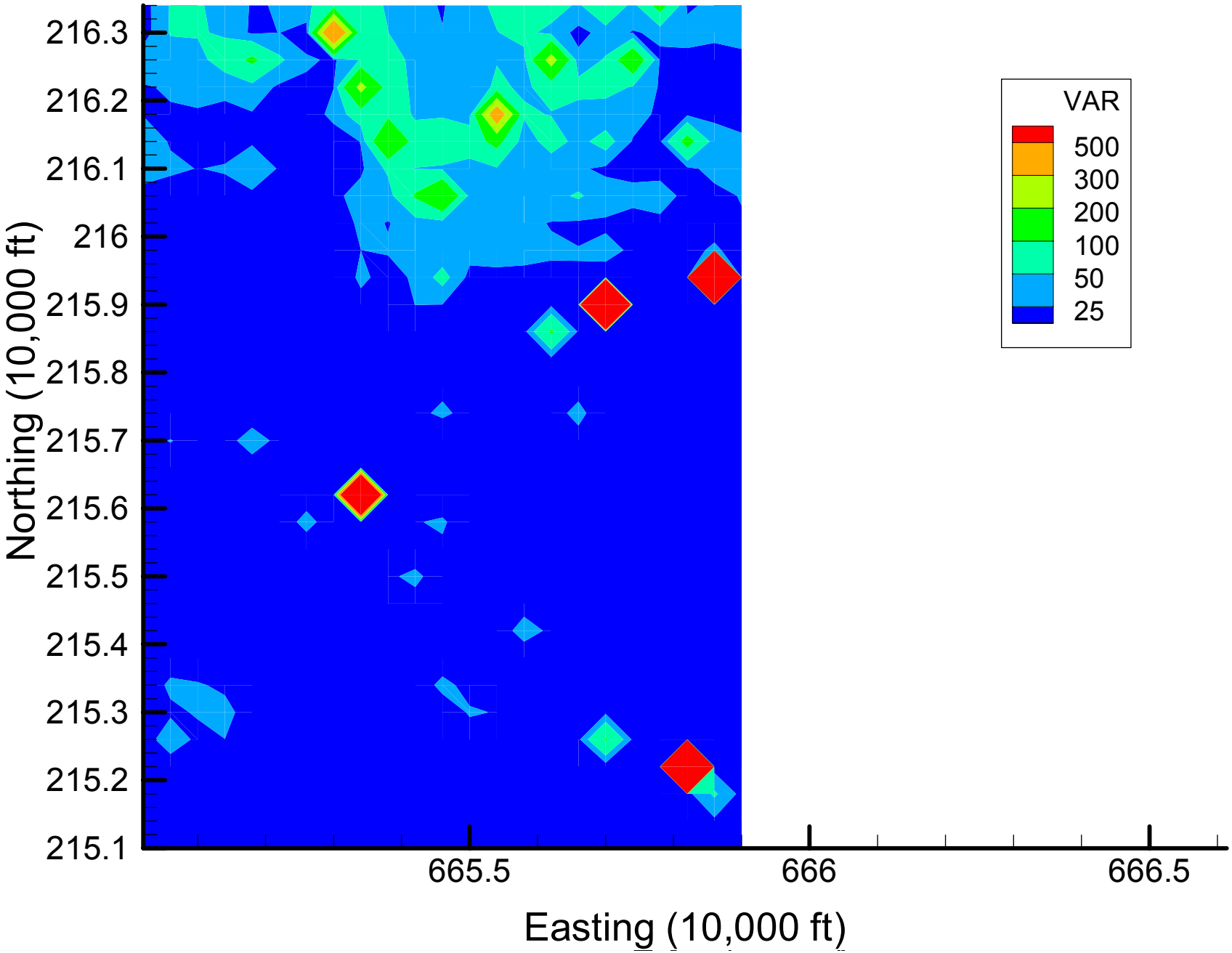

Site 133: MN Local Variances, 1999-2000, 67% Removal

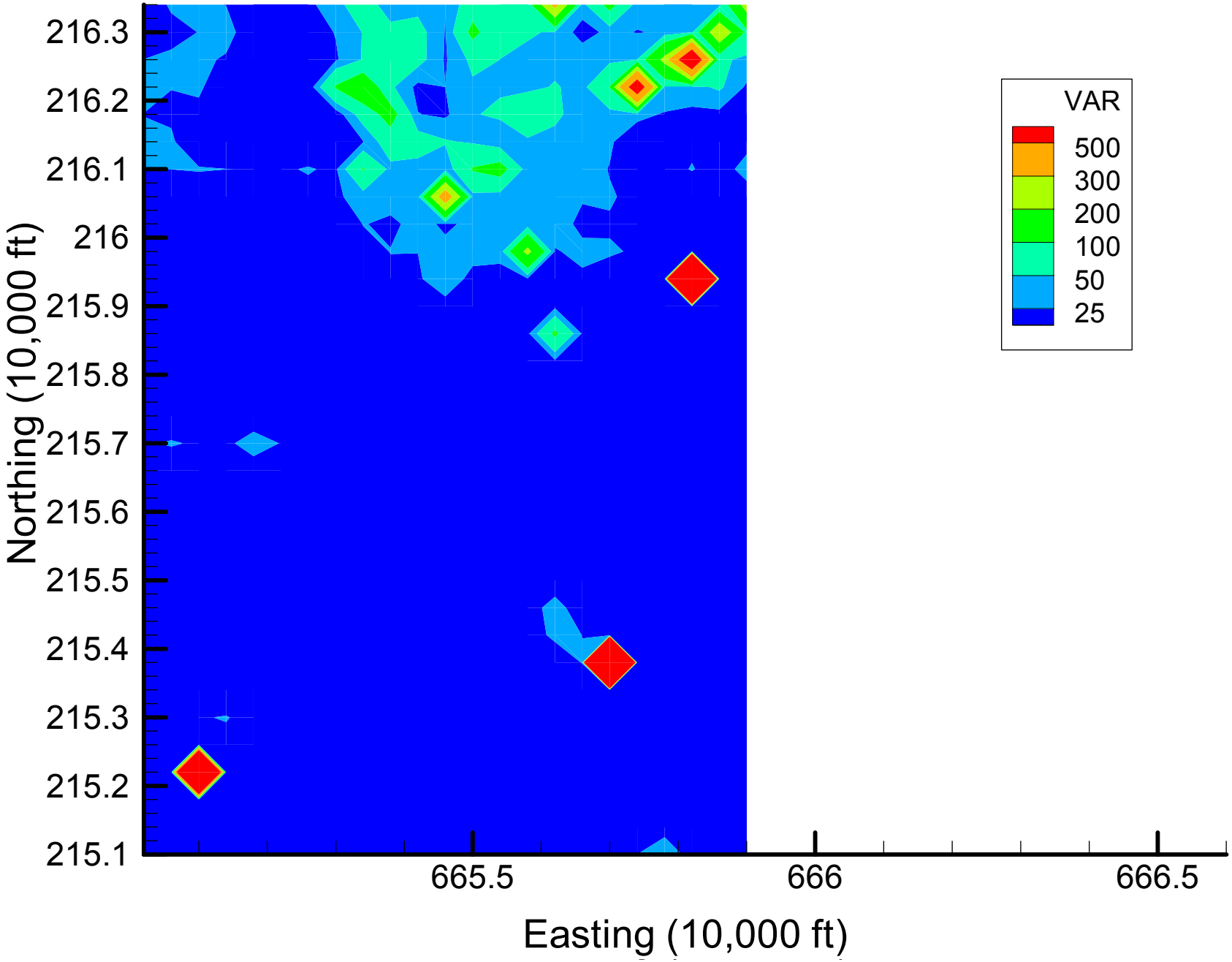

Appendix 4.3
MN Local Variance Maps
Time Slice 2

Site 133: MN Local Variances, 2001-2002, Base Map

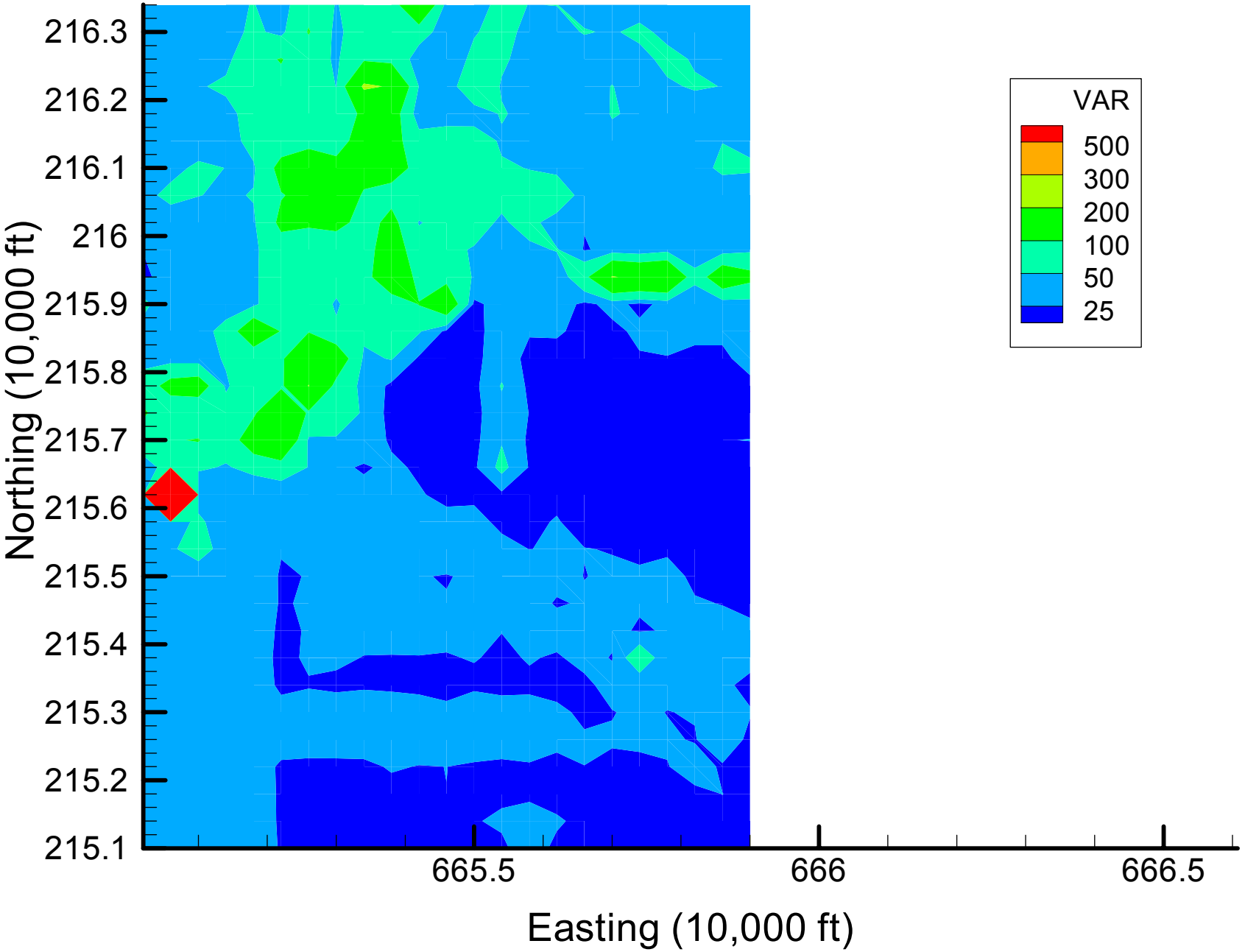

Site 133: MN Local Variances, 2001-2002, 7% Removal

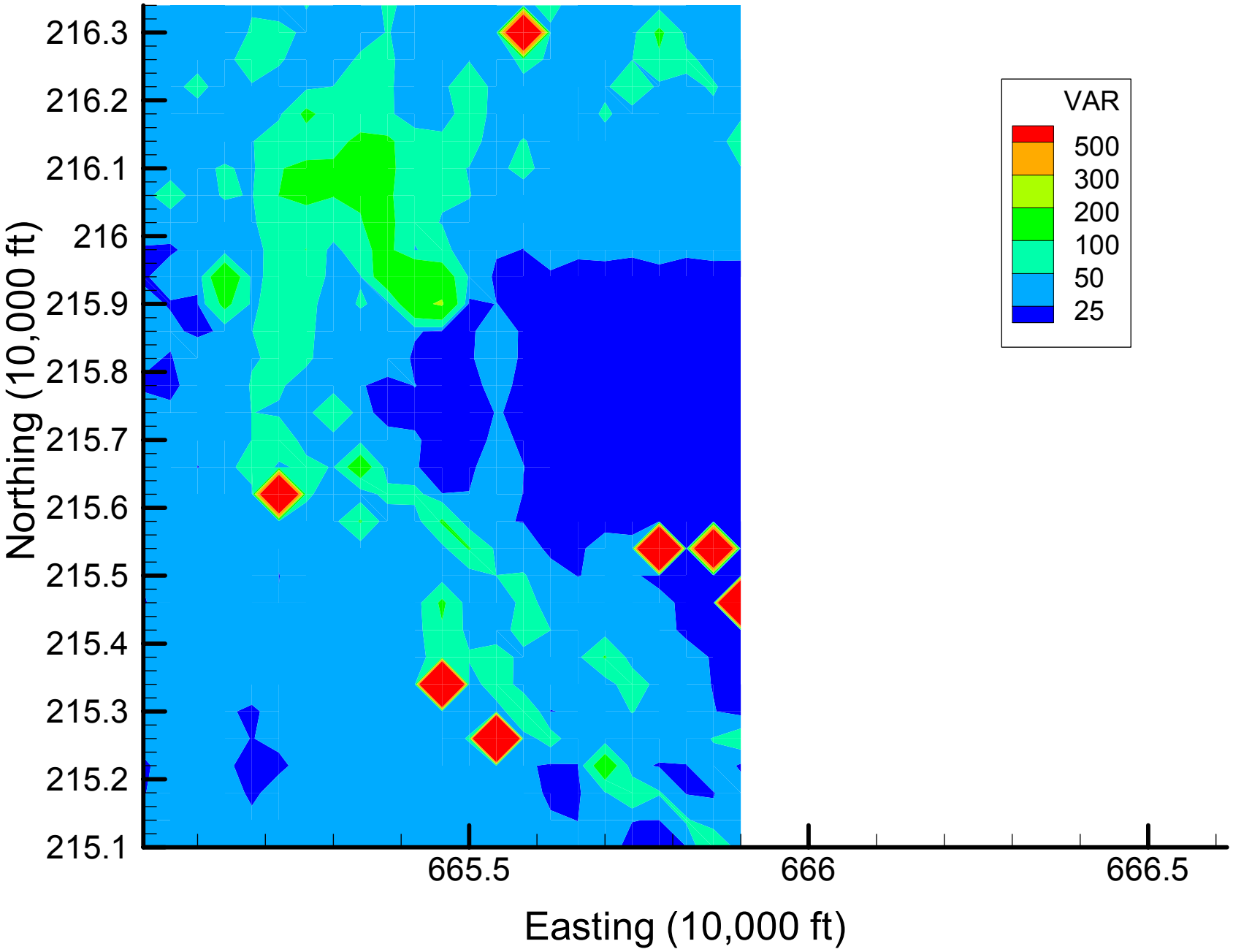

Site 133: MN Local Variances, 2001-2002, 13% Removal

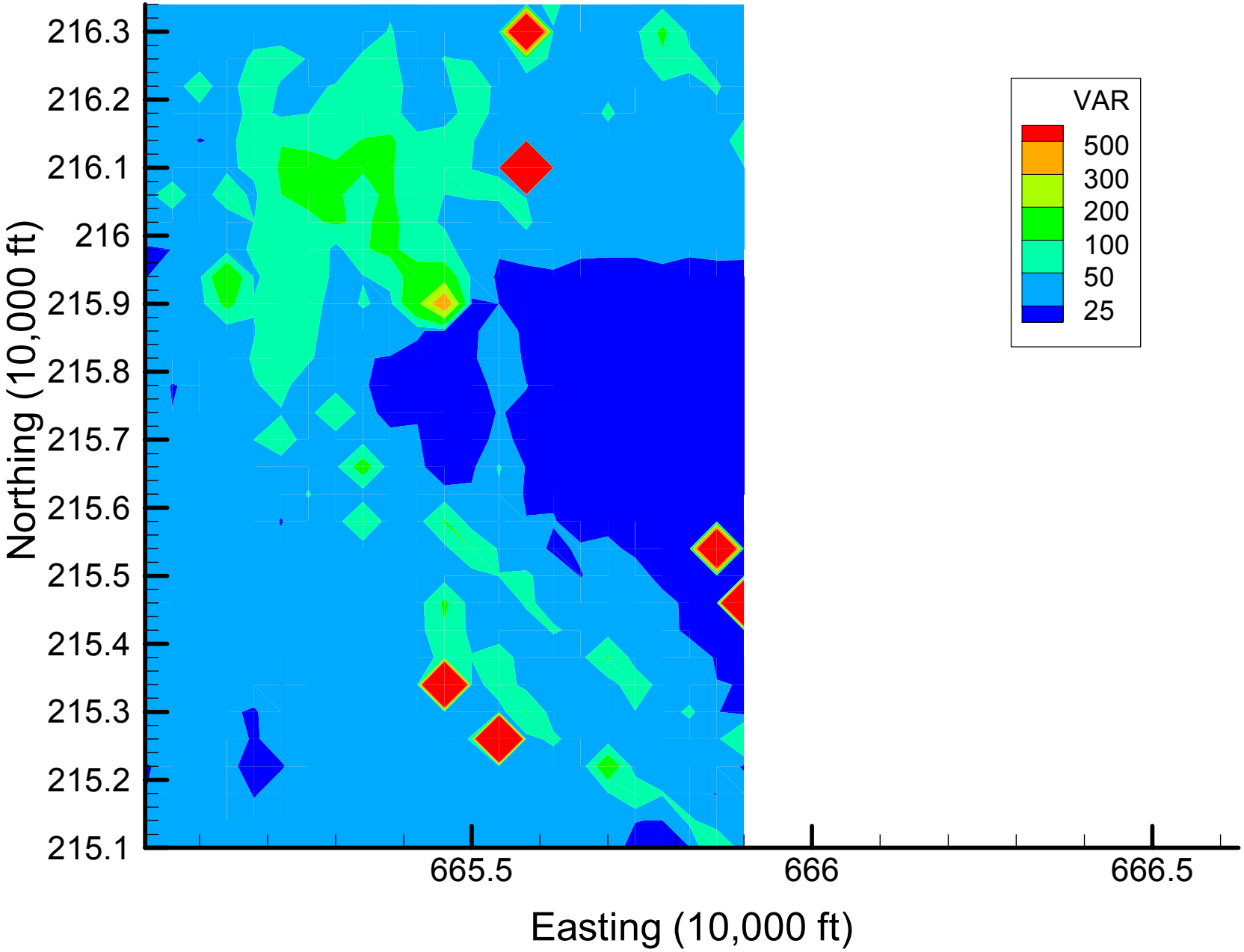

Site 133: MN Local Variances, 2001-2002, 20% Removal

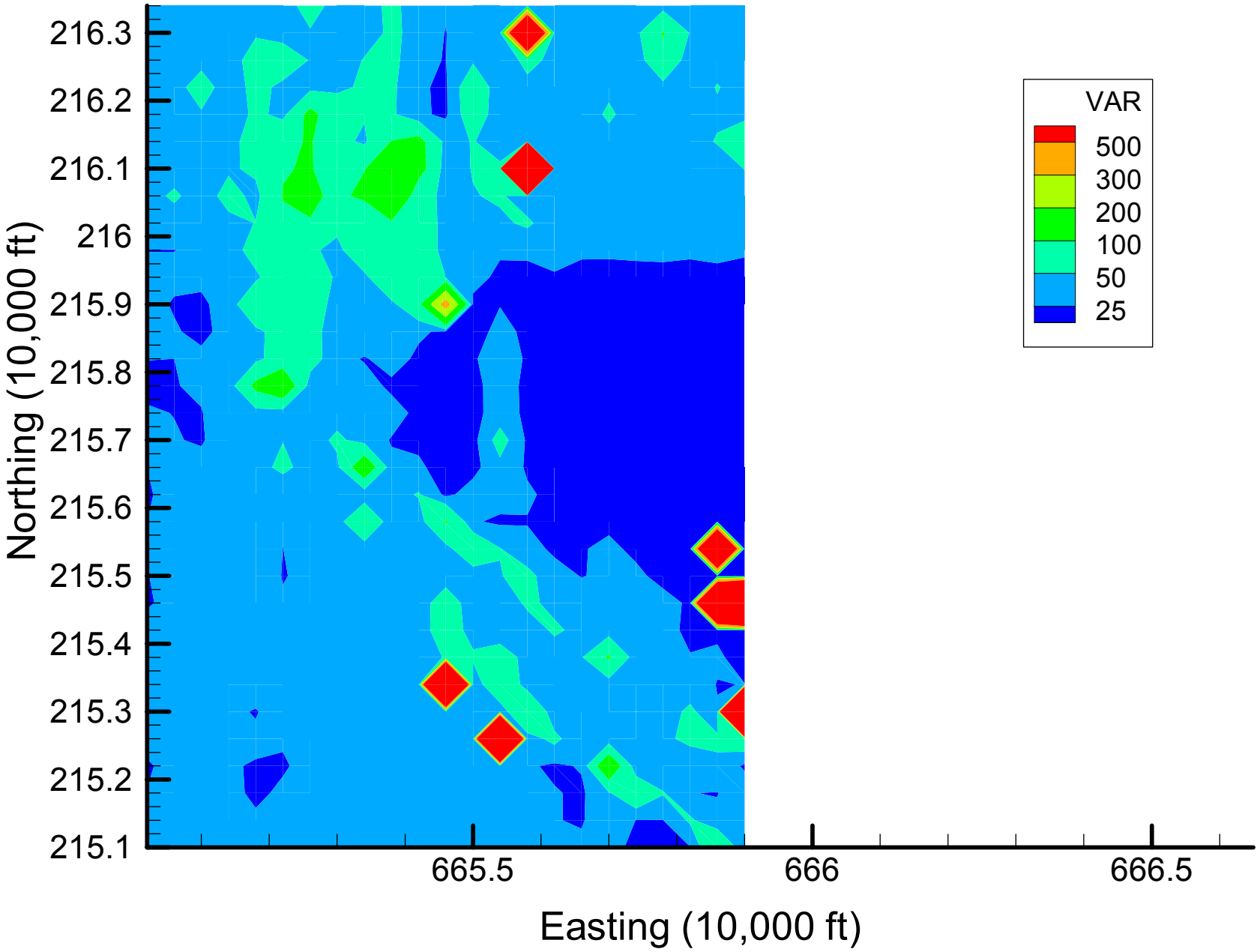

Site 133: MN Local Variances, 2001-2002, 27% Removal

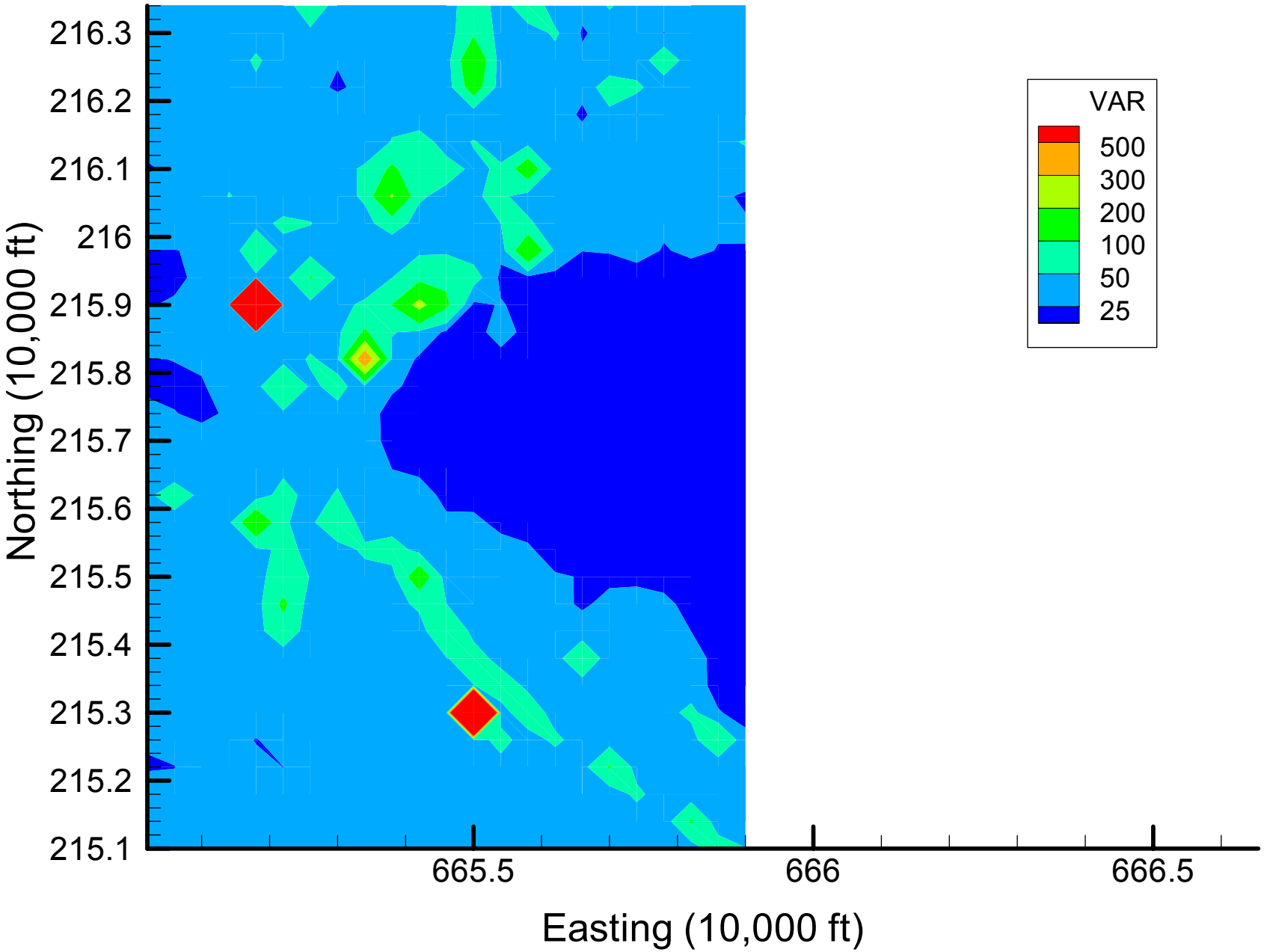

Site 133: MN Local Variances, 2001-2002, 33% Removal

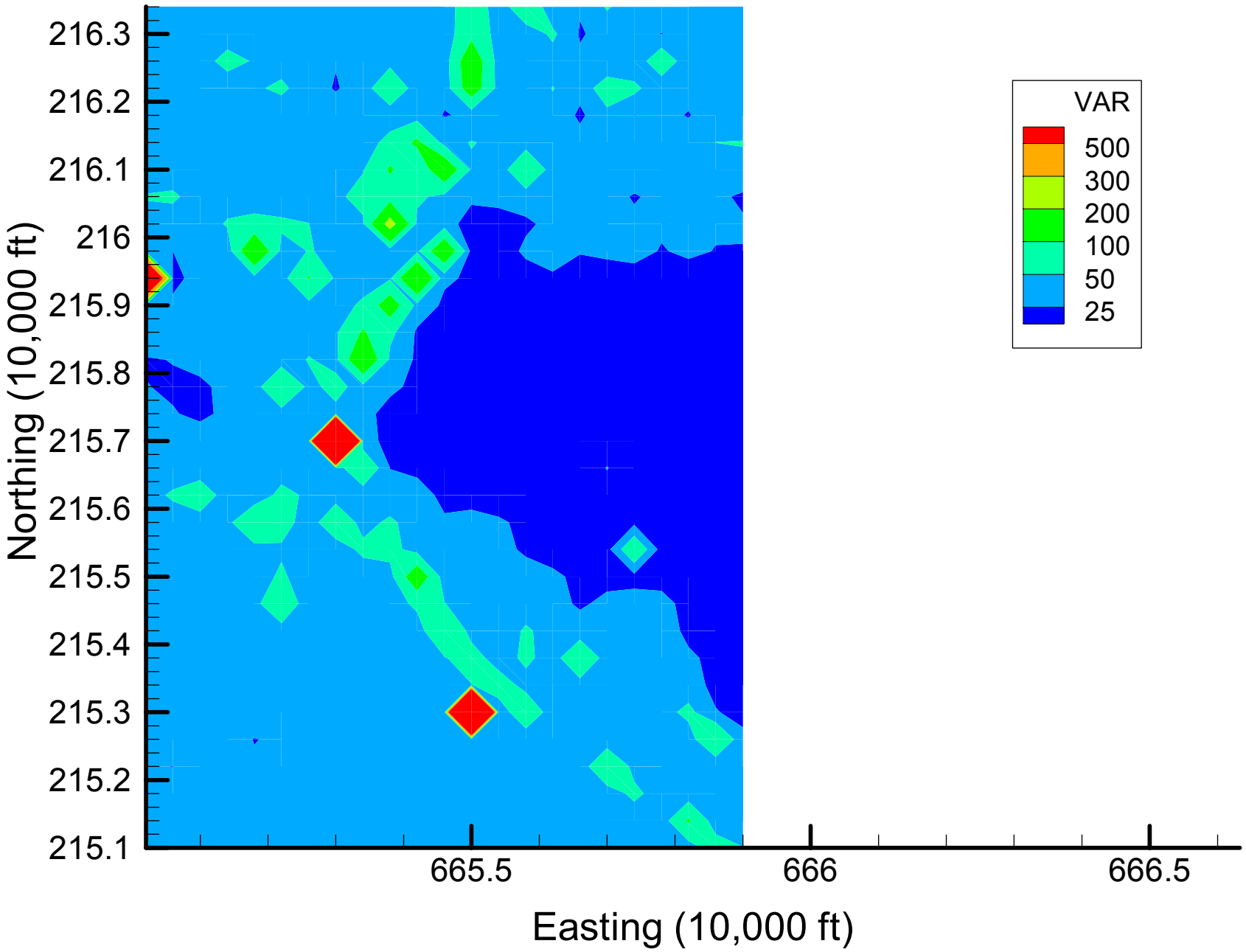

Site 133: MN Local Variances, 2001-2002, 40% Removal

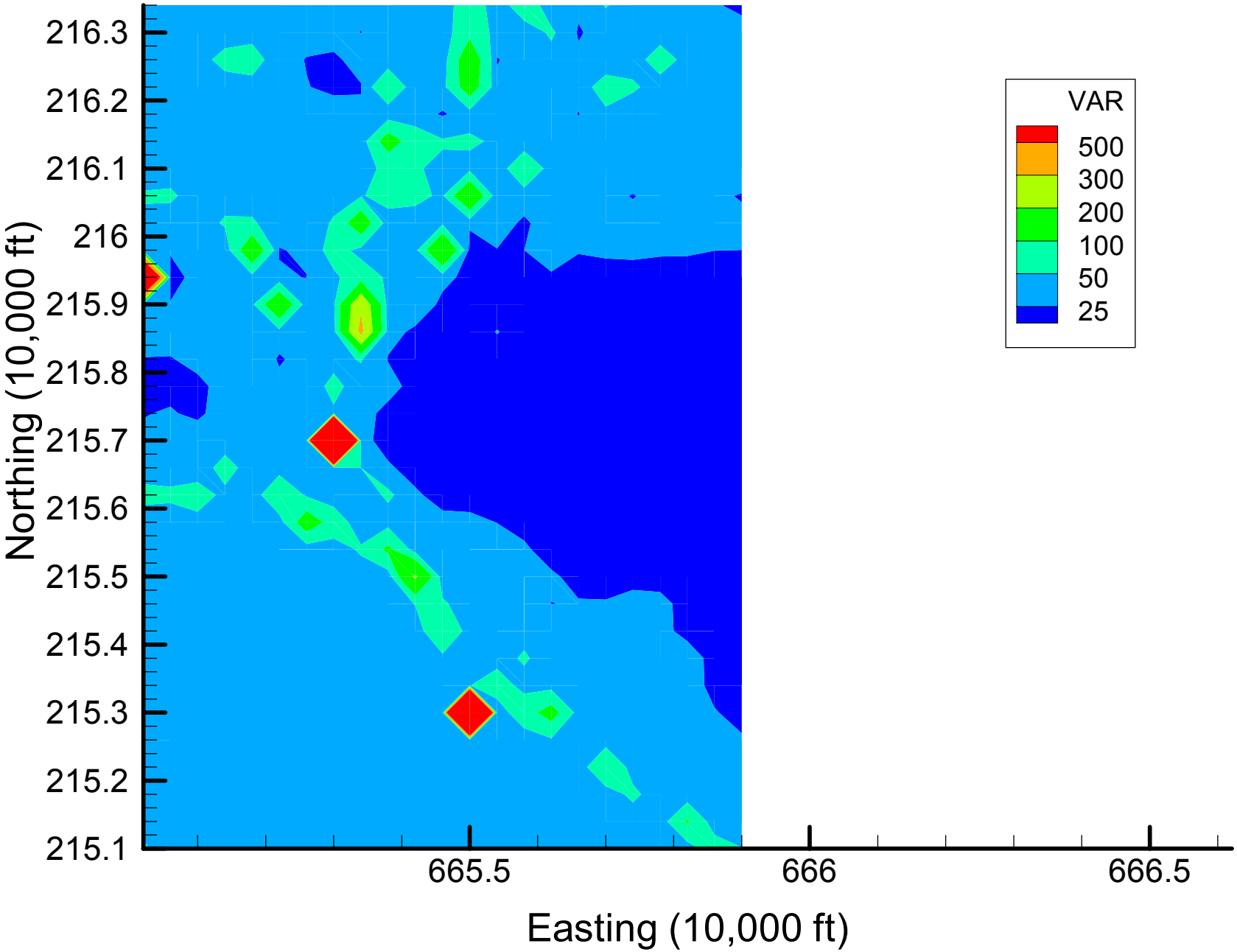

Site 133: MN Local Variances, 2001-2002, 47% Removal

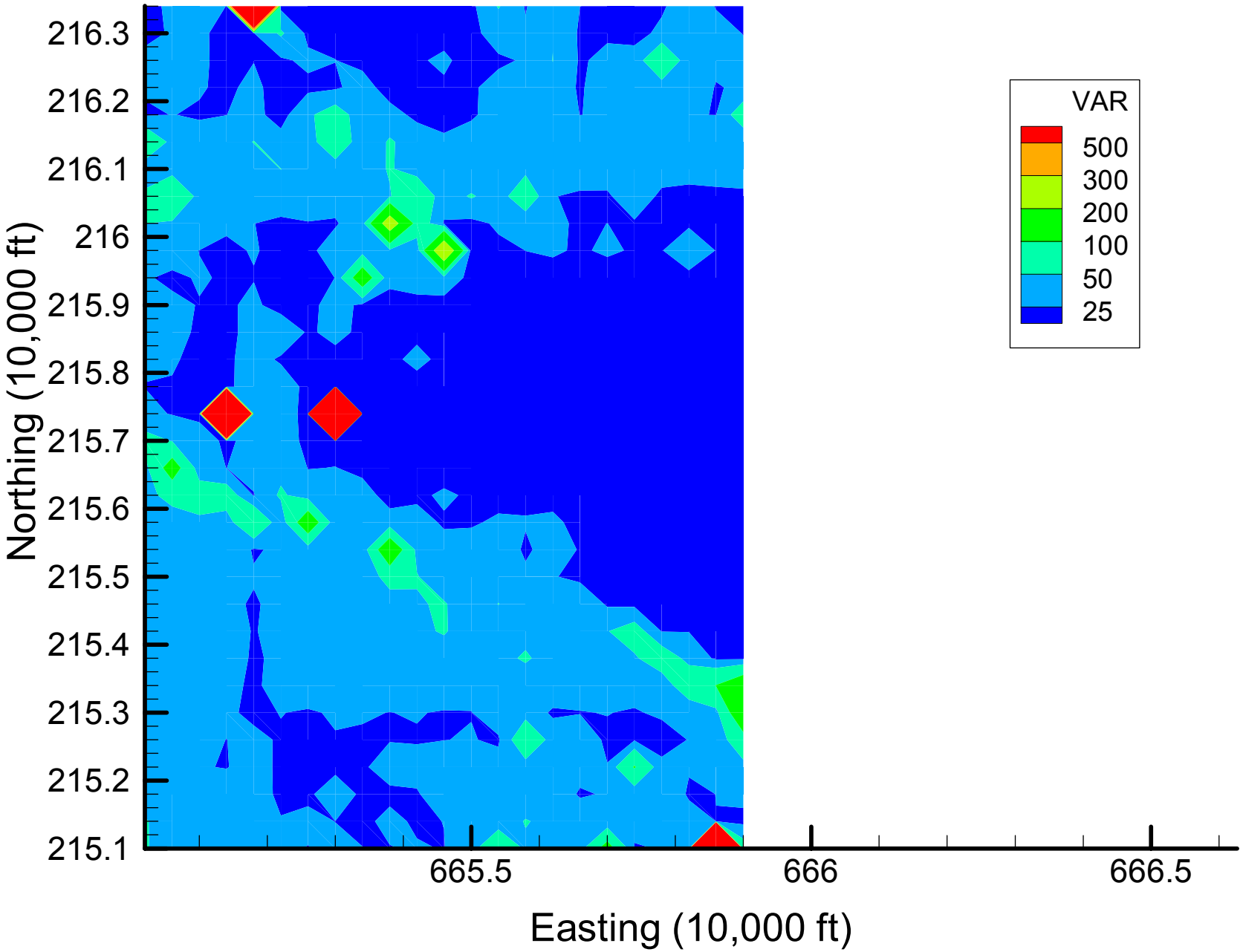

Site 133: MN Local Variances, 2001-2002, 53% Removal

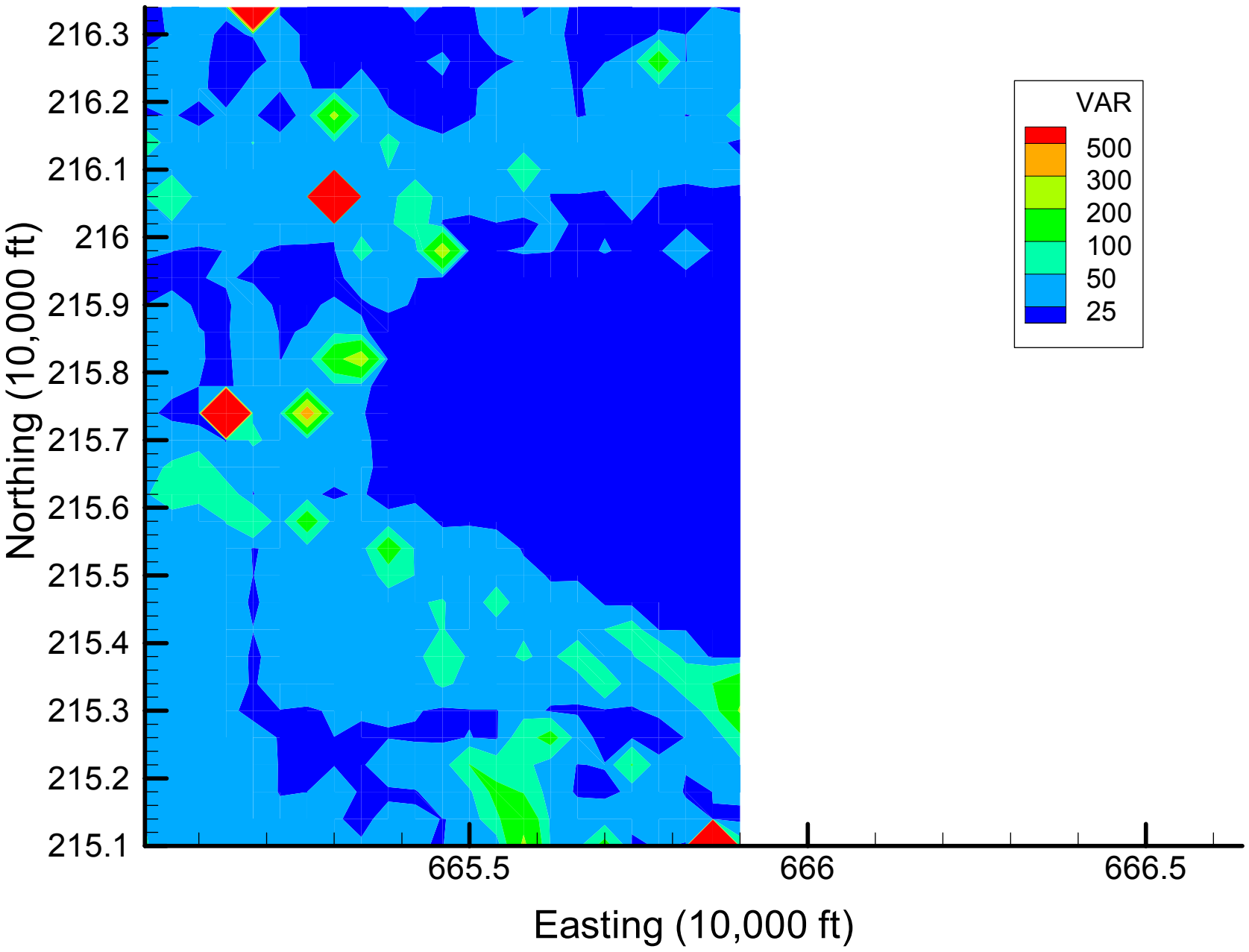

Site 133: MN Local Variances, 2001-2002, 60% Removal

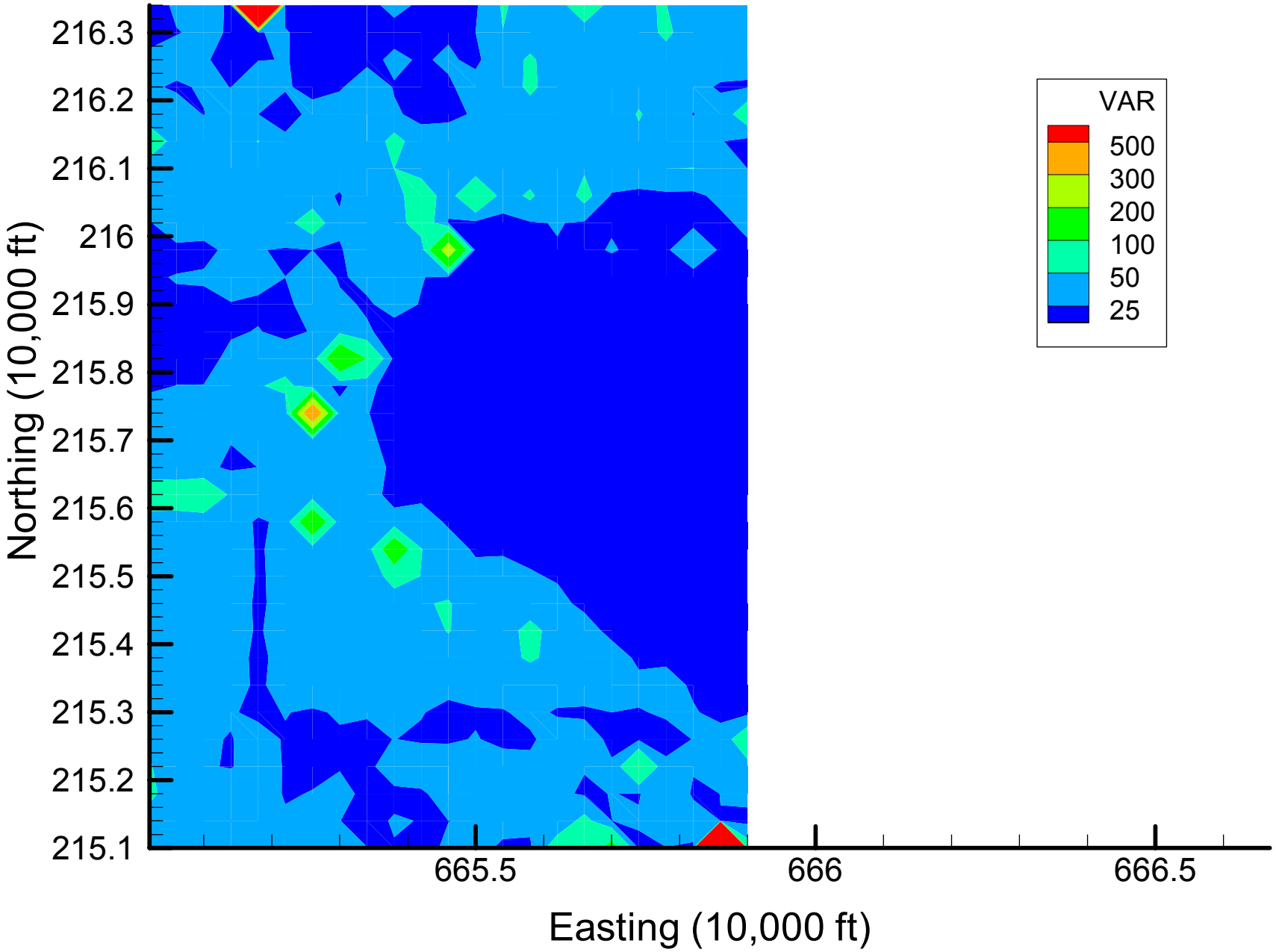

Site 133: MN Local Variances, 2001-2002, 67% Removal

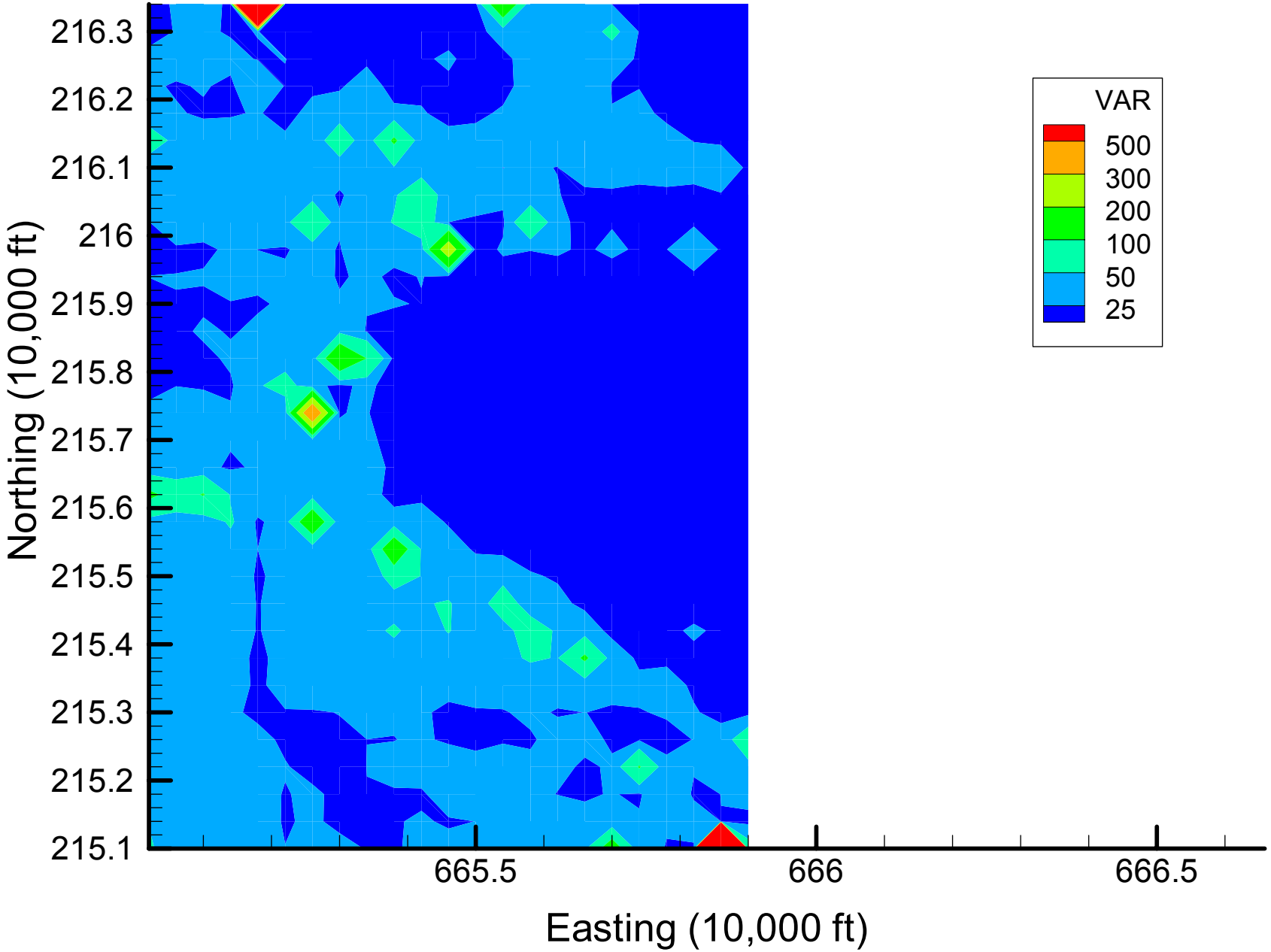

Appendix 4.3
TCE Local Variance Maps
Time Slice 1

Site 133: TCE Local Variances, 1999-2000, Base Map

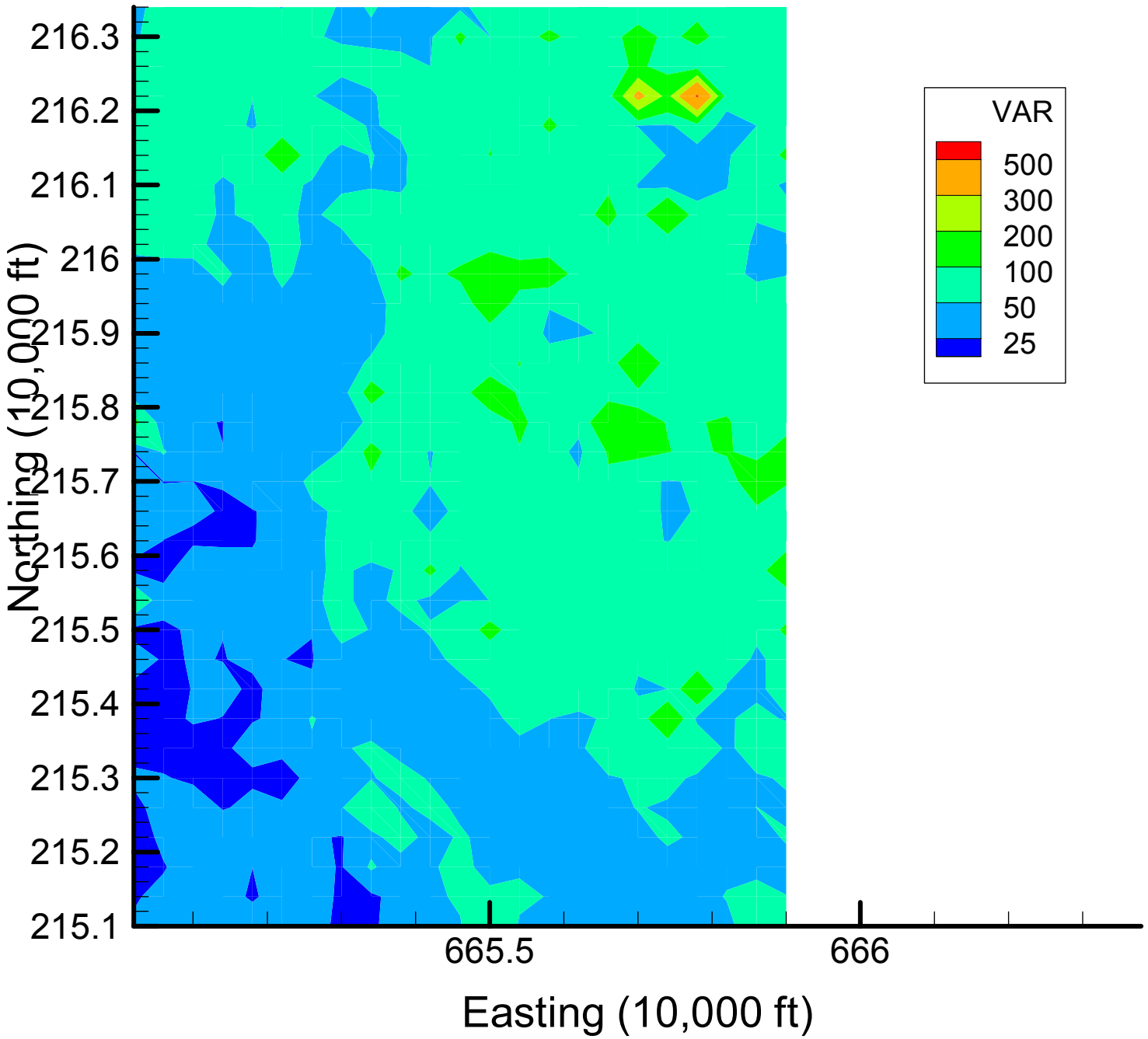

Site 133: TCE Local Variances, 1999-2000, 7% Removal

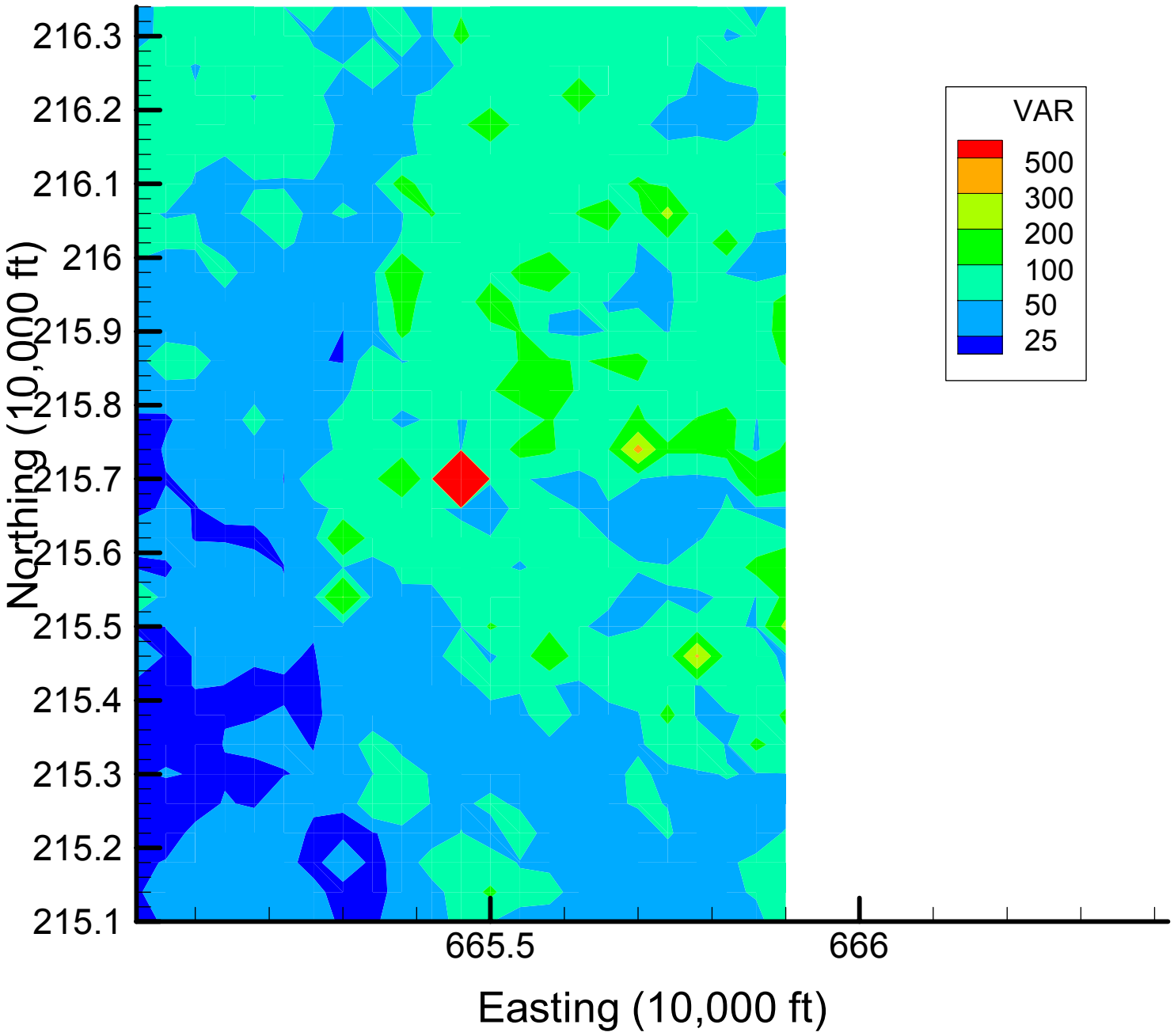

Site 133: TCE Local Variances, 1999-2000, 13% Removal

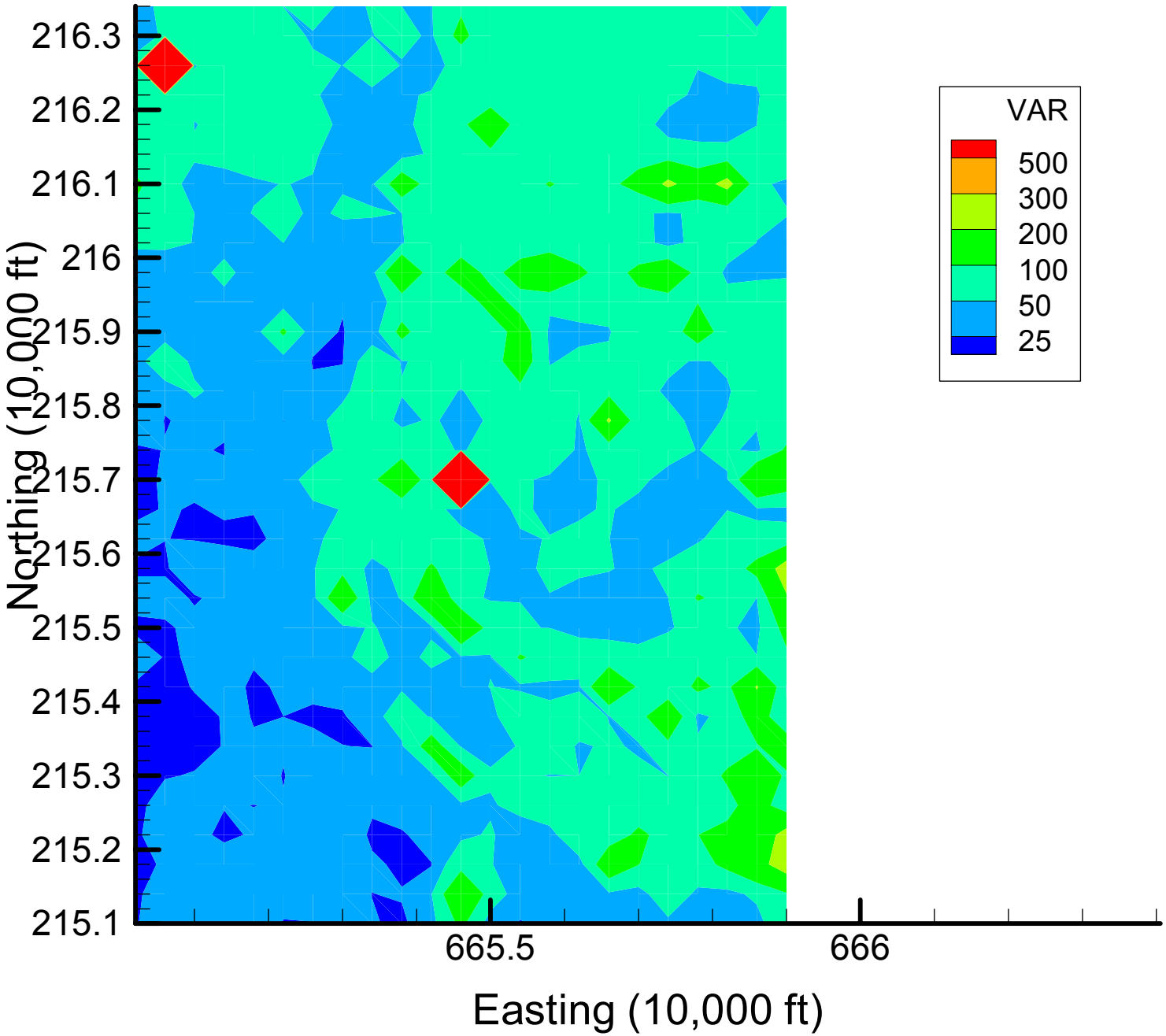

Site 133: TCE Local Variances, 1999-2000, 20% Removal

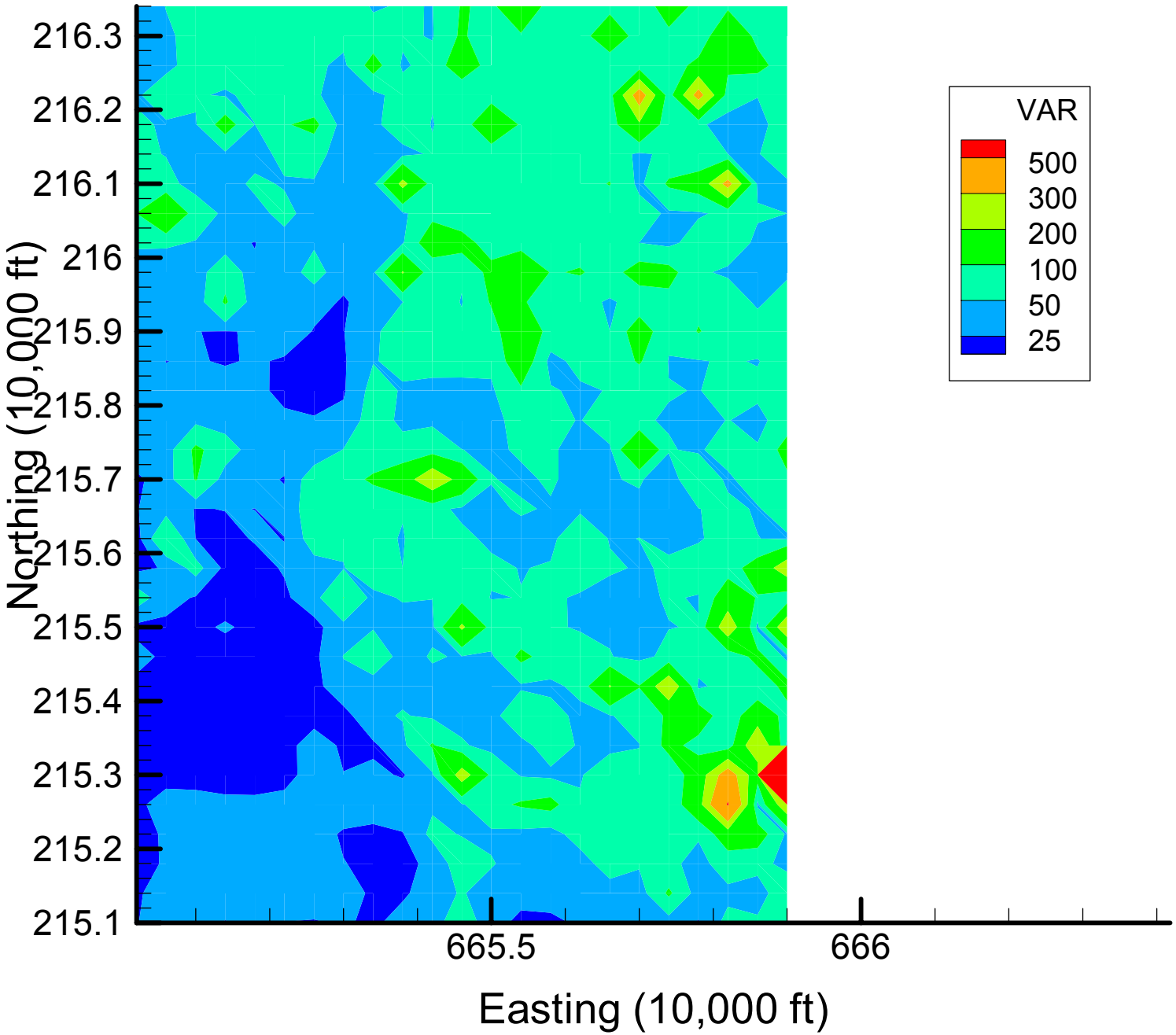

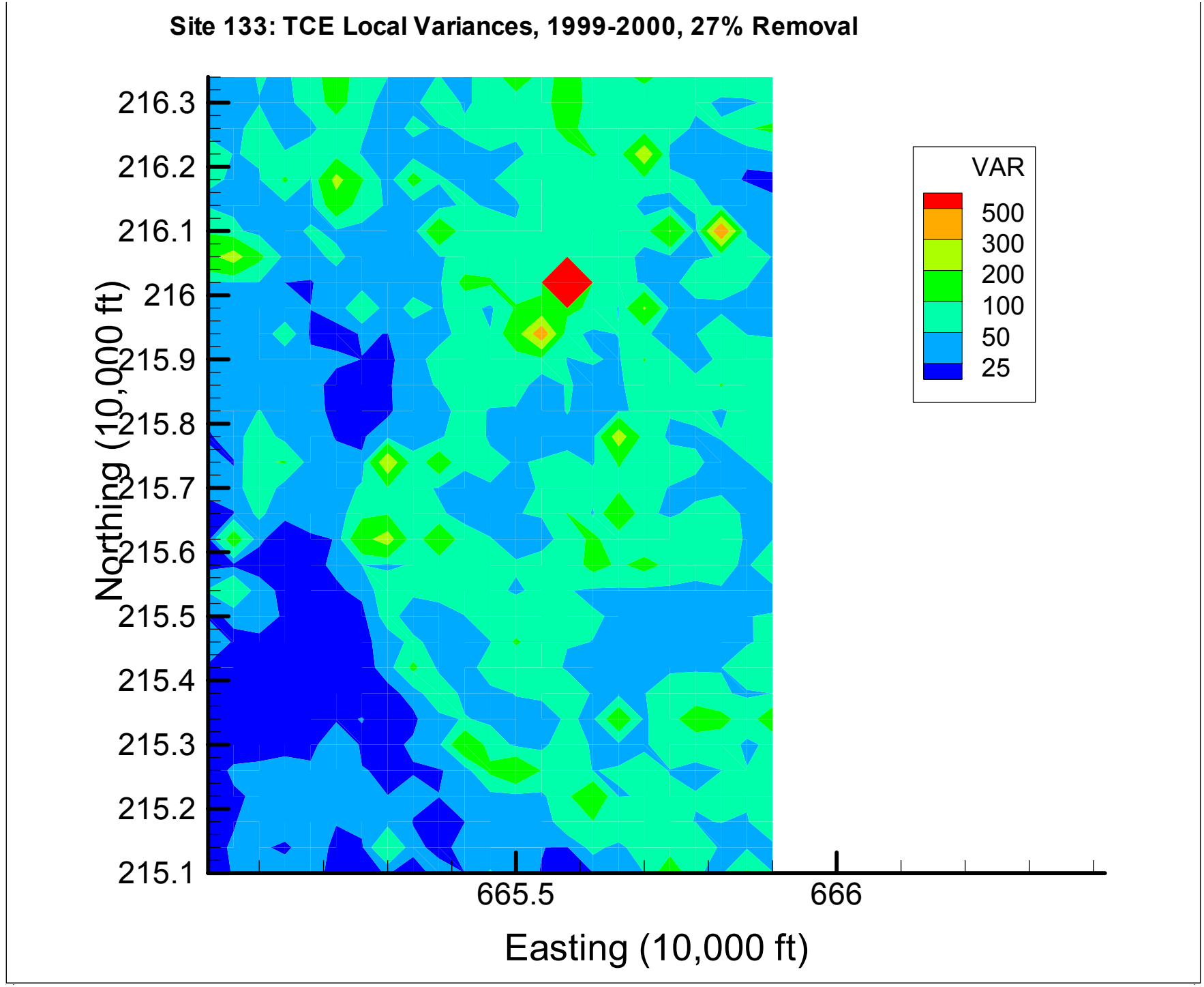
Site 133: TCE Local Variances, 1999-2000, 27% Removal
216.3
216.2
216.1
216
215.9
215.8
215.7
215.6
215.5
215.4
215.3
215.2
215.1
Northing (10,000 ft)
665.5
666
Easting (10,000 ft)
VAR
500
300
200
100
50
25

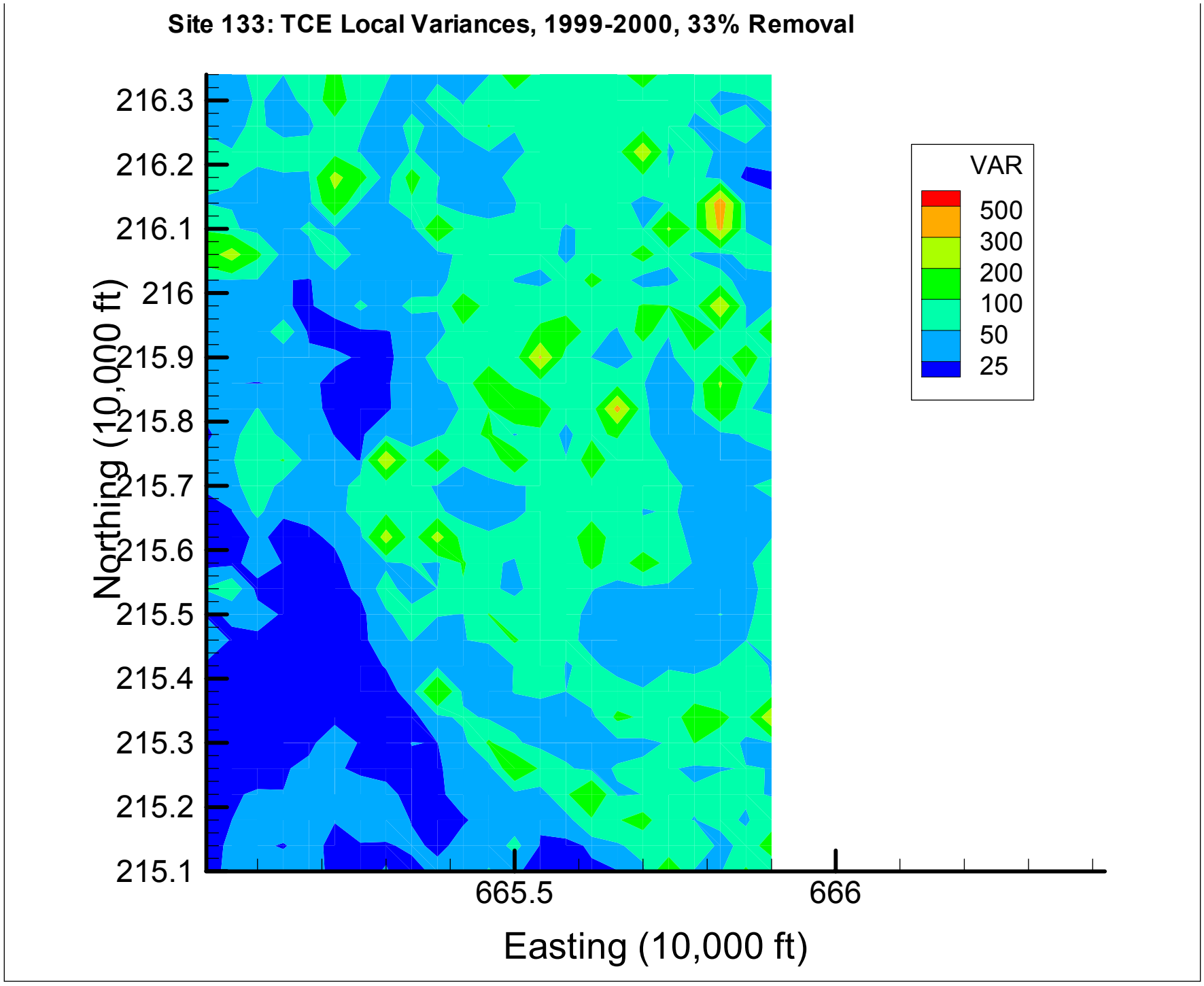
Site 133: TCE Local Variances, 1999-2000, 33% Removal
VAR
500
300
200
100
50
25
216.3
216.2
216.1
216
215.9
215.8
215.7
215.6
215.5
215.4
215.3
215.2
215.1
Northing (10,000 ft)
665.5
666
Easting (10,000 ft)

Site 133: TCE Local Variances, 1999-2000, 40% Removal

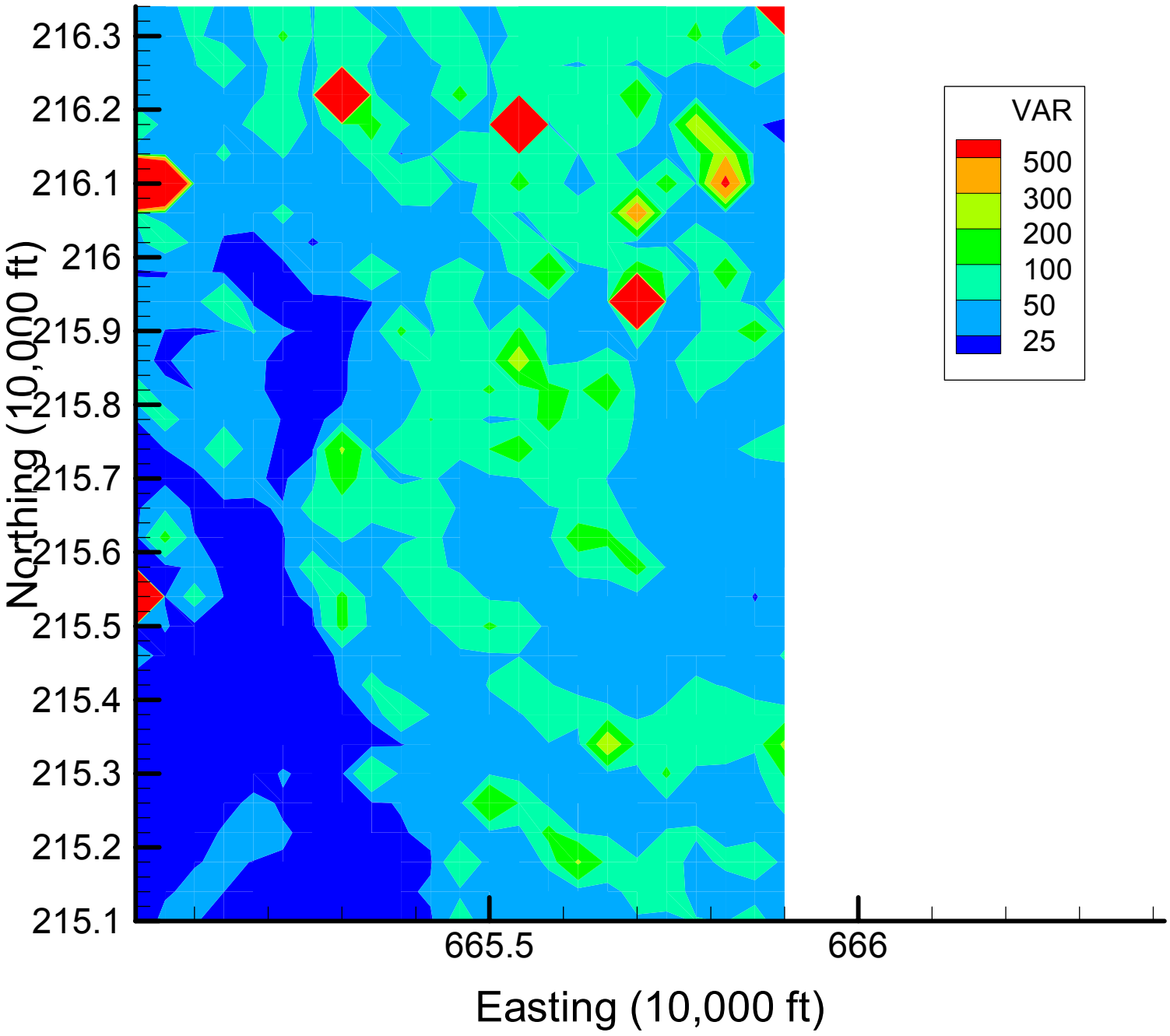

Site 133: TCE Local Variances, 1999-2000, 47% Removal

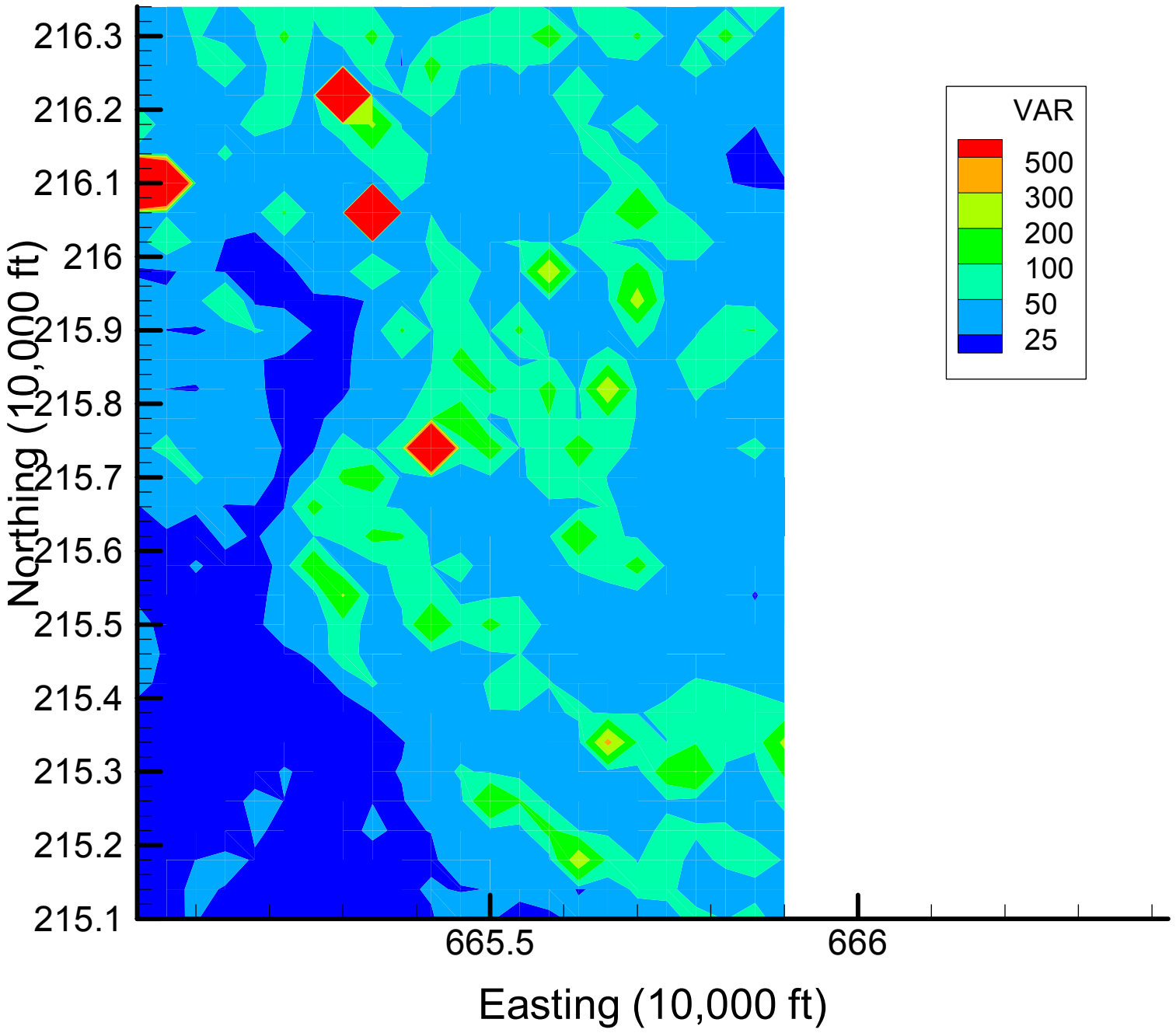

Site 133: TCE Local Variances, 1999-2000, 53% Removal

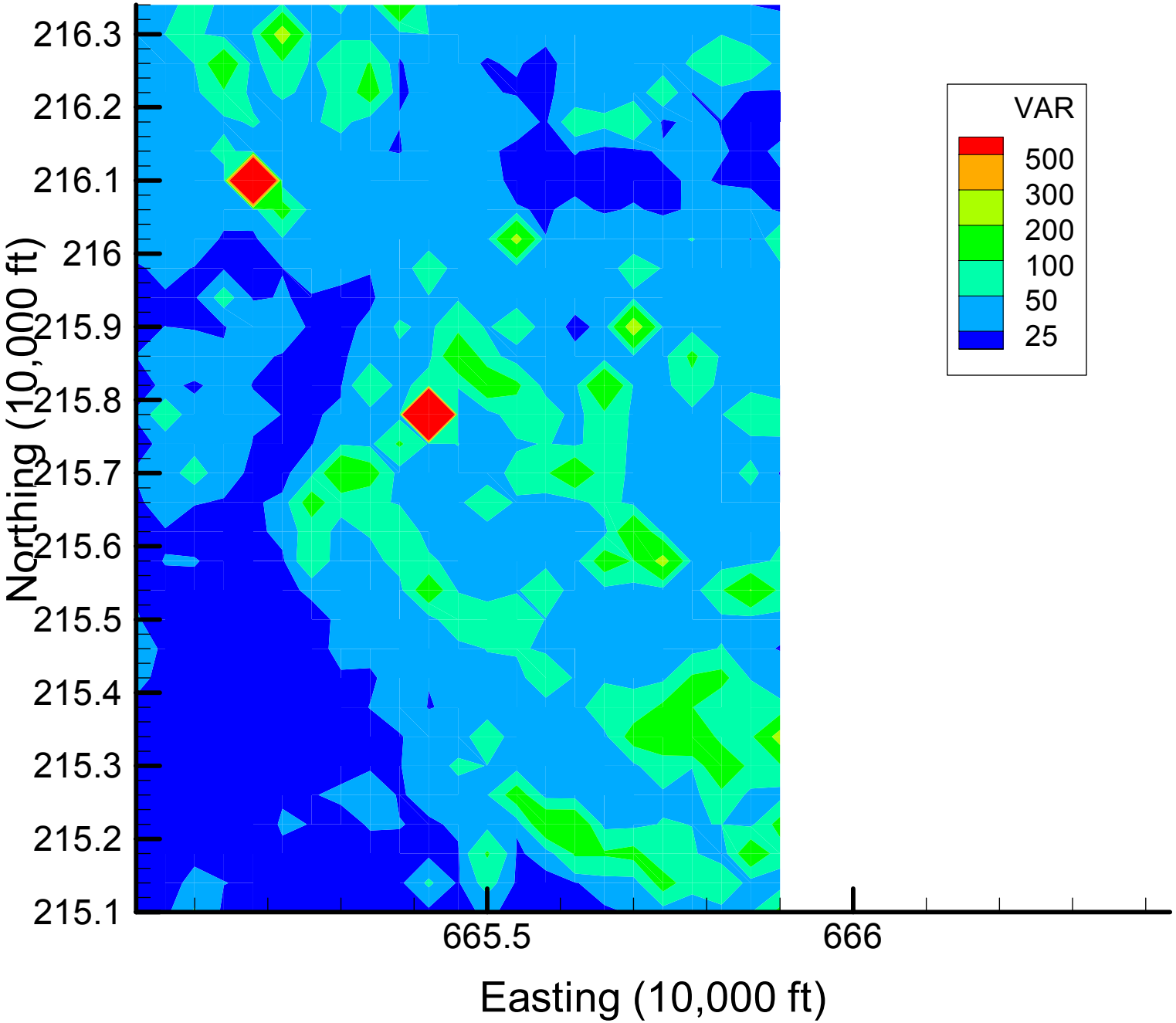

Site 133: TCE Local Variances, 1999-2000, 60% Removal

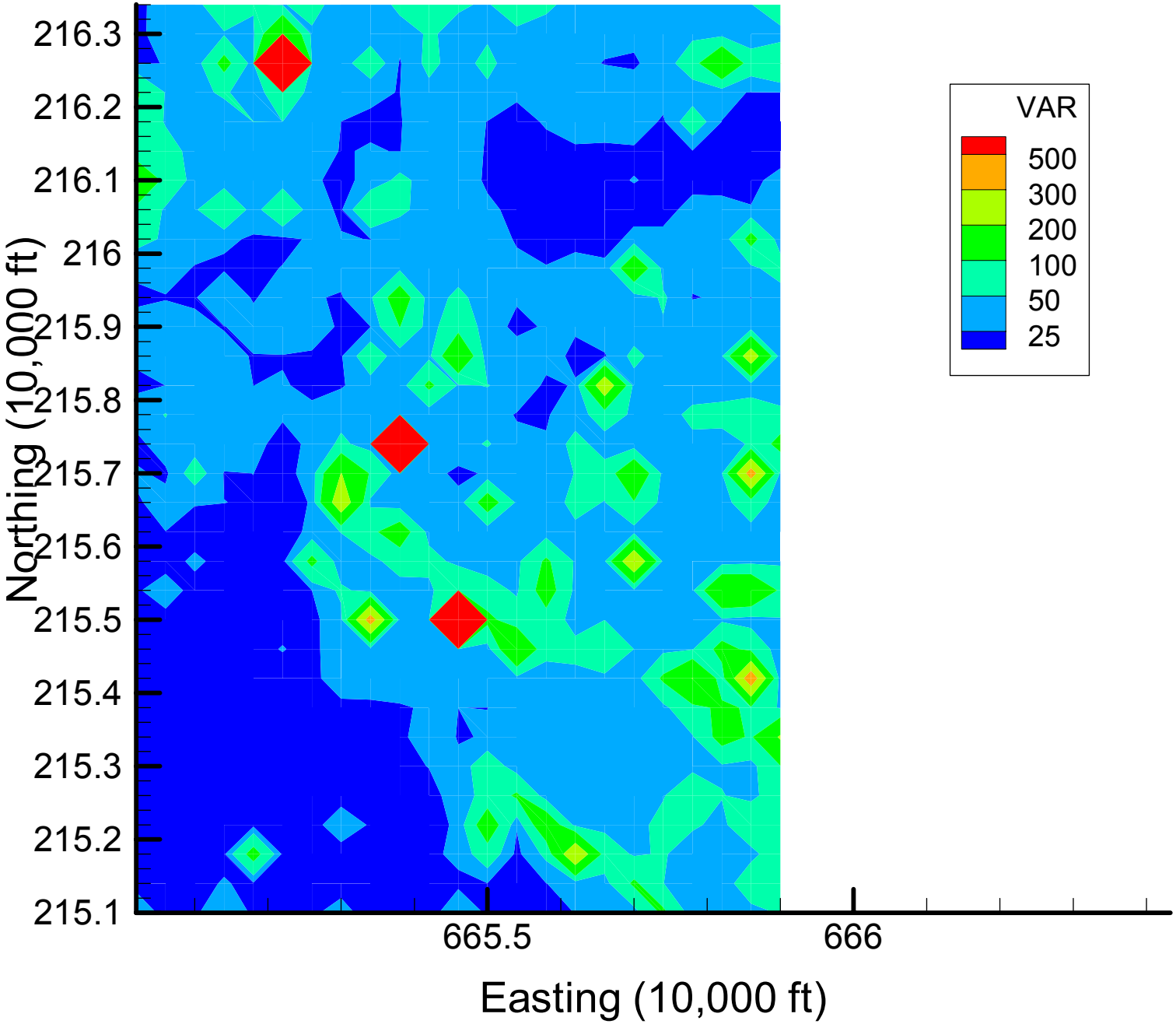

Site 133: TCE Local Variances, 1999-2000, 67% Removal

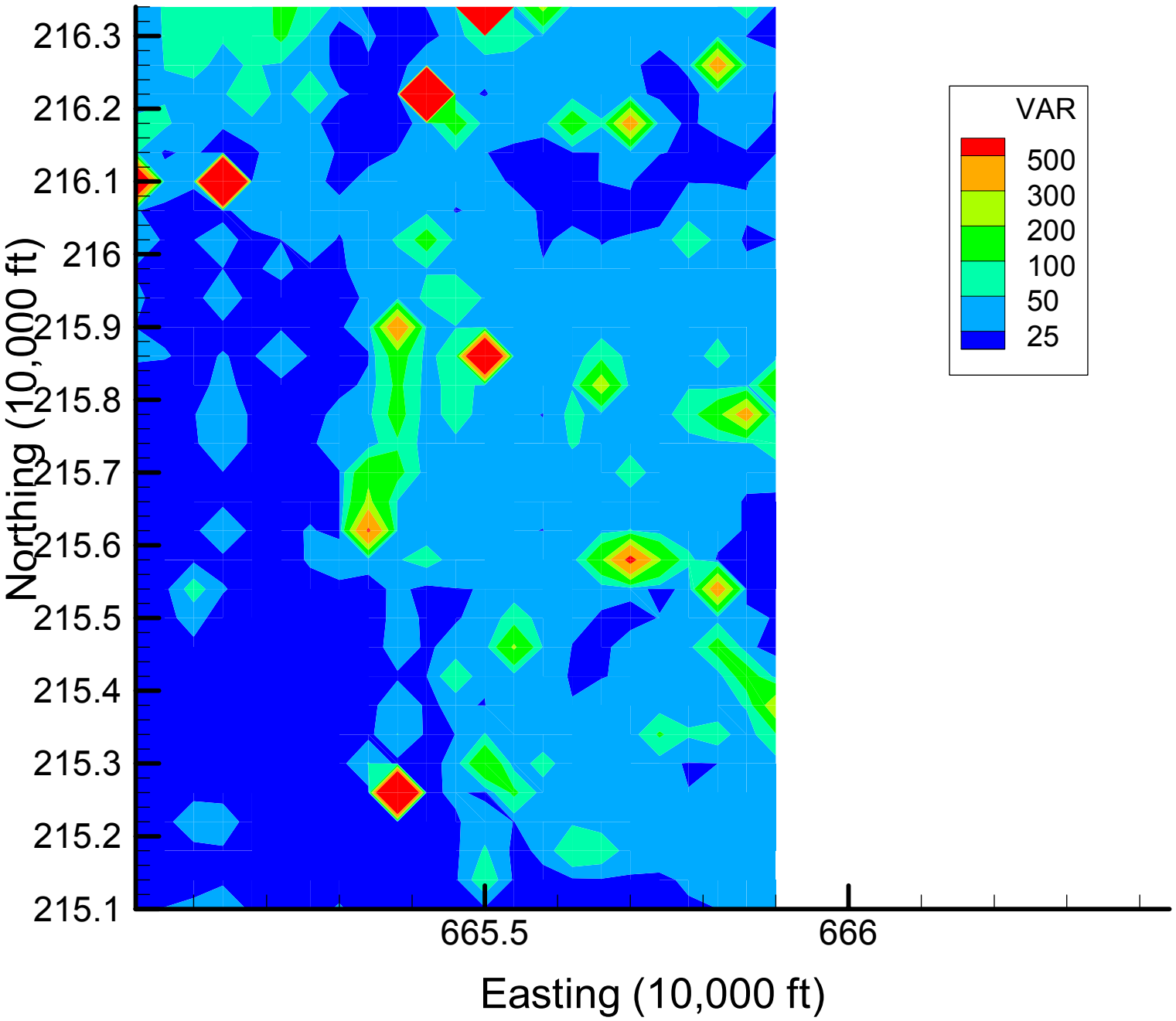

Appendix 4.3
TCE Local Variance Maps
Time Slice 2

Site 133: TCE Local Variances, 2001-2002, Base Map

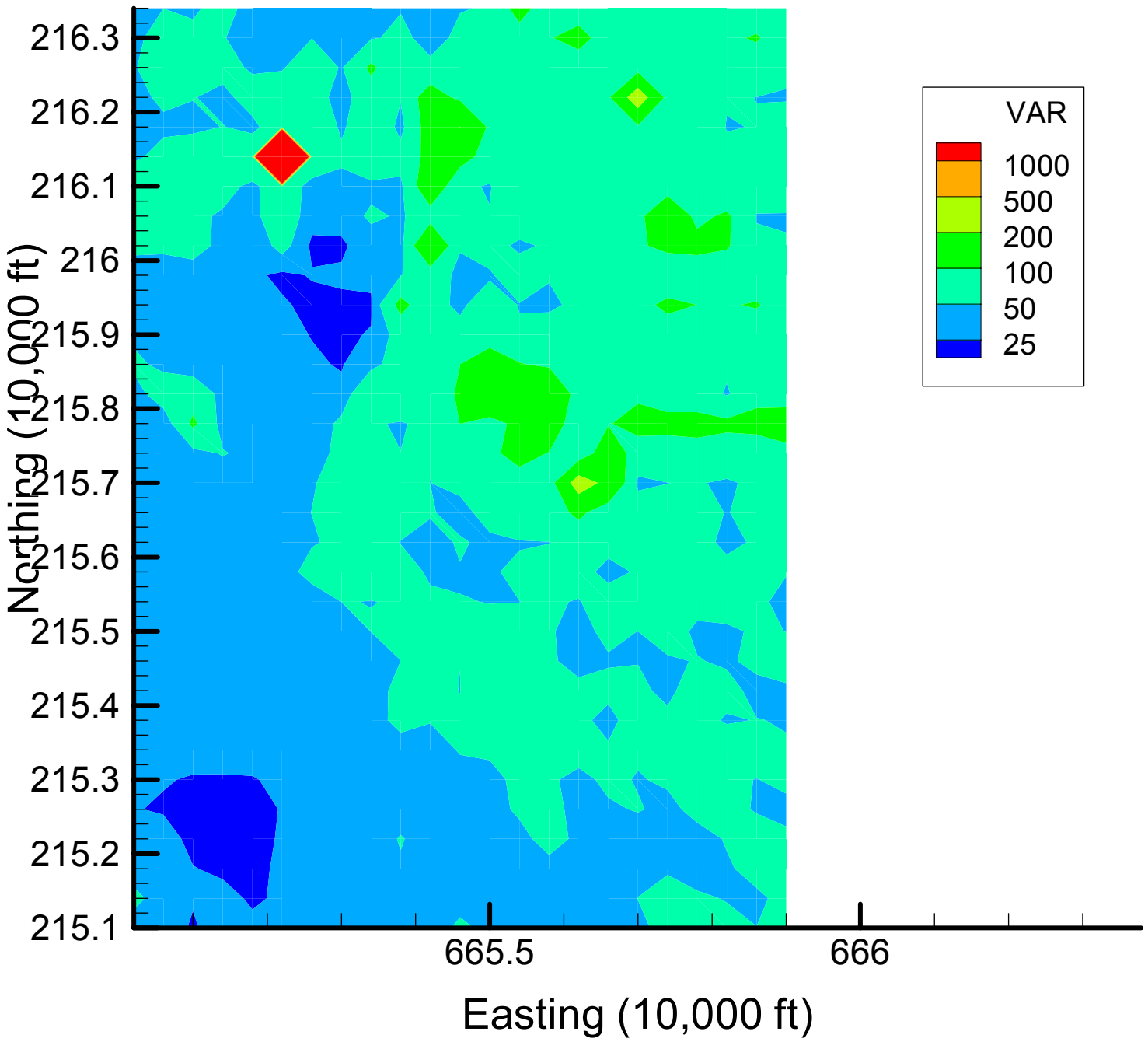

Site 133: TCE Local Variances, 2001-2002, 7% Removal

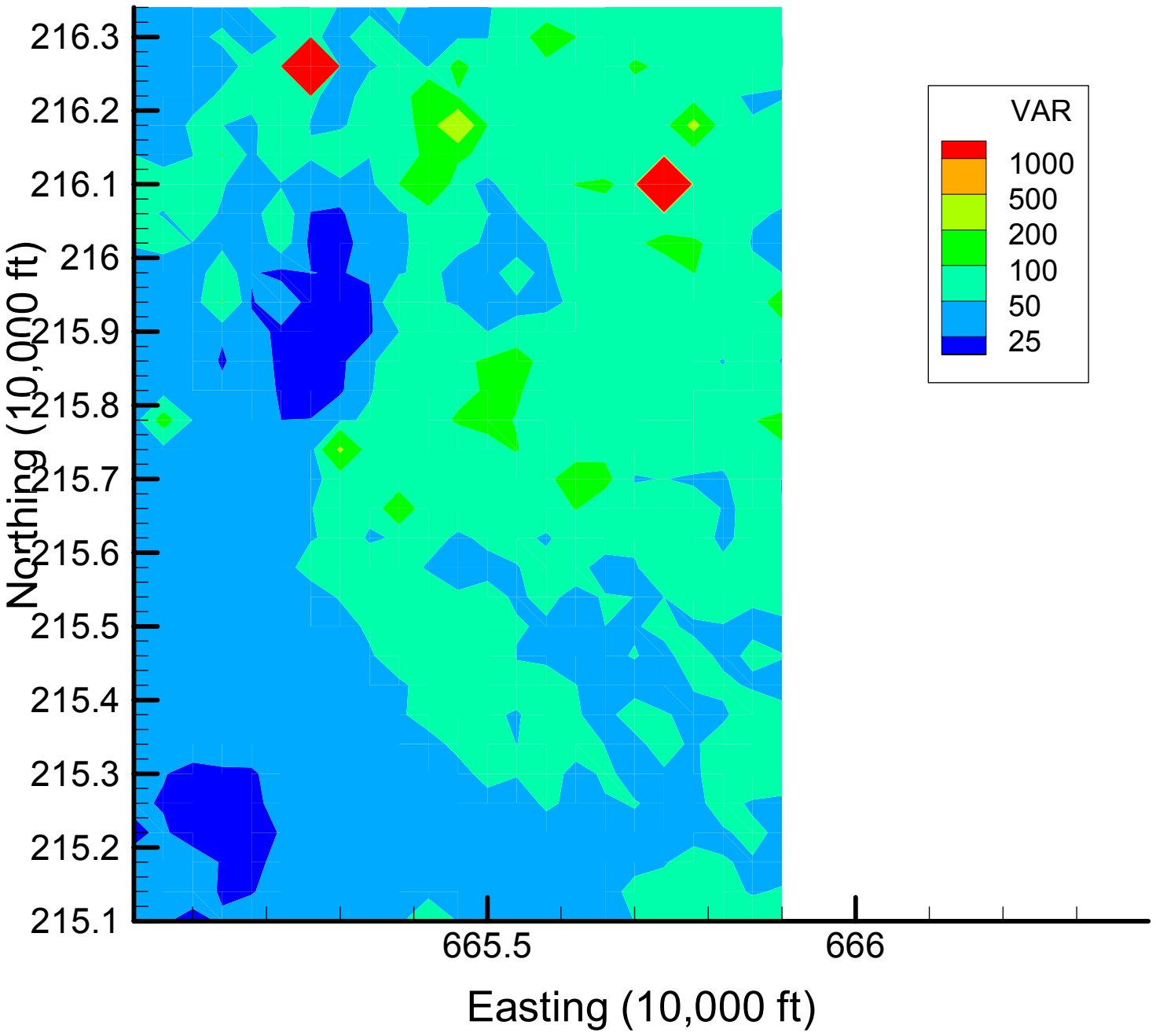

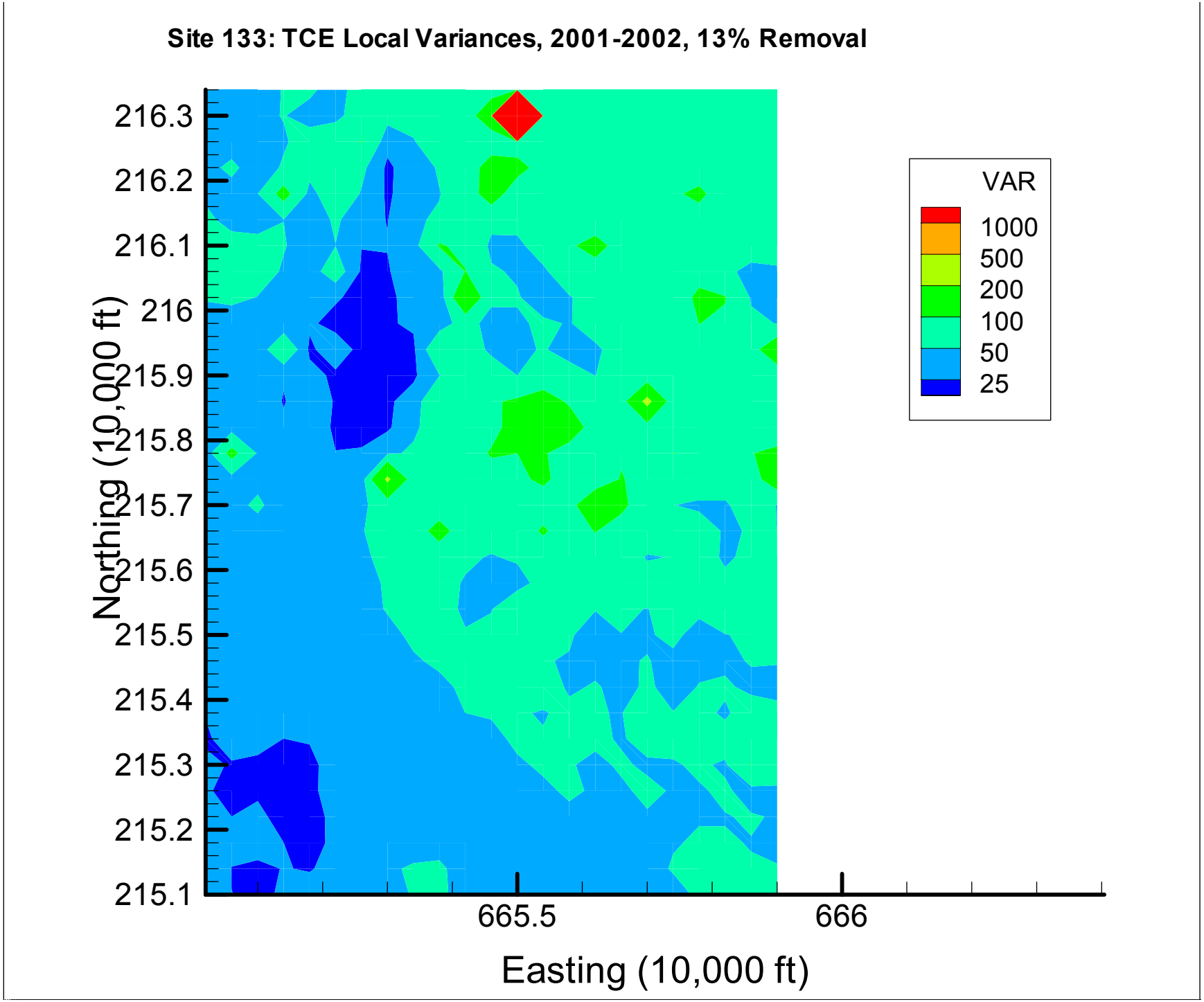
Site 133: TCE Local Variances, 2001-2002, 13% Removal
VAR
1000
500
200
100
50
25
216.3
216.2
216.1
216
215.9
215.8
215.7
215.6
215.5
215.4
215.3
215.2
215.1
Northing (10,000 ft)
665.5
666
Easting (10,000 ft)

Site 133: TCE Local Variances, 2001-2002, 20% Removal

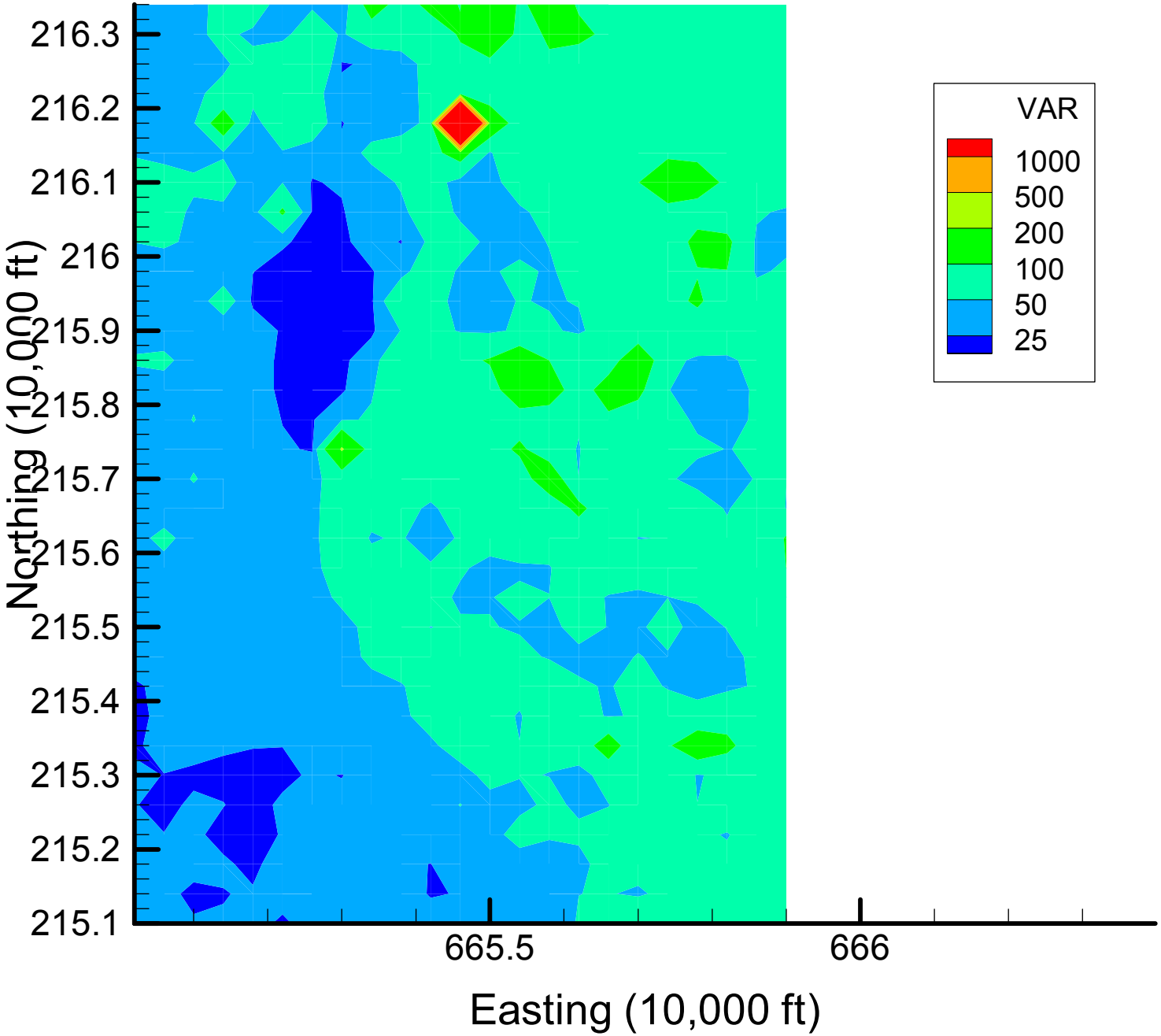

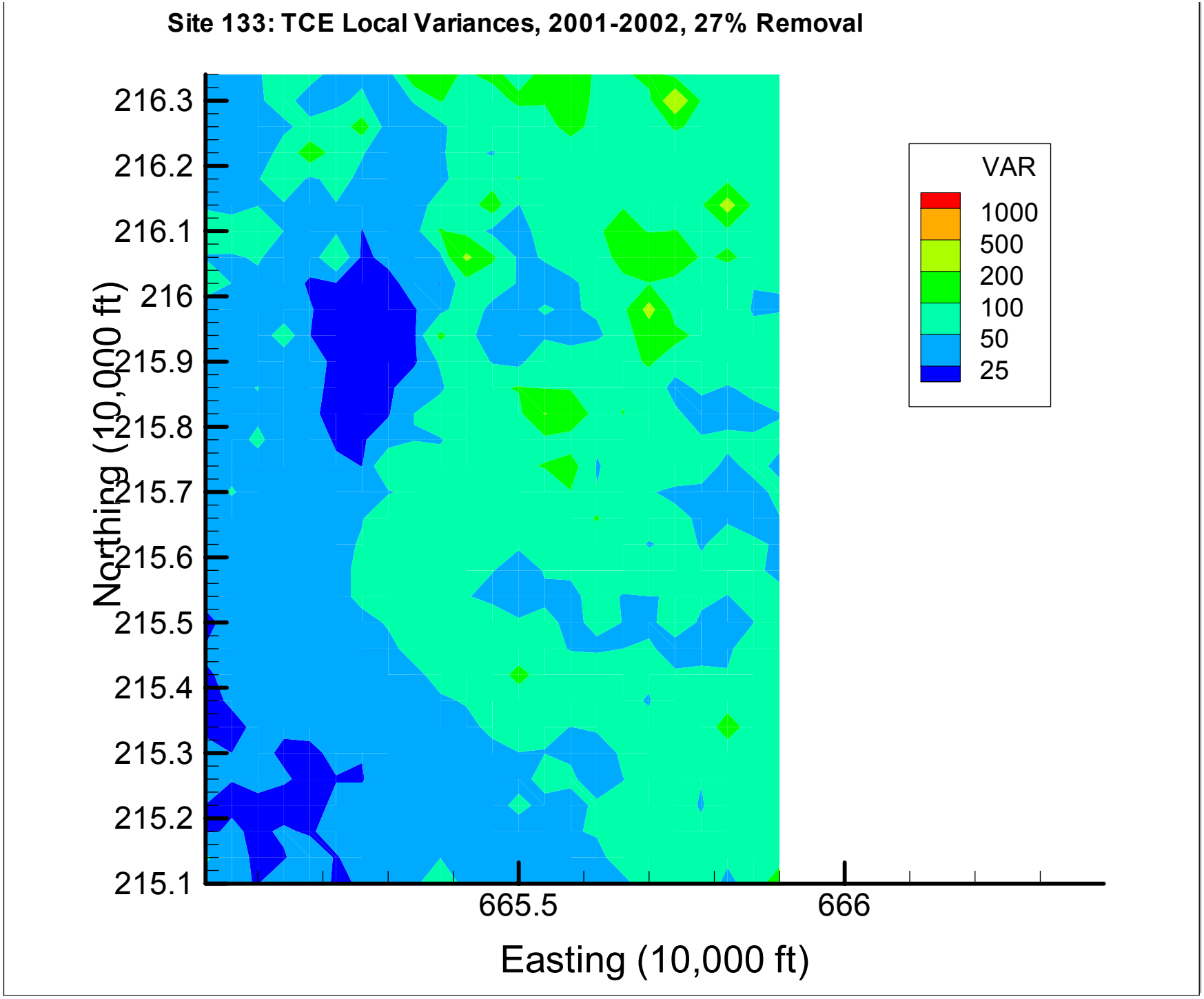
Site 133: TCE Local Variances, 2001-2002, 27% Removal
VAR
1000
500
200
100
50
25
216.3
216.2
216.1
216
215.9
215.8
215.7
215.6
215.5
215.4
215.3
215.2
215.1
Northing (10,000 ft)
665.5
666
Easting (10,000 ft)

Site 133: TCE Local Variances, 2001-2002, 33% Removal

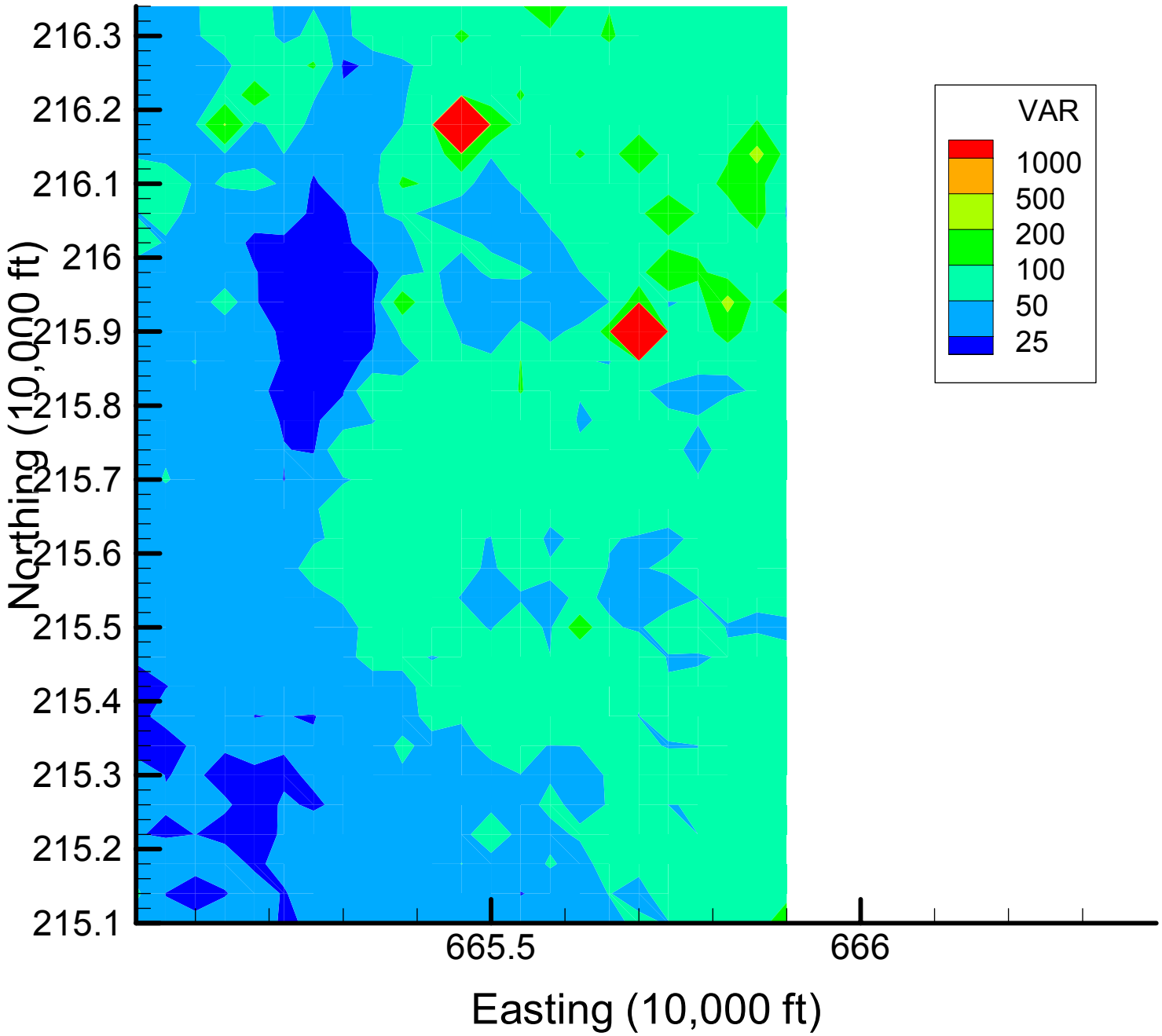

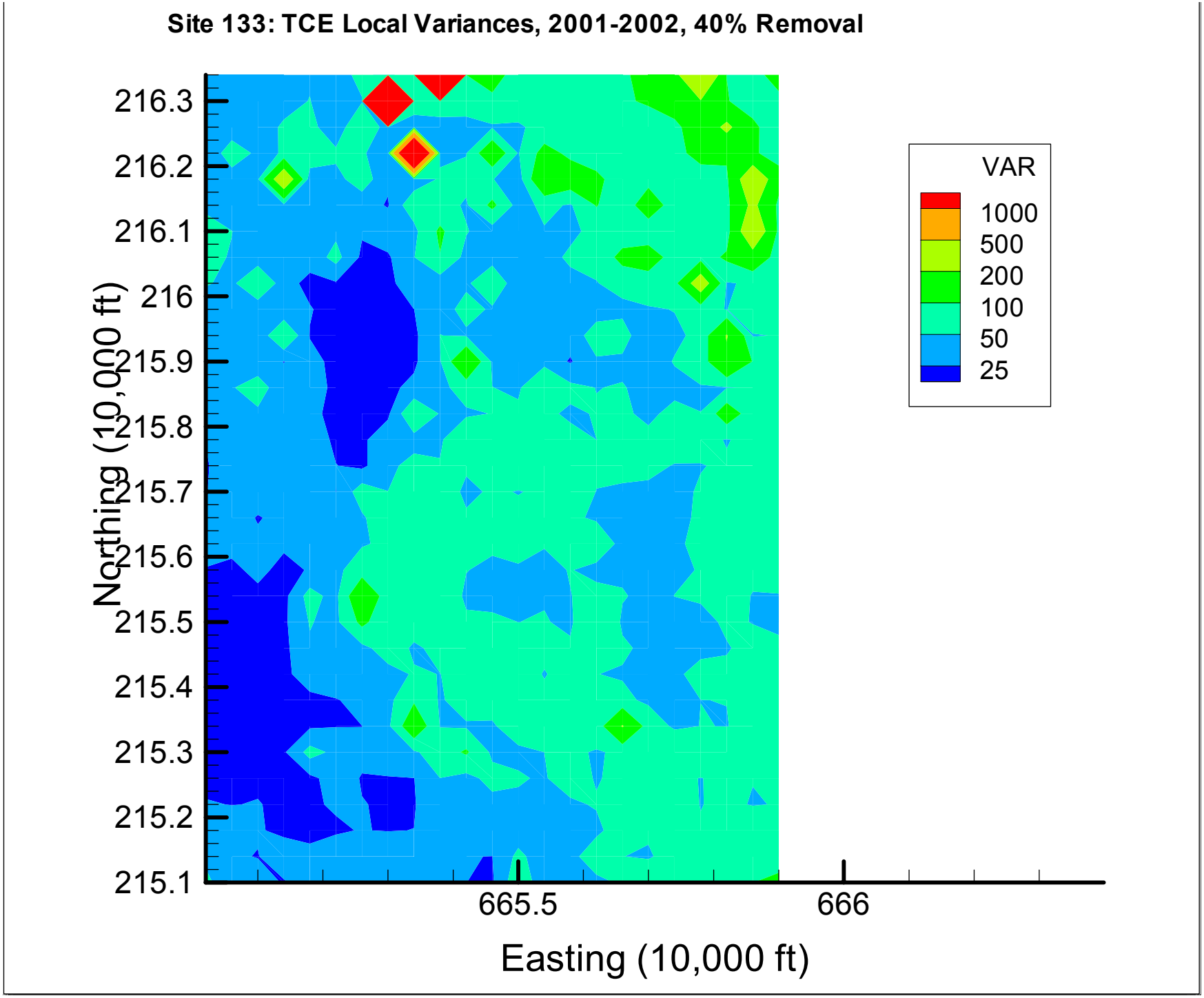
Site 133: TCE Local Variances, 2001-2002, 40% Removal
216.3
216.2
216.1
216
215.9
215.8
215.7
215.6
215.5
215.4
215.3
215.2
215.1
Northing (10,000 ft)
665.5
666
Easting (10,000 ft)
VAR
1000
500
200
100
50
25

Site 133: TCE Local Variances, 2001-2002, 47% Removal

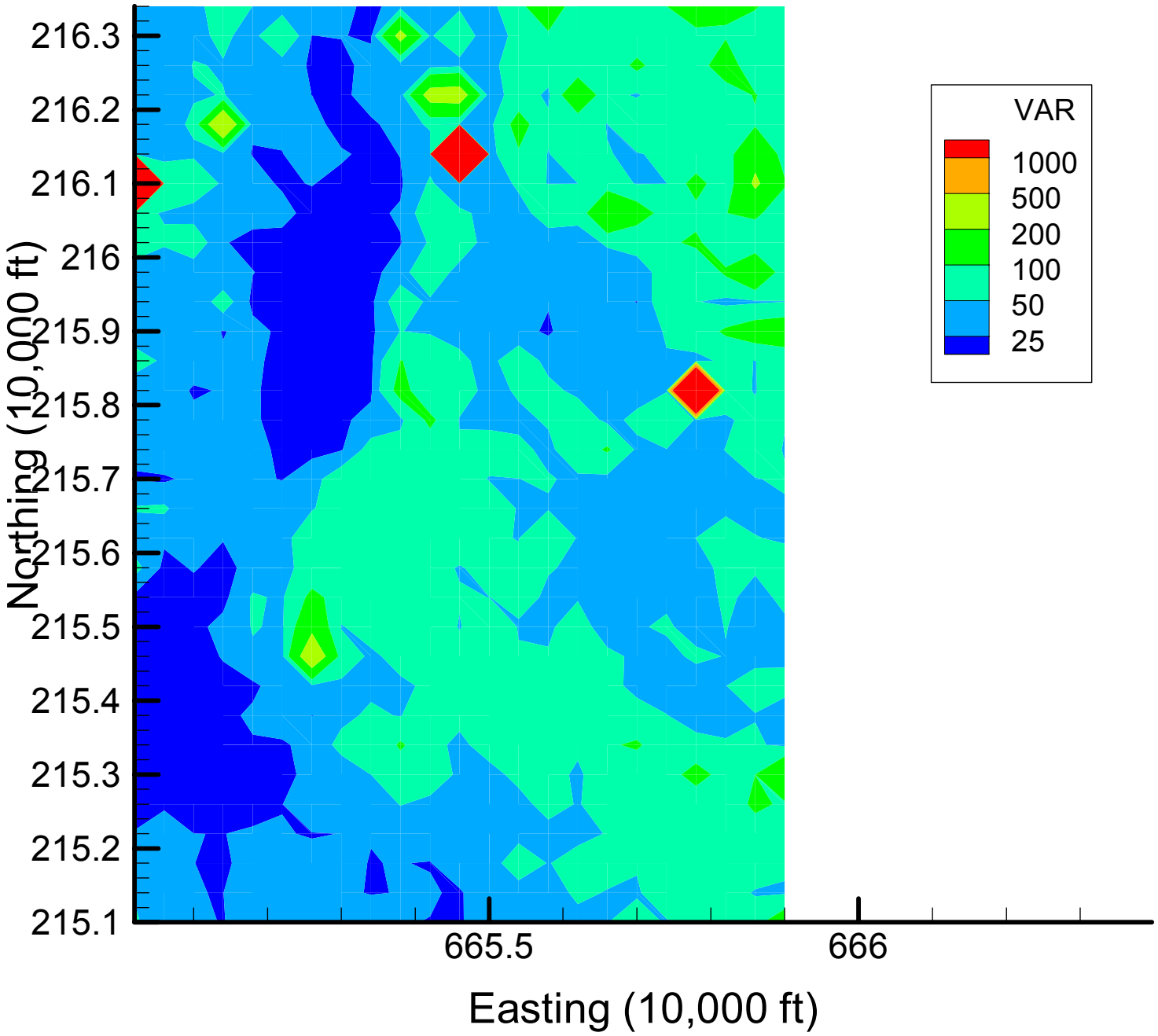

Site 133: TCE Local Variances, 2001-2002, 53% Removal

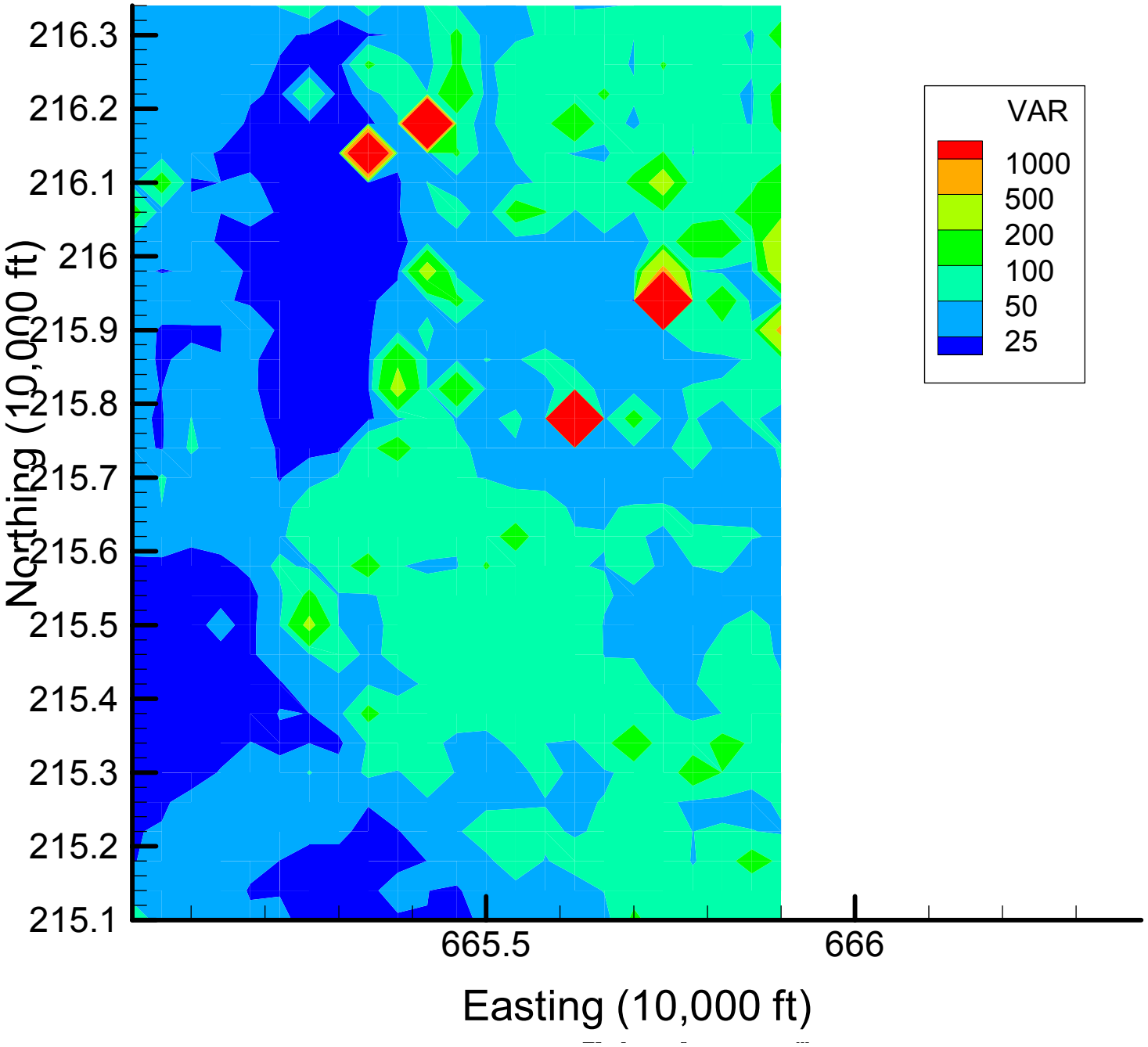

Site 133: TCE Local Variances, 2001-2002, 60% Removal

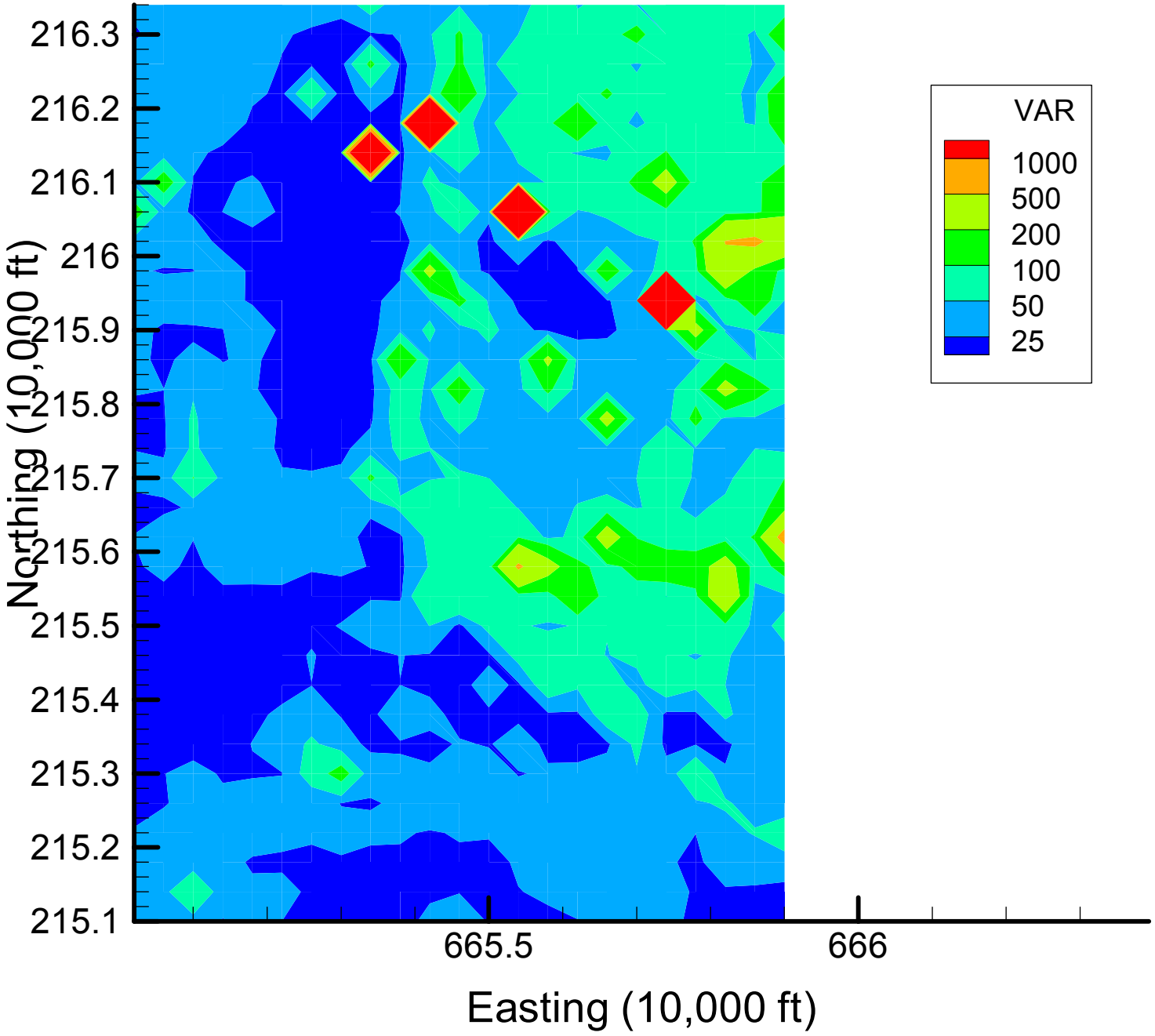

Site 133: TCE Local Variances, 2001-2002, 67% Removal

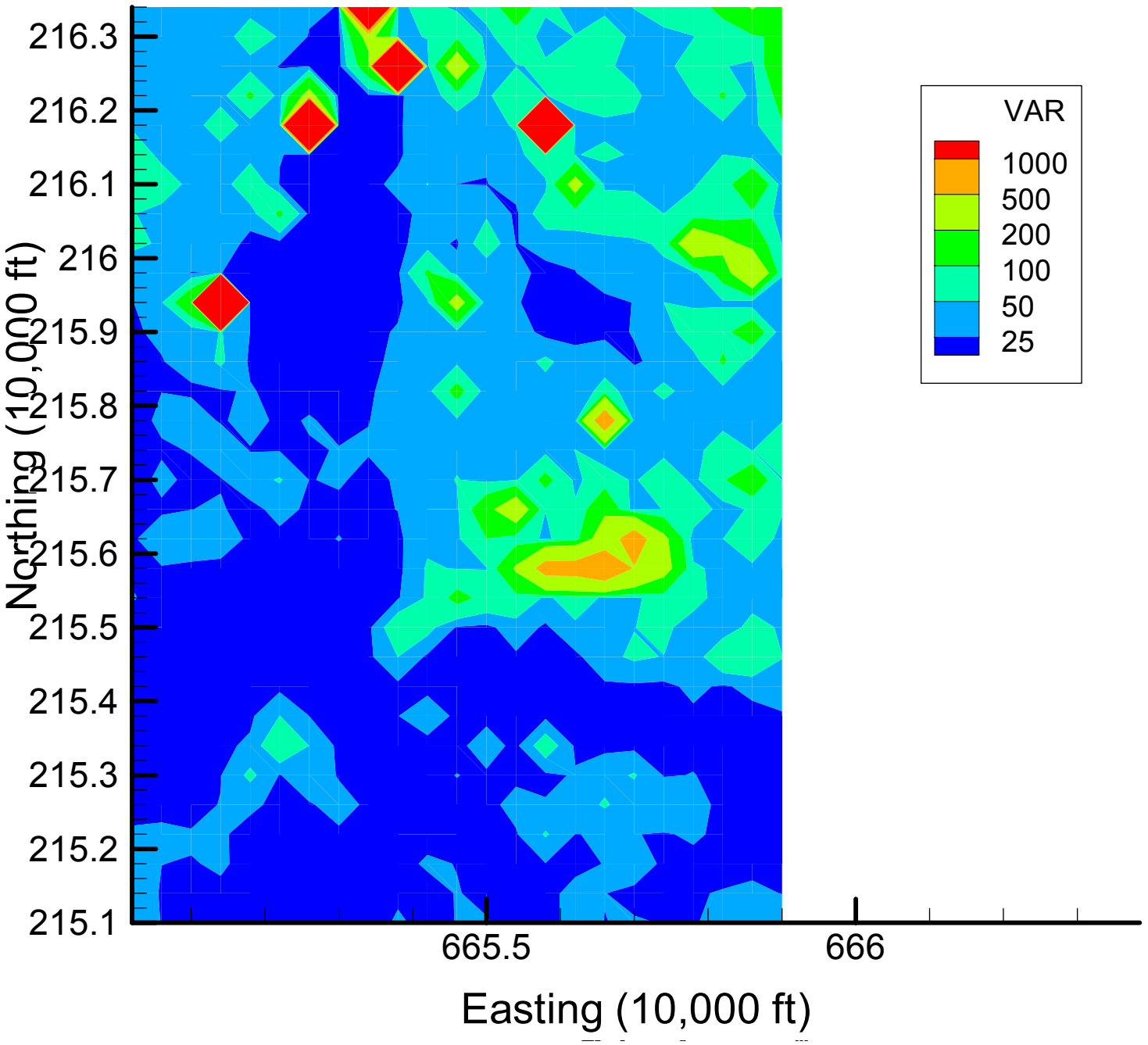

Appendix 4.4
Base Concentration Maps

TCE

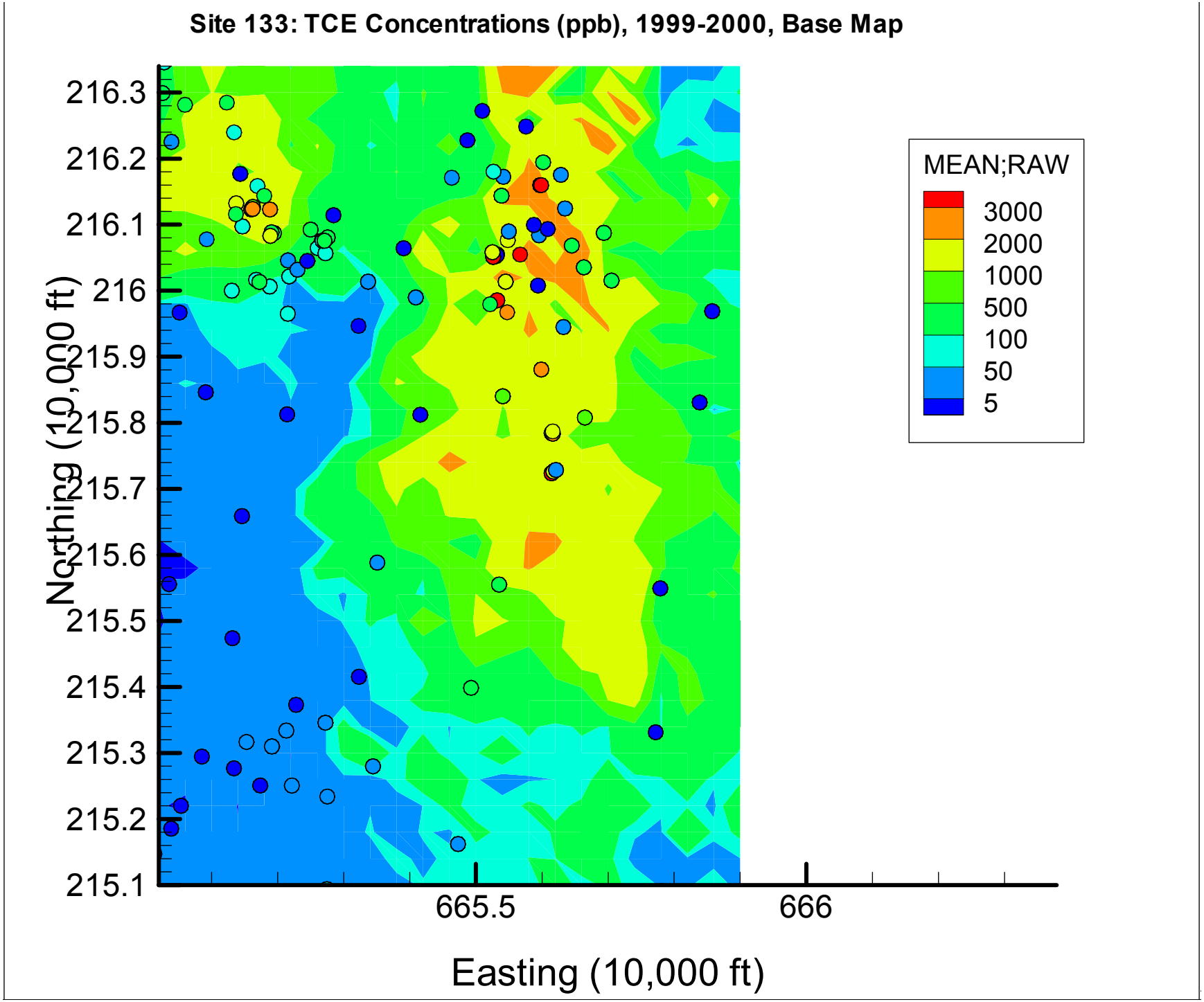
Site 133: TCE Concentrations (ppb), 1999-2000, Base Map
MEAN;RAW
3000
2000
1000
500
100
50
5
216.3
216.2
216.1
216
215.9
215.8
215.7
215.6
215.5
215.4
215.3
215.2
215.1
Northing (10,000 ft)
665.5
666
Easting (10,000 ft)

Site 133: TCE Concentrations (ppb), 2001-2002, Base Map

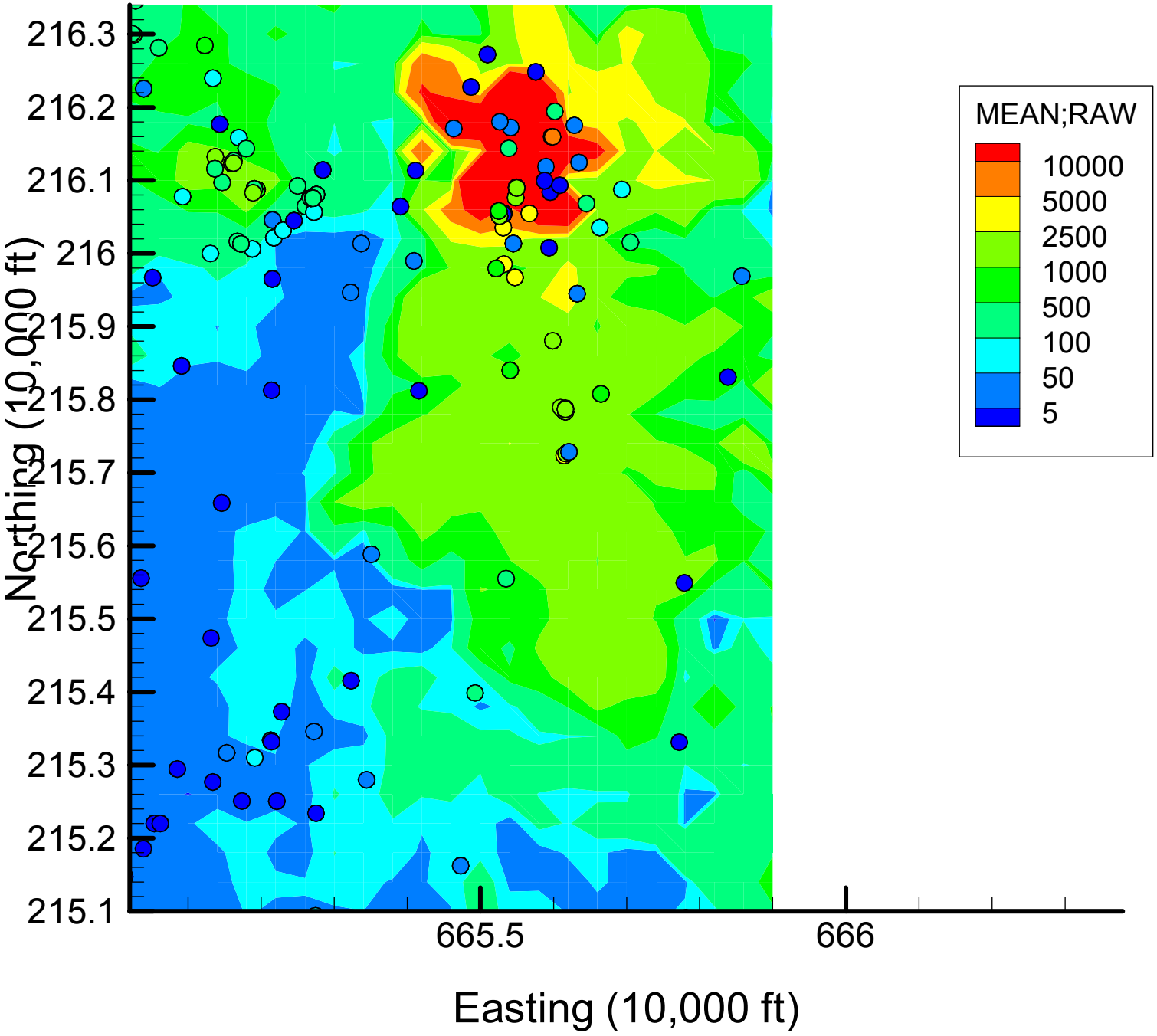

MN

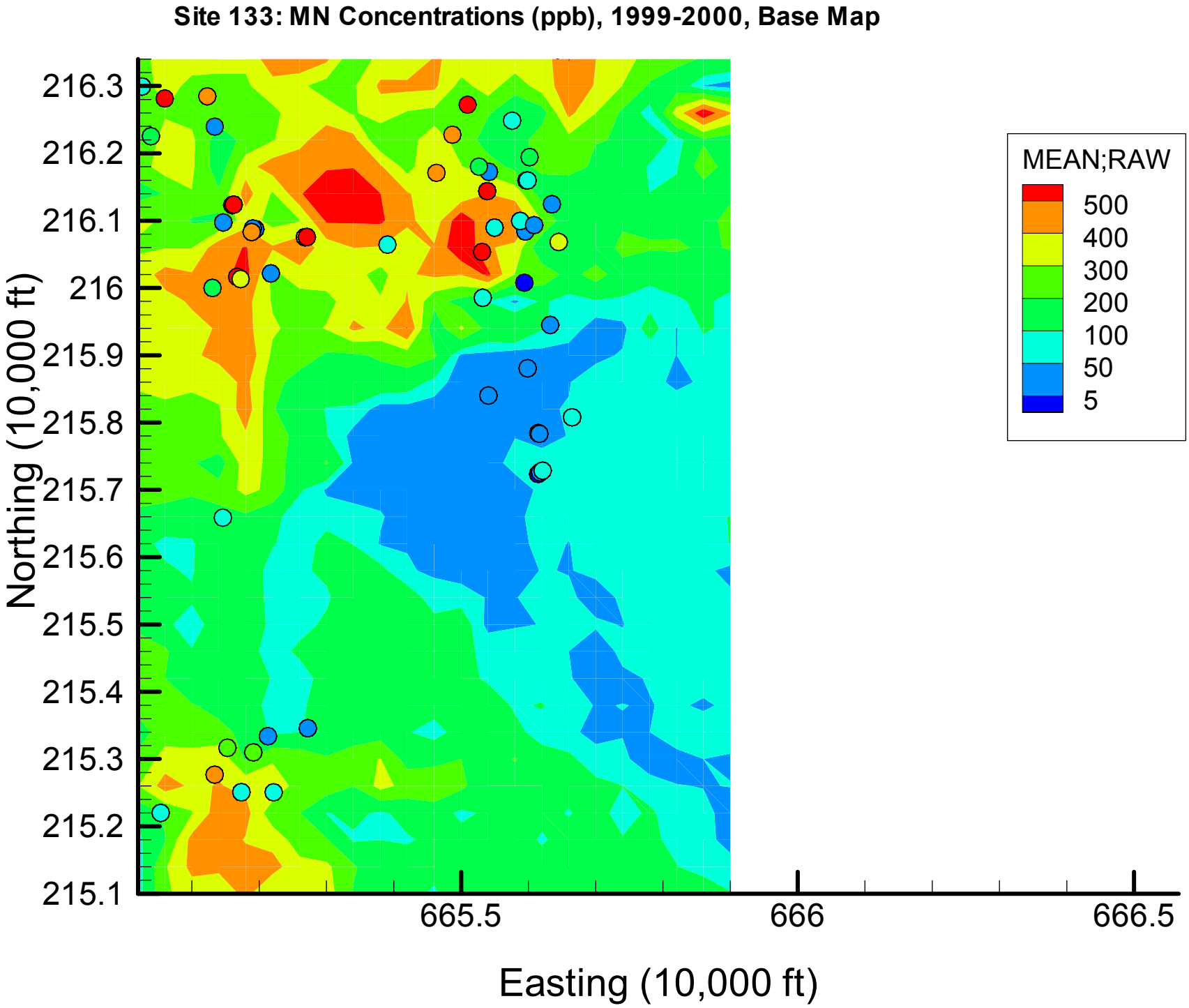
Site 133: MN Concentrations (ppb), 1999-2000, Base Map
MEAN;RAW
500
400
300
200
100
50
5
216.3
216.2
216.1
216
215.9
215.8
215.7
215.6
215.5
215.4
215.3
215.2
215.1
Northing (10,000 ft)
665.5
666
666.5
Easting (10,000 ft)

Site 133: MN Concentrations (ppb), 2001-2002, Base Map

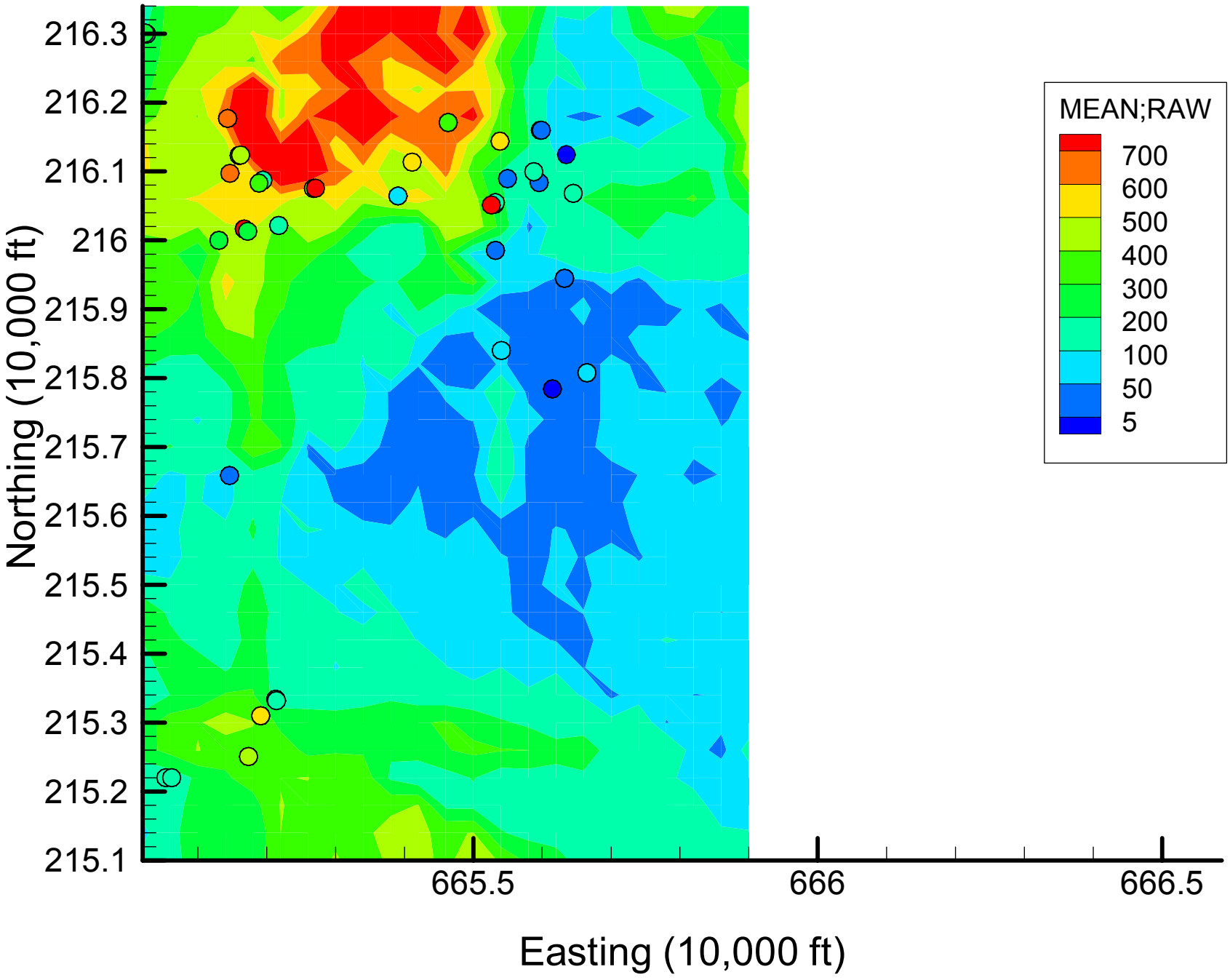

DIOXANE14

Site 133: DIOXANE14 Concentrations (ppb), 1999-2000, Base Map

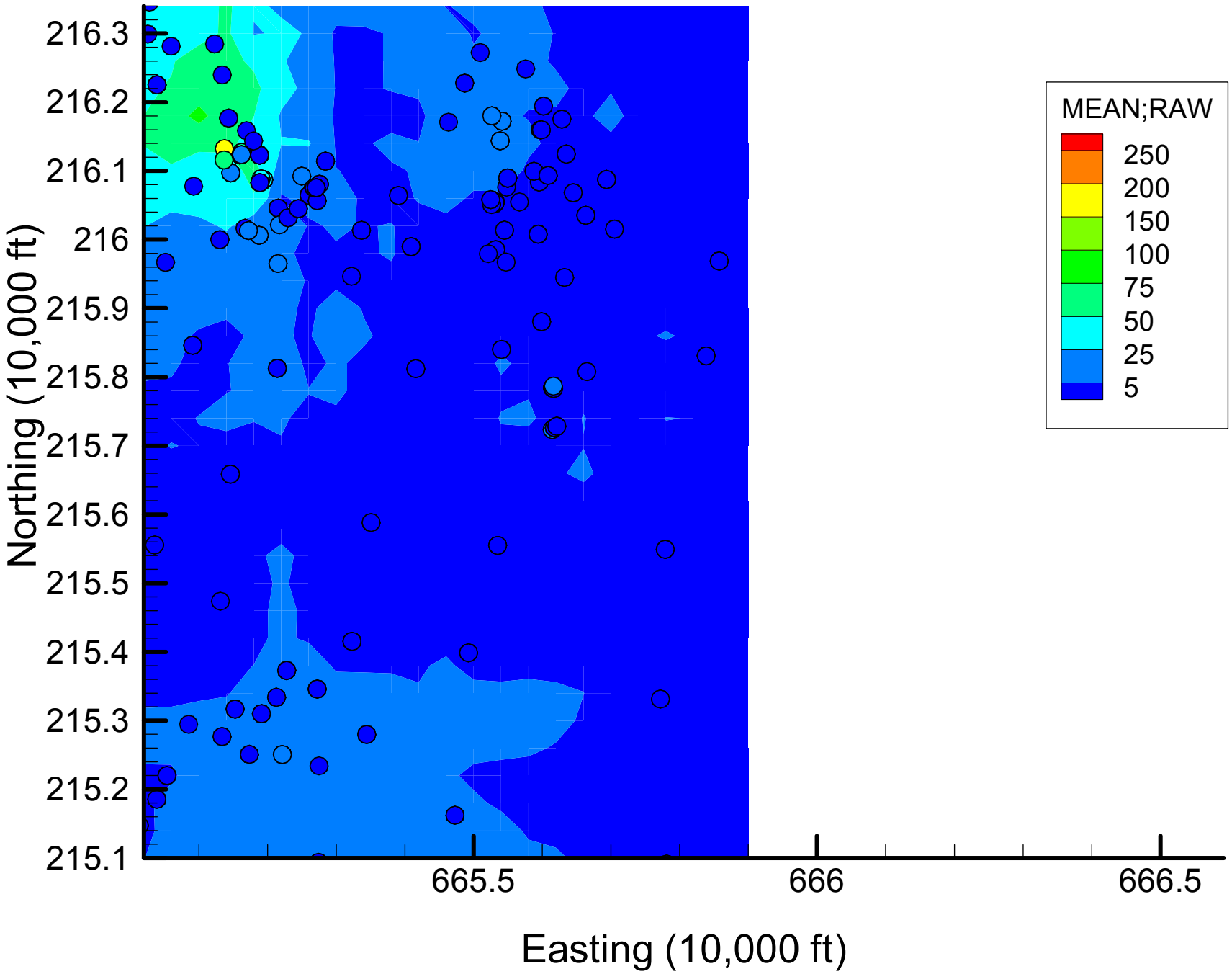

Site 133: DIOXANE14 Concentrations (ppb), 2001-2002, Base Map